

AFRL-RX-WP-TR-2012-0238

QUICK REACTION EVALUATION OF MATERIALS AND PROCESSES (QRE)

Task Order 0008: Titanium Billet Characterization and Materials Properties Development (Nonconforming Titanium) – Executive Summary

John J. Ruschau and Nicholas J. Jacobs

University of Dayton Research Institute

Steven R. Thompson

Materials Integrity Branch
Systems Support Division

JANUARY 2012

Approved for public release; distribution unlimited.

See additional restrictions described on inside pages

STINFO COPY

AIR FORCE RESEARCH LABORATORY
MATERIALS AND MANUFACTURING DIRECTORATE
WRIGHT-PATTERSON AIR FORCE BASE, OH 45433-7750
AIR FORCE MATERIEL COMMAND
UNITED STATES AIR FORCE

NOTICE AND SIGNATURE PAGE

Using Government drawings, specifications, or other data included in this document for any purpose other than Government procurement does not in any way obligate the U.S. Government. The fact that the Government formulated or supplied the drawings, specifications, or other data does not license the holder or any other person or corporation; or convey any rights or permission to manufacture, use, or sell any patented invention that may relate to them.

This report was cleared for public release by the USAF 88th Air Base Wing (88 ABW) Public Affairs (AFRL/PA) Office and is available to the general public, including foreign nationals. Copies may be obtained from the Defense Technical Information Center (DTIC) (http://www.dtic.mil).

AFRL-RX-WP-TR-2012-0238 HAS BEEN REVIEWED AND IS APPROVED FOR PUBLICATION IN ACCORDANCE WITH THE ASSIGNED DISTRIBUTION STATEMENT.

*//Signature//

STEVEN R. THOMPSON
Senior Materials Engineer
Structural Materials Evaluation Team
Materials Integrity Branch

//Signature//

LAWRENCE M. BUTKUS
Acting Chief
Materials Integrity Branch
Systems Support Division

//Signature//

MARY ANN PHILLIPS
Acting Deputy Chief
Systems Support Division
Propulsion Directorate

This report is published in the interest of scientific and technical information exchange, and its publication does not constitute the Government's approval or disapproval of its ideas or findings.

*Disseminated copies will show "//Signature//" stamped or typed above the signature blocks.

REPORT DOCUMENTATION PAGE

Form Approved
OMB No. 0704-0188

The public reporting burden for this collection of information is estimated to average 1 hour per response, including the time for reviewing instructions, searching existing data sources, gathering and maintaining the data needed, and completing and reviewing the collection of information. Send comments regarding this burden estimate or any other aspect of this collection of information, including suggestions for reducing this burden, to Department of Defense, Washington Headquarters Services, Directorate for Information Operations and Reports (0704-0188), 1215 Jefferson Davis Highway, Suite 1204, Arlington, VA 22202-4302. Respondents should be aware that notwithstanding any other provision of law, no person shall be subject to any penalty for failing to comply with a collection of information if it does not display a currently valid OMB control number. **PLEASE DO NOT RETURN YOUR FORM TO THE ABOVE ADDRESS**.

1. REPORT DATE *(DD-MM-YY)*	2. REPORT TYPE	3. DATES COVERED *(From - To)*
January 2012	Final	29 October 2009 – 31 January 2012

4. TITLE AND SUBTITLE

QUICK REACTION EVALUATION OF MATERIALS AND PROCESSES (QRE)
Task Order 0008: Titanium Billet Characterization and Materials Properties Development (Nonconforming Titanium) – Executive Summary

5a. CONTRACT NUMBER
FA8650-09-D-5600-0008

5b. GRANT NUMBER

5c. PROGRAM ELEMENT NUMBER
62102F

6. AUTHOR(S)

John J. Ruschau and Nicholas J. Jacobs (University of Dayton Research Institute)
Steven R. Thompson (AFRL/RXSA)

5d. PROJECT NUMBER
4349

5e. TASK NUMBER
56

5f. WORK UNIT NUMBER
SC101300

7. PERFORMING ORGANIZATION NAME(S) AND ADDRESS(ES)

University of Dayton Research Institute
300 College Park
Dayton, OH 45469

Materials Integrity Branch (AFRL/RXSA)
Systems Support Division, Air Force Research Laboratory
Materials and Manufacturing Directorate
Wright-Patterson Air Force Base, OH 45433-7750
Air Force Materiel Command, United States Air Force

8. PERFORMING ORGANIZATION REPORT NUMBER

9. SPONSORING/MONITORING AGENCY NAME(S) AND ADDRESS(ES)

Air Force Research Laboratory
Materials and Manufacturing Directorate
Wright-Patterson Air Force Base, OH 45433-7750
Air Force Materiel Command
United States Air Force

10. SPONSORING/MONITORING AGENCY ACRONYM(S)
AFRL/RXSA

11. SPONSORING/MONITORING AGENCY REPORT NUMBER(S)
AFRL-RX-WP-TR-2012-0238

12. DISTRIBUTION/AVAILABILITY STATEMENT

Approved for public release; distribution unlimited.

13. SUPPLEMENTARY NOTES

PAO Case Number: 88ABW 2012- 1065; Clearance Date: 28 Feb 2012. Document contains color.

- This information consists of reasonable lower bound properties for titanium billet.
- This information should be used only to evaluate the potential impact of improperly substituted titanium.
- This information should not be used for design purposes in place of material properties from specifications or MMPDS entries covering titanium plate, bar, or other product forms.
- This information should not be used to analyze components manufactured from titanium stock that is known to be compliant with applicable specifications.

14. ABSTRACT

A previous federal investigation identified a risk associated with improperly processed titanium (Ti) material being used in the fabrication of critical components in several USAF and DoD systems. To investigate the potential for major mishaps, a USAF Titanium Task Force was formed to further define risk to USAF systems and to assist with mitigation efforts. An R&D testing program was designed to develop reasonable lower bound property data on a heretofore not fully characterized form of Ti for two alloys: Ti-6Al-4V and Ti-6Al-6V-2Sn. Such data was developed on both properly processed plate materials along with billet material, representing the improperly processed material.

Key results obtained in this investigation have shown that improperly processed materials can have properties that do not meet specifications and requirements. Engineers and designers must account for reduced properties when assessing the integrity and safety of components that are, or may have been, made with the improperly processed materials described herein. This report provides data that should be used in such assessments.

15. SUBJECT TERMS

Titanium 6Al-4V, Ti-6Al-6V-2Sn, billet, plate, tensile, fatigue, fracture toughness, design allowable, fatigue crack growth

16. SECURITY CLASSIFICATION OF:			17. LIMITATION OF ABSTRACT:	18. NUMBER OF PAGES	19a. NAME OF RESPONSIBLE PERSON (Monitor)
a. REPORT	b. ABSTRACT	c. THIS PAGE			Steven R. Thompson
Unclassified	Unclassified	Unclassified	SAR	372	19b. TELEPHONE NUMBER *(Include Area Code)* N/A

TABLE OF CONTENTS

PREFACE iii
SECTION 1 INTRODUCTION 1
SECTION 2 MATERIALS AND SPECIMENS 2
Ti-6Al-4V Billets 2
Ti-6Al-6V-2Sn Billets 3
Ti-6Al-4V & Ti-6Al-6V-2Sn Control Plates 5
SECTION 3 EVALUATIONS PERFORMED 10
Tension (Modulus) 10
Tension 10
Fatigue (Force-controlled) 11
Fatigue (Strain-controlled) 11
Fatigue Crack Growth Rate 11
Fracture Toughness 11
Stress Corrosion Cracking (SCC) 11
SECTION 4 RESULTS 13
SECTION 5 CONCLUSIONS 16
SECTION 6 REFERENCES 17
APPENDICES 18

APPENDIX A - NON-CONFORMING TITANIUM - BILLET CHARACTERIZATION (TI-6AL-4V BILLET) AFRL/RXS 10-057 19

APPENDIX B - NON-CONFORMING TITANIUM – CONTROL PLATE CHARACTERIZATION (TI-6AL-4V & TI-6AL-6V-2SN PLATE) AFRL/RXS 10-072 71

APPENDIX C - NON-CONFORMING TITANIUM - BILLET CHARACTERIZATION (TI-6AL-4V BILLET) AFRL/RXS 10-087 135

APPENDIX D - NON CONFORMING TITANIUM – BILLET CHARACTERIZATION (TI-6AL-6V-2SN BILLETS) AFRL/RXS 11-009 195

APPENDIX E - NON CONFORMING TITANIUM – REASONABLE LOWER BOUND ANALYSES AFRK/RXS 11-051 307

APPENDIX F - STATISTICAL EVALUATION OF FATIGUE CRACK GROWTH RATE DATA FROM TITANIUM BILLETS/PLATES UDR-TR-2011-258 346

Approved for public release; distribution unlimited.

LIST OF FIGURES

Figure 1. Ti-6Al-4V billet (#75838) indicating dimensions, orientations, and sectioning plan prior to specimen extraction 2
Figure 2. Ti-6Al-4V billet (#K27P) indicating dimensions, orientations, and sectioning plan prior to specimen extraction 3
Figure 3. (a) Ti-6Al-6V-2Sn billet (14824) and (b) Ti-6Al-6V-2Sn billet (14828) indicating dimensions and orientations prior to specimen extraction [Note: All dimensions in inches] 4
Figure 4. (a) Ti-6Al-4V plate (J91K) and (b) Ti-6Al-6V-2Sn plate (1247) indicating dimensions and orientations prior to specimen extraction 6
Figure 5. Tensile Specimen Configuration 7
Figure 6. Fatigue Specimen Configuration 7
Figure 7. Eccentrically-Loaded Single Edge Crack Tension (ESE(T)) Geometry used for da/dN Determination 8
Figure 8. Compact (C(T)) Specimen Configuration for Fracture Toughness Determination 8
Figure 9. Stress Corrosion Cracking (SCC) Specimen Configuration 9

LIST OF TABLES

Table 1. Test Methodology 10
Table 2. Summary of Mechanical Property Data on Improperly Processed Titanium 14

Approved for public release; distribution unlimited.

PREFACE

This effort was performed under United States Air Force (USAF) Contract FA8650-09-D-5600, Task Order 0008 entitled "Titanium Billet Characterization & Material Properties Development." The government contract monitor during the period of performance was Mr. Steven Thompson of AFRL/RXSA. Mr. John Ruschau was the UDRI program manager. Special thanks and recognition go to Drs. Larry Butkus and Jeffrey Calcaterra of AFRL/RXSA for their overall guidance and expertise throughout this program.

The bulk of testing described in this report was performed at the Systems Support Division of AFRL, and at Kettering Laboratories located at the University of Dayton Research Institute, Dayton Ohio. The authors would like to extend special recognition to the following UDRI staff who performed the bulk of mechanical testing: Donald Woleslagle, Patricia Youngerman, Eric Soppe, Cris Williams, and Ron Glett. Additional thanks go Dan Laufersweiler and Ed Porter of UTC who performed all of the NDI of the plate and billet materials; Brad Pinnell and Adam Long of UDRI who provided microstructural examinations; Timothy Klopfenstein, Jesse Thumser, and Gary Acton of UDRI who provided machining support; Sarah Kuhlman and Gerald Shaughnessy of the University of Dayton for their development and statistical analysis of the fatigue crack growth rate data, respectively; and Mr. Richard Rice of Battelle Laboratories, Columbus, OH for his support in developing statistical design data consistent with that in the MMPDS Handbook. Finally, special thanks also go to Ms. Cynthia Smith of UDRI who handled the financial aspects of this contract and to Ms. Lou Cooper of UDRI for all administrative support and preparation of final manuscript.

SECTION 1
INTRODUCTION

A federal investigation identified a risk associated with improperly processed (i.e. "nonconforming") titanium (Ti) material being used in the fabrication of critical safety items and safety-of-flight components in USAF, DoD, NASA, FAA, and other systems. At the direction of AFMC/CC, a USAF Titanium Task Force, led by AFMC/EN, was formed to further define risk to USAF systems and to assist with mitigation efforts. The suspect Ti material (e.g., "billet," "reforging stock") was never intended to be machined to the final forms in which it is now possibly being used. This R&D testing program was therefore designed to develop new baseline (reasonable lower bound) properties on a heretofore not fully characterized form of Ti. The decision to refer to these baseline values as "reasonable lower bounds" (RLBs) is based on the fact that an insufficient quantity of material heats and lots were represented for the calculation of traditional MMPDS [1] A- or B-, or even S-basis allowables. However, the number of specimens tested (often in replicate) is significant. Thus "reasonable lower bound" was chosen by the USAF Ti Task Force as an acceptable term to describe properties derived from the testing of multiple specimens from the two heats (per alloy) of material in this program. While these do not meet the requirements for standard baseline property determination, they are, nevertheless, significant. Under normal circumstances, three heats of material would be needed for establishing a specification minimum (S-basis) value; whereas 10 heats of material would be required for A- and B-basis allowables.

Approved for public release; distribution unlimited.

SECTION 2
MATERIALS AND SPECIMENS

Ti-6Al-4V Billets - The first Ti-6Al-4V billet was purchased from Titanium Industries, Inc. As shown in Figure 1, the section received had nominal dimensions of 24”(w) x 19”(l) x 6.5”(t) and had been produced per the AMS 4928R and AMS-T-9047 specifications. The billet’s pedigree traces back to an ingot heat HC-14177 produced by Howmet Castings. (Note: In this report, the billet has been identified through the number 75838, rather than the heat number.) The billet was delivered in the mill-annealed heat treat condition.

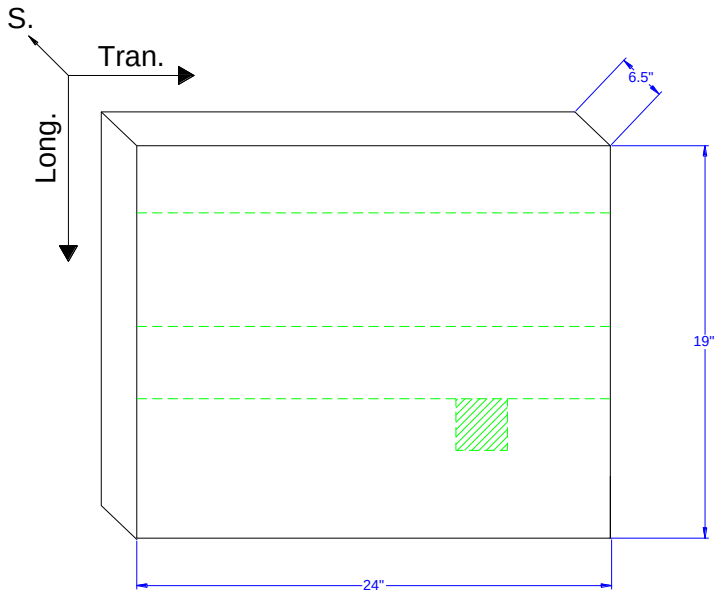


Figure 1. Ti-6Al-4V billet (#75838) indicating dimensions, orientations, and sectioning plan prior to specimen extraction

The second Ti-6Al-4V billet was purchased from Titanium Industries, Inc. and had nominal dimensions of 24”(w) x 45”(l) x 6.5”(t) and had been produced per the AMS 4928R and AMS-T-9047 specifications. The billet’s pedigree traces back to an ingot heat K27P produced by ATI Allvac. This heat number was used in this report for identification of this billet. The billet was delivered in the mill-annealed heat treat condition.

Upon receipt of the second billet, a 4-inch wide section was cut along the length of the billet. The face of this section through the thickness was machined to a 32 RA surface finish and macro-etched using Avesta Pickling Paste 101 to determine forging flowlines. No anomalous microstructure was noticed during this examination. This 4”(w) x 45”(l) x 6.5”(t) section of billet was not used for subsequent mechanical testing. The rest of the billet was further sectioned as indicated in Figure 2.

Approved for public release; distribution unlimited.

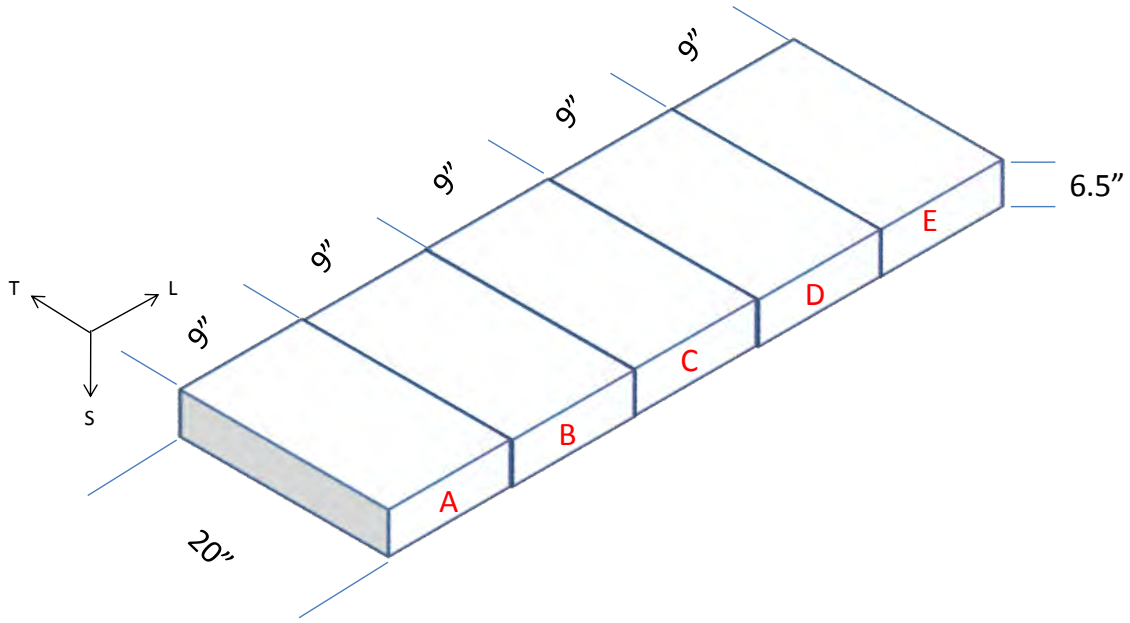
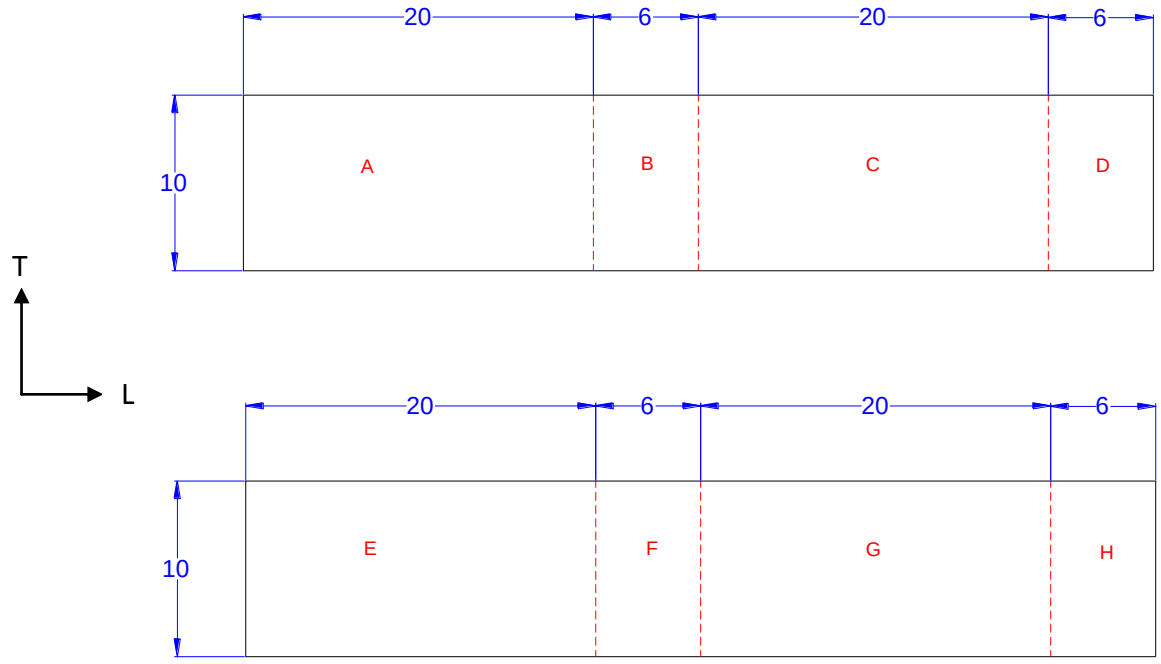


Figure 2. Ti-6Al-4V billet (#K27P) indicating dimensions, orientations, and sectioning plan prior to specimen extraction

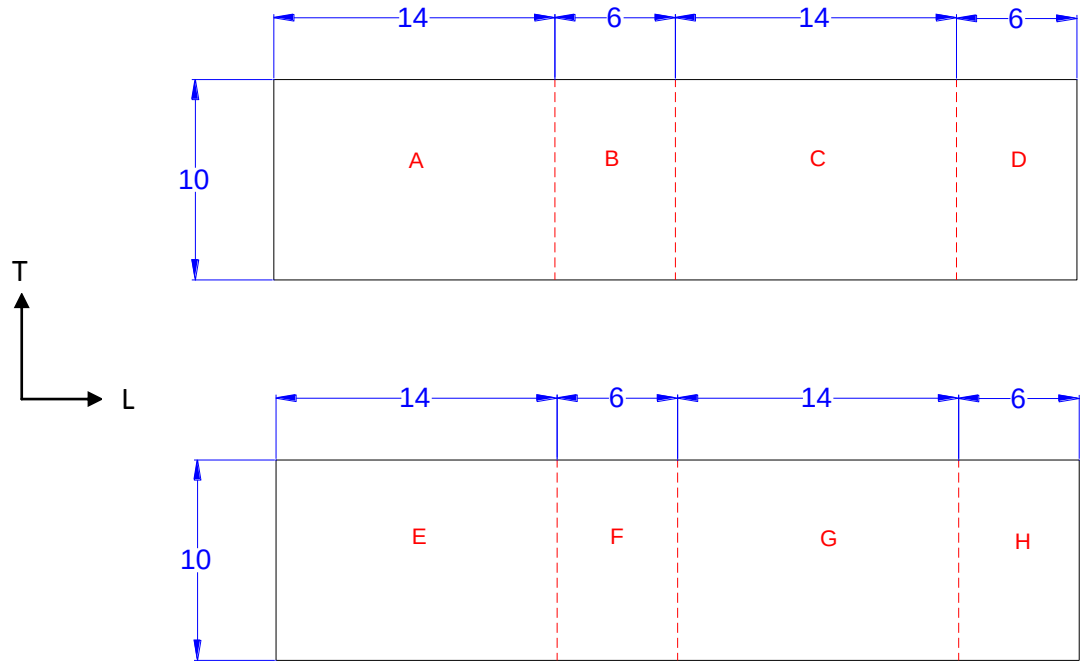
Ti-6Al-6V-2Sn Billets - The Ti-6Al-6V-2Sn billets were purchased from Sierra Alloys of Irwindale, CA. The billets were fabricated for this program to thicknesses prescribed by AFRL/RXS in order to produce two different levels of hot working in the material. Upon receipt from Sierra Alloys, the billets had nominal dimensions of 12"(w) x 105"(l) x 4.5"(t), identified throughout this report as billet number 14824, and 12"(w) x 80"(l) x 8"(t), identified throughout this report as billet number 14828. The billets had been produced per the AMS-T-9047G specification. The billets' pedigree trace back to an ingot heat HC14820 produced by Howmet. The billets were delivered in the mill-annealed heat treat condition.

Upon receipt of the billets, a 2-inch wide section was cut along the length of the billet. The face of this section through the thickness was machined to a 32 RA surface finish and macro-etched using Avesta Pickling Paste 101 to determine forging flowlines. No anomalous microstructure was noticed during this examination. These sections of the billets were not used for subsequent mechanical testing. The dimensions and sectioning plan for both of these products are illustrated in Figure 3.

Approved for public release; distribution unlimited.



(a)



(b)

Figure 3. (a) Ti-6Al-6V-2Sn billet (14824) and (b) Ti-6Al-6V-2Sn billet (14828) indicating dimensions and orientations prior to specimen extraction [Note: All dimensions in inches]

Approved for public release; distribution unlimited.

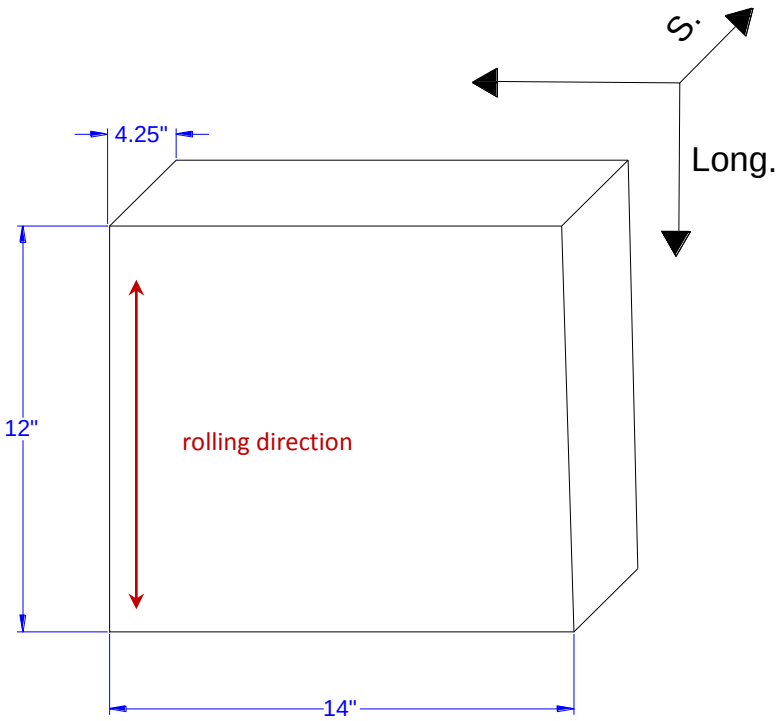
Ti-6Al-4V & Ti-6Al-6V-2Sn Control Plates – The Ti-6Al-4V plate was purchased from Titanium Industries, Inc. As shown in Figure 4(a), the section of plate received had nominal dimensions of 14”(w) x 12”(l) x 4.25”(t) and had been produced per the AMS-T-9046 specification. The plate’s pedigree traces back to ingot heat J91K produced by ATI Allvac. The plate was delivered in the mill-annealed heat treat condition.

The Ti-6Al-6V-2Sn plate had originally been purchased for a similar investigation in 2005. The plate was obtained from RJ Enterprise, Inc. and had original nominal dimensions of 12”(w) x 12”(l) x 4”(t), as illustrated in Figure 4(b), and had been produced per the AMS-T-9046 specification. The plate’s pedigree traces back to ingot heat 855401-01 produced by RMI. (Note: Upon receipt, the plate had been given an internal designation of M1247, and specimens from this plate used the 1247 for identification.) The plate was delivered in the mill annealed heat treat condition.

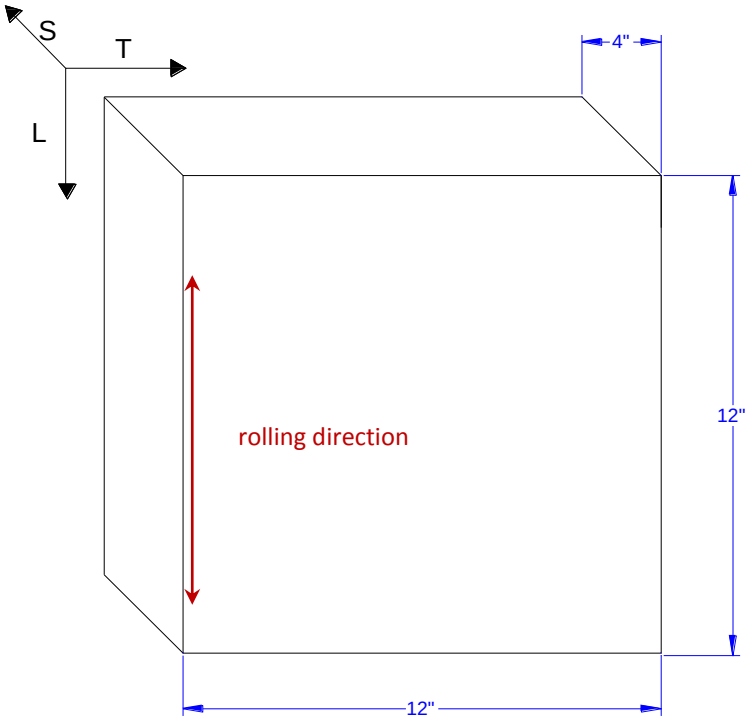
Prior to test specimen extraction, the billets were sectioned so that they could be subjected to non-destructive evaluation (NDE) using ultrasonic transmission (UT). The two control plates were also subjected to UT inspection prior to specimen extraction. After the test specimens were machined, they were once again examined using NDE techniques. All specimens, except the fracture toughness, were examined using x-ray and fluorescent penetrant inspection (FPI). Fracture toughness specimens had UT and FPI examinations. Any resultant indications were noted and photographed for use in analysis of anomalous test results.

Due to the fact that billet material is intended to be an intermediate product form and not meant for use in component fabrication, a specimen orientation system needed to be established. The standard designations of longitudinal (L), long transverse (T), and short transverse (S) coordinate system were employed in this investigation in order to establish a consistency with plate and bar product forms.

Approved for public release; distribution unlimited.



(a)

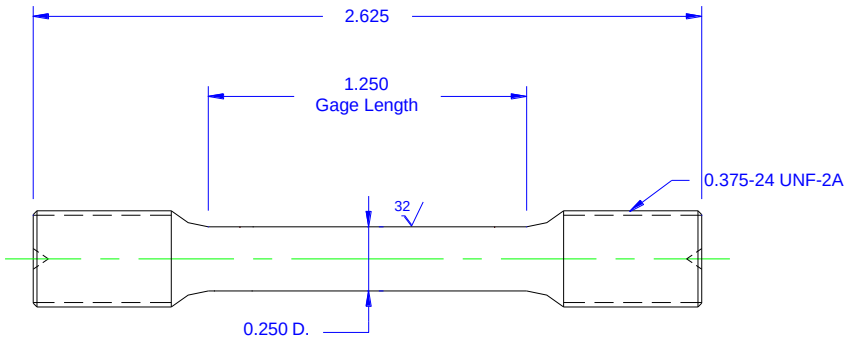


(b)

Figure 4. (a) Ti-6Al-4V plate (J91K) and (b) Ti-6Al-6V-2Sn plate (1247) indicating dimensions and orientations prior to specimen extraction

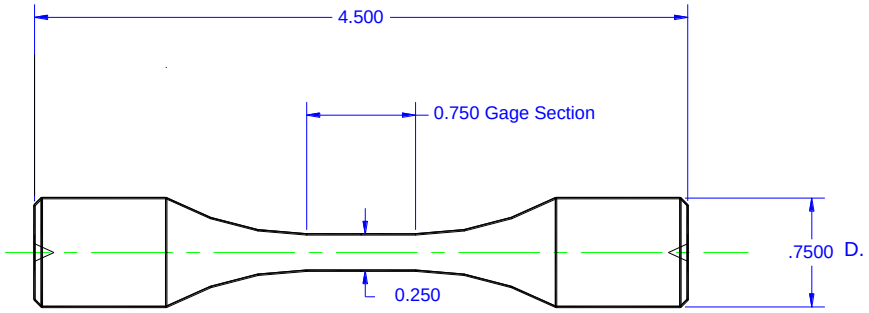
Approved for public release; distribution unlimited.

Test specimens were machined to the final required geometries as shown in the Figures 5 through 9. All of the geometries were in accordance with the applicable test method (as described in the next section). Specimens were generally removed from three planes through the thickness where possible: the two quarter points (t/4 and 3t/4) and the midplane (t/2). For short-transverse (S or S-L) oriented specimens, the location was determined by either the center of the gage length or the crack plane. All of the specimens were fabricated using the same machine shop per specimen drawings provided by AFRL/RXS, in order to minimize possibility of variability due to specimen machining. Special care was given to the traceability of the specimen back to a general location within the billet. Test specimens were given a unique identification that would allow for this tracking.



all dimensions in inches

Figure 5. Tensile Specimen Configuration



all dimensions in inches

Figure 6. Fatigue Specimen Configuration

Approved for public release; distribution unlimited.

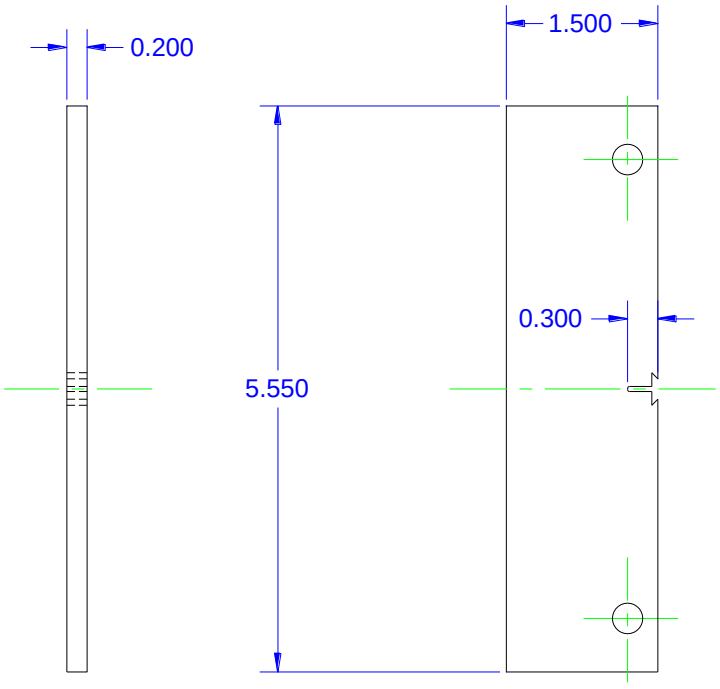


Figure 7. Eccentrically-Loaded Single Edge Crack Tension (ESE(T)) Geometry used for da/dN Determination

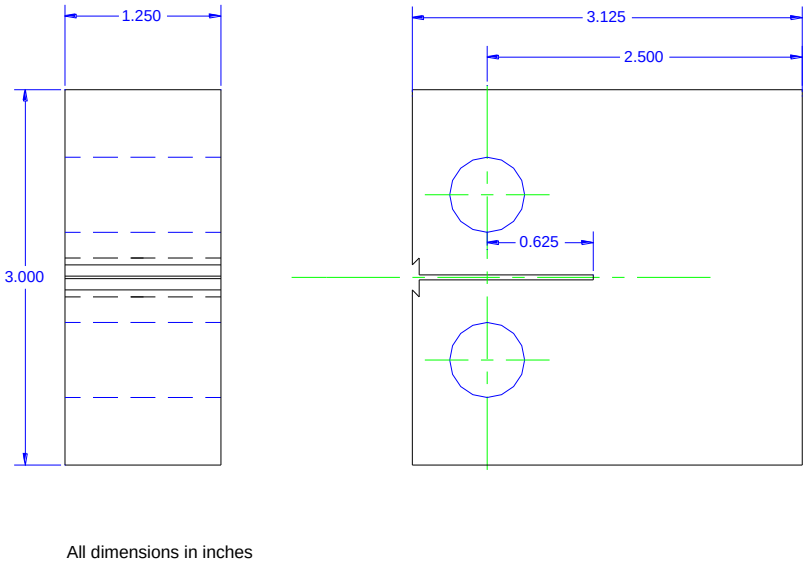


Figure 8. Compact (C(T)) Specimen Configuration for Fracture Toughness Determination

Approved for public release; distribution unlimited.

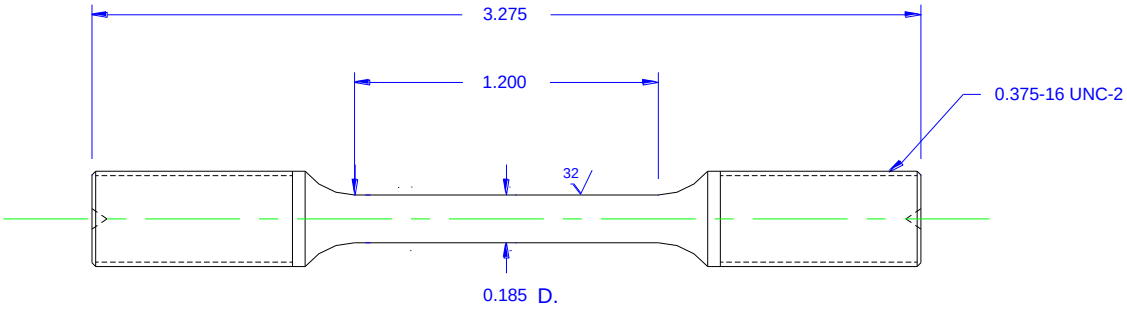


Figure 9. Stress Corrosion Cracking (SCC) Specimen Configuration

Approved for public release; distribution unlimited.

SECTION 3
EVALUATIONS PERFORMED

The test methodologies employed in this investigation are listed in Table 1. With the exception of stress corrosion cracking, all of the tests were performed in accordance with applicable ASTM standards as referenced in the table. All testing was performed in ambient laboratory conditions (approximately 72°F and 50% relative humidity).

Table 1. Test Methodology

Test	ASTM Method
Tension (Modulus)	E111-04 "Standard Test Method for Young's Modulus, Tangent Modulus, and Chord Modulus"
Tension	E8/E8M-08 "Standard Test Methods for Tension Testing of Metallic Materials"
Fatigue (force-controlled)	E466-07 "Standard Practice for Conducting Force Controlled Constant Amplitude Axial Fatigue Tests of Metallic Materials"
Fatigue (strain-controlled)	E606-04 "Standard Practice for Strain-Controlled Fatigue Testing"
Fatigue Crack Growth Rate	E647-08 "Standard Test Method for Measurement of Fatigue Crack Growth Rates"
Fracture Toughness	E399-08 "Standard Test Method for Linear-Elastic Plane-Strain Fracture Toughness KIc of Metallic Materials"
Stress Corrosion Cracking	Similar to G64-99 "Standard Classification of Resistance to Stress-Corrosion Cracking of Heat-Treatable Aluminum Alloys" Applied stress = 75% of specification tensile yield strength / 40 days 3.5% NaCl solution – alternate immersion (10 min wet/50 min dry)

Tension (Modulus) – Prior to performing full-range tension testing, approximately 10% of the machined tension specimens were used to generate modulus data using the procedures outlined in ASTM E111. For this testing the specimens were loaded to a maximum stress below the proportional limit, so as to remain within the linear region of the stress-strain curve. The test was repeated three times per specimen, with the specimen being rotated 120° between test runs. Strain was measured using an MTS averaging extensometer (B-1 classification) with a one-inch gage length. The average modulus from the three runs was recorded as the final elastic modulus.

Tension – Tension testing was performed on an Instron electro-mechanical test machine in accordance with ASTM E8. Strain was measured using an Instron one-inch gage length extensometer. The extensometer was removed from the specimen prior to reaching ultimate load

Approved for public release; distribution unlimited.

to prevent damage to the instrument during specimen breakage. Elongation and reduction of area measurements were made using the "fit-back" method.

Fatigue (Force-controlled) – Axial fatigue testing was performed under force-controlled conditions using an MTS servo-hydraulic test machine in accordance with ASTM E466. Stress ratios (R) of 0.05 and -1 were used in this investigation. Replicate specimens were tested at four applied stress levels for each of the stress ratios.

Fatigue (Strain-controlled) – Axial fatigue testing was performed under strain-controlled conditions using an MTS servo-hydraulic test machine in accordance with ASTM E606. An MTS one-inch gage length extensometer was used for strain measurement. The testing frequency used was 1 Hz. Strain ratios ($R\varepsilon = \varepsilon min/\varepsilon max$) of 0.05 and -1 (or A-ratios of 0.90 and ∞, respectively) was examined for both alloys. Replicate specimens were tested at four applied strain levels for each of the ratios.

Fatigue Crack Growth Rate – Fatigue crack growth rate testing was performed on MTS servo-hydraulic test machines per ASTM E647 using computer data acquisition and control systems developed in-house. Crack length was measured using compliance techniques with standard crack-opening-displacement (COD) gages. Testing was performed under decreasing K-control (C = -2) until a near-threshold growth rate (~5x10-8 in/cycle) was obtained, at which point the test was then run under constant amplitude load control (ΔK-increasing) for the remainder of the test. Initial and final crack lengths were measured optically for use in post-test crack correlation calculations. A test frequency of 25 Hz was used throughout the test, with humidity maintained at 50%, ±10% for the duration of the test. Specimens were tested using stress ratios (R) of 0.1 and 0.7. Two orientations were tested for this program, L-T and S-L, where the first letter indicates the loading direction and the second letter indicates the direction of crack propagation. The ESE(T) specimen geometry was utilized for the billet material in order to minimize any potential for out-of-plane cracking due to anisotropy in the material.

Fracture Toughness – Plane-strain fracture toughness testing was performed in accordance with ASTM E399 on a Tinius-Olsen electro-mechanical test machine. Specimen precracking was performed on an MTS servo-hydraulic test machine. Crack length was monitored via compliance techniques using an MTS COD gage as previously described. Initial and final crack lengths were measured optically post-test.

Stress Corrosion Cracking (SCC) – The rationale for performing this type of test was that since the billet material had not been subject to final hot working, the microstructure may not have been fully homogenized, leading to the potential for localized aluminum segregation. If this were to occur, those areas would be more susceptible to the effect of stress corrosion cracking, particularly at this applied stress level.

For this investigation, stress corrosion cracking tests were therefore performed in order to simply give pass/fail results. As there is no ASTM test method for SCC of titanium alloys in a salt water environment, the procedure outlined in ASTM G64 ("A" level) was used. This procedure has been adopted for use within AFRL/RXS as a standard SCC test. Specimens were axially loaded (statically) in an alternate immersion, 3.5% NaCl solution such that the specimens

were submerged in the solution for 10 minutes and then dry air for the remaining 50 minutes of an hour. Samples were loaded at 75% of the specification yield strength (for plate and bar). For the Ti-6Al-4V alloy, the applied stress was 90 ksi; for the Ti-6Al-6V-2Sn the applied stress was 101.3 ksi. The test duration for all tests was 40 days or approximately 1000 hours. Failure criterion was no failure of the specimen during the 40 day period.

Approved for public release; distribution unlimited.

SECTION 4
RESULTS

Individual reports [2-7] covering the specific test and analysis of each of the materials are furnished in Appendices A-E at the end of this report. Key results of the testing described in this report are summarized in Table 2.

Statistical analyses were utilized to determine RLBs/life factors for tensile strength (ultimate and yield), fatigue, and fatigue crack growth rate. Tensile ductility (elongation and reduction of area), elastic modulus, and fracture toughness RLBs were determined by the lowest value in the test population.

Results of testing performed on improperly processed titanium material have shown that material properties often do not meet specifications and requirements. This report has documented this for the titanium alloys Ti-6Al-4V and Ti-6Al-6V-2Sn.

Engineers and designers must account for reduced properties when assessing the integrity and safety of components that are, or may have been, made with improperly processed materials. This report provides data for Ti-6Al-4V and Ti-6Al-6V-2Sn that should be used in such assessments.

Table 2. Summary of Mechanical Property Data on Improperly Processed Titanium

Property	Alloy	Reasonable Lower Bound / Life Factor	Difference from Specification Minimum Value
F_{tu}	Ti-6Al-4V	130 ksi	MMPDS A-basis
	Ti-6Al-6V-2Sn	137 ksi	8 ksi lower than AMS-T-9046 (2”-4”)
F_{ty}	Ti-6Al-4V	118 ksi	MMPDS A-basis
	Ti-6Al-6V-2Sn	131 ksi	4 ksi lower than AMS-T-9046 (2”-4”)
% elongation	Ti-6Al-4V	6.7%	3.3% lower than AMS-T-9046, 9047
	Ti-6Al-6V-2Sn	8%	AMS-T-9046 (2”-4”) Spec Min
% reduction of area	Ti-6Al-4V	10%	15% lower than AMS-T-9047 (<4”)
	Ti-6Al-6V-2Sn	19%	1% lower than AMS-T-9047 (L-orientation)
E	Ti-6Al-4V	15.3 msi	0.7 msi lower than MMPDS typical
	Ti-6Al-6V-2Sn	14.2 msi	1.8 msi lower than MMPDS typical
K_{Ic}	Ti-6Al-4V	59.8 ksi√in	n/a†
	Ti-6Al-6V-2Sn	55.7 ksi√in	
S-N Fatigue*	Ti-6Al-4V	0.61	n/a†
	Ti-6Al-6V-2Sn	0.14	
ε-N Fatigue*	Ti-6Al-4V	0.70	n/a†
	Ti-6Al-6V-2Sn	0.69	
Fatigue Crack Growth Rate*	Ti-6Al-4V	1x	n/a†
	Ti-6Al-6V-2Sn	2x	

where:
F_{tu}: ultimate tensile strength
F_{ty}: tensile yield strength
E: elastic modulus
K_{Ic}: plane strain fracture toughness

Approved for public release; distribution unlimited.

†: No specification minimum value exists for this property. Data from tested control plates were used in the determination of RLB or life factor.

*: Fatigue & crack growth rate life factors discussed in this report that describe the relationship between titanium billet and plate should be used for initial screening purposes only. These factors represent worst case comparisons FOR ONLY TWO STRESS RATIOS (R=0.05 and -1 for fatigue, R=0.1 and 0.7 for fatigue crack growth rate); factors approach 1.0 at certain regions of the curves from which the factors were derived. If a program's initial screening indicates that sufficient maintenance intervals continue to exist for titanium components, no further analysis is required. However, if maintenance intervals are found to be unacceptable during an initial screening using the published factors, a program may conduct further analysis using the full range of the test data provided by AFRL supplemented, as appropriate, with test data and analysis generated by the program.

Approved for public release; distribution unlimited.

SECTION 5
CONCLUSIONS

Improperly processed materials can have material properties that do not meet specifications and requirements. This report has documented this effect for improperly processed titanium alloys Ti-6Al-4V and Ti-6Al-6V-2Sn.

Engineers and designers must account for reduced properties when assessing the integrity and safety of components that are, or may have been, made with improperly processed materials. This report provides data for Ti-6Al-4V and Ti-6Al-6V-2Sn that should be used in such assessments.

SECTION 6
REFERENCES

1. Metallic Materials Properties Development and Standardization (MMPDS) Handbook, MMPDS-04, April 2008, copyright 2008 Federal Aviation Administration.
2. Non-Conforming Titanium - Billet Characterization (TI-6AL-4V Billet), Evaluation Report, Steven R. Thompson, AFRL/RXS 10-057, July 15, 2010.
3. Non-Conforming Titanium - Control Plate Characterization (TI-6AL-4V & TI-6AL-6V-2SN Plate), Evaluation Report, Steven R. Thompson, AFRL/RXS 10-072, August 31, 2010.
4. Non-Conforming Titanium - Billet Characterization (TI-6AL-4V Billet), Evaluation Report, AFRL/RXS 10-087, Steven R. Thompson, AFRL/RXS 10-087, November 5, 2010.
5. Non Conforming Titanium - Billet Characterization (TI-6AL-6V-2SN Billets), Evaluation Report, Steven R. Thompson, AFRL/RXS 11-009, January 31, 2011.
6. Non Conforming Titanium - Reasonable Lower Bound Analyses, Evaluation Report, Steven R. Thompson, AFRL/RXS 11-051, August 12, 2011.
7. Statistical Evaluation of Fatigue Crack Growth Rate Data from Titanium Billets/Plates, Evaluation Report, UDR-TR-2011-258, Gerry Shaughnessy and John J. Ruschau, August 2011.

APPENDICES

Approved for public release; distribution unlimited.

APPENDIX A

NON-CONFORMING TITANIUM - BILLET CHARACTERIZATION (TI-6AL-4V BILLET)

15 JULY 2010

EVALUATION REPORT

REPORT NO. AFRL/RXS 10-057

AUTHOR

Steven R. Thompson
Acquisition Systems Support Branch (AFRL/RXSCE)

Building 652, Room 122
2179 12th Street
Wright-Patterson AFB, Ohio 45433-7718

REQUESTER
AFMC/EN (Thomas Fischer)

CAUTION

This information consists of PRELIMINARY reasonable lower bound properties for titanium billet. (Fully analyzed data, labeled FINAL, will be forthcoming.)
This information should be used **only** to evaluate the potential impact of improperly substituted titanium.
This information should **not** be used for design purposes in place of material properties from specifications or MMPDS entries covering titanium plate, bar, or other product forms.
This information should **not** be used to analyze components manufactured from titanium stock that is known to be compliant with applicable specifications.

CAUTION

DISTRIBUTION STATEMENT A: Approved for public release; distribution unlimited.

BACKGROUND

An ongoing federal investigation has identified a risk associated with improperly processed titanium (Ti) material being used in the fabrication of critical safety items and safety-of-flight components in USAF, DoD, NASA, FAA, and other systems. At the direction of AFMC/CC, a Titanium Task Force (led by AFMC/EN) was formed to further define risk to USAF systems and to assist with mitigation efforts. The suspect Ti material (e.g., "billet," "reforging stock") was never intended to be machined to the final forms in which it is now possibly being used. This R&D testing program will develop new baseline (reasonable lower bound) properties on a heretofore not fully characterized form of Ti. The decision to refer to these baseline values as "reasonable lower bounds" is based on the fact that an insufficient quantity of material heats and lots were represented for the calculation of traditional MMPDS **[*1*]** A- or B-, or even S-basis allowables. However, the number specimens tested (often in replicate) is significant. Thus "reasonable lower bound" was chosen as the proper phrase to describe properties derived from the testing of multiple specimens from the two heats (per alloy) of material in this program. While these do not meet the requirements for standard baseline property determination, they are, nevertheless, significant.

This report is intended to summarize the mechanical testing of one Ti-6Al-4V billet. The data presented in this report is shown on a "preliminary" basis and should not be used for design purposes.

MATERIAL DESCRIPTION

The Ti-6Al-4V billet summarized in this report was purchased from Titanium Industries, Inc. As shown in Figure 1, the section received had nominal dimensions of 24"(w) x 18.5"(l) x 6.5"(t) and had been produced per the AMS 4928R and AMS-T-9047 specifications. The billet's pedigree traces back to an ingot heat HC-14177 produced by Howmet Castings. (Note: In this report, the billet has been identified through the number 75838, rather than the heat number.) The billet was delivered in the mill-annealed heat treat condition.

Due to the fact that billet material is intended to be an intermediate product form and not meant for use in component fabrication, a specimen orientation system needed to be established. The standard designations of longitudinal (L), long transverse (T), and short transverse (S) coordinate system were employed in this investigation in order to establish a consistency with plate and bar product forms. For this billet, the L-orientation was assigned to the billet length, the T-orientation to the billet width, and the S-orientation to the billet thickness as illustrated in Figure 1.

Prior to test specimen extraction, the billet was sub-sectioned (per the dashed lines shown in Fig. 1) so that it could be subjected to non-destructive evaluation (NDE) using

Approved for public release; distribution unlimited.

ultrasonic transmission (UT). One relevant indication was noted during this evaluation and the location was removed from the billet for further examination (as indicated by the hatched region in Fig. 1). After the test specimens were machined, they were once again examined using NDE techniques. All specimens, except the fracture toughness, were examined using x-ray and fluorescent penetrant inspection (FPI). Fracture toughness specimens had UT and FPI examinations. Any resultant indications were noted and photographed for use in analysis of anomalous test results.

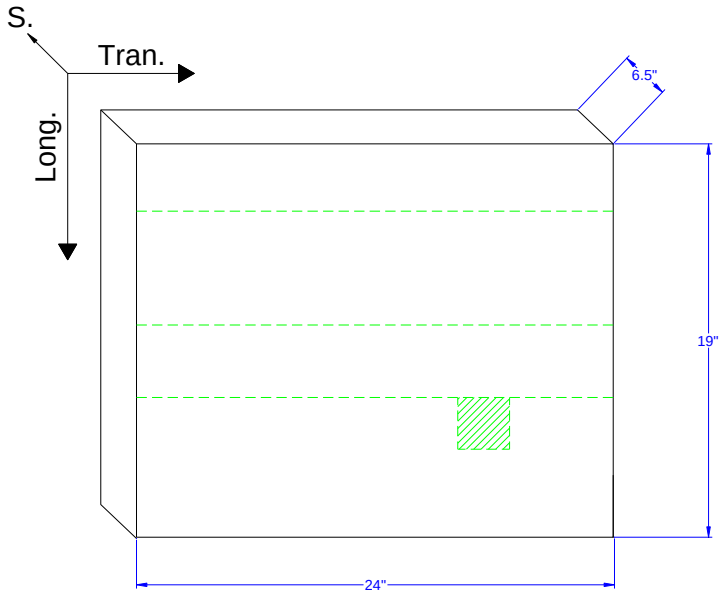


Figure 1. Ti-6Al-4V billet (#75838) indicating dimensions, orientations, and sectioning plan prior to specimen extraction.

TEST PLAN

Test Specimens – The test specimens were excised approximately from the locations shown in Figure 2. Specimens were removed from three planes through the thickness where possible: the two quarter points (t/4 and 3t/4) and the midplane (t/2). Throughout this report, specimen location within the thickness is designated by either "A" (t/4), "B" (t/2), or "C" (3t/4). For short-transverse (S or S-L) oriented specimens, the location was determined by either the center of the gage length or the crack plane.

Approved for public release; distribution unlimited.

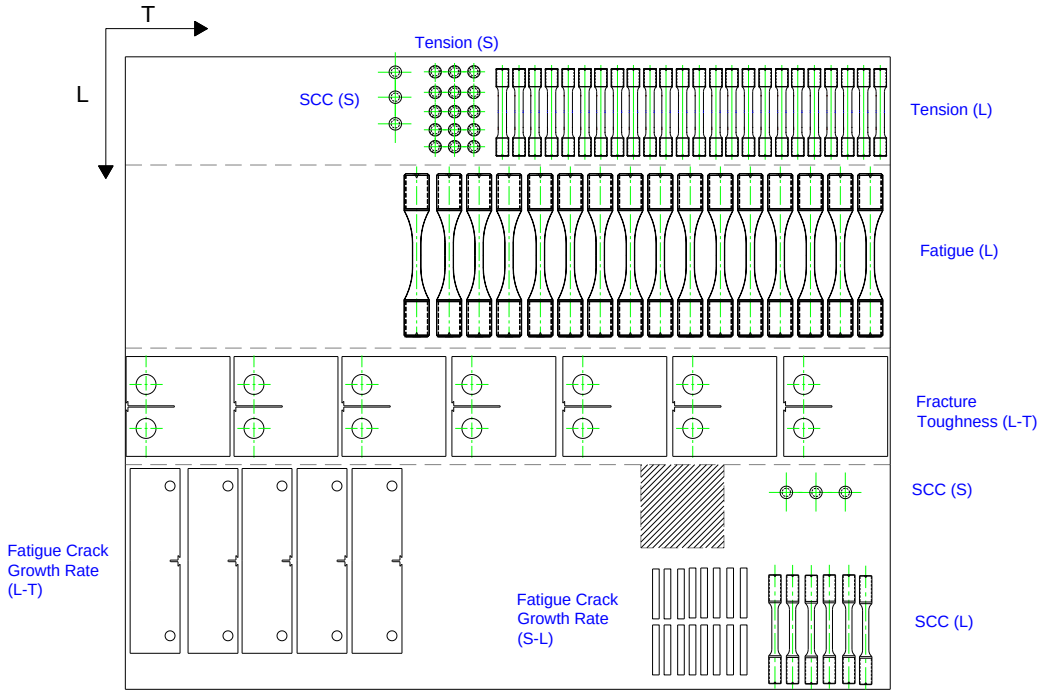


Figure 2. Specimen location layout drawing.

Test specimens were machined to the final required geometries as shown in the Figures 3 through 7. All of the geometries were in accordance with the applicable test method (as described in the next section). All of the specimens were fabricated using the same machine shop per specimen drawings provided by AFRL/RXSCE, in order to minimize possibility of variability due to specimen machining. Special care was given to the traceability of the specimen back to a general location within the billet. Test specimens were given a unique identification that would allow for this tracking.

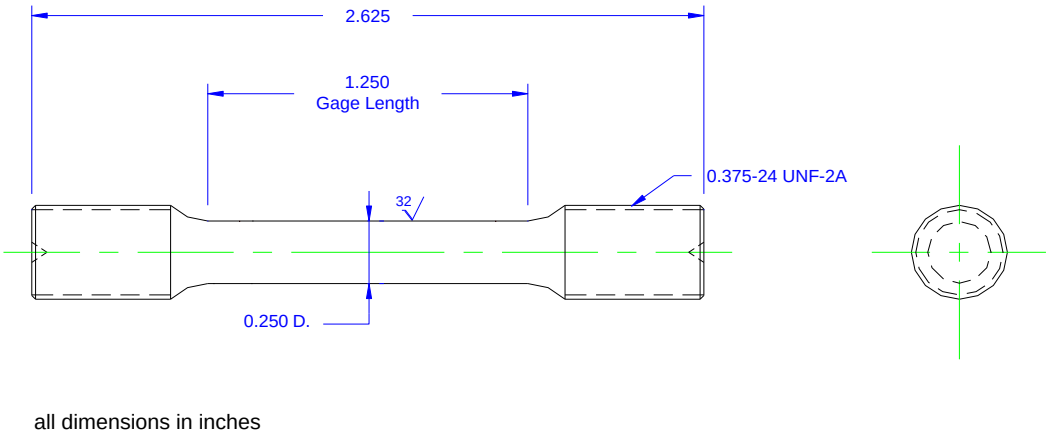


Figure 3. Geometry of tensile test specimen.

Approved for public release; distribution unlimited.

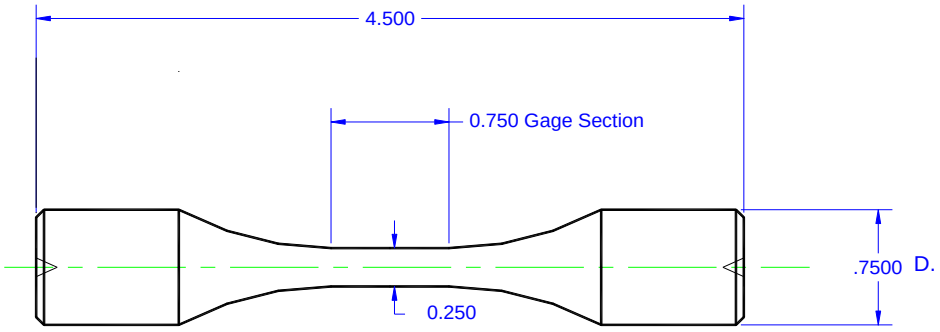


Figure 4. Geometry of fatigue test specimen. (Note: gage section was low-stress ground to a final surface finish of 8 Ra and then hand-polished longitudinally to remove all circumferential scratches.)

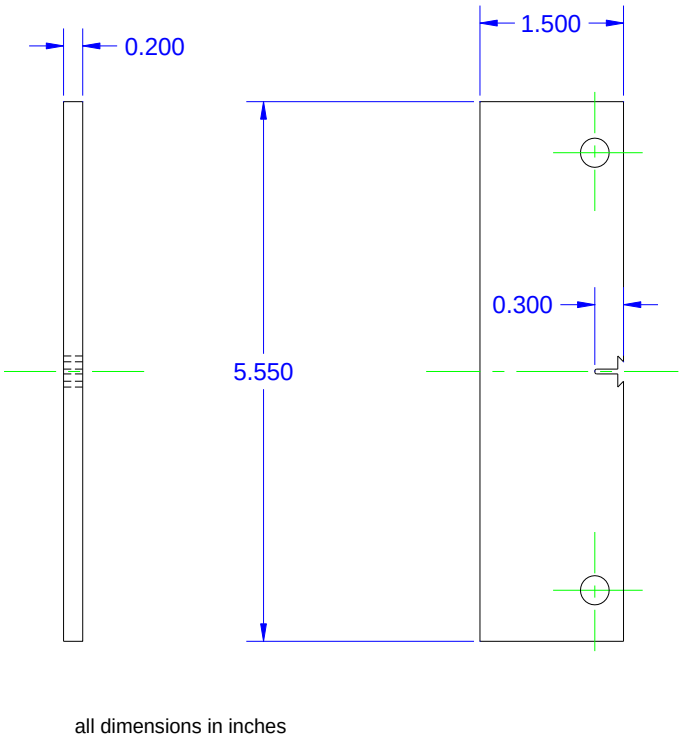


Figure 5. Geometry of fatigue crack growth rate ESE(T) test specimen.

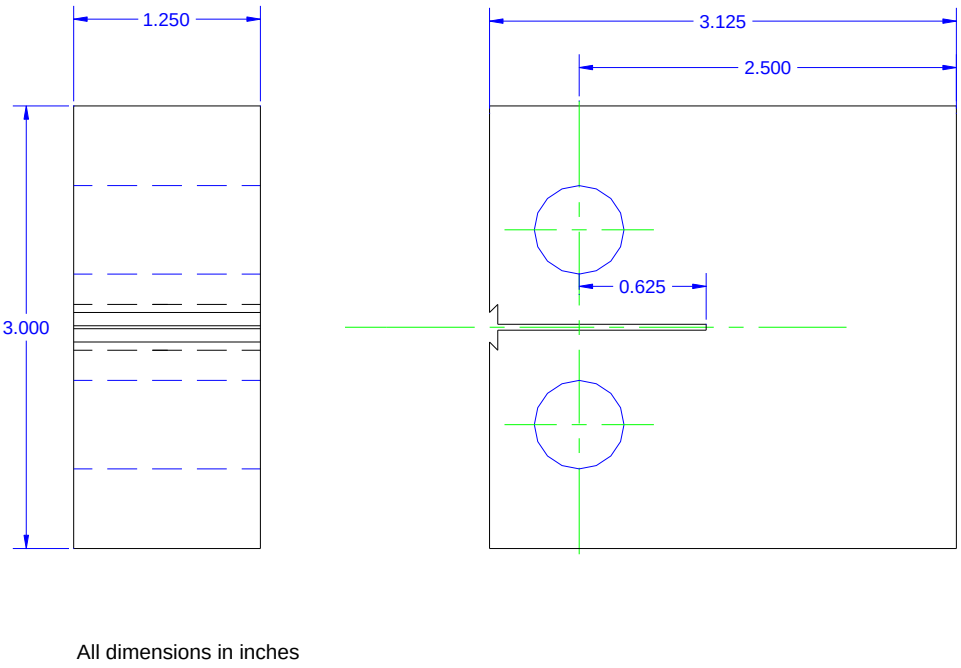


Figure 6. Geometry of fracture toughness C(T) test specimen.

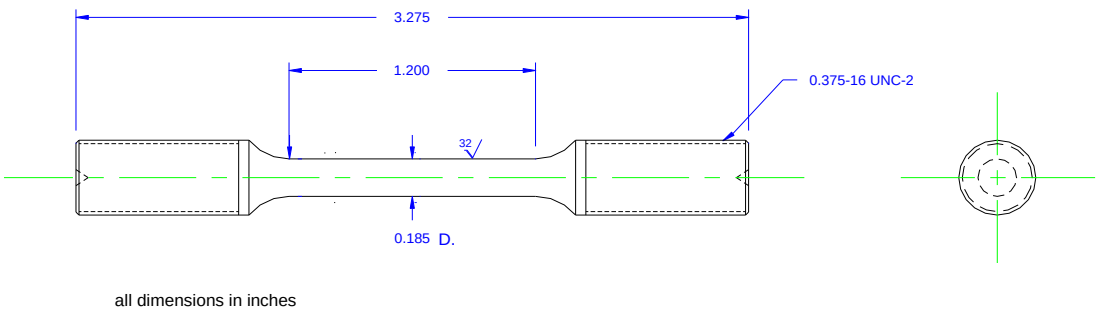


Figure 7. Geometry of stress corrosion cracking (SCC) test specimen.

Test Methods – The test methodologies used in this investigation are listed in Table 1. With the exception of stress corrosion cracking, all of the tests were performed in accordance with applicable ASTM standards. All testing was performed in ambient laboratory conditions (approximately 72°F and 50% relative humidity).

Table 1. Test Methodology

Test	ASTM Method
Tension (Modulus)	E 111-04 "Standard Test Method for Young's Modulus, Tangent Modulus, and Chord Modulus"
Tension	E 8/E 8M-08 "Standard Test Methods for Tension Testing of Metallic Materials"
Fatigue (force-controlled)	E 466-07 "Standard Practice for Conducting Force Controlled Constant Amplitude Axial Fatigue Tests of Metallic Materials"
Fatigue (strain-controlled)	E606-04 "Standard Practice for Strain-Controlled Fatigue Testing"
Fatigue Crack Growth Rate	E 647-08 "Standard Test Method for Measurement of Fatigue Crack Growth Rates"
Fracture Toughness	E 399-08 "Standard Test Method for Linear-Elastic Plane-Strain Fracture Toughness K_{Ic} of Metallic Materials"
Stress Corrosion Cracking	Similar to G 64-99 "Standard Classification of Resistance to Stress-Corrosion Cracking of Heat-Treatable Aluminum Alloys" Applied stress = 75% of specification tensile yield strength / 40 days 3.5% NaCl solution – alternate immersion (10 min wet/50 min dry)

Tension (Modulus) – Prior to performing full-range tension testing, 10% of the machined tension specimens were used to generate modulus data using the procedures outlined in ASTM E111. For this testing the specimens were loaded to a maximum stress below the proportional limit, so as to remain within the linear region of the stress-strain curve. The test was repeated three times per specimen, with the specimen being rotated 120° between test runs. Strain was measured using an MTS averaging extensometer (B-1 classification) with a one-inch gage length. The average modulus from the three runs was recorded as the final elastic modulus.

Tension – Tension testing was performed on an Instron electro-mechanical test machine in accordance with ASTM E8. Strain was measured using an Instron one-inch gage length extensometer. The extensometer was removed from the specimen prior to reaching ultimate load to prevent damage to the instrument during specimen breakage. Elongation and reduction of area measurements were made using the "fit-back" method.

Fatigue (Force-controlled) – Axial fatigue testing was performed under force-controlled conditions using an MTS servo-hydraulic test machine in accordance with ASTM

E466. Stress ratios (R) of 0.05 and -1 were used in this investigation. Replicate specimens were tested at four applied stress levels for each of the stress ratios.

Fatigue (Strain-controlled) – Axial fatigue testing was performed under strain-controlled conditions using an MTS servo-hydraulic test machine in accordance with ASTM E606. An MTS one-inch gage length extensometer was used for strain measurement. The testing frequency used was 1 Hz. A strain ratio ($R_\varepsilon = \varepsilon_{min}/\varepsilon_{max}$) of -1 was used for these specimens. Due to the limited number of specimens available from this particular billet, only a limited amount of replicate testing was performed.

Fatigue Crack Growth Rate – Fatigue crack growth rate testing was performed on an MTS servo-hydraulic test machine per ASTM E647 using computer data acquisition and control systems developed in-house. Crack length was measured via using compliance techniques with standard crack-opening-displacement (COD) gages. Testing was performed under K-control (C=-2) until a near-threshold growth rate was obtained, at which point the test was then run under constant amplitude (constant load) conditions for the remainder of the test. Initial and final crack lengths were measured optically for use in post-test crack correlation calculations. A test frequency of 25 Hz was used throughout the test, with humidity maintained at 50%, ±10% for the duration of the test. Specimens were tested using stress ratios (R) of 0.1 and 0.7. Two orientations were tested for this program, L-T and S-L, where the first letter indicates the loading direction and the second letter indicates the direction of crack propagation. The ESE(T) specimen geometry was utilized for the billet material in order to minimize any potential for out-of-plane cracking due to anisotropy in the material.

Fracture Toughness – Plane-strain fracture toughness tests were performed in accordance with ASTM E399 on a Tinius-Olsen electro-mechanical test machine. Specimen precracking was performed on an MTS servo-hydraulic test machine. Crack length was monitored via compliance techniques using an MTS COD gage as previously described. Initial and final crack lengths were measured optically post-test.

Stress corrosion cracking – The theory behind this testing was that since the billet material had not been subject to final hot working, the microstructure would not be fully homogenized, leading to the potential for localized aluminum segregation. If this were to occur, those areas would be more susceptible to the effect of stress corrosion cracking, particularly at this applied stress level.

For this investigation, stress corrosion cracking tests were therefore performed in order to simply give pass/fail results. As there is currently no ASTM test method for SCC of titanium alloys, the procedure outlined in ASTM G64 ("A" level) was used. This procedure has been adopted for use within AFRL/RXSCE as a standard SCC test. Specimens were axially loaded (statically) in an alternate immersion, 3.5% NaCl solution such that the specimens were submerged in the solution for 10 minutes and then allowed to dry for the next 50 minutes each hour. The specimens were loaded at 75% of the specification yield strength (for plate and bar). For this alloy, the applied stress was 90 ksi. The test duration

was set at 40 days. To pass the test, no failure of the specimen could occur during the 40 loading cycle.

FACTUAL DATA

Tension – The results of tensile testing are shown in Tables 2(a) through 2(e). Strength levels for all specimens were above the specification minimum values shown in AMS-T-9046 (plate) or AMS-T-9047 (bar) for this alloy. However, some of the specimens did have ductility (elongation and reduction of area) results that fell below the specification minimum values (highlighted in red in the tables); particularly in the short-transverse orientation. Elastic modulus values were all within the range expected for this alloy. There was also very little difference between those modulus results from ASTM E111 tests and those obtained from the E8 tensile test record. In addition, there did not appear to be a difference between specimens excised from the three different thickness locations.

Although the "reasonable lower bound" for the alloy will be calculated after the completion of testing of a second Ti-6Al-4V billet and identified in a future report, for this billet a preliminary reasonable lower bound was calculated using the procedures described in MMPDS Section 9.4.1 and assuming normality in the data population. The equation used for the calculation of these preliminary values (for strength only) was:

$$Minimum\ S = \overline{X} - s * k_{99}$$

where

$\overline{X}$ = sample mean

s = standard deviation

k_{99} = one-sided tolerance-limit factor corresponding to a proportion at least 0.99 of a normal distribution and a confidence coefficient of 0.95 based on the number of specimens in the given population. For this report, a k_{99} factor of 2.68 was used, representing a population size of 101.

It should be noted that the AMS-T-9046 specification does not list minimum properties for the short-transverse orientation. Due to evidence indicating that non-conforming materials have been cut-down from billet and purported as plate or bar, the expected orientation system may not have been known during component fabrication. Therefore, the results from the two orientations tested have been grouped together in order to provide reasonable lower bound properties. After calculating these values, they were compared with both the specification minimums and MMPDS A-basis allowables. The lesser of the values were established as the reasonable lower bound property. These preliminary reasonable lower bound properties are shown in Table 3. For modulus, elongation, and reduction of area, the minimum value from the data has been used as the preliminary reasonable lower bound.

Approved for public release; distribution unlimited.

Table 2. Tensile test results.
(a) Longitudinal orientation, t/4 thickness location

	Orientation	Thickness Location	Yield Strength (ksi)	Ultimate Tensile Strength (ksi)	% Elongation	% Reduction of Area	Elastic Modulus, E111 (msi)	Elastic Modulus, E8 (msi)
75838-T-L-1-A	L	t/4	131.2	139.0	14.6%	26.6%	16.6	16.9
L-2-A	L	t/4	130.5	138.2	14.5%	28.7%		16.9
L-3-A	L	t/4	130.4	137.9	12.6%	24.6%		17.0
L-4-A	L	t/4	*a*	*a*	*a*	*a*	17.2	*a*
L-5-A	L	t/4	128.4	136.9	13.7%	21.4%		17.4
L-6-A	L	t/4	129.5	137.3	13.4%	25.7%		17.5
L-7-A	L	t/4	128.9	137.1	15.2%	23.4%		16.9
L-8-A	L	t/4	127.9	135.6	13.9%	26.4%		17.1
L-9-A	L	t/4	126.9	134.5	13.2%	26.3%		17.2
L-10-A	L	t/4	128.2	135.3	16.2%	22.3%		17.2
L-11-A	L	t/4	127.9	137.1	14.3%	26.1%		17.2
L-12-A	L	t/4	126.2	135.8	13.7%	21.1%		17.2
L-13-A	L	t/4	126.7	134.0	12.0%	21.2%		16.7
L-14-A	L	t/4	127.8	135.6	15.4%	25.1%		17.2
L-15-A	L	t/4	126.4	135.9	15.3%	25.8%		17.5
L-16-A	L	t/4	126.8	135.4	13.7%	21.1%		17.3
L-17-A	L	t/4	126.8	135.5	15.2%	27.1%		17.3
L-18-A	L	t/4	126.2	134.3	15.2%	22.3%		17.1
L-19-A	L	t/4	127.9	136.0	12.3%	22.3%		17.6
L-20-A	L	t/4	126.3	134.8	13.3%	25.9%		17.2
L-21-A	L	t/4	127.0	135.6	12.7%	19.6%		17.1
L-22-A	L	t/4	126.3	133.8	12.9%	26.3%		17.5
L-23-A	L	t/4	126.5	134.3	13.3%	29.2%		16.9
L-24-A	L	t/4	127.3	135.9	11.7%	23.1%		17.2
AMS-T-9046			120	130	10%			
AMS-T-9047 (4" & under)			120	130	10%	25%		
AMS-T-9047 (4"-6")			120	130	10% [8%][b]	20% [15%][b]		
MMPDS A-basis			118	130	10			16.0

(a) Specimen damaged prior to ASTM E8 tensile test.
(b) Values in brackets [ ] apply to the short transverse orientation for short transverse dimensions of 3.0 inches or greater.

(b) Longitudinal orientation, t/2 thickness location

	Orientation	Thickness Location	Yield Strength (ksi)	Ultimate Tensile Strength (ksi)	% Elongation	% Reduction of Area	Elastic Modulus, E111 (Msi)	Elastic Modulus, E8 (Msi)
75838-T-L-1-B	L	t/2	130.3	138.1	8.3%	12.4%		17.1
L-2-B	L	t/2	128.2	135.9	14.3%	23.8%		16.9
L-3-B	L	t/2	129.8	137.6	13.6%	22.8%		16.8
L-4-B	L	t/2	128.0	135.6	13.0%	25.2%		17.0
L-5-B	L	t/2	125.7	133.4	11.3%	19.9%		16.4
L-6-B	L	t/2	125.9	133.5	14.9%	33.2%		16.8
L-7-B	L	t/2	127.6	136.0	13.0%	24.0%		17.7
L-8-B	L	t/2	127.4	135.5	12.0%	25.5%		17.6
L-9-B	L	t/2	126.1	133.9	11.7%	26.4%		17.3
L-10-B	L	t/2	126.0	133.6	11.1%	22.9%		17.0
L-11-B	L	t/2	126.5	134.5	11.6%	22.3%		16.9
L-12-B	L	t/2	125.1	133.2	11.8%	25.9%		17.2
L-13-B	L	t/2	124.0	132.0	12.2%	26.5%		16.7
L-14-B	L	t/2	126.1	134.5	16.5%	23.4%		17.1
L-15-B	L	t/2	123.9	130.9	13.5%	22.6%		16.5
L-16-B	L	t/2	125.2	133.6	12.1%	23.3%	17.1	17.3
L-17-B	L	t/2	124.4	132.6	11.8%	18.6%	16.9	17.3
L-18-B	L	t/2	123.5	132.3	14.6%	21.5%		16.3
L-19-B	L	t/2	124.1	130.9	15.7%	27.4%		16.3
L-20-B	L	t/2	126.6	133.9	11.6%	23.1%		16.6
L-21-B	L	t/2	125.1	131.2	14.2%	26.9%		17.0
L-22-B	L	t/2	124.2	133.4	15.6%	27.0%		16.4
L-23-B	L	t/2	127.7	135.6	15.9%	22.9%		17.3
L-24-B	L	t/2	126.4	132.9	12.9%	24.2%		17.2
AMS-T-9046			120	130	10			
AMS-T-9047 (4" & under)			120	130	10%	25%		
AMS-T-9047 (4"-6")			120	130	10% [8%][a]	20% [15%][a]		
MMPDS A-basis			118	130	10			16.0

(a) Values in brackets [ ] apply to the short transverse orientation for short transverse dimensions of 3.0 inches or greater.

Approved for public release; distribution unlimited.

(c) Longitudinal orientation, 3t/4 thickness location

	Orientation	Thickness Location	Yield Strength (ksi)	Ultimate Tensile Strength (ksi)	% Elongation	% Reduction of Area	Elastic Modulus, E111 (msi)	Elastic Modulus, E8 (msi)
75838-T-L-1-C	L	3t/4	129.4	137.2	10.1%	19.5%		16.6
L-2-C	L	3t/4	130.4	137.7	13.0%	27.9%		16.8
L-3-C	L	3t/4	129.0	136.5	13.3%	29.3%		16.8
L-4-C	L	3t/4	129.6	137.2	14.0%	25.3%		17.5
L-5-C	L	3t/4	128.6	135.9	11.6%	22.0%		17.2
L-6-C	L	3t/4	129.1	136.9	14.8%	26.4%		17.0
L-7-C	L	3t/4	126.4	134.4	12.6%	19.7%		16.8
L-8-C	L	3t/4	126.8	135.2	11.0%	21.6%	17.0	17.0
L-9-C	L	3t/4	127.1	135.1	12.2%	26.4%		16.9
L-10-C	L	3t/4	127.5	135.3	13.4%	26.6%		17.3
L-11-C	L	3t/4	127.6	135.2	13.1%	26.4%		17.1
L-12-C	L	3t/4	128.9	136.7	14.5%	22.5%		17.8
L-13-C	L	3t/4	125.9	134.3	17.7%	24.3%		16.9
L-14-C	L	3t/4	127.3	135.2	15.0%	23.5%		17.4
L-15-C	L	3t/4	126.7	134.3	13.2%	21.6%		17.2
L-16-C	L	3t/4	125.7	134.5	15.1%	24.0%	16.8	17.1
L-17-C	L	3t/4	128.5	135.6	13.6%	22.9%		17.4
L-18-C	L	3t/4	127.6	134.3	12.7%	26.1%		16.6
L-19-C	L	3t/4	128.0	135.6	13.5%	20.9%		16.7
L-20-C	L	3t/4	127.9	135.6	15.9%	19.5%		16.7
L-21-C	L	3t/4	125.9	135.2	13.0%	21.2%		16.6
L-22-C	L	3t/4	129.2	134.9	14.1%	24.8%		16.6
L-23-C	L	3t/4	127.6	136.4	13.5%	23.1%		17.5
L-24-C	L	3t/4	129.0	136.5	18.3%	24.8%		17.1
AMS-T-9046			120	130	10			
AMS-T-9047 (4" & under)			120	130	10%	25%		
AMS-T-9047 (4"-6")			120	130	10% [8%][a]	20% [15%][a]		
MMPDS A-basis			118	130	10			16.0

(a) Values in brackets [ ] apply to the short transverse orientation for short transverse dimensions of 3.0 inches or greater.

Approved for public release; distribution unlimited.

(d) Short-transverse orientation, t/4 thickness location

	Orientation	Thickness Location	Yield Strength (ksi)	Ultimate Tensile Strength (ksi)	% Elongation	% Reduction of Area	Elastic Modulus, E111 (Msi)	Elastic Modulus, E8 (Msi)
75838-T-S-1-A	S	t/4	128.9	139.7	10.4%	22.1%	16.5	16.0
S-2-A	S	t/4	128.2	137.7	6.7%	24.6%	16.4	16.5
S-3-A	S	t/4	127.1	140.2	10.5%	17.6%		16.4
S-4-A	S	t/4	128.2	139.6	10.0%	14.3%		17.0
S-5-A	S	t/4	128.7	139.6	7.9%	10.0%		16.5
S-6-A	S	t/4	126.3	140.0	11.0%	14.9%		16.5
S-7-A	S	t/4	127.6	139.4	8.5%	14.8%		16.5
S-8-A	S	t/4	126.8	139.8	9.3%	19.8%		16.2
S-9-A	S	t/4	126.6	139.1	10.2%	16.5%		16.5
S-10-A	S	t/4	128.4	139.3	8.8%	18.6%		16.7
S-11-A	S	t/4	127.9	140.3	10.4%	19.9%		16.6
S-12-A	S	t/4	126.7	139.0	11.8%	17.9%		16.3
S-13-A	S	t/4	126.0	138.7	10.4%	18.7%		16.6
S-14-A	S	t/4	128.3	138.3	9.5%	16.5%		16.0
S-15-A	S	t/4	127.8	137.4	7.8%	13.4%		16.5
AMS-T-9046			120	130	10			
AMS-T-9047 (4" & under)			120	130	10%	25%		
AMS-T-9047 (4"-6")			120	130	10% [8%][a]	20% [15%][a]		
MMPDS A-basis			118	130	10			16.0

(a) Values in brackets [ ] apply to the short transverse orientation for short transverse dimensions of 3.0 inches or greater.

Approved for public release; distribution unlimited.

(e) Short-transverse orientation, 3t/4 thickness location

	Orientation	Thickness Location	Yield Strength (ksi)	Ultimate Tensile Strength (ksi)	% Elongation	% Reduction of Area	Elastic Modulus, E111 (Msi)	Elastic Modulus, E8 (Msi)
75838-T-S-1-C	S	3t/4	127.5	139.1	9.9%	24.2%		16.7
S-2-C	S	3t/4	129.6	140.1	11.9%	19.9%	16.5	16.6
S-3-C	S	3t/4	129.4	140.5	10.0%	17.7%	16.5	16.8
S-4-C	S	3t/4	128.9	140.7	11.5%	19.5%		17.2
S-5-C	S	3t/4	127.9	136.7	9.9%	16.8%		16.2
S-6-C	S	3t/4	127.2	140.7	10.2%	18.9%		16.4
S-7-C	S	3t/4	126.8	140.3	9.7%	21.5%		16.3
S-8-C	S	3t/4	128.6	139.3	9.8%	15.2%		16.3
S-9-C	S	3t/4	127.2	140.8	*a*	11.2%		16.5
S-10-C	S	3t/4	129.9	140.4	9.7%	15.0%		16.4
S-11-C	S	3t/4	129.1	139.6	9.5%	16.7%		16.3
S-12-C	S	3t/4	128.1	141.1	10.1%	20.6%		16.9
S-13-C	S	3t/4	128.7	140.4	10.9%	13.4%		16.8
S-14-C	S	3t/4	128.6	137.7	9.0%	19.3%		16.3
S-15-C	S	3t/4	129.5	138.9	7.6%	14.6%		16.5
AMS-T-9046			120	130	10			
AMS-T-9047 (4" & under)			120	130	10%	25%		
AMS-T-9047 (4"-6")			120	130	10% [8%][b]	20% [15%][b]		
MMPDS A-basis			118	130	10			16.0

(a) Specimen failed at gage punch location.
(b) Values in brackets [ ] apply to the short transverse orientation for short transverse dimensions of 3.0 inches or greater.

Table 3. Preliminary reasonable lower bound tensile properties for Ti-6Al-4V billet (#75838).

Yield Strength (ksi)	Ultimate Tensile Strength (ksi)	% Elongation	% Reduction of Area	Elastic Modulus (msi)
118	130	6.7%	10%	16

Approved for public release; distribution unlimited.

Fatigue (force-controlled) – The results of force-controlled axial fatigue testing are shown graphically in Figure 8. Individual results are tabulated in Table 4. In Fig. 8, the results for each stress ratio (R) have been fit with a best-fit power-law curve for graphical purposes only. Also included in this figure is a curve based on an equivalent stress equation from MMPDS Figure 5.4.1.1.8(a) for a mean stress of zero (R = -1). This curve is for comparison with the R = -1 data generated in this investigation. As stated in Fig. 4, the fatigue specimens used herein were manufactured using low-stress-grinding operations to a surface finish (Ra) of 8 per ASTM E466 Standard. The MMPDS reference data curve was generated from specimens having a surface roughness of 32. Furthermore, it is not known whether low-stress grinding was used on these specimens. These aspects could quite easily have contributed to the difference between the data sets.

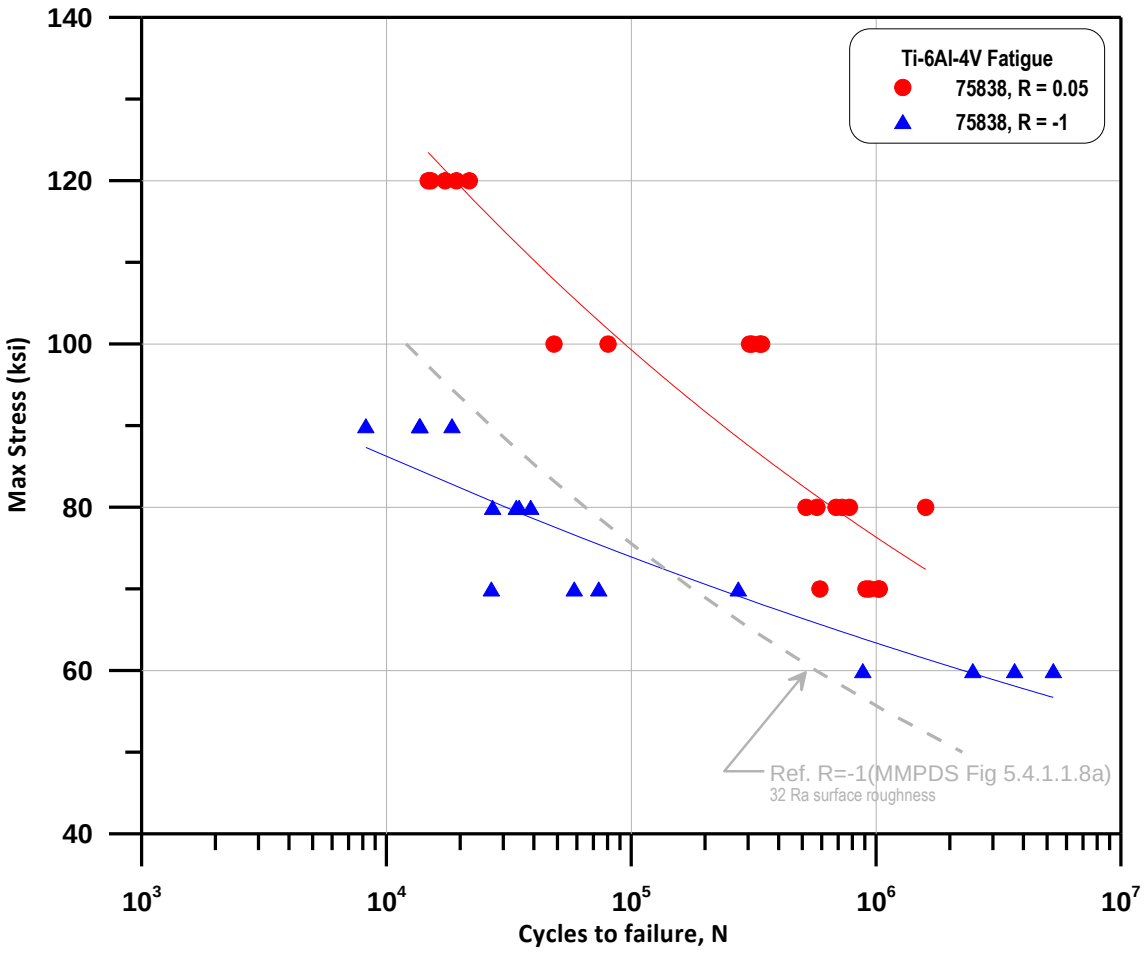


Figure 8. Force-controlled axial fatigue test results.

Approved for public release; distribution unlimited.

Table 4. Force-controlled axial fatigue test results.

	Thickness Location	Max Stress (ksi)	Stress Ratio, R	Cycles to Failure
75838-F-L-12-A	t/4	120	0.05	17,360
L-9-A	t/4	120	0.05	19,278
L-12-B	t/2	120	0.05	14,798
L-13-C	3t/4	120	0.05	15,190
L-11-C	3t/4	120	0.05	21,770
L-15-A	t/4	100	0.05	334,340
L-16-A	t/4	100	0.05	48,280
L-13-A	t/4	100	0.05	304,010
L-14-B	t/2	100	0.05	340,300
L-10-B	t/2	100	0.05	80,236
L-14-C	3t/4	100	0.05	310,817
L-11-A	t/4	80	0.05	777,980
L-14-A	t/4	80	0.05	725,010
L-16-B	t/2	80	0.05	572,558
L-16-C	3t/4	80	0.05	516,664
L-9-C	3t/4	80	0.05	1,593,000
L-10-C	3t/4	80	0.05	685,215
L-10-A	t/4	70	0.05	1,029,437
L-15-B	t/2	70	0.05	939,640
L-11-B	t/2	70	0.05	588,859
L-15-C	3t/4	70	0.05	1,020,840
L-12-C	3t/4	70	0.05	907,710
75838-F-L-8-A	t/4	90	-1	18,498
L-1-B	t/2	90	-1	8,223
L-6-C	3t/4	90	-1	13,625
L-8-C	3t/4	90	-1	13,696
L-1-A	t/4	80	-1	27,138
L-3-A	t/4	80	-1	33,882
L-3-B	t/2	80	-1	38,813
L-2-C	3t/4	80	-1	34,762
L-4-A	t/4	70	-1	58,442
L-4-B	t/2	70	-1	273,475
L-7-B	t/2	70	-1	73,600
L-1-C	3t/4	70	-1	26,776
L-6-A	t/4	60	-1	5,291,838
L-5-B	t/2	60	-1	881,434
L-4-C	3t/4	60	-1	3,674,814
L-7-C	3t/4	60	-1	2,480,572

Approved for public release; distribution unlimited.

Fatigue (strain-controlled) – The results of strain-controlled axial fatigue testing are shown graphically in Figure 9, with individual results tabulated in Table 5. A limited quantity of specimens was available for this testing from this billet, therefore only a strain-ratio (R_ε) of -1 was used.

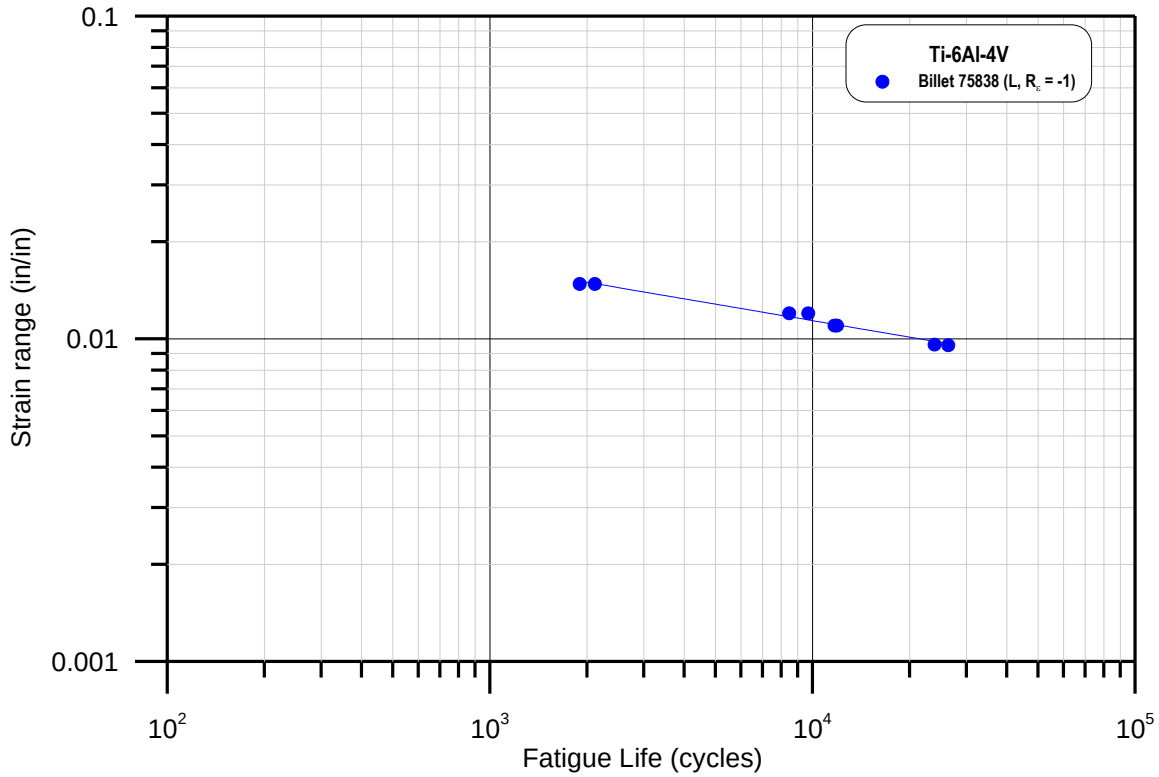


Figure 9. Strain-controlled axial fatigue test results.

Table 5. Strain-controlled axial fatigue test results.

	Thickness Location	Strain Range (in/in)	Strain Ratio, R_ε	Cycles to Failure
75838-F-L-2-A	t/4	0.0148	-1	2,113
L-6-B	t/2	0.0148	-1	1,896
L-8-B	t/2	0.0120	-1	8,466
L-3-C	3t/4	0.0120	-1	9,695
L-5-C	3t/4	0.0110	-1	11,696
L-7-A	t/4	0.0110	-1	11,900
L-5-A	t/4	0.0096	-1	23,880
L-2-B	t/2	0.0096	-1	26,338

Approved for public release; distribution unlimited.

Fatigue Crack Growth Rate – Fatigue crack growth rate test result summary curves are shown in Figures 10 and 11 for stress ratios (R) of 0.1 and 0.7, respectively. Individual specimen curves are located in Appendix A of this report. For both stress ratios, the S-L orientation specimens tended to have faster growth rates than the L-T specimens. Also included on these summary curves are best-fit mean curves from MMPDS-04 Figure 5.4.1.1.9(a1) for 0.25 inch thick Ti-6Al-4V plate (L-T orientation). Comparing the data generated from billet specimens with the MMPDS reference data, the combined orientation billet data generally exhibits slower growth rates over the range of stress intensities examined. Fractographic and metallographic examinations of the failed specimens will be performed to investigate possible reasons for this difference in growth rates. For example, larger grain (or colony) sizes in the billet material could lead to slower growth rates.

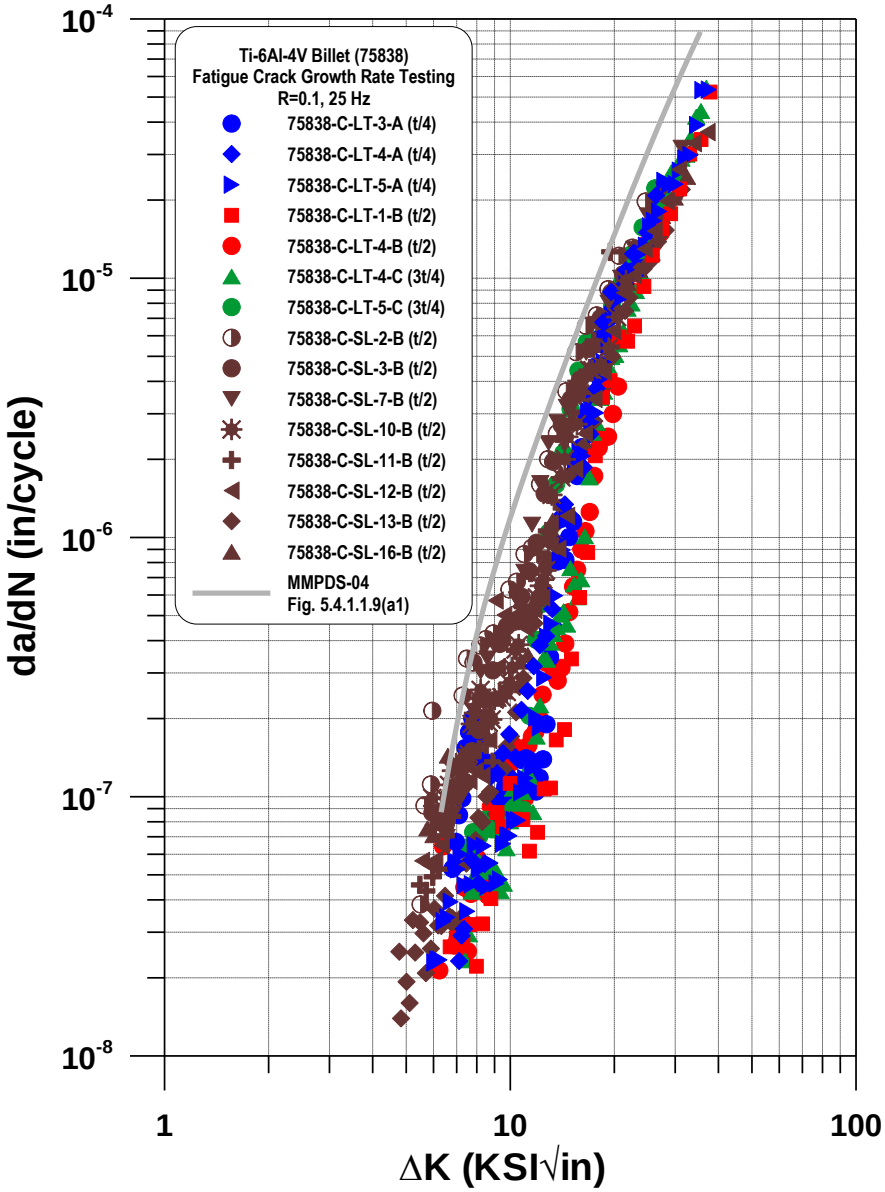


Figure 10. Fatigue crack growth rate test results (R=0.1).

Approved for public release; distribution unlimited.

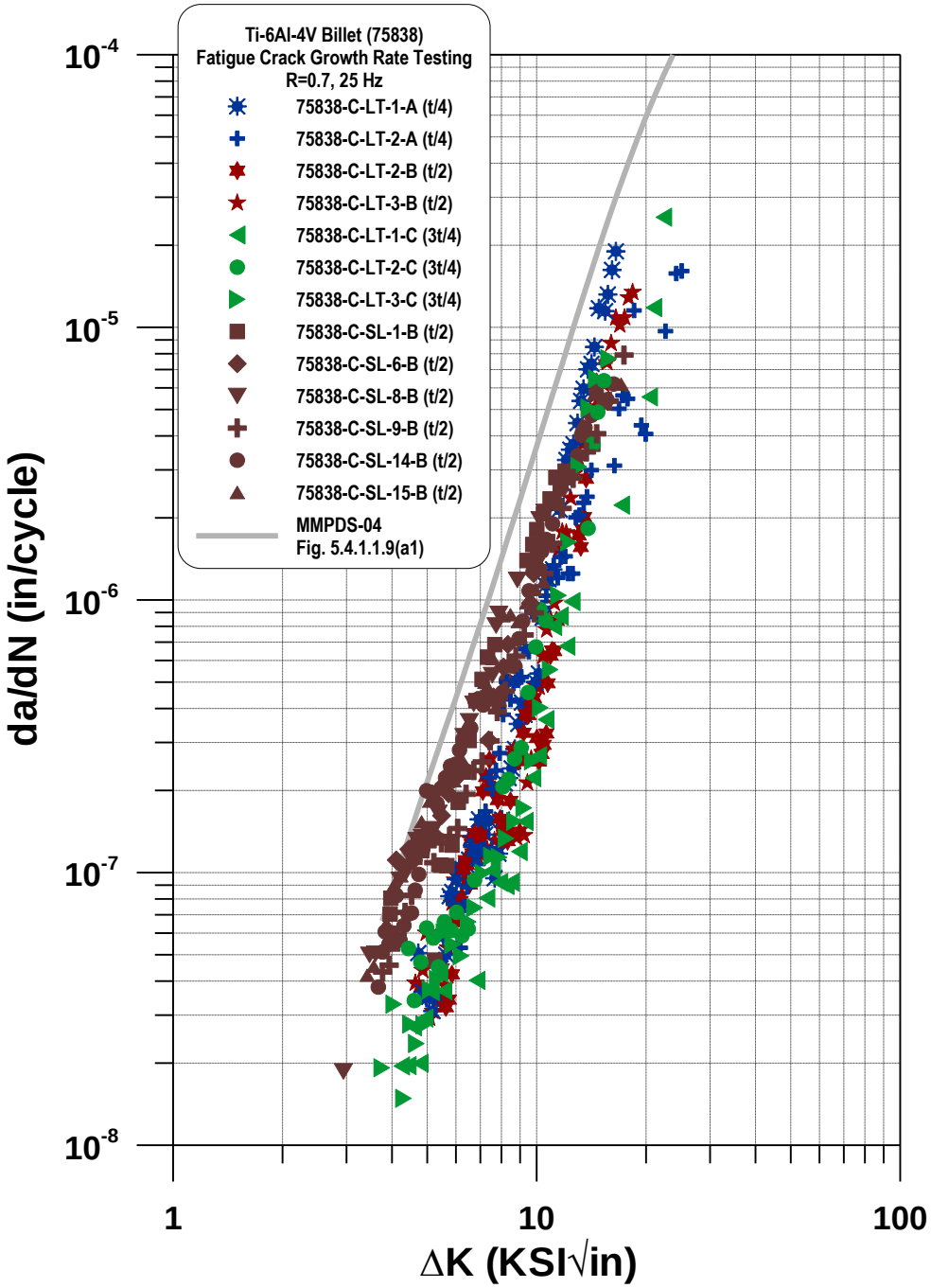


Figure 11. Fatigue crack growth rate test results (R=0.7).

Approved for public release; distribution unlimited.

Fracture Toughness – Plane-strain fracture toughness test results are shown in Table 6. Only valid K_{Ic} values (per ASTM E399) are shown. Four test specimens produced invalid results, having failed the "$P_{max}/P_q < 1.1$" validity check, and have not been included in the table. For this investigation, only the L-T orientation was tested.

From this data, it is readily apparent that the t/2 thickness location produced higher fracture toughness results than the two quarter point locations, by approximately 7 ksi√in on average. Considering that other results from this effort did not show the same type of trend with respect to thickness location, the reason for this difference is currently unknown and will be investigated and reported on in a future report on the metallurgy of this billet.

Also shown in this table are reference values from MMPDS-04 and the Damage Tolerant Design Handbook **[*2*]** for forged bar and plate product forms, respectively. Despite the variability shown in the test data, these results generally correspond with those referenced data points, especially since those references indicate a high degree of variability as well.

As there is no accepted standard for the development of a reasonable lower bound for fracture toughness and the fact that the material specifications do not specify minimum properties for this test, the lowest value of the data set was selected as the "preliminary reasonable lower bound" fracture toughness on this billet.

Approved for public release; distribution unlimited.

Table 6. Fracture toughness test results.

	Thickness Location	K_{Ic} (ksi√in)	
75838-K-LT-1-A	t/4	60.8	
LT-2-A	t/4	66.8	
LT-3-A	t/4	66.4	
LT-6-A	t/4	68.0	
LT-7-A	t/4	65.1	
LT-1-B	t/2	66.2	
LT-2-B	t/2	79.1	
LT-3-B	t/2	76.8	
LT-5-B	t/2	77.9	
LT-6-B	t/2	74.5	
LT-7-B	t/2	63.0	
LT-1-C	3t/4	64.1	
LT-2-C	3t/4	69.4	
LT-4-C	3t/4	68.1	
LT-5-C	3t/4	67.6	
LT-6-C	3t/4	64.5	
LT-7-C	3t/4	59.8	← Preliminary reasonable lower bound
MMPDS-04 *Table 5.1.2.1.1 (Forged Bar) Avg.*		60	
Damage Tolerant Design Handbook *Table 6.16.1.1 (Plate) Mean*		74.4	

Stress Corrosion Cracking – Axial, smooth bar stress corrosion cracking tests were performed on 29 test specimens, representing all three thickness locations and two orientations (L and S). As stated previously, the specimens were loaded at a stress of 90 ksi (75% of the specification yield strength of 120 ksi) for 40 days in an alternate immersion 3.5% NaCl solution. No failures occurred during testing. After testing, specimens were rinsed in deionized water and visually inspected for evidence of corrosion damage. No evidence of pitting or other corrosion-related damage was indicated.

Approved for public release; distribution unlimited.

CONCLUSIONS AND RECOMMENDATIONS

As this report dealt with mechanical properties from only one Ti-6Al-4V billet, no specific conclusions or recommendations will be made, other than comparisons to material specifications or available reference data. With the exception of tensile ductility (elongation and reduction of area) results, the material was generally equivalent to the reference data noted throughout the report. The lower ductility results should not be overlooked however when evaluating this material with respect to properly processed plate or bar.

REFERENCES

1. *Metallic Materials Properties Development and Standardization (MMPDS)*, MMPDS-04; April 2008; Federal Aviation Administration.
2. *Damage Tolerant Design Handbook: A Compilation of Fracture and Crack Growth Data for High Strength Alloys*; Compiled by D.A. Skinn, J.P. Gallagher, A.P. Berens, P.D. Huber, J. Smith; University of Dayton Research Institute, May 1994.

ACKNOWLEDGEMENTS

The author wishes to thank Mssrs. John Ruschau, Nick Jacobs, Don Woleslagle, Eric Soppe, Cris Williams, Ron Glett, Ms. Pat Youngerman, and Ms. Sarah Kuhlman, all of the University of Dayton Research Institute (UDRI); Mssrs. Dan Laufersweiler, Ed Porter, and Dave Roberts of Universal Technology Corporation (UTC); and Mssrs. Keith Vehorn and Nick Blommel of AFRL/RXSCE for their engineering and technical support of this program. Acknowledgement is also given to Westmoreland Mechanical Testing & Research, Inc. for the machining of all of the test specimens.

PREPARED BY

SIGNED

STEVEN R. THOMPSON, Senior Materials Engineer
Materials Test & Evaluation Team
Acquisition Systems Support Branch
Systems Support Division

REVIEWED BY

SIGNED

NEAL R. ONTKO, Team Lead
Materials Test & Evaluation Team
Acquisition Systems Support Branch
Systems Support Division

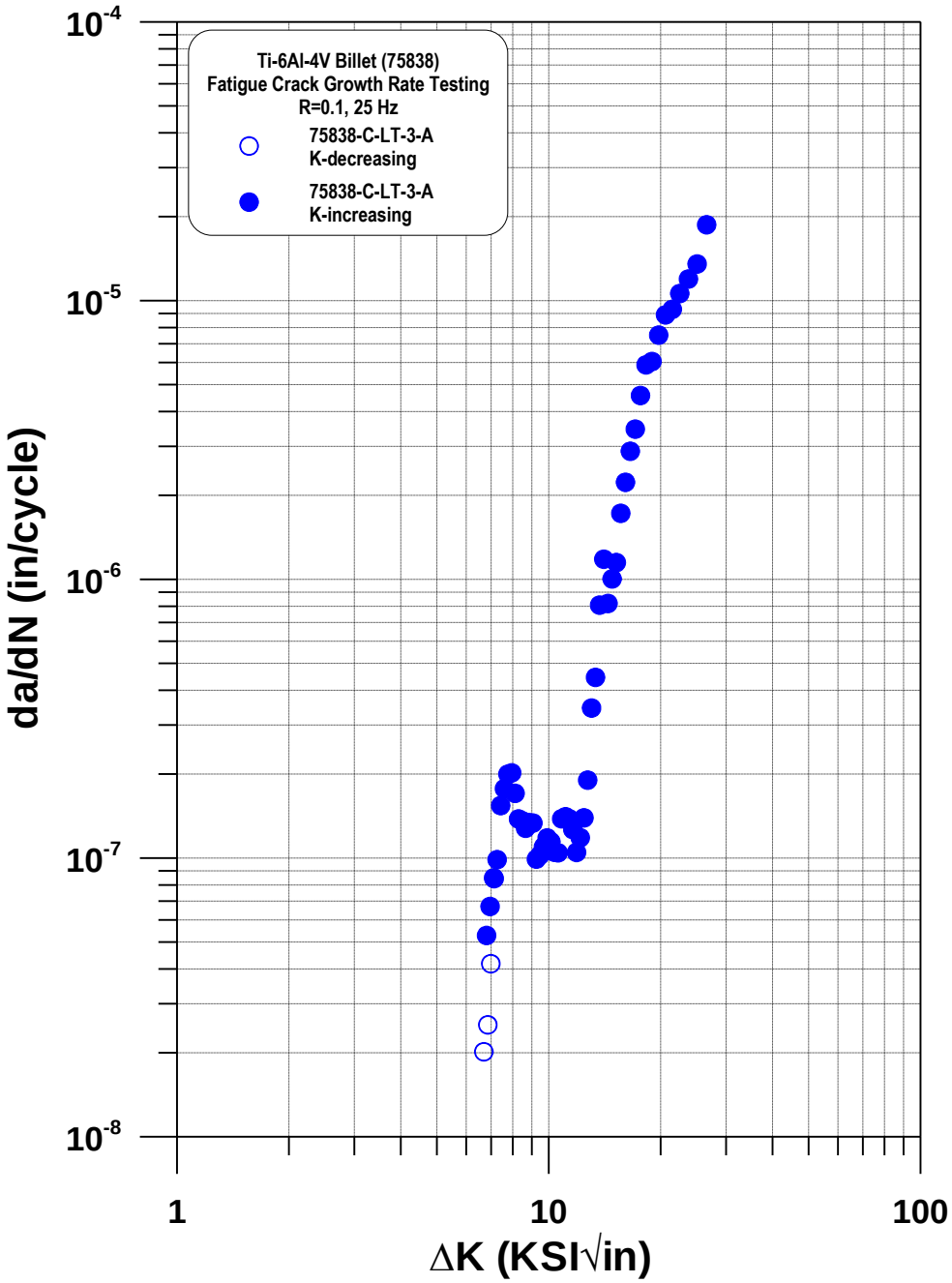
PUBLICATION REVIEW: This report has been reviewed and approved.

SIGNED

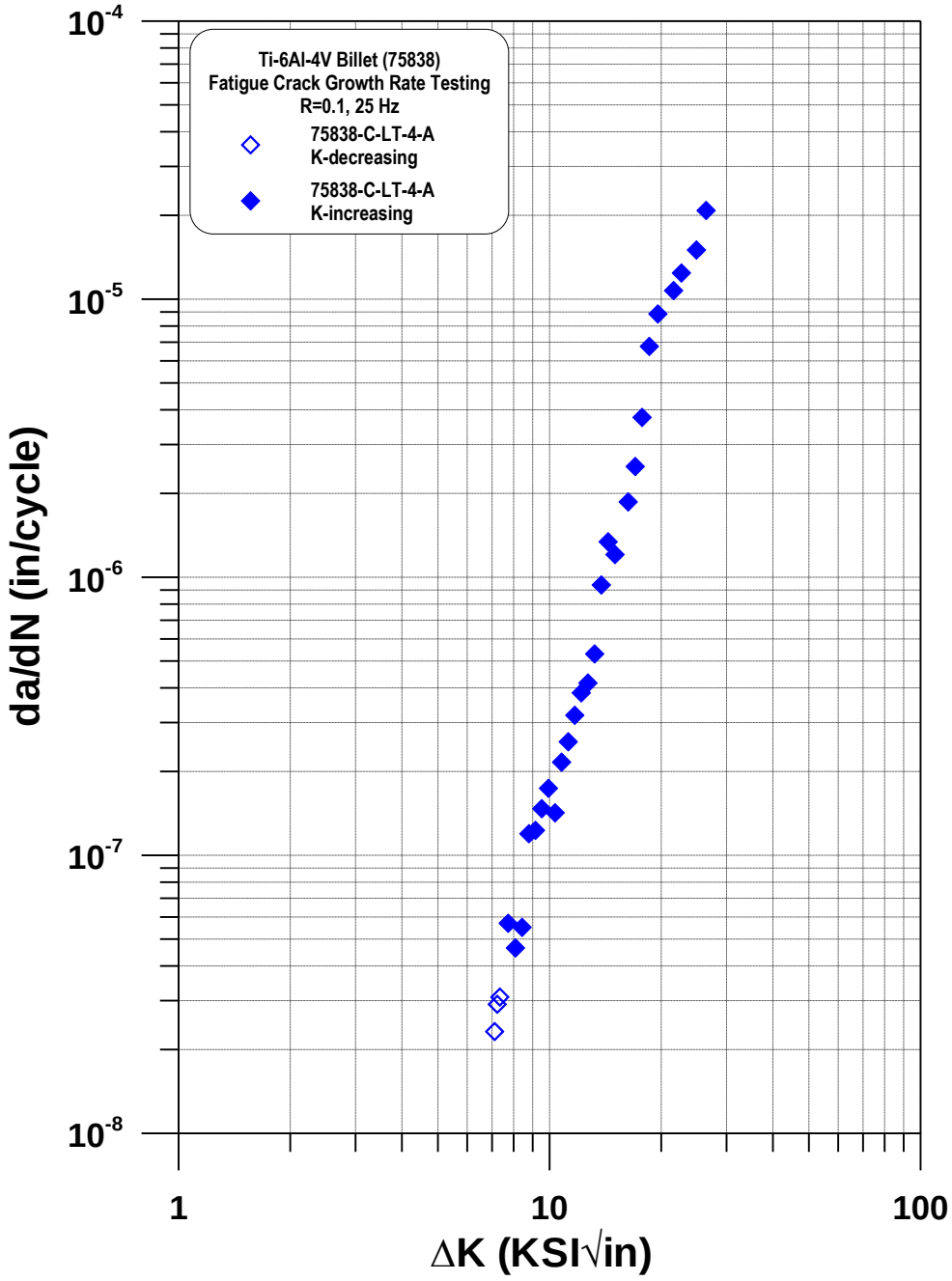
CHARLES E. WAGNER, Chief
Acquisition Systems Support Branch
Systems Support Division
Materials and Manufacturing Directorate

Appendix A
Individual fatigue crack growth rate curves for Ti-6Al-4V billet (75838).

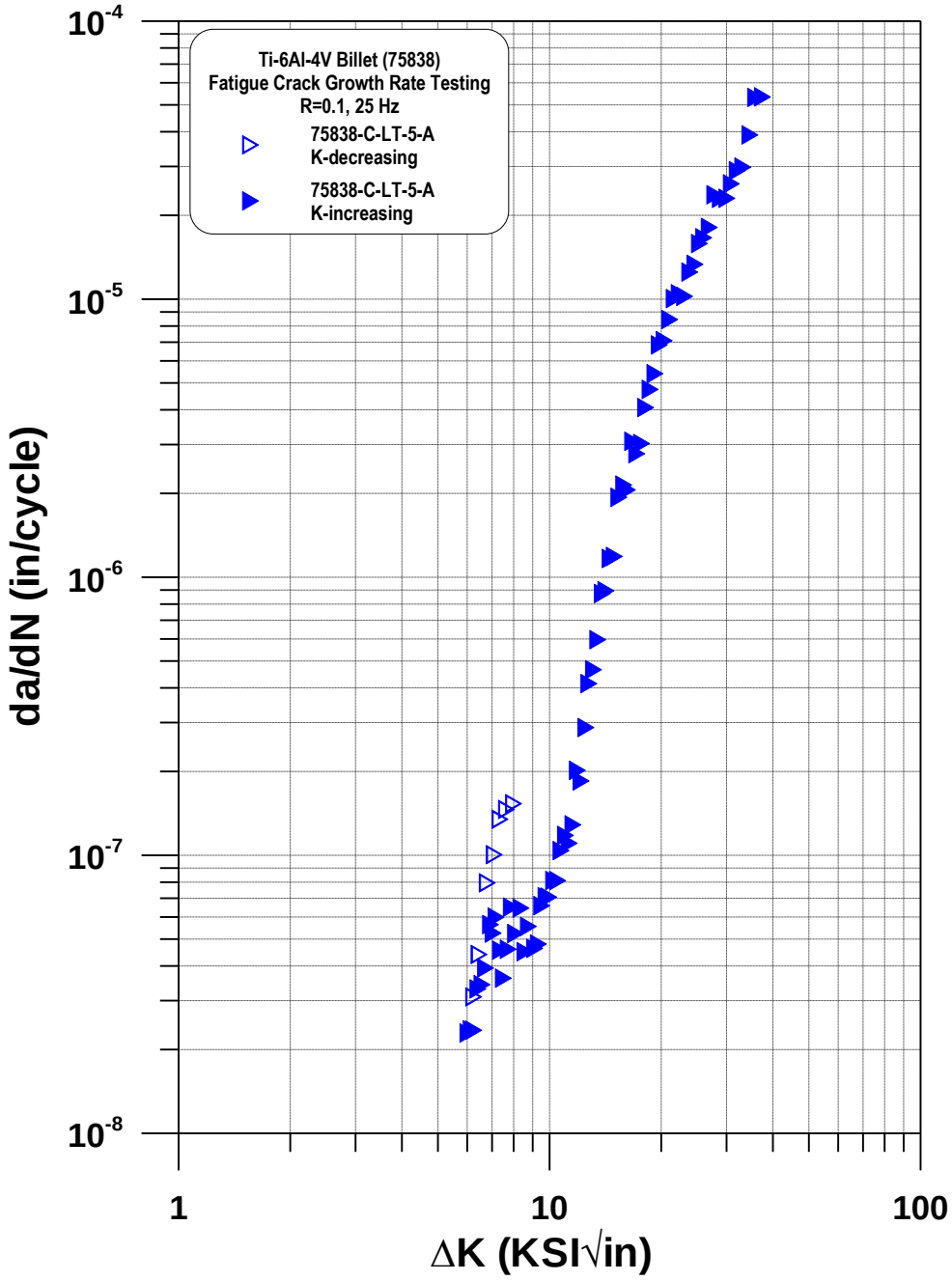
Approved for public release; distribution unlimited.



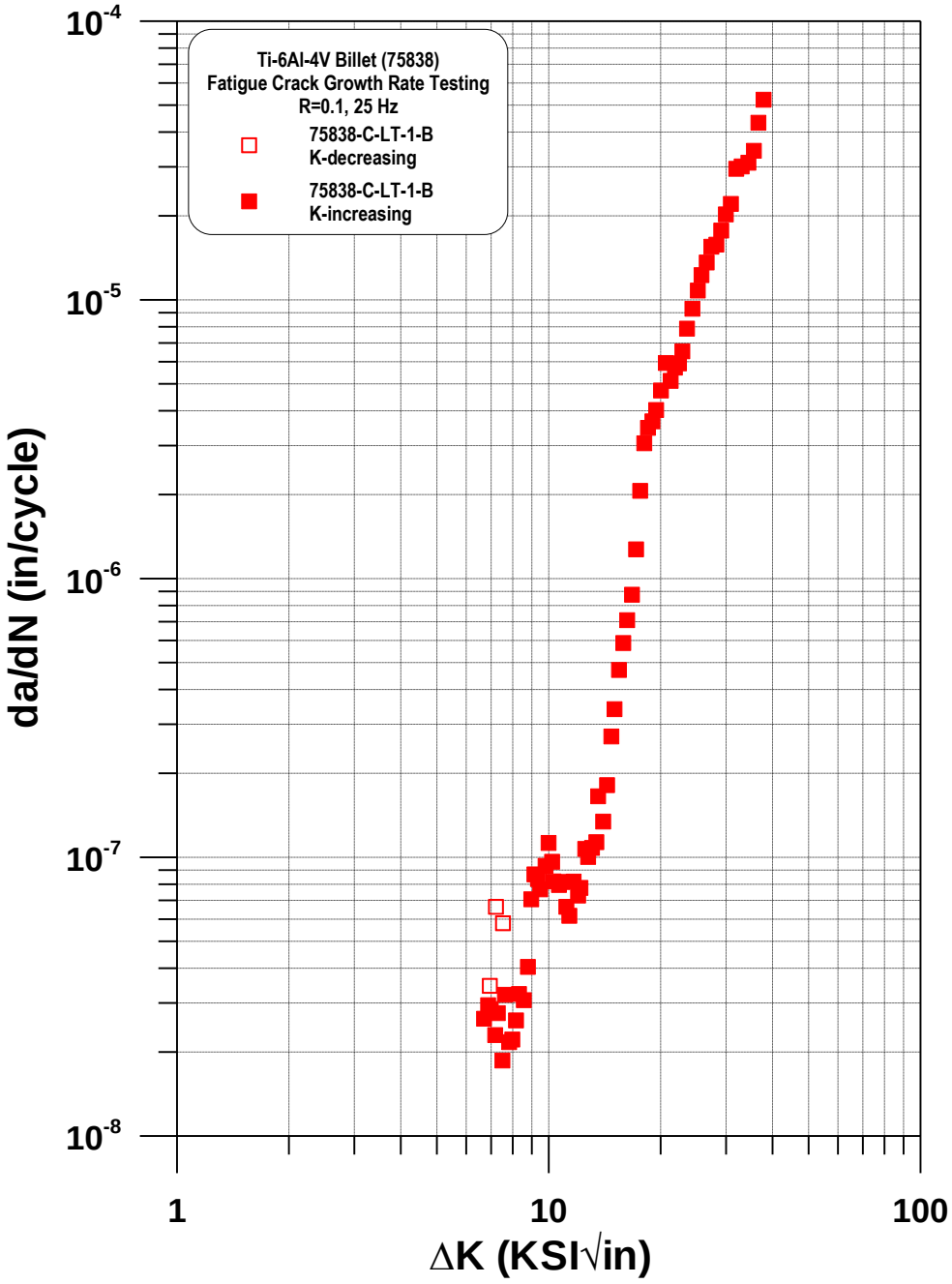
Approved for public release; distribution unlimited.



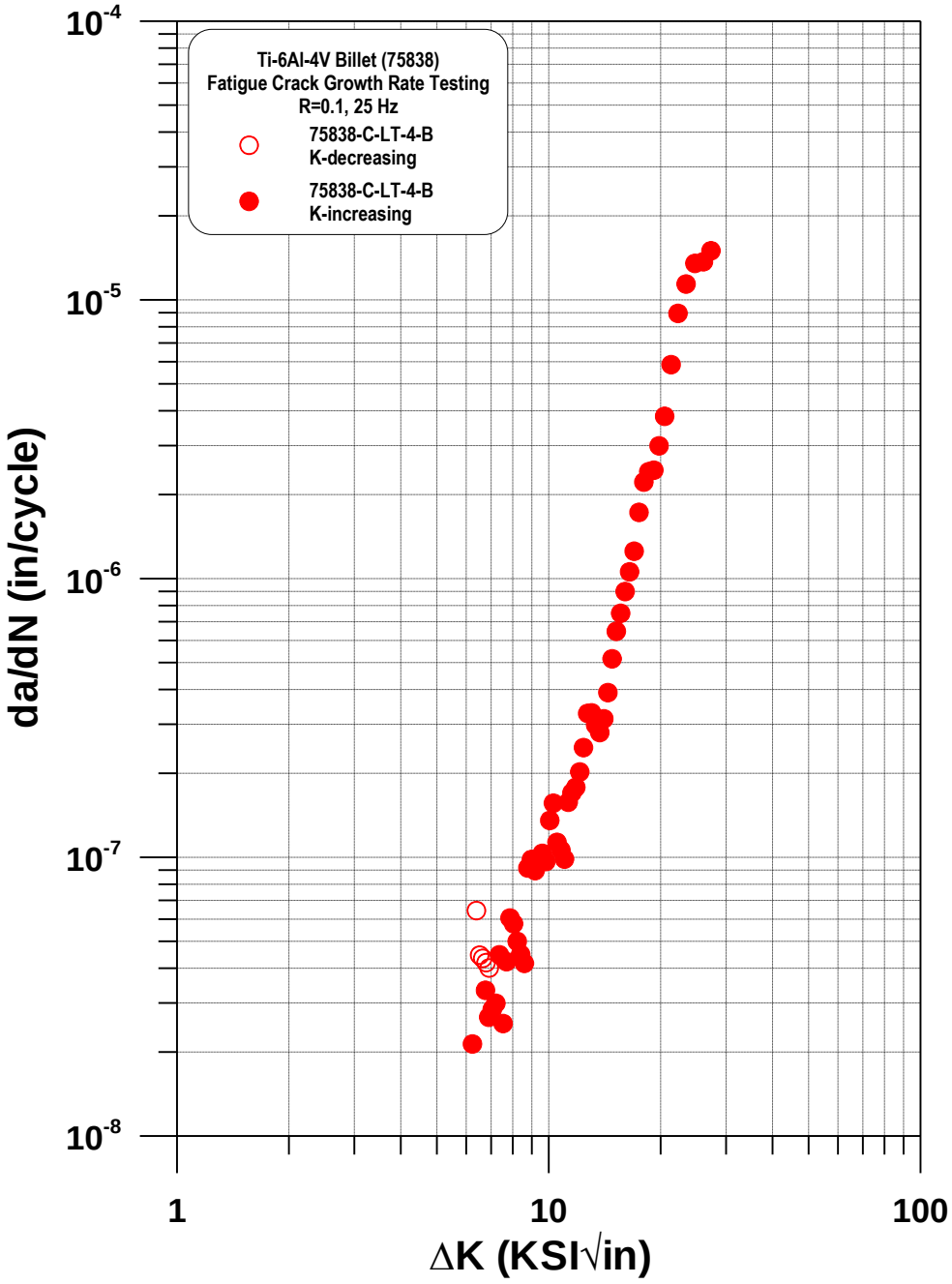
Approved for public release; distribution unlimited.



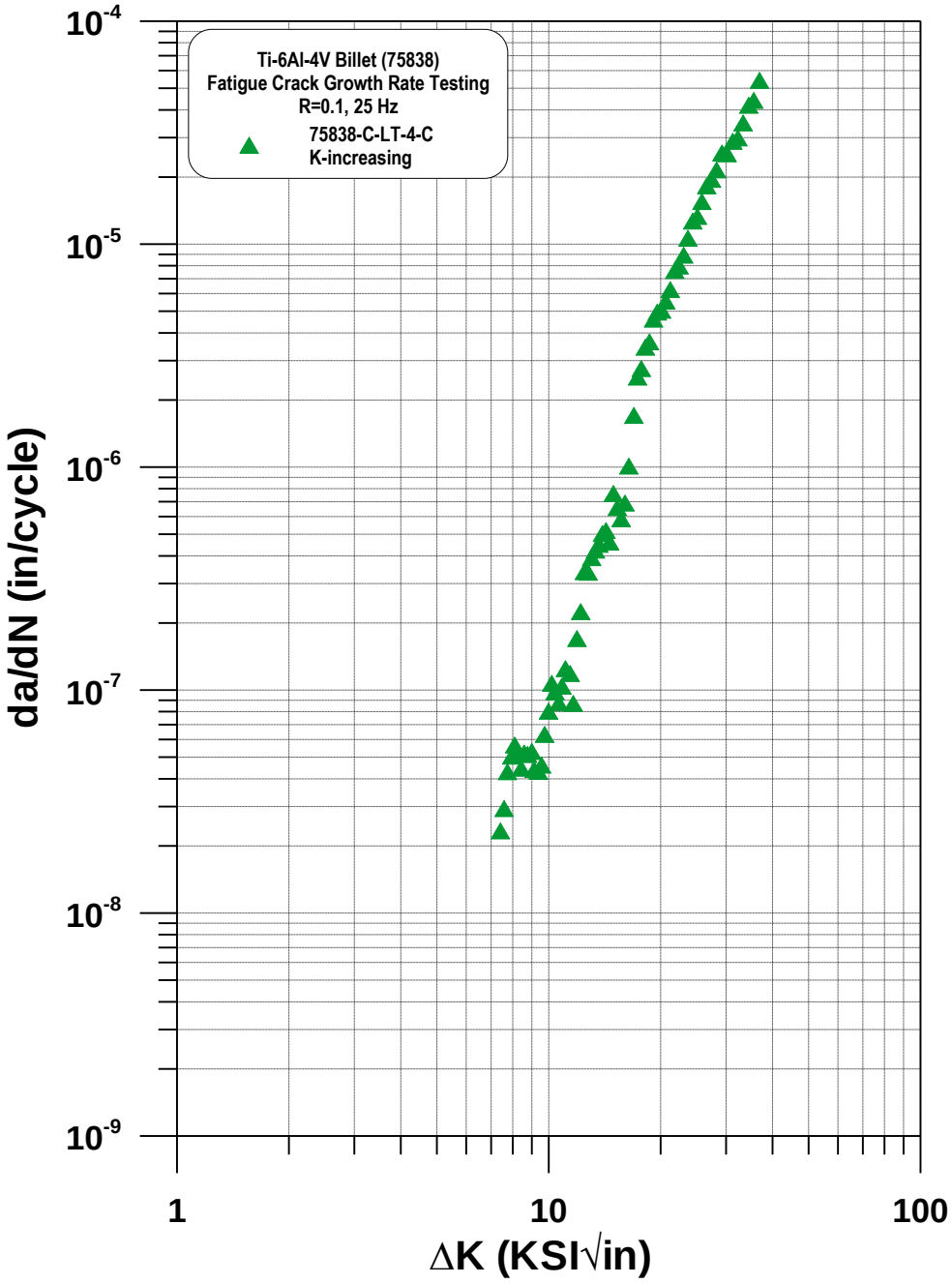
Approved for public release; distribution unlimited.



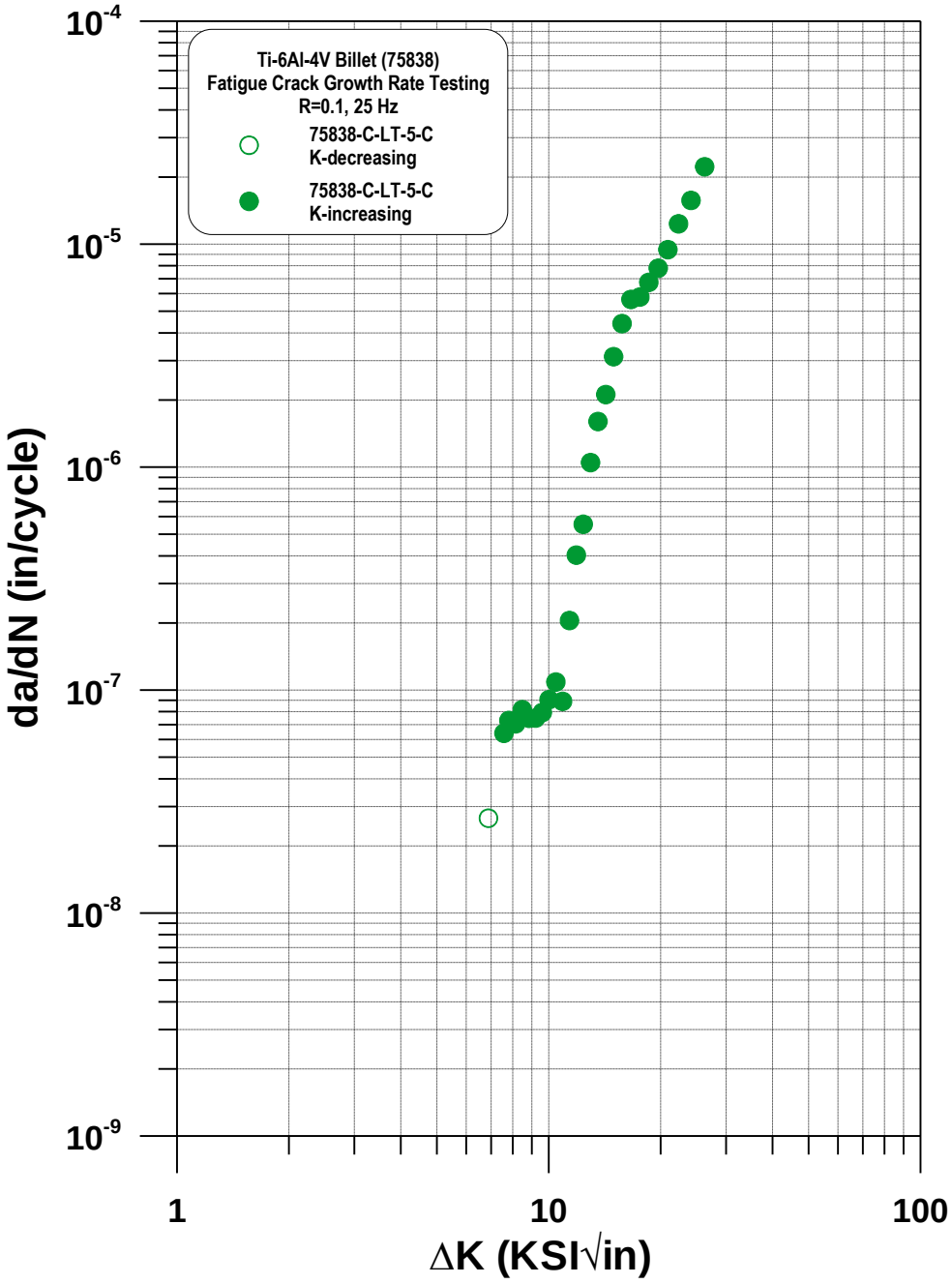
Approved for public release; distribution unlimited.



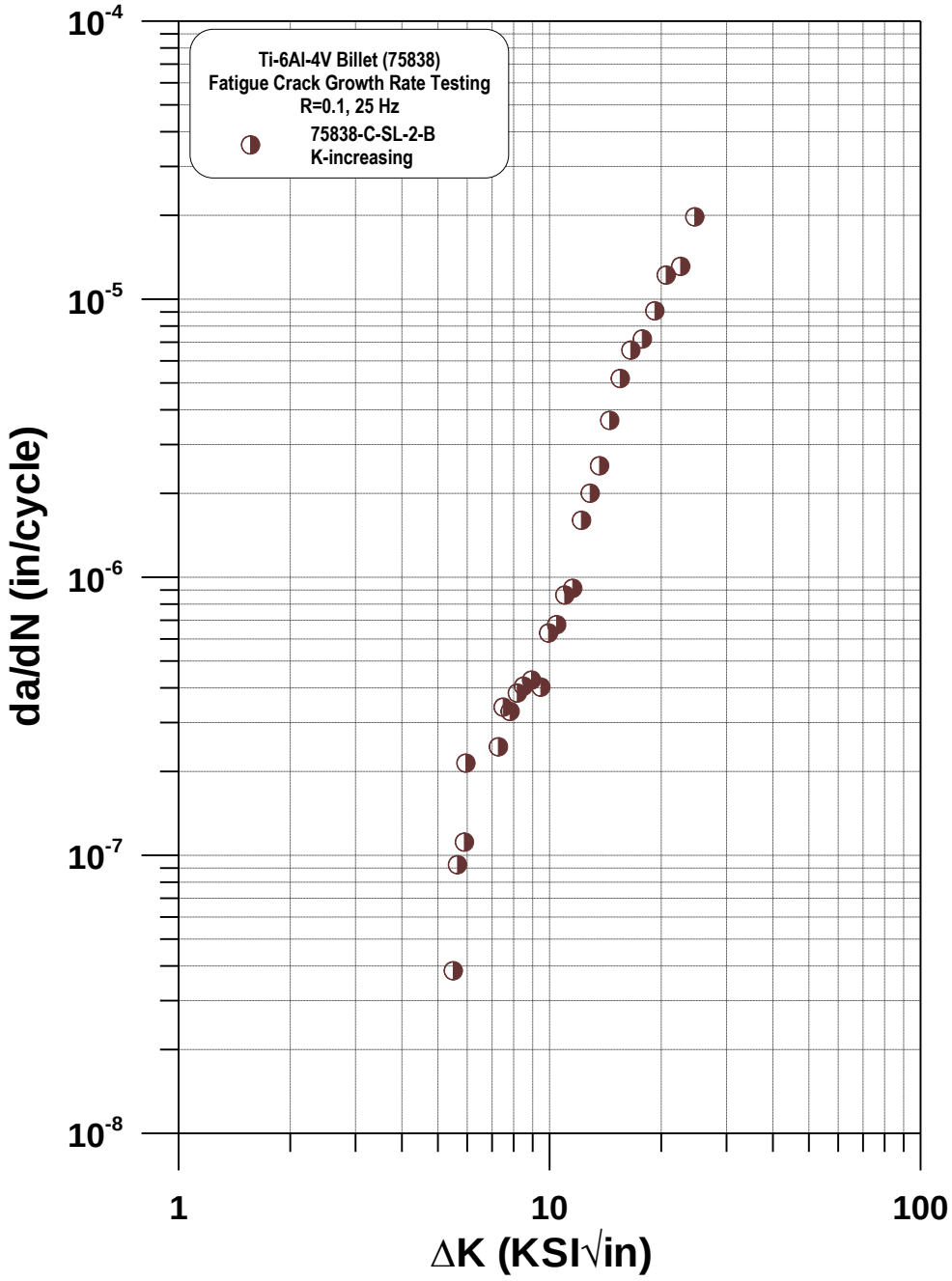
Approved for public release; distribution unlimited.



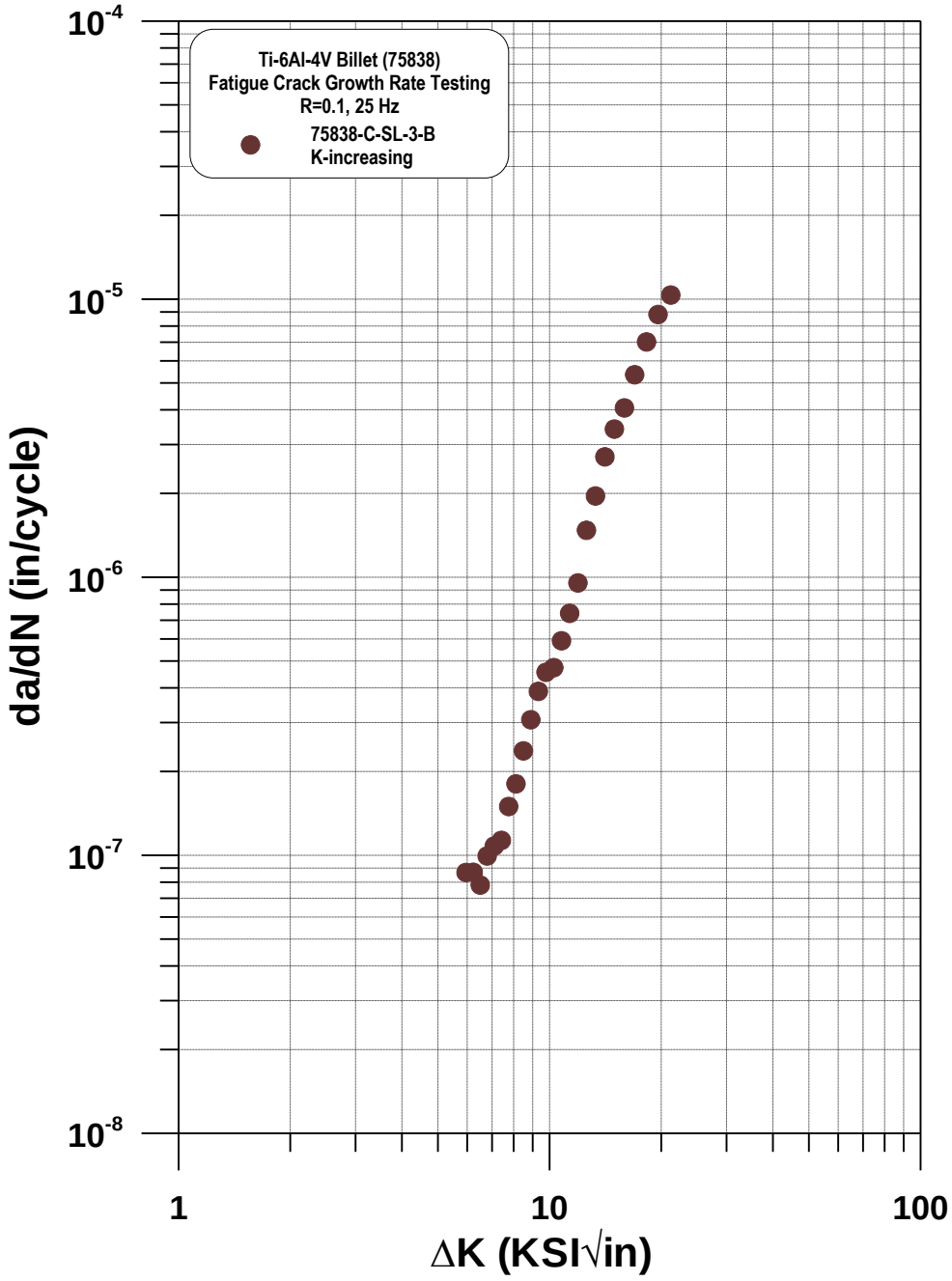
Approved for public release; distribution unlimited.



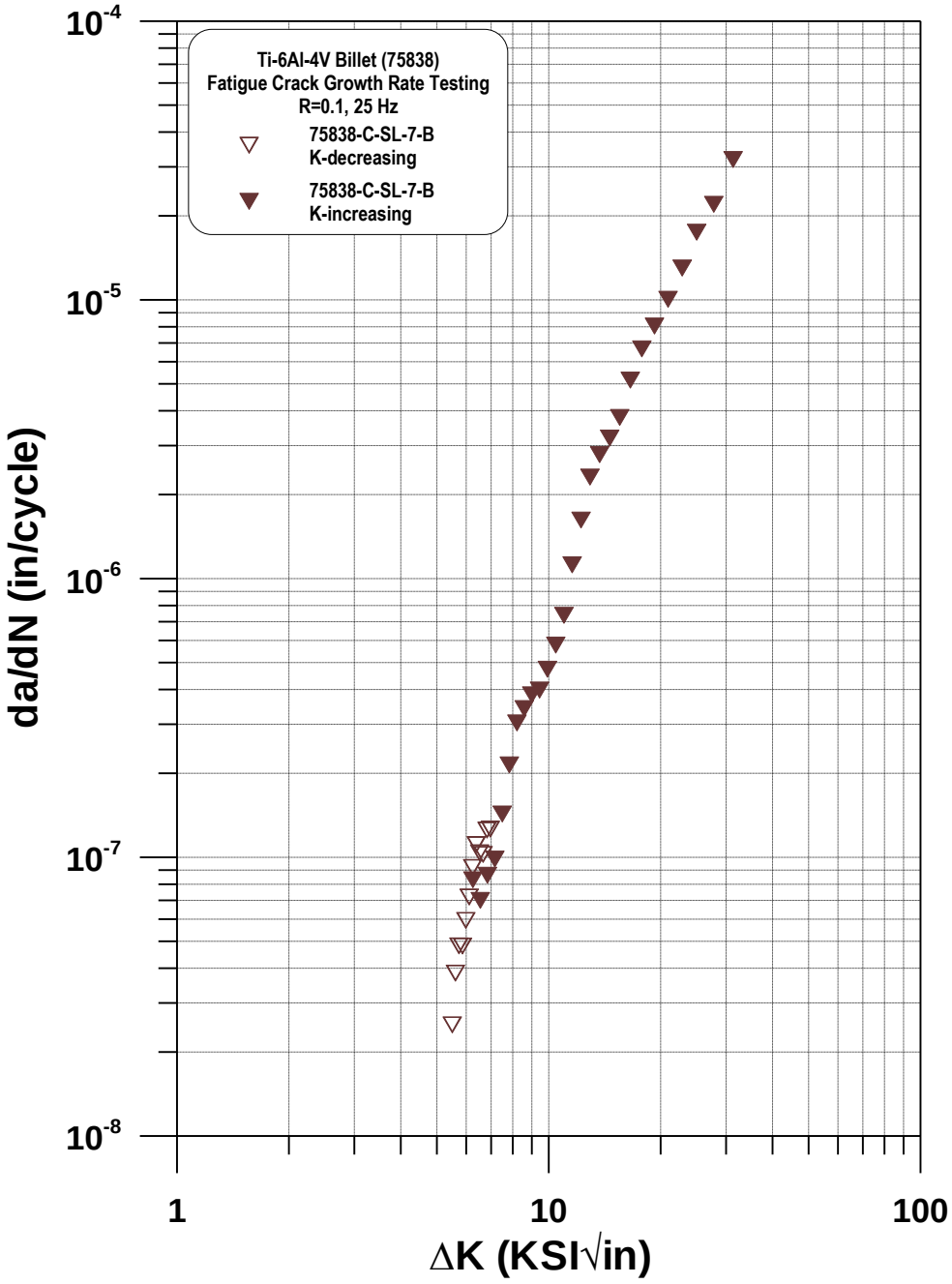
Approved for public release; distribution unlimited.



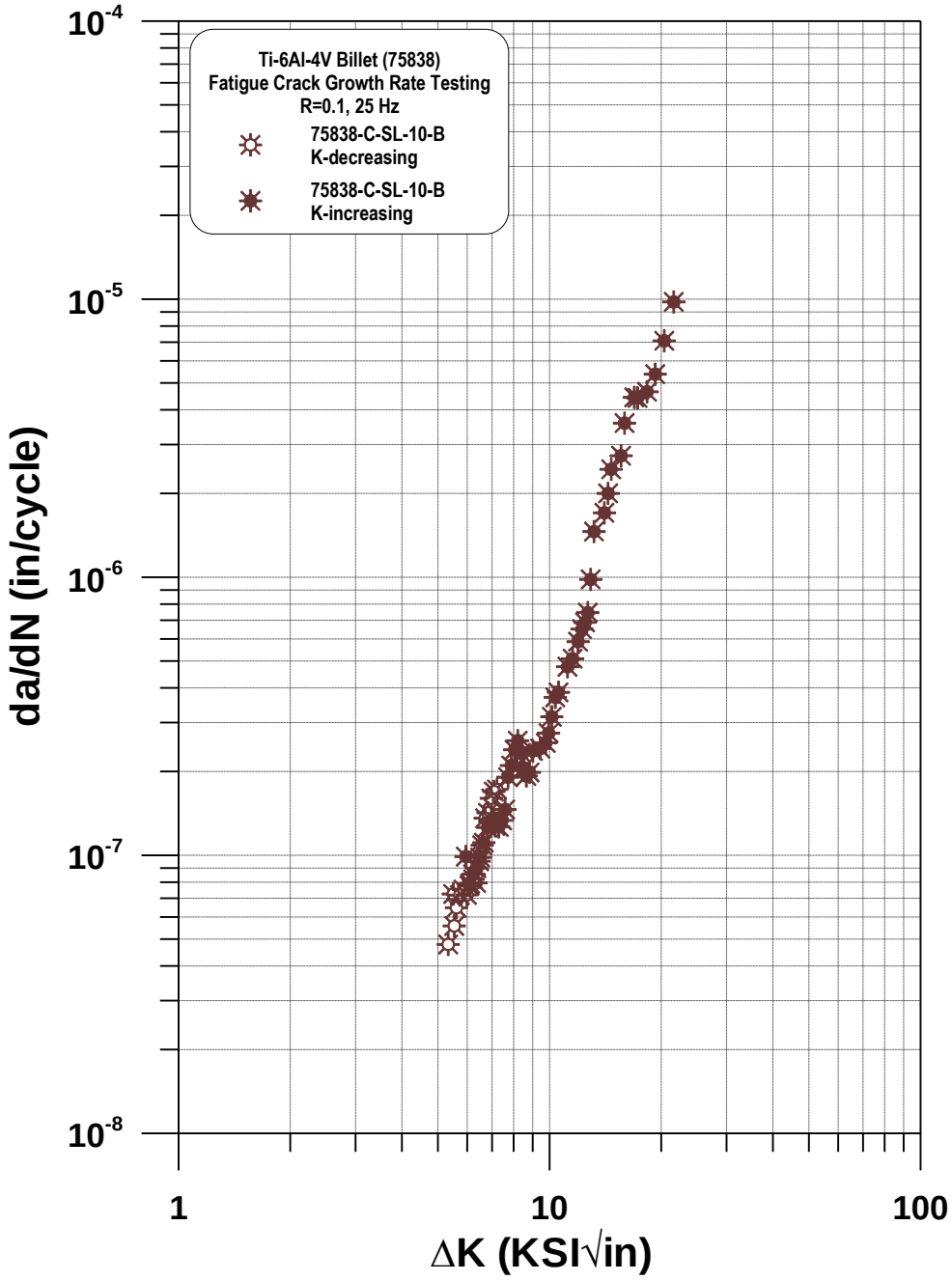
Approved for public release; distribution unlimited.



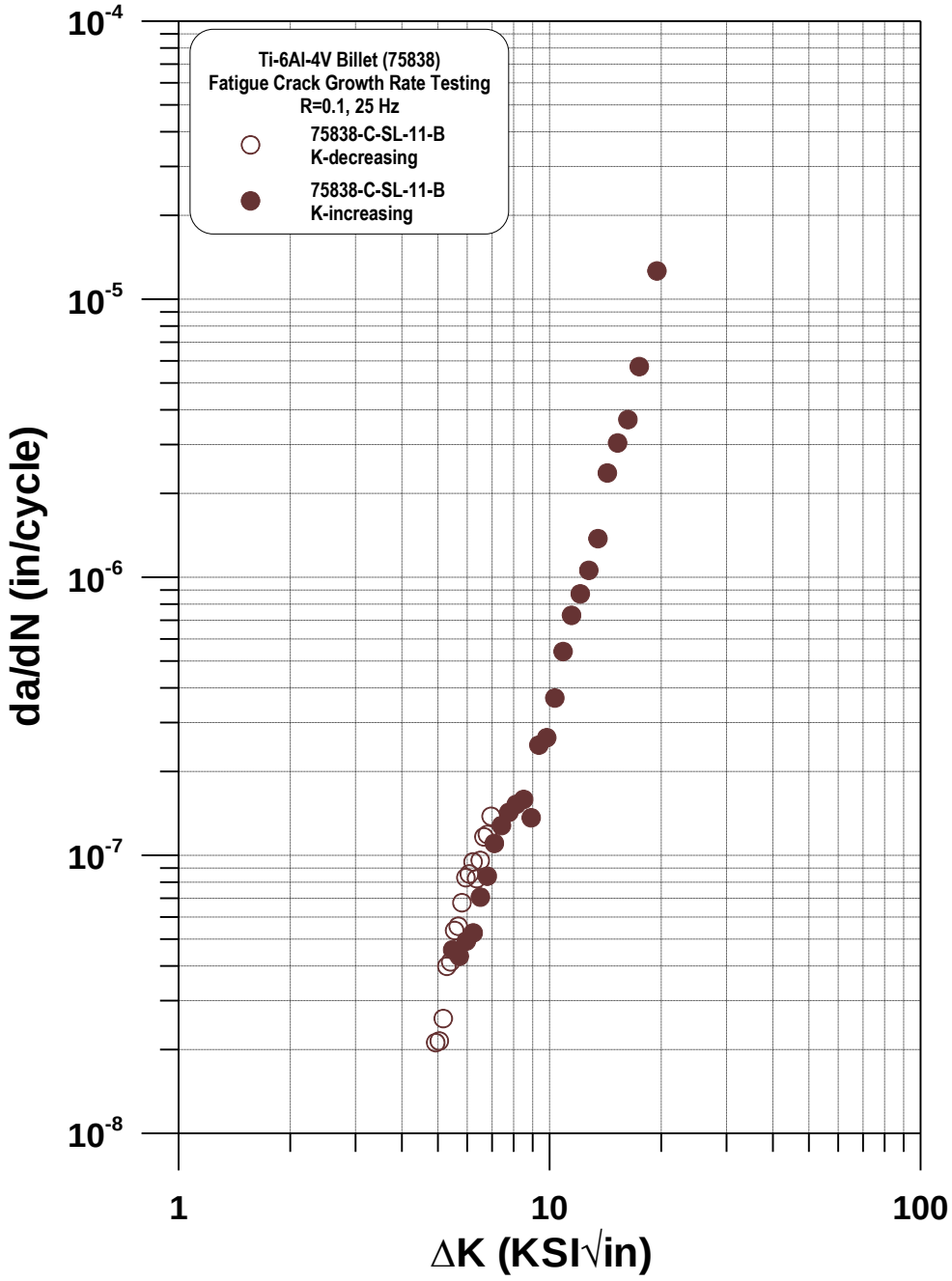
Approved for public release; distribution unlimited.



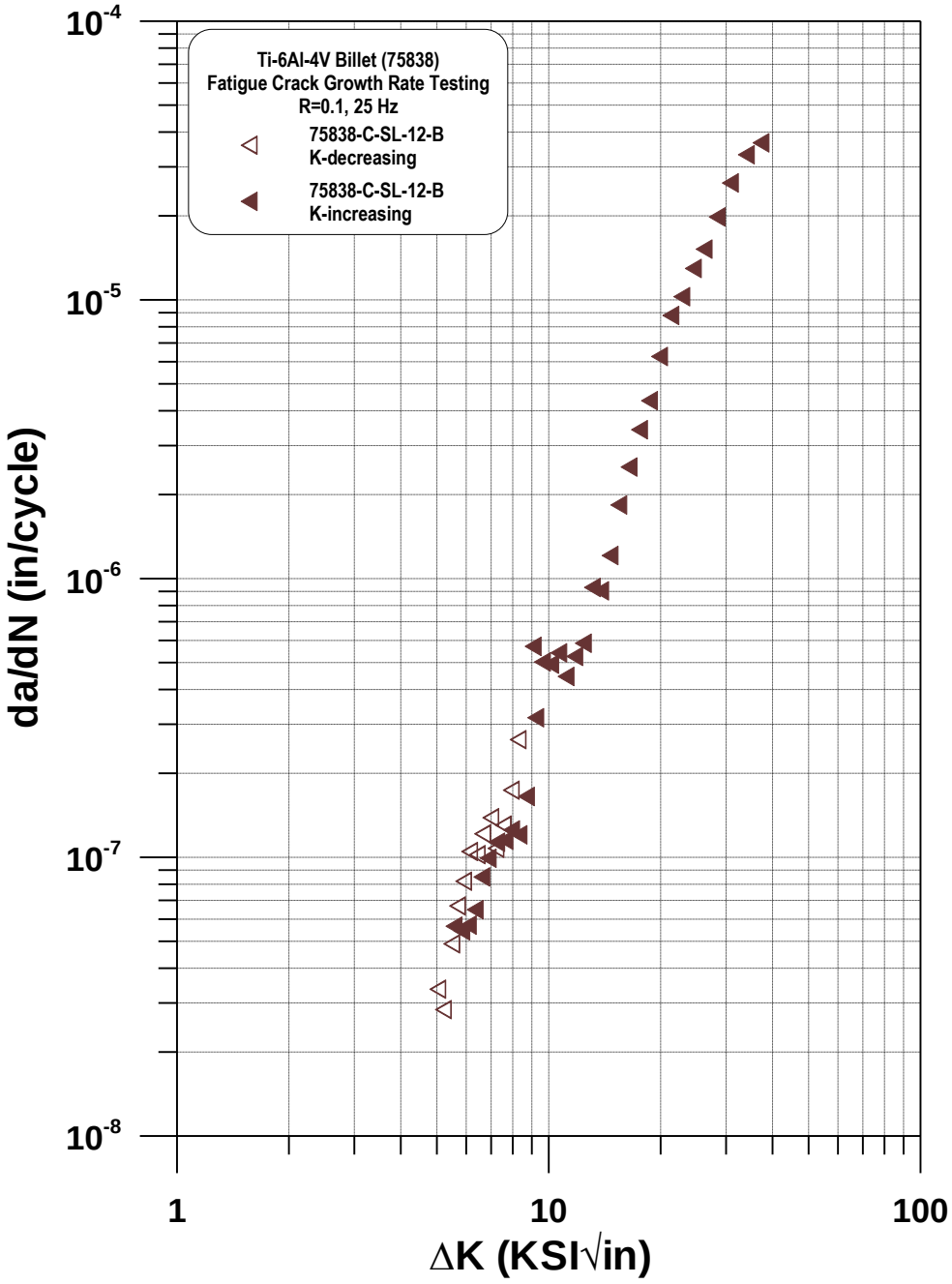
Approved for public release; distribution unlimited.



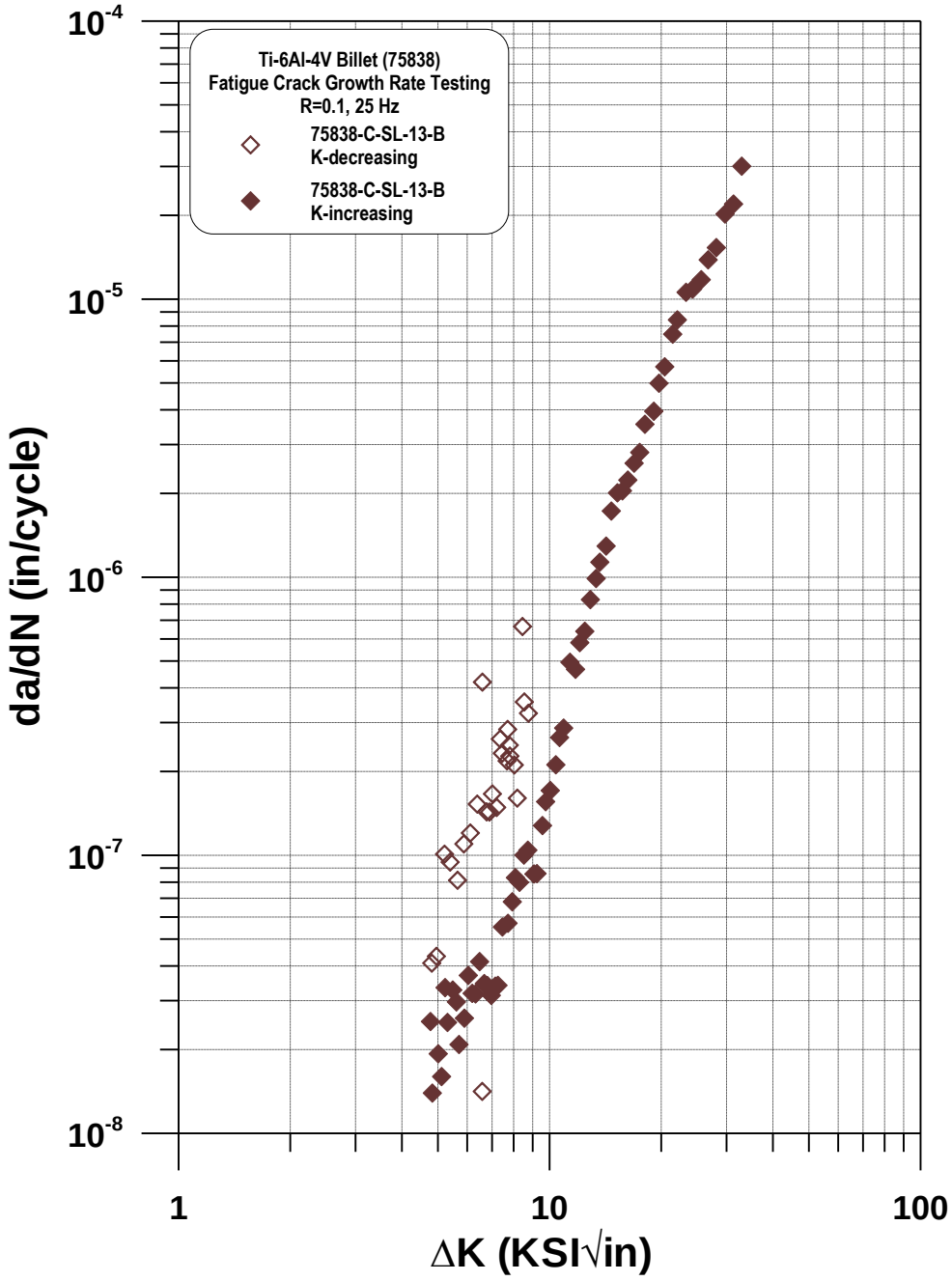
Approved for public release; distribution unlimited.



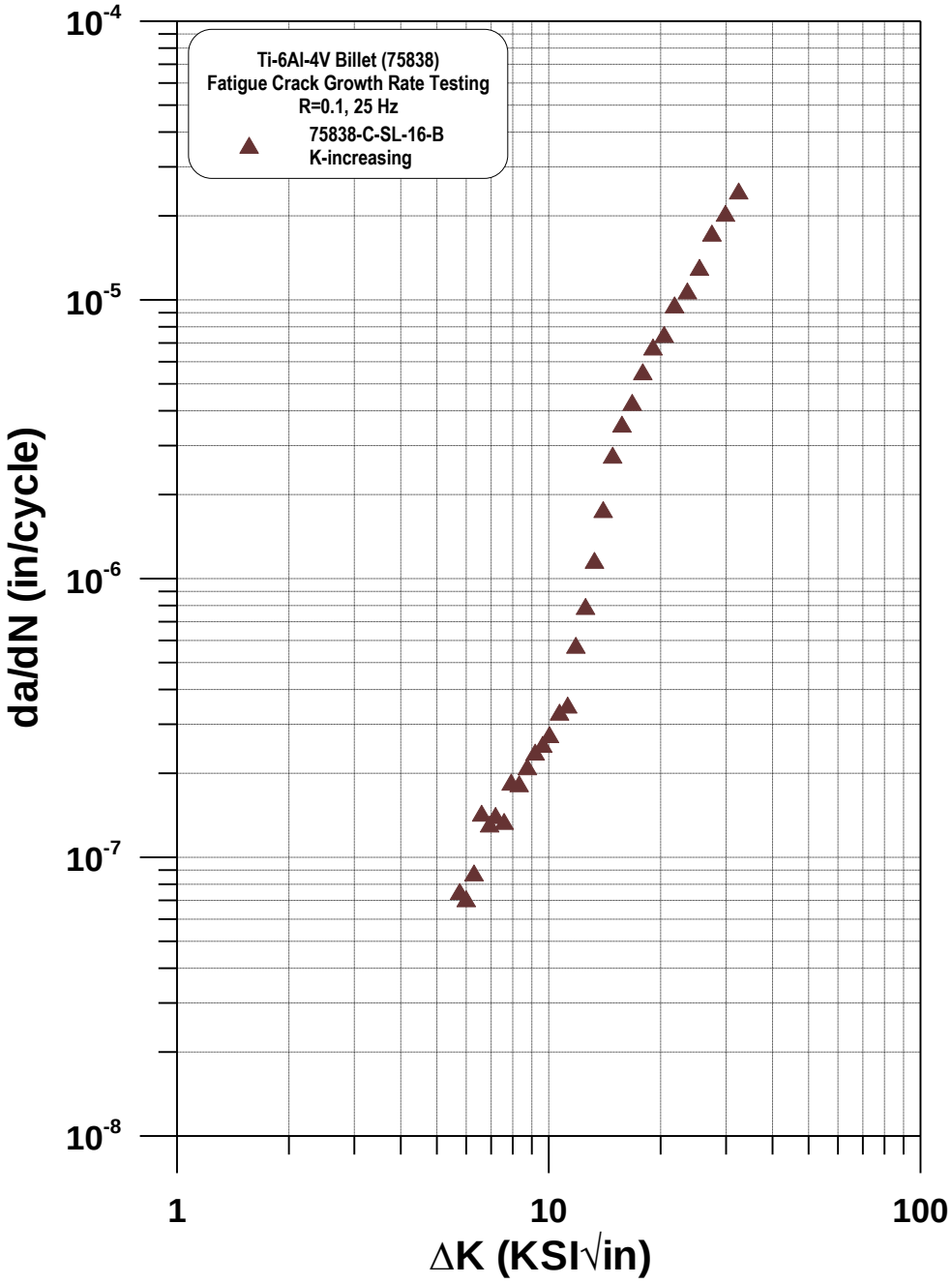
Approved for public release; distribution unlimited.



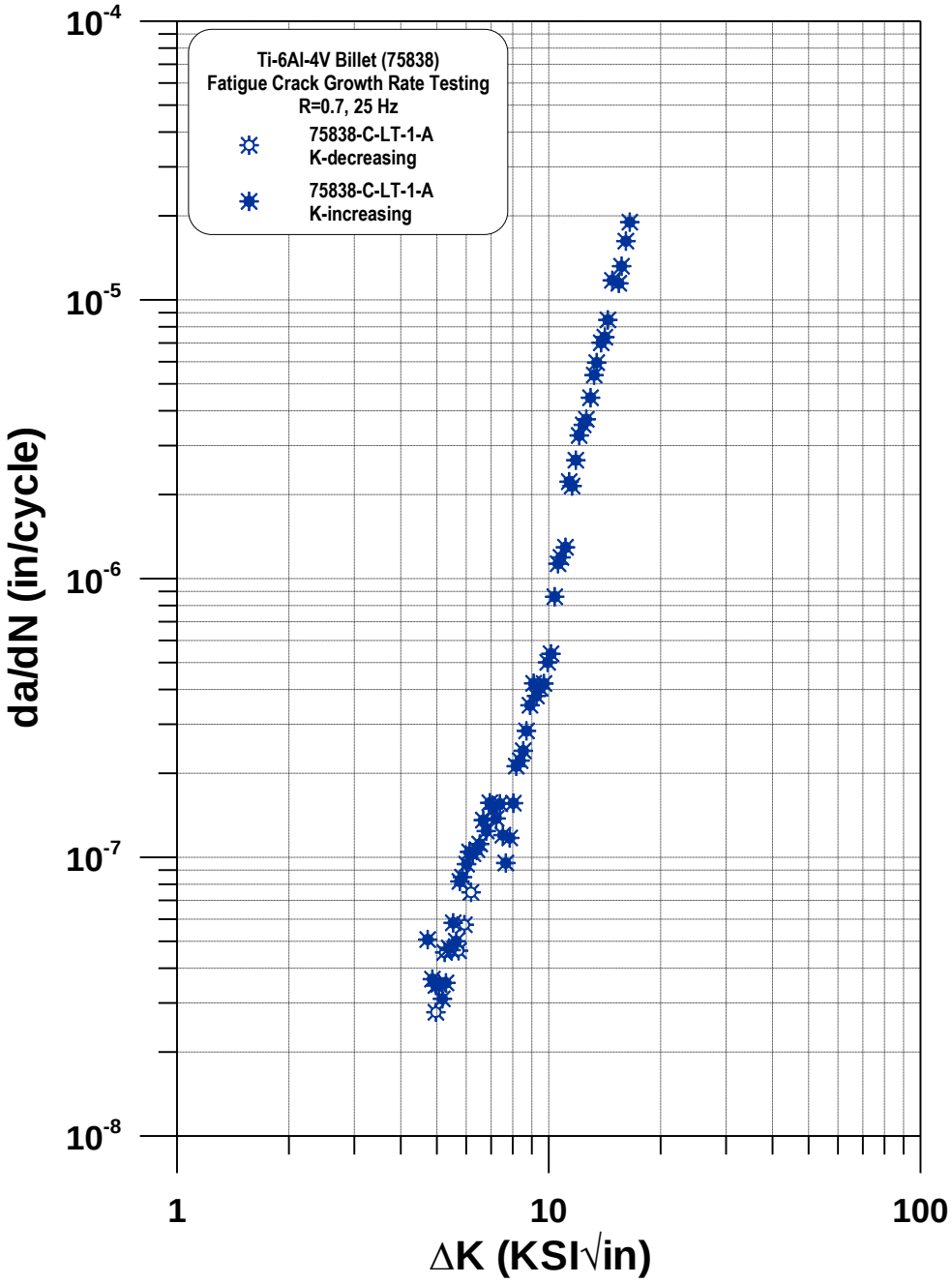
Approved for public release; distribution unlimited.



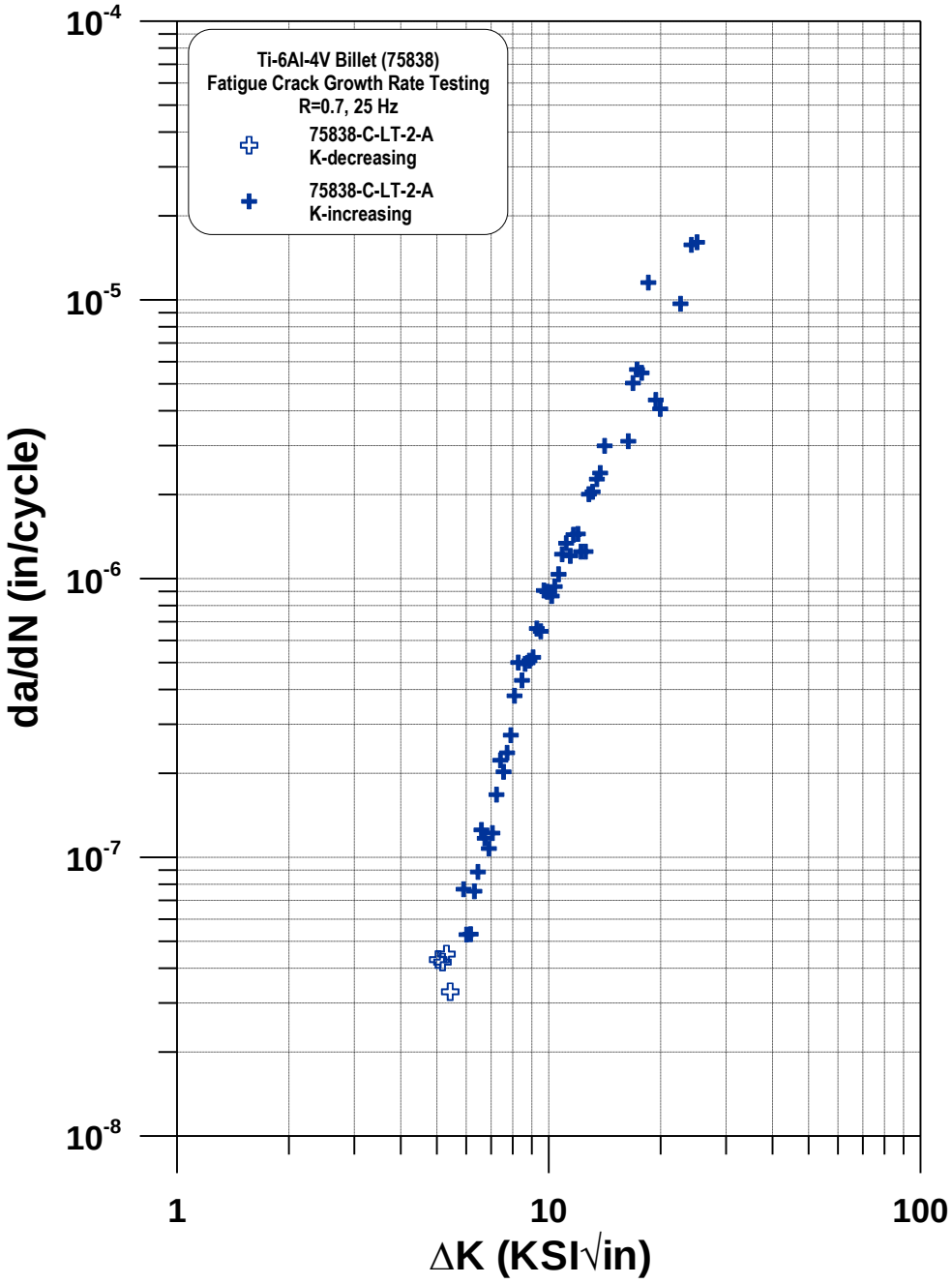
Approved for public release; distribution unlimited.



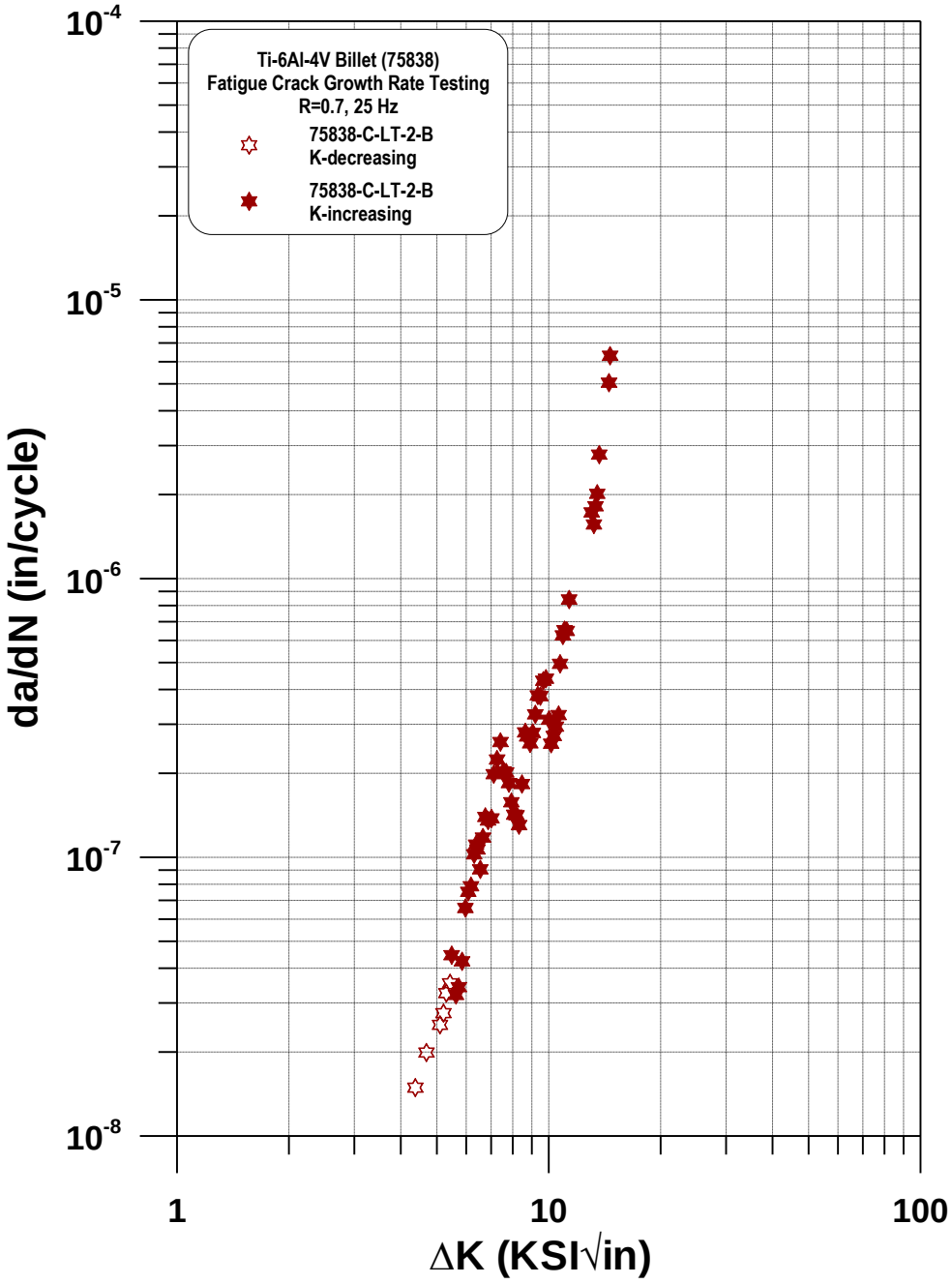
Approved for public release; distribution unlimited.



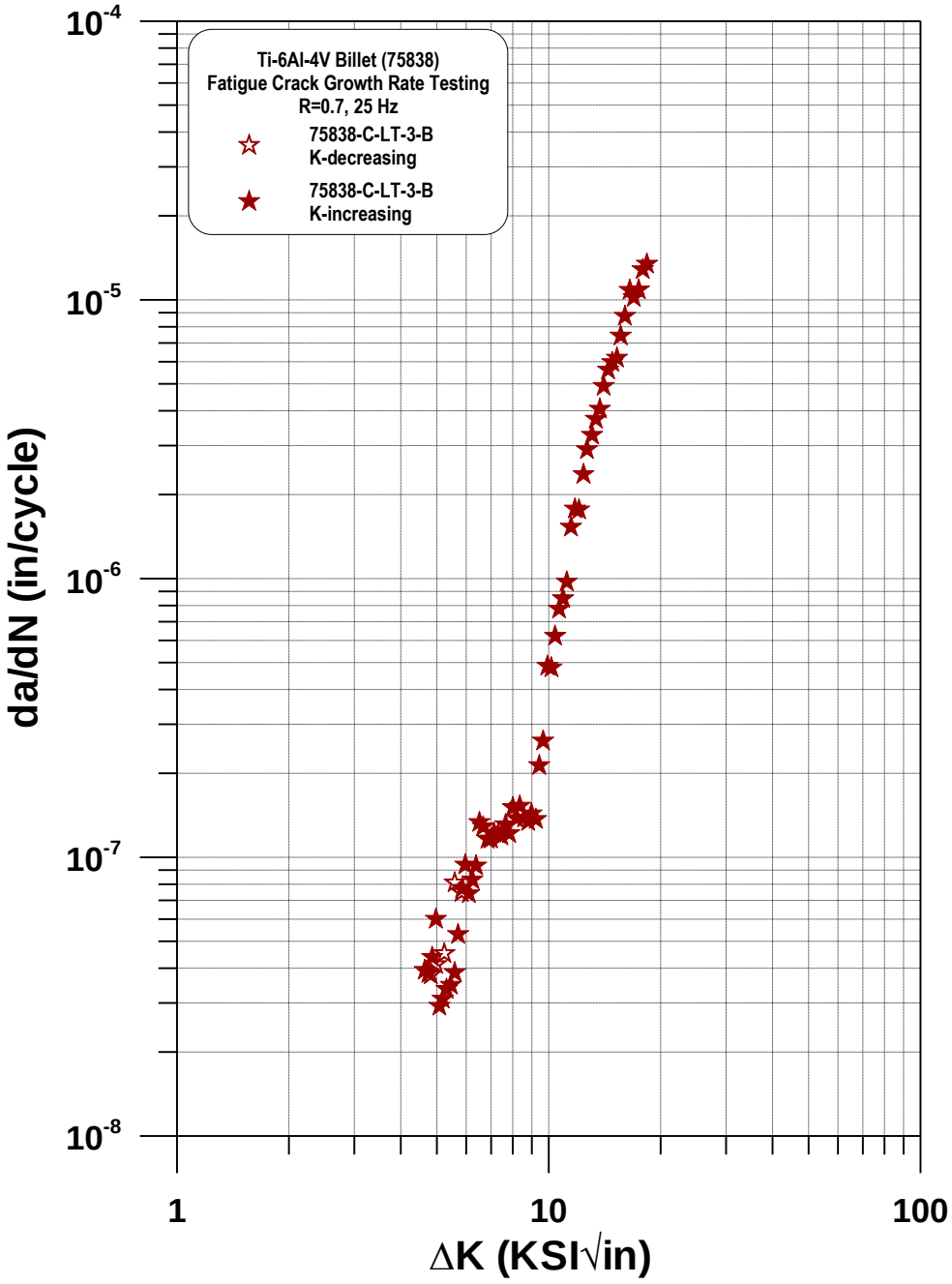
Approved for public release; distribution unlimited.



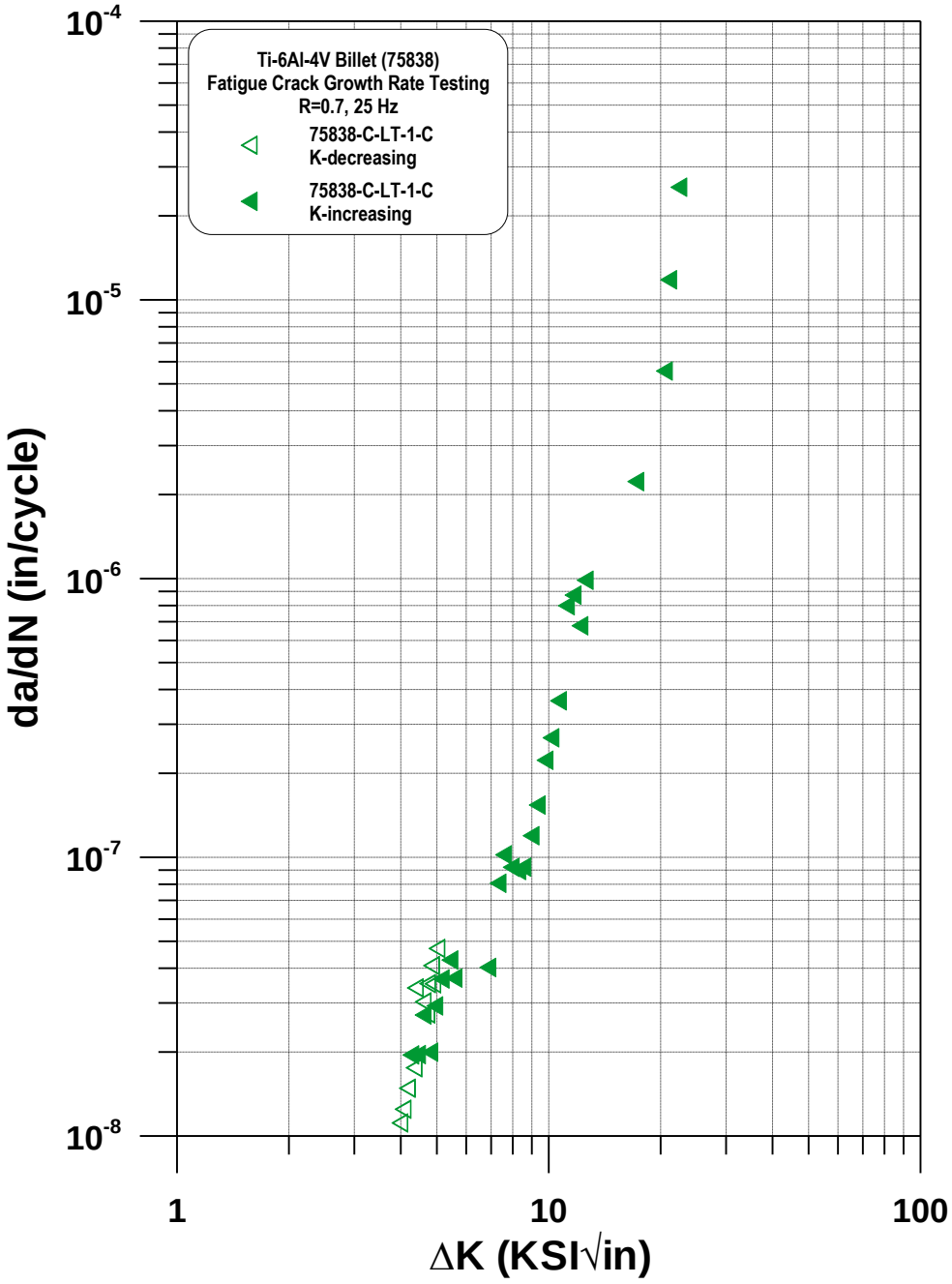
Approved for public release; distribution unlimited.



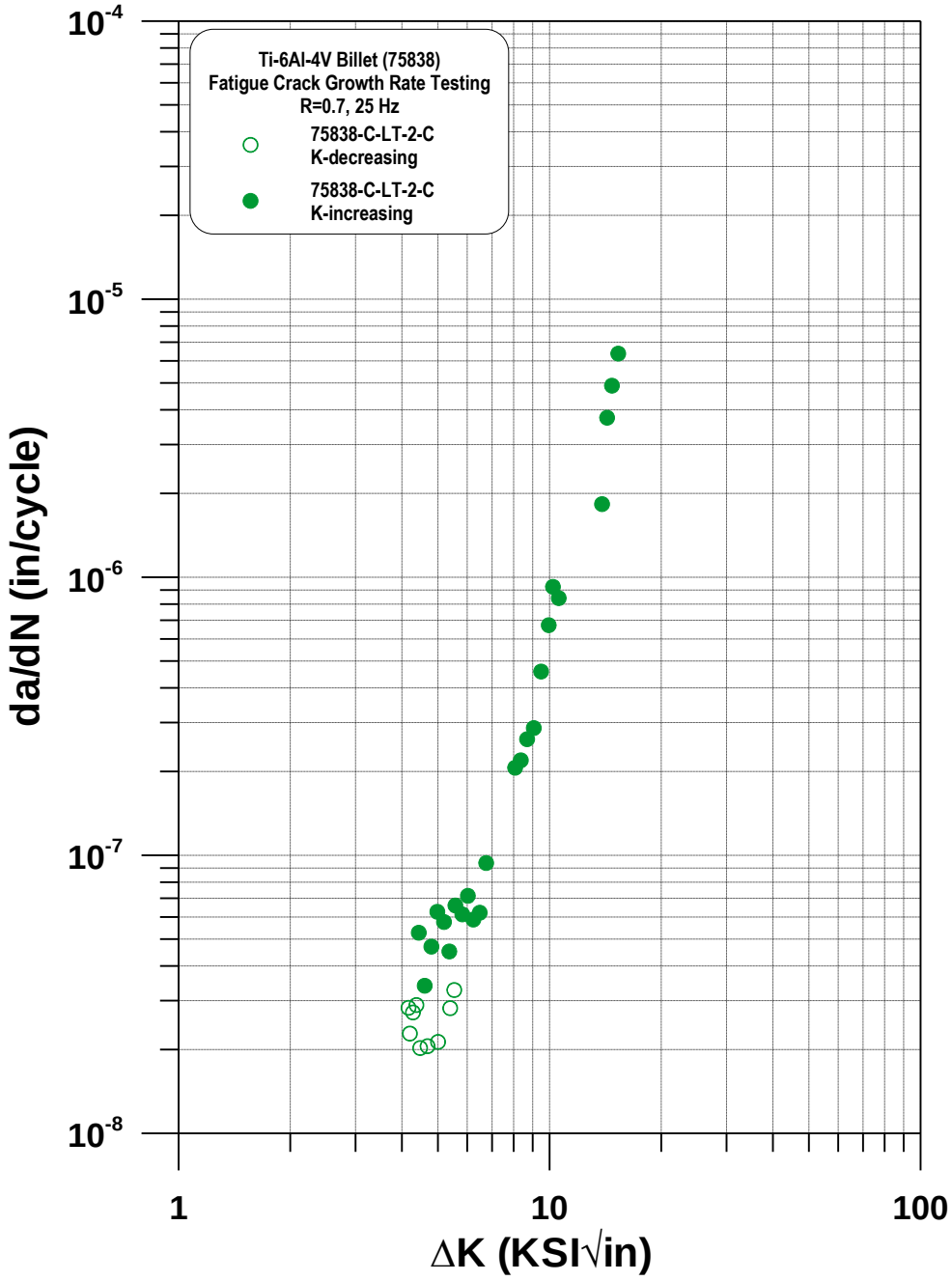
Approved for public release; distribution unlimited.



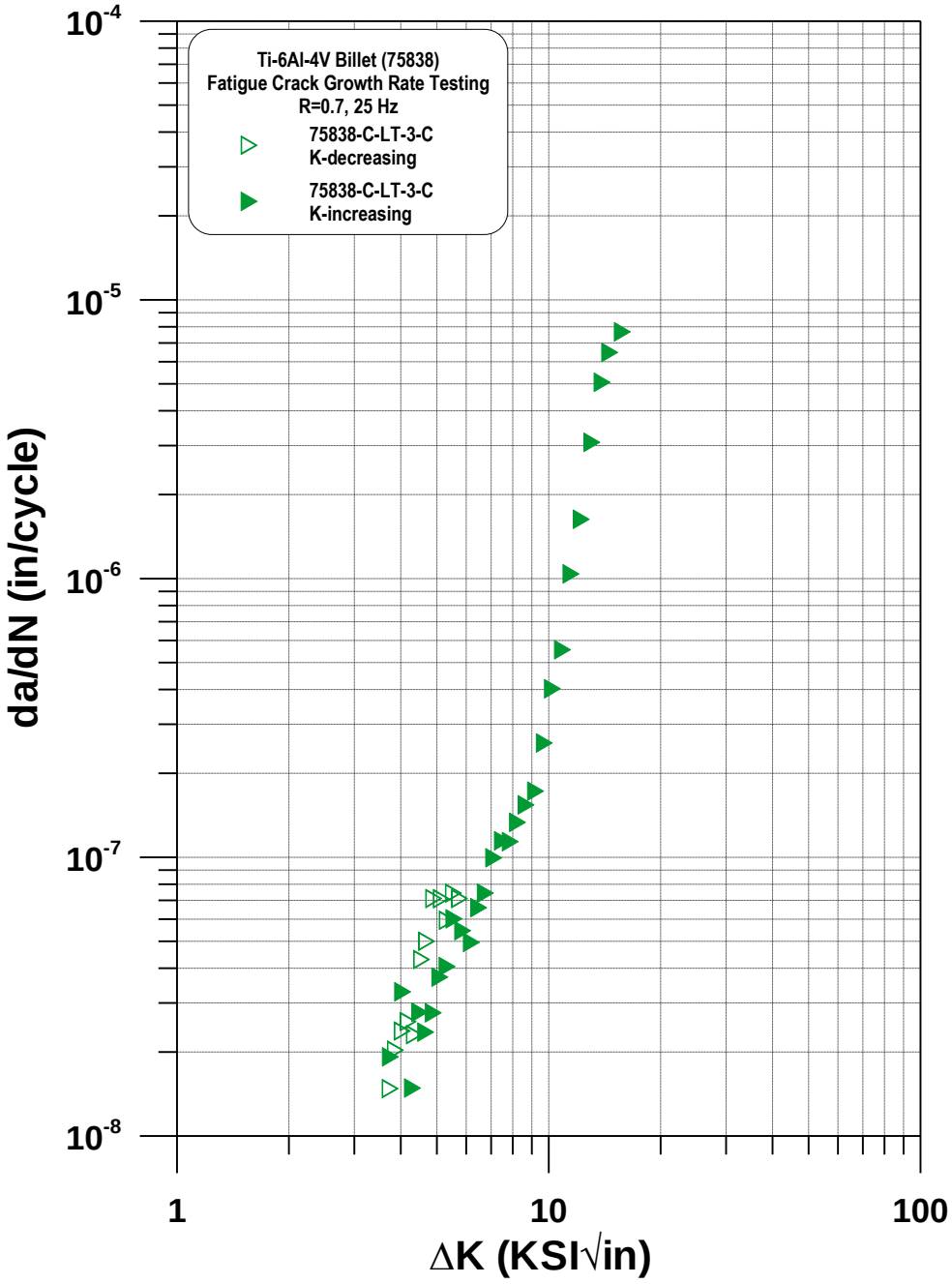
Approved for public release; distribution unlimited.



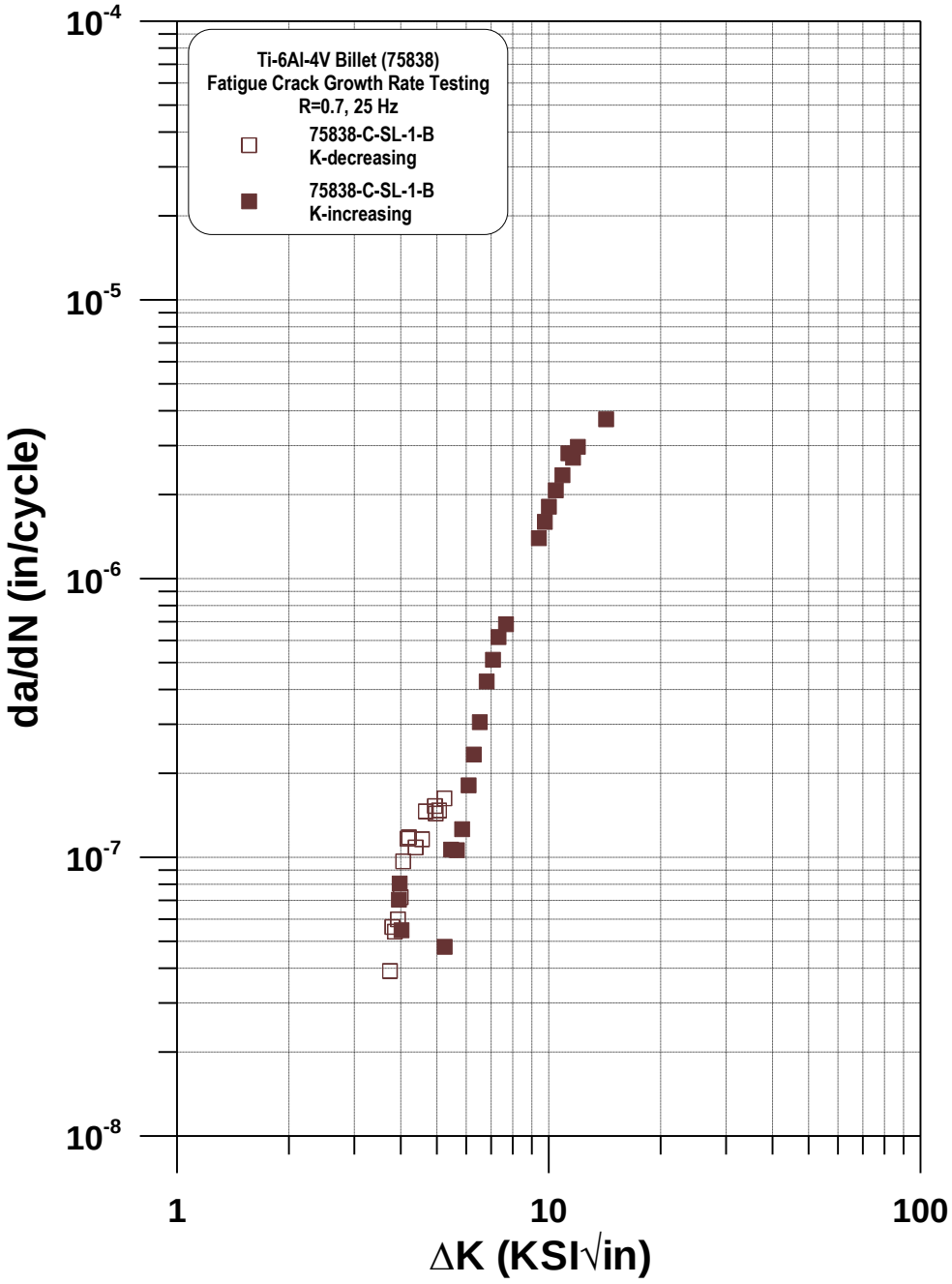
Approved for public release; distribution unlimited.



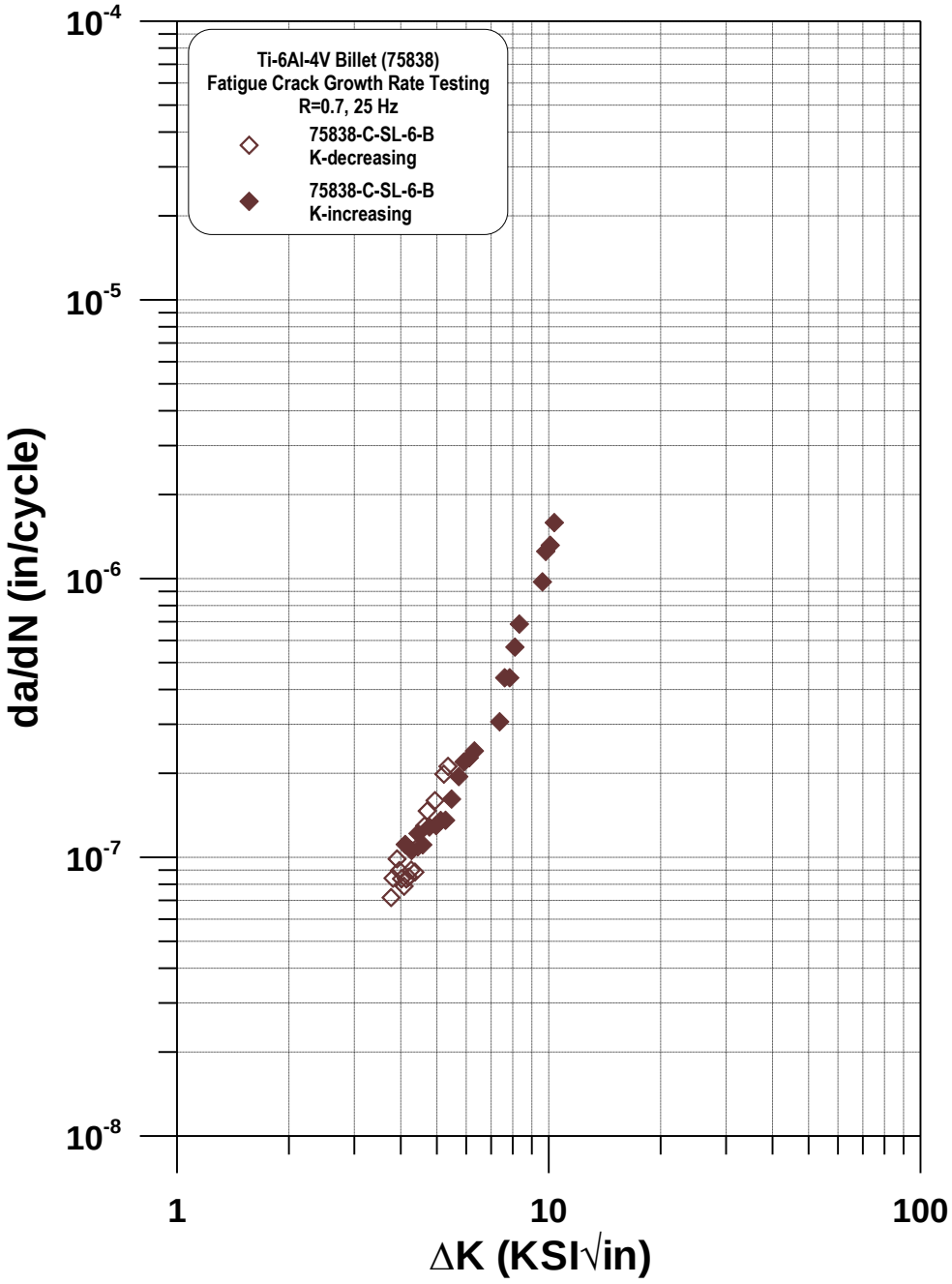
Approved for public release; distribution unlimited.



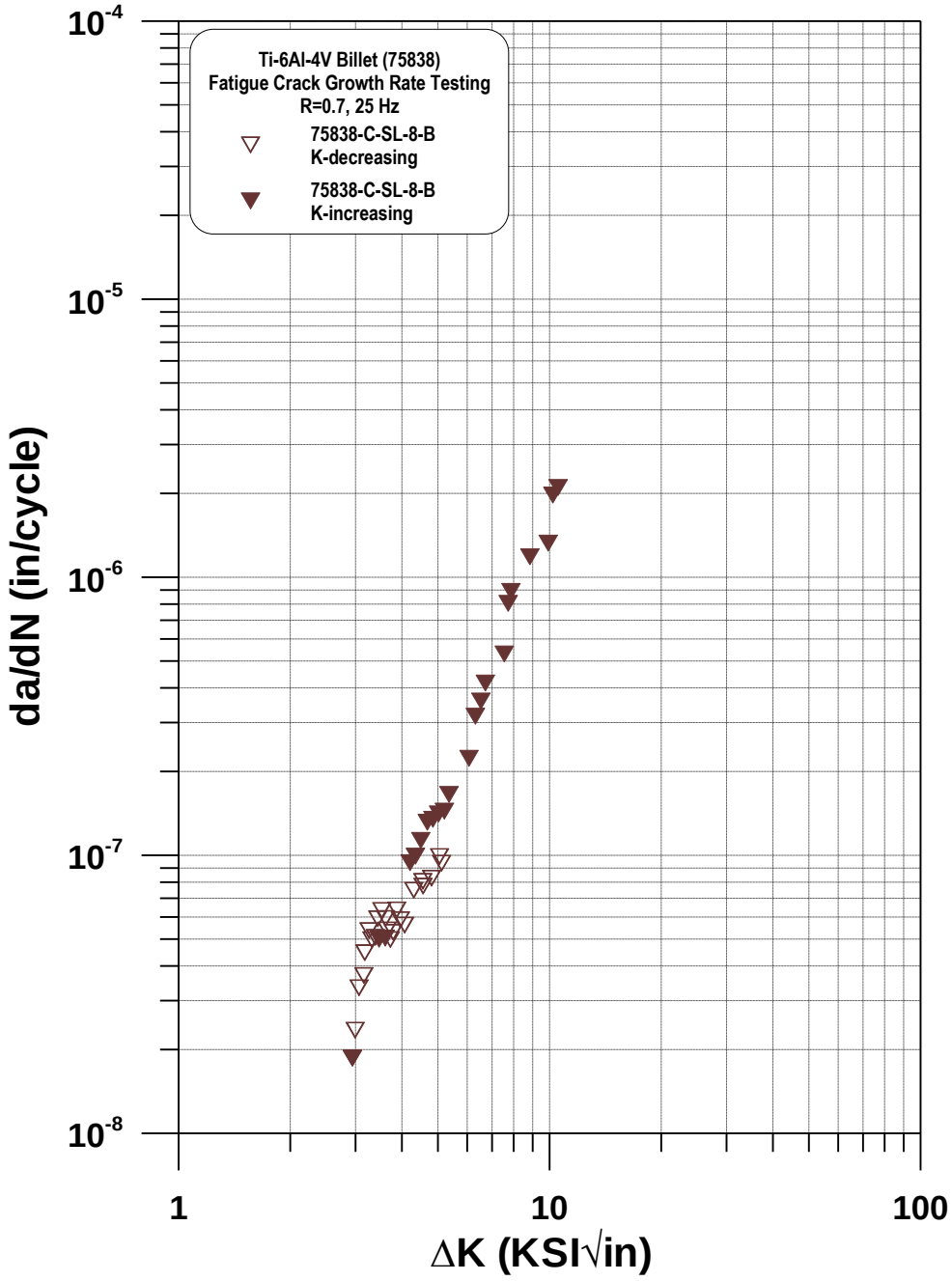
Approved for public release; distribution unlimited.



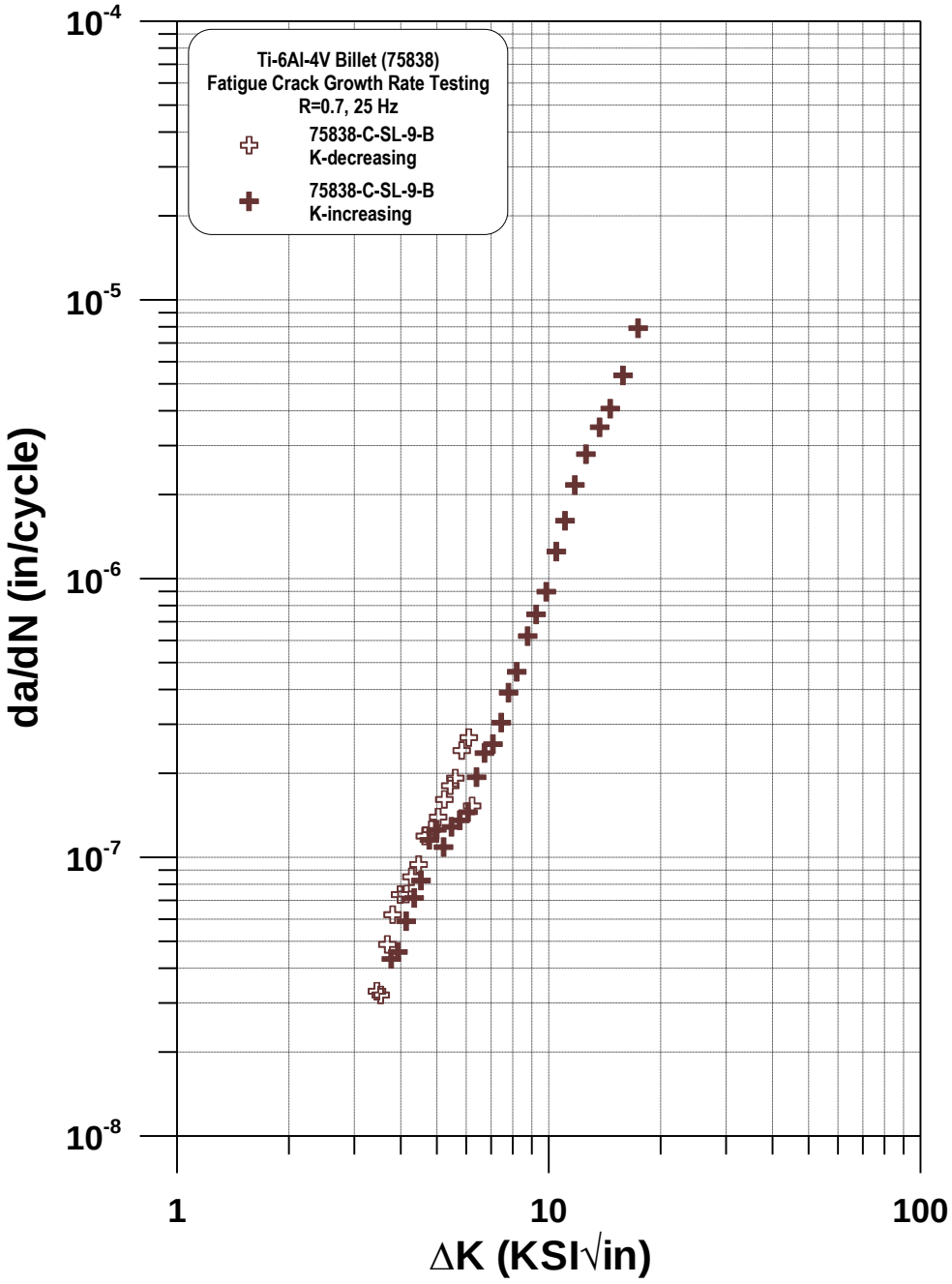
Approved for public release; distribution unlimited.



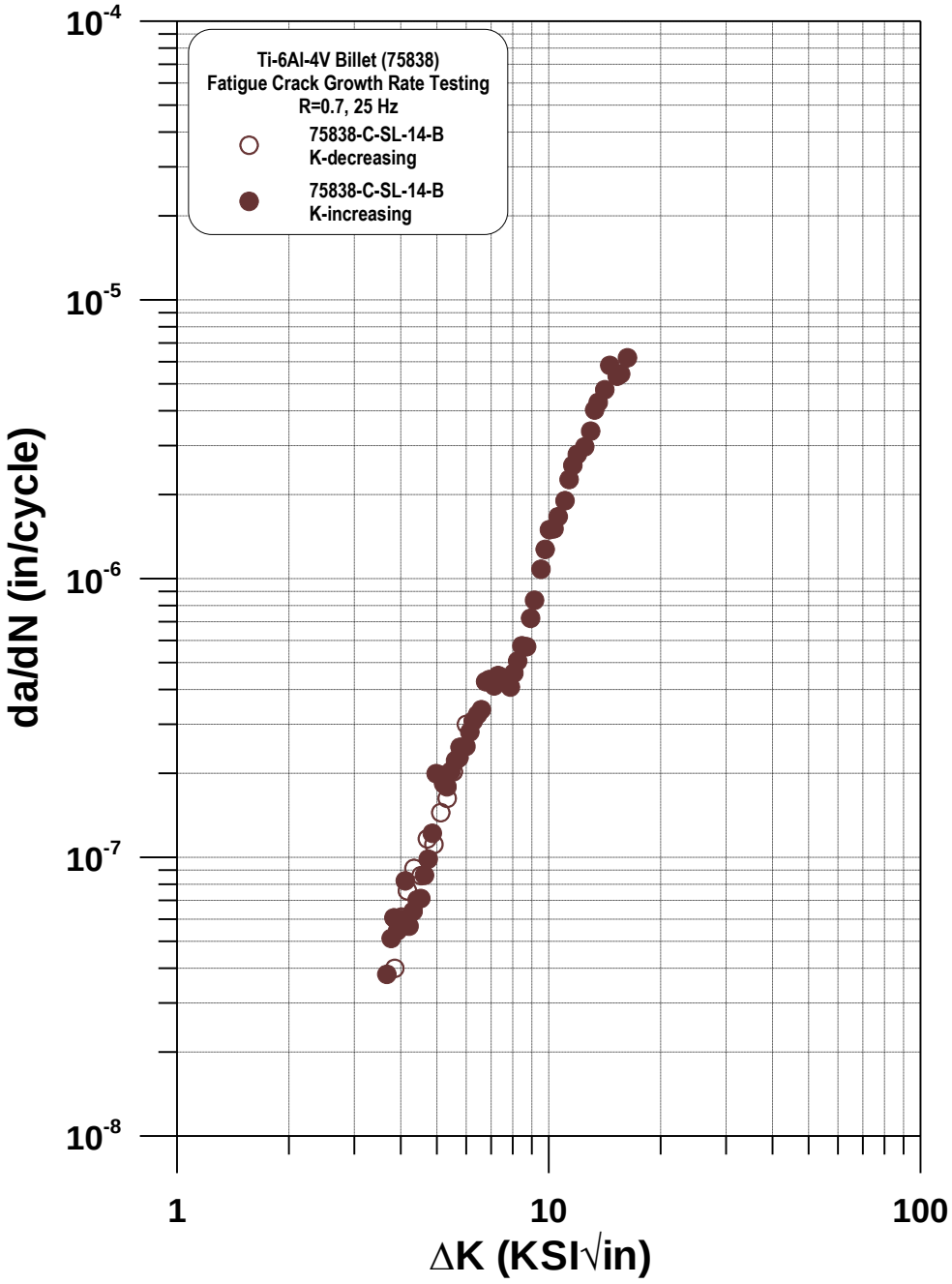
Approved for public release; distribution unlimited.



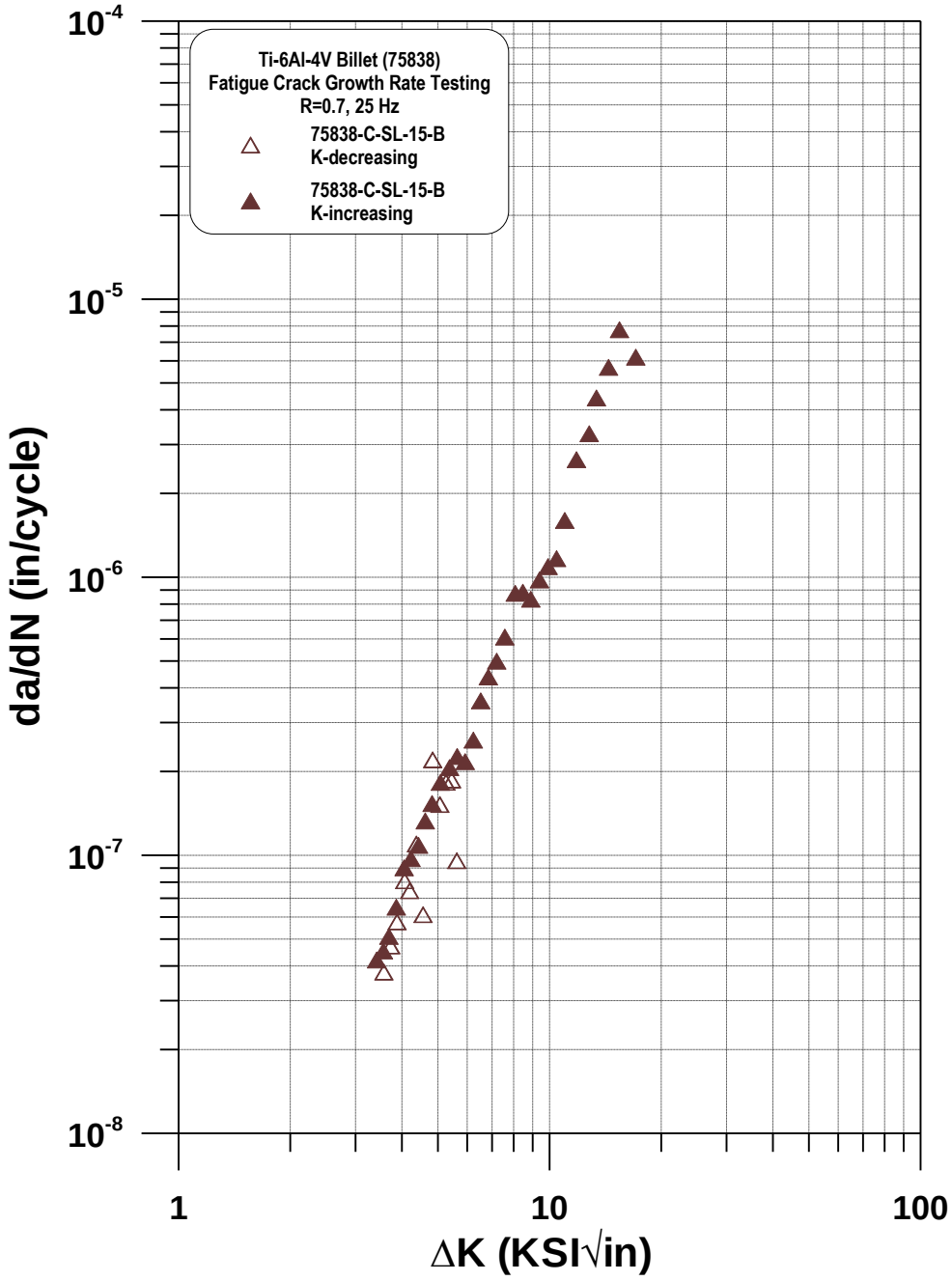
Approved for public release; distribution unlimited.



Approved for public release; distribution unlimited.



Approved for public release; distribution unlimited.



Approved for public release; distribution unlimited.

APPENDIX B

NON-CONFORMING TITANIUM – CONTROL PLATE CHARACTERIZATION (TI-6AL-4V & TI-6AL-6V-2SN PLATE)

31 AUGUST 2010

EVALUATION REPORT

REPORT NO. AFRL/RXS 10-072

AUTHOR

Steven R. Thompson
Acquisition Systems Support Branch (AFRL/RXSCE)

Building 652, Room 122
2179 12th Street
Wright-Patterson AFB, Ohio 45433-7718

REQUESTER
AFMC/EN (Thomas Fischer)

CAUTION

This information consists of PRELIMINARY reasonable lower bound properties for titanium billet. (Fully analyzed data, labeled FINAL, will be forthcoming.)
This information should be used **only** to evaluate the potential impact of improperly substituted titanium.
This information should **not** be used for design purposes in place of material properties from specifications or MMPDS entries covering titanium plate, bar, or other product forms.
This information should **not** be used to analyze components manufactured from titanium stock that is known to be compliant with applicable specifications.

CAUTION

DISTRIBUTION STATEMENT A: Approved for public release; distribution unlimited.

BACKGROUND

An ongoing federal investigation has identified a risk associated with improperly processed titanium (Ti) material being used in the fabrication of critical safety items and safety-of-flight components in USAF, DoD, NASA, FAA, and other systems. At the direction of AFMC/CC, a Titanium Task Force (led by AFMC/EN) was formed to further define risk to USAF systems and to assist with mitigation efforts. The suspect Ti material (e.g., "billet," "reforging stock") was never intended to be machined to the final forms in which it is now possibly being used. This R&D testing program will develop new baseline (reasonable lower bound) properties on a heretofore not fully characterized form of Ti. The decision to refer to these baseline values as "reasonable lower bounds" is based on the fact that an insufficient quantity of material heats and lots were represented for the calculation of traditional MMPDS **[*1*]** A- or B-, or even S-basis allowables. However, the number of specimens tested (often in replicate) is significant. Thus "reasonable lower bound" was chosen as the proper phrase to describe properties derived from the testing of multiple specimens from the two heats (per alloy) of material in this program. While these do not meet the requirements for standard baseline property determination, they are, nevertheless, significant.

This report is intended to summarize the mechanical testing of one Ti-6Al-4V plate and one Ti-6Al-6V-2Sn plate. The data obtained from these plates will be used as "control" information for comparison with the data obtained from the billet material. The data contained herein is not intended to replace currently established design allowables.

MATERIAL DESCRIPTION

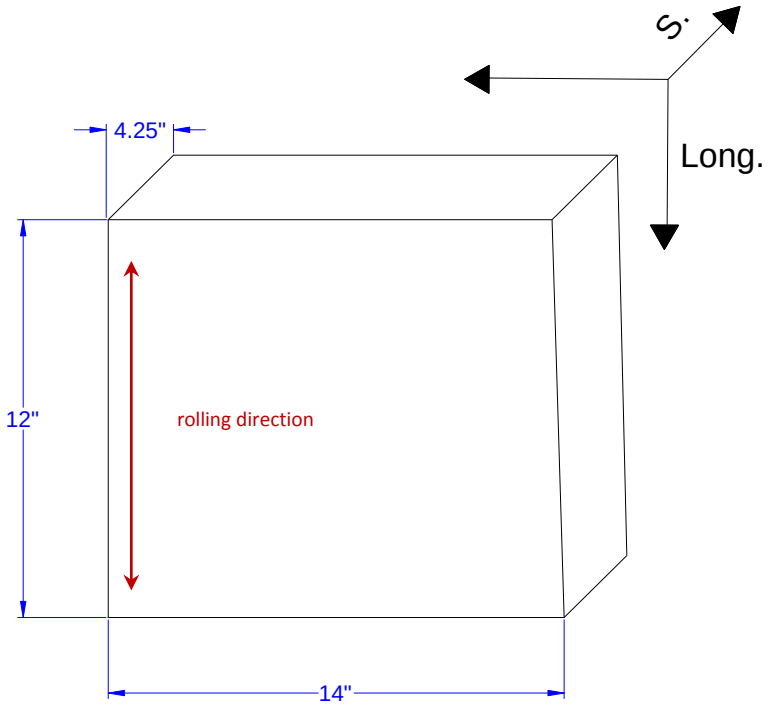
Ti-6Al-4V – The Ti-6Al-4V plate summarized in this report was purchased from Titanium Industries, Inc. As shown in Figure 1(a), the section of plate received had nominal dimensions of 14"(w) x 12"(l) x 4.25"(t) and had been produced per the AMS-T-9046 specification. The plate's pedigree traces back to ingot heat J91K produced by ATI Allvac. The plate was delivered in the mill-annealed heat treat condition.

Ti-6Al-6V-2Sn – The Ti-6Al-6V-2Sn plate summarized in this report had originally been purchased for a similar investigation in 2005. The plate was obtained from RJ Enterprise, Inc. and had original nominal dimensions of 12"(w) x 12"(l) x 4"(t) and had been produced per the AMS-T-9046 specification. The plate's pedigree traces back to ingot heat 855401-01 produced by RMI. (Note: Upon receipt, the plate had been given an internal designation of M1247, and specimens from this plate used the 1247 for identification.) The plate was delivered in the mill annealed heat treat condition.

The standard designations of longitudinal (L), long transverse (T), and short transverse (S) coordinate system were employed in the investigation of these plates.

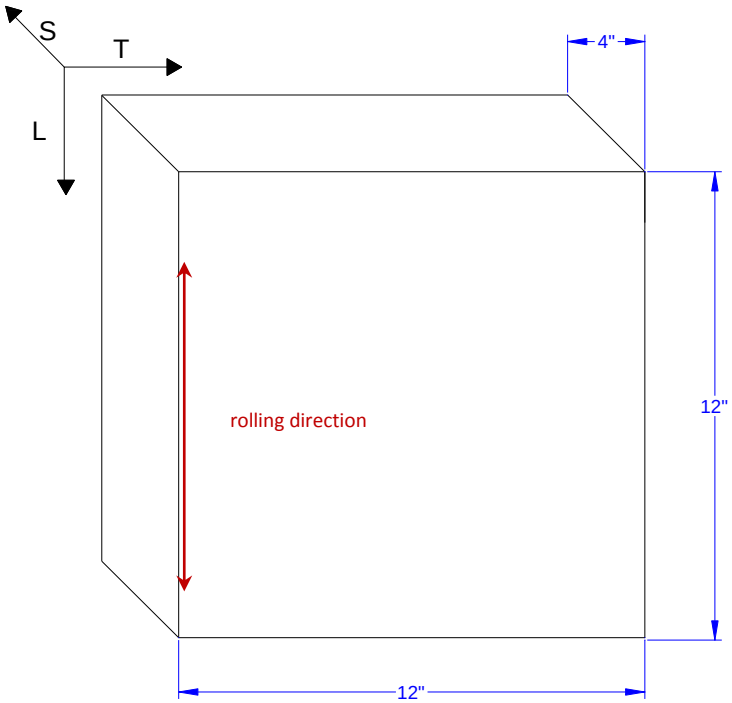
Approved for public release; distribution unlimited.

Prior to test specimen extraction, the plates were subjected to non-destructive evaluation (NDE) using ultrasonic transmission (UT). No relevant indications were noted during this evaluation. After the test specimens were machined, they were once again examined using NDE techniques. All specimens, except the fracture toughness, were examined using x-ray and fluorescent penetrant inspection (FPI). Fracture toughness specimens had UT and FPI examinations. Any resultant indications were noted and photographed for use in analysis of anomalous test results.



(a)

Approved for public release; distribution unlimited.

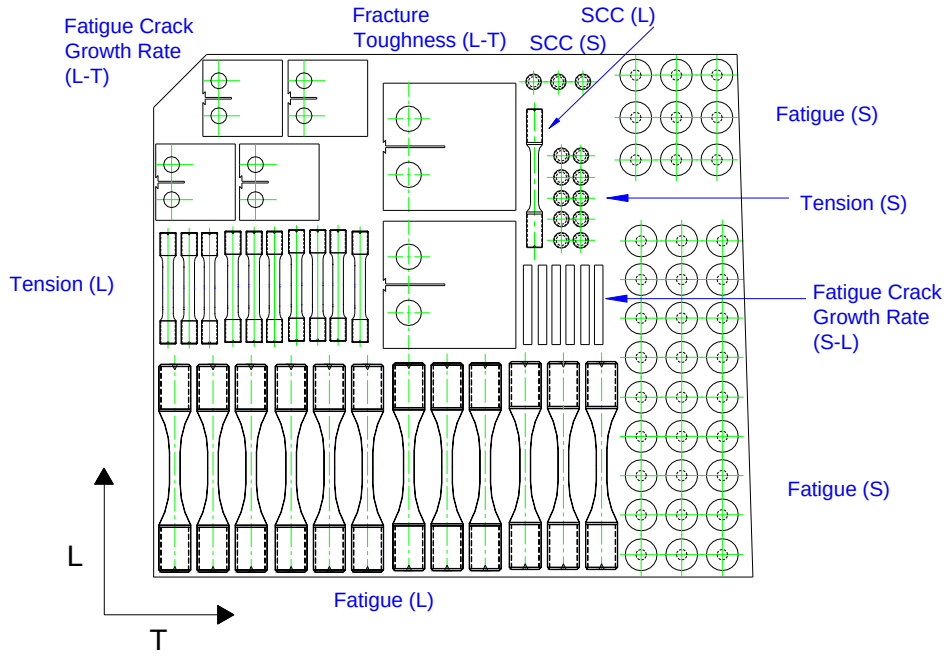


(b)

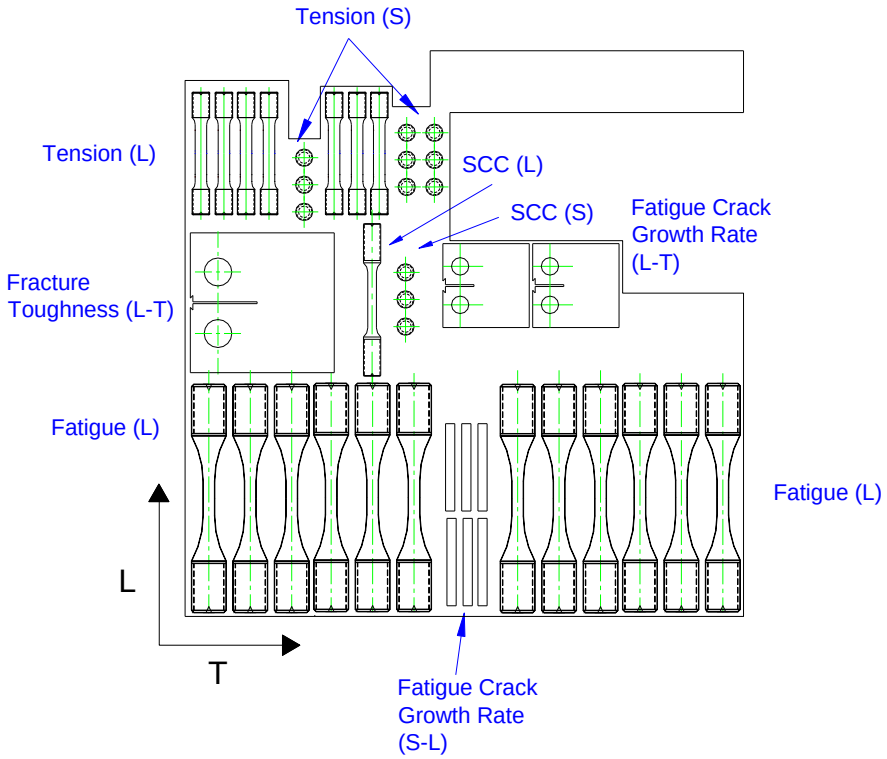
Figure 1. (a) Ti-6Al-4V plate (J91K) and (b) Ti-6Al-6V-2Sn plate (1247) indicating dimensions and orientations prior to specimen extraction.

TEST PLAN

Test Specimens – The test specimens were excised approximately from the locations shown in Figure 2(a) for the Ti-6Al-4V plate and Figure 2(b) for the Ti-6Al-6V-2Sn plate. For the Ti-6Al-6V-2Sn plate, the layout shows the portion of plate remaining after the 2005 investigation. Specimens were removed from three planes through the thickness where possible: the two quarter points (t/4 and 3t/4) and the midplane (t/2). Throughout this report, specimen location within the thickness is designated by either "A" (t/4), "B" (t/2), or "C" (3t/4). For short-transverse (S or S-L) oriented specimens, the location was determined by either the center of the gage length or the crack plane.



(a)



(b)

Figure 2. Specimen location layout drawings for (a) Ti-6Al-4V and (b) Ti-6Al-6V-2Sn plates.

Approved for public release; distribution unlimited.

Test specimens were machined to the final required geometries as shown in Figures 3 through 7. All of the geometries were in accordance with the applicable test method (as described in the next section). All of the specimens were fabricated using the same machine shop per specimen drawings provided by AFRL/RXSCE, in order to minimize possibility of variability due to specimen machining. Special care was given to the traceability of the specimen back to a general location within the billet. Test specimens were given a unique identification that would allow for this tracking.

Due to an error during the machining of the fatigue specimens from the Ti-6Al-4V plate (J91K), the fatigue specimen geometry had to be modified from that shown in Figure 4. The resultant test section diameter was 0.200 inches with a 0.626 inch diameter grip section. The modified specimen geometry was still in compliance with ASTM E466.

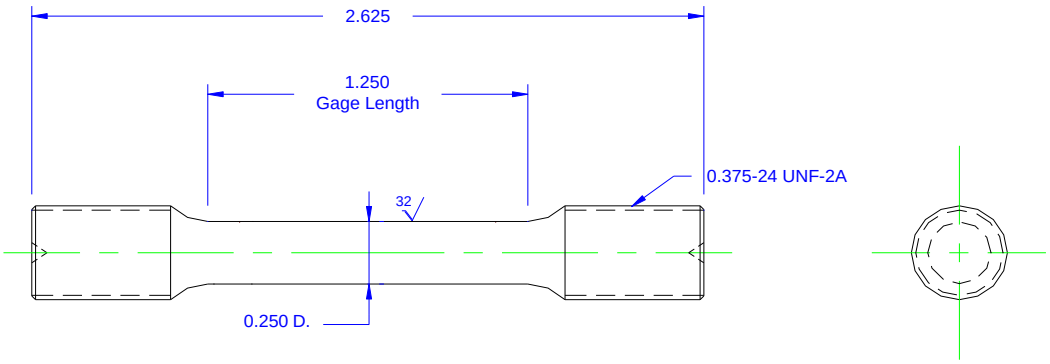


Figure 3. Geometry of tensile test specimen.

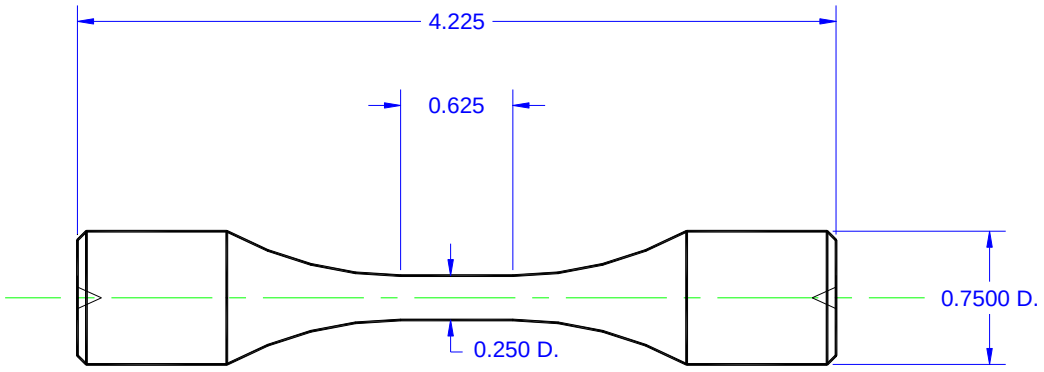
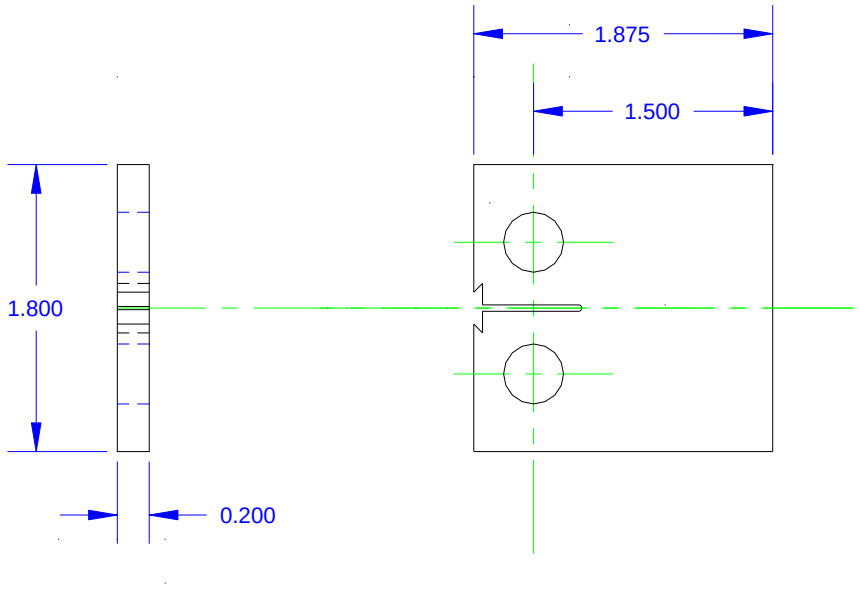


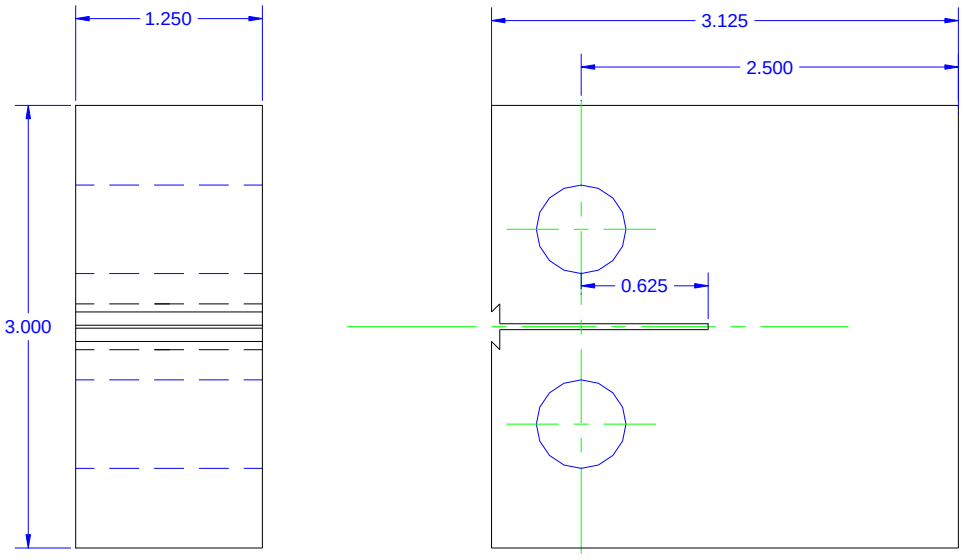
Figure 4. Geometry of fatigue test specimen. (Note: gage section was low-stress ground to a final surface finish of 8 Ra and then hand-polished longitudinally to remove all circumferential scratches.)

Approved for public release; distribution unlimited.



All dimensions in inches.

Figure 5. Geometry of fatigue crack growth rate C(T) test specimen.



All dimensions in inches

Figure 6. Geometry of fracture toughness C(T) test specimen.

Approved for public release; distribution unlimited.

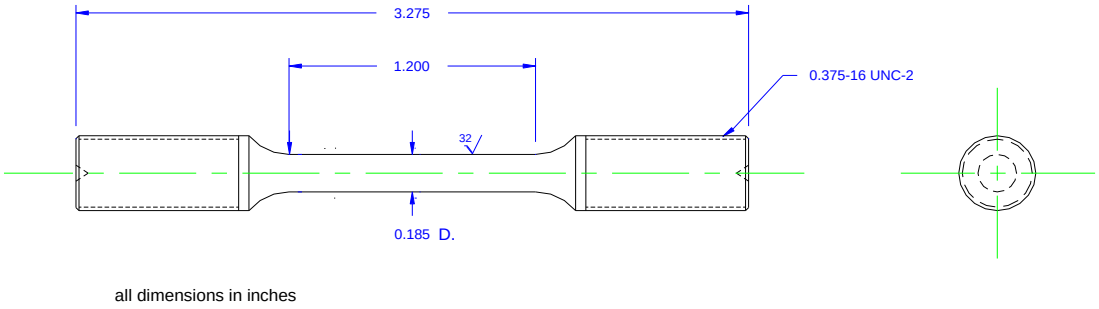


Figure 7. Geometry of stress corrosion cracking (SCC) test specimen.

Test Methods – The test methodologies used in this investigation are listed in Table 1. With the exception of stress corrosion cracking, all of the tests were performed in accordance with applicable ASTM standards. All testing was performed in ambient laboratory conditions (approximately 72°F and 50% relative humidity).

Table 1. Test Methodology

Test	ASTM Method
Tension (Modulus)	E 111-04 "Standard Test Method for Young's Modulus, Tangent Modulus, and Chord Modulus"
Tension	E 8/E 8M-08 "Standard Test Methods for Tension Testing of Metallic Materials"
Fatigue (force-controlled)	E 466-07 "Standard Practice for Conducting Force Controlled Constant Amplitude Axial Fatigue Tests of Metallic Materials"
Fatigue (strain-controlled)	E606-04 "Standard Practice for Strain-Controlled Fatigue Testing"
Fatigue Crack Growth Rate	E 647-08 "Standard Test Method for Measurement of Fatigue Crack Growth Rates"
Fracture Toughness	E 399-08 "Standard Test Method for Linear-Elastic Plane-Strain Fracture Toughness K_{Ic} of Metallic Materials"
Stress Corrosion Cracking	Similar to G 64-99 "Standard Classification of Resistance to Stress-Corrosion Cracking of Heat-Treatable Aluminum Alloys" Applied stress = 75% of specification tensile yield strength / 40 days 3.5% NaCl solution – alternate immersion (10 min wet/50 min dry)

Tension (Modulus) – Prior to performing full-range tension testing, 10% of the machined tension specimens were used to generate modulus data using the procedures outlined in ASTM E111. For this testing the specimens were loaded to a maximum stress below the proportional limit, so as to remain within the linear region of the stress-strain curve. The test was repeated three times per specimen, with the specimen being rotated 120° between test runs. Strain was measured using an MTS averaging extensometer (B-1 classification) with a one-inch gage length. The average modulus from the three runs was recorded as the final elastic modulus.

Tension – Tension testing was performed on an Instron electro-mechanical test machine in accordance with ASTM E8. Strain was measured using an Instron one-inch gage length extensometer. The extensometer was removed from the specimen prior to reaching ultimate load to prevent damage to the instrument during specimen breakage. Elongation and reduction of area measurements were made using the "fit-back" method.

Fatigue (Force-controlled) – Axial fatigue testing was performed under force-controlled conditions using an MTS servo-hydraulic test machine in accordance with ASTM

E466. Stress ratios (R) of 0.05 and -1 were used in this investigation. Replicate specimens were tested at four applied stress levels for each of the stress ratios.

Fatigue (Strain-controlled) – Axial fatigue testing was performed under strain-controlled conditions using an MTS servo-hydraulic test machine in accordance with ASTM E606. An MTS one-inch gage length extensometer was used for strain measurement. The testing frequency used was 1 Hz. Strain ratios ($R_\varepsilon = \varepsilon_{min}/\varepsilon_{max}$) of 0.05 and -1 were used for these specimens.

Fatigue Crack Growth Rate – Fatigue crack growth rate testing was performed on an MTS servo-hydraulic test machine per ASTM E647 using computer data acquisition and control systems developed in-house. Crack length was measured via compliance techniques with standard crack-opening-displacement (COD) gages. Testing was performed under K-control (C=-2) until a near-threshold growth rate was obtained, at which point the test was then run under constant amplitude (constant load) conditions for the remainder of the test. Initial and final crack lengths were measured optically for use in post-test crack correlation calculations. A test frequency of 25 Hz was used throughout the test, with humidity maintained at 50% ±10% for the duration of the test. Specimens were tested using stress ratios (R) of 0.1 and 0.7. Two orientations were tested for this program, L-T and S-L, where the first letter indicates the loading direction and the second letter indicates the direction of crack propagation. The C(T) specimen geometry was utilized for the plate material due to thickness limitations which would prevent the ESE(T) specimen from being used in the S-L orientation.

Fracture Toughness – Plane-strain fracture toughness tests were performed in accordance with ASTM E399 on a Tinius-Olsen electro-mechanical test machine. Specimen precracking was performed on an MTS servo-hydraulic test machine. Crack length was monitored via compliance techniques using an MTS COD gage as previously described. Initial and final crack lengths were measured optically post-test.

Stress Corrosion Cracking – The theory behind this testing was that since the billet material had not been subject to final hot working, the microstructure would not be fully homogenized, leading to the potential for localized aluminum segregation. If this were to occur, those areas would be more susceptible to the effect of stress corrosion cracking, particularly at these applied stress levels.

For this investigation, stress corrosion cracking tests were therefore performed in order to simply give pass/fail results. As there is currently no ASTM test method for SCC of titanium alloys, the procedure outlined in ASTM G64 ("A" level) was used. This procedure has been adopted for use within AFRL/RXSCE as a standard SCC test. Specimens were axially loaded (statically) in an alternate immersion, 3.5% NaCl solution such that the specimens were submerged in the solution for 10 minutes and then allowed to dry for the next 50 minutes each hour. The specimens were loaded at 75% of the specification yield strength (for plate and bar). For the Ti-6Al-4V plate, the applied stress was 90 ksi whereas for the Ti-6Al-6V-2Sn plate, the applied stress was 101.3 ksi. The test duration was set at

Approved for public release; distribution unlimited.

40 days. To pass the test, no failure of the specimen could occur during the 40 loading cycle.

FACTUAL DATA

Ti-6Al-4V Plate

Tension – The results of tensile testing are shown in Tables 2(a) through 2(d). Strength levels for all L-orientation specimens were above the specification minimum values shown in AMS-T-9046 (plate) for this alloy. S-orientation specimens exhibited lower ductility and slightly lower elastic modulus than specimens from the L-orientation. Elastic modulus values were all within the range expected for this alloy. There was a less than 5% difference between those modulus results from ASTM E111 tests and those obtained from the E8 tensile test record. In addition, there did not appear to be a difference between specimens excised from the three different thickness locations.

As this piece of material was properly processed plate, it would not be appropriate to combine the two orientations into one population. Also, since there are specification minimum values and MMPDS A-basis allowables for this alloy, reasonable lower bound properties will not be calculated from the obtained data set. The data will be used to show compliance with the specification and will be used in further analyses for comparison with billet material.

It should be noted that the AMS-T-9046 specification does not list minimum properties for the short-transverse orientation, therefore the values shown at the bottom of Table 2(d) are for comparison only.

Approved for public release; distribution unlimited.

Table 2. Ti-6Al-4V plate tensile test results.

(a) Longitudinal orientation, t/4 thickness location

	Orientation	Thickness Location	Yield Strength (ksi)	Ultimate Tensile Strength (ksi)	% Elongation	% Reduction of Area	Elastic Modulus, E111 (msi)	Elastic Modulus, E8 (msi)
J91K-T-L-1-A	L	t/4	132.4	139.5	15.5%	21.2%	17.60	17.63
L-2-A	L	t/4	132.9	139.9	16.4%	28.1%		17.80
L-3-A	L	t/4	132.1	139.0	15.3%	19.5%		17.20
L-4-A	L	t/4	133.1	140.2	15.6%	25.8%		16.80
L-5-A	L	t/4	132.4	138.7	15.4%	26.0%		17.10
L-6-A	L	t/4	132.4	139.1	13.4%	18.4%		17.10
L-7-A	L	t/4	133.1	140.2	16.4%	24.1%		17.10
L-8-A	L	t/4	131.8	139.0	15.8%	25.2%		17.30
L-9-A	L	t/4	132.8	139.5	14.8%	22.2%		17.00
L-10-A	L	t/4	133.3	140.9	16.0%	26.0%		17.92
AMS-T-9046 (L)			120	130	10%			
MMPDS A-basis (L)			118	130	10%			16.0

(b) Longitudinal orientation, t/2 thickness location

	Orientation	Thickness Location	Yield Strength (ksi)	Ultimate Tensile Strength (ksi)	% Elongation	% Reduction of Area	Elastic Modulus, E111 (msi)	Elastic Modulus, E8 (msi)
J91K-T-L-1-B	L	t/2	133.0	142.1	17.4%	21.4%	18.15	17.50
L-2-B	L	t/2	132.7	141.0	14.3%	21.9%		18.40
L-3-B	L	t/2	132.7	141.4	13.9%	19.3%		17.80
L-4-B	L	t/2	132.3	140.8	13.4%	23.8%		17.60
L-5-B	L	t/2	132.1	140.4	15.2%	21.3%		17.10
L-6-B	L	t/2	130.9	138.6	13.7%	19.7%		17.30
L-7-B	L	t/2	131.4	139.2	15.5%	24.8%		18.20
L-8-B	L	t/2	131.3	139.1	15.6%	20.4%		17.40
L-9-B	L	t/2	130.8	138.7	13.4%	24.7%		16.70
L-10-B	L	t/2	131.6	139.2	13.4%	22.7%		17.80
AMS-T-9046 (L)			120	130	10%			
MMPDS A-basis (L)			118	130	10%			16.0

Approved for public release; distribution unlimited.

(c) Longitudinal orientation, 3t/4 thickness location

	Orientation	Thickness Location	Yield Strength (ksi)	Ultimate Tensile Strength (ksi)	% Elongation	% Reduction of Area	Elastic Modulus, E111 (msi)	Elastic Modulus, E8 (msi)
J91K-T-L-1-C	L	3t/4	133.0	140.2	14.5%	26.7%	17.96	17.20
L-2-C	L	3t/4	133.0	140.4	16.7%	24.9%		18.00
L-3-C	L	3t/4	133.3	141.1	15.0%	23.4%		17.30
L-4-C	L	3t/4	132.1	139.2	14.9%	26.3%		17.20
L-5-C	L	3t/4	131.9	138.6	16.3%	24.4%		17.20
L-6-C	L	3t/4	132.4	139.4	15.4%	26.2%		17.10
L-7-C	L	3t/4	132.2	139.3	15.4%	22.0%		17.30
L-8-C	L	3t/4	132.3	139.1	15.0%	23.2%		17.50
L-9-C	L	3t/4	132.0	139.2	18.9%	23.0%		17.70
L-10-C	L	3t/4	133.0	140.2	16.5%	22.9%		17.10
AMS-T-9046 (L)			120	130	10%			
MMPDS A-basis (L)			118	130	10%			16.0

(d) Short-transverse orientation, t/2 thickness location

	Orientation	Thickness Location	Yield Strength (ksi)	Ultimate Tensile Strength (ksi)	% Elongation	% Reduction of Area	Elastic Modulus, E111 (msi)	Elastic Modulus, E8 (msi)
J91K-T-S-1-A	S	t/2	127.3	142.3	11.7%	15.8%	16.27	15.47
S-2-A	S	t/2	127.4	142.4	10.5%	14.3%		15.90
S-3-A	S	t/2	127.1	142.4	9.5%	15.1%		16.10
S-4-A	S	t/2	127.6	142.2	10.4%	14.1%		15.10
S-5-A	S	t/2	127.0	142.5	10.9%	15.5%		15.90
S-6-A	S	t/2	127.1	141.8	10.4%	16.9%		16.60
S-7-A	S	t/2	127.5	142.0	10.7%	14.8%		15.40
S-8-A	S	t/2	127.4	141.7	10.2%	14.6%		16.00
S-9-A	S	t/2	127.5	142.4	9.9%	12.3%		15.50
S-10-A	S	t/2	127.2	142.0	9.3%	16.7%		16.50
AMS-T-9046 (L)			120	130	10%			
MMPDS A-basis (L)			118	130	10%			16.0

Approved for public release; distribution unlimited.

Fatigue (force-controlled) – The results of force-controlled axial fatigue testing are shown graphically in Figure 8. Individual results are tabulated in Table 3. In Figure 8, the results for each stress ratio (R) have been fit with a best-fit power-law curve for graphical purposes only. Also included in this figure is a curve based on an equivalent stress equation from MMPDS Figure 5.4.1.1.8(a) for a mean stress of zero (R = -1). This curve is for comparison with the R = -1 data generated in this investigation. As stated in Figure 4, the fatigue specimens used herein were manufactured using low-stress grinding operations to a surface finish (Ra) of 8 per the ASTM E466 standard. The MMPDS reference data curve was generated from Ti-6Al-4V bar material using specimens having a surface roughness of 32. Although the specimens used in this effort had a smoother surface finish that those used in the reference data, and a longer life would typically be expected, it is not known whether low-stress grinding was used on those specimens. This aspect, along with inherent processing differences between plate and bar materials, could potentially have contributed to the difference between the data sets.

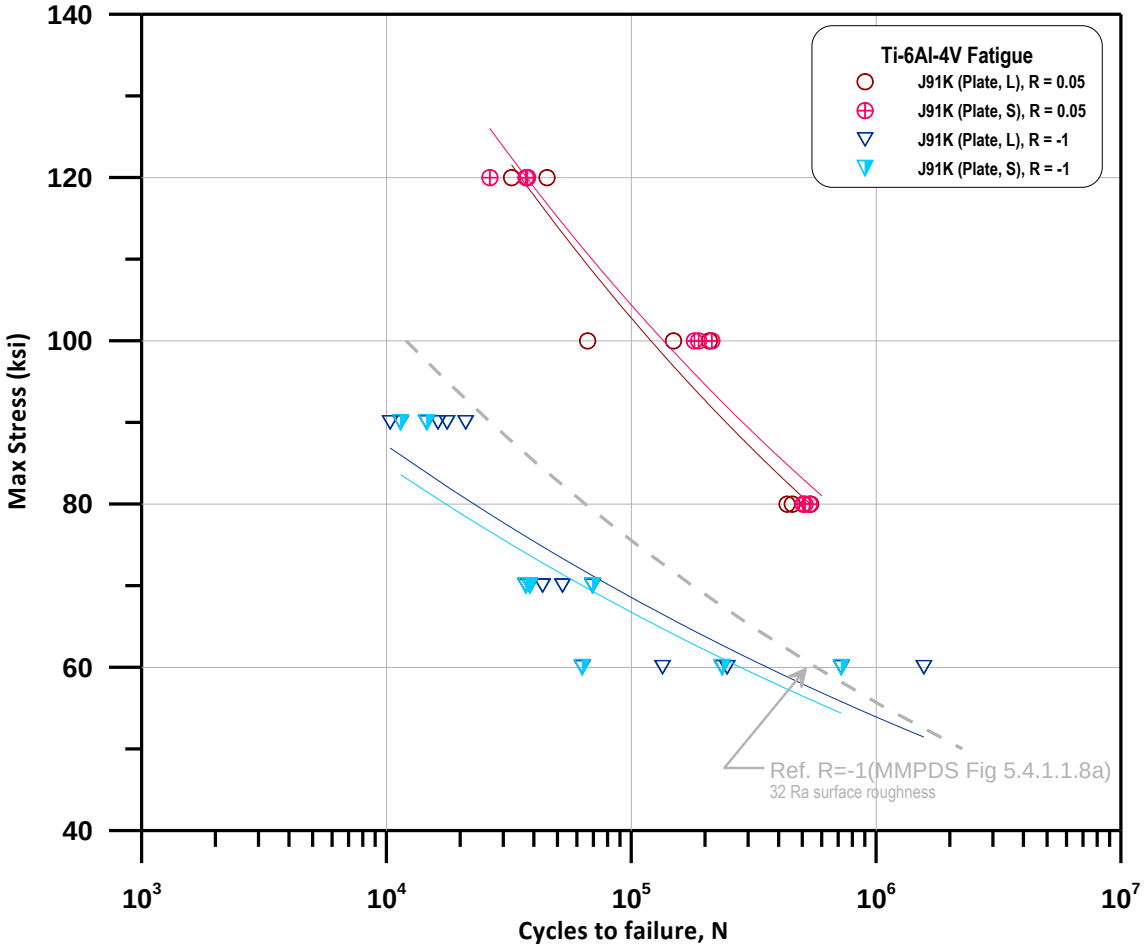


Figure 8. Ti-6Al-4V plate force-controlled axial fatigue test results.

Approved for public release; distribution unlimited.

Table 3. Ti-6Al-4V plate force-controlled axial fatigue test results.

	Thickness Location	Orientation	Max Stress (ksi)	Stress Ratio, R	Cycles to Failure
J91K-F-L-11-A	t/4	L	120	0.05	45,230
L-12-B	t/2	L	120	0.05	32,410
L-10-C	3t/4	L	120	0.05	37,600
L-10-A	t/4	L	100	0.05	66,290
L-10-B	t/2	L	100	0.05	208,140
L-12-C	3t/4	L	100	0.05	148,690
L-12-A	t/4	L	80	0.05	432,620
L-11-B	t/2	L	80	0.05	454,400
L-11-C	3t/4	L	80	0.05	539,120
J91K-F-S-34-B	t/2	S	120	0.05	26,410
S-35-B	t/2	S	120	0.05	37,070
S-36-B	t/2	S	120	0.05	37,600
S-32-B	t/2	S	100	0.05	188,080
S-30-B	t/2	S	100	0.05	212,980
S-29-B	t/2	S	100	0.05	180,730
S-31-B	t/2	S	80	0.05	502,570
S-33-B	t/2	S	80	0.05	511,950
S-28-B	t/2	S	80	0.05	533,570
J91K-F-L-2-A	t/4	L	90	-1	21,048
L-8-B	t/2	L	90	-1	16,229
L-5-C	3t/4	L	90	-1	17,672
L-5-A	t/4	L	70	-1	43,354
L-8-C	3t/4	L	70	-1	52,337
L-8-A	t/4	L	60	-1	1,564,688
L-5-B	t/2	L	60	-1	246344
L-2-C	3t/4	L	60	-1	134,143
J91K-F-S-2-B	t/2	S	90	-1	10,337
S-17-B	t/2	S	90	-1	11,414
S-23-B	t/2	S	90	-1	14,594
S-5-B	t/2	S	70	-1	69,413
S-11-B	t/2	S	70	-1	37,026
S-26-B	t/2	S	70	-1	38,472
S-8-B	t/2	S	60	-1	719,475
S-14-B	t/2	S	60	-1	63,015
S-20-B	t/2	S	60	-1	234,617

Approved for public release; distribution unlimited.

Fatigue (strain-controlled) – The results of strain-controlled axial fatigue testing are shown graphically in Figure 9, with individual results tabulated in Table 4.

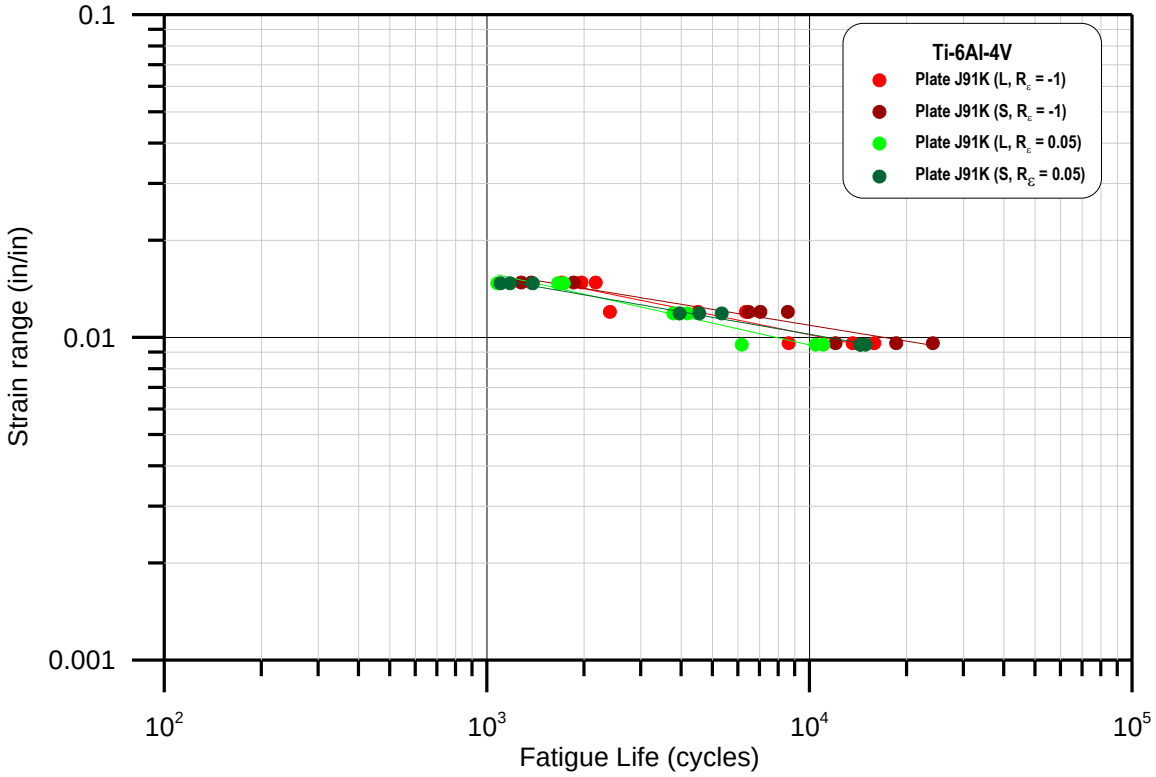


Figure 9. Ti-6Al-4V plate strain-controlled axial fatigue test results.

Approved for public release; distribution unlimited.

Table 4. Ti-6Al-4V plate strain-controlled axial fatigue test results.

	Thickness Location	Orientation	Strain Range (in/in)	Strain Ratio, R_ε	Cycles to Failure
J91K-F-L-1-B	t/2	L	0.0148	-1	2,172
F-L-3-C	3t/4	L	0.0148	-1	1,709
F-L-4-A	t/4	L	0.0148	-1	1,964
F-L-3-A	t/4	L	0.0120	-1	4,507
F-L-3-B	t/2	L	0.0120	-1	6,346
F-L-9-C	3t/4	L	0.0120	-1	2,404
F-L-6-C	3t/4	L	0.0096	-1	8,614
F-L-9-A	t/4	L	0.0096	-1	15,870
F-L-9-B	t/2	L	0.0096	-1	13,603
J91K-F-S-3-B	t/2	S	0.0148	-1	1,373
F-S-12-B	t/2	S	0.0148	-1	1,858
F-S-24-B	t/2	S	0.0148	-1	1,277
F-S-6-B	t/2	S	0.0120	-1	7,041
F-S-18-B	t/2	S	0.0120	-1	8,563
F-S-27-B	t/2	S	0.0120	-1	6,471
F-S-9-B	t/2	S	0.0096	-1	24,091
F-S-15-B	t/2	S	0.0096	-1	12,041
F-S-21-B	t/2	S	0.0096	-1	18,558
F-S-3-B	t/2	S	0.0148	-1	1,373
J91K-F-L-1-C	3t/4	L	0.0147	0.05	1,729
F-L-6-A	t/4	L	0.0147	0.05	1,077
F-L-7-B	t/2	L	0.0147	0.05	1,662
F-L-4-C	3t/4	L	0.0119	0.05	3,782
F-L-6-B	t/2	L	0.0119	0.05	3,934
F-L-7-A	t/4	L	0.0119	0.05	4,182
F-L-1-A	t/4	L	0.0095	0.05	10,440
F-L-4-B	t/2	L	0.0095	0.05	11,023
F-L-7-C	3t/4	L	0.0095	0.05	6,161
J91K-F-S-1-B	t/2	S	0.0147	0.05	1,102
F-S-13-B	t/2	S	0.0147	0.05	1,387
F-S-22-B	t/2	S	0.0147	0.05	1,179
F-S-7-B	t/2	S	0.0119	0.05	3,954
F-S-10-B	t/2	S	0.0119	0.05	5,342
F-S-19-B	t/2	S	0.0119	0.05	4,550
F-S-4-B	t/2	S	0.0095	0.05	14,348
F-S-16-B	t/2	S	0.0095	0.05	14,911
F-S-25-B	t/2	S	0.0095	0.05	14,380

Approved for public release; distribution unlimited.

Fatigue Crack Growth Rate – Fatigue crack growth rate test result summary curves are shown in Figures 10 and 11 for stress ratios (R) of 0.1 and 0.7, respectively. Individual specimen curves are located in Appendix A of this report. For both stress ratios, the S-L orientation specimens tended to have faster growth rates than the L-T specimens. Also included on these summary curves are best-fit mean curves from MMPDS-04 Figure 5.4.1.1.9(a1) for 0.25 inch thick Ti-6Al-4V plate (L-T orientation). Comparing the data generated from plate specimens with the MMPDS reference data, the combined orientation plate data generally exhibits slower growth rates over the range of stress intensities examined. Fractographic and metallographic examinations of the failed specimens will be performed to investigate possible reasons for this difference in growth rates.

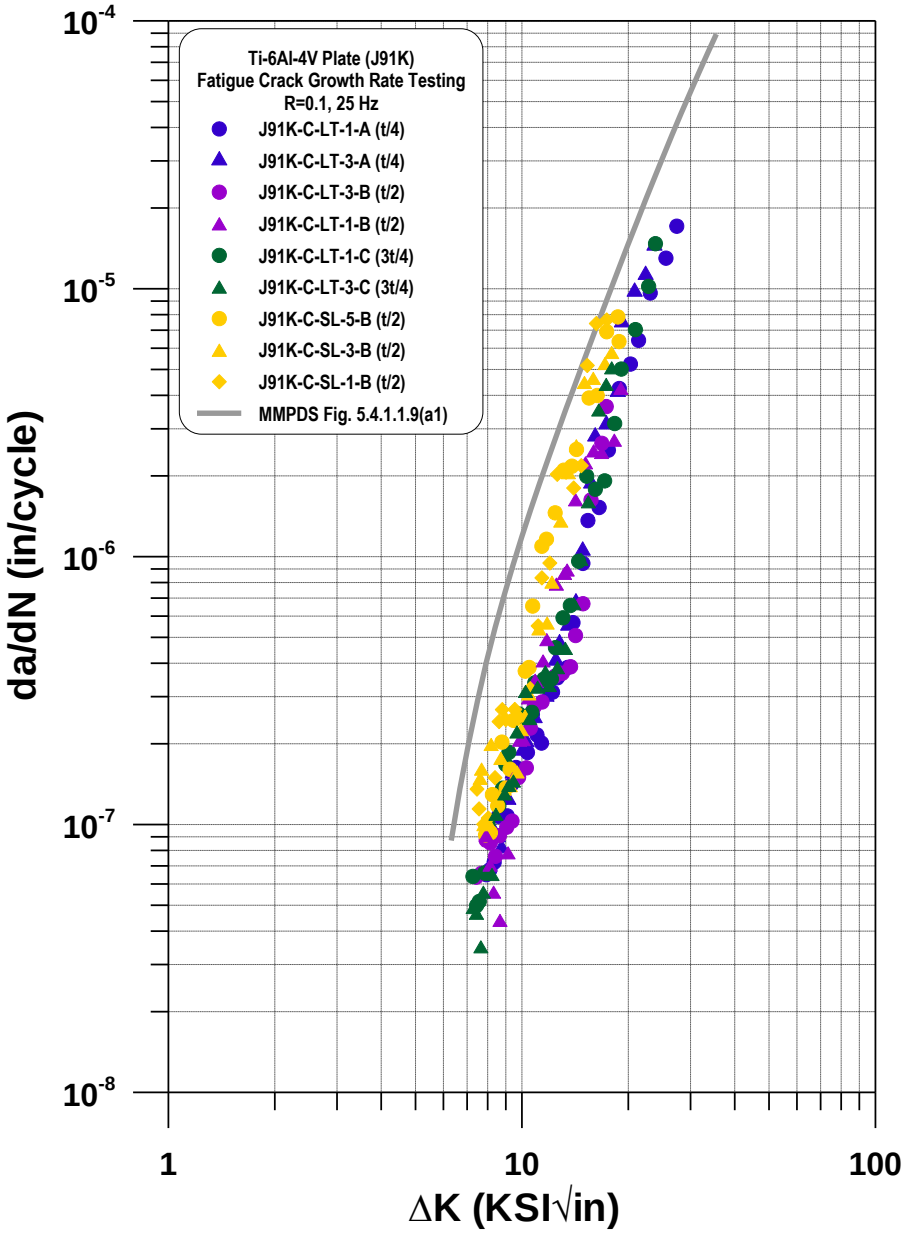


Figure 10. Ti-6Al-4V plate fatigue crack growth rate test results (R=0.1).

Approved for public release; distribution unlimited.

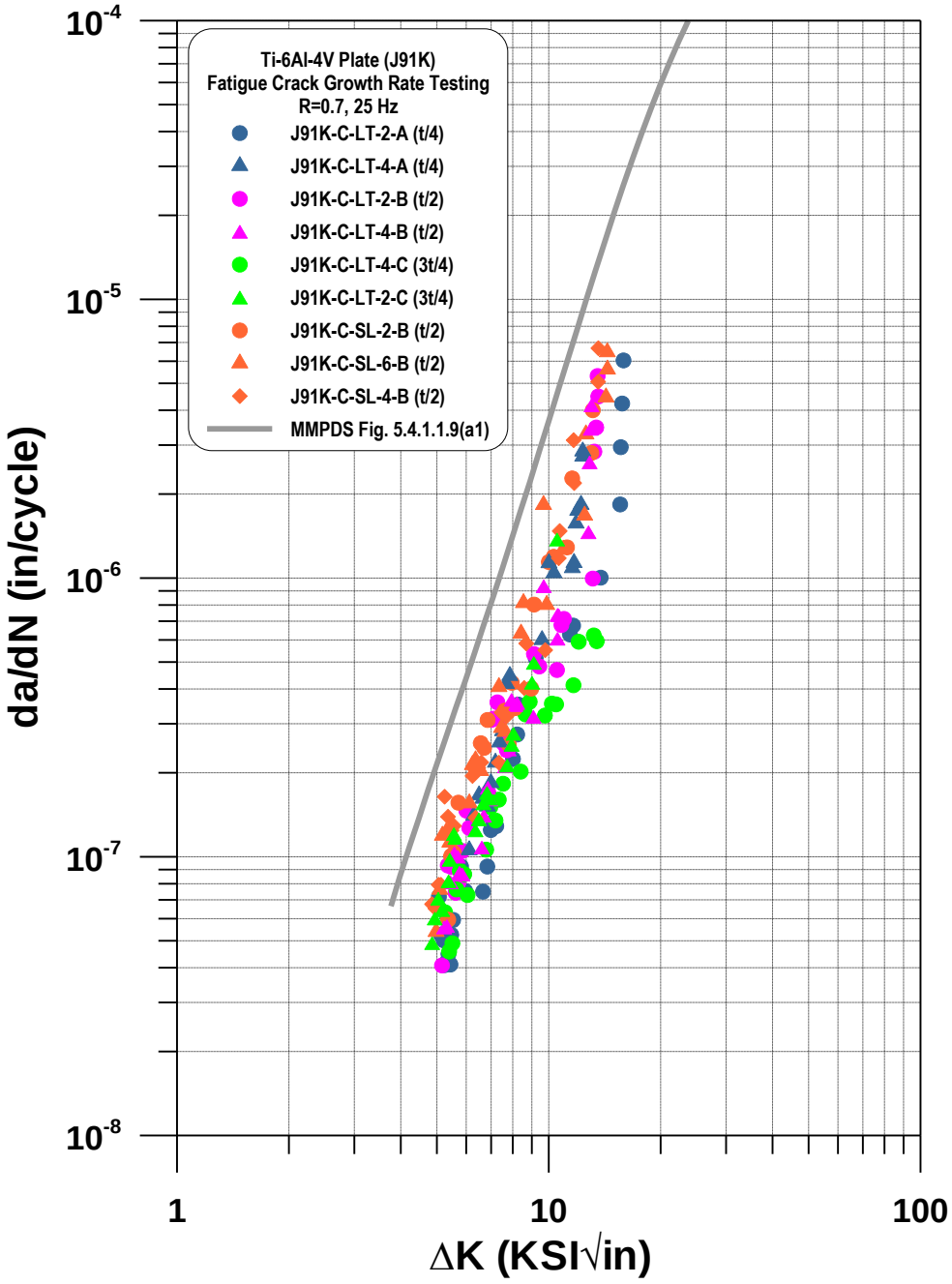


Figure 11. Ti-6Al-4V plate fatigue crack growth rate test results (R=0.7).

Approved for public release; distribution unlimited.

Fracture Toughness – Plane-strain fracture toughness test results are shown in Table 6. For this investigation, only the L-T orientation was tested.

Also shown in this table are reference values from MMPDS-04 and the Damage Tolerant Design Handbook **[*2*]** for forged bar and plate product forms, respectively. The test results generally correspond with those referenced data points considering those references indicate a high degree of variability.

Table 6. Ti-6Al-4V plate fracture toughness test results.

	Thickness Location	K_{Ic} (ksi√in)
J91K-K-LT-1-A	t/4	67.1
LT-2-A	t/4	66.1
LT-1-C	3t/4	64.6
LT-2-C	3t/4	64.6
MMPDS-04 *Table 5.1.2.1.1 (Forged Bar) Avg.*		60
Damage Tolerant Design Handbook *Table 6.16.1.1 (Plate) Mean*		74.4

Stress Corrosion Cracking – Axial, smooth bar stress corrosion cracking tests were performed on 4 test specimens, representing two orientations (L and S). As stated previously, the specimens were loaded at a stress of 90 ksi (75% of the specification yield strength of 120 ksi) for 40 days in an alternate immersion 3.5% NaCl solution. No failures occurred during testing. After testing, specimens were rinsed in deionized water and visually inspected for evidence of corrosion damage. No evidence of pitting or other corrosion-related damage was indicated.

Ti-6Al-6V-2Sn Plate

Tension – The results of tensile testing are shown in Tables 7(a) through 7(d). Also included in these tables are results from a 2005 test program that involved this particular section of plate. Yield strength and ductility levels for all L-orientation specimens were above the specification minimum values shown in AMS-T-9046 (plate) for this alloy. It should be pointed out that there were specimens from this section of plate that did not meet specification minimum properties for ultimate tensile strength. Those values are highlighted in red in the tables. S-orientation specimens exhibited lower ductility and slightly lower elastic modulus than specimens from the L-orientation. Average elastic modulus values were within the range expected for this alloy. The maximum difference between those modulus results from ASTM E111 tests and those obtained from the E8 tensile test record was approximately 6.1%. In addition, there did not appear to be a difference between specimens excised from the three different thickness locations.

As this piece of material was properly processed plate, it would not be appropriate to combine the two orientations into one population. Also, since the alloy has specification minimum values, reasonable lower bound properties will not be calculated from the obtained data set. The data will be used to show compliance with the specification and will be used in further analyses for comparison with billet material.

It should be noted that the AMS-T-9046 specification does not list minimum properties for the short-transverse orientation, therefore the values shown at the bottom of Table 7(d) are for comparison only.

Table 7. Ti-6Al-6V-2Sn plate tensile test results.
(a) Longitudinal orientation, t/4 thickness location

	Orientation	Thickness Location	Yield Strength (ksi)	Ultimate Tensile Strength (ksi)	% Elongation	% Reduction of Area	Elastic Modulus, E111 (msi)	Elastic Modulus, E8 (msi)
1247-T-L-1-A	L	t/4	140.6	147.5	16.1%	28.7%	16.80	16.60
L-2-A	L	t/4	139.8	146.3	14.7%	23.7%		16.60
L-3-A	L	t/4	140.4	147.5	19.7%	27.8%		16.72
L-4-A	L	t/4	141.1	148.3	15.8%	27.4%		16.67
L-5-A	L	t/4	139.6	145.9	15.8%	30.1%		16.07
L-6-A	L	t/4	140.5	147.4	16.4%	26.5%		16.02
L-7-A	L	t/4	140.0	146.9	17.2%	22.6%		16.76
AMS-T-9046 (L) (2"-4" plate)			135	145	8%			16.0[a]

(a): Typical value per MMPDS-04

Approved for public release; distribution unlimited.

(b) Longitudinal orientation, t/2 thickness location

	Orientation	Thickness Location	Yield Strength (ksi)	Ultimate Tensile Strength (ksi)	% Elongation	% Reduction of Area	Elastic Modulus, E111 (msi)	Elastic Modulus, E8 (msi)
1247-T-L-1-B	L	t/2	141.3	149.5	15.4%	24.5%	17.14	16.10
L-2-B	L	t/2	140.6	148.2	15.5%	23.8%		16.49
L-3-B	L	t/2	140.3	148.2	15.7%	24.5%		15.50
L-4-B	L	t/2	140.5	148.1	16.4%	24.8%		15.40
L-5-B	L	t/2	139.9	147.6	17.2%	20.4%		16.40
L-6-B	L	t/2	140.1	148.1	16.7%	21.6%		16.90
L-7-B	L	t/2	139.5	146.8	15.8%	24.4%		16.90
1247TL1	L	t/2	138.8	144.9	17.8%			16.81
TL2	L	t/2	138.9	144.2	14.0%			16.75
TL3	L	t/2	140.5	146.7	15.2%			16.34
TL4	L	t/2	139.9	145.3	14.0%			16.08
TL5	L	t/2	140.5	147.1	15.3%			17.01
AMS-T-9046 (L) (2"-4" plate)			135	145	8%			16.0[a]

(a): Typical value per MMPDS-04

(c) Longitudinal orientation, 3t/4 thickness location

	Orientation	Thickness Location	Yield Strength (ksi)	Ultimate Tensile Strength (ksi)	% Elongation	% Reduction of Area	Elastic Modulus, E111 (msi)	Elastic Modulus, E8 (msi)
1247-T-L-1-C	L	3t/4	139.7	144.8	15.3%	27.9%	16.49	15.60
L-2-C	L	3t/4	138.6	144.1	14.5%	27.7%		16.50
L-3-C	L	3t/4	139.5	145.1	17.5%	29.1%		16.80
L-4-C	L	3t/4	139.1	144.3	15.2%	29.4%		15.30
L-5-C	L	3t/4	139.9	145.2	16.3%	29.5%		15.90
L-6-C	L	3t/4	139.3	144.9	15.1%	25.6%		15.70
L-7-C	L	3t/4	139.2	144.6	17.2%	28.6%		16.40
AMS-T-9046 (L) (2"-4" plate)			135	145	8%			16.0[a]

(a): Typical value per MMPDS-04

Approved for public release; distribution unlimited.

(d) Short-transverse orientation, t/2 thickness location

	Orientation	Thickness Location	Yield Strength (ksi)	Ultimate Tensile Strength (ksi)	% Elongation	% Reduction of Area	Elastic Modulus, E111 (msi)	Elastic Modulus, E8 (msi)
1247-T-S-1-A	S	t/2	140.0	150.3	12.0%	20.6%	15.8	15.70
S-2-A	S	t/2	140.3	150.7	11.9%	17.2%		14.99
S-3-A	S	t/2	140.6	151.3	12.5%	21.7%		15.70
S-4-A	S	t/2	138.9	148.9	12.3%	21.4%		16.50
S-5-A	S	t/2	139.2	148.8	9.4%	17.1%		15.46
S-6-A	S	t/2	139.3	149.7	11.3%	16.9%		16.00
S-7-A	S	t/2	139.1	148.8	9.6%	16.1%		14.80
S-8-A	S	t/2	139.8	149.3	11.8%	19.2%		16.80
S-9-A	S	t/2	139.8	149.4	10.8%	19.7%		15.30
1247TS1	S	t/2	139.4	147.5	10.7%			15.80
TS2	S	t/2	137.5	147.5	10.1%			18.95
TS3	S	t/2	139.2	147.4	11.7%			15.93
TS4	S	t/2	138.6	146.4	11.3%			15.80
TS5	S	t/2	138.6	147.2	9.8%			17.09
TS6	S	t/2	140.1	148.1	9.2%			15.59
TS7	S	t/2	139.8	147.9	9.0%			16.00
TS8	S	t/2	140.0	148.1	9.8%			15.84
TS9	S	t/2	140.8	148.7	9.1%			15.75
AMS-T-9046 (L) (2"-4" plate)			135	145	8%			16.0[a]

(a): Typical value per MMPDS-04

Approved for public release; distribution unlimited.

Fatigue (force-controlled) – The results of force-controlled axial fatigue testing are shown graphically in Figure 12. Individual results are tabulated in Table 8. In Figure 8, the results for each stress ratio (R) have been fit with a best-fit power-law curve for graphical purposes only. Also included in this figure is a curve based on an equivalent stress equation from MMPDS Figure 5.4.2.1.8(a). As stated in Figure 4, the fatigue specimens used herein were manufactured using low-stress grinding operations to a surface finish (Ra) of 8 per the ASTM E466 standard. The MMPDS reference data curve was generated from specimens having a surface roughness of 32. Furthermore, it is not known whether low-stress grinding was used on these specimens. Also, the reference data that produced the equivalent stress equation in MMPDS was generated using 1.5 inch thick plate, which has higher specification minimum tensile values of 150 ksi (ultimate tensile strength) and 140 ksi (tensile yield strength). These aspects could have contributed to the difference between the data sets.

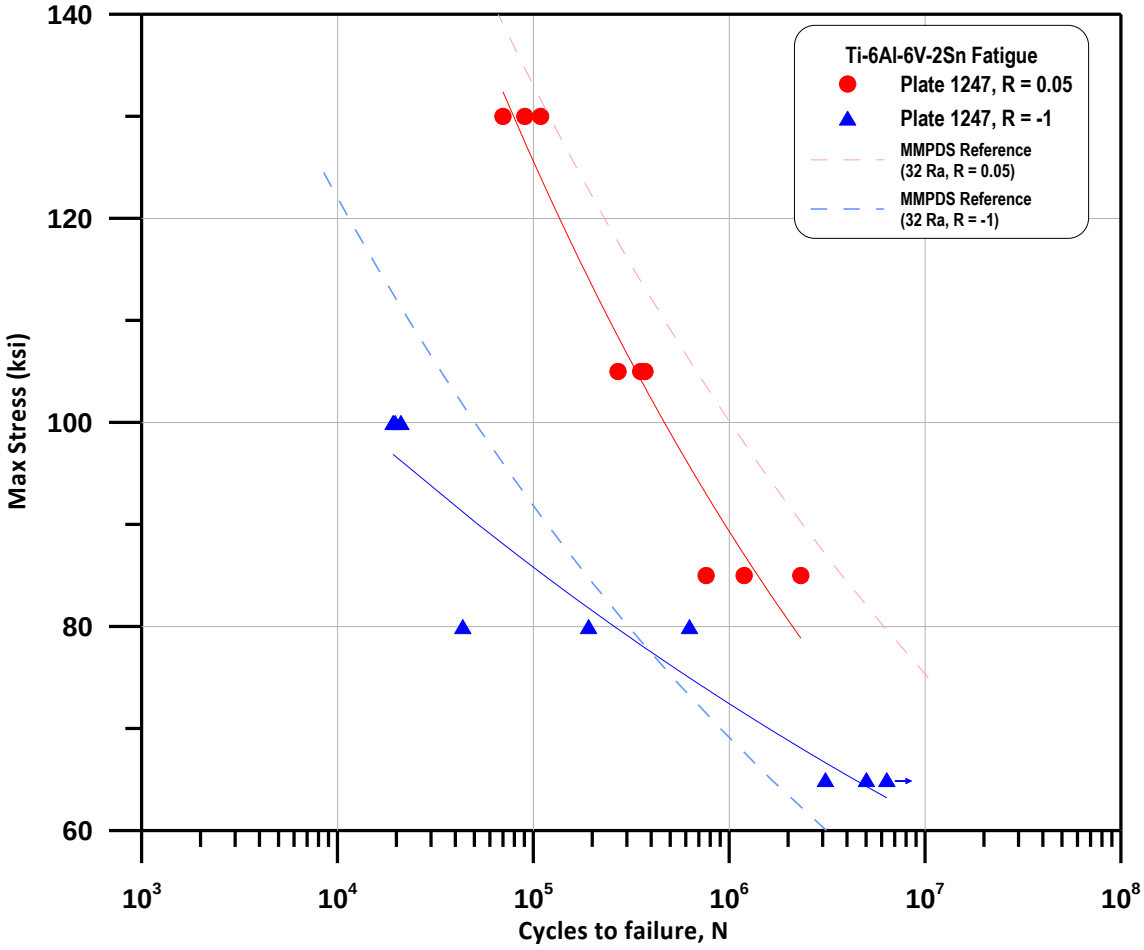


Figure 12. Ti-6Al-6V-2Sn plate force-controlled axial fatigue test results.

Approved for public release; distribution unlimited.

Table 8. Ti-6Al-6V-2Sn plate force-controlled axial fatigue test results.

	Thickness Location	Max Stress (ksi)	Stress Ratio, R	Cycles to Failure
1247-F-L-10-A	t/4	130	0.05	108,890
L-12-B	t/2	130	0.05	69,910
L-12-C	3t/4	130	0.05	90,400
L-11-A	t/4	105	0.05	270,390
L-10-B	t/2	105	0.05	370,510
L-10-C	3t/4	105	0.05	352,810
L-12-A	t/4	85	0.05	1,191,750
L-11-B	t/2	85	0.05	761,770
L-11-C	3t/4	85	0.05	2,318,800
1247-F-L-8-A	t/4	100	-1	19,202
L-3-B	t/2	100	-1	21,057
L-4-C	3t/4	100	-1	19,681
L-5-A	t/4	80	-1	43,572
L-6-B	t/2	80	-1	191,278
L-1-C	3t/4	80	-1	626,054
L-2-A	t/4	65	-1	3,098,503
L-9-B	t/2	65	-1	5,009,816
L-7-C	3t/4	65	-1	>6,000,000*

**: indicates run-out*

Fatigue (strain-controlled) – The results of strain-controlled axial fatigue testing are shown graphically in Figure 13, with individual results tabulated in Table 9. Due to material limitations, only longitudinal specimens were tested.

Approved for public release; distribution unlimited.

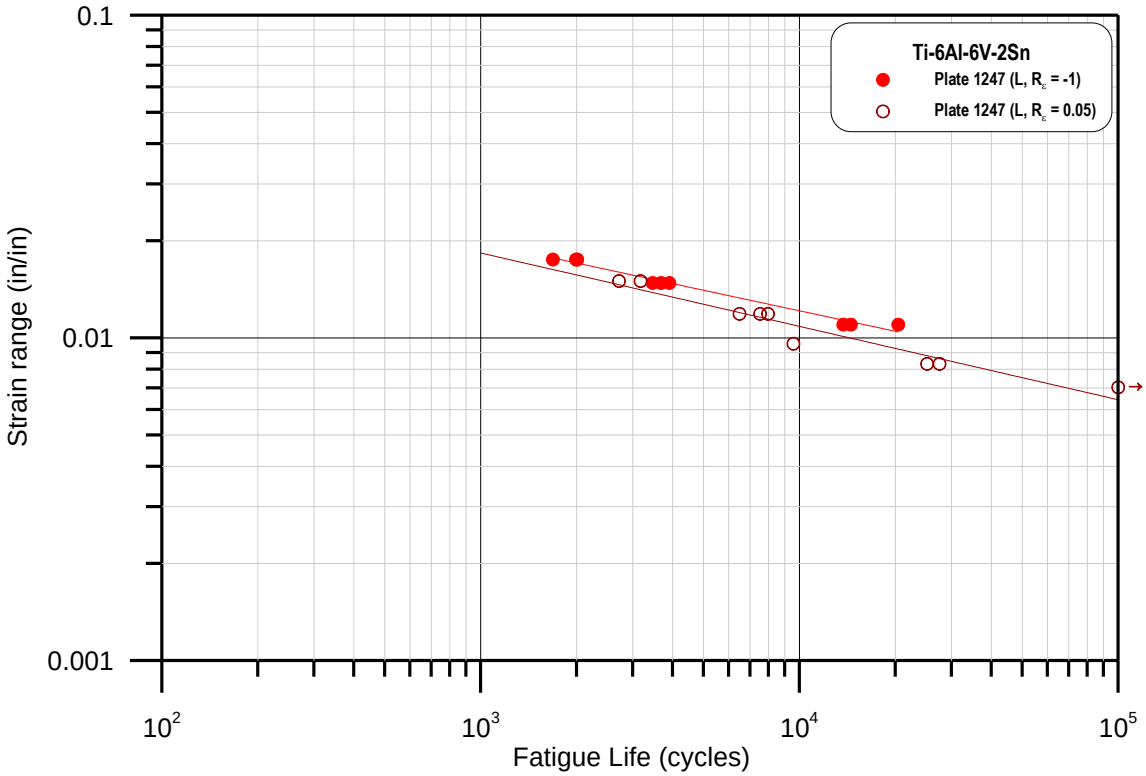


Figure 13. Ti-6Al-6V-2Sn plate strain-controlled axial fatigue test results.

Table 9. Ti-6Al-6V-2Sn plate strain-controlled axial fatigue test results.

	Thickness Location	Orientation	Strain Range (in/in)	Strain Ratio, R_ε	Cycles to Failure
1247-F-L-2-B	t/2	L	0.0175	-1	1,684
F-L-4-A	t/4	L	0.0175	-1	2,009
F-L-9-C	3t/4	L	0.0175	-1	1,990
F-L-3-C	3t/4	L	0.0148	-1	3,910
F-L-7-A	t/4	L	0.0148	-1	3,462
F-L-8-B	t/2	L	0.0148	-1	3,682
F-L-1-A	t/4	L	0.0110	-1	13,727
F-L-5-B	t/2	L	0.0110	-1	20,417
F-L-6-C	3t/4	L	0.0110	-1	14,511
1247-F-L-4-B	t/2	L	0.0150	0.05	3,172
F-L-6-A	t/4	L	0.0150	0.05	2,716
F-L-1-B	t/2	L	0.0119	0.05	6,489
F-L-8-C	3t/4	L	0.0119	0.05	7,526
F-L-9-A	t/4	L	0.0119	0.05	7,972
F-L-3-A	t/4	L	0.0096	0.05	9,576
F-L-2-C	3t/4	L	0.0083	0.05	25,157
F-L-7-B	t/2	L	0.0083	0.05	27,499
F-L-5-C	3t/4	L	0.0070	0.05	100,000

Approved for public release; distribution unlimited.

Fatigue Crack Growth Rate – Fatigue crack growth rate test result summary curves are shown in Figures 14 and 15 for stress ratios (R) of 0.1 and 0.7, respectively. Individual specimen curves are located in Appendix B of this report. For both stress ratios, the S-L orientation specimens tended to have faster growth rates than the L-T specimens. Fractographic and metallographic examinations of the failed specimens will be performed to investigate possible reasons for this difference in growth rates.

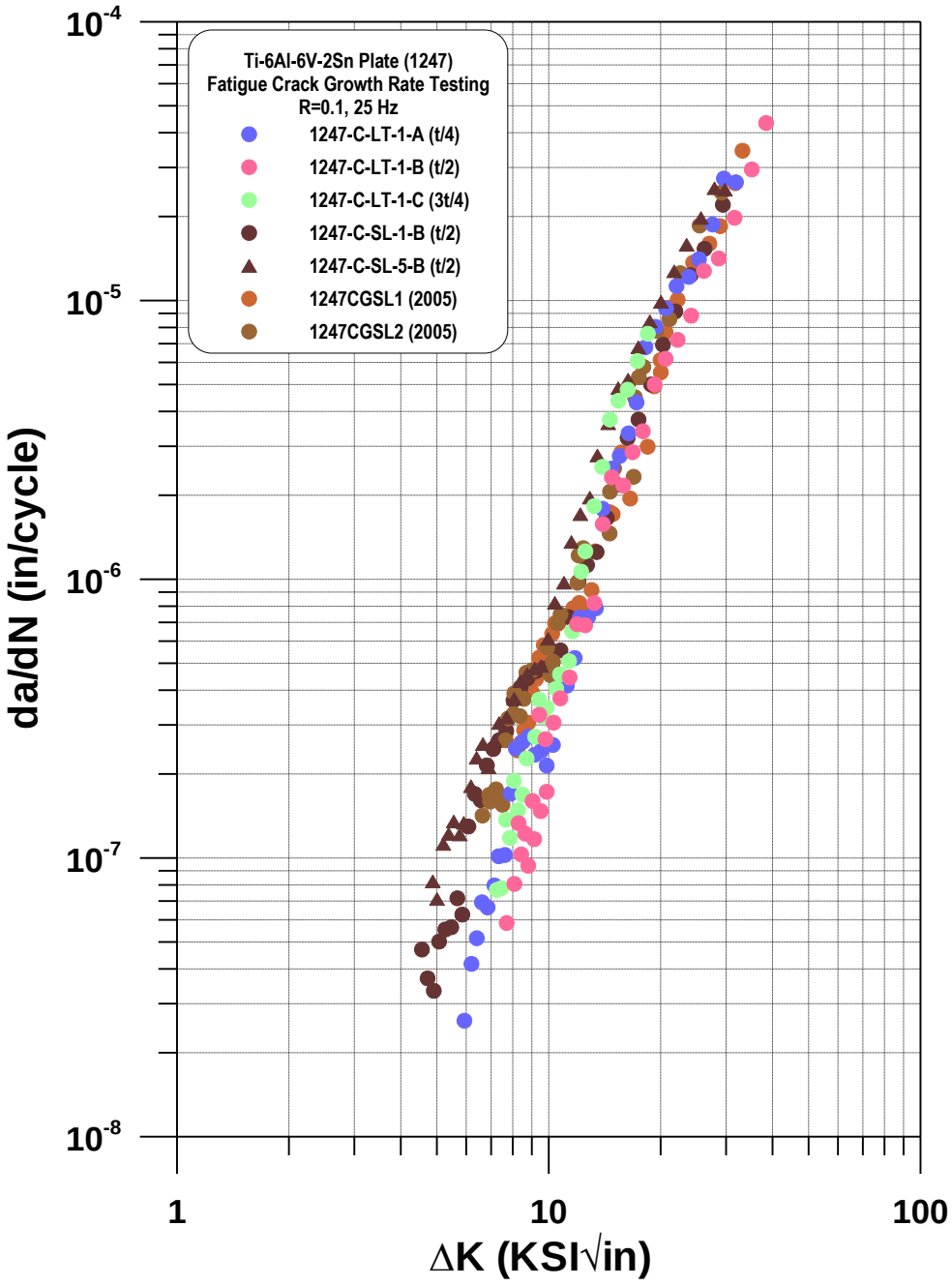


Figure 14. Ti-6Al-6V-2Sn plate fatigue crack growth rate test results (R=0.1).

Approved for public release; distribution unlimited.

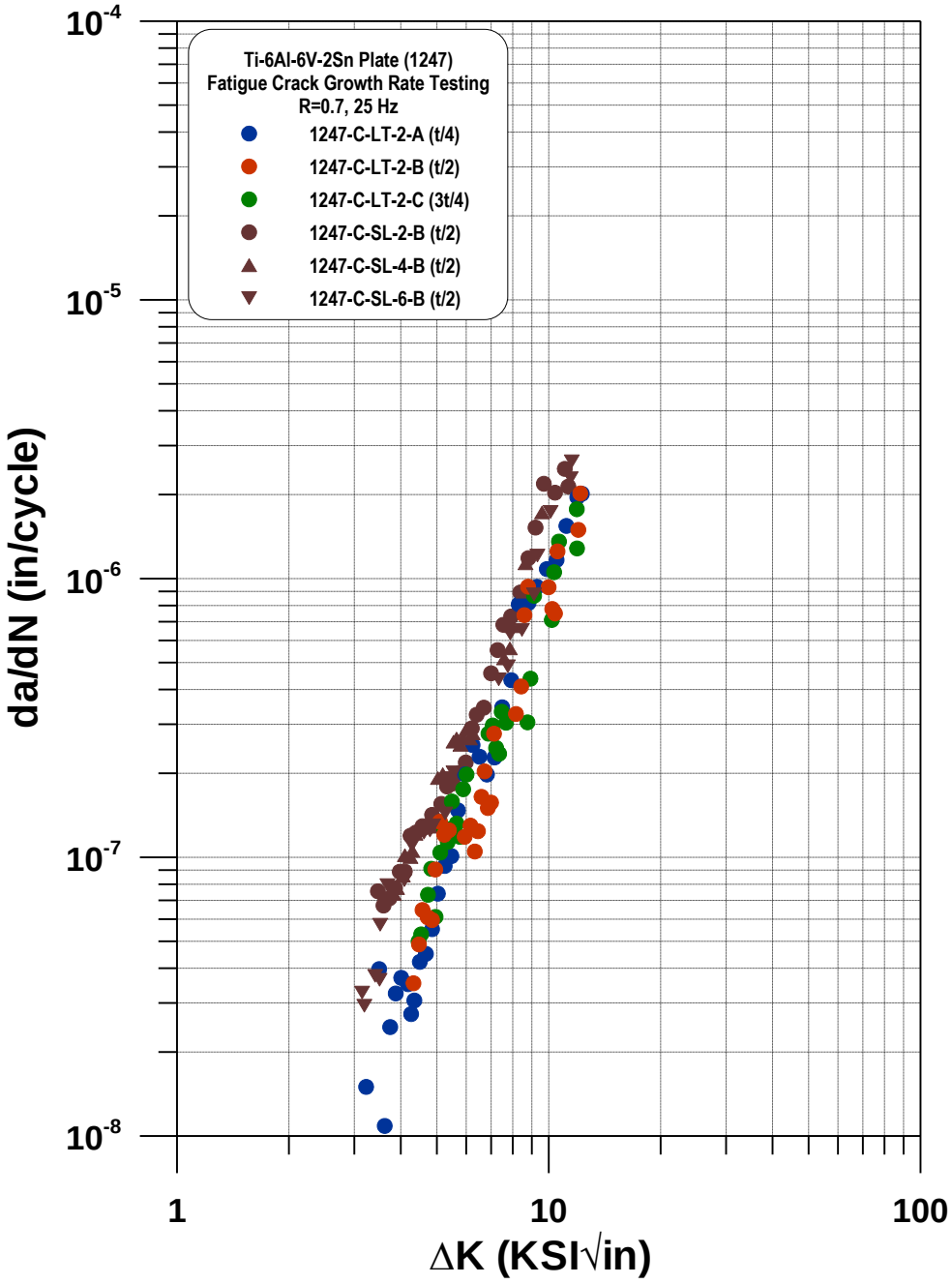


Figure 15. Ti-6Al-6V-2Sn plate fatigue crack growth rate test results (R=0.7).

Approved for public release; distribution unlimited.

Fracture Toughness – Plane-strain fracture toughness test results are shown in Table 10. For this investigation, only the L-T orientation was tested. Due to material limitations, only two specimens were tested. Of these two, one specimen had an invalid result, having failed the "$P_{max}/P_q < 1.1$" validity check, and has been included in the table as a K_q value for reference purposes only.

Table 10. Ti-6Al-6V-2Sn plate fracture toughness test results.

	Thickness Location	K_{Ic} (ksi√in)
1247-K-LT-1-A	t/4	55.7
LT-1-C	3t/4	53.9*

**: Kq value.*

Stress Corrosion Cracking – Axial, smooth bar stress corrosion cracking tests were performed on 6 test specimens, representing two orientations (L and S). As stated previously, the specimens were loaded at a stress of 101.3 ksi (75% of the specification yield strength of 135 ksi) for 40 days in an alternate immersion 3.5% NaCl solution. No failures occurred during testing. After testing, specimens were rinsed in deionized water and visually inspected for evidence of corrosion damage. No evidence of pitting or other corrosion-related damage was indicated.

Approved for public release; distribution unlimited.

CONCLUSIONS AND RECOMMENDATIONS

As this report dealt with mechanical properties from only one lot each of Ti-6Al-4V plate and Ti-6Al-6V-2Sn plate, no specific conclusions or recommendations will be made, other than comparisons to material specifications or available reference data. Had the goal of this program been to develop statistically significant datasets, a larger population of data would have been required that represented multiple heats and lots of material. With the exception of some ultimate tensile strength results for the Ti-6Al-6V-2Sn plate, the materials were generally equivalent to the reference data noted throughout the report.

It is recommended that A- and B-basis MMPDS design allowables be developed for the Ti-6Al-6V-2Sn alloy in the plate product form. Currently, these allowables do not exist. Although the majority of the strength results for this alloy met or exceeded the specification minimum values, the author believes that the material specifications may not provide sufficient coverage for the statistical lower bounds of the population of recent production heats and lots.

REFERENCES

3. *Metallic Materials Properties Development and Standardization (MMPDS)*, MMPDS-04; April 2008; Federal Aviation Administration.
4. *Damage Tolerant Design Handbook: A Compilation of Fracture and Crack Growth Data for High Strength Alloys*; Compiled by D.A. Skinn, J.P. Gallagher, A.P. Berens, P.D. Huber, J. Smith; University of Dayton Research Institute, May 1994.

ACKNOWLEDGEMENTS

The author wishes to thank Mssrs. John Ruschau, Nick Jacobs, Don Woleslagle, Eric Soppe, Cris Williams, Ron Glett, Ms. Pat Youngerman, and Ms. Sarah Kuhlman, all of the University of Dayton Research Institute (UDRI); Mssrs. Dan Laufersweiler, Ed Porter, and Dave Roberts of Universal Technology Corporation (UTC); and Mssrs. Keith Vehorn and Nick Blommel of AFRL/RXSCE for their engineering and technical support of this program. Acknowledgement is also given to Westmoreland Mechanical Testing & Research, Inc. for the machining of all of the test specimens.

PREPARED BY

SIGNED

_____

STEVEN R. THOMPSON, Senior Materials Engineer
Materials Test & Evaluation Team
Acquisition Systems Support Branch
Systems Support Division
Manufacturing and Manufacturing Directorate

REVIEWED BY

SIGNED

_____

NEAL R. ONTKO, Team Lead
Materials Test & Evaluation Team
Acquisition Systems Support Branch
Systems Support Division
Manufacturing and Manufacturing Directorate

PUBLICATION REVIEW: This report has been reviewed and approved.

SIGNED

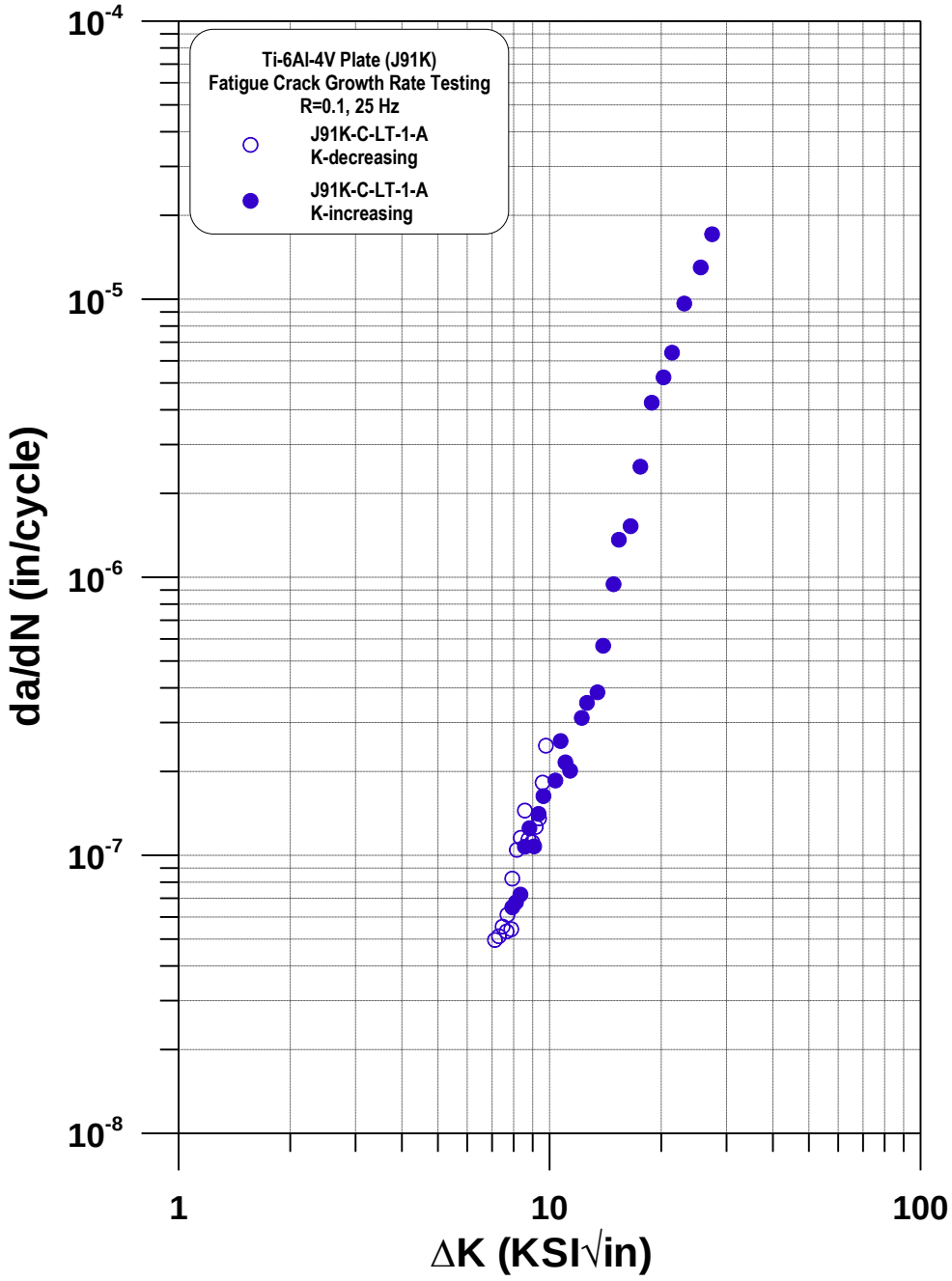
_____

CHARLES E. WAGNER, Chief
Acquisition Systems Support Branch
Systems Support Division
Manufacturing and Manufacturing Directorate

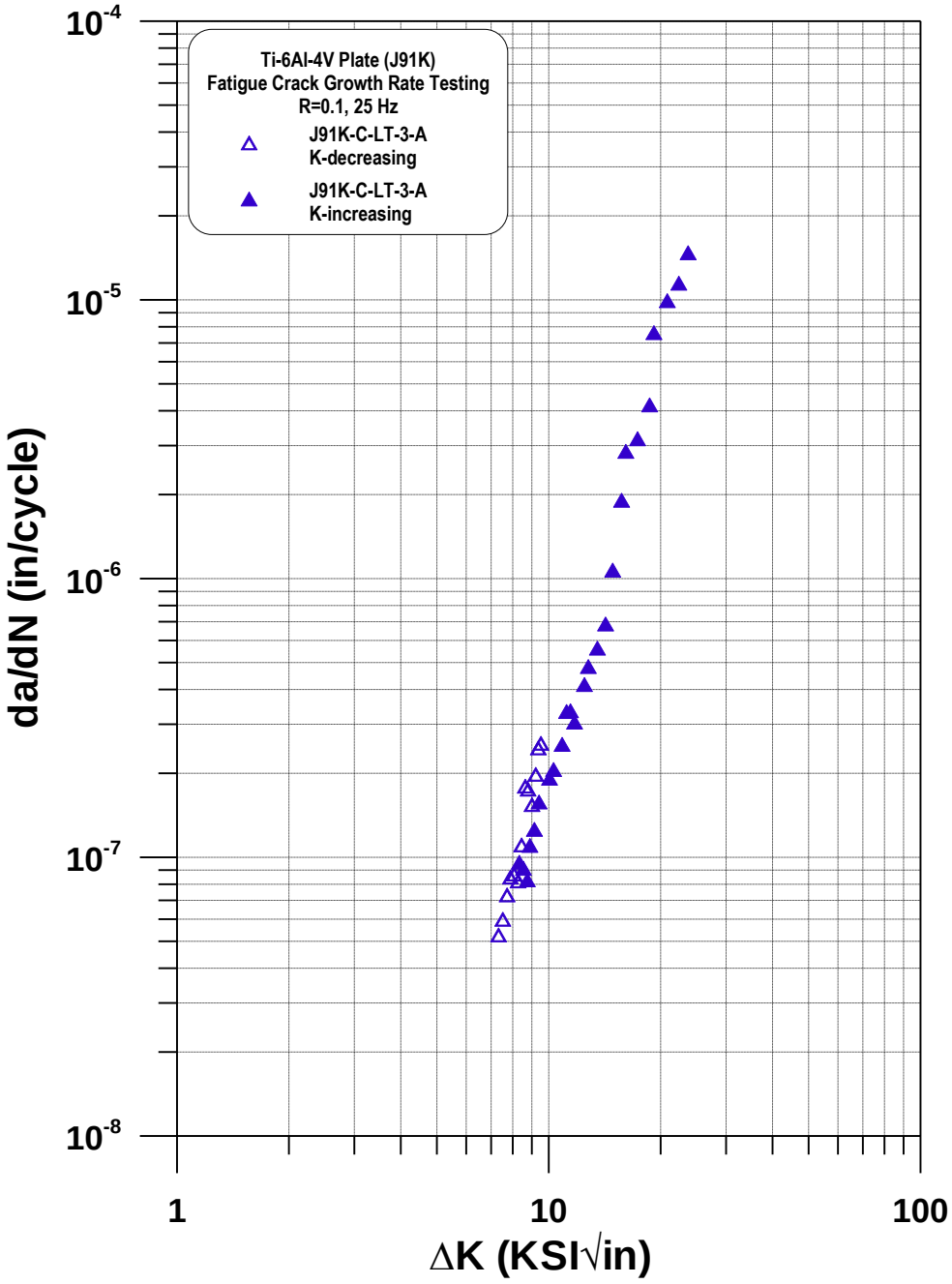
Approved for public release; distribution unlimited.

Appendix A
Individual fatigue crack growth rate curves for Ti-6Al-4V plate (J91K).

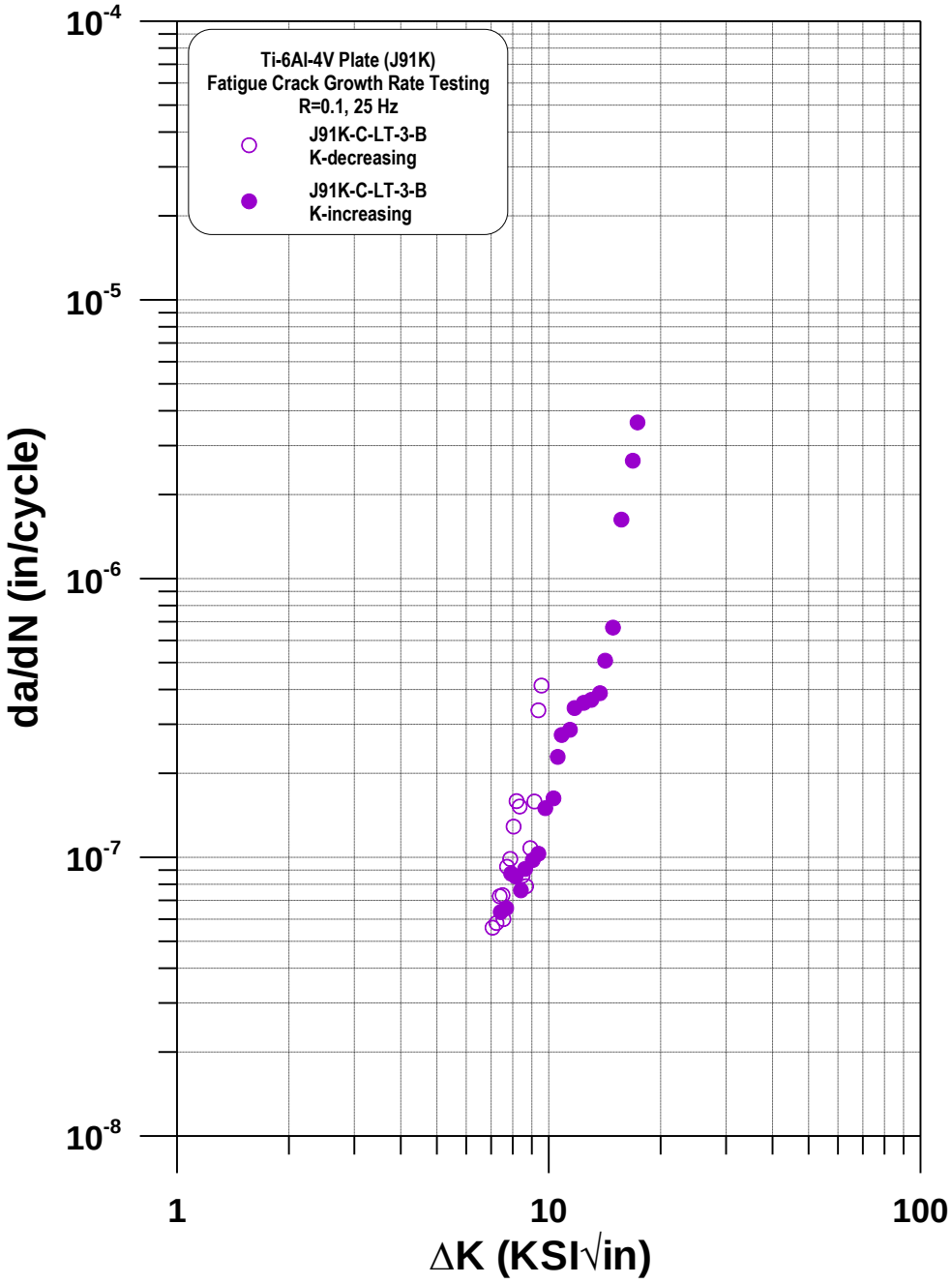
Approved for public release; distribution unlimited.



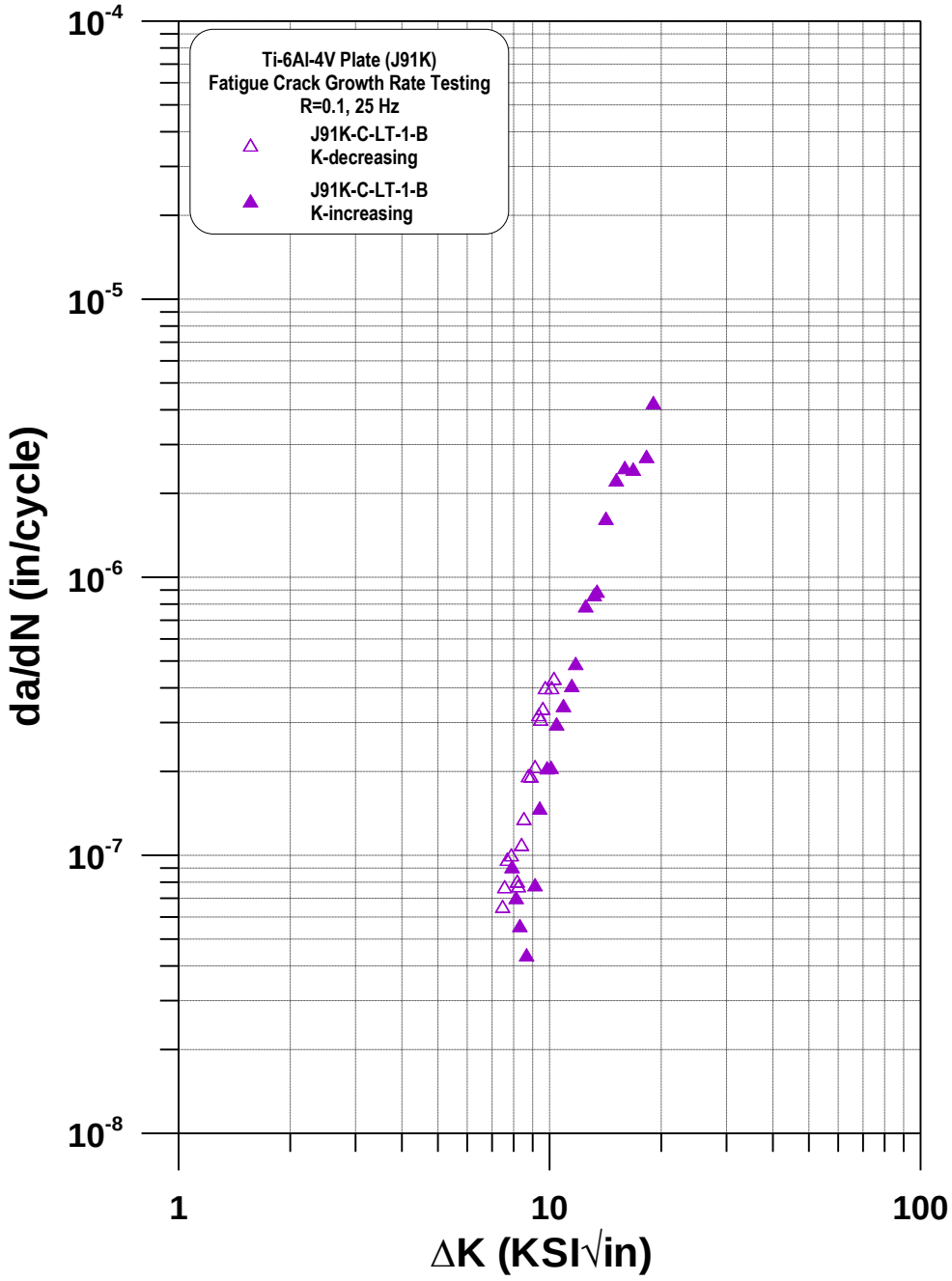
Approved for public release; distribution unlimited.



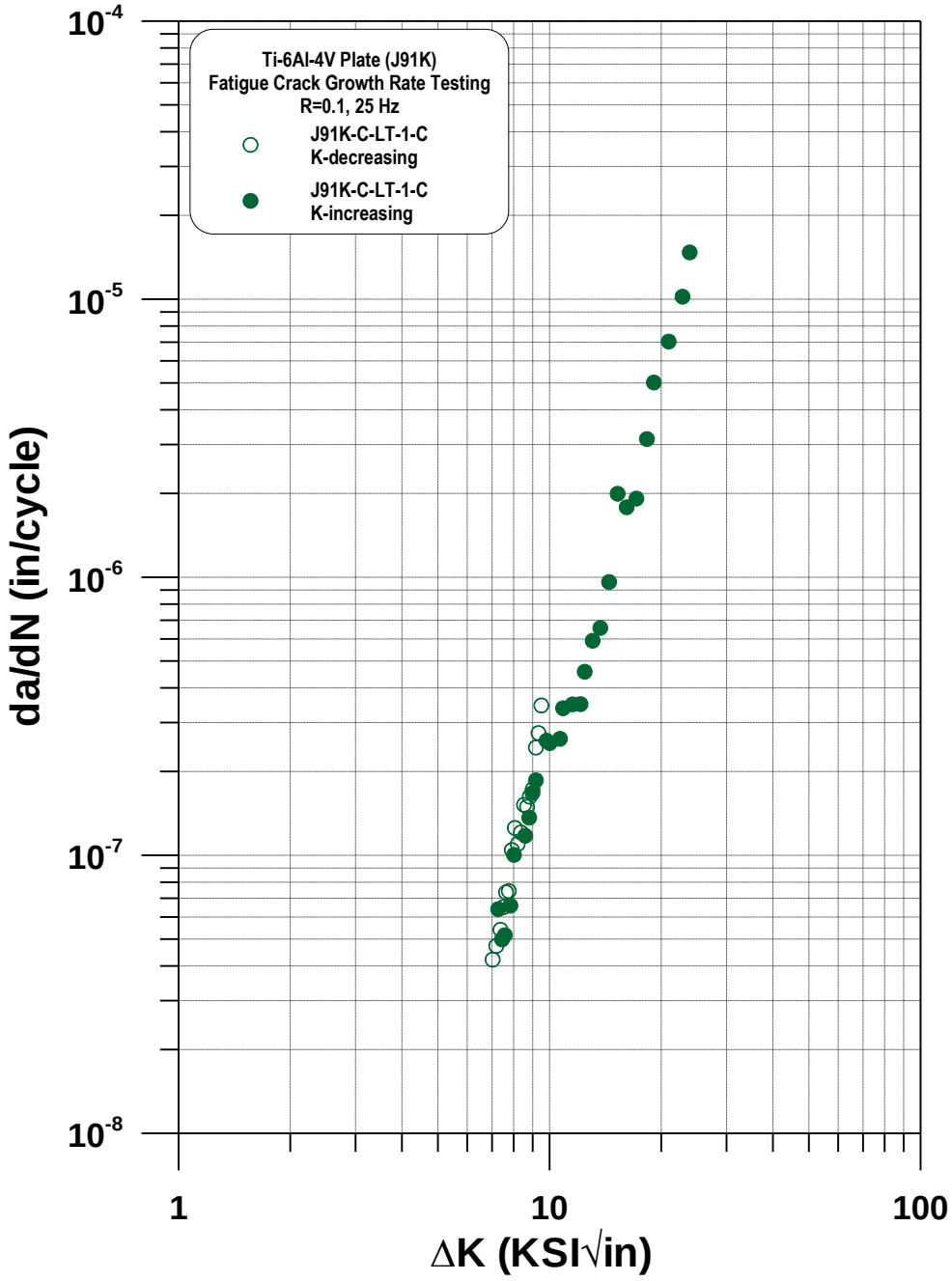
Approved for public release; distribution unlimited.



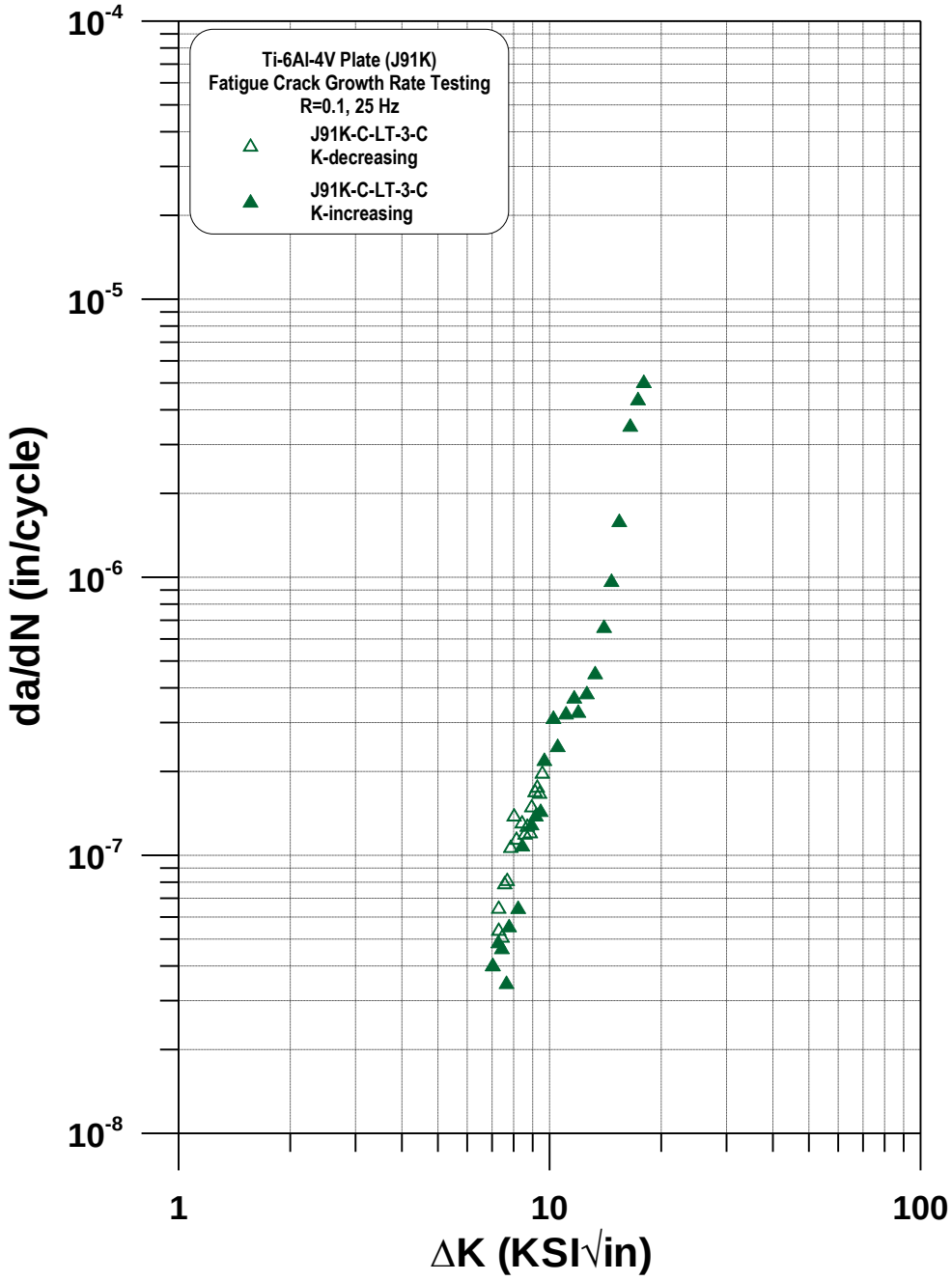
Approved for public release; distribution unlimited.



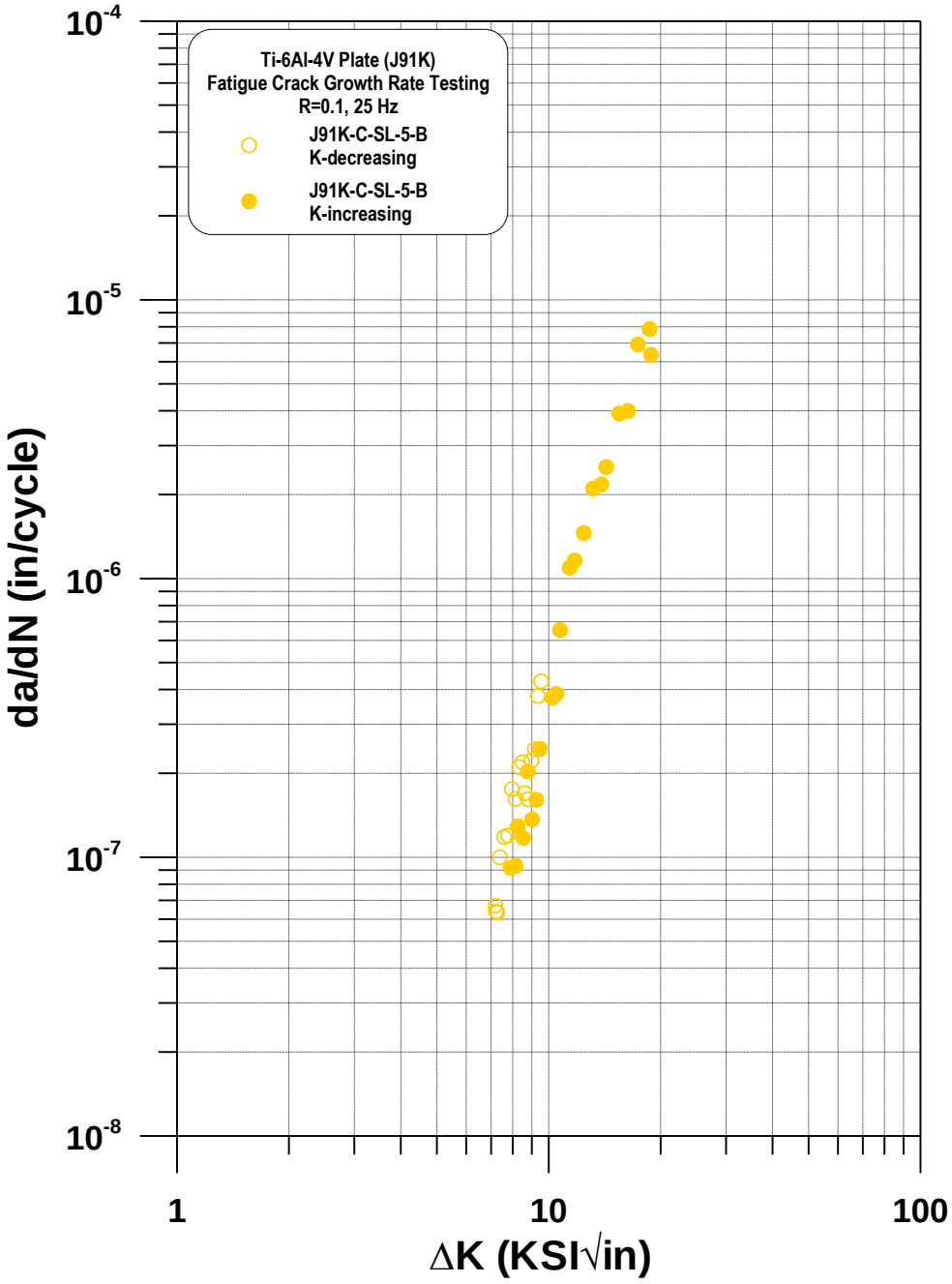
Approved for public release; distribution unlimited.



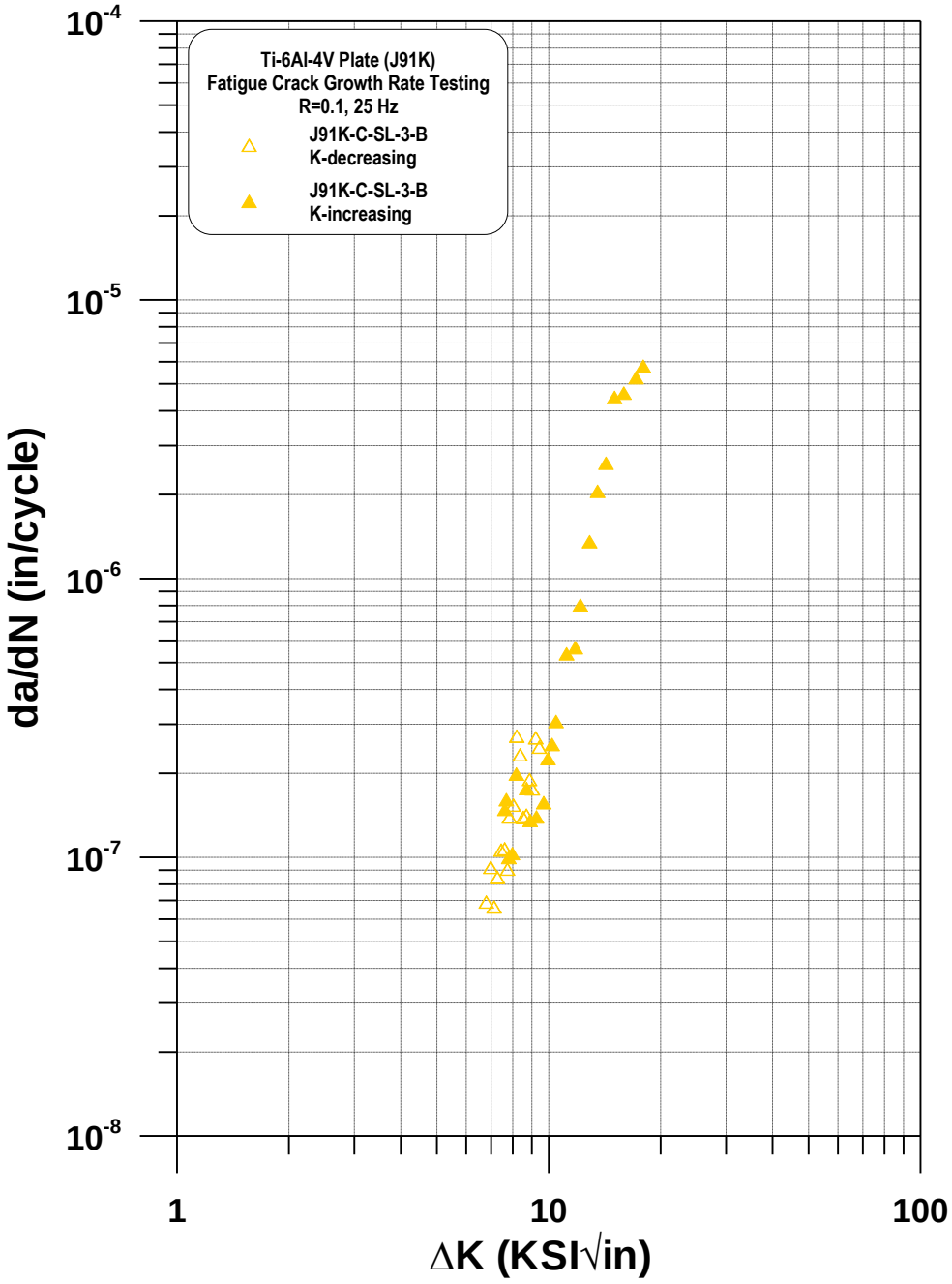
Approved for public release; distribution unlimited.



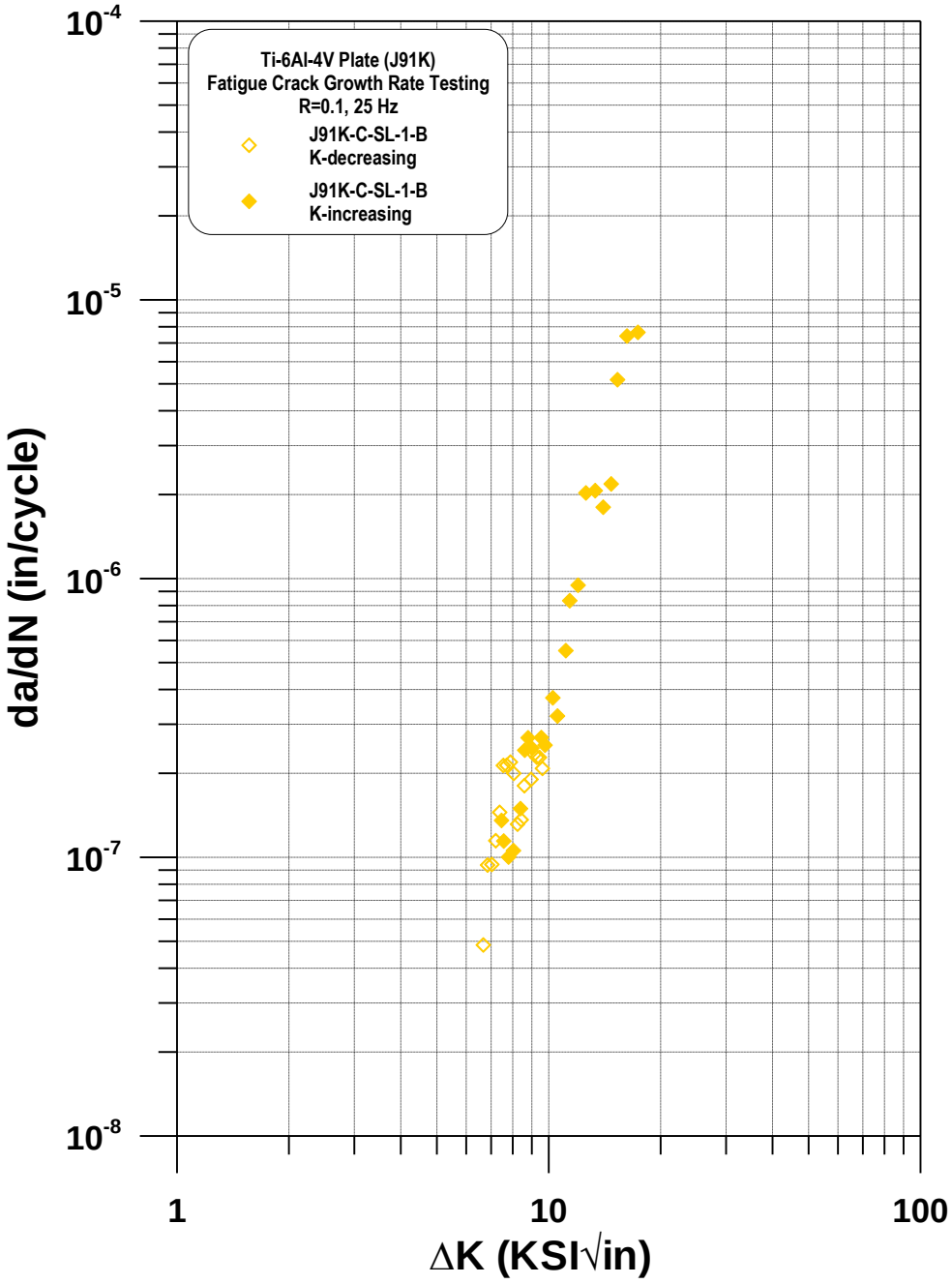
Approved for public release; distribution unlimited.



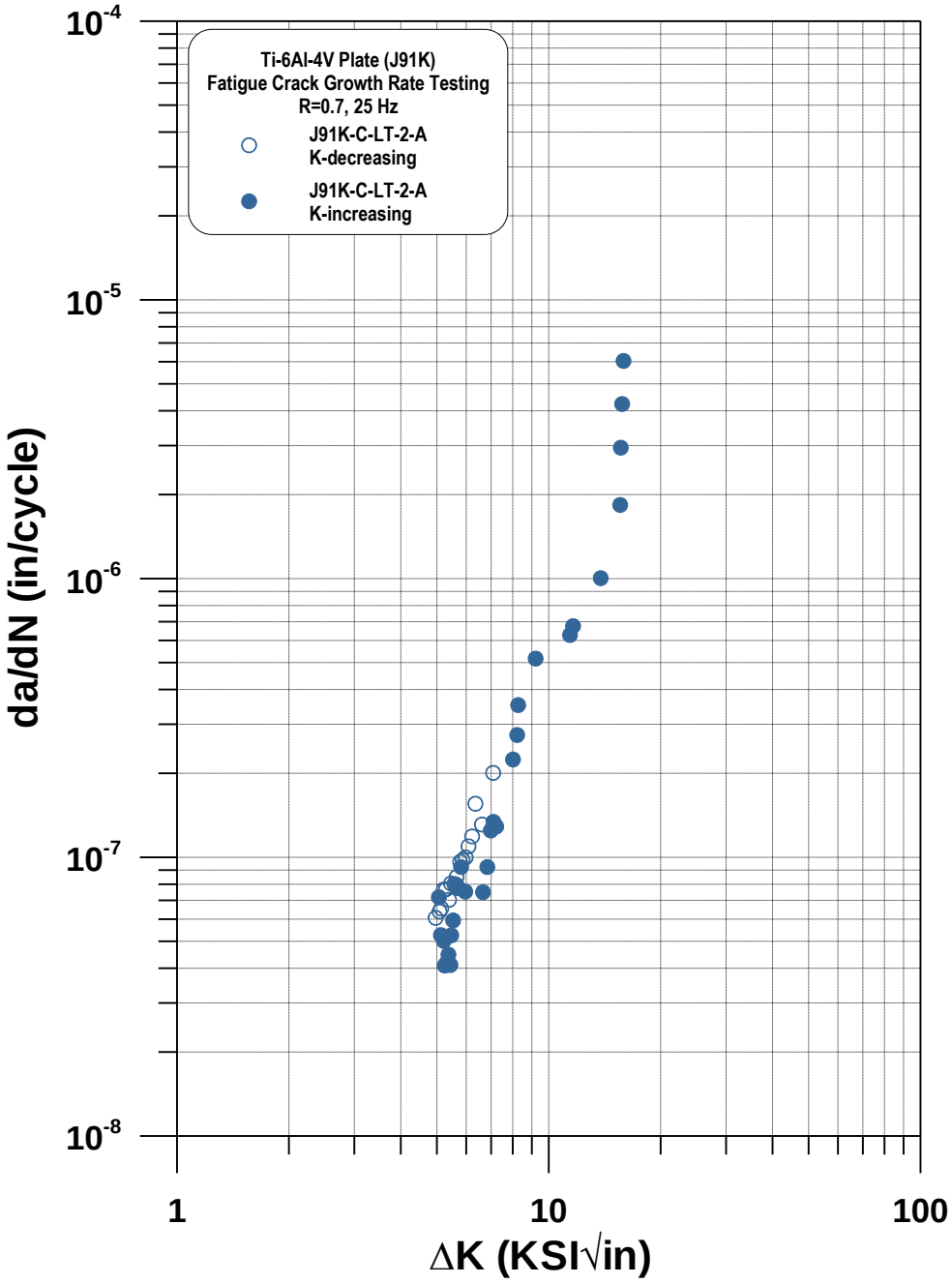
Approved for public release; distribution unlimited.



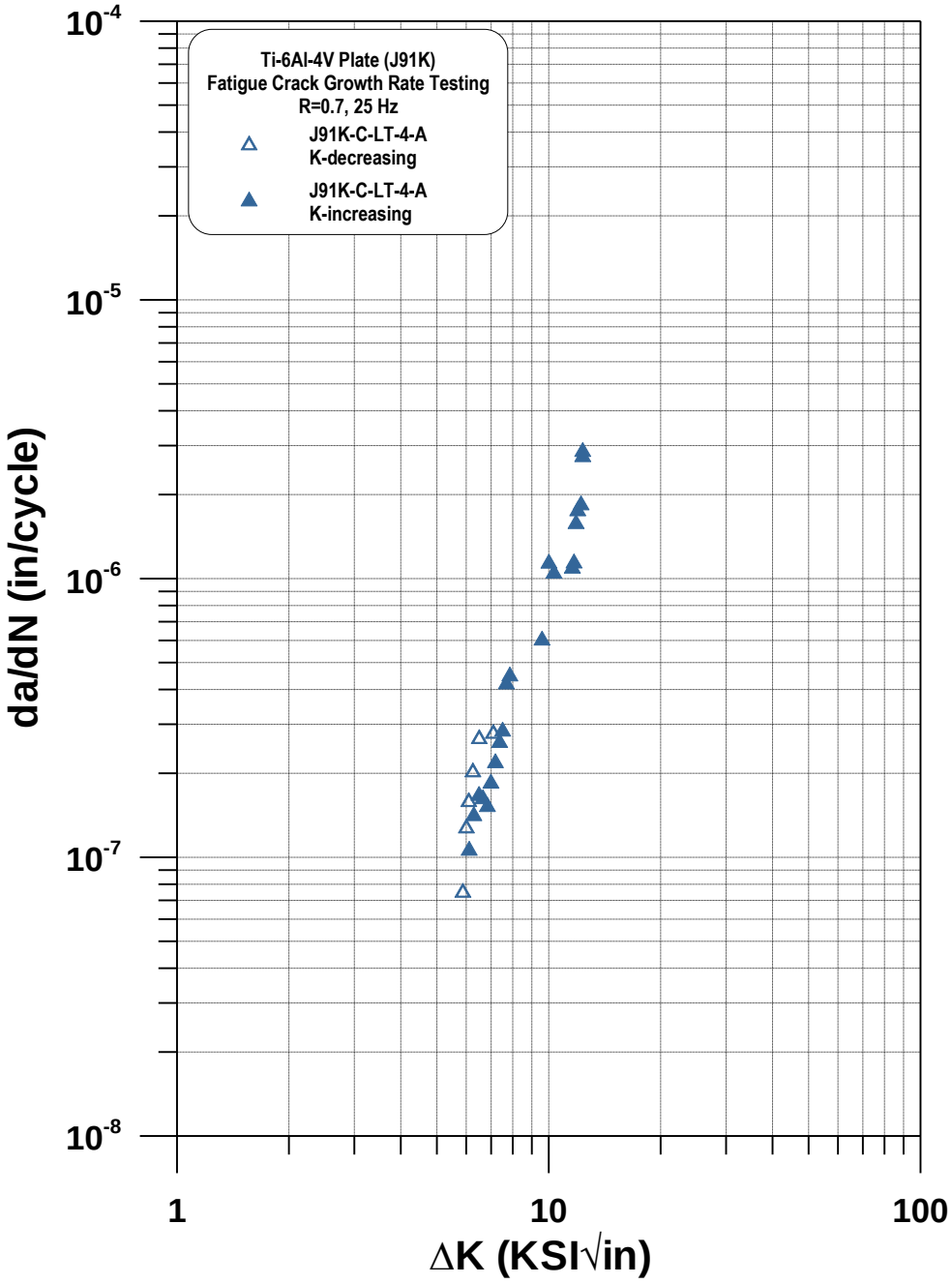
Approved for public release; distribution unlimited.



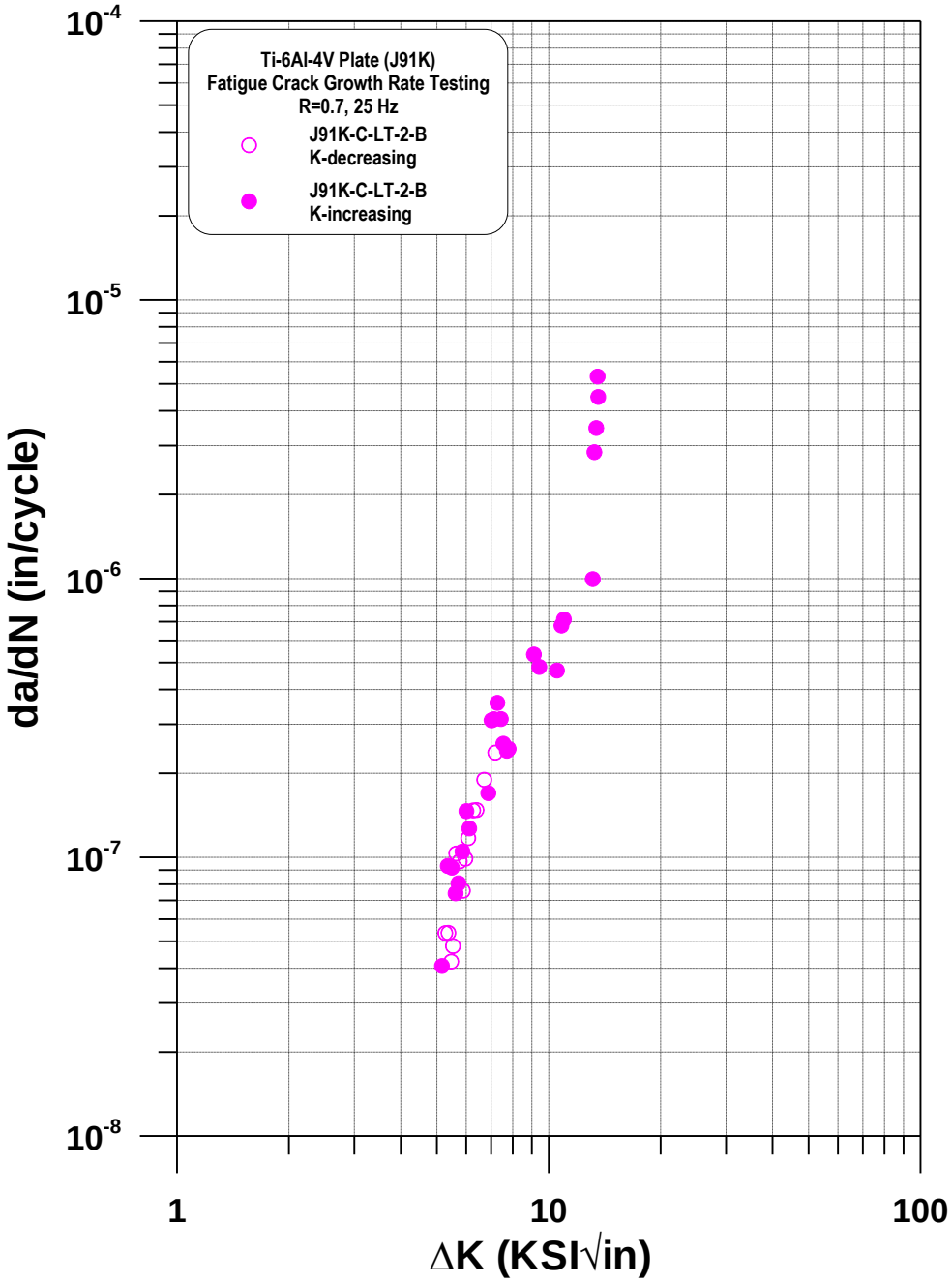
Approved for public release; distribution unlimited.



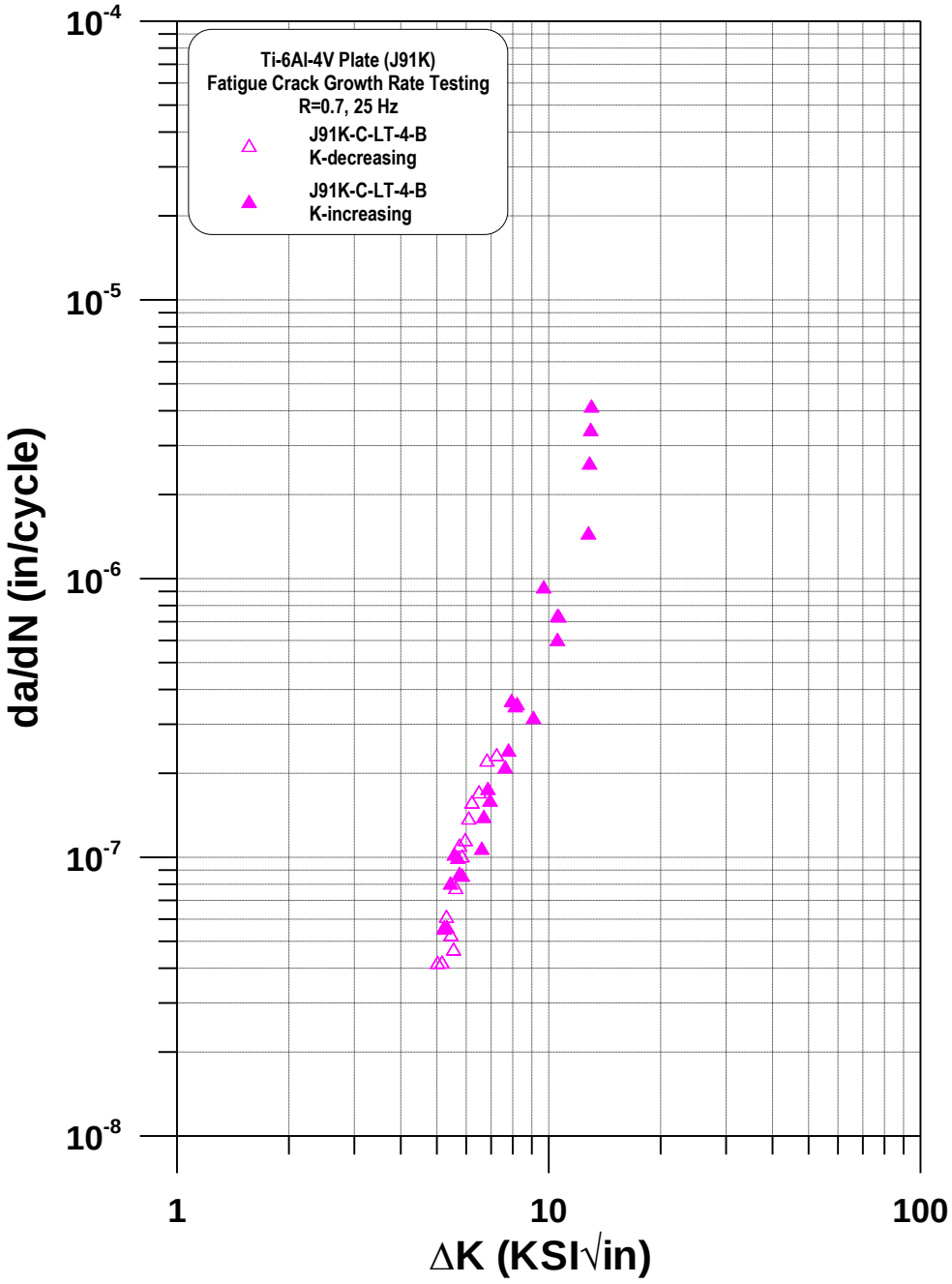
Approved for public release; distribution unlimited.



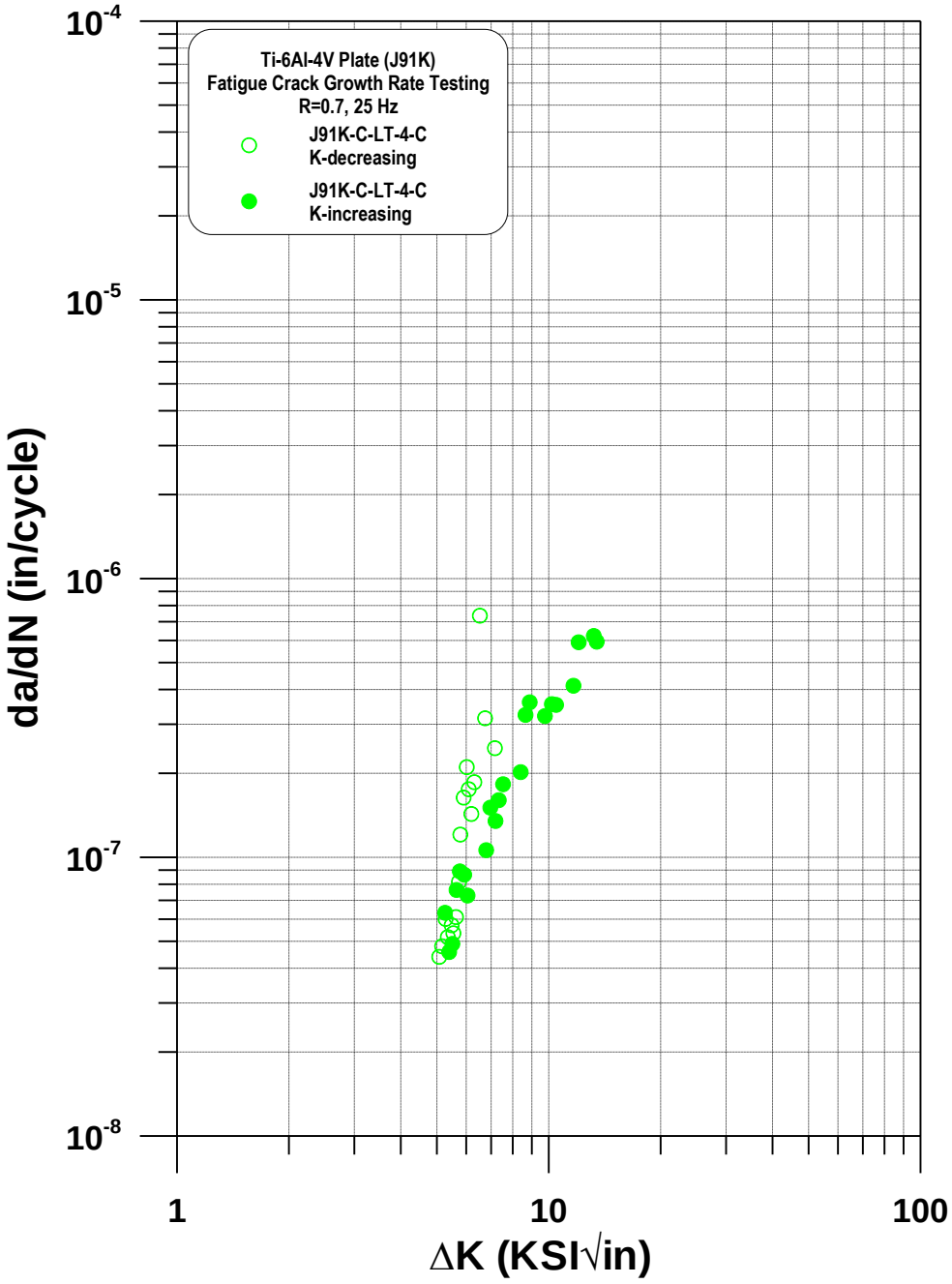
Approved for public release; distribution unlimited.



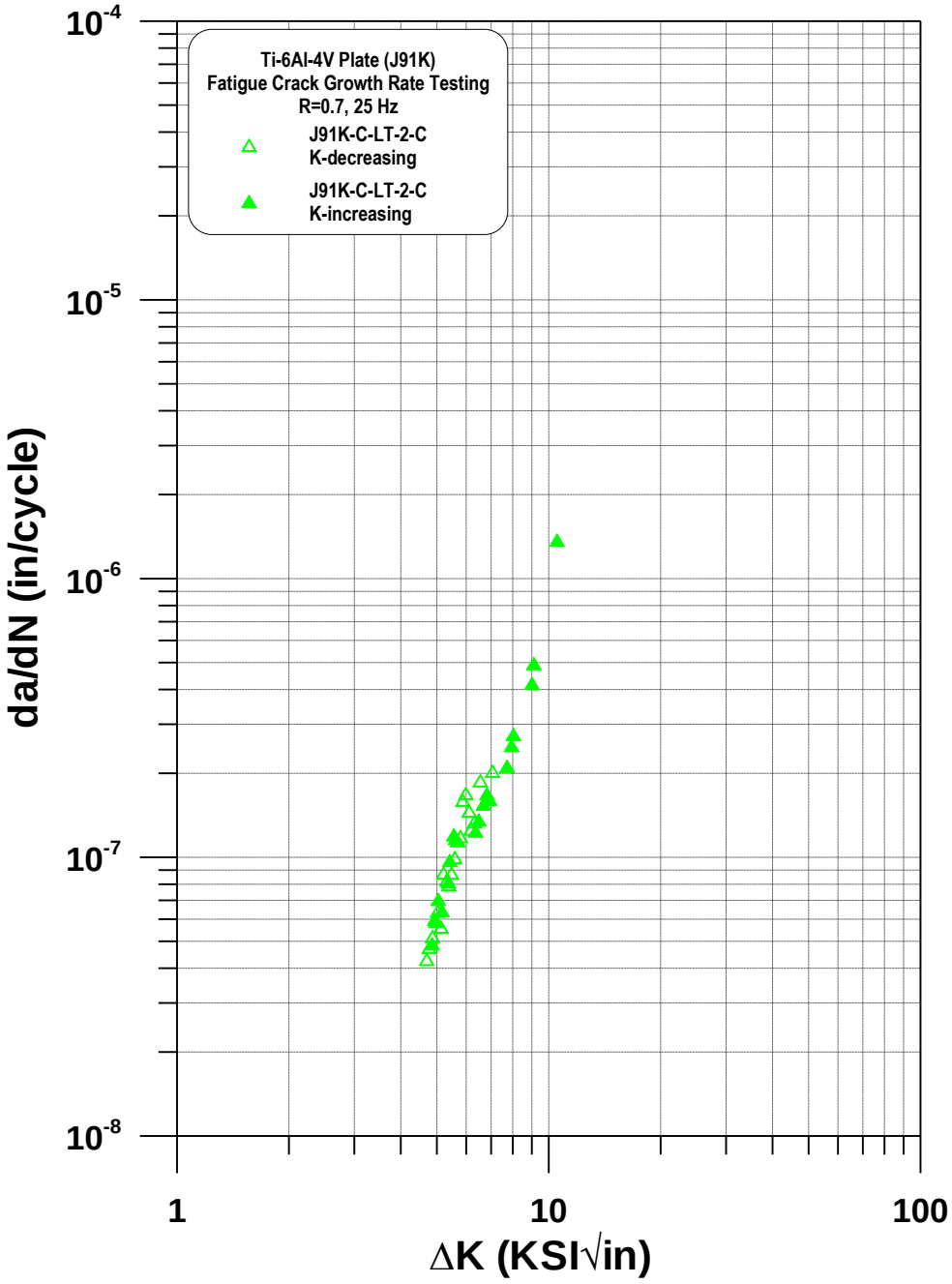
Approved for public release; distribution unlimited.



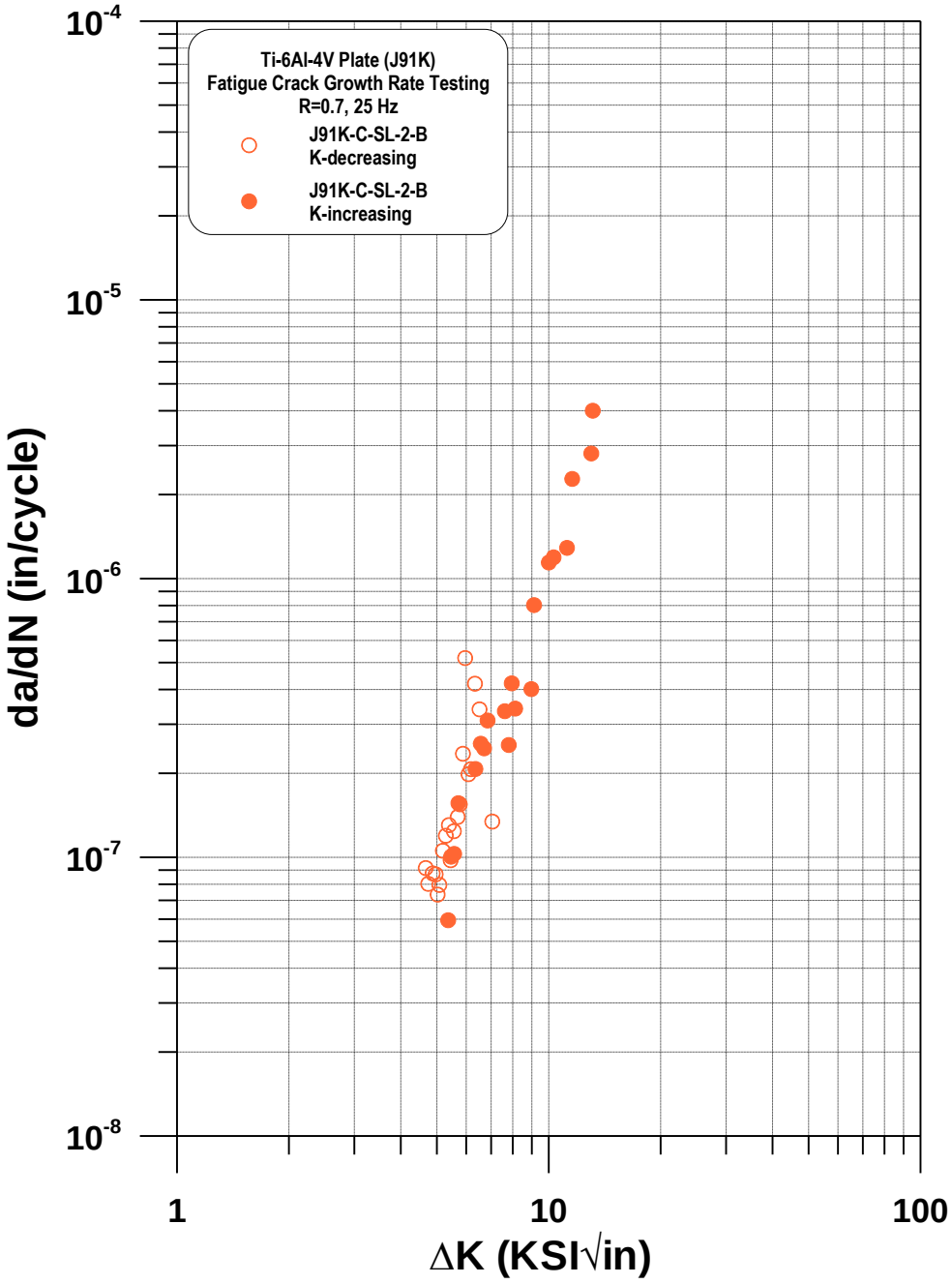
Approved for public release; distribution unlimited.



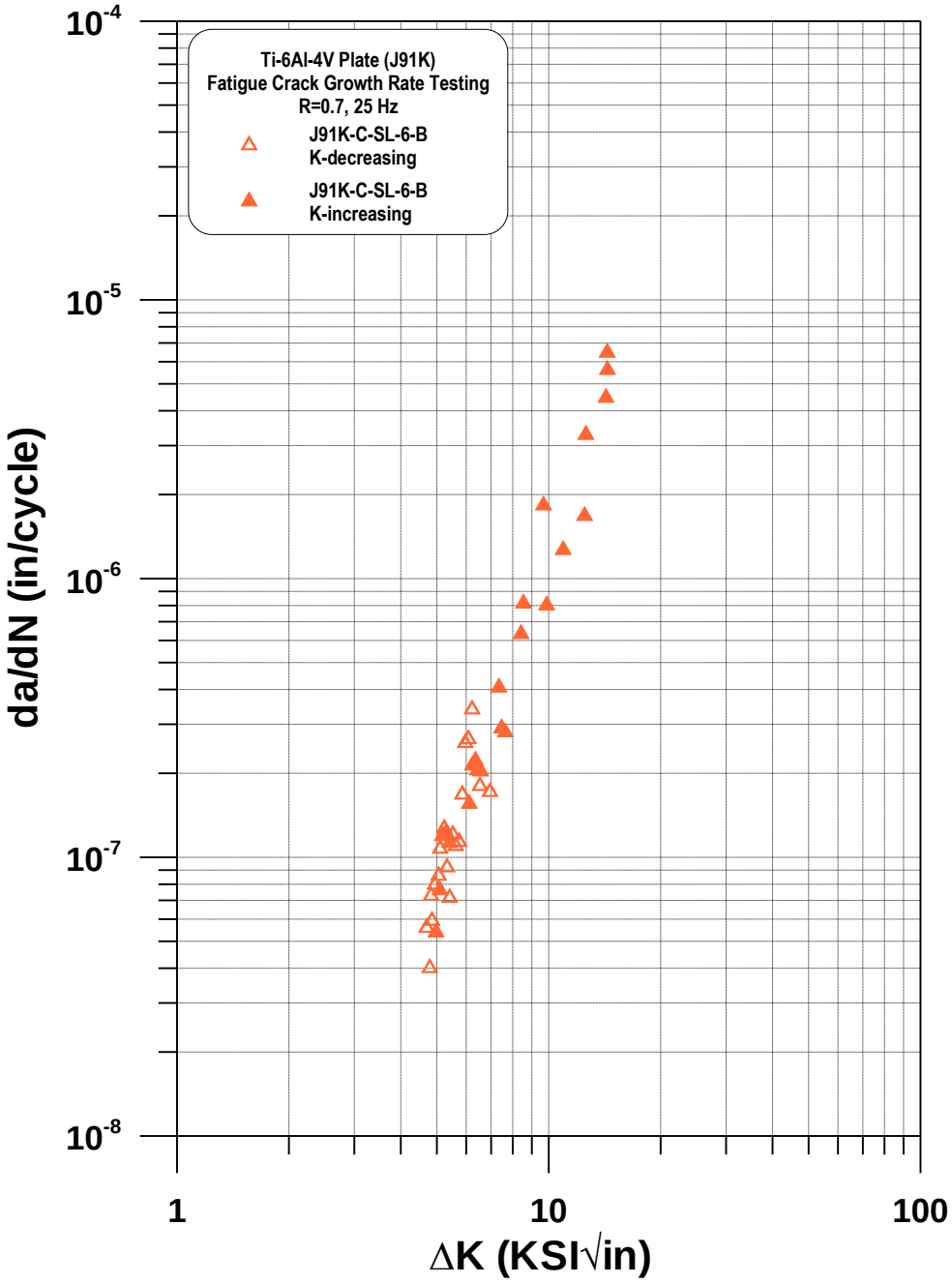
Approved for public release; distribution unlimited.



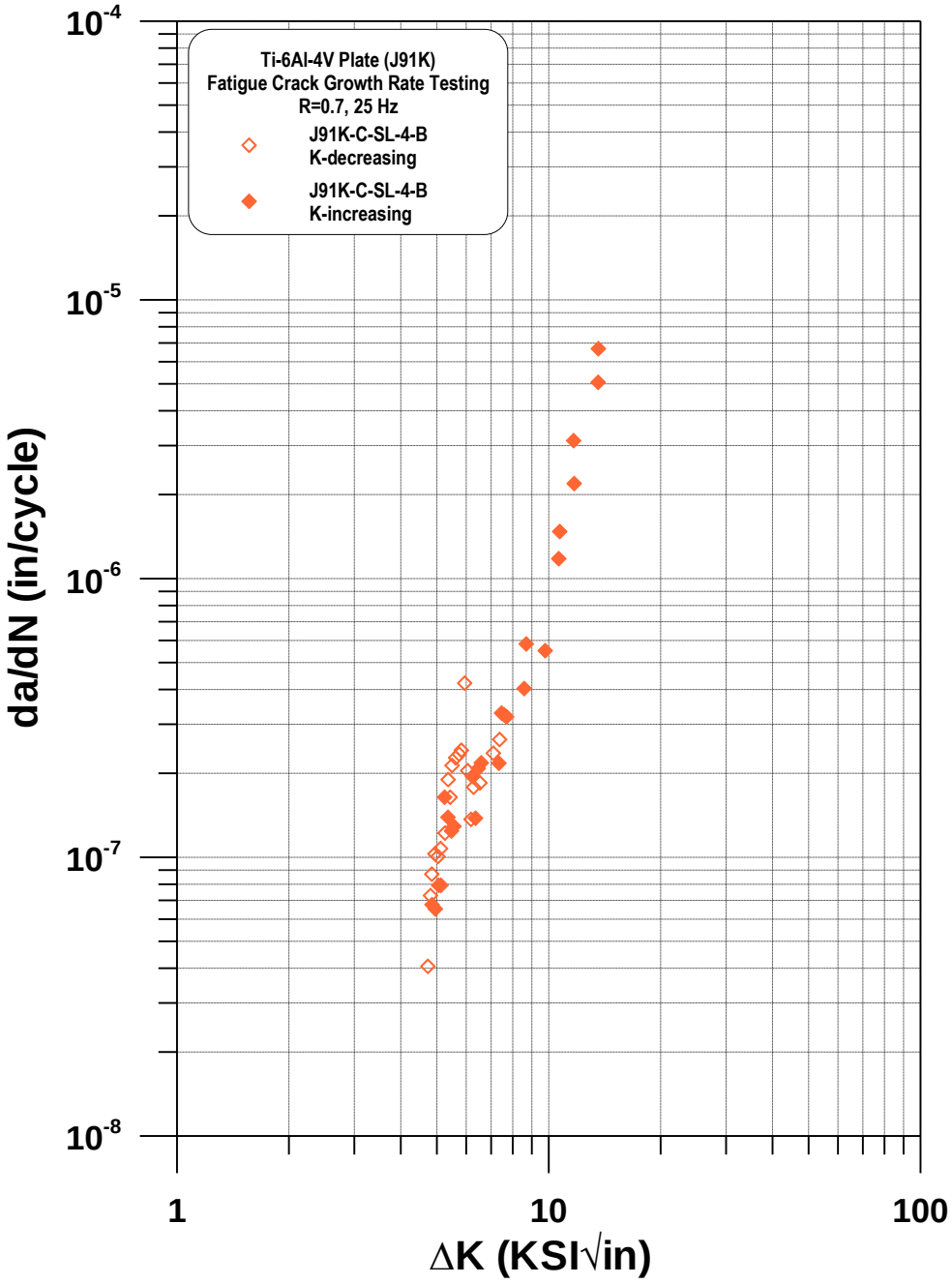
Approved for public release; distribution unlimited.



Approved for public release; distribution unlimited.



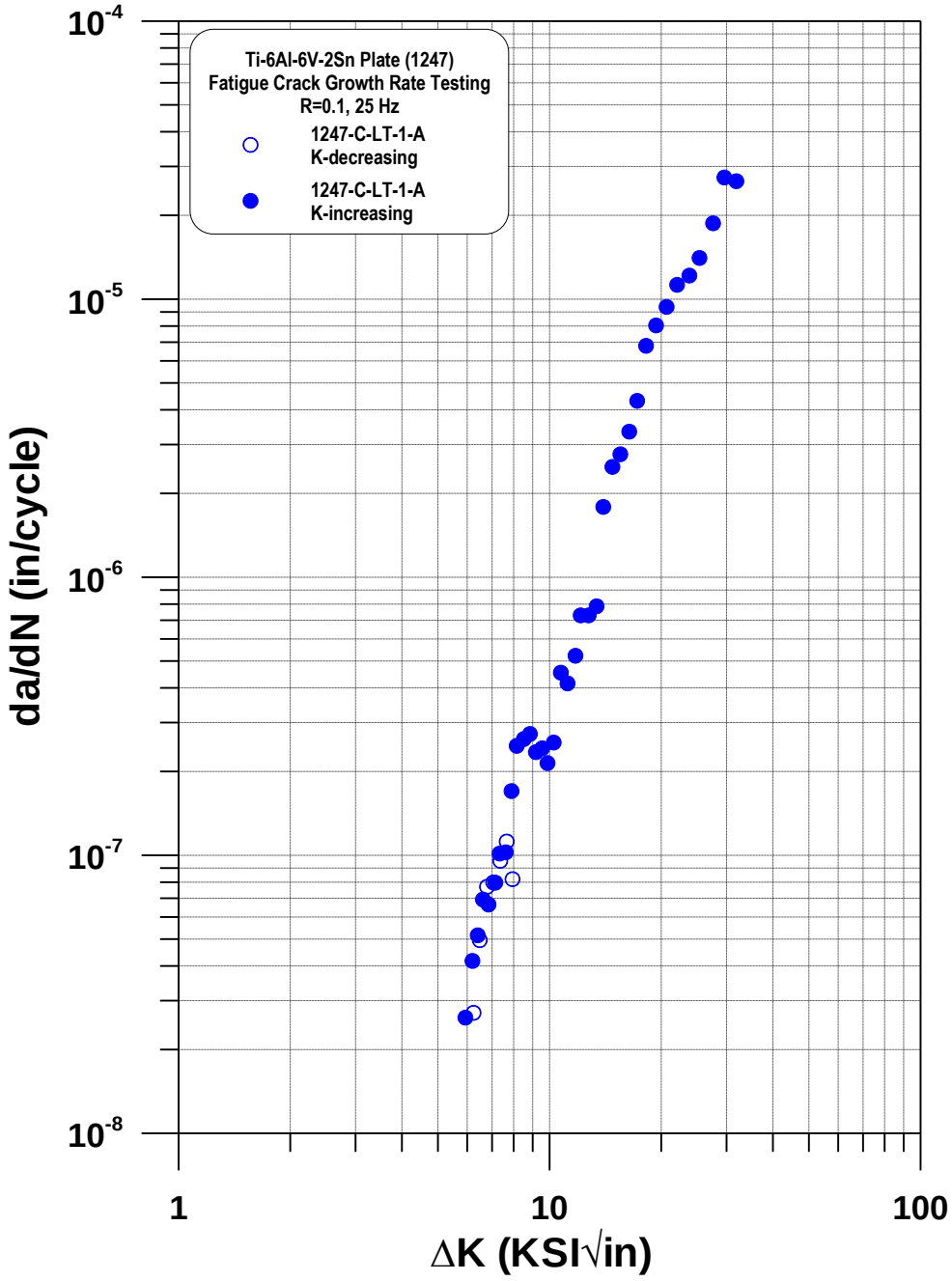
Approved for public release; distribution unlimited.



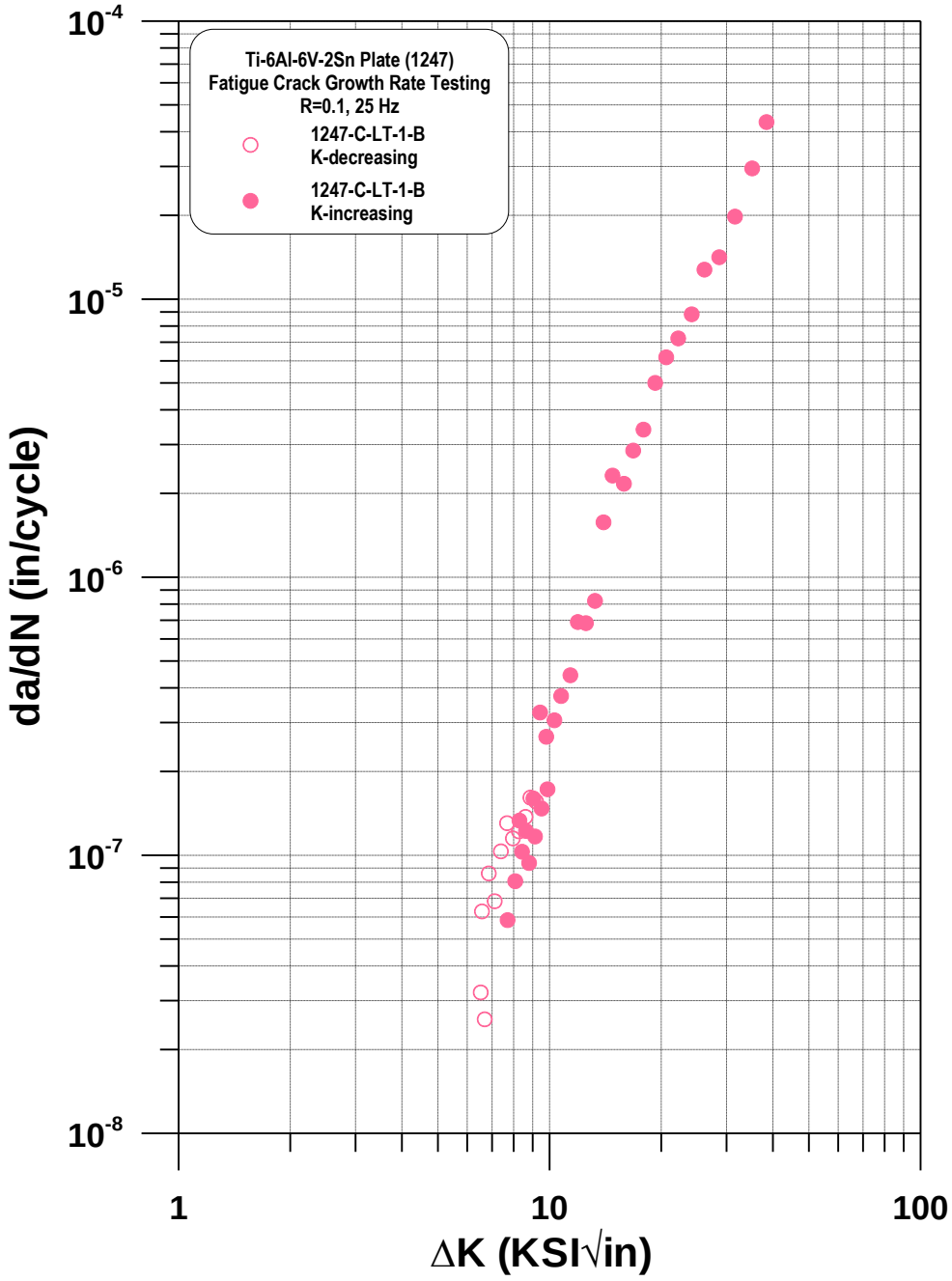
Approved for public release; distribution unlimited.

Appendix B
Individual fatigue crack growth rate curves for Ti-6Al-6V-2Sn plate (1247).

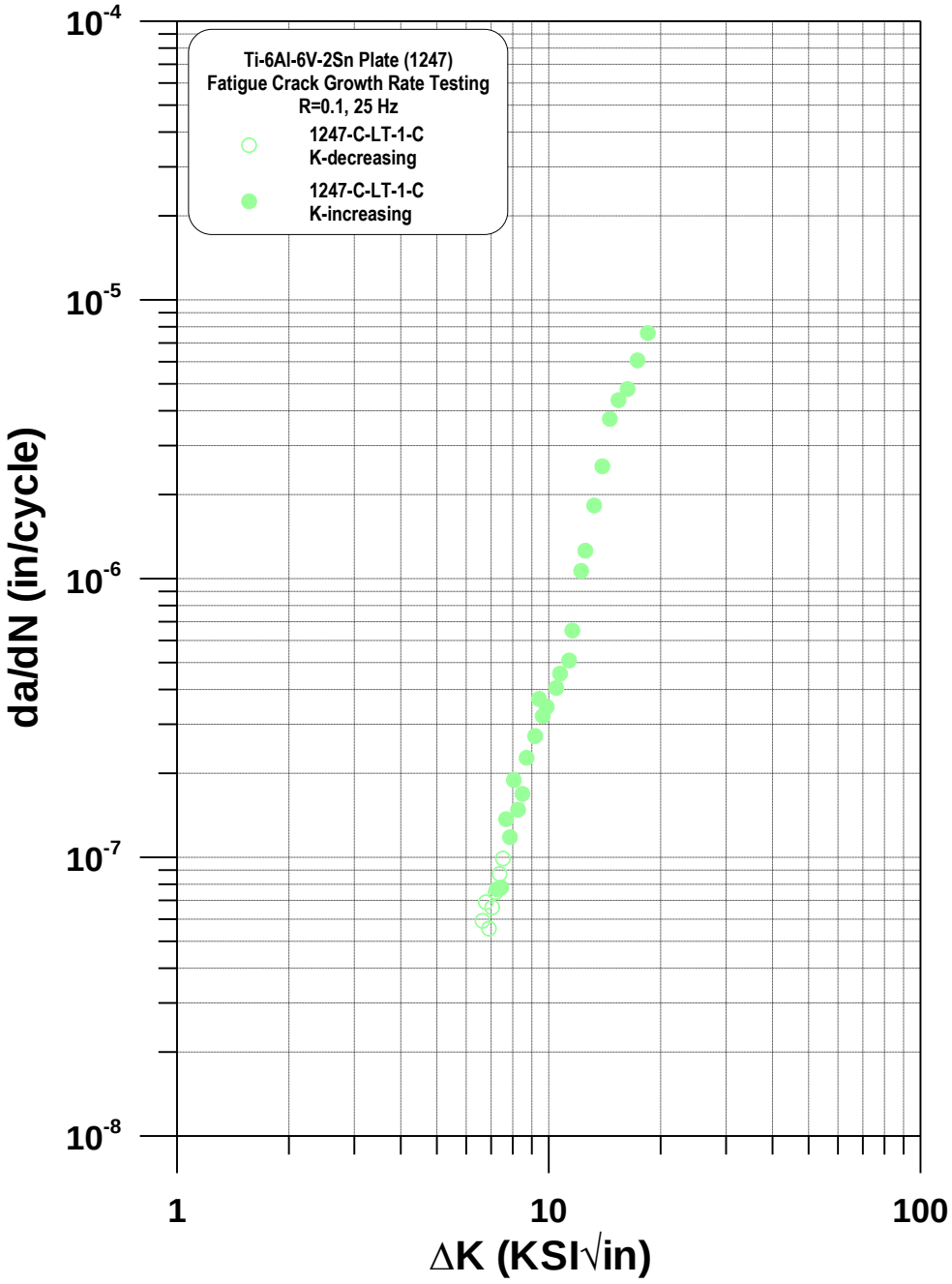
Approved for public release; distribution unlimited.



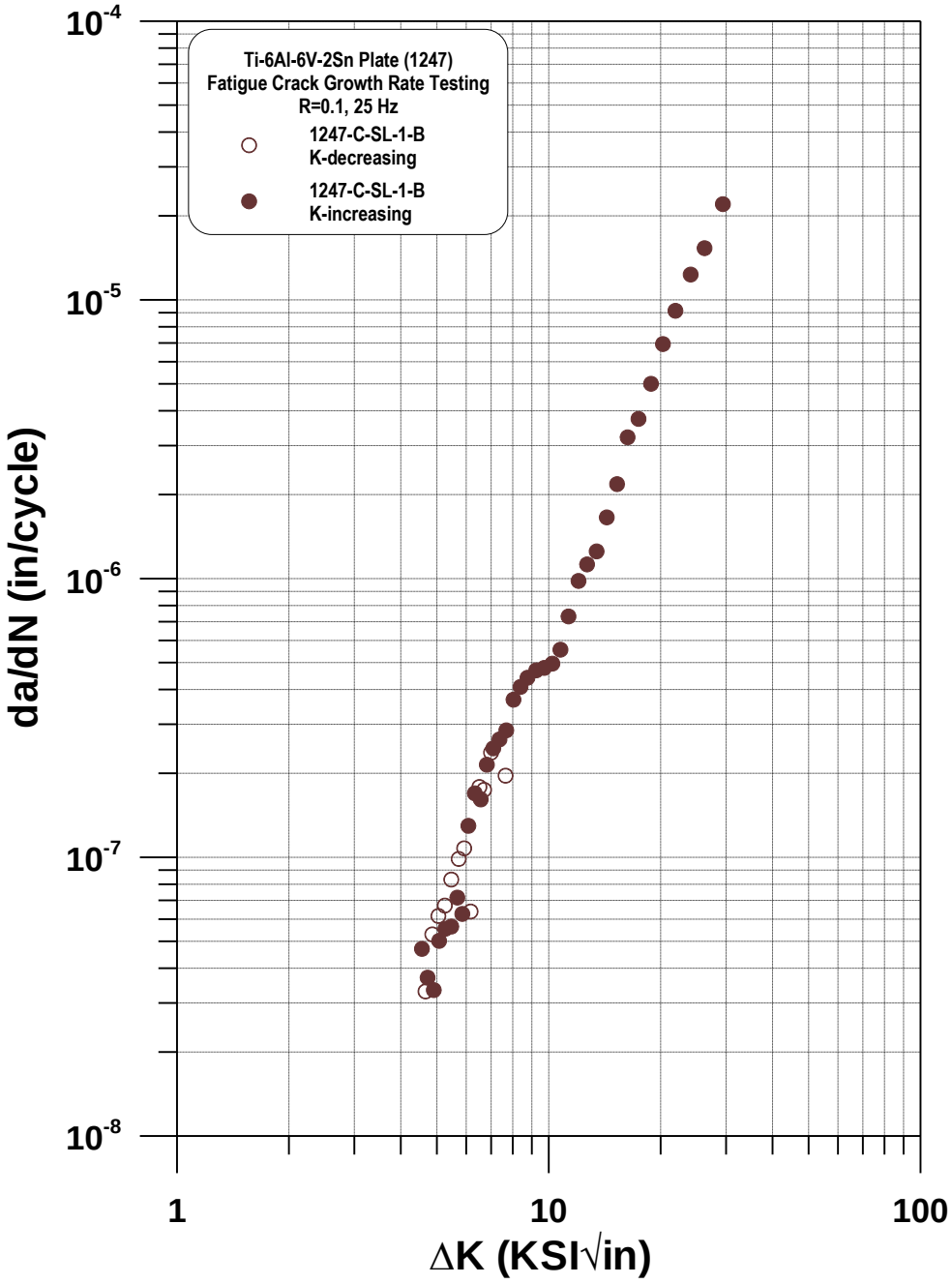
Approved for public release; distribution unlimited.



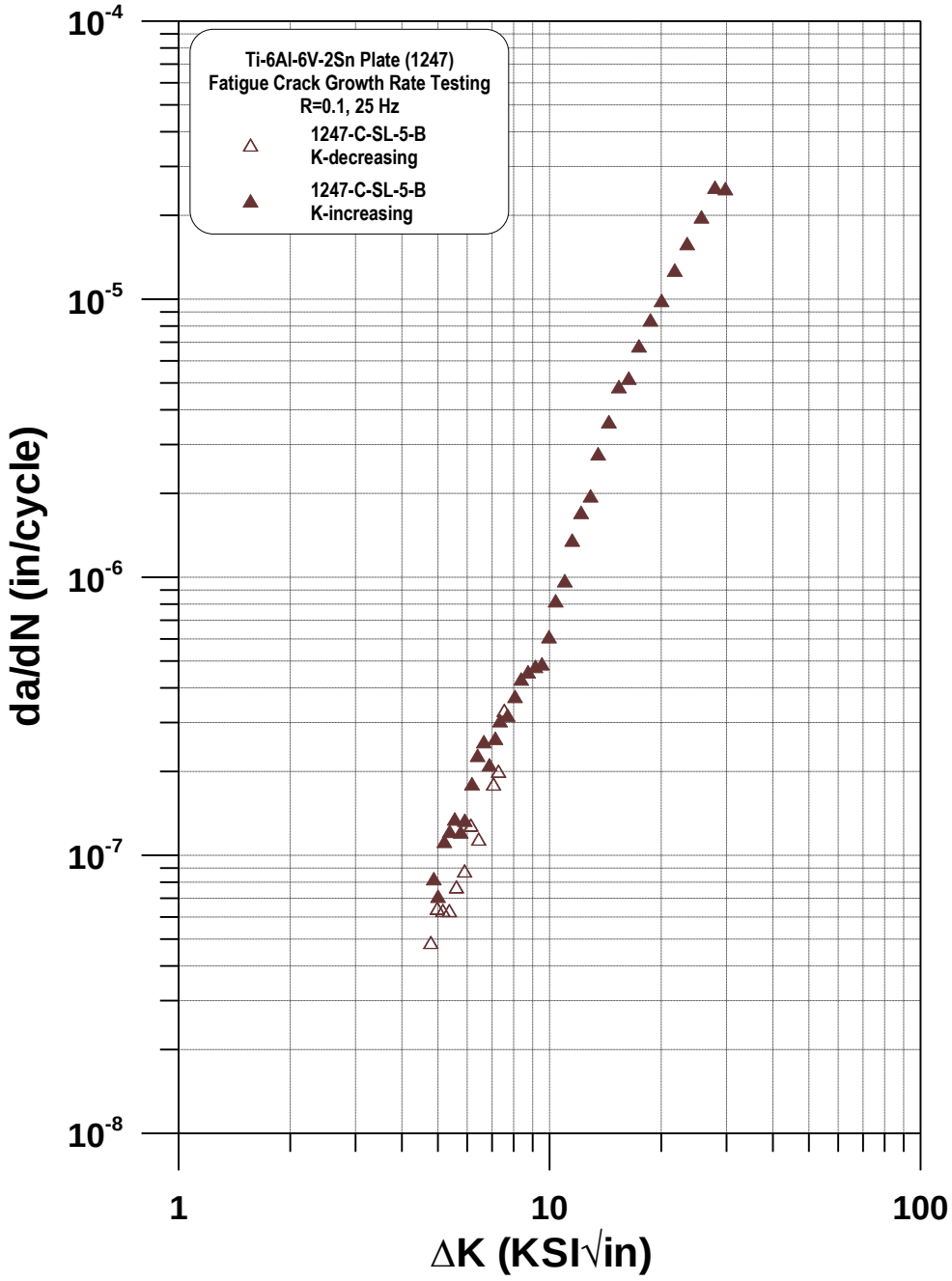
Approved for public release; distribution unlimited.



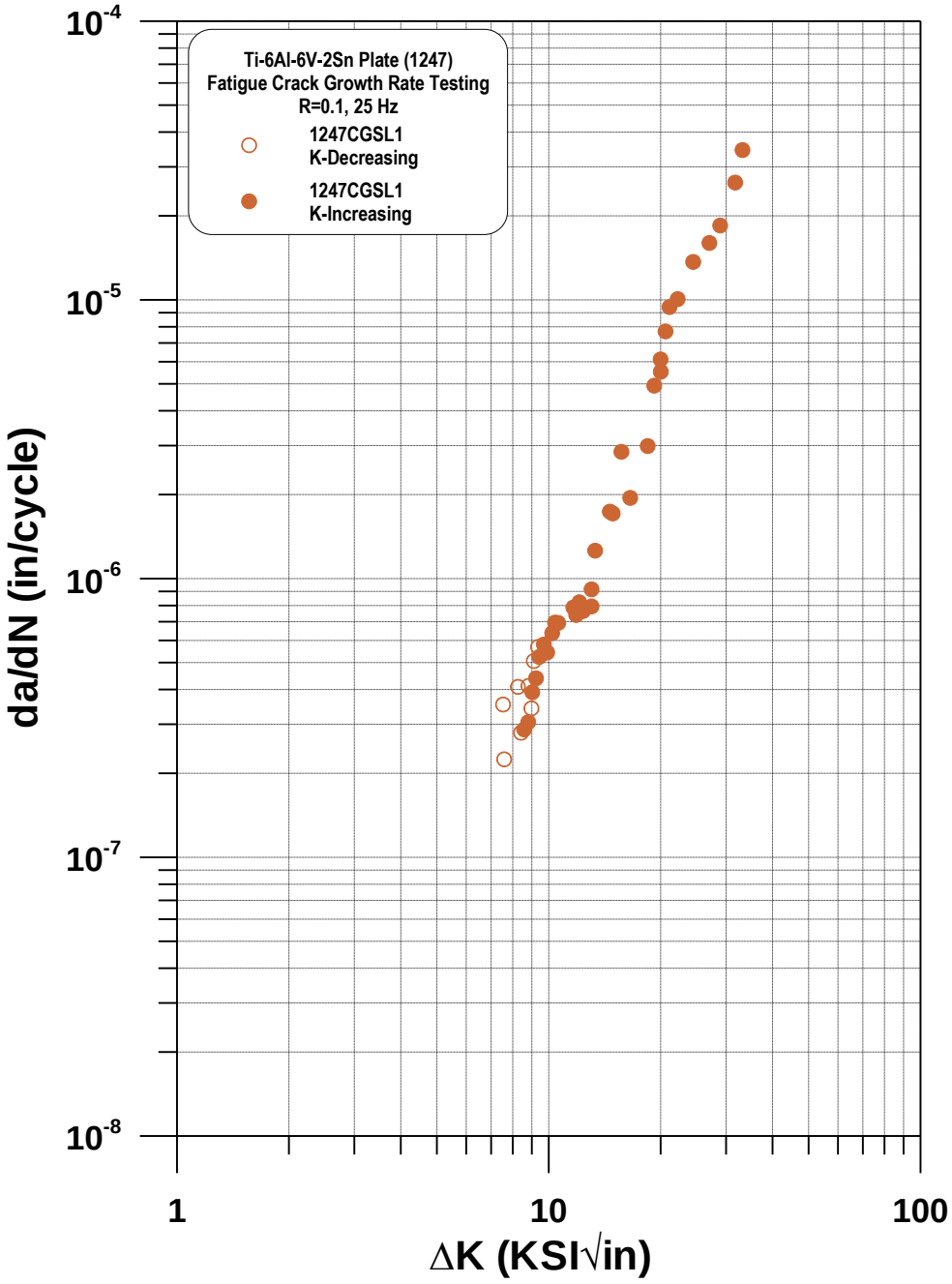
Approved for public release; distribution unlimited.



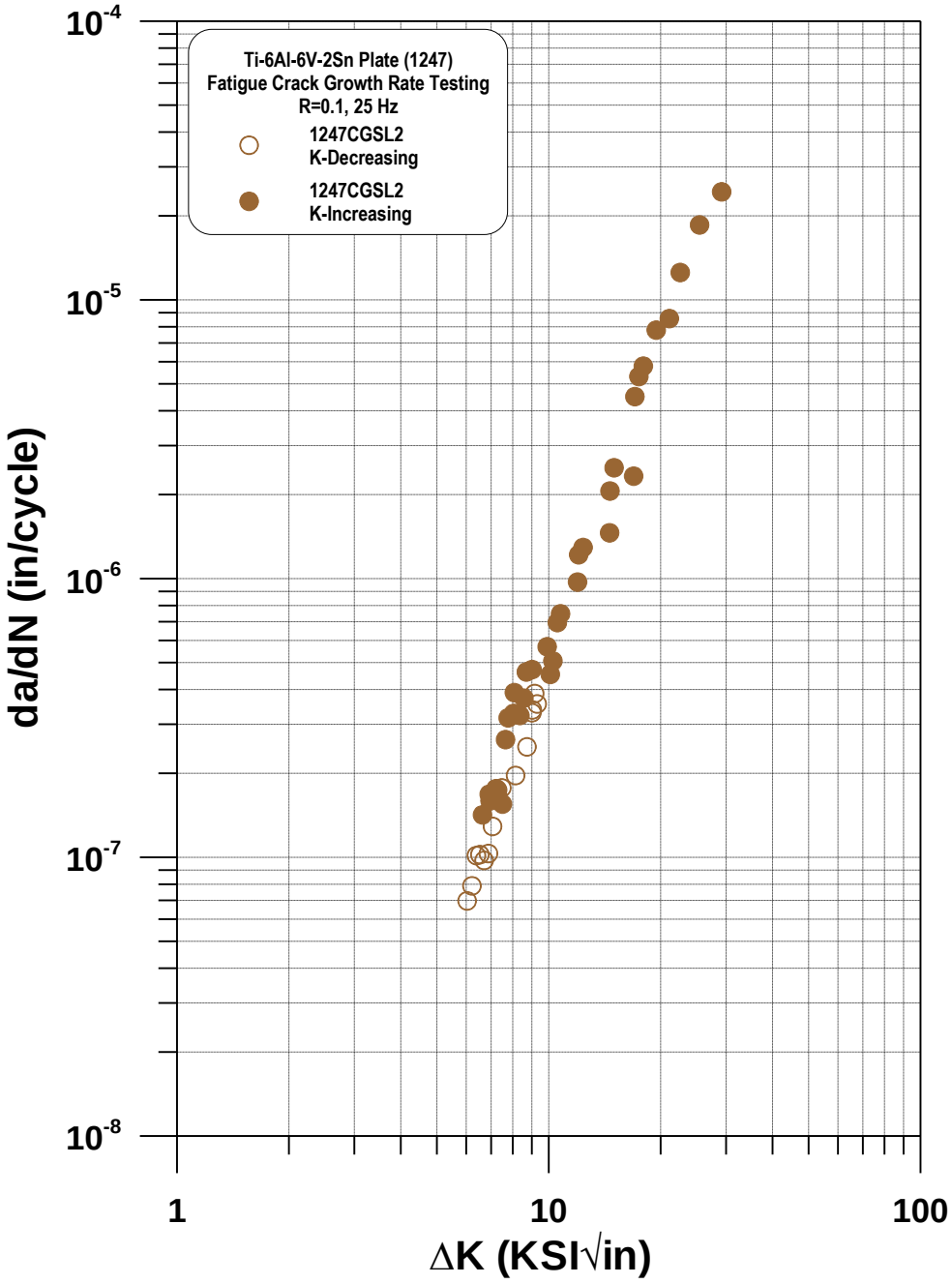
Approved for public release; distribution unlimited.



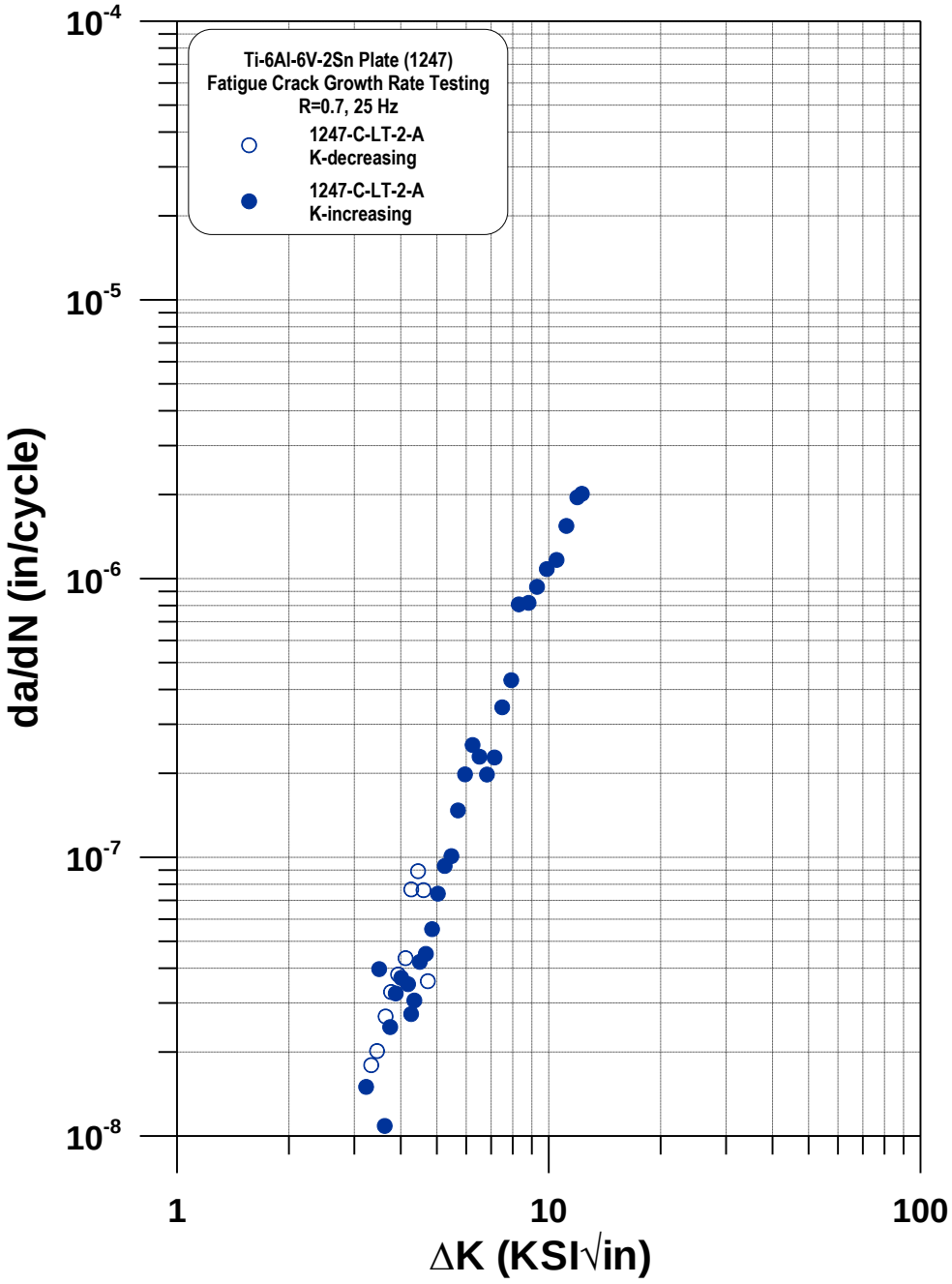
Approved for public release; distribution unlimited.



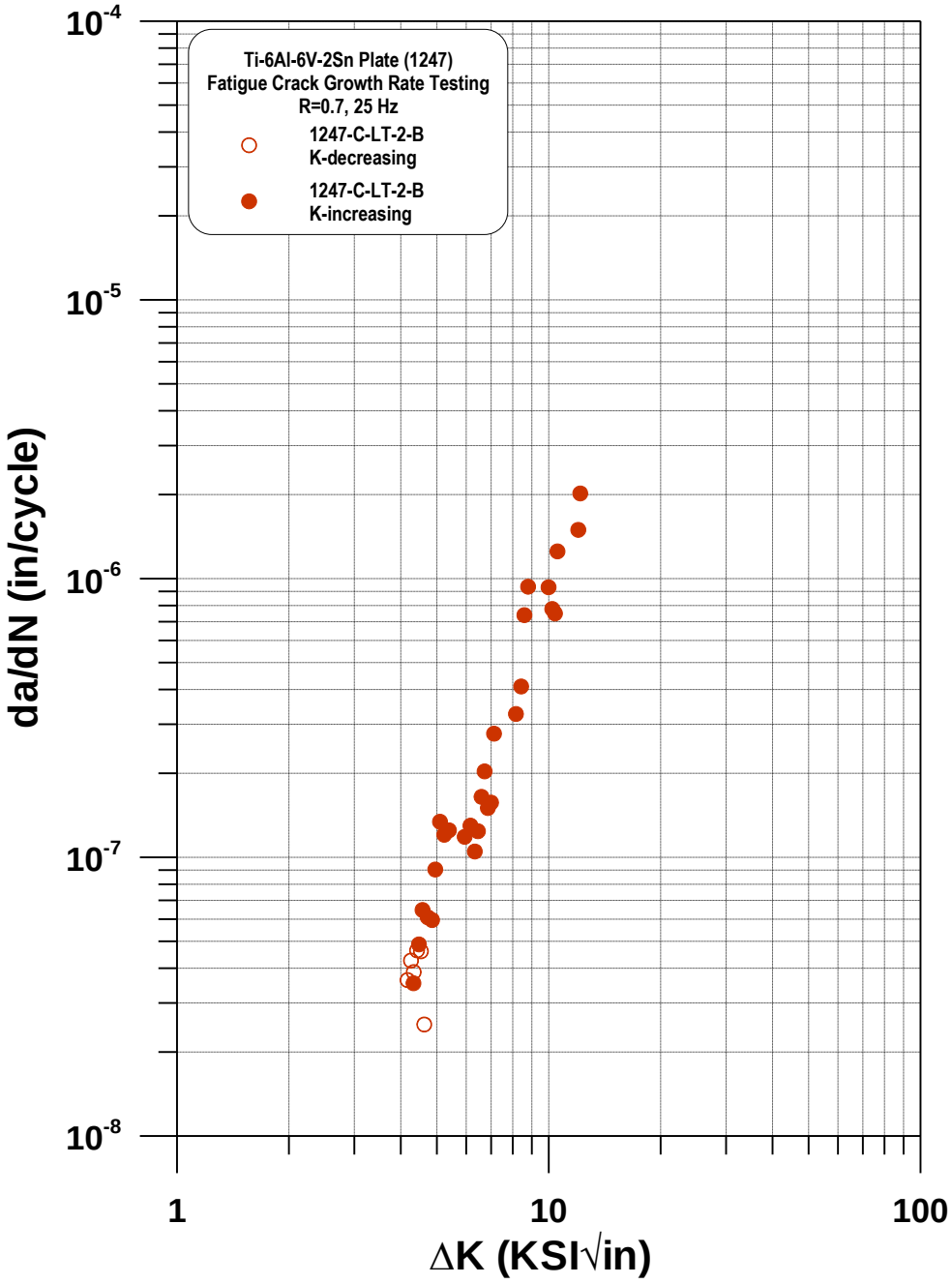
Approved for public release; distribution unlimited.



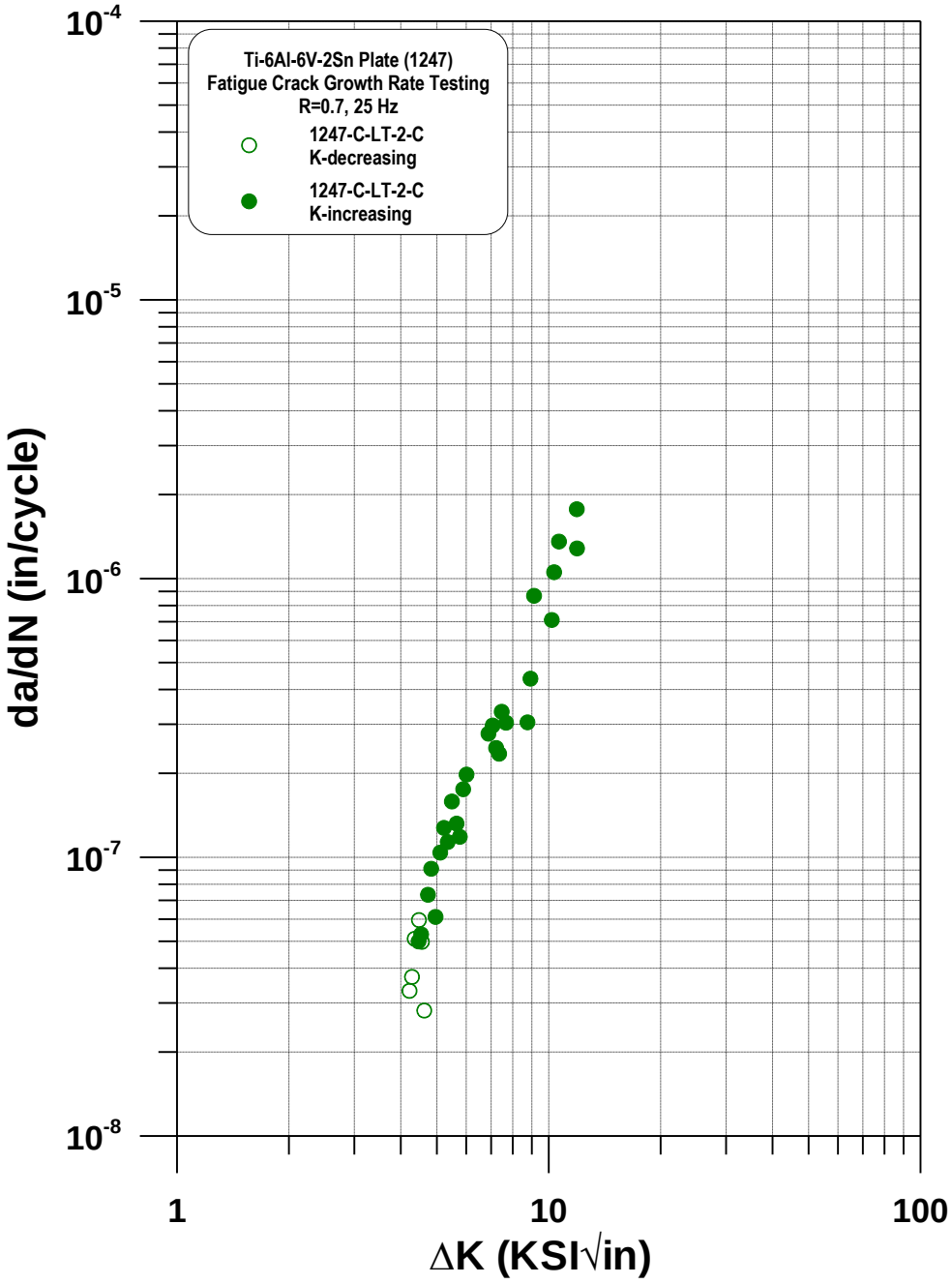
Approved for public release; distribution unlimited.



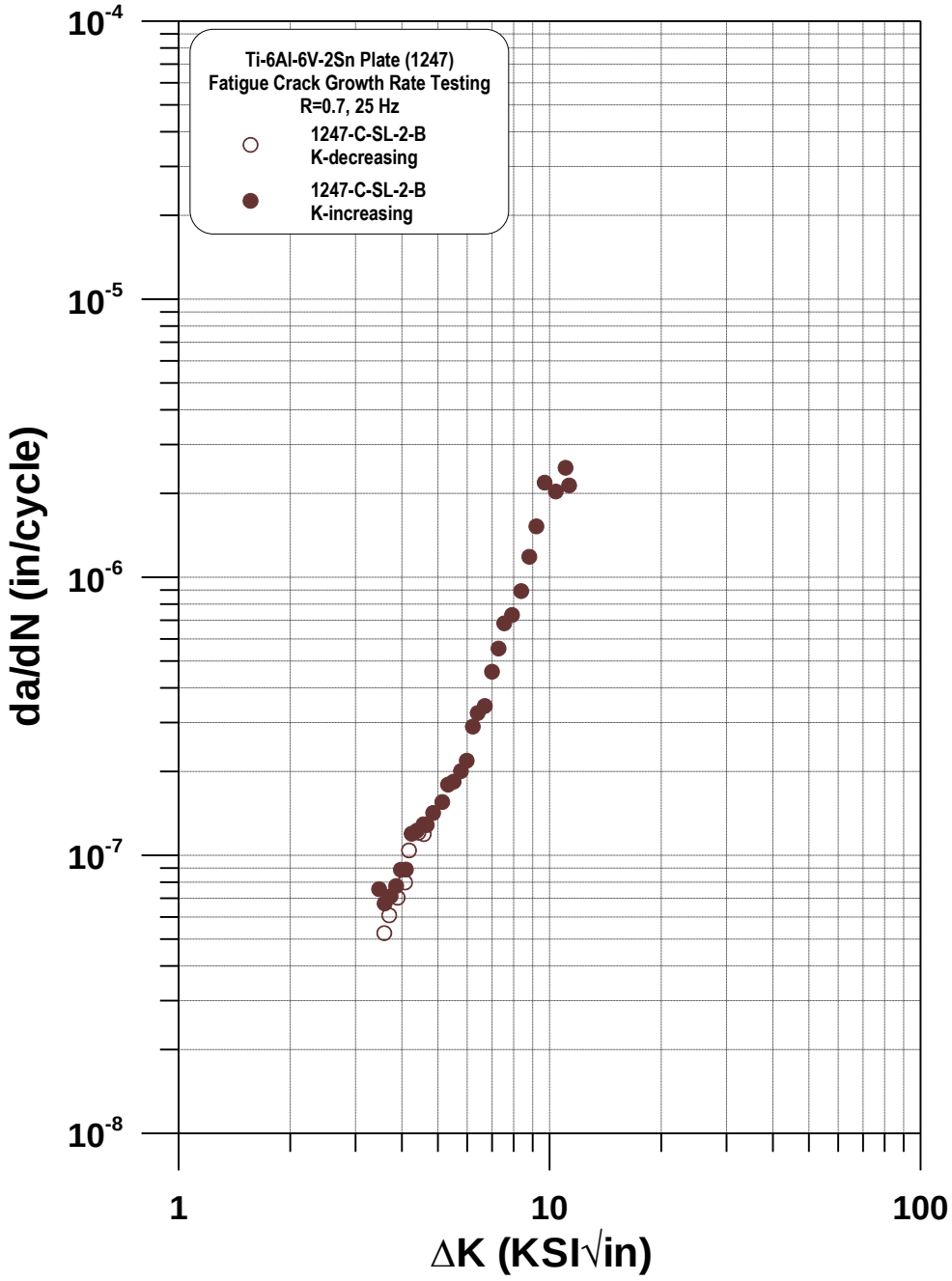
Approved for public release; distribution unlimited.



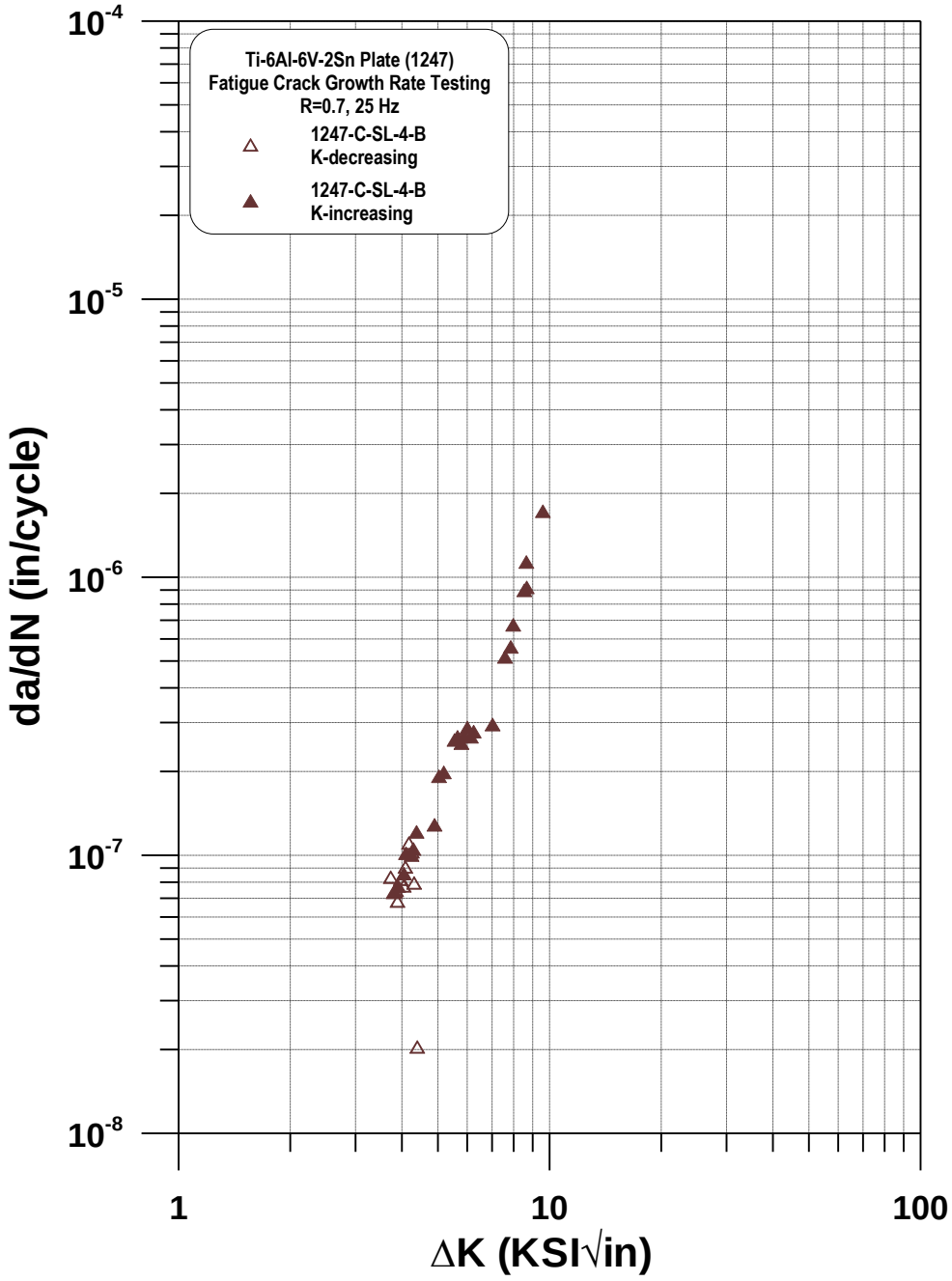
Approved for public release; distribution unlimited.



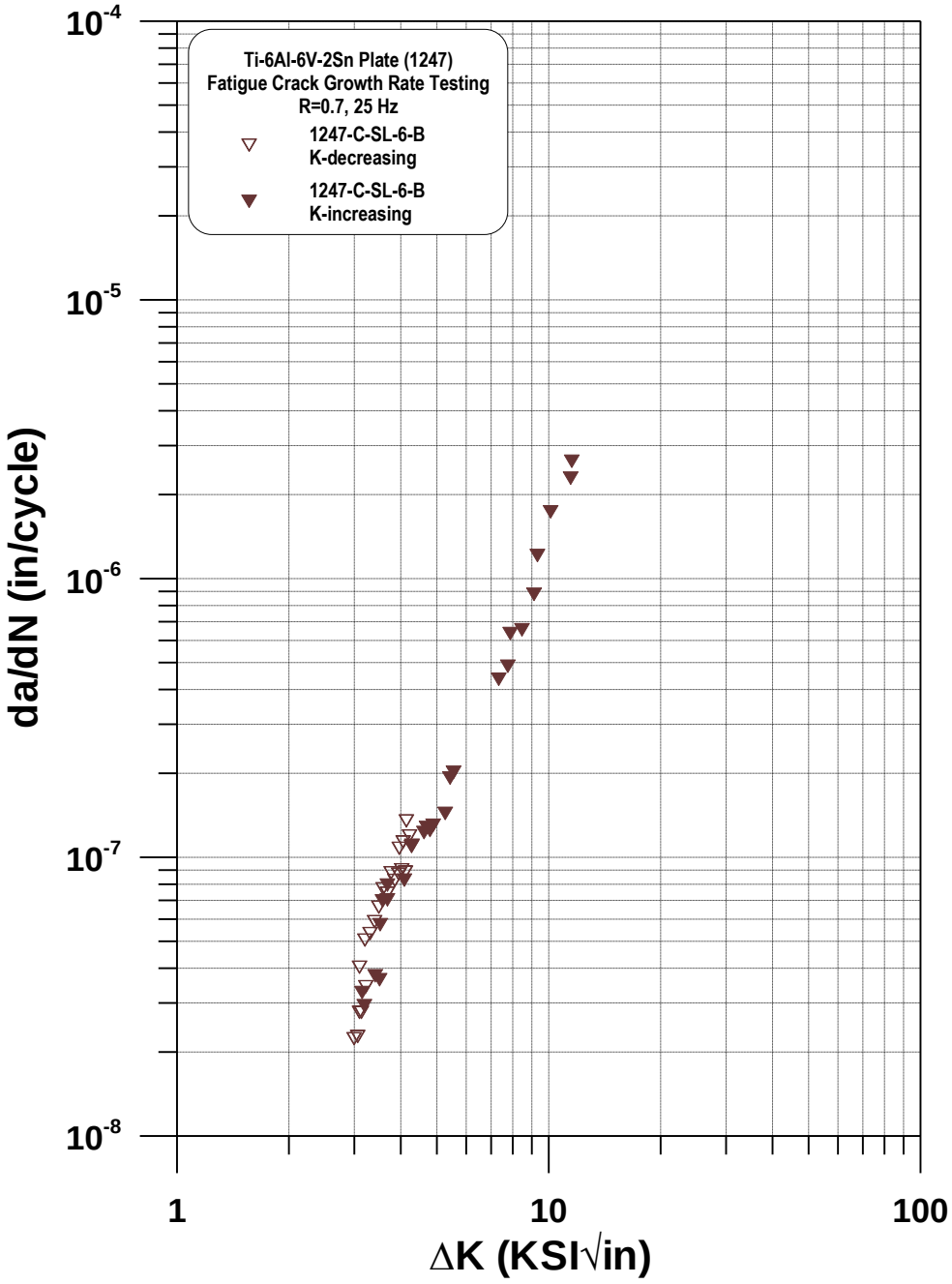
Approved for public release; distribution unlimited.



Approved for public release; distribution unlimited.



Approved for public release; distribution unlimited.



Approved for public release; distribution unlimited.

APPENDIX C

NON-CONFORMING TITANIUM - BILLET CHARACTERIZATION (TI-6AL-4V BILLET)

5 November 2010

EVALUATION REPORT

REPORT NO. AFRL/RXS 10-087

AUTHOR

Steven R. Thompson
Acquisition Systems Support Branch (AFRL/RXSCE)

Building 652, Room 122
2179 12th Street
Wright-Patterson AFB, Ohio 45433-7718

REQUESTER
AFMC/EN (Thomas Fischer)

CAUTION

This information consists of PRELIMINARY reasonable lower bound properties for titanium billet. (Fully analyzed data, labeled FINAL, will be forthcoming.)
This information should be used **only** to evaluate the potential impact of improperly substituted titanium.
This information should **not** be used for design purposes in place of material properties from specifications or MMPDS entries covering titanium plate, bar, or other product forms.
This information should **not** be used to analyze components manufactured from titanium stock that is known to be compliant with applicable specifications.

CAUTION

DISTRIBUTION STATEMENT A: Approved for public release; distribution unlimited.

BACKGROUND

An ongoing federal investigation has identified a risk associated with improperly processed titanium (Ti) material being used in the fabrication of critical safety items and safety-of-flight components in USAF, DoD, NASA, FAA, and other systems. At the direction of AFMC/CC, a Titanium Task Force (led by AFMC/EN) was formed to further define risk to USAF systems and to assist with mitigation efforts. The suspect Ti material (e.g., "billet," "reforging stock") was never intended to be machined to the final forms in which it is now possibly being used. This R&D testing program will develop new baseline (reasonable lower bound) properties on a heretofore not fully characterized form of Ti. The decision to refer to these baseline values as "reasonable lower bounds" is based on the fact that an insufficient quantity of material heats and lots were represented for the calculation of traditional MMPDS **[*1*]** A- or B-, or even S-basis allowables. However, the number of specimens tested (often in replicate) is significant. Thus "reasonable lower bound" was chosen as the proper phrase to describe properties derived from the testing of multiple specimens from the two heats (per alloy) of material in this program. While these do not meet the requirements for standard baseline property determination, they are, nevertheless, significant.

This report is intended to summarize the mechanical testing of one Ti-6Al-4V billet. The data presented in this report is shown on a "preliminary" basis and should not be used for design purposes.

MATERIAL DESCRIPTION

The Ti-6Al-4V billet summarized in this report was purchased from Titanium Industries, Inc. As shown in Figure 1, the section received had nominal dimensions of 24"(w) x 45"(l) x 6.5"(t) and had been produced per the AMS 4928R and AMS-T-9047 specifications. The billet's pedigree traces back to an ingot heat K27P produced by ATI Allvac. The billet was delivered in the mill-annealed heat treat condition.

Upon receipt of the billet, a 4-inch wide section was cut along the length of the billet. The face of this section through the thickness was machined to a 32 Ra surface finish and macro-etched to determine forging flowlines. No anomalous behavior was noticed during this examination. This 4"(w) x 45"(l) x 6.5"(t) section of billet was not used for subsequent mechanical testing.

Due to the fact that billet material is intended to be an intermediate product form and not meant for use in component fabrication, a specimen orientation system needed to be established. The standard designations of longitudinal (L), long transverse (T), and short transverse (S) coordinate system were employed in this investigation in order to establish a consistency with plate and bar product forms. For this billet, the L-orientation was assigned to the billet length, the T-orientation to the billet width, and the S-orientation to the billet thickness as illustrated in Figure 1.

Approved for public release; distribution unlimited.

Prior to test specimen extraction, the remaining billet was sub-sectioned (as shown in Figure 1) so that it could be subjected to non-destructive evaluation (NDE) using ultrasonic transmission (UT). The individual sections were designated as A through E and these designations were used in the specimen numbering schema. Some relevant, below threshold indications were noted during this evaluation, particularly in Section E. These areas were noted for further examination in the event of anomalous test results. After the test specimens were machined, they were once again examined using NDE techniques. All specimens, except the fracture toughness, were examined using x-ray and fluorescent penetrant inspection (FPI). Fracture toughness specimens had UT and FPI examinations. Any resultant indications were noted and photographed for use in analysis of anomalous test results.

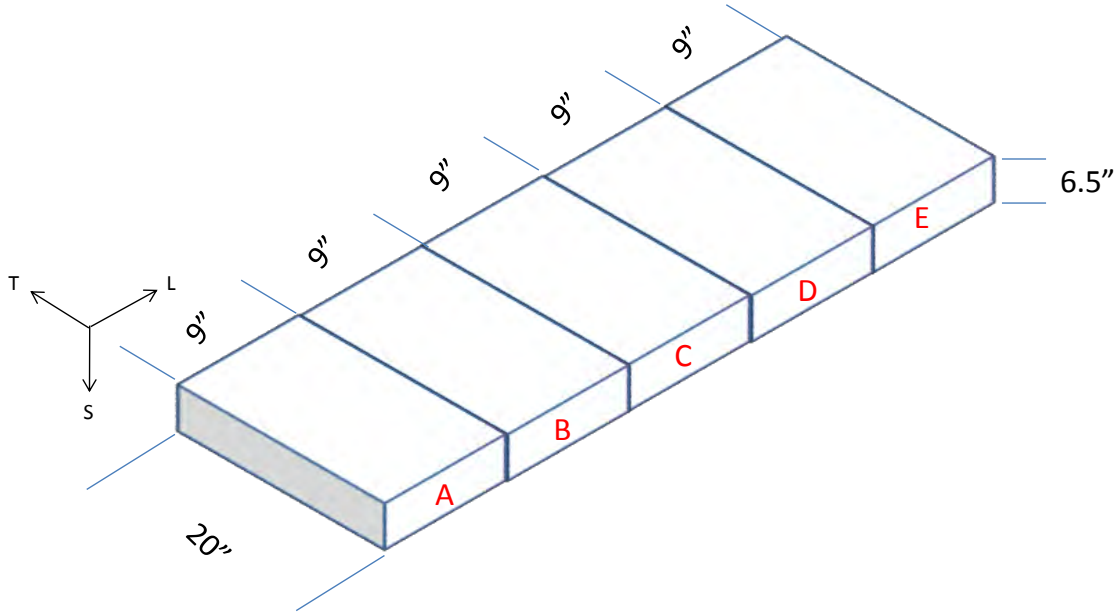
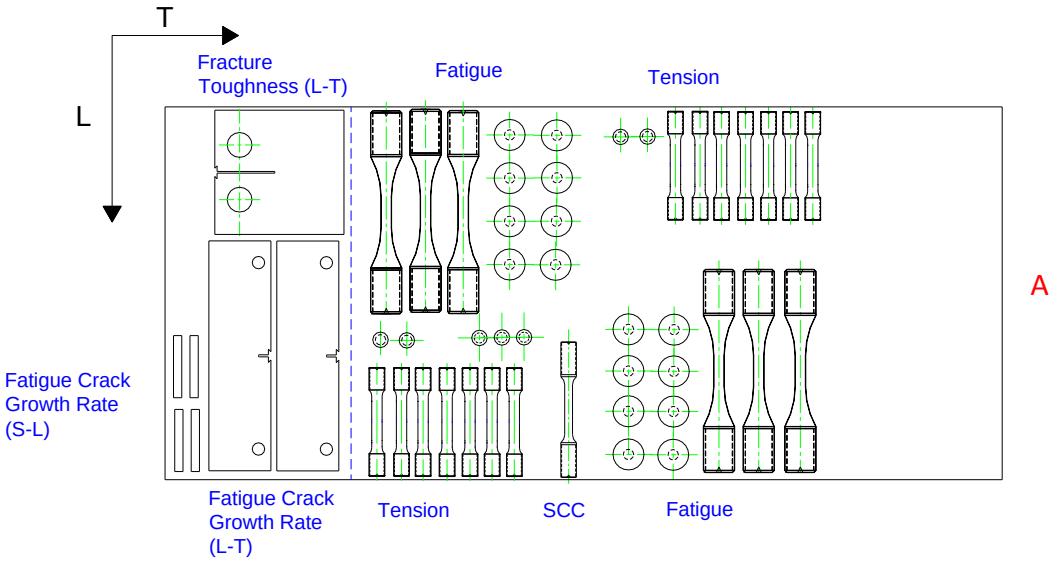


Figure 1. Ti-6Al-4V billet (#K27P) indicating dimensions, orientations, and sectioning plan prior to specimen extraction.

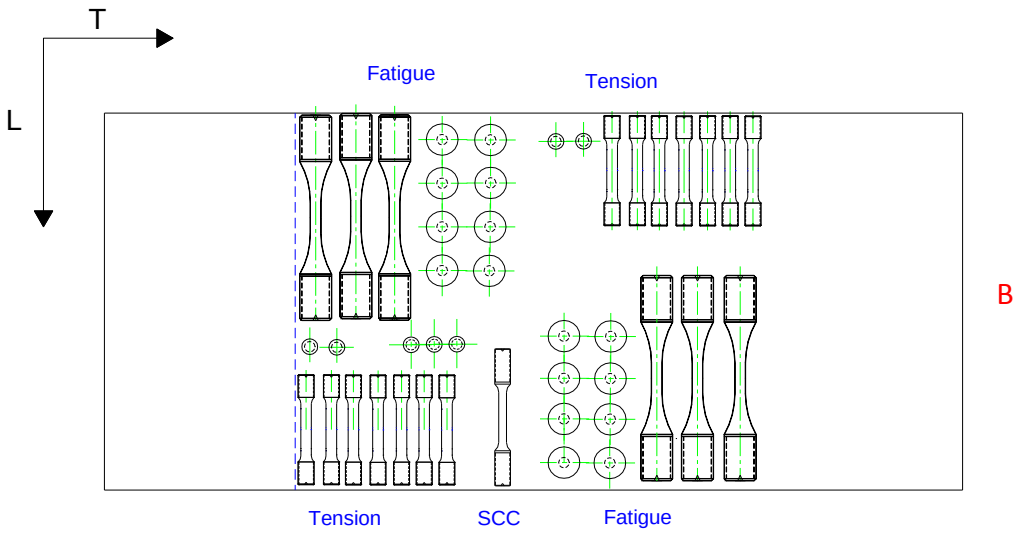
TEST PLAN

Test Specimens – The test specimens were excised approximately from the locations shown in Figure 2. Specimens were removed from three planes through the thickness where possible: the two quarter points (t/4 and 3t/4) and the midplane (t/2). Throughout this report, specimen location within the thickness is designated by either "A" (t/4), "B" (t/2), or "C" (3t/4). For short-transverse (S or S-L) oriented specimens, the location was determined by either the center of the gage length or the crack plane.

Approved for public release; distribution unlimited.

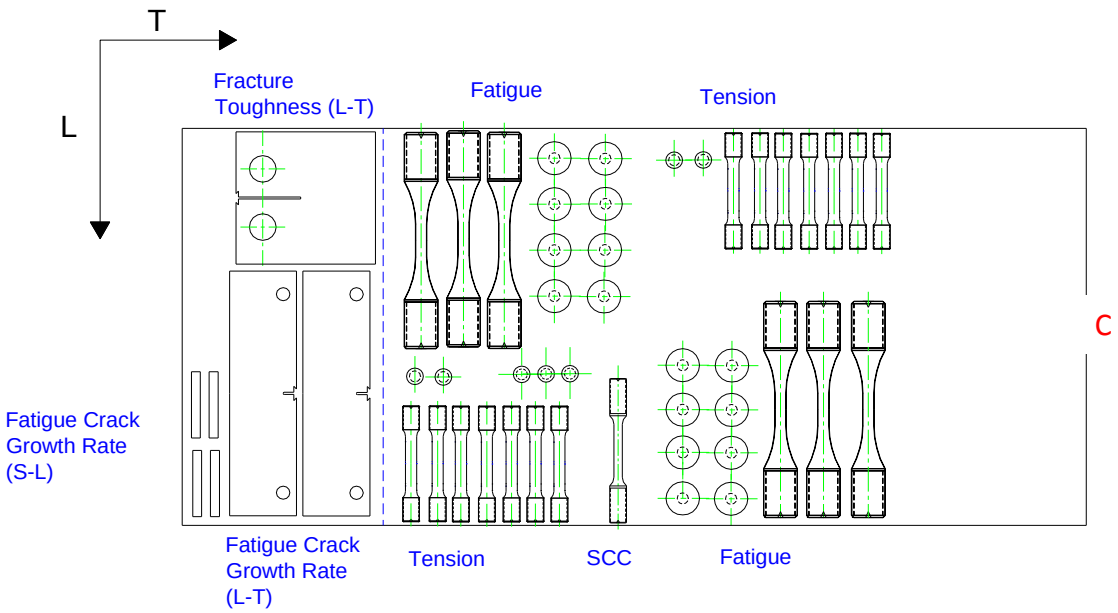


(a)

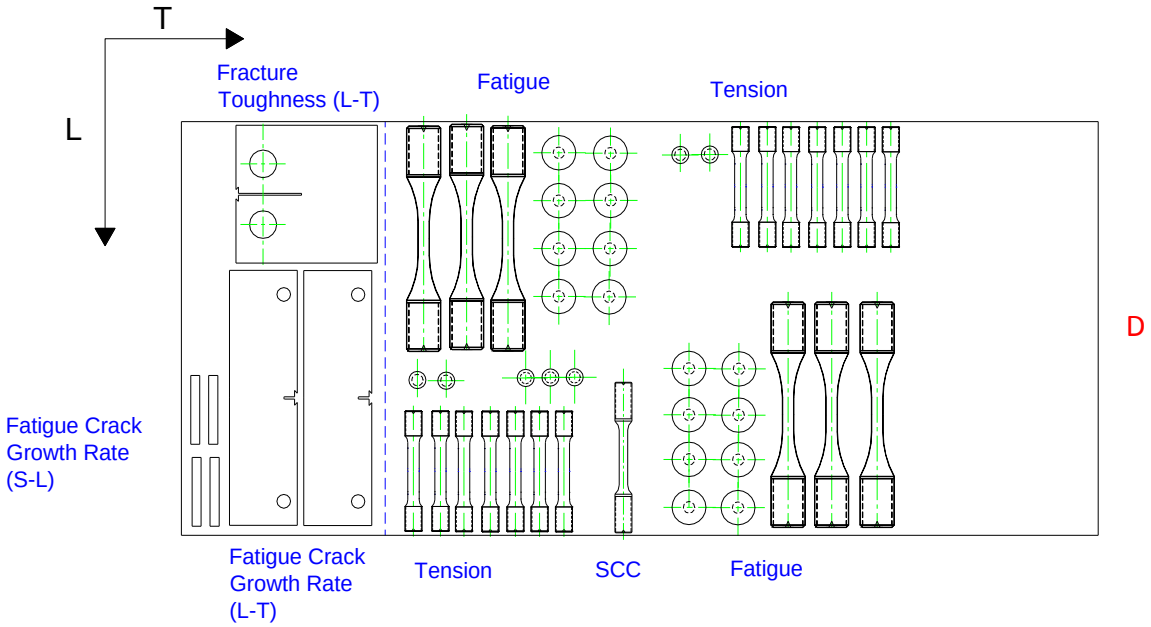


(b)

Approved for public release; distribution unlimited.

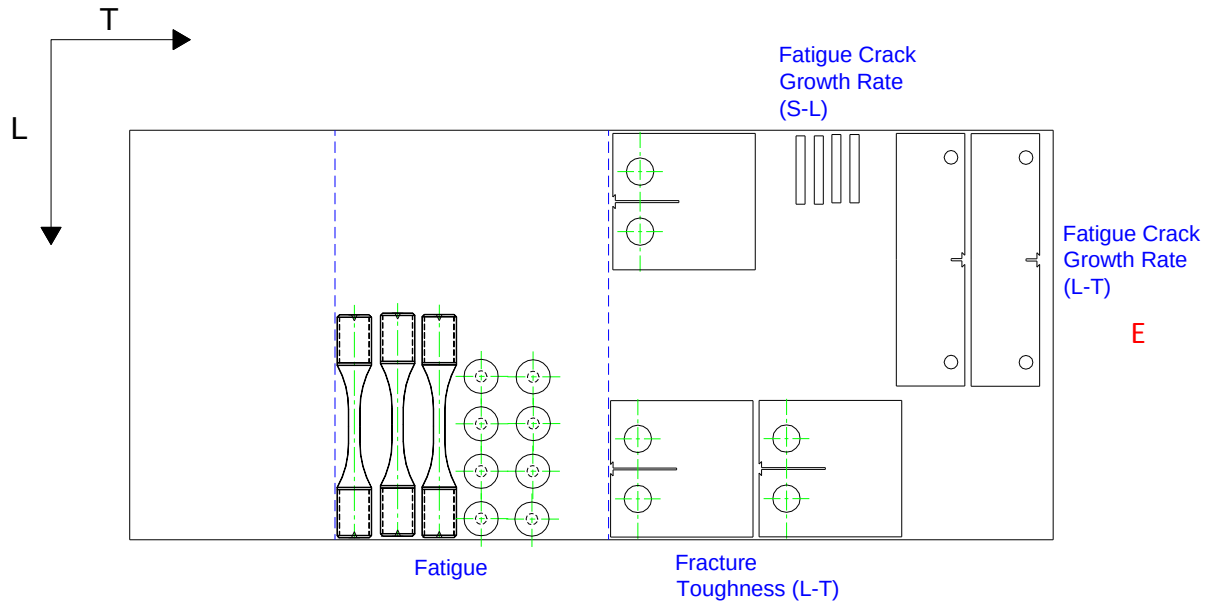


(c)



(d)

Approved for public release; distribution unlimited.



(e)

Figure 2. Specimen location layout drawings for sections (a) A, (b) B, (c) C, (d) D, and (e) E.

Test specimens were machined to the final required geometries as shown in the Figures 3 through 7. All of the geometries were in accordance with the applicable test method (as described in the next section). All of the specimens were fabricated using the same machine shop per specimen drawings provided by AFRL/RXSCE, in order to minimize possibility of variability due to specimen machining. Special care was given to the traceability of the specimen back to a general location within the billet. Test specimens were given a unique identification that would allow for this tracking.

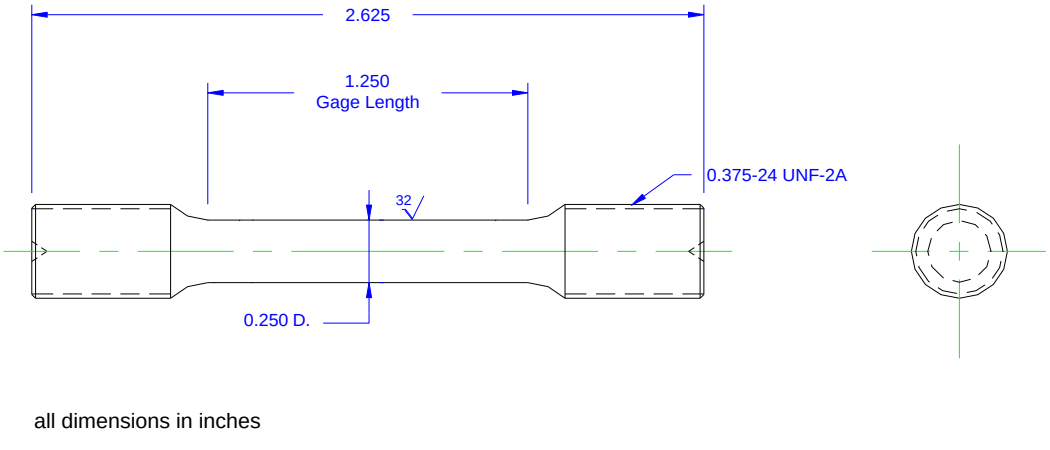


Figure 3. Geometry of tensile test specimen.

Approved for public release; distribution unlimited.

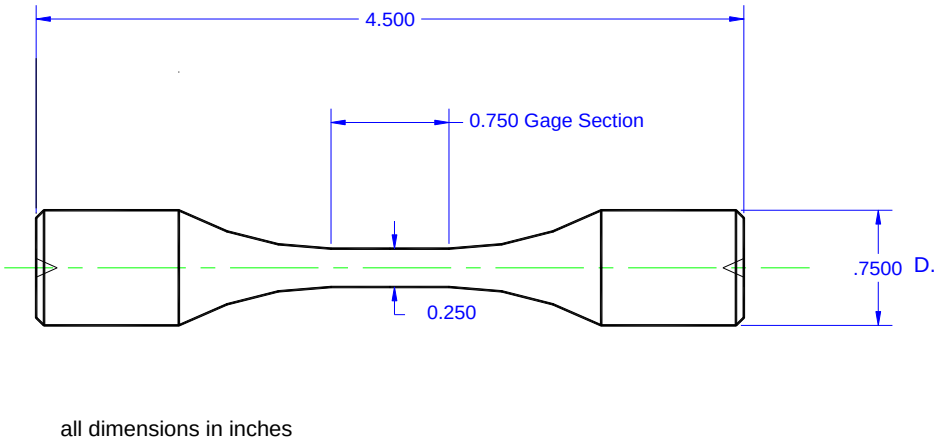


Figure 4. Geometry of fatigue test specimen. (Note: gage section was low-stress ground to a final surface finish of 8 Ra and then hand-polished longitudinally to remove all circumferential scratches.)

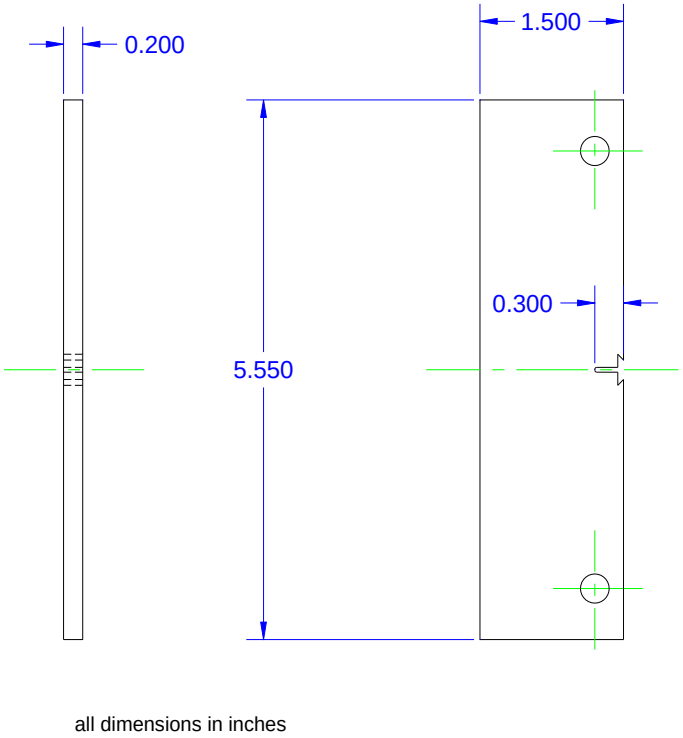


Figure 5. Geometry of fatigue crack growth rate ESE(T) test specimen.

Approved for public release; distribution unlimited.

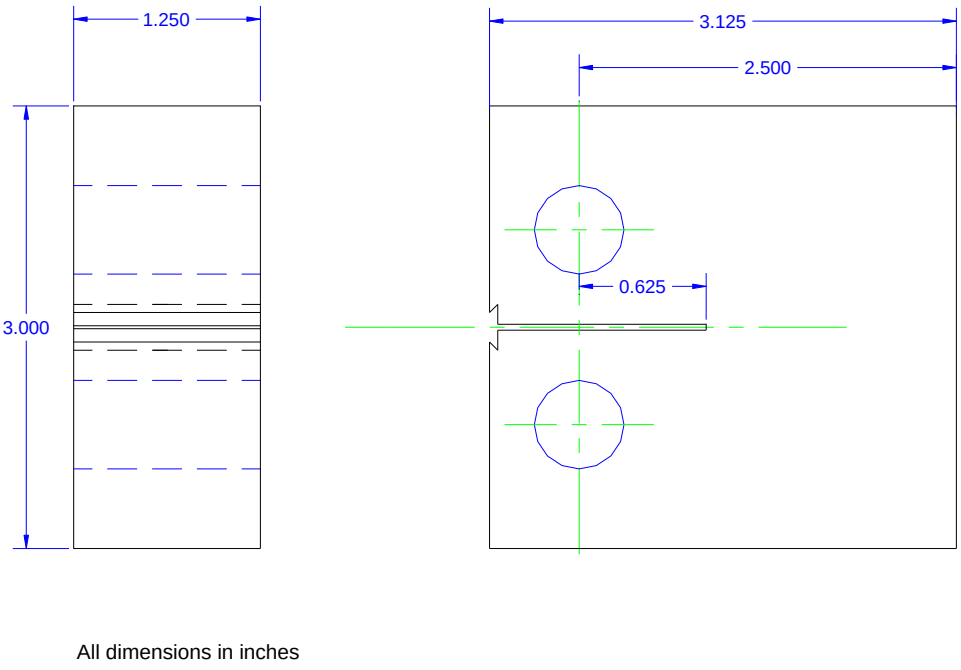


Figure 6. Geometry of fracture toughness C(T) test specimen.

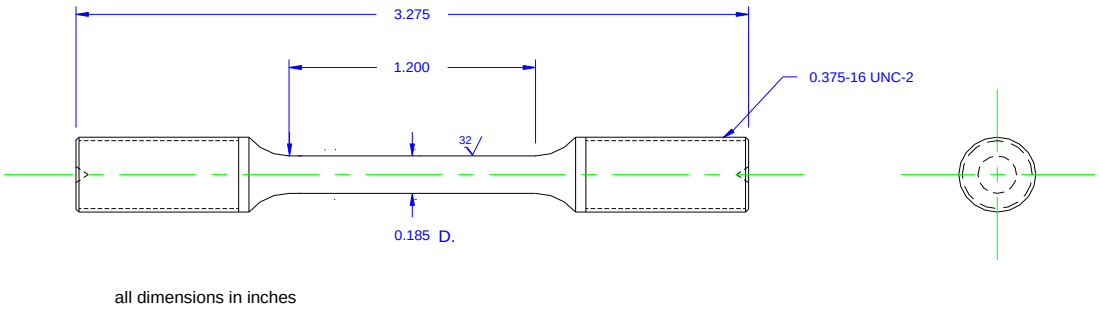


Figure 7. Geometry of stress corrosion cracking (SCC) test specimen.

Test Methods – The test methodologies used in this investigation are listed in Table 1. With the exception of stress corrosion cracking, all of the tests were performed in accordance with applicable ASTM standards. All testing was performed in ambient laboratory conditions (approximately 72°F and 50% relative humidity).

Table 1. Test Methodology

Test	ASTM Method
Tension (Modulus)	E 111-04 "Standard Test Method for Young's Modulus, Tangent Modulus, and Chord Modulus"
Tension	E 8/E 8M-08 "Standard Test Methods for Tension Testing of Metallic Materials"
Fatigue (force-controlled)	E 466-07 "Standard Practice for Conducting Force Controlled Constant Amplitude Axial Fatigue Tests of Metallic Materials"
Fatigue (strain-controlled)	E606-04 "Standard Practice for Strain-Controlled Fatigue Testing"
Fatigue Crack Growth Rate	E 647-08 "Standard Test Method for Measurement of Fatigue Crack Growth Rates"
Fracture Toughness	E 399-08 "Standard Test Method for Linear-Elastic Plane-Strain Fracture Toughness K_{Ic} of Metallic Materials"
Stress Corrosion Cracking	Similar to G 64-99 "Standard Classification of Resistance to Stress-Corrosion Cracking of Heat-Treatable Aluminum Alloys" Applied stress = 75% of specification tensile yield strength / 40 days 3.5% NaCl solution – alternate immersion (10 min wet/50 min dry)

Tension (Modulus) – Prior to performing full-range tension testing, approximately 10% of the machined tension specimens were used to generate modulus data using the procedures outlined in ASTM E111. For this testing the specimens were loaded to a maximum stress below the proportional limit, so as to remain within the linear region of the stress-strain curve. The test was repeated three times per specimen, with the specimen being rotated 120° between test runs. Strain was measured using an MTS averaging extensometer (B-1 classification) with a one-inch gage length. The average modulus from the three runs was recorded as the final elastic modulus.

Tension – Tension testing was performed on an Instron electro-mechanical test machine in accordance with ASTM E8. Strain was measured using an Instron one-inch gage length extensometer. The extensometer was removed from the specimen prior to reaching ultimate load to prevent damage to the instrument during specimen breakage. Elongation and reduction of area measurements were made using the "fit-back" method.

Fatigue (Force-controlled) – Axial fatigue testing was performed under force-controlled conditions using an MTS servo-hydraulic test machine in accordance with ASTM

E466. Stress ratios (R) of 0.05 and -1 were used in this investigation. Replicate specimens were tested at four applied stress levels for each of the stress ratios.

Fatigue (Strain-controlled) – Axial fatigue testing was performed under strain-controlled conditions using an MTS servo-hydraulic test machine in accordance with ASTM E606. An MTS one-inch gage length extensometer was used for strain measurement. The testing frequency used was 1 Hz. Strain ratios ($R_\varepsilon = \varepsilon_{min}/\varepsilon_{max}$) of 0.05 and -1 was used for these specimens. Replicate specimens were tested at four applied strain levels for each of the strain ratios.

Fatigue Crack Growth Rate – Fatigue crack growth rate testing was performed on an MTS servo-hydraulic test machine per ASTM E647 using computer data acquisition and control systems developed in-house. Crack length was measured via using compliance techniques with standard crack-opening-displacement (COD) gages. Testing was performed under K-control (C=-2) until a near-threshold growth rate ($\sim 5 \times 10^{-8}$ in/cycle) was obtained, at which point the test was then run under constant amplitude (constant load) conditions for the remainder of the test. Initial and final crack lengths were measured optically for use in post-test crack correlation calculations. A test frequency of 25 Hz was used throughout the test, with humidity maintained at 50%, ±10% for the duration of the test. Specimens were tested using stress ratios (R) of 0.1 and 0.7. Two orientations were tested for this program, L-T and S-L, where the first letter indicates the loading direction and the second letter indicates the direction of crack propagation. The ESE(T) specimen geometry was utilized for the billet material in order to minimize any potential for out-of-plane cracking due to anisotropy in the material.

Fracture Toughness – Plane-strain fracture toughness tests were performed in accordance with ASTM E399 on a Tinius-Olsen electro-mechanical test machine. Specimen precracking was performed on an MTS servo-hydraulic test machine. Crack length was monitored via compliance techniques using an MTS COD gage as previously described. Initial and final crack lengths were measured optically post-test.

Stress corrosion cracking – The theory behind this testing was that since the billet material had not been subject to final hot working, the microstructure would not be fully homogenized, leading to the potential for localized aluminum segregation. If this were to occur, those areas would be more susceptible to the effect of stress corrosion cracking, particularly at this applied stress level.

For this investigation, stress corrosion cracking tests were therefore performed in order to simply give pass/fail results. As there is currently no ASTM test method for SCC of titanium alloys, the procedure outlined in ASTM G64 ("A" level) was used. This procedure has been adopted for use within AFRL/RXSCE as a standard SCC test. Specimens were axially loaded (statically) in an alternate immersion, 3.5% NaCl solution such that the specimens were submerged in the solution for 10 minutes and then allowed to dry for the next 50 minutes each hour. The specimens were loaded at 75% of the specification yield strength (for plate and bar). For this alloy, the applied stress was 90 ksi. The test duration

was set at 40 days. To pass the test, no failure of the specimen could occur during the 40 loading cycle.

FACTUAL DATA

Tension – The results of tensile testing are shown in Tables 2(a) through 2(e). With the exception of one specimen, strength levels for all specimens were above the specification minimum values shown in AMS-T-9046 (plate) or AMS-T-9047 (bar) for this alloy, after rounding rules were applied. However, some of the specimens did have reduction of area results that fell below the minimum properties of AMS-T-9047, particularly in the short transverse orientation. All properties that fell below a specification minimum value are highlighted in red in the tables. Also, some of the short transverse elastic modulus values were slightly lower than expected for this alloy. In general, there was less than a 5% average difference between those modulus results from ASTM E111 tests and those obtained from the E8 tensile test record, with the latter results typically being lower. In addition, there did not appear to be a significant difference between specimens excised from the three different thickness locations.

Although the "reasonable lower bound" for the alloy will be calculated and identified in a future report, for this billet a preliminary reasonable lower bound was calculated using the procedures described in MMPDS Section 9.4.1 and assuming normality in the data population. The equation used for the calculation of these preliminary values (for strength only) was:

$$Minimum\ S = \overline{X} - s * k_{99}$$

where

$\overline{X}$ = sample mean

s = standard deviation

k_{99} = one-sided tolerance-limit factor corresponding to a proportion at least 0.99 of a normal distribution and a confidence coefficient of 0.95 based on the number of specimens in the given population. For this report, a k_{99} factor of 2.68 was used, representing a population size of 101.

It should be noted that the AMS-T-9046 specification does not list minimum properties for the short-transverse orientation. Due to evidence indicating that non-conforming materials have been cut-down from billet and purported as plate or bar, the expected orientation system may not have been known during component fabrication. Therefore, the results from the two orientations tested have been grouped together in order to provide reasonable lower bound properties. After calculating these values, they were compared with both the specification minimums and MMPDS A-basis allowables. The lesser of the values were established as the reasonable lower bound property. These preliminary reasonable lower bound properties are shown in Table 3. For modulus, elongation, and reduction of area, the minimum value from the data has been used as the preliminary reasonable lower bound.

Approved for public release; distribution unlimited.

Table 2. Tensile test results.
(a) Longitudinal orientation, t/4 thickness location

	Orientation	Thickness Location	Yield Strength (ksi)	Ultimate Tensile Strength (ksi)	% Elongation	% Reduction of Area	Elastic Modulus, E111 (msi)	Elastic Modulus, E8 (msi)
K27PA-T-L-1-A	L	t/4	126.4	134.7	14.8%	27.9%	17.4	16.6
L-2-A	L	t/4	126.4	134.4	15.3%	27.9%	17.4	16.3
L-3-A	L	t/4	127.2	134.8	17.7%	26.1%		16.3
L-4-A	L	t/4	127.5	136.5	15.6%	27.8%		17.1
L-5-A	L	t/4	126.1	133.8	16.1%	28.7%		17.0
L-6-A	L	t/4	126.6	135.0	16.2%	29.1%		16.3
L-7-A	L	t/4	126.7	134.9	14.6%	25.0%		16.3
L-8-A	L	t/4	126.7	134.3	14.2%	27.1%		16.3
L-9-A	L	t/4	125.9	133.8	16.3%	26.0%		16.3
L-10-A	L	t/4	125.8	133.7	12.1%	26.0%		17.7
L-11-A	L	t/4	126.7	134.6	15.1%	30.0%		17.8
L-12-A	L	t/4	127.3	135.2	15.1%	27.4%		17.4
L-13-A	L	t/4	128.6	137.1	14.9%	25.9%		17.8
L-14-A	L	t/4	126.1	133.8	16.0%	29.2%		17.1
K27PB-T-L-15-A	L	t/4	126.1	134.3	15.7%	24.1%	17.4	16.8
L-16-A	L	t/4	125.4	133.5	15.3%	26.6%	17.4	16.7
L-17-A	L	t/4	125.7	134.6	13.7%	22.0%		16.7
L-18-A	L	t/4	127.2	135.9	15.2%	25.8%		17.1
L-19-A	L	t/4	126.2	134.2	17.2%	26.4%		16.3
L-20-A	L	t/4	126.4	134.6	14.1%	24.5%		17.3
L-21-A	L	t/4	126.4	134.8	14.6%	27.3%		17.1
L-22-A	L	t/4	125.7	133.8	13.9%	25.8%		17.0
L-23-A	L	t/4	124.1	132.1	13.8%	26.6%		17.1
L-24-A	L	t/4	126.0	134.1	13.5%	24.9%		17.3
L-25-A	L	t/4	125.1	132.5	14.0%	27.5%		16.5
L-26-A	L	t/4	125.0	132.6	13.7%	24.7%		16.7
L-27-A	L	t/4	126.4	134.1	16.3%	22.9%		16.4
L-28-A	L	t/4	128.0	135.6	16.5%	31.0%		17.2

Approved for public release; distribution unlimited.

K27PC-T-L-29-A	L	t/4	126.5	134.4	15.6%	29.7%	17.4	16.2
L-30-A	L	t/4	126.9	135.1	13.8%	24.7%	17.6	17.0
L-31-A	L	t/4	126.8	134.9	14.7%	23.5%		17.0
L-32-A	L	t/4	126.7	134.8	14.4%	27.4%		16.5
L-33-A	L	t/4	126.5	134.1	16.5%	23.4%		16.6
L-34-A	L	t/4	127.4	135.3	16.2%	23.4%		16.8
L-35-A	L	t/4	128.2	136.0	14.4%	27.9%		17.1
L-36-A	L	t/4	126.7	134.4	16.0%	32.2%		16.6
L-37-A	L	t/4	125.0	133.3	15.3%	28.0%		16.9
L-38-A	L	t/4	125.9	132.7	15.5%	28.6%		17.2
L-39-A	L	t/4	127.3	134.8	17.2%	24.2%		17.1
L-40-A	L	t/4	128.4	136.1	15.2%	28.4%		17.3
L-41-A	L	t/4	127.7	135.2	15.3%	29.5%		17.0
L-42-A	L	t/4	127.5	134.9	13.8%	30.6%		17.0
K27PD-T-L-43-A	L	t/4	127.3	134.7	14.7%	28.7%	17.5	16.5
L-44-A	L	t/4	126.6	133.8	11.9%	21.0%	17.4	16.1
L-45-A	L	t/4	127.3	134.7	14.4%	27.2%		17.0
L-46-A	L	t/4	126.6	133.9	16.2%	24.2%		16.9
L-47-A	L	t/4	126.3	133.3	15.8%	27.4%		17.0
L-48-A	L	t/4	126.7	133.8	14.9%	28.8%		16.2
L-49-A	L	t/4	126.1	133.8	11.0%	19.4%		16.5
L-50-A	L	t/4	126.5	134.8	15.2%	27.7%		17.0
L-51-A	L	t/4	126.3	133.6	14.9%	27.0%		16.8
L-52-A	L	t/4	126.6	133.6	14.1%	29.5%		15.9
L-53-A	L	t/4	129.2	137.1	13.8%	27.0%		16.5
L-54-A	L	t/4	127.4	134.6	18.3%	25.0%		16.6
L-55-A	L	t/4	127.2	135.1	16.1%	30.3%		17.0
L-56-A	L	t/4	128.3	135.3	15.1%	28.5%		16.6
AMS-T-9046			120	130	10%			
AMS-T-9047 (4" & under)			120	130	10%	25%		
AMS-T-9047 (4"-6")			120	130	10% [8%][a]	20% [15%][a]		
MMPDS A-basis			118	130	10			16.0

(a) Values in brackets [ ] apply to the short transverse orientation for short transverse dimensions of 3.0 inches or greater.

Approved for public release; distribution unlimited.

(b) Longitudinal orientation, t/2 thickness location

	Orientation	Thickness Location	Yield Strength (ksi)	Ultimate Tensile Strength (ksi)	% Elongation	% Reduction of Area	Elastic Modulus, E111 (msi)	Elastic Modulus, E8 (msi)
K27PA-T-L-1-B	L	t/2	125.6	134.8	15.9%	23.4%	17.8	17.0
L-2-B	L	t/2	126.2	135.6	13.0%	26.2%	17.7	16.8
L-3-B	L	t/2	124.6	132.7	13.7%	30.5%		16.6
L-4-B	L	t/2	123.5	132.4	14.4%	23.3%		16.1
L-5-B	L	t/2	123.2	131.6	15.2%	31.0%		17.1
L-6-B	L	t/2	123.3	131.2	16.5%	34.3%		16.4
L-7-B	L	t/2	125.9	135.1	12.6%	29.0%		17.2
L-8-B	L	t/2	125.2	133.9	14.6%	28.8%		17.0
L-9-B	L	t/2	126.5	134.8	13.5%	28.7%		17.2
L-10-B	L	t/2	126.9	135.0	13.9%	26.8%		16.1
L-11-B	L	t/2	127.1	135.6	16.3%	29.7%		16.1
L-12-B	L	t/2	126.6	135.1	17.6%	34.9%		16.6
L-13-B	L	t/2	127.7	136.6	18.6%	29.3%		16.7
L-14-B	L	t/2	127.5	135.8	15.3%	28.2%		17.3
K27PB-T-L-15-B	L	t/2	124.6	133.0	14.2%	26.5%	17.2	17.1
L-16-B	L	t/2	123.9	132.4	15.4%	28.5%	17.2	16.3
L-17-B	L	t/2	125.0	134.5	15.3%	24.3%		16.6
L-18-B	L	t/2	122.3	130.1	13.0%	25.9%		16.9
L-19-B	L	t/2	122.1	129.8	14.7%	33.3%		16.4
L-20-B	L	t/2	123.8	132.6	15.8%	26.2%		16.1
L-21-B	L	t/2	121.8	129.9	12.0%	29.7%		16.3
L-22-B	L	t/2	124.5	133.1	13.8%	23.3%		16.1
L-23-B	L	t/2	125.1	133.5	17.0%	24.9%		16.2
L-24-B	L	t/2	126.1	133.5	13.7%	29.0%		16.2
L-25-B	L	t/2	126.8	134.8	18.1%	33.0%		17.0
L-26-B	L	t/2	127.3	135.0	14.3%	31.4%		16.8
L-27-B	L	t/2	127.6	135.6	14.4%	28.0%		16.2
L-28-B	L	t/2	128.1	136.5	16.7%	29.0%		16.5

Approved for public release; distribution unlimited.

K27PC-T-L-29-B	L	t/2	123.4	131.2	14.2%	24.1%	17.3	16.8
L-30-B	L	t/2	124.2	132.0	15.6%	31.8%	17.3	16.2
L-31-B	L	t/2	123.6	131.4	14.5%	34.6%		15.8
L-32-B	L	t/2	123.1	130.4	13.1%	30.2%		16.0
L-33-B	L	t/2	124.1	132.4	16.2%	27.8%		16.8
L-34-B	L	t/2	124.1	132.2	14.4%	31.7%		17.1
L-35-B	L	t/2	122.9	130.4	14.4%	29.5%		16.0
L-36-B	L	t/2	126.4	134.7	15.6%	31.5%		16.8
L-37-B	L	t/2	126.2	134.1	13.0%	29.2%		16.8
L-38-B	L	t/2	126.3	135.2	16.6%	32.7%		16.4
L-39-B	L	t/2	126.4	134.8	15.5%	25.1%		15.9
L-40-B	L	t/2	126.3	134.7	14.2%	23.4%		16.2
L-41-B	L	t/2	127.7	133.9	14.3%	31.7%		16.2
L-42-B	L	t/2	128.0	136.7	14.1%	22.7%		16.9
K27PD-T-L-43-B	L	t/2	126.0	133.8	17.3%	32.5%	17.8	16.4
L-44-B	L	t/2	123.7	131.5	12.1%	26.9%	17.3	16.6
L-45-B	L	t/2	123.4	131.4	14.4%	24.2%		17.0
L-46-B	L	t/2	121.5	128.7	*a*	23.9%		15.7
L-47-B	L	t/2	123.2	130.6	16.2%	31.8%		16.4
L-48-B	L	t/2	123.1	130.5	15.7%	30.5%		15.8
L-49-B	L	t/2	124.6	132.8	16.9%	31.2%		16.9
L-50-B	L	t/2	123.9	131.8	14.6%	27.0%		16.4
L-51-B	L	t/2	125.2	134.0	16.4%	24.6%		16.6
L-52-B	L	t/2	125.6	133.8	14.8%	24.7%		16.2
L-53-B	L	t/2	124.9	133.2	15.5%	28.0%		17.1
L-54-B	L	t/2	126.5	134.1	13.9%	25.7%		16.3
L-55-B	L	t/2	126.5	134.4	13.7%	29.5%		17.2
L-56-B	L	t/2	127.5	135.3	15.0%	32.1%		16.0
AMS-T-9046			120	130	10%			
AMS-T-9047 (4" & under)			120	130	10%	25%		
AMS-T-9047 (4"-6")			120	130	10% [8%][b]	20% [15%][b]		
MMPDS A-basis			118	130	10%			16.0

(a) Specimen broke at gage punch location.
(b) Values in brackets [ ] apply to the short transverse orientation for short transverse dimensions of 3.0 inches or greater.

Approved for public release; distribution unlimited.

(c) Longitudinal orientation, 3t/4 thickness location

	Orientation	Thickness Location	Yield Strength (ksi)	Ultimate Tensile Strength (ksi)	% Elongation	% Reduction of Area	Elastic Modulus, E111 (msi)	Elastic Modulus, E8 (msi)
K27PA-T-L-1-C	L	3t/4	127.3	135.6	15.8%	32.3%		17.4
L-2-C	L	3t/4	125.8	133.8	12.7%	26.1%		16.7
L-3-C	L	3t/4	127.2	135.8	16.6%	28.8%	17.6	17.3
L-4-C	L	3t/4	126.4	135.1	16.2%	29.6%	17.4	17.0
L-5-C	L	3t/4	126.9	135.2	15.3%	26.2%		16.4
L-6-C	L	3t/4	127.3	135.7	14.4%	31.0%		17.2
L-7-C	L	3t/4	127.7	136.2	15.7%	29.8%		17.0
L-8-C	L	3t/4	127.0	135.8	14.0%	27.4%		17.6
L-9-C	L	3t/4	127.5	136.6	15.3%	25.0%		17.1
L-10-C	L	3t/4	128.5	138.5	15.7%	26.5%		17.3
L-11-C	L	3t/4	127.4	136.2	12.9%	23.8%		17.9
L-12-C	L	3t/4	126.2	134.1	14.6%	28.3%		16.1
L-13-C	L	3t/4	126.9	134.5	15.6%	29.2%		16.4
L-14-C	L	3t/4	127.0	135.7	17.2%	30.1%		17.5
K27PB-T-L-15-C	L	3t/4	126.8	135.3	16.9%	28.6%		17.1
L-16-C	L	3t/4	128.0	136.2	15.7%	27.6%		17.2
L-17-C	L	3t/4	126.5	134.8	16.8%	24.0%		17.5
L-18-C	L	3t/4	128.0	136.3	14.1%	27.2%		16.7
L-19-C	L	3t/4	127.4	136.1	15.2%	24.6%		17.3
L-20-C	L	3t/4	126.8	135.1	14.9%	26.0%	17.4	16.2
L-21-C	L	3t/4	127.5	136.1	16.0%	27.9%	17.5	16.2
L-22-C	L	3t/4	128.4	137.4	15.0%	29.7%		16.8
L-23-C	L	3t/4	128.0	136.7	15.1%	24.0%		16.6
L-24-C	L	3t/4	126.9	135.4	14.8%	27.1%		17.1
L-25-C	L	3t/4	127.6	135.7	15.6%	30.6%		16.1
L-26-C	L	3t/4	128.3	137.7	16.0%	20.6%		16.8
L-27-C	L	3t/4	128.3	137.1	16.9%	30.8%		16.9
L-28-C	L	3t/4	128.2	135.9	13.6%	27.5%		16.3

Approved for public release; distribution unlimited.

K27PC-T-L-29-C	L	3t/4	128.0	136.1	13.1%	25.4%	17.8	16.9
L-30-C	L	3t/4	127.3	135.6	15.2%	24.0%	17.6	16.3
L-31-C	L	3t/4	126.5	134.4	15.1%	30.0%		17.3
L-32-C	L	3t/4	127.1	134.9	16.6%	32.1%		17.1
L-33-C	L	3t/4	127.3	135.0	16.5%	30.0%		16.6
L-34-C	L	3t/4	127.6	135.6	13.5%	29.7%		16.6
L-35-C	L	3t/4	127.6	135.7	15.9%	31.4%		17.0
L-36-C	L	3t/4	128.6	136.5	15.5%	27.4%		16.8
L-37-C	L	3t/4	129.7	138.9	14.9%	25.3%		17.0
L-38-C	L	3t/4	131.0	140.8	16.9%	29.1%		16.9
L-39-C	L	3t/4	131.5	140.6	17.5%	26.6%		17.2
L-40-C	L	3t/4	128.2	136.4	16.5%	29.2%		16.9
L-41-C	L	3t/4	128.9	137.1	14.7%	31.7%		16.9
L-42-C	L	3t/4	127.9	135.8	14.8%	22.6%		17.3
K27PD-T-L-43-C	L	3t/4	124.7	131.6	12.9%	31.1%	17.1	16.6
L-44-C	L	3t/4	123.0	131.4	13.7%	28.1%	17.0	15.8
L-45-C	L	3t/4	125.5	133.0	15.6%	29.0%		16.2
L-46-C	L	3t/4	124.9	132.8	16.6%	30.6%		16.6
L-47-C	L	3t/4	124.3	131.2	15.0%	27.2%		16.4
L-48-C	L	3t/4	126.1	134.7	14.7%	27.6%		16.6
L-49-C	L	3t/4	125.8	133.8	16.0%	27.7%		16.0
L-50-C	L	3t/4	125.5	132.2	16.5%	29.5%		16.2
L-51-C	L	3t/4	128.8	137.7	16.1%	24.3%		17.1
L-52-C	L	3t/4	130.1	139.1	13.8%	26.9%		16.8
L-53-C	L	3t/4	128.5	136.6	14.8%	26.3%		16.9
L-54-C	L	3t/4	128.5	136.5	15.9%	28.7%		17.0
L-55-C	L	3t/4	127.6	134.6	14.5%	27.5%		16.5
L-56-C	L	3t/4	128.9	136.2	15.5%	27.3%		16.7
AMS-T-9046			120	130	10%			
AMS-T-9047 (4" & under)			120	130	10%	25%		
AMS-T-9047 (4"-6")			120	130	10% [8%][a]	20% [15%][a]		
MMPDS A-basis			118	130	10%			16.0

(a) Values in brackets [ ] apply to the short transverse orientation for short transverse dimensions of 3.0 inches or greater.

Approved for public release; distribution unlimited.

(d) Short-transverse orientation, t/4 thickness location

	Orientation	Thickness Location	Yield Strength (ksi)	Ultimate Tensile Strength (ksi)	% Elongation	% Reduction of Area	Elastic Modulus, E111 (Msi)	Elastic Modulus, E8 (Msi)
K27PA-T-S-1-A	S	t/4	125.5	137.7	10.9%	17.1%	16.7	15.8
S-2-A	S	t/4	125.7	137.3	11.6%	20.0%	16.7	16.0
S-3-A	S	t/4	124.3	135.2	10.3%	21.3%		15.8
S-4-A	S	t/4	124.7	136.9	9.7%	17.9%		16.1
K27PB-T-S-5-A	S	t/4	125.9	137.3	11.3%	18.0%	16.8	16.1
S-6-A	S	t/4	127.1	135.5	11.8%	18.1%	16.8	16.0
S-7-A	S	t/4	124.5	136.2	10.7%	16.0%		16.5
S-8-A	S	t/4	124.9	135.5	11.6%	18.4%		15.8
K27PC-T-S-9-A	S	t/4	125.6	135.7	13.1%	21.6%	16.7	15.7
S-10-A	S	t/4	124.1	135.5	11.0%	17.9%	16.6	15.3
S-11-A	S	t/4	126.5	138.0	13.2%	16.8%		15.7
S-12-A	S	t/4	125.4	136.8	13.7%	21.8%		16.1
K27PD-T-S-13-A	S	t/4	125.2	135.6	11.6%	21.9%	16.5	15.4
S-14-A	S	t/4	125.2	135.1	12.8%	14.1%	16.7	15.5
S-15-A	S	t/4	126.0	136.9	11.7%	18.4%		15.6
S-16-A	S	t/4	125.4	136.8	11.0%	20.1%		15.5
AMS-T-9046			120	130	10%			
AMS-T-9047 (4" & under)			120	130	10%	25%		
AMS-T-9047 (4"-6")			120	130	10% [8%][a]	20% [15%][a]		
MMPDS A-basis			118	130	10%			16.0

(a) Values in brackets [ ] apply to the short transverse orientation for short transverse dimensions of 3.0 inches or greater.

(e) Short-transverse orientation, 3t/4 thickness location

	Orientation	Thickness Location	Yield Strength (ksi)	Ultimate Tensile Strength (ksi)	% Elongation	% Reduction of Area	Elastic Modulus, E111 (Msi)	Elastic Modulus, E8 (Msi)
K27PA-T-S-1-C	S	3t/4	125.4	137.1	10.9%	16.2%		15.4
S-2-C	S	3t/4	124.5	136.7	12.4%	18.0%	16.5	15.7
S-3-C	S	3t/4	125.3	138.0	10.2%	14.5%	16.6	15.6
S-4-C	S	3t/4	125.9	137.7	12.6%	19.3%		15.7
K27PB-T-S-5-C	S	3t/4	125.9	137.1	12.9%	19.6%	16.7	15.9
S-6-C	S	3t/4	124.5	136.1	11.1%	17.1%	16.4	15.7
S-7-C	S	3t/4	125.8	137.1	11.7%	14.8%		15.6
S-8-C	S	3t/4	126.3	138.4	10.9%	14.3%		15.6
K27PC-T-S-9-C	S	3t/4	123.6	134.3	10.5%	21.4%	16.6	15.6
S-10-C	S	3t/4	125.1	135.9	11.8%	19.8%	16.8	15.6
S-11-C	S	3t/4	124.6	136.9	13.1%	20.7%		16.5
S-12-C	S	3t/4	125.5	137.3	11.8%	20.2%		15.6
K27PD-T-S-13-C	S	3t/4	122.0	132.3	10.5%	19.8%	16.7	15.4
S-14-C	S	3t/4	121.8	132.1	12.9%	20.2%	16.5	15.3
S-15-C	S	3t/4	125.6	137.1	10.8%	22.3%		16.3
S-16-C	S	3t/4	125.7	137.0	10.8%	21.5%		16.3
AMS-T-9046			120	130	10%			
AMS-T-9047 (4" & under)			120	130	10%	25%		
AMS-T-9047 (4"-6")			120	130	10% [8%][b]	20% [15%][b]		
MMPDS A-basis			118	130	10%			16.0

(a) Specimen failed at gage punch location.
(b) Values in brackets [ ] apply to the short transverse orientation for short transverse dimensions of 3.0 inches or greater.

Table 3. Preliminary reasonable lower bound tensile properties for Ti-6Al-4V billet (#K27P).

Yield Strength (ksi)	Ultimate Tensile Strength (ksi)	% Elongation	% Reduction of Area	Elastic Modulus (msi)
118	130	10%	14%	15.3

Approved for public release; distribution unlimited.

Fatigue (force-controlled) – The results of force-controlled axial fatigue testing are shown graphically in Figure 8. Individual results are tabulated in Tables 4 (a) and (b). In Figure 8, the results for each stress ratio (R) and orientation have been fit with a best-fit power-law curve for graphical purposes only. Also included in this figure is a curve based on an equivalent stress equation from MMPDS Figure 5.4.1.1.8(a) for a mean stress of zero (R = -1). This curve is for comparison with the R = -1 data generated in this investigation. As stated in Figure 4, the fatigue specimens used herein were manufactured using low-stress-grinding operations to a surface finish (Ra) of 8 per the ASTM E466 Standard. The MMPDS reference data curve was generated from specimens having a surface roughness of 32. Furthermore, it is not known whether low-stress grinding was used on these specimens. These aspects could quite easily have contributed to the difference between the data sets.

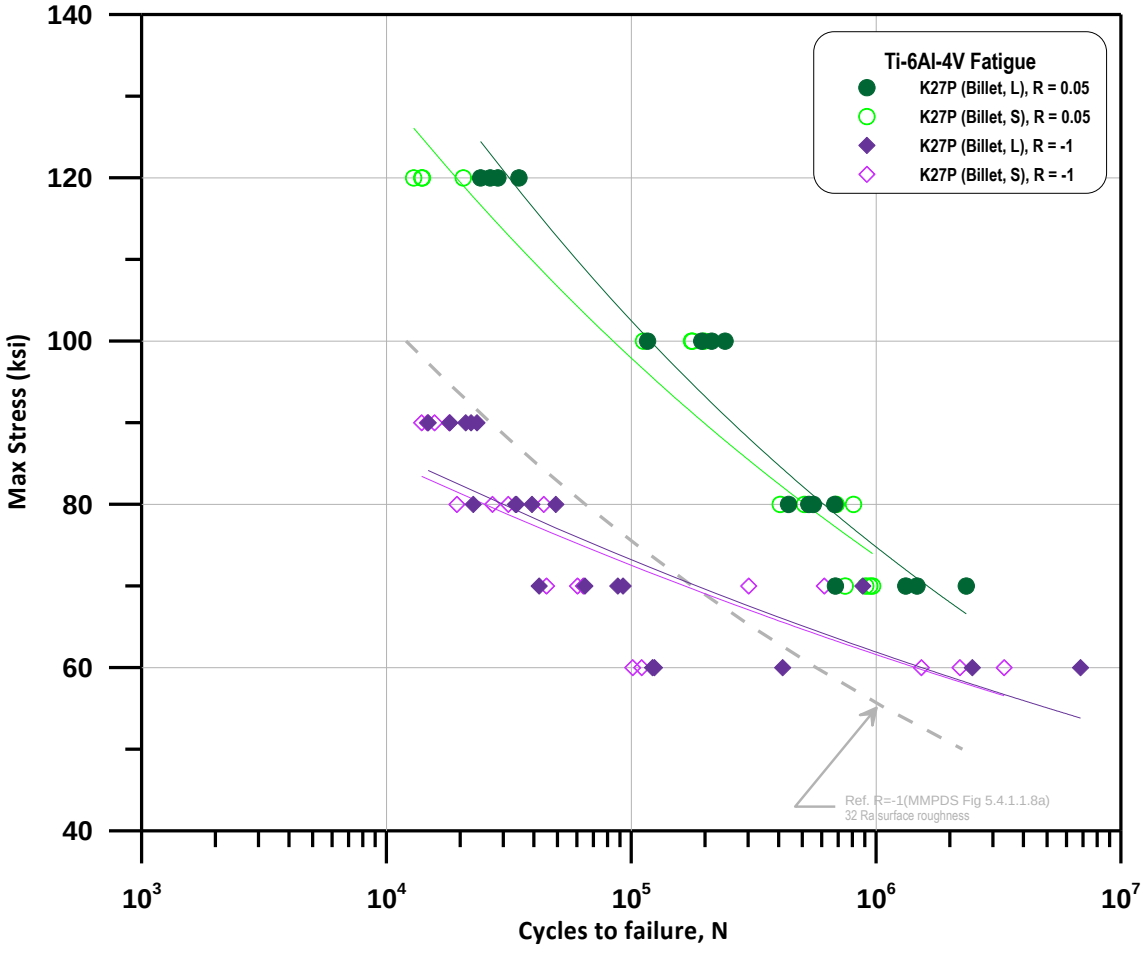


Figure 8. Force-controlled axial fatigue test results.

Approved for public release; distribution unlimited.

Table 4. Force-controlled axial fatigue test results.
(a) R = 0.05

	Thickness Location	Orientation	Max Stress (ksi)	Stress Ratio, R	Cycles to Failure
K27PC-F-L-18-A	t/4	L	120	0.05	26,510
K27PD-F-L-22-A	t/4	L	120	0.05	28,500
K27PB-F-L-12-B	t/2	L	120	0.05	24,210
K27PC-F-L-18-C	3t/4	L	120	0.05	34,710
K27PA-F-L-6-A	t/4	L	100	0.05	193,690
K27PA-F-L-6-B	t/2	L	100	0.05	212,970
K27PD-F-L-23-B	t/2	L	100	0.05	241,290
K27PB-F-L-12-C	3t/4	L	100	0.05	116,430
K27PB-F-L-12-A	t/4	L	80	0.05	530,520
K27PC-F-L-18-B	t/2	L	80	0.05	553,540
K27PD-F-L-22-B	t/2	L	80	0.05	677,000
K27PD-F-L-22-C	3t/4	L	80	0.05	438,490
K27PD-F-L-24-A	t/4	L	70	0.05	1,467,700
K27PD-F-L-24-B	t/2	L	70	0.05	681,030
K27PA-F-L-6-C	3t/4	L	70	0.05	2,332,410
K27PD-F-L-23-C	3t/4	L	70	0.05	1,319,690
K27PD-F-S-61-B	t/2	S	120	0.05	12,910
K27PC-F-S-47-B	t/2	S	120	0.05	13,920
K27PA-F-S-13-B	t/2	S	120	0.05	20,580
K27PC-F-S-45-B	t/2	S	120	0.05	14,010
K27PD-F-S-63-B	t/2	S	100	0.05	112,110
K27PC-F-S-46-B	t/2	S	100	0.05	176,010
K27PD-F-S-64-B	t/2	S	100	0.05	198,140
K27PA-F-S-16-B	t/2	S	100	0.05	177,530
K27PD-F-S-62-B	t/2	S	80	0.05	686,950
K27PC-F-S-48-B	t/2	S	80	0.05	508,620
K27PA-F-S-15-B	t/2	S	80	0.05	807,970
K27PB-F-S-31-B	t/2	S	80	0.05	405,590
K27PA-F-S-14-B	t/2	S	70	0.05	746,580
K27PB-F-S-30-B	t/2	S	70	0.05	941,580
K27PB-F-S-29-B	t/2	S	70	0.05	905,960
K27PB-F-S-32-B	t/2	S	70	0.05	966,380

Approved for public release; distribution unlimited.

(b) R = -1

	Thickness Location	Orientation	Max Stress (ksi)	Stress Ratio, R	Cycles to Failure
K27PA-F-L-1-A	t/4	L	90	-1	21,057
K27PB-F-L-8-A	t/4	L	90	-1	23,392
K27PB-F-L-10-A	t/4	L	90	-1	14,784
K27PA-F-L-3-B	t/2	L	90	-1	18,124
K27PC-F-L-13-B	t/2	L	90	-1	22,153
K27PA-F-L-5-A	t/4	L	80	-1	22,582
K27PA-F-L-1-B	t/2	L	80	-1	33,604
K27PB-F-L-10-B	t/2	L	80	-1	33,945
K27PA-F-L-3-C	3t/4	L	80	-1	39,256
K27PC-F-L-13-C	3t/4	L	80	-1	49,095
K27PC-F-L-15-A	t/4	L	70	-1	88,100
K27PB-F-L-8-B	t/2	L	70	-1	881,164
K27PA-F-L-1-C	3t/4	L	70	-1	64,604
K27PA-F-L-5-C	3t/4	L	70	-1	42,025
K27PB-F-L-10-C	3t/4	L	70	-1	92,443
K27PA-F-L-3-A	t/4	L	60	-1	124,153
K27PC-F-L-13-A	t/4	L	60	-1	414,646
K27PA-F-L-5-B	t/2	L	60	-1	6,836,683
K27PC-F-L-15-B	t/2	L	60	-1	122,060
K27PB-F-L-8-C	3t/4	L	60	-1	2,468,536
K27PA-F-S-2-B	t/2	S	90	-1	18,058
K27PE-F-S-67-B	t/2	S	90	-1	15,694
K27PD-F-S-52-B	t/2	S	90	-1	14,670
K27PB-F-S-20-B	t/2	S	90	-1	13,903
K27PB-F-S-18-B	t/2	S	80	-1	19,384
K27PE-F-S-66-B	t/2	S	80	-1	27,065
K27PB-F-S-17-B	t/2	S	80	-1	31,424
K27PA-F-S-4-B	t/2	S	80	-1	43,866
K27PE-F-S-65-B	t/2	S	70	-1	63,686
K27PB-F-S-19-B	t/2	S	70	-1	301,379
K27PD-F-S-50-B	t/2	S	70	-1	614,040
K27PC-F-S-35-B	t/2	S	70	-1	45,034
K27PA-F-S-3-B	t/2	S	70	-1	60,254
K27PC-F-S-33-B	t/2	S	60	-1	1,529,071
K27PD-F-S-51-B	t/2	S	60	-1	2,198,996
K27PC-F-S-34-B	t/2	S	60	-1	110,116
K27PD-F-S-49-B	t/2	S	60	-1	101,203
K27PA-F-S-1-B	t/2	S	60	-1	3,334,177

Approved for public release; distribution unlimited.

Fatigue (strain-controlled) – The results of strain-controlled axial fatigue testing are shown graphically in Figure 9, with individual results tabulated in Table 5. In Figure 9, the results for each strain ratio (R_ε) and orientation have been fit with a best-fit power-law curve for graphical purposes only.

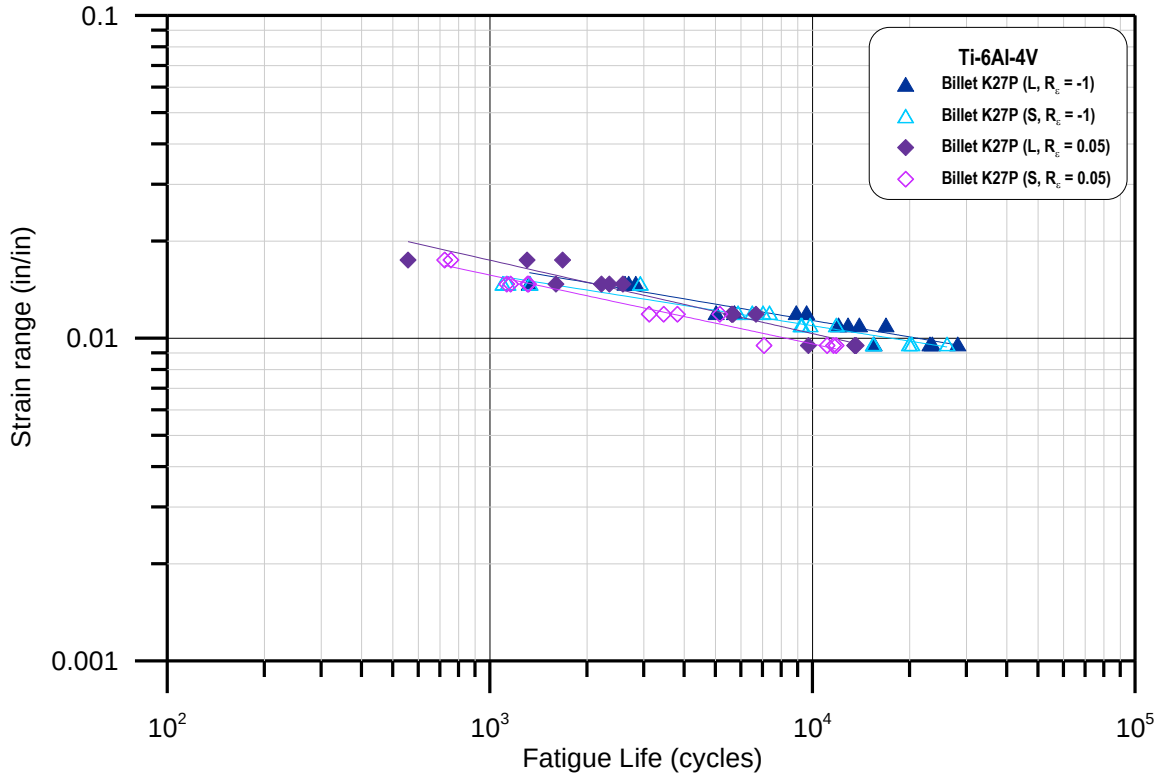


Figure 9. Strain-controlled axial fatigue test results.

Approved for public release; distribution unlimited.

Table 5. Strain-controlled axial fatigue test results.
(a) $R_\varepsilon = 0.05$

	Thickness Location	Orientation	Strain Range (in/in)	Strain Ratio, R_ε	Cycles to Failure
K27PA-F-L-4-A	t/4	L	0.0175	0.05	1,474
K27PE-F-L-25-A	t/4	L	0.0175	0.05	1,678
K27PB-F-L-7-B	t/2	L	0.0175	0.05	1,006
K27PD-F-L-21-B	t/2	L	0.0175	0.05	557
K27PC-F-L-17-C	3t/4	L	0.0175	0.05	1,303
K27PE-F-L-25-C	3t/4	L	0.0175	0.05	1,664
K27PA-F-L-2-A	t/4	L	0.0147	0.05	2,344
K27PD-F-L-20-A	t/4	L	0.0147	0.05	1,602
K27PE-F-L-27-A	t/4	L	0.0147	0.05	2,566
K27PA-F-L-4-B	t/2	L	0.0147	0.05	2,215
K27PB-F-L-7-C	3t/4	L	0.0147	0.05	2,583
K27PC-F-L-17-A	t/4	L	0.0119	0.05	5,631
K27PA-F-L-2-B	t/2	L	0.0119	0.05	5,671
K27PD-F-L-20-B	t/2	L	0.0119	0.05	6,679
K27PE-F-L-25-B	t/2	L	0.0119	0.05	7,376
K27PA-F-L-4-C	3t/4	L	0.0119	0.05	5,618
K27PB-F-L-7-A	t/4	L	0.0095	0.05	13,522
K27PC-F-L-17-B	t/2	L	0.0095	0.05	9,700
K27PE-F-L-27-B	t/2	L	0.0095	0.05	11,057
K27PA-F-L-2-C	3t/4	L	0.0095	0.05	13,516
K27PD-F-L-20-C	3t/4	L	0.0095	0.05	13,651
K27PE-F-L-27-C	3t/4	L	0.0095	0.05	14,525
K27PB-B-S-21-B	t/2	S	0.0175	0.05	706
K27PC-F-S-37-B	t/2	S	0.0175	0.05	757
K27PD-F-S-53-B	t/2	S	0.0175	0.05	724
K27PE-F-S-69-B	t/2	S	0.0175	0.05	946
K27PE-F-S-70-B	t/2	S	0.0175	0.05	901
K27PA-F-S-6-B	t/2	S	0.0147	0.05	1,308
K27PB-F-S-22-B	t/2	S	0.0147	0.05	1,159
K27PC-F-S-38-B	t/2	S	0.0147	0.05	1,127
K27PD-F-S-54-B	t/2	S	0.0147	0.05	1,317
K27PA-F-S-7-B	t/2	S	0.0119	0.05	5,157
K27PB-F-S-23-B	t/2	S	0.0119	0.05	3,115
K27PC-F-S-39-B	t/2	S	0.0119	0.05	3,456
K27PD-F-S-55-B	t/2	S	0.0119	0.05	3,812
K27PA-F-S-8-B	t/2	S	0.0095	0.05	7,068
K27PC-F-S-40-B	t/2	S	0.0095	0.05	11,092
K27PD-F-S-56-B	t/2	S	0.0095	0.05	11,836
K27PD-F-S-60-B	t/2	S	0.0095	0.05	11,620
K27PE-F-S-71-B	t/2	S	0.0095	0.05	13,012

Approved for public release; distribution unlimited.

(b) R_ε = -1

	Thickness Location	Orientation	Strain Range (in/in)	Strain Ratio, R_ε	Cycles to Failure
K27PB-F-L-9-A	t/4	L	0.0148	-1	2,833
K27PC-F-L-16-A	t/4	L	0.0148	-1	2,621
K27PE-F-L-26-A	t/4	L	0.0148	-1	2,909
K27PB-F-L-11-B	t/2	L	0.0148	-1	1,324
K27PC-F-L-14-C	3t/4	L	0.0148	-1	2,691
K27PB-F-L-11-A	t/4	L	0.0120	-1	5,725
K27PB-F-L-9-B	t/2	L	0.0120	-1	9,583
K27PC-F-L-16-B	t/2	L	0.0120	-1	5,022
K27PE-F-L-26-B	t/2	L	0.0120	-1	11,267
K27PB-F-L-11-C	3t/4	L	0.0120	-1	8,900
K27PC-F-L-14-A	t/4	L	0.0110	-1	13,970
K27PD-F-L-19-B	t/2	L	0.0110	-1	12,034
K27PB-F-L-9-C	3t/4	L	0.0110	-1	16,884
K27PD-F-L-19-C	3t/4	L	0.0110	-1	12,879
K27PD-F-L-21-C	3t/4	L	0.0110	-1	7,659
K27PD-F-L-19-A	t/4	L	0.0096	-1	23,493
K27PD-F-L-21-A	t/4	L	0.0096	-1	23,124
K27PC-F-L-14-B	t/2	L	0.0096	-1	28,168
K27PC-F-L-16-C	3t/4	L	0.0096	-1	15,511
K27PE-F-L-26-C	3t/4	L	0.0096	-1	18,754
K27PA-F-S-5-B	t/2	S	0.0148	-1	1,336
K27PA-F-S-12-B	t/2	S	0.0148	-1	1,332
K27PB-F-S-28-B	t/2	S	0.0148	-1	1,096
K27PC-F-S-43-B	t/2	S	0.0148	-1	1,138
K27PE-F-S-68-B	t/2	S	0.0148	-1	2,925
K27PA-F-S-9-B	t/2	S	0.0120	-1	6,499
K27PB-F-S-25-B	t/2	S	0.0120	-1	7,351
K27PC-F-S-36-B	t/2	S	0.0120	-1	7,026
K27PC-F-S-44-B	t/2	S	0.0120	-1	5,877
K27PA-F-S-10-B	t/2	S	0.0110	-1	9,208
K27PB-F-S-26-B	t/2	S	0.0110	-1	9,831
K27PC-F-S-41-B	t/2	S	0.0110	-1	9,270
K27PD-F-S-57-B	t/2	S	0.0110	-1	11,845
K27PA-F-S-11-B	t/2	S	0.0096	-1	15,422
K27PC-F-S-42-B	t/2	S	0.0096	-1	20,320
K27PD-F-S-58-B	t/2	S	0.0096	-1	15,478
K27PD-F-S-59-B	t/2	S	0.0096	-1	19,944
K27PE-F-S-72-B	t/2	S	0.0096	-1	26,116

Approved for public release; distribution unlimited.

Fatigue Crack Growth Rate – Fatigue crack growth rate test result summary curves are shown in Figures 10 and 11 for stress ratios (R) of 0.1 and 0.7, respectively. Individual specimen curves are located in Appendix A of this report. For both stress ratios, the S-L orientation specimens tended to have faster growth rates than the L-T specimens. Also included on these summary curves are best-fit mean curves from MMPDS-04 Figure 5.4.1.1.9(a1) for 0.25 inch thick Ti-6Al-4V plate (L-T orientation). Comparing the data generated from billet specimens with the MMPDS reference data, the combined orientation billet data generally exhibits slower growth rates over the range of stress intensities examined. Fractographic and metallographic examinations of the failed specimens will be performed to investigate possible reasons for this difference in growth rates. For example, larger grain (or colony) sizes in the billet material could lead to slower growth rates.

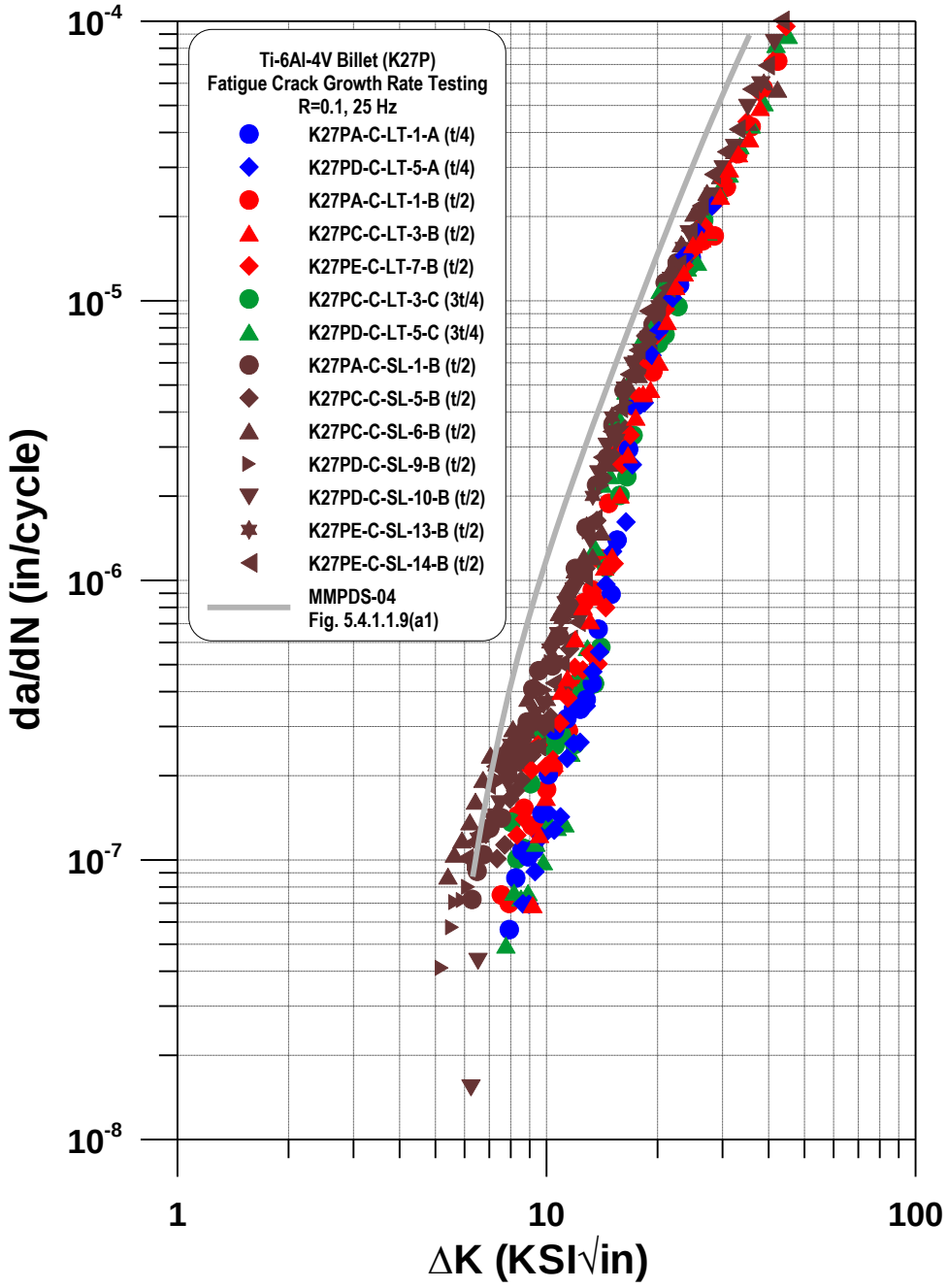


Figure 10. Fatigue crack growth rate test results (R=0.1).

Approved for public release; distribution unlimited.

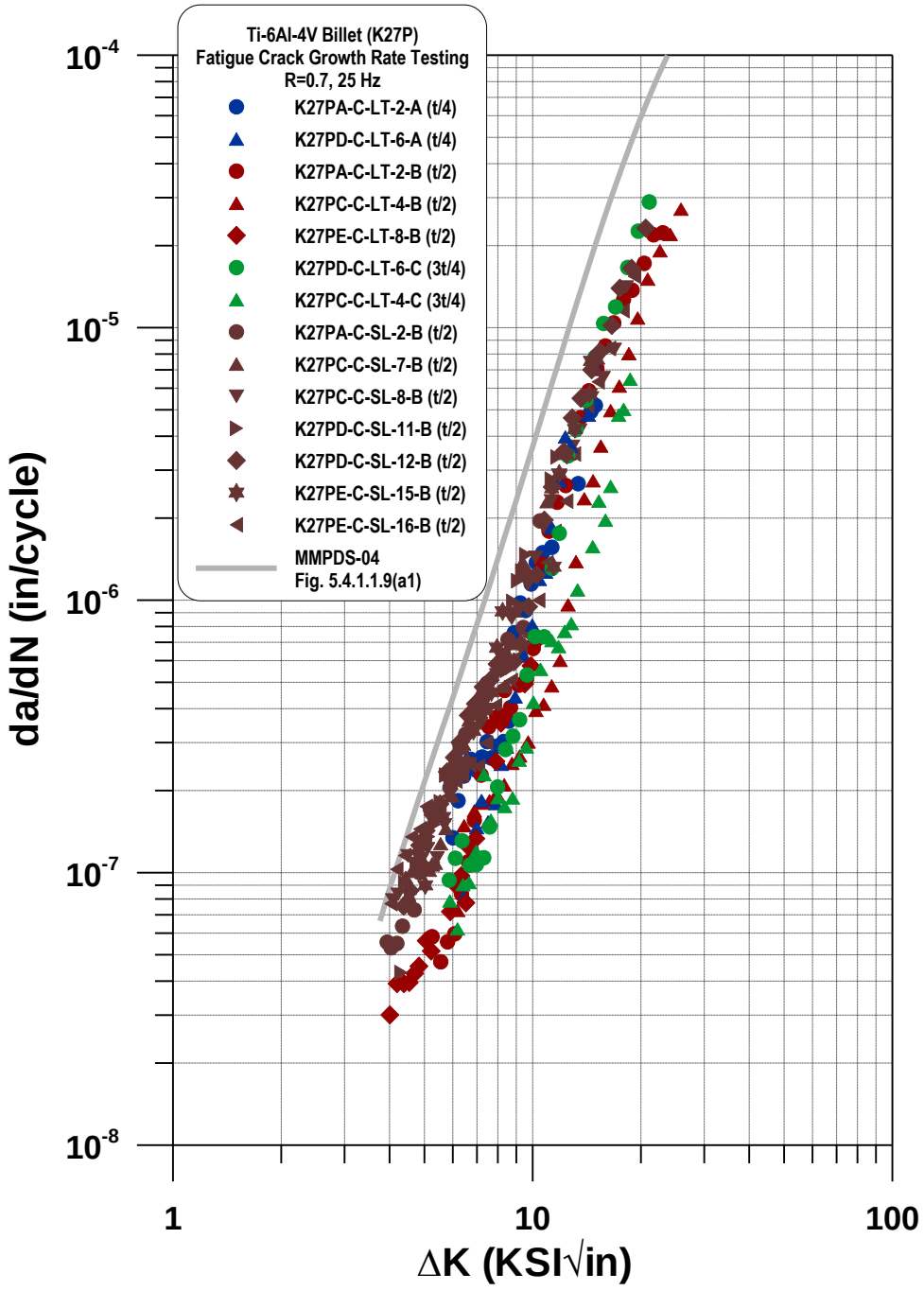


Figure 11. Fatigue crack growth rate test results (R=0.7).

Approved for public release; distribution unlimited.

Fracture Toughness – Plane-strain fracture toughness test results are shown in Table 6. Only valid K_{Ic} values (per ASTM E399) are shown. Five test specimens produced invalid results, having failed the "$P_{max}/P_q < 1.1$" validity check, and have not been included in the table. Two other specimens were damaged during precracking. For this investigation, only the L-T orientation was tested.

The data does not show a difference based upon the thickness location in the billet from where the specimens were extracted.

Also shown in this table are reference values from the Damage Tolerant Design Handbook **[*2*]** for mill-annealed billet. The pedigree of the billet in this handbook is not known. All of the data generated for this report is significantly higher than the reference data.

As there is no accepted standard for the development of a reasonable lower bound for fracture toughness and the fact that the material specifications do not specify minimum properties for this test, the lowest value of the data set was selected as the "preliminary reasonable lower bound" fracture toughness on this billet.

Table 6. Fracture toughness test results.

	Thickness Location	K_{Ic} (ksi√in)	
K27PC-K-LT-2-A	t/4	84.1	
LT-2-C	3t/4	80.7	
K27PD-K-LT-3-A	t/4	79.4	
LT-3-C	3t/4	74.6	
K27PE-K-LT-4-C	3t/4	85.1	
LT-5-A	t/4	79.7	
LT-5-B	t/2	81.5	
LT-5-C	3t/4	80.6	
LT-6-A	t/4	71.3	← Preliminary reasonable lower bound
LT-6-B	t/2	77.7	
LT-6-C	3t/4	75.0	
Damage Tolerant Design Handbook *Table 6.18.1.1 (Billet) Mean*		52.3	

Stress Corrosion Cracking – Axial, smooth bar stress corrosion cracking tests were performed on 24 test specimens, representing all three thickness locations and two

Approved for public release; distribution unlimited.

orientations (L and S). As stated previously, the specimens were loaded at a stress of 90 ksi (75% of the specification yield strength of 120 ksi) for 40 days in an alternate immersion 3.5% NaCl solution. No failures occurred during testing. After testing, specimens were rinsed in deionized water and visually inspected for evidence of corrosion damage. No evidence of pitting or other corrosion-related damage was indicated.

CONCLUSIONS AND RECOMMENDATIONS

As this report dealt with mechanical properties from only one Ti-6Al-4V billet, no specific conclusions or recommendations will be made, other than comparisons to material specifications or available reference data. With the exception of tensile ductility (reduction of area) results, the material was generally equivalent to the reference data noted throughout the report. The lower ductility results should not be overlooked however when evaluating this material with respect to properly processed plate or bar.

REFERENCES

5. *Metallic Materials Properties Development and Standardization (MMPDS)*, MMPDS-04; April 2008; Federal Aviation Administration.
6. *Damage Tolerant Design Handbook: A Compilation of Fracture and Crack Growth Data for High Strength Alloys*; Compiled by D.A. Skinn, J.P. Gallagher, A.P. Berens, P.D. Huber, J. Smith; University of Dayton Research Institute, May 1994.

ACKNOWLEDGEMENTS

The author wishes to thank Mssrs. John Ruschau, Nick Jacobs, Don Woleslagle, Eric Soppe, Cris Williams, Ron Glett, Ms. Pat Youngerman, and Ms. Sarah Kuhlman, all of the University of Dayton Research Institute (UDRI); Mssrs. Dan Laufersweiler, Ed Porter, and Dave Roberts of Universal Technology Corporation (UTC); and Mssrs. Keith Vehorn and Nick Blommel of AFRL/RXSCE for their engineering and technical support of this program. Acknowledgement is also given to Westmoreland Mechanical Testing & Research, Inc. for the machining of all of the test specimens.

PREPARED BY

SIGNED

_____

STEVEN R. THOMPSON, Senior Materials Engineer
Materials Test & Evaluation Team
Acquisition Systems Support Branch
Systems Support Division

REVIEWED BY

SIGNED

_____

NEAL R. ONTKO, Team Lead
Materials Test & Evaluation Team
Acquisition Systems Support Branch
Systems Support Division

PUBLICATION REVIEW: This report has been reviewed and approved.

SIGNED

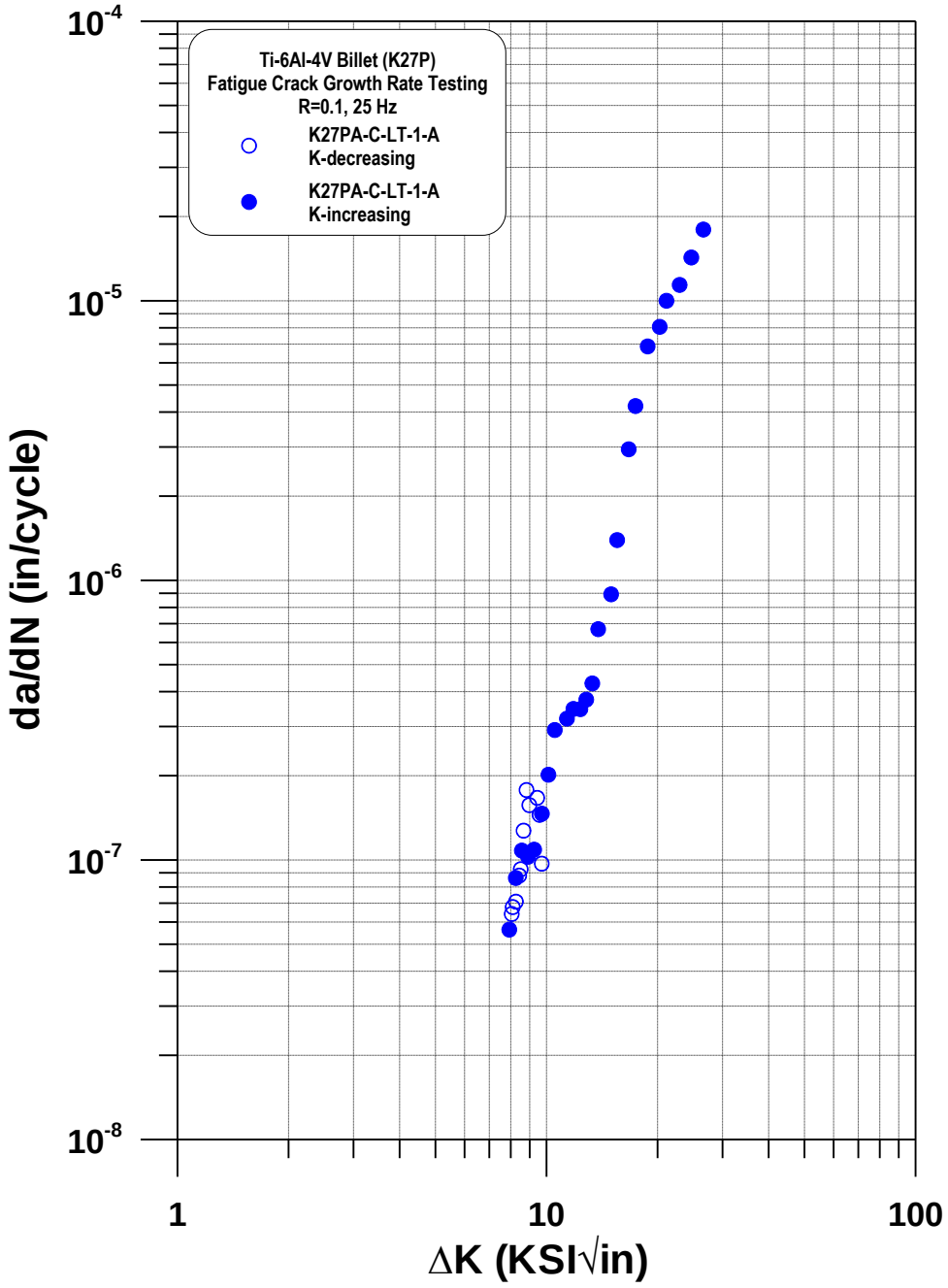
_____

CHARLES E. WAGNER, Chief
Acquisition Systems Support Branch
Systems Support Division
Materials and Manufacturing Directorate

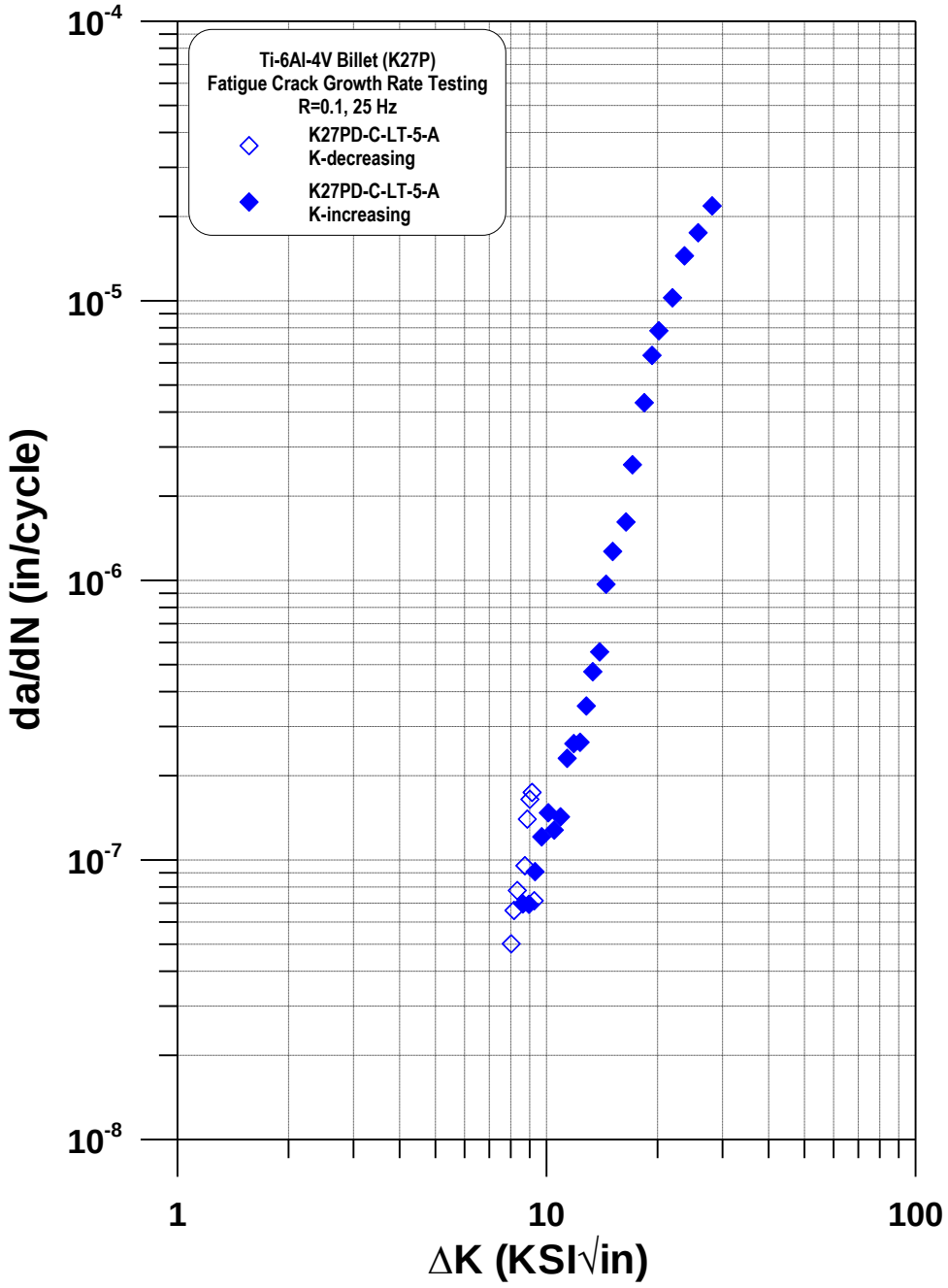
Approved for public release; distribution unlimited.

Appendix A
Individual fatigue crack growth rate curves for Ti-6Al-4V billet (K27P).

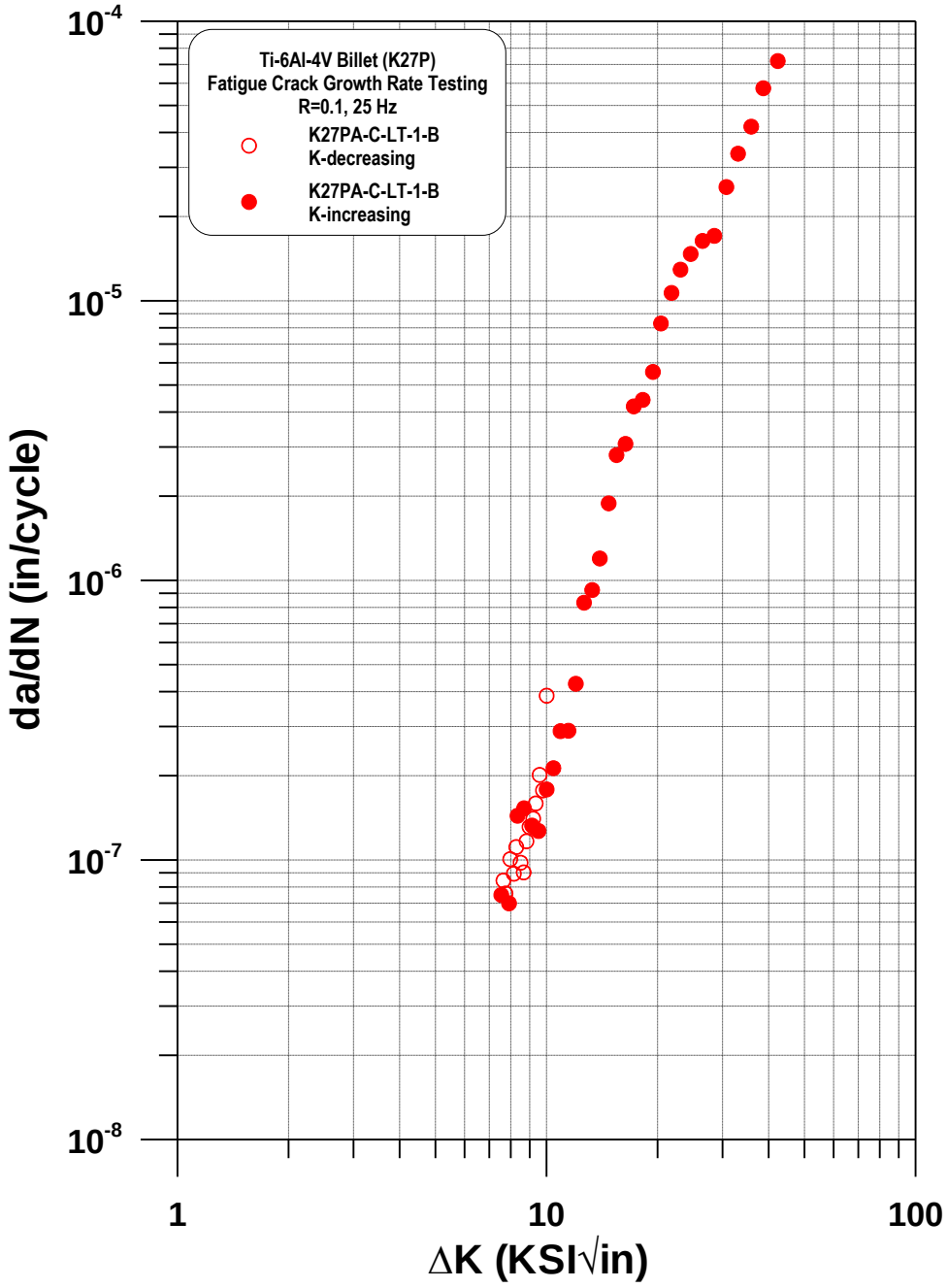
Approved for public release; distribution unlimited.



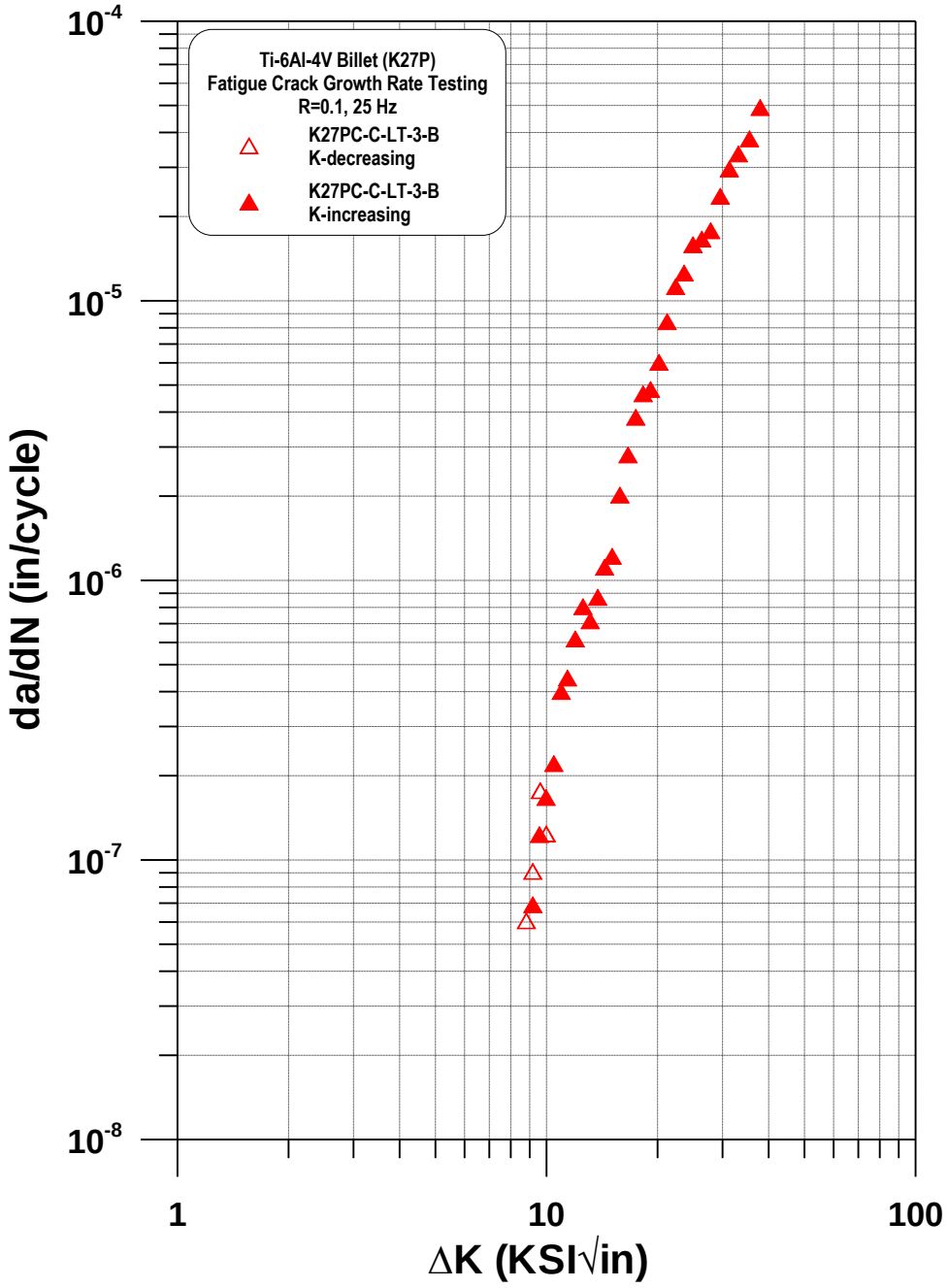
Approved for public release; distribution unlimited.



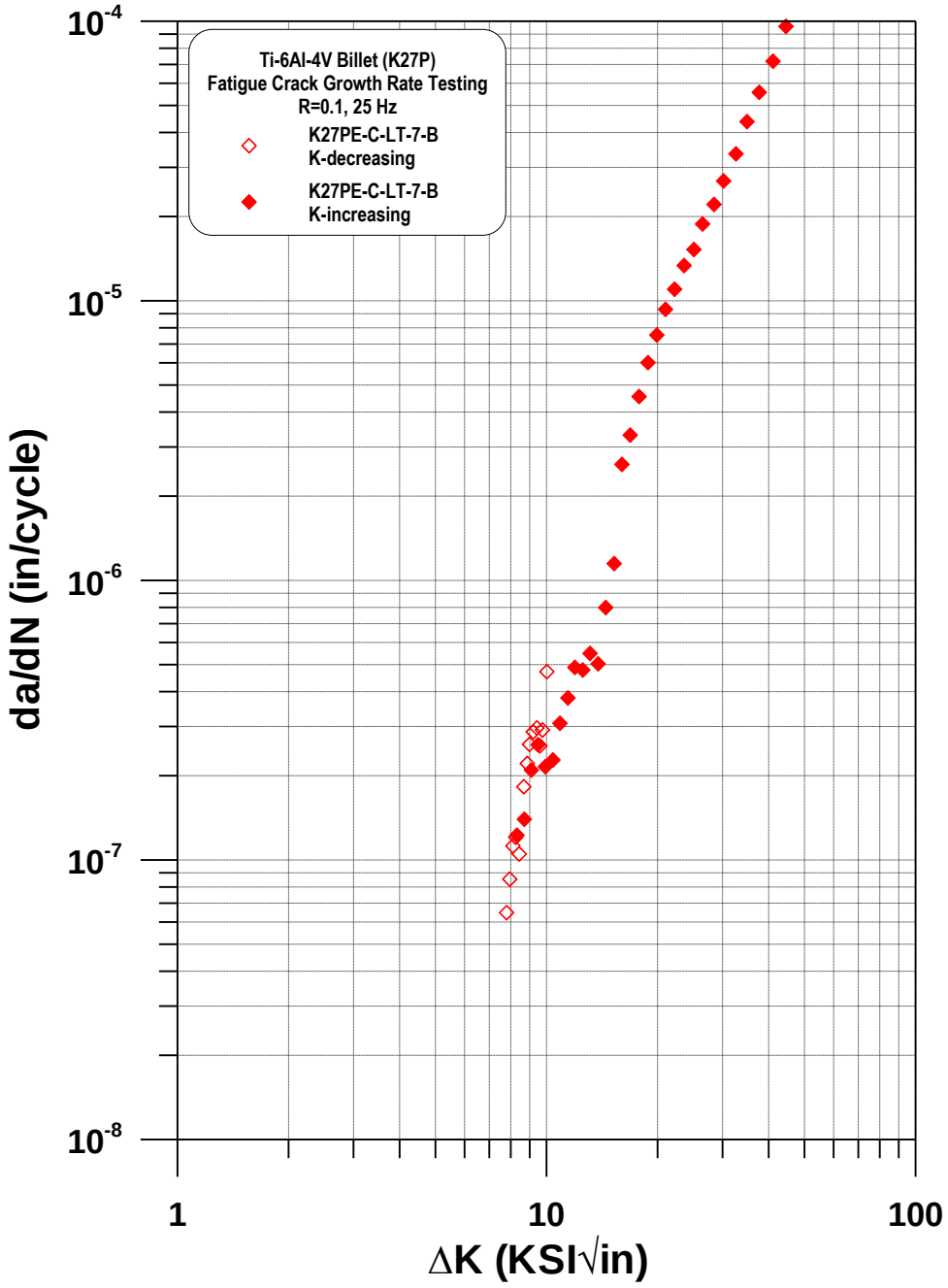
Approved for public release; distribution unlimited.



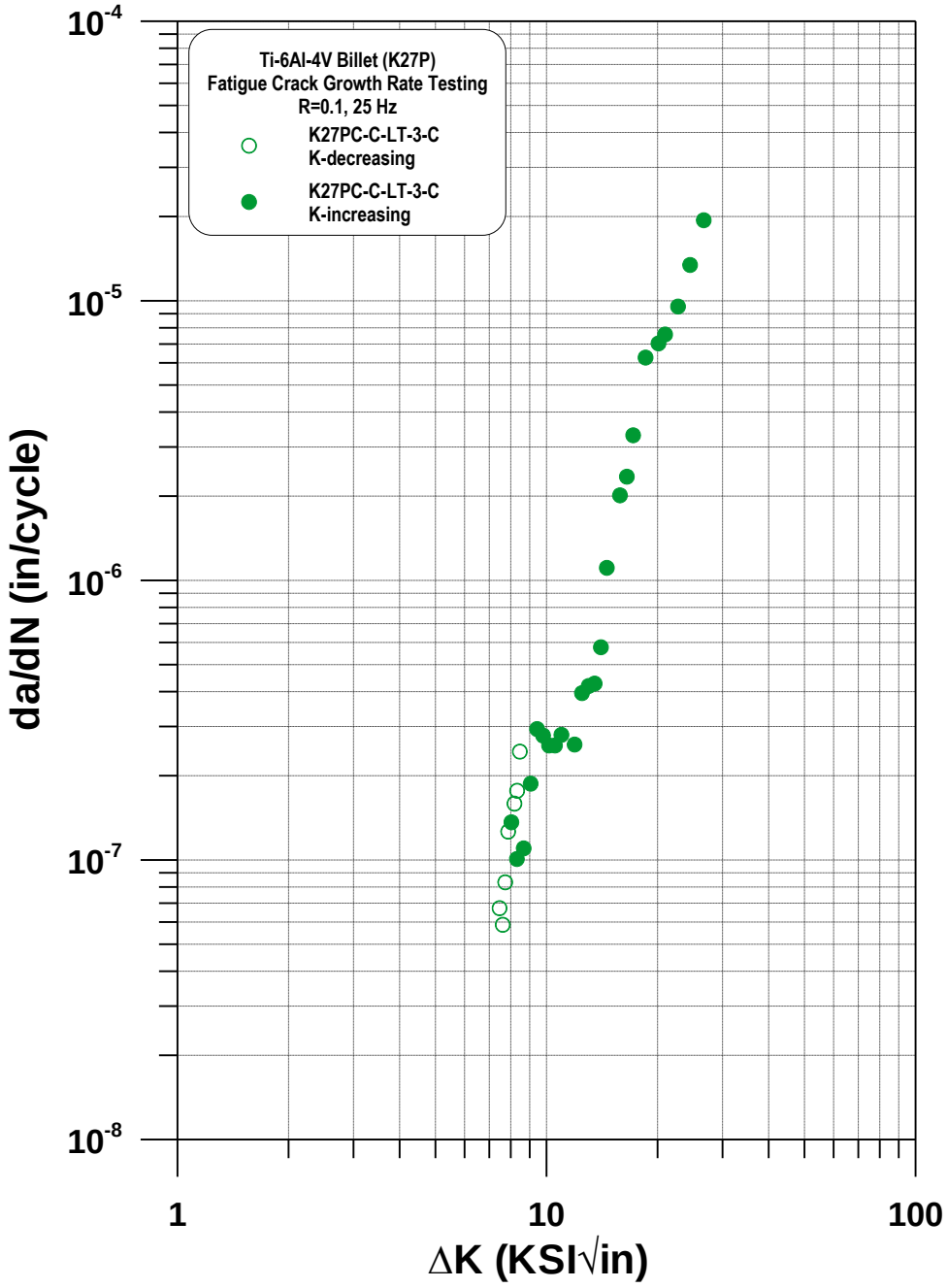
Approved for public release; distribution unlimited.



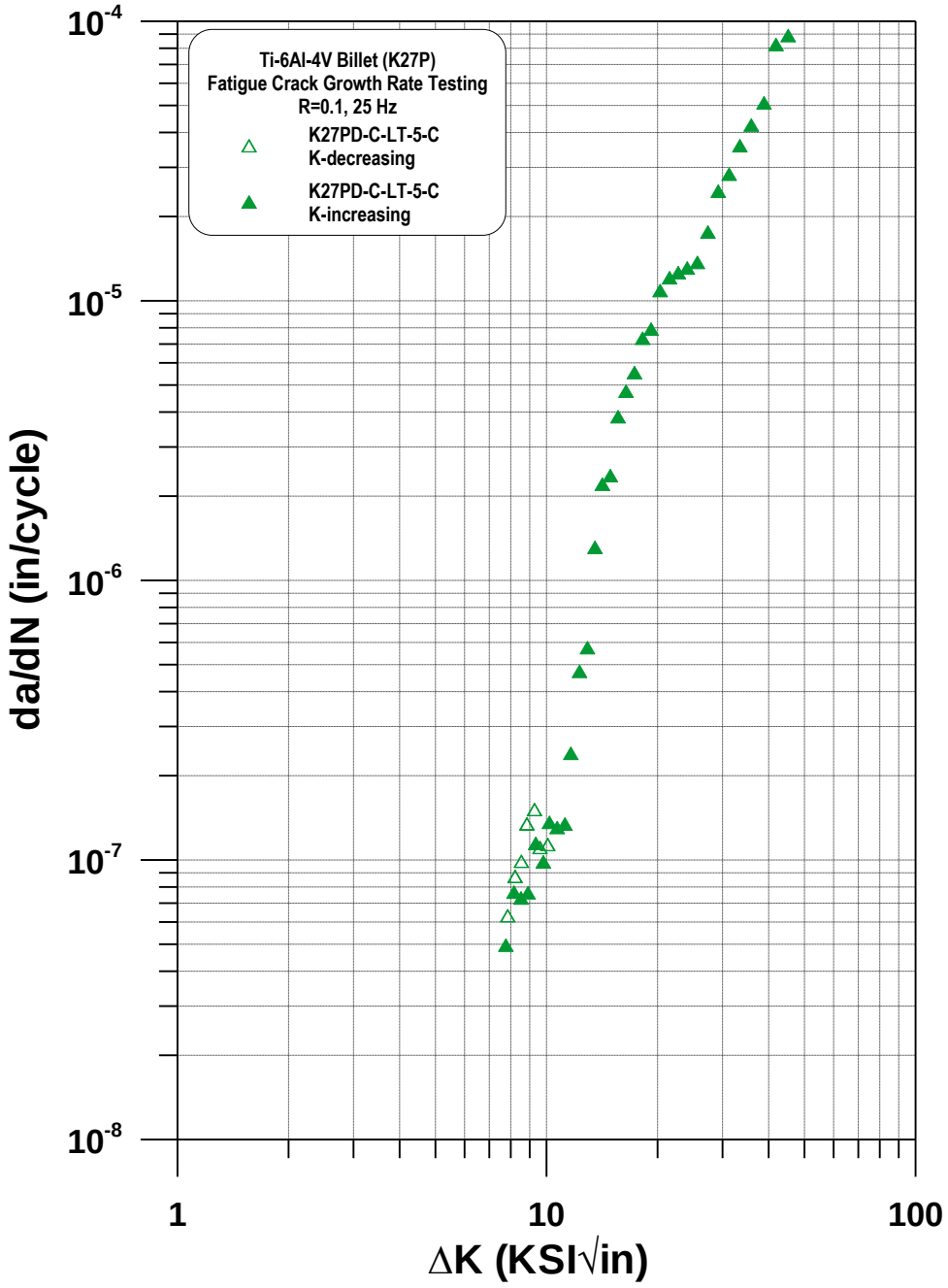
Approved for public release; distribution unlimited.



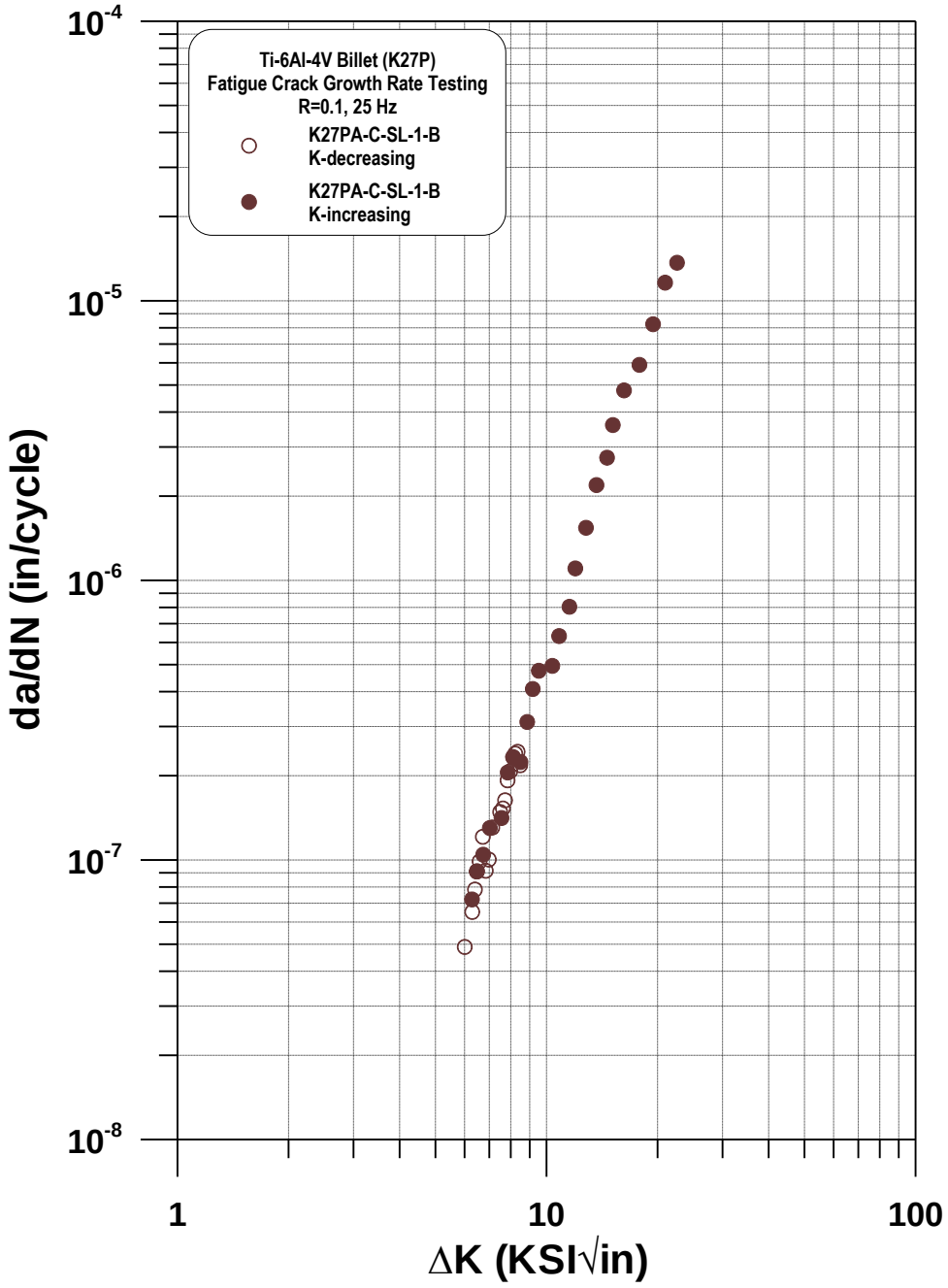
Approved for public release; distribution unlimited.



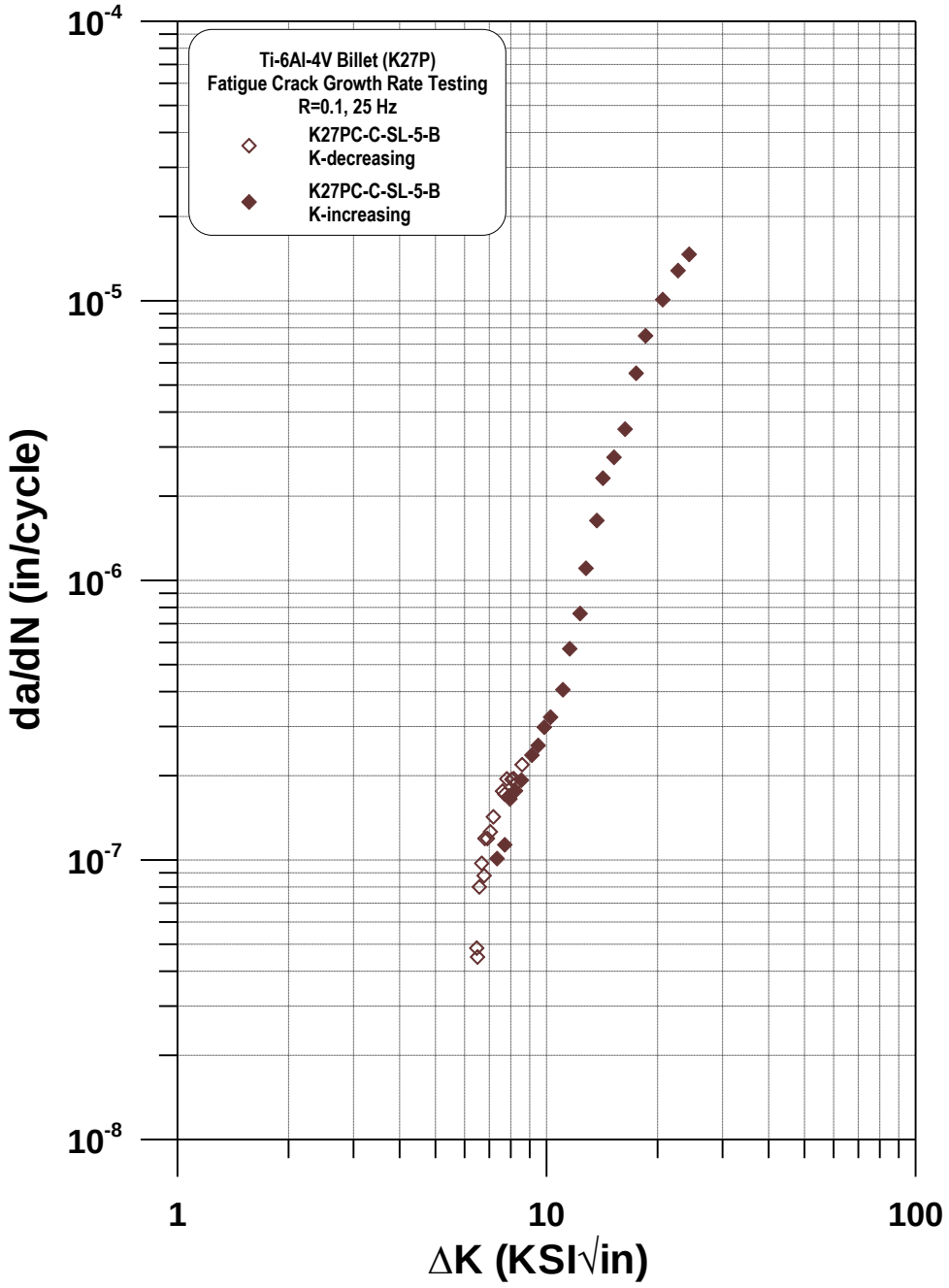
Approved for public release; distribution unlimited.



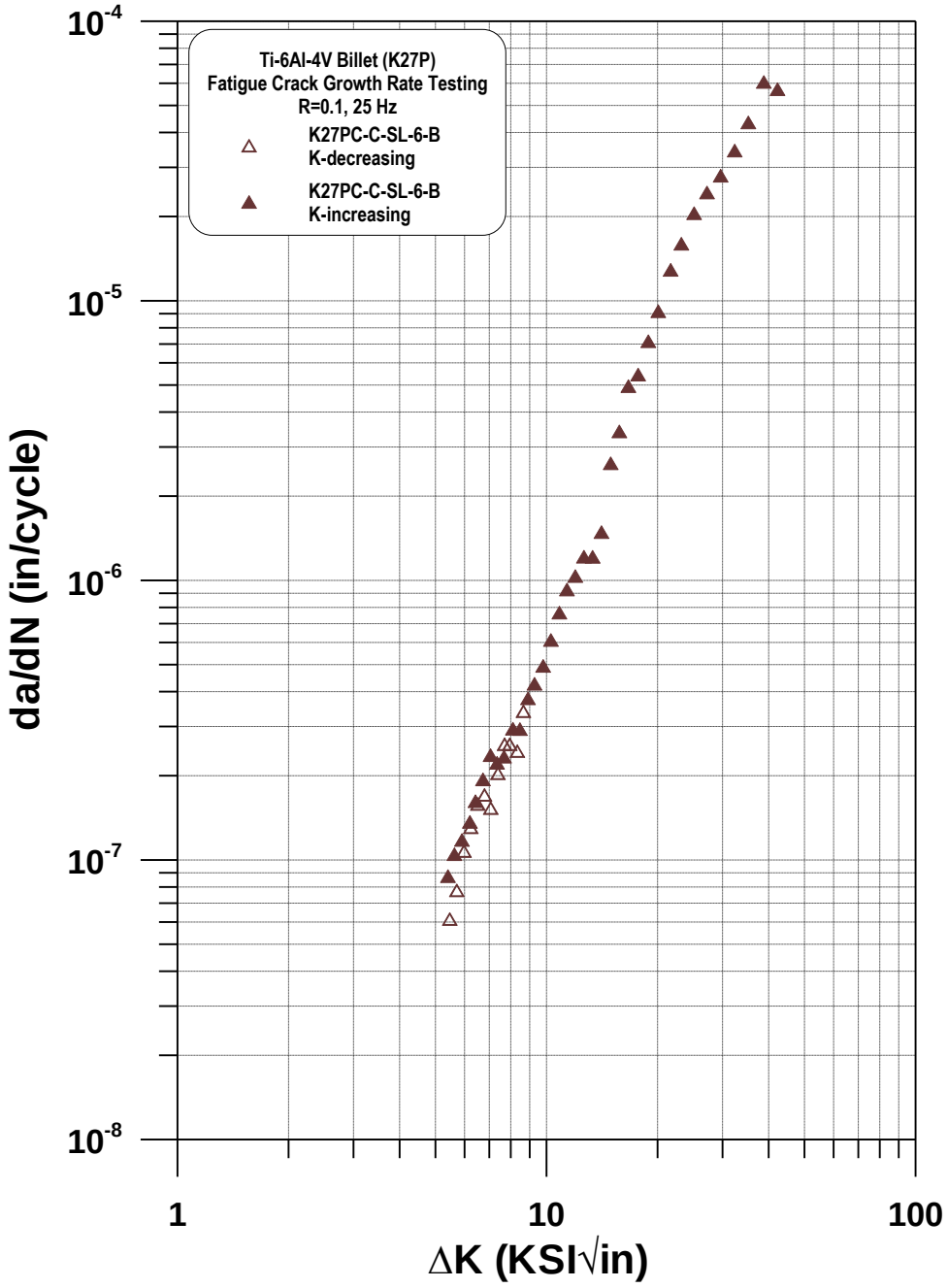
Approved for public release; distribution unlimited.



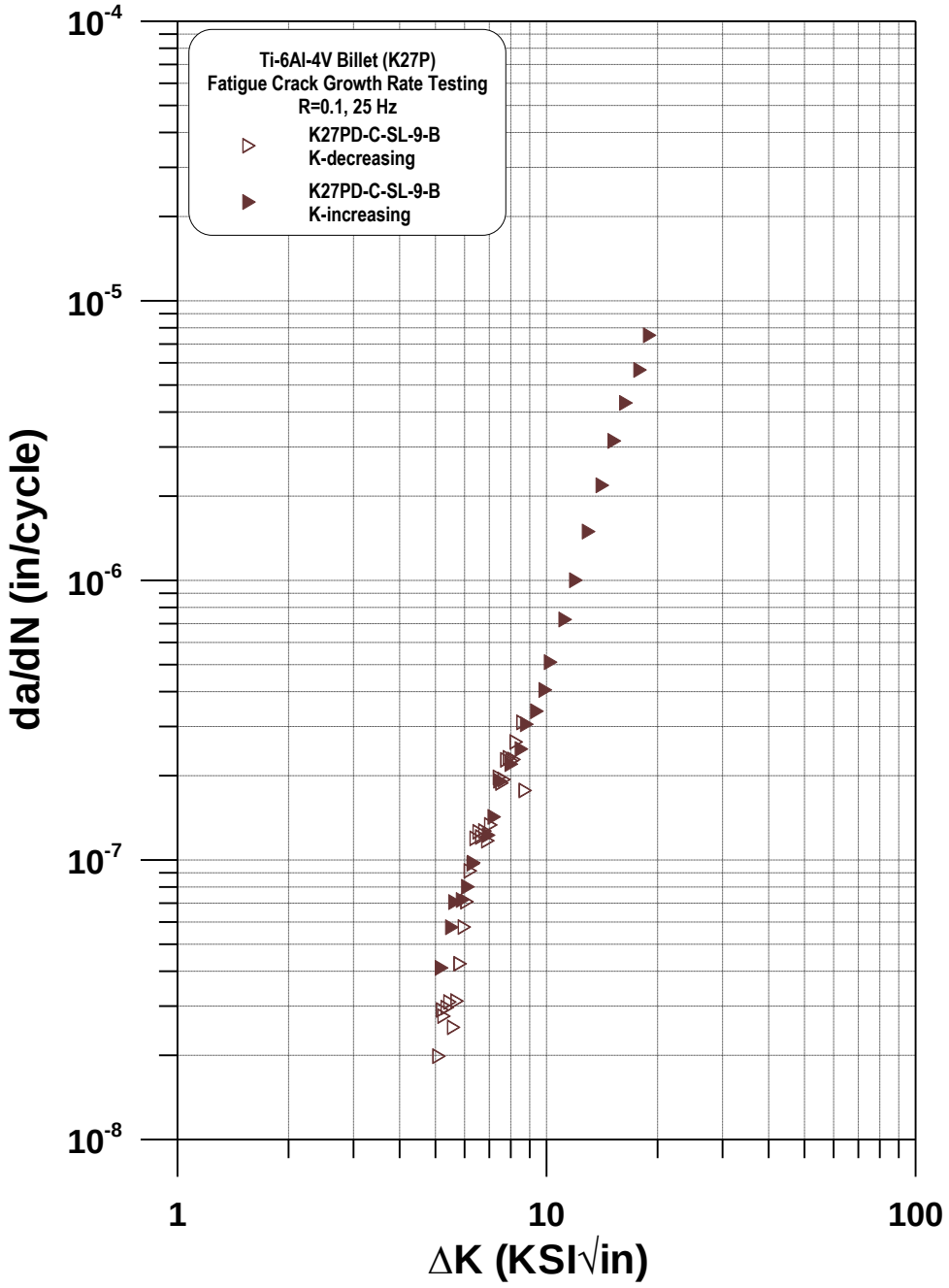
Approved for public release; distribution unlimited.



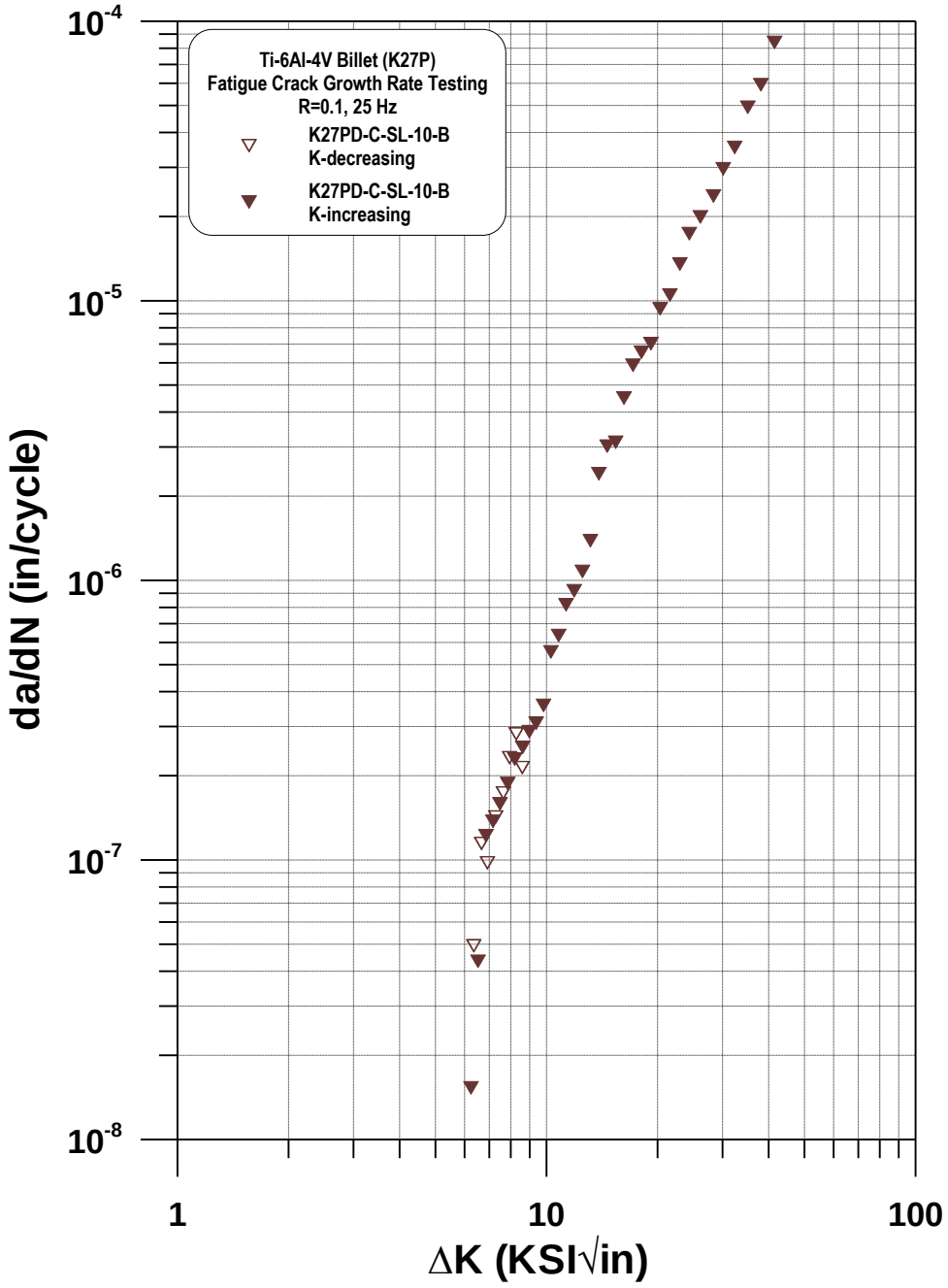
Approved for public release; distribution unlimited.



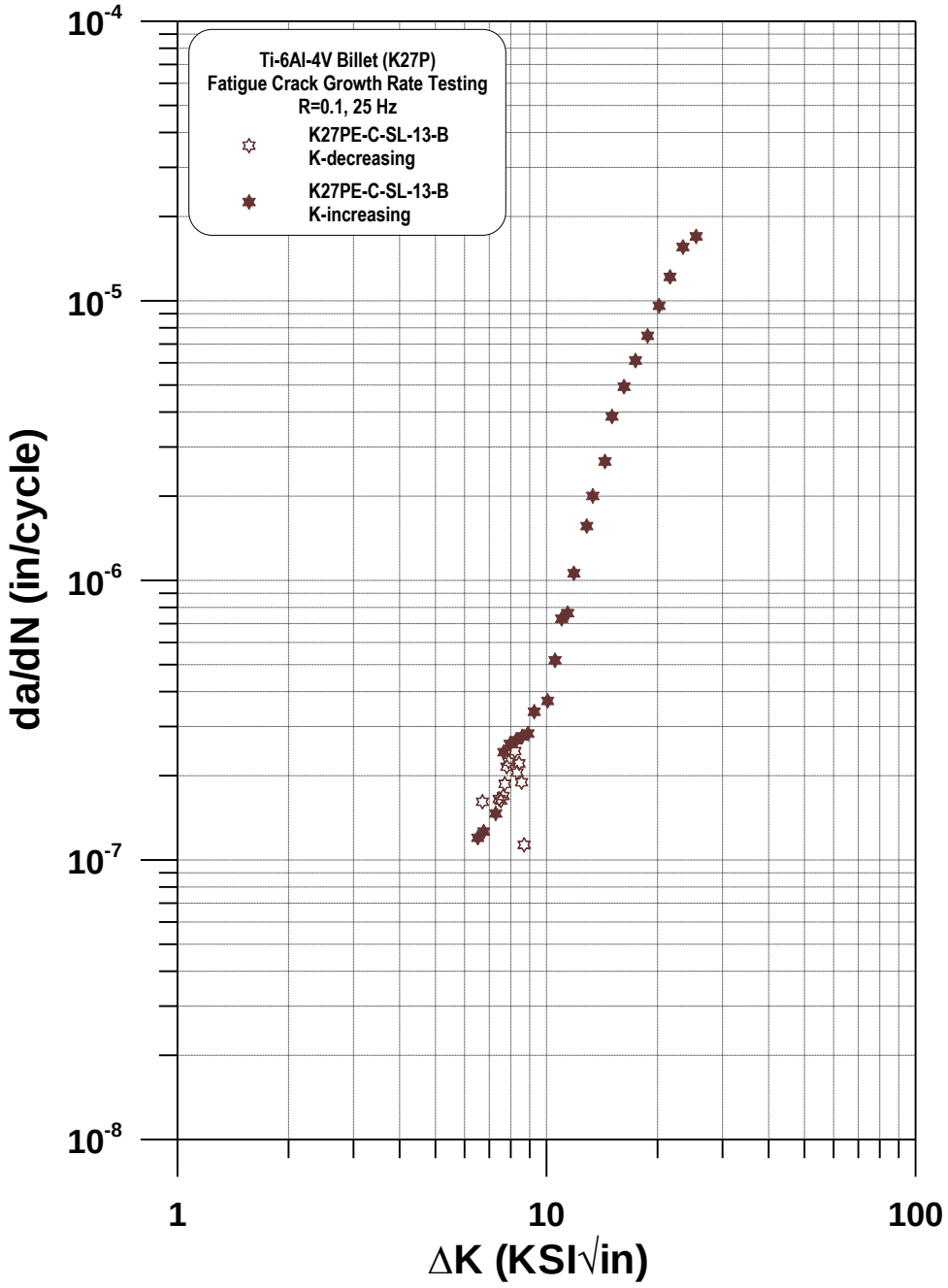
Approved for public release; distribution unlimited.



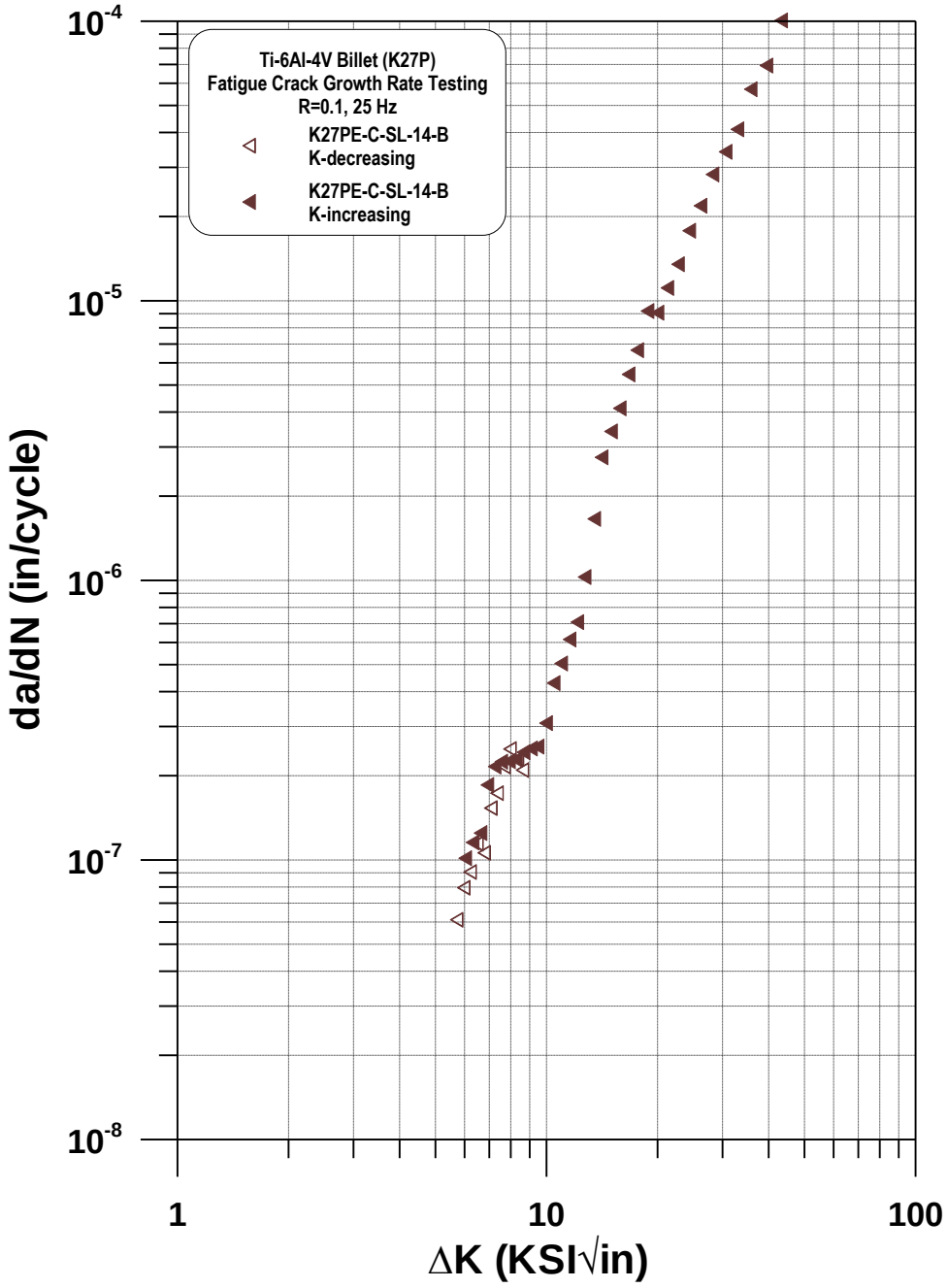
Approved for public release; distribution unlimited.



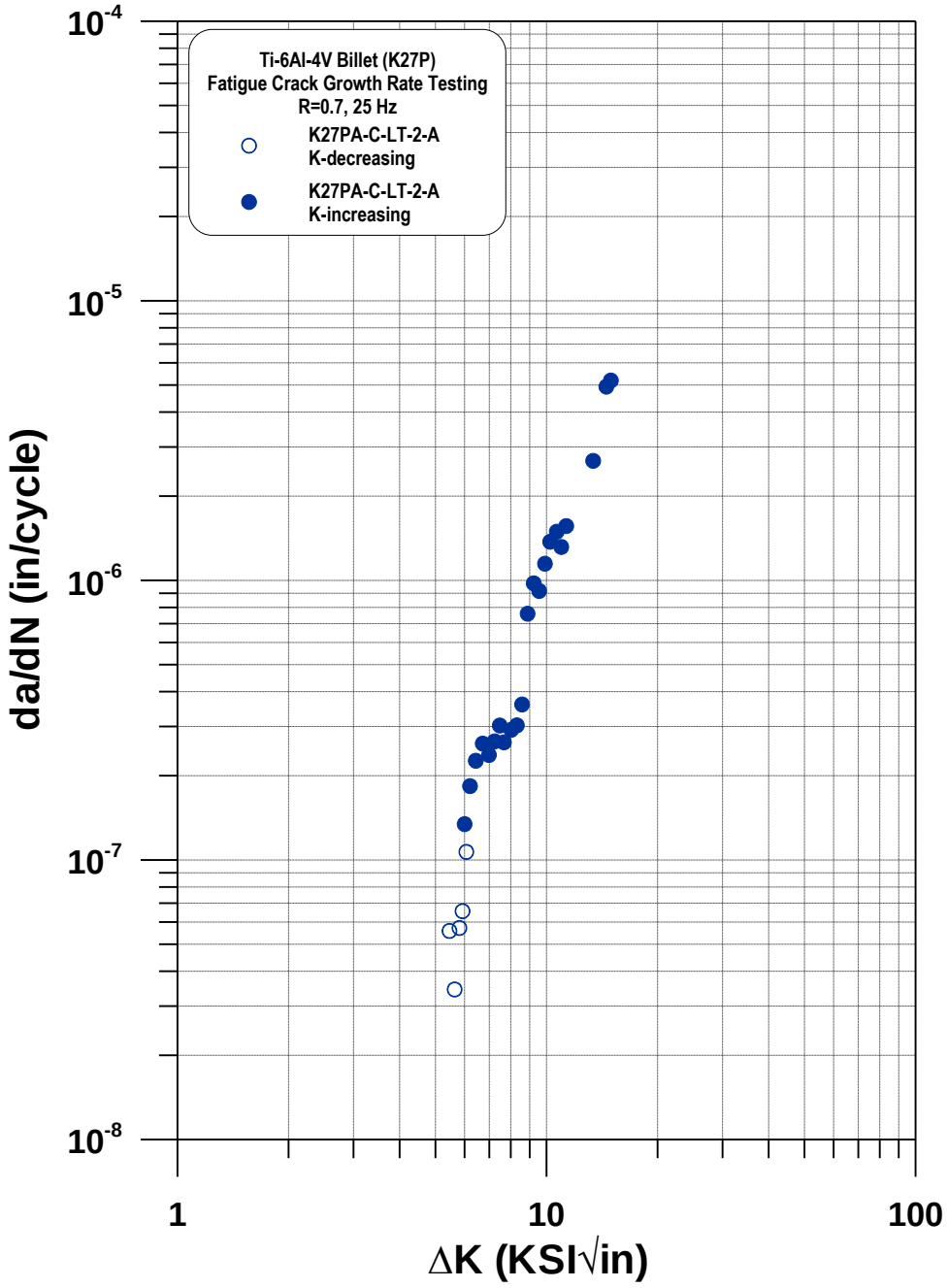
Approved for public release; distribution unlimited.



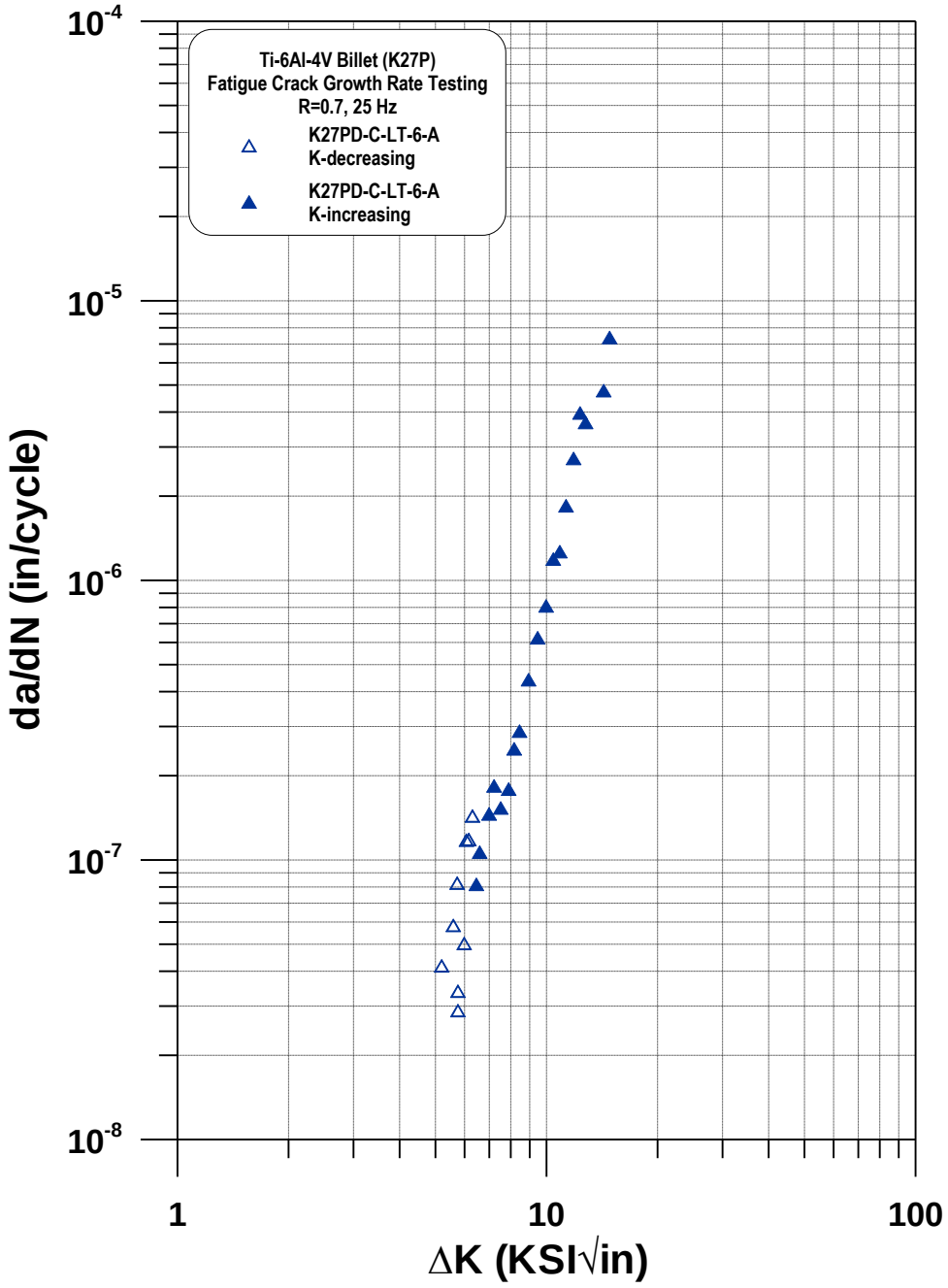
Approved for public release; distribution unlimited.



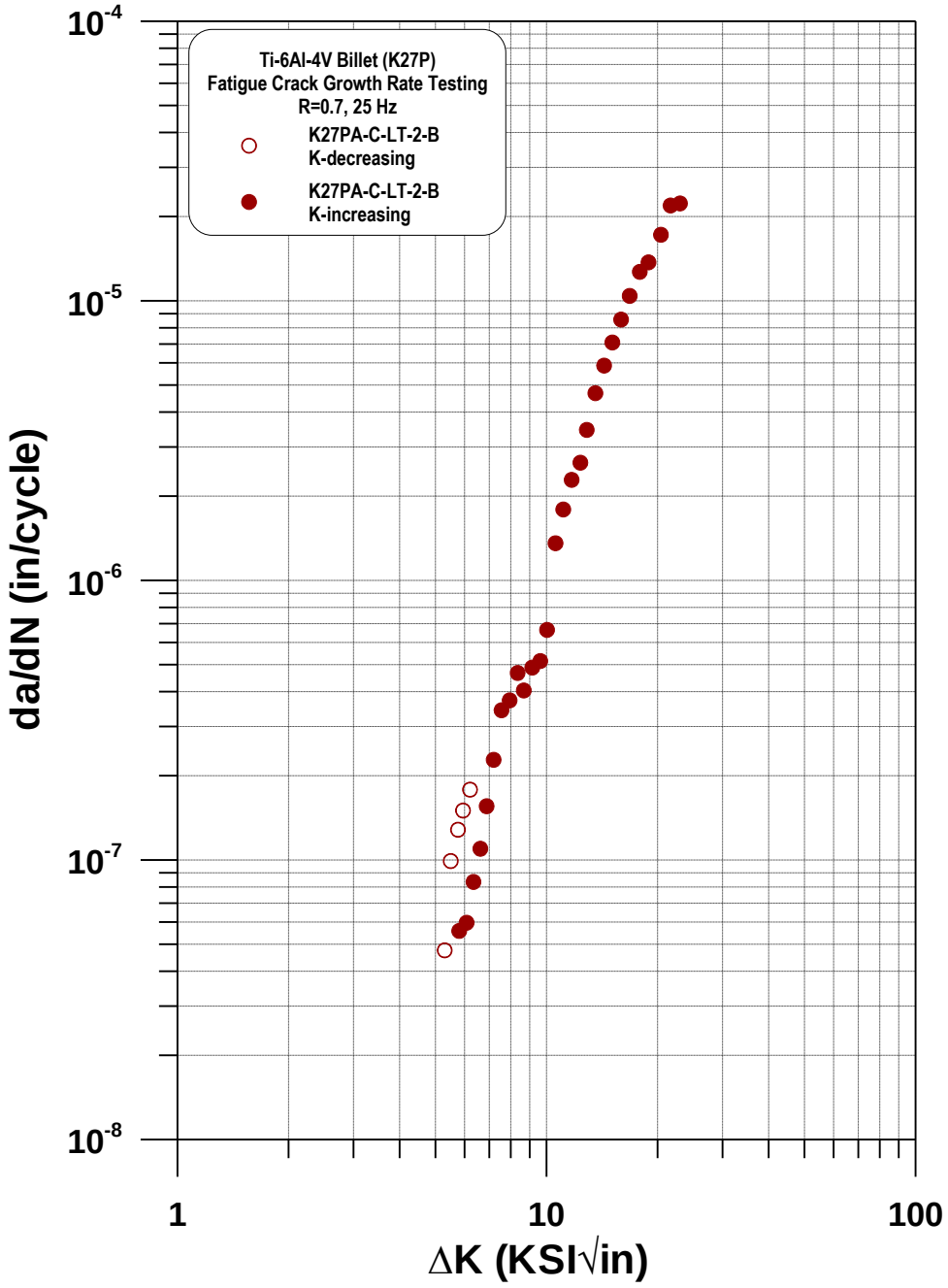
Approved for public release; distribution unlimited.



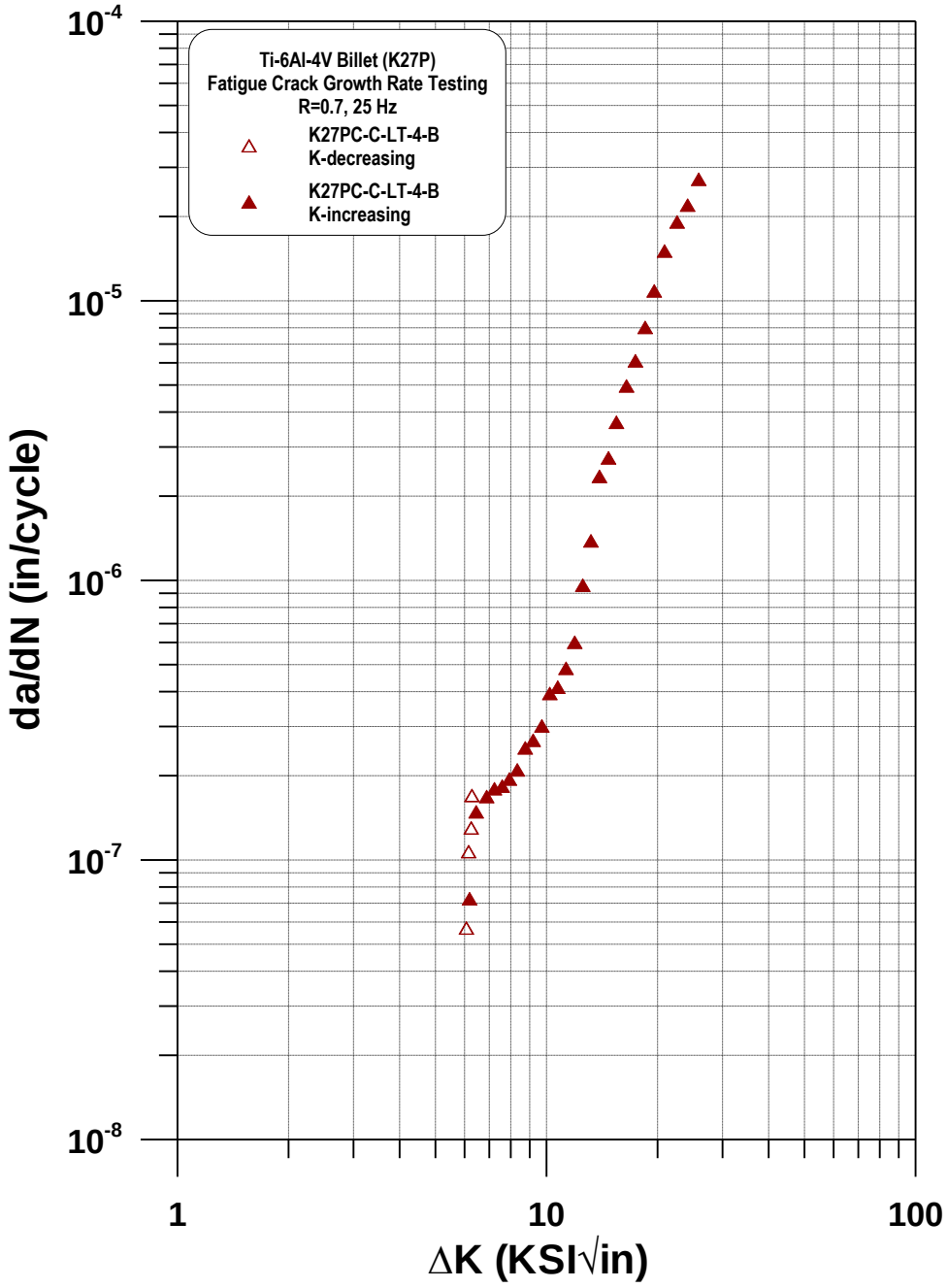
Approved for public release; distribution unlimited.



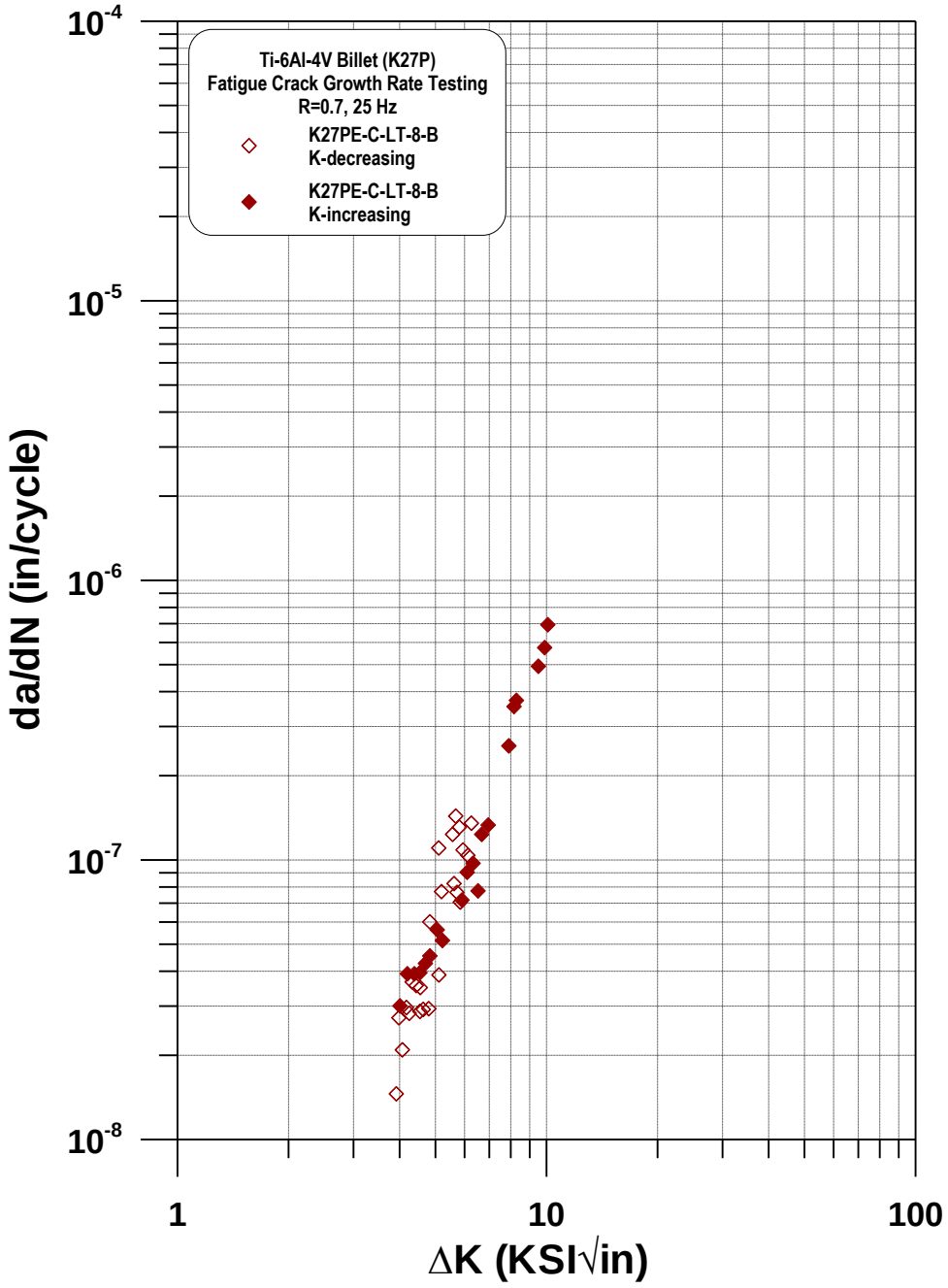
Approved for public release; distribution unlimited.



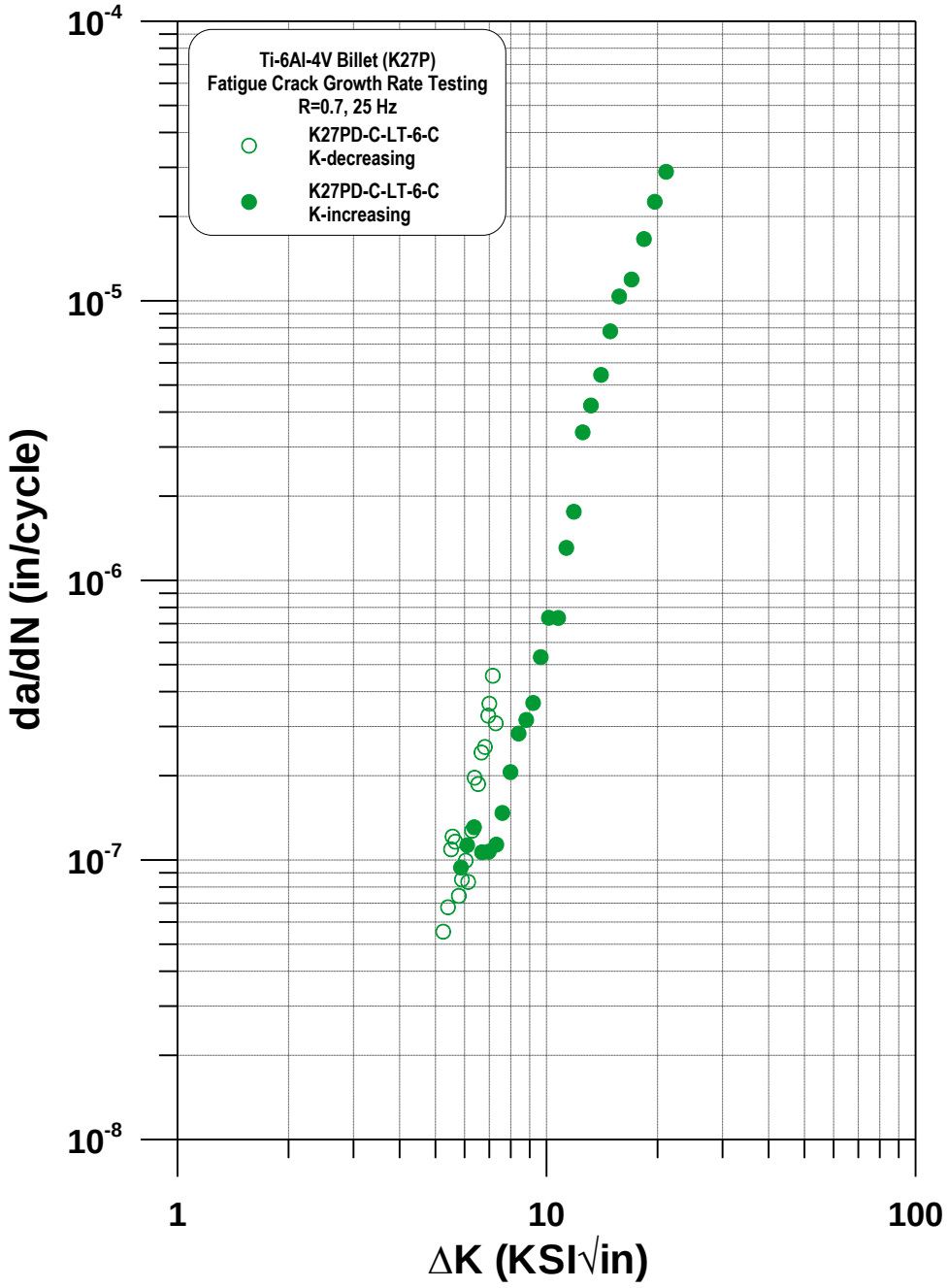
Approved for public release; distribution unlimited.



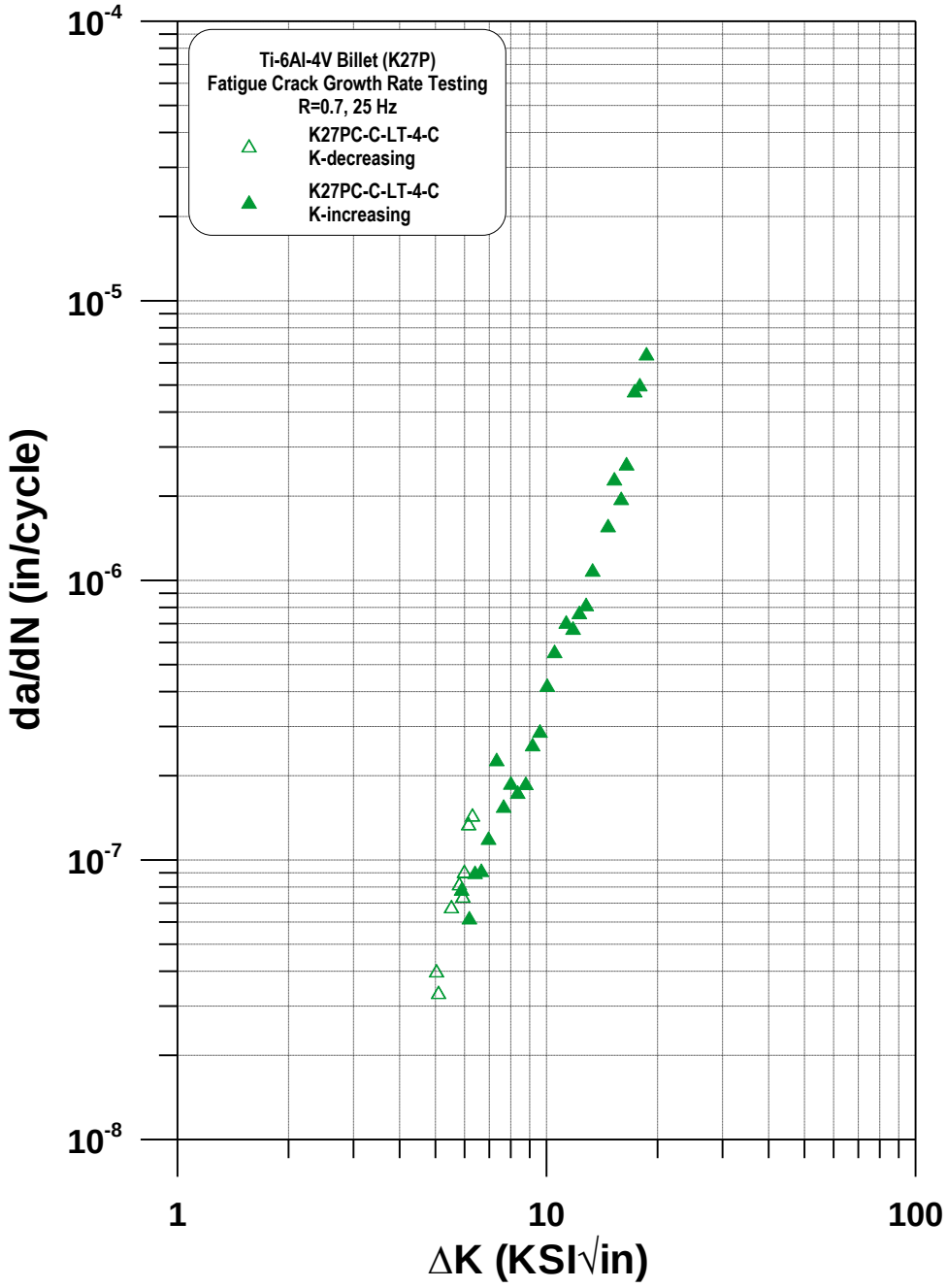
Approved for public release; distribution unlimited.



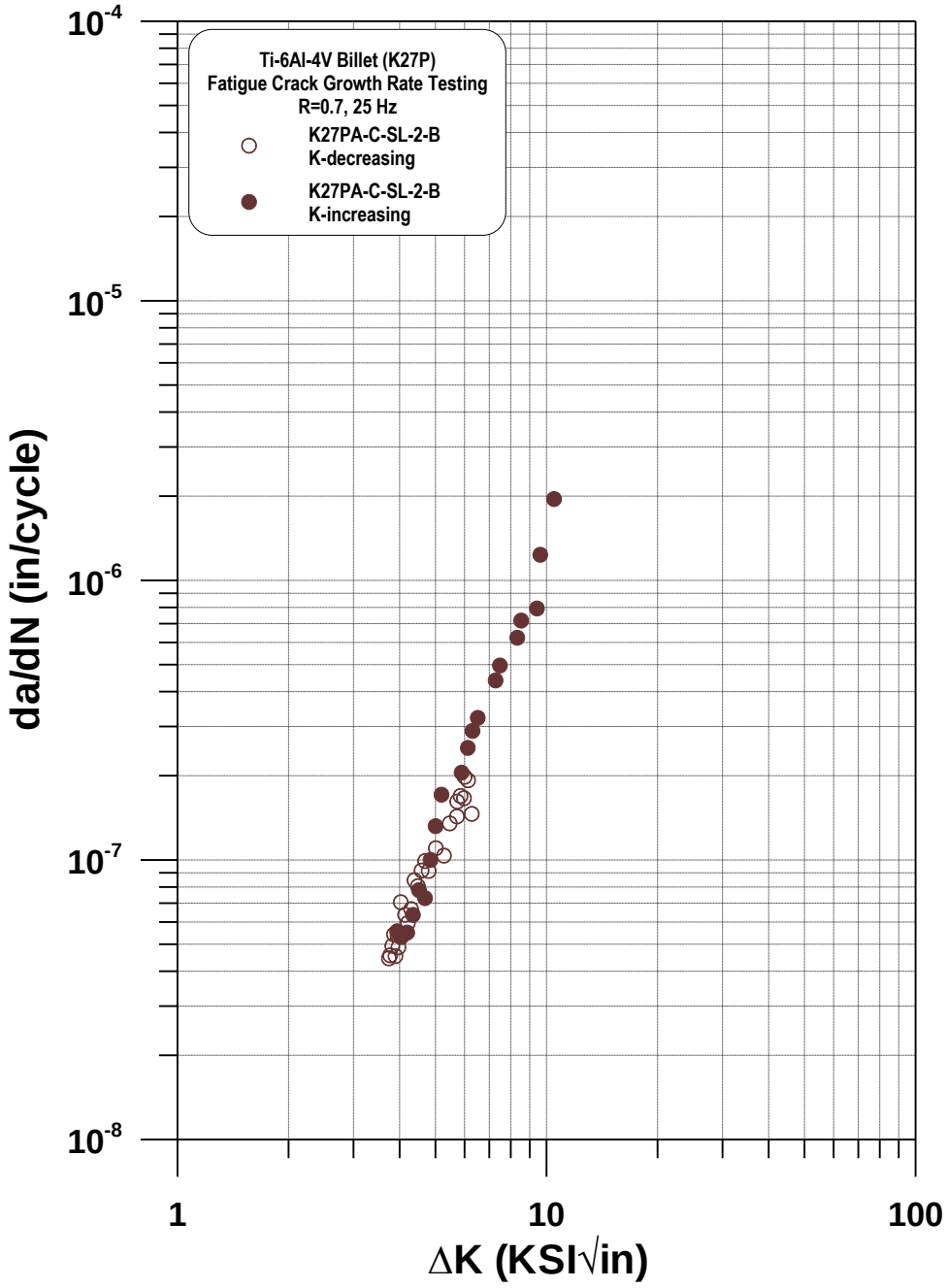
Approved for public release; distribution unlimited.



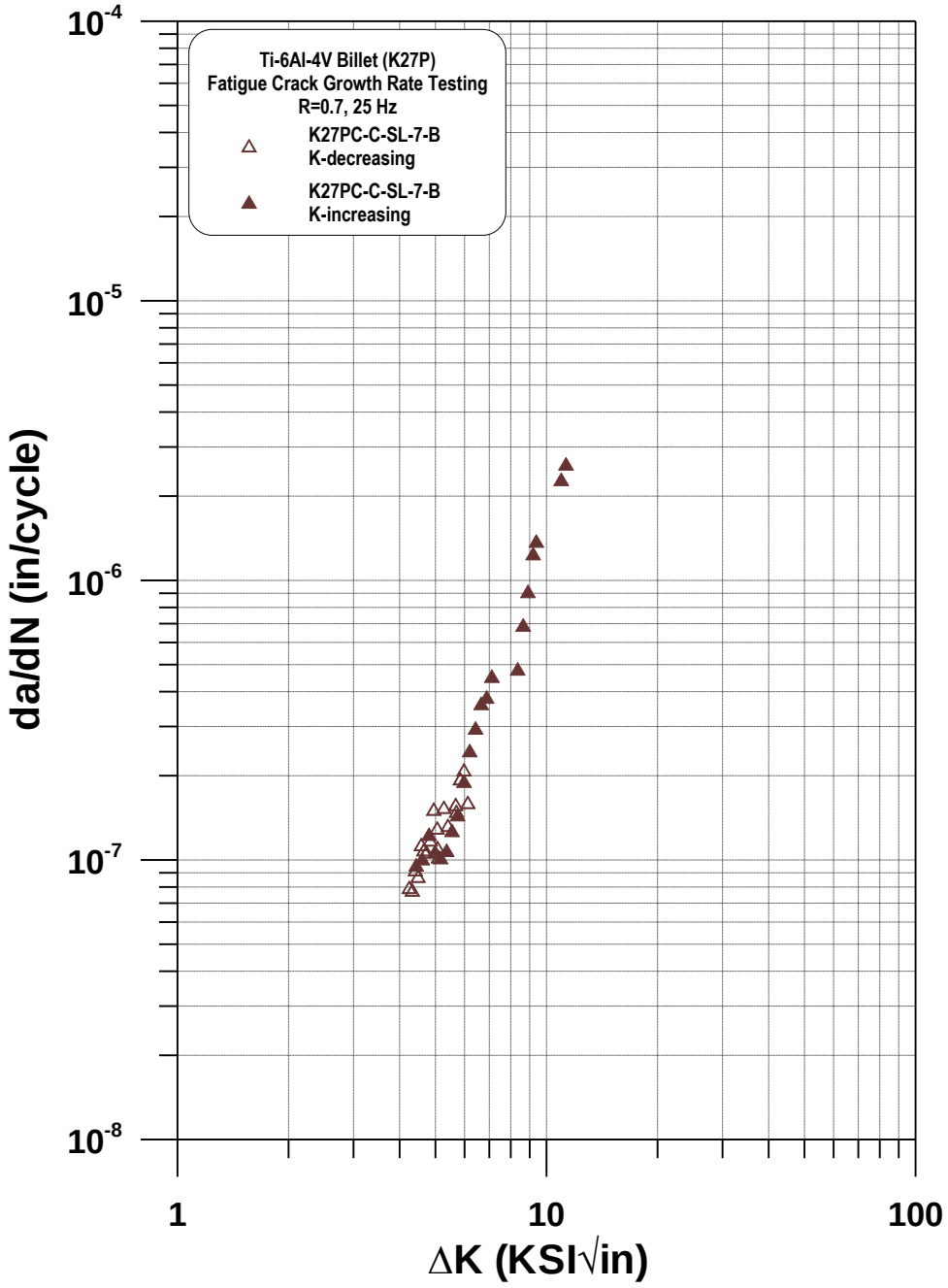
Approved for public release; distribution unlimited.



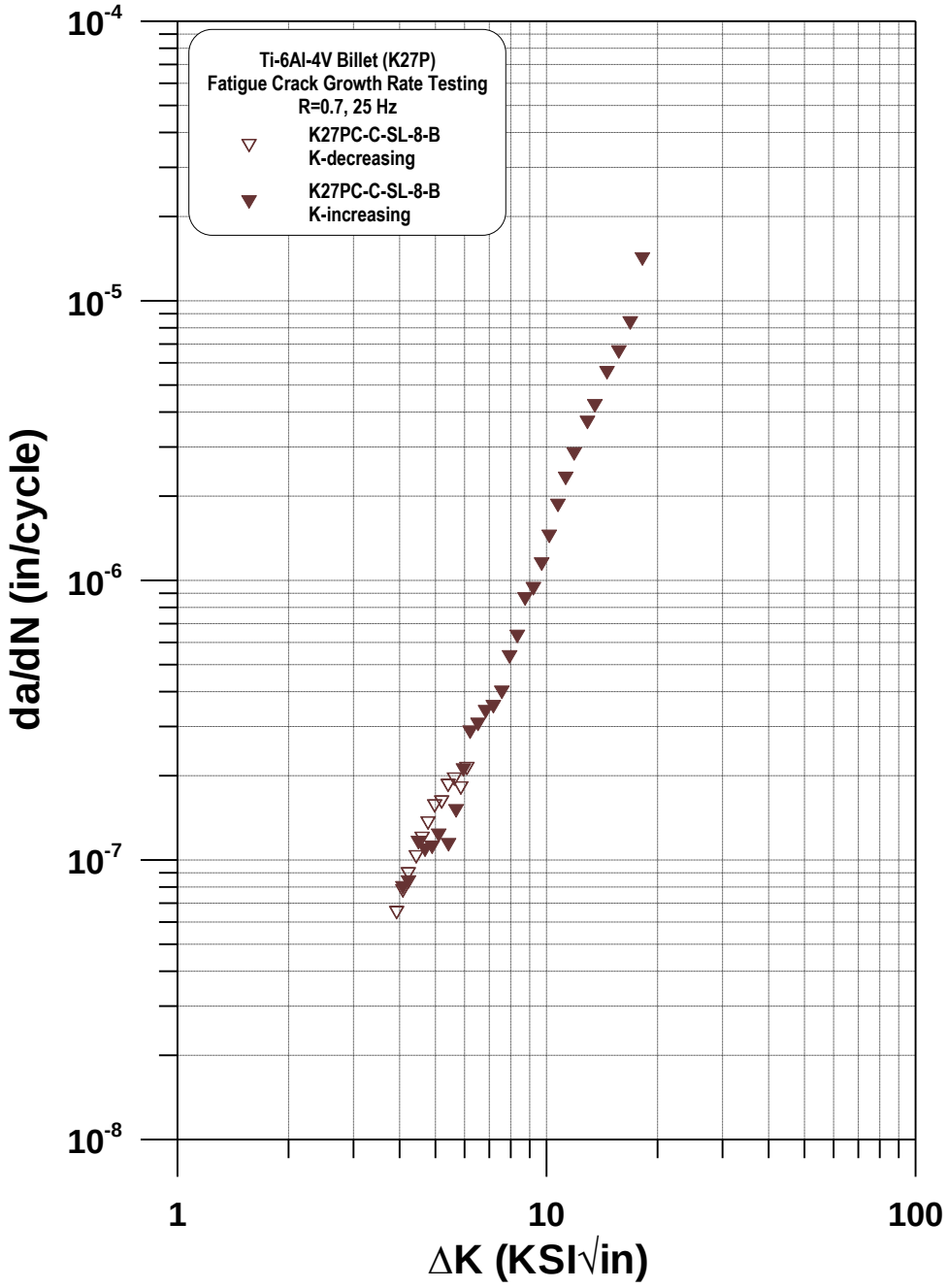
Approved for public release; distribution unlimited.



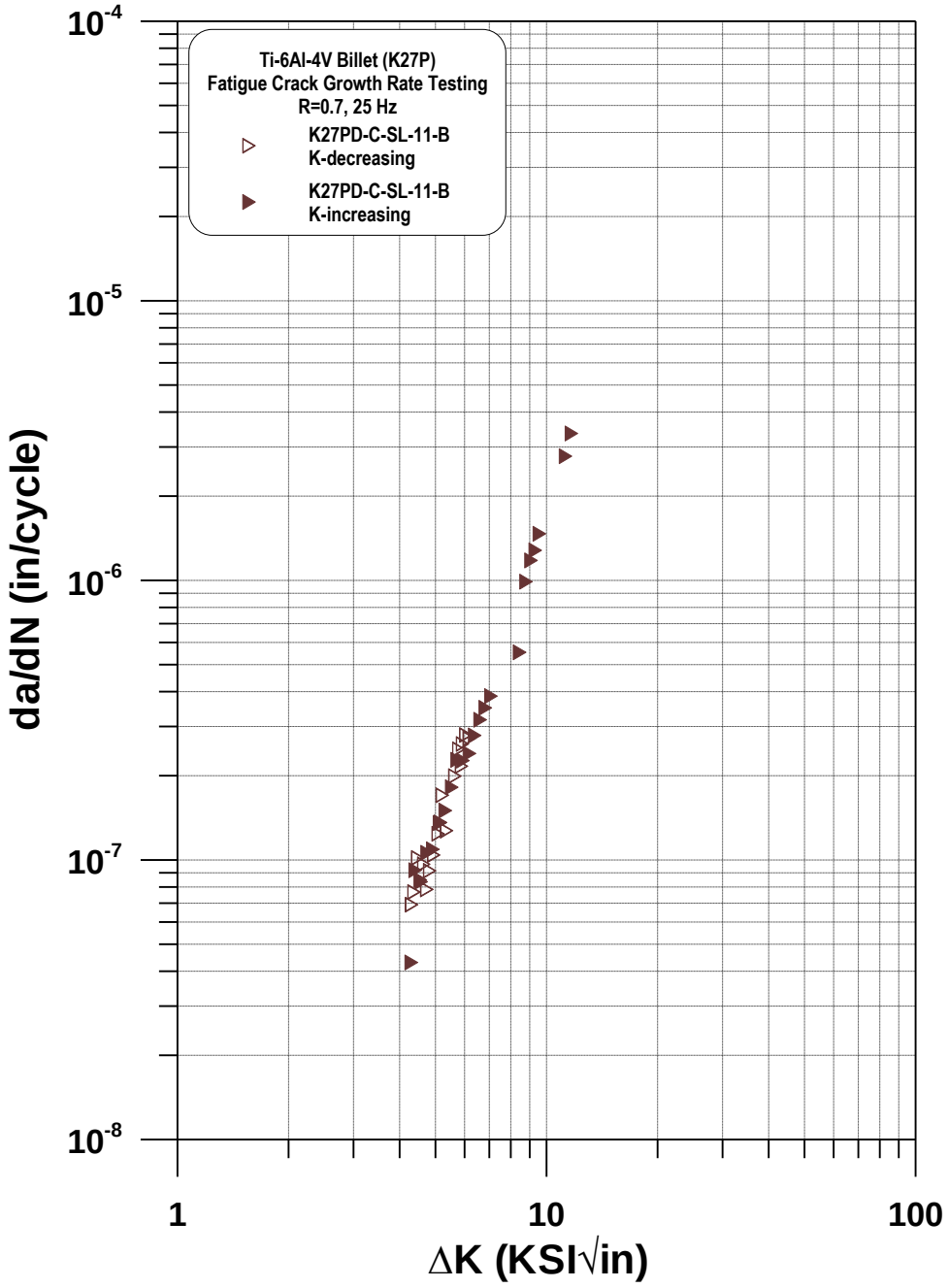
Approved for public release; distribution unlimited.



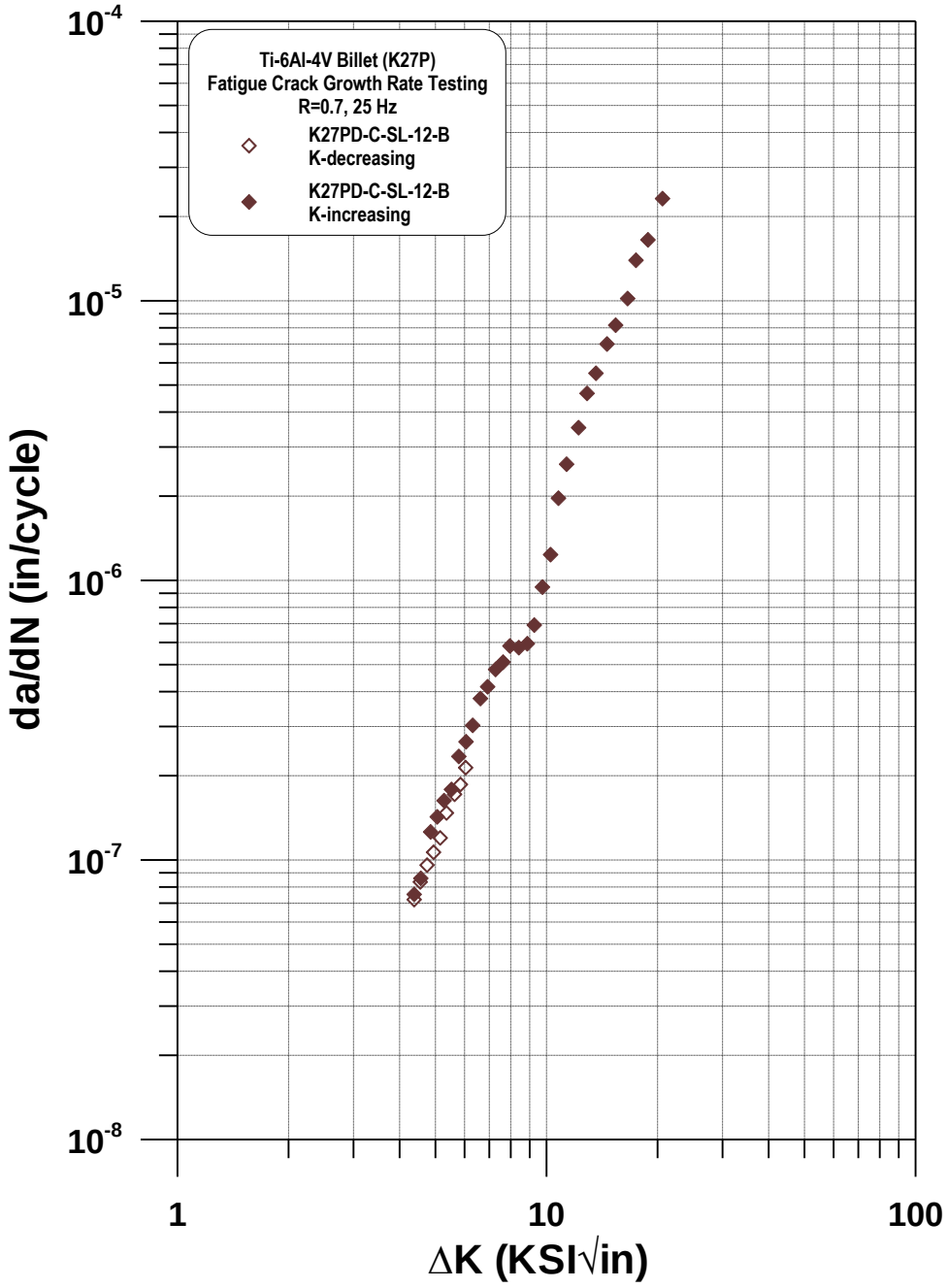
Approved for public release; distribution unlimited.



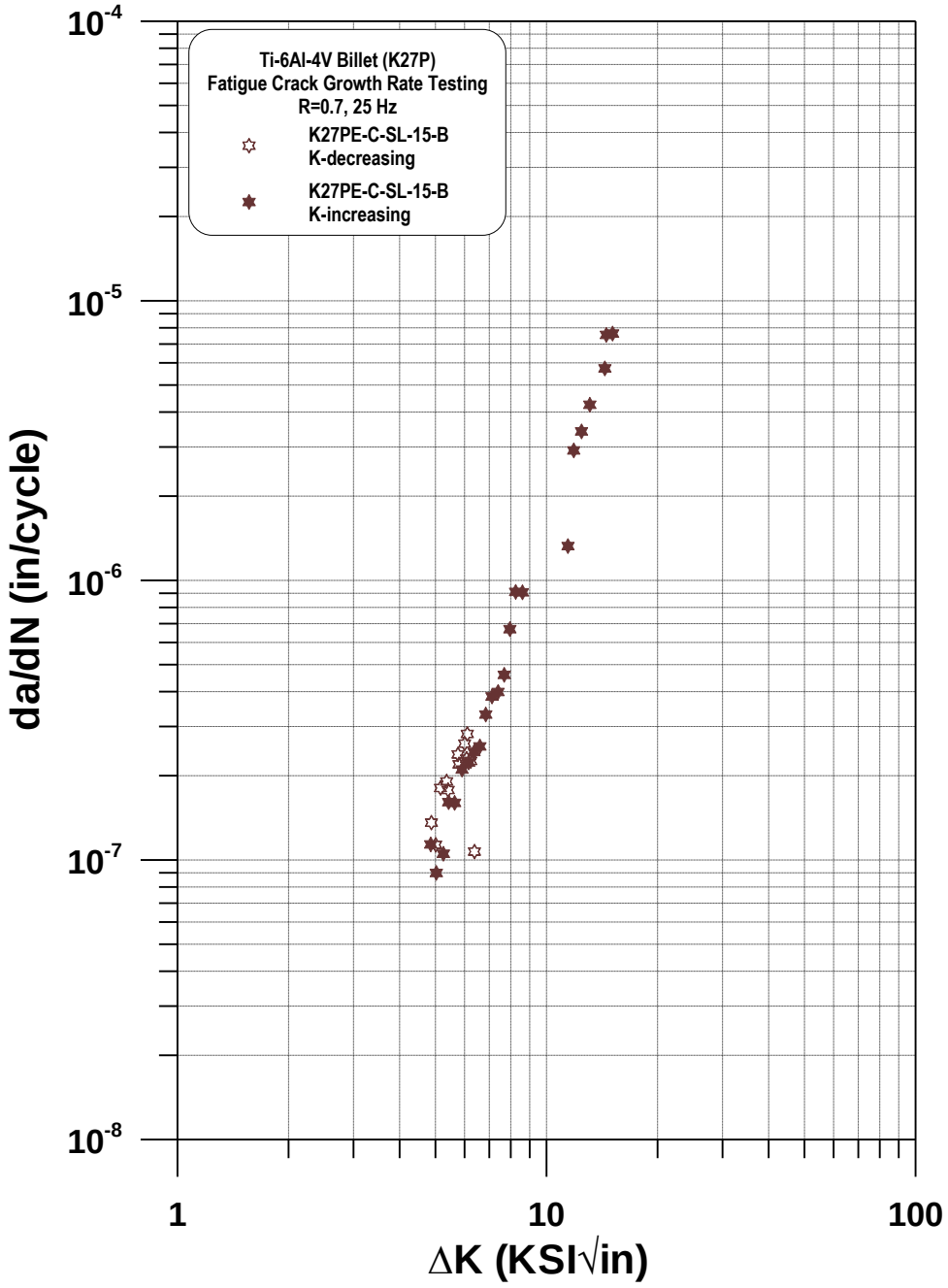
Approved for public release; distribution unlimited.



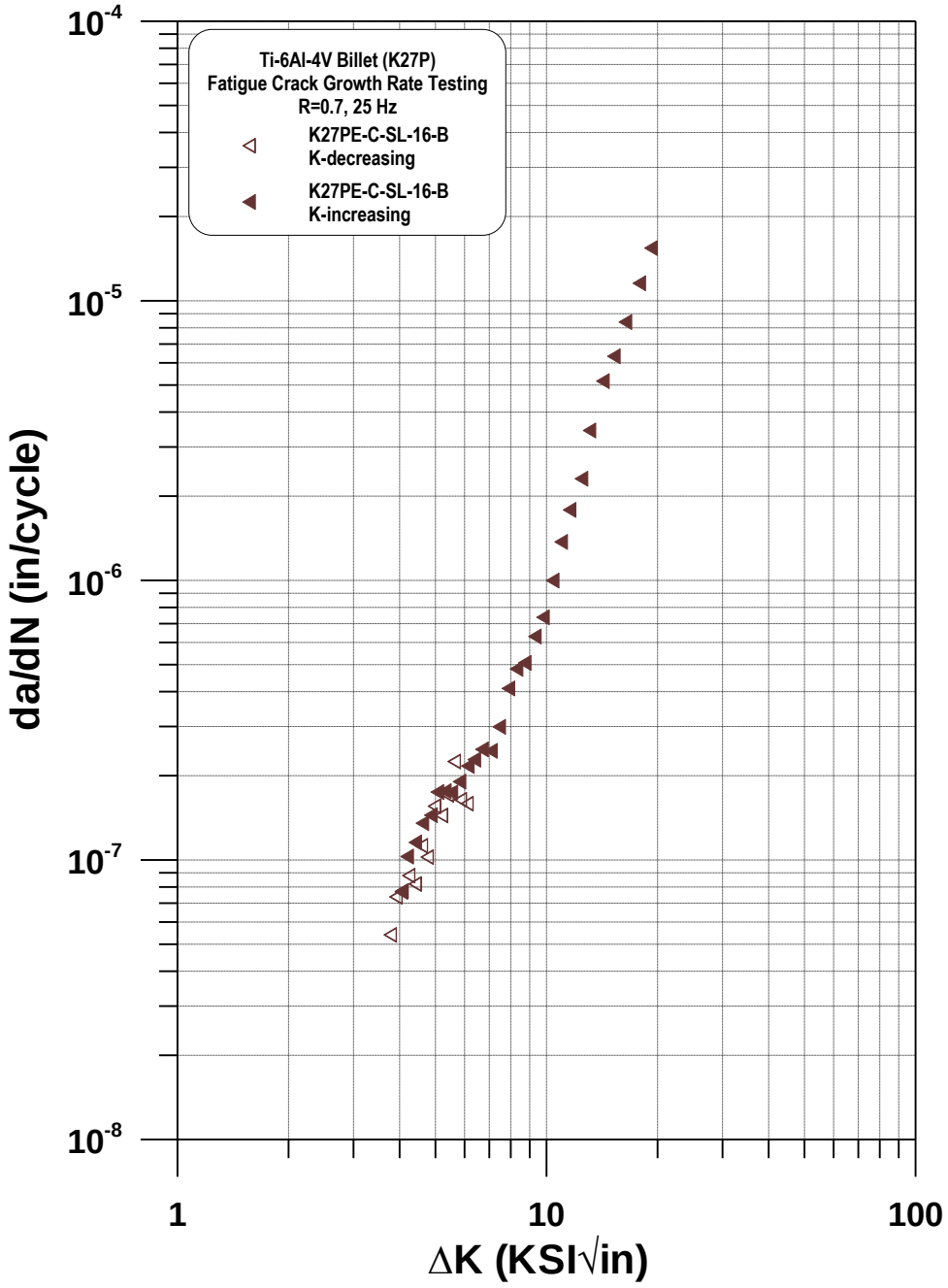
Approved for public release; distribution unlimited.



Approved for public release; distribution unlimited.



Approved for public release; distribution unlimited.



Approved for public release; distribution unlimited.

APPENDIX D

NON CONFORMING TITANIUM – BILLET CHARACTERIZATION (TI-6AL-6V-2SN BILLETS)

31 January 2011

EVALUATION REPORT

REPORT NO. AFRL/RXS 11-009

AUTHOR

Steven R. Thompson
Acquisition Systems Support Branch (AFRL/RXSCE)

Building 652, Room 122
2179 12th Street
Wright-Patterson AFB, Ohio 45433-7718

REQUESTER

AFMC/EN (Thomas Fischer)

CAUTION

This information consists of PRELIMINARY reasonable lower bound properties for titanium billet. (Fully analyzed data, labeled FINAL, will be forthcoming.)
This information should be used **only** to evaluate the potential impact of improperly substituted titanium.
This information should **not** be used for design purposes in place of material properties from specifications or MMPDS entries covering titanium plate, bar, or other product forms.
This information should **not** be used to analyze components manufactured from titanium stock that is known to be compliant with applicable specifications.

CAUTION

DISTRIBUTION STATEMENT A: Approved for public release; distribution unlimited.

EXECUTIVE SUMMARY

This report is intended to summarize the mechanical testing of two Ti-6Al-6V-2Sn billets. The data presented in this report is shown on a "preliminary" basis and should not be used for design purposes. Preliminary reasonable lower bounds are given for tensile and fracture toughness test results. Ultimate tensile strength and tensile yield strength preliminary reasonable lower bounds are based on a statistical analysis (described herein). Elastic modulus, ductility, and fracture toughness preliminary reasonable lower bounds are based on the lowest value in the population for that billet. Fatigue and fatigue crack growth results are presented in this report without discussion of lower bounds, as these properties will have further analyses (to be discussed in a future report) that will establish a delta in "life" based on comparison with control plate properties.

Key results of the testing described in this report are shown in the table below. For tensile results, specification minimum properties (for properly processed materials) are also shown for comparison purposes.

Property	Billet Number	Preliminary Reasonable Lower Bound	Specification Minimum Value
F_{tu}	14824	139 ksi	AMS-T-9046: 145 ksi AMS-T-9047 (1"-3"): 143 ksi AMS-T-9047 (3"-4"): 137 ksi
	14828	137 ksi	
F_{ty}	14824	131 ksi	AMS-T-9046: 135 ksi AMS-T-9047 (1"-3"): 131 ksi AMS-T-9047 (3"-4"): 129 ksi
	14828	131 ksi	
% elongation	14824	10%	AMS-T-9046: 8% AMS-T-9047 (1"-3"): 10% AMS-T-9047 (3"-4"): 10%
	14828	11%	
% reduction of area	14824	19%	AMS-T-9046: n/a AMS-T-9047 (1"-3"): 20% AMS-T-9047 (3"-4"): 20%
	14828	19%	
E	14824	14.2 msi	MMPDS04 (typical): 16.0 msi
	14828	14.3 msi	
K_{Ic}	14824	79.5 ksi$\sqrt{in}$	n/a
	14828	71.8 ksi$\sqrt{in}$	

where:
F_{tu}*: ultimate tensile strength*
F_{ty}*: tensile yield strength*
E*: elastic modulus*
K_{Ic}*: plane strain fracture toughness*

Approved for public release; distribution unlimited.

BACKGROUND

A federal investigation identified a risk associated with improperly processed titanium (Ti) material being used in the fabrication of critical safety items and safety-of-flight components in USAF, DoD, NASA, FAA, and other systems. At the direction of AFMC/CC, a Titanium Task Force (led by AFMC/EN) was formed to further define risk to USAF systems and to assist with mitigation efforts. The suspect Ti material (e.g., "billet," "reforging stock") was never intended to be machined to the final forms in which it is now possibly being used. This R&D testing program will develop new baseline (reasonable lower bound) properties on a heretofore not fully characterized form of Ti. The decision to refer to these baseline values as "reasonable lower bounds" is based on the fact that an insufficient quantity of material heats and lots were represented for the calculation of traditional MMPDS **[*1*]** A- or B-, or even S-basis allowables. However, the number specimens tested (often in replicate) is significant. Thus "reasonable lower bound" was chosen as the proper phrase to describe properties derived from the testing of multiple specimens from the two heats (per alloy) of material in this program. While these do not meet the requirements for standard baseline property determination, they are, nevertheless, significant.

This report is intended to summarize the mechanical testing of two Ti-6Al-6V-2Sn billets. The data presented in this report is shown on a "preliminary" basis and should not be used for design purposes.

Approved for public release; distribution unlimited.

MATERIAL DESCRIPTION

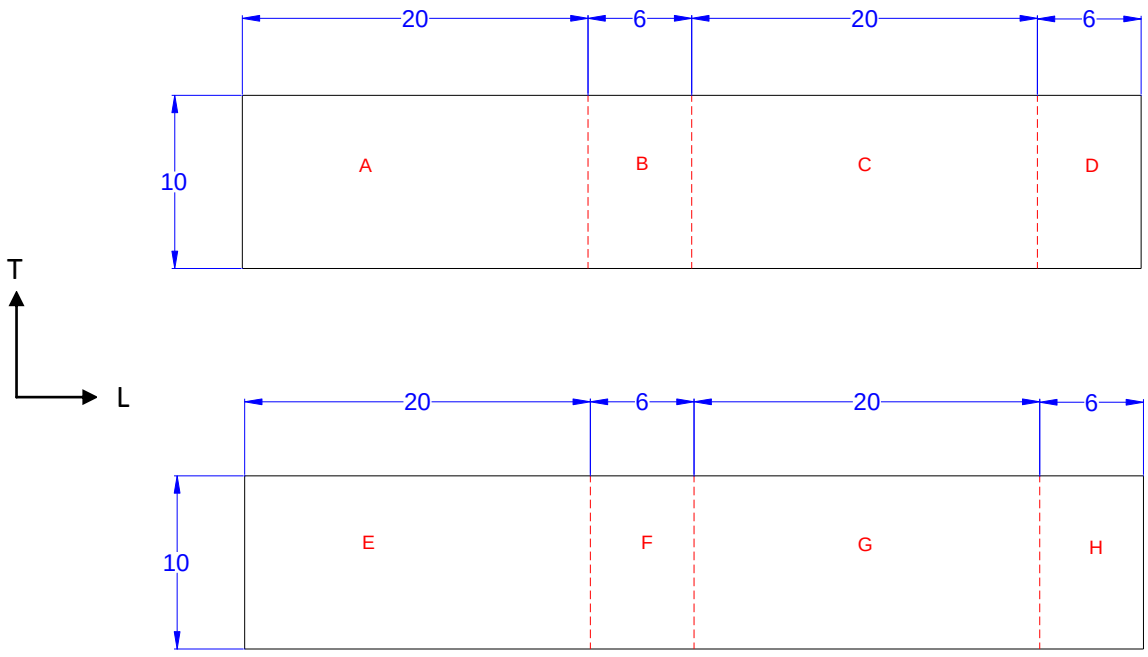
The Ti-6Al-6V-2Sn billets summarized in this report were purchased from Sierra Alloys. The billets were fabricated for this program to thicknesses prescribed by AFRL/RXS in order to produce two different levels of hot working in the material. Upon receipt from Sierra Alloys, the billets had nominal dimensions of 12”(w) x 105”(l) x 4.5”(t), identified throughout this report as billet number 14824, and 12”(w) x 80”(l) x 8”(t), identified throughout this report as billet number 14828. The billets had been produced per the AMS-T-9047G specification. The billets’ pedigree trace back to an ingot heat HC14820 produced by Howmet. The billets were delivered in the mill-annealed heat treat condition.

Upon receipt of the billets, a 2-inch wide section was cut along the length of the billet. The face of this section through the thickness was machined to a 32 Ra surface finish and macro-etched to determine forging flowlines. No anomalous microstructure was noticed during this examination. These sections of the billets were not used for subsequent mechanical testing.

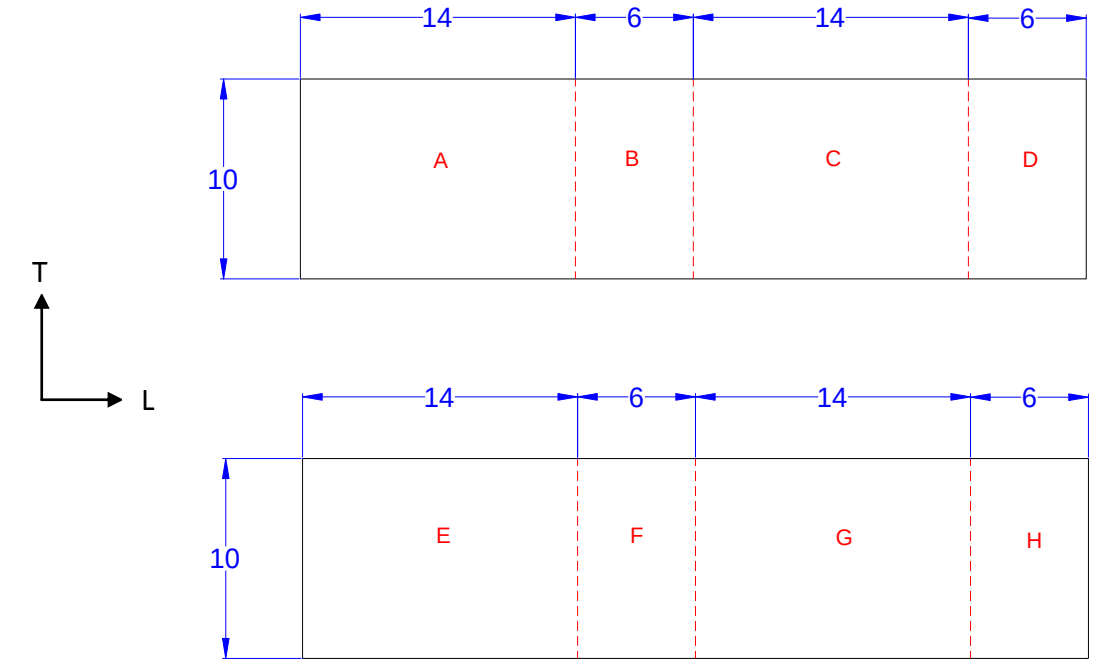
Due to the fact that billet material is intended to be an intermediate product form and not meant for use in component fabrication, a specimen orientation system needed to be established. The standard designations of longitudinal (L), long transverse (T), and short transverse (S) coordinate system were employed in this investigation in order to establish a consistency with plate and bar product forms. For this billet, the L-orientation was assigned to the billet length, the T-orientation to the billet width, and the S-orientation to the billet thickness as illustrated in Figure 1.

Prior to test specimen extraction, the remaining billet was sub-sectioned (as shown in Fig. 1) so that it could be subjected to non-destructive evaluation (NDE) using ultrasonic transmission (UT). The individual sections were designated as A through H and these designations were used in the specimen numbering schema. Any relevant, below threshold, indications were noted during this evaluation in the event of anomalous test results. After the test specimens were machined, they were once again examined using NDE techniques. All specimens, except the fracture toughness, were examined using x-ray and fluorescent penetrant inspection (FPI). Fracture toughness specimens had UT and FPI examinations. Any resultant indications were noted and photographed for use in analysis of anomalous test results.

Approved for public release; distribution unlimited.



(a)



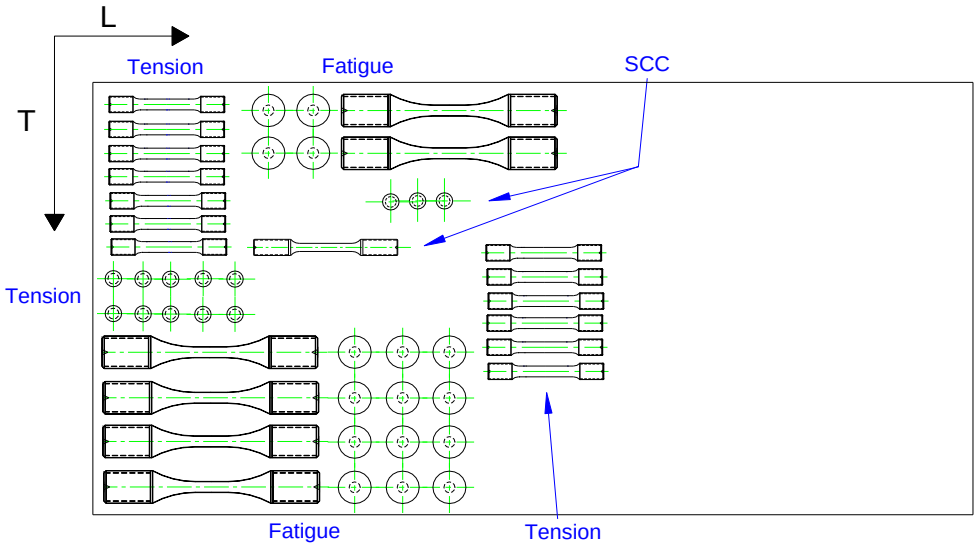
(b)

Figure 1. (a) Ti-6Al-6V-2Sn billet (14824) and (b) Ti-6Al-6V-2Sn billet (14828) indicating dimensions and orientations prior to specimen extraction. *[Note: All dimensions in inches.]*

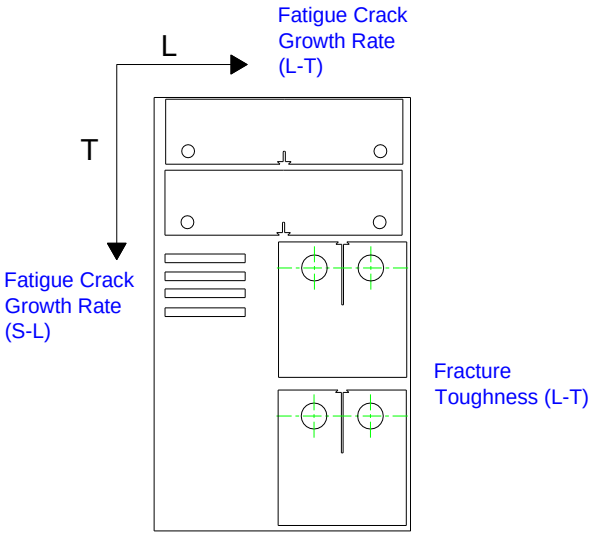
Approved for public release; distribution unlimited.

TEST PLAN

Test Specimens – The test specimens were excised from approximately the locations shown in Figures 2(a) and (b) for the 4.5" thick Ti-6Al-6V-2Sn billet and Figures 3(a) and (b) for the 8" thick Ti-6Al-6V-2Sn billet. Specimens were removed from three planes through the thickness where possible: the two quarter points (t/4 and 3t/4) and the midplane (t/2). Throughout this report, specimen location within the thickness is designated by either "A" (t/4), "B" (t/2), or "C" (3t/4). For short-transverse (S or S-L) oriented specimens, the location was determined by either the center of the gage length or the crack plane.



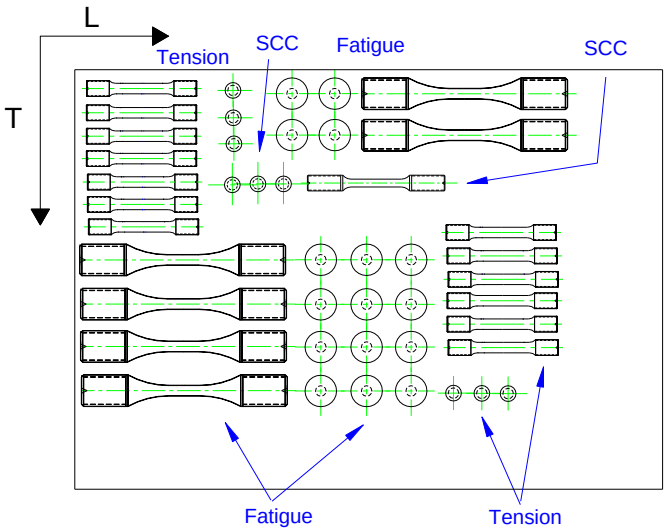
(a) Sections A, C, E, G



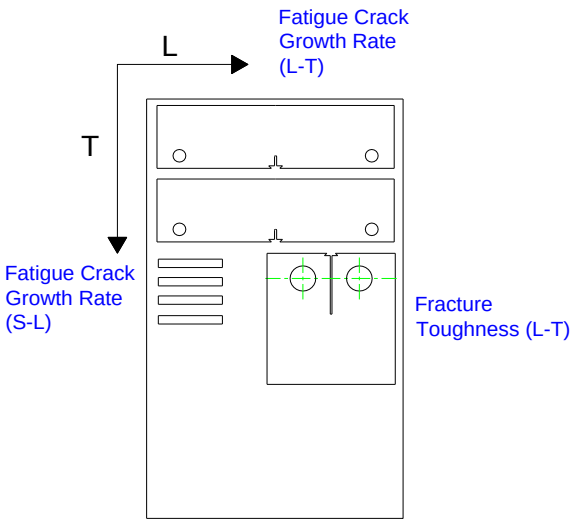
(b) Sections B, D, F, H

Figure 2. Specimen location layout drawings for Ti-6Al-6V-2Sn billet (14824).

Approved for public release; distribution unlimited.



(a) Sections A, C, E, G



(b) Sections B, D, F, H

Figure 3. Specimen location layout drawings for Ti-6Al-6V-2Sn billet (14828).

Test specimens were machined to the final required geometries as shown in Figures 4 through 8. All of the geometries were in accordance with the applicable test method (as described in the next section). All of the specimens were fabricated using the same machine shop per specimen drawings provided by AFRL/RXSCE, in order to minimize possibility of variability due to specimen machining. Special care was given to the traceability of the specimen back to a general location within the billet. Test specimens were given a unique identification that would allow for this tracking.

Approved for public release; distribution unlimited.

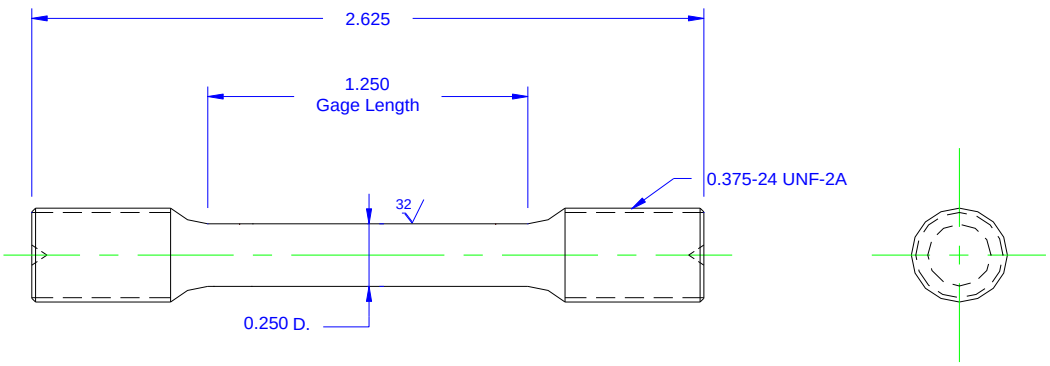


Figure 4. Geometry of tensile test specimen.

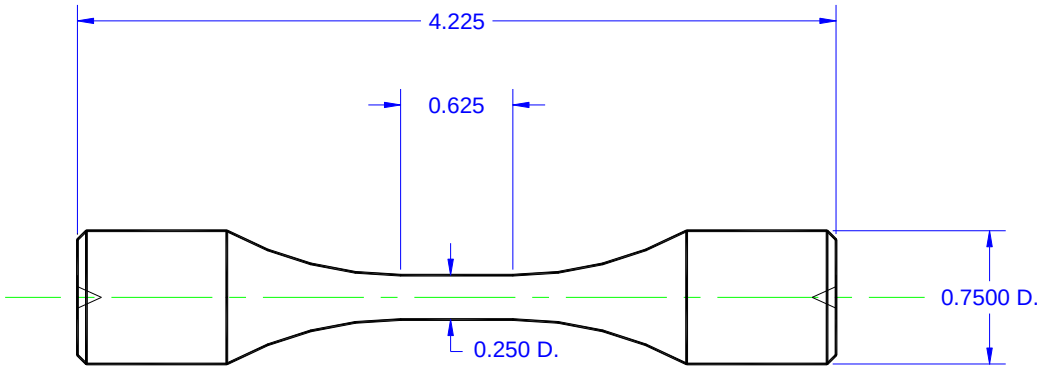
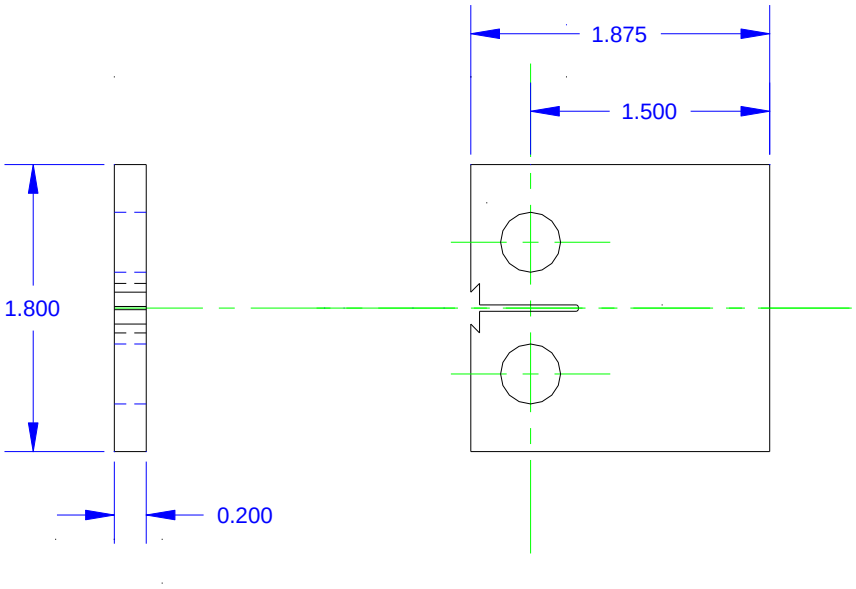
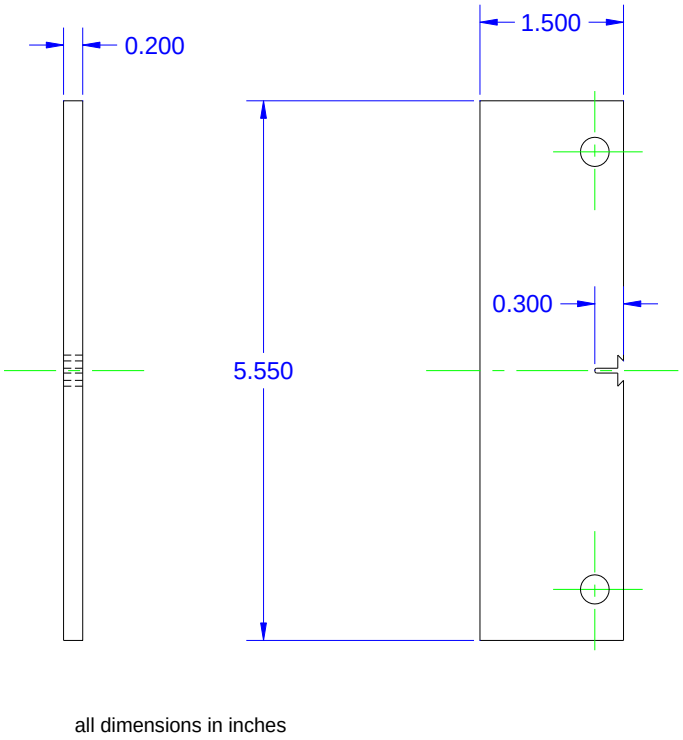


Figure 5. Geometry of fatigue test specimen. (Note: gage section was low-stress ground to a final surface finish of 8 Ra and then hand-polished longitudinally to remove all circumferential scratches.)



(a)



(b)

Figure 6. Geometry of fatigue crack growth rate (a) C(T) and (b) ESE(T) test specimens.

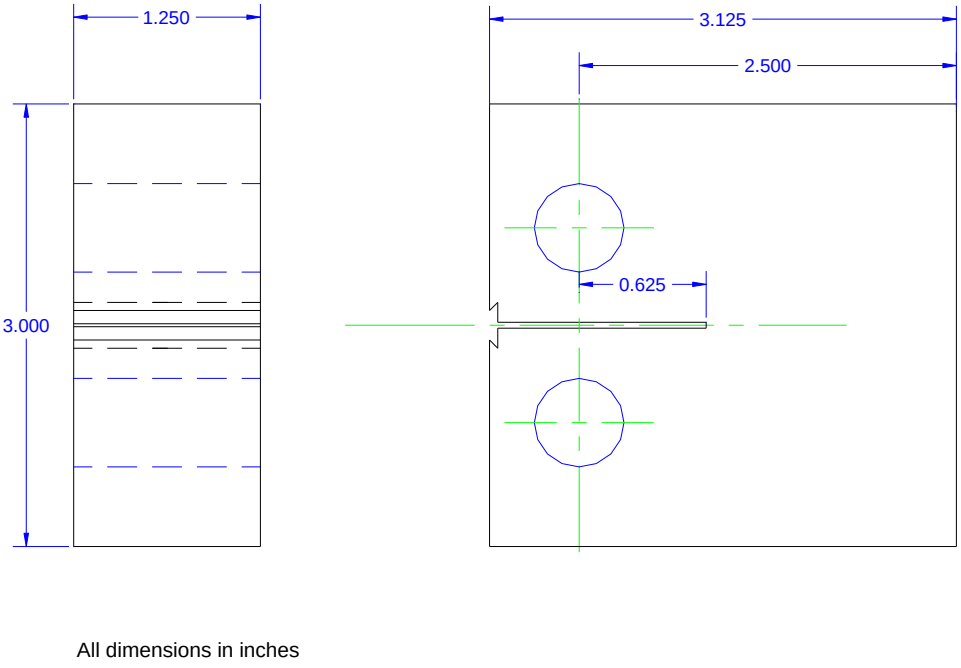


Figure 7. Geometry of fracture toughness C(T) test specimen.

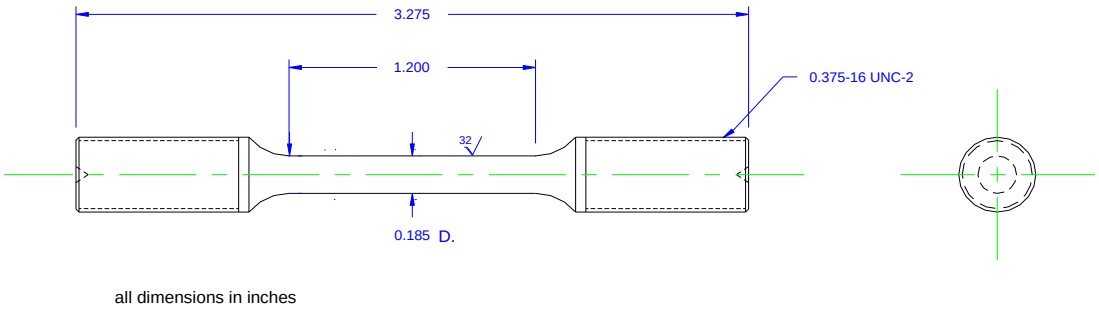


Figure 8. Geometry of stress corrosion cracking (SCC) test specimen.

Test Methods – The test methodologies used in this investigation are listed in Table 1. With the exception of stress corrosion cracking, all of the tests were performed in accordance with applicable ASTM standards. All testing was performed in ambient laboratory conditions (approximately 72°F and 50% relative humidity).

Table 1. Test Methodology

Test	ASTM Method
Tension (Modulus)	E 111-04 "Standard Test Method for Young's Modulus, Tangent Modulus, and Chord Modulus"
Tension	E 8/E 8M-08 "Standard Test Methods for Tension Testing of Metallic Materials"
Fatigue (force-controlled)	E 466-07 "Standard Practice for Conducting Force Controlled Constant Amplitude Axial Fatigue Tests of Metallic Materials"
Fatigue (strain-controlled)	E606-04 "Standard Practice for Strain-Controlled Fatigue Testing"
Fatigue Crack Growth Rate	E 647-08 "Standard Test Method for Measurement of Fatigue Crack Growth Rates"
Fracture Toughness	E 399-08 "Standard Test Method for Linear-Elastic Plane-Strain Fracture Toughness K_{Ic} of Metallic Materials"
Stress Corrosion Cracking	Similar to G 64-99 "Standard Classification of Resistance to Stress-Corrosion Cracking of Heat-Treatable Aluminum Alloys" Applied stress = 75% of specification tensile yield strength / 40 days 3.5% NaCl solution – alternate immersion (10 min wet/50 min dry)

Tension (Modulus) – Prior to performing full-range tension testing, approximately 10% of the machined tension specimens were used to generate modulus data using the procedures outlined in ASTM E111. For this testing the specimens were loaded to a maximum stress below the proportional limit, so as to remain within the linear region of the stress-strain curve. The test was repeated three times per specimen, with the specimen being rotated 120° between test runs. Strain was measured using an MTS averaging extensometer (B-1 classification) with a one-inch gage length. The average modulus from the three runs was recorded as the final elastic modulus.

Tension – Tension testing was performed on an Instron electro-mechanical test machine in accordance with ASTM E8. Strain was measured using an Instron one-inch gage length extensometer. The extensometer was removed from the specimen prior to reaching ultimate load to prevent damage to the instrument during specimen breakage. Elongation and reduction of area measurements were made using the "fit-back" method.

Fatigue (Force-controlled) – Axial fatigue testing was performed under force-controlled conditions using an MTS servo-hydraulic test machine in accordance with ASTM

E466. Stress ratios (R) of 0.05 and -1 were used in this investigation. Replicate specimens were tested at four applied stress levels for each of the stress ratios.

Fatigue (Strain-controlled) – Axial fatigue testing was performed under strain-controlled conditions using an MTS servo-hydraulic test machine in accordance with ASTM E606. An MTS one-inch gage length extensometer was used for strain measurement. The testing frequency used was 1 Hz. Strain ratios ($R_\varepsilon = \varepsilon_{min}/\varepsilon_{max}$) of 0.05 and -1 were used for these specimens.

Fatigue Crack Growth Rate – Fatigue crack growth rate testing was performed on an MTS servo-hydraulic test machine per ASTM E647 using computer data acquisition and control systems developed in-house. Crack length was measured via compliance techniques with standard crack-opening-displacement (COD) gages. Testing was performed under K-control (normalized K-gradient, C=-2) until a near-threshold growth rate was obtained, at which point the test was then run under constant amplitude (constant load) conditions for the remainder of the test. Initial and final crack lengths were measured optically for use in post-test crack correlation calculations. A test frequency of 25 Hz was used throughout the test, with humidity maintained at 50% ±10% for the duration of the test. Specimens were tested using stress ratios (R) of 0.1 and 0.7. Two orientations were tested for this program, L-T and S-L, where the first letter indicates the loading direction and the second letter indicates the direction of crack propagation. The compact, C(T), specimen geometry was utilized for the S-L orientation specimens extracted from the 4.5" thick billet material (14824) due to thickness limitations which would prevent the eccentrically-loaded single edge crack tension, ESE(T), specimen from being used.

Fracture Toughness – Plane-strain fracture toughness tests were performed in accordance with ASTM E399 on a Tinius-Olsen electro-mechanical test machine. Specimen precracking was performed on an MTS servo-hydraulic test machine. Crack length was monitored via compliance techniques using an MTS COD gage as previously described. Initial and final crack lengths were measured optically post-test.

Stress Corrosion Cracking – The theory behind this testing was that since the billet material had not been subject to final hot working, the microstructure may not have been fully homogenized, increasing the potential for localized aluminum segregation. If this were to occur, aluminum-rich areas would be more susceptible to the effect of stress corrosion cracking, particularly at these applied stress levels.

For this investigation, stress corrosion cracking tests were therefore performed to obtain pass/fail results. As there is currently no ASTM test method for SCC of titanium alloys, the procedure outlined in ASTM G64 ("A" level) was used. This procedure was previously adopted for use within AFRL/RXSCE as a standard SCC test. Specimens were axially loaded (statically) in an alternate immersion, 3.5% NaCl solution such that the specimens were submerged in the solution for 10 minutes and then allowed to dry for the next 50 minutes each hour. The specimens were loaded at 75% of the specification yield

strength (for plate and bar). For this alloy, the applied stress was 101.3 ksi. The test duration was set at 40 days. To pass the test, no specimen could fail during this 40 day loading cycle; failure being breakage of the test specimen or evidence of corrosion-related damage (i.e pitting).

FACTUAL DATA

4.5" Ti-6Al-6V-2Sn Billet (14824)

Tension – The results of tensile testing are shown in Tables 2(a) through 2(d). Strength levels for a portion of specimens from both orientations were below the specification minimum values shown in AMS-T-9046 (plate) and AMS-T-9047 (1"-3" bar) for this alloy. Elastic modulus values (based on E8 tensile test results) were generally below the range expected for this alloy, particularly for specimens in the S-orientation. On average, there was a less than 5% difference between those modulus results from ASTM E111 tests and those obtained from the E8 tensile test record. In addition, there did not appear to be a difference between specimens excised from the three different thickness locations.

Although the "reasonable lower bound" for the alloy will be calculated and identified in a future report, for this billet a preliminary reasonable lower bound was calculated using the procedures described in MMPDS Section 9.4.1 and assuming normality in the data population. The equation used for the calculation of these preliminary values (for strength only) was:

$$Minimum\ S = \overline{X} - s * k_{99}$$

where

$\overline{X}$ = sample mean

s = standard deviation

k_{99} = one-sided tolerance-limit factor corresponding to a proportion at least 0.99 of a normal distribution and a confidence coefficient of 0.95 based on the number of specimens in the given population. For this billet, a k_{99} factor of 2.57 was used, representing a population size of 196.

It should be noted that the AMS-T-9046 specification does not list minimum properties for the short-transverse orientation. Due to information indicating that non conforming materials have been cut-down from billet and purported as plate or bar, the expected orientation system may not have been known during component fabrication. Therefore, the results from the two orientations tested have been grouped together in order to provide reasonable lower bound properties. These preliminary reasonable lower bound properties are shown in Table 3. For modulus, elongation, and reduction of area, the minimum value from the data has been used as the preliminary reasonable lower bound.

Approved for public release; distribution unlimited.

Table 2. Ti-6Al-6V-2Sn billet (14824) tensile test results.

(a) Longitudinal orientation, t/4 thickness location

	Orientation	Thickness Location	Yield Strength (ksi)	Ultimate Tensile Strength (ksi)	% Elongation	% Reduction of Area	Elastic Modulus, E111 (msi)	Elastic Modulus, E8 (msi)
14824A-T-L-1-A	L	t/4	138.9	146.5	17.8%	38.2%	16.2	15.6
L-2-A	L	t/4	138.1	146.0	18.5%	42.5%	16.4	15.6
L-3-A	L	t/4	137.5	145.4	16.5%	35.1%		15.6
L-4-A	L	t/4	136.4	144.9	18.5%	40.3%		15.7
L-5-A	L	t/4	136.5	144.6	16.7%	36.6%		16.0
L-6-A	L	t/4	136.0	144.4	16.8%	36.7%		15.9
L-7-A	L	t/4	135.1	143.9	14.1%	25.0%		15.7
L-8-A	L	t/4	134.1	145.4	16.7%	34.5%		15.7
L-9-A	L	t/4	133.0	144.7	16.4%	37.1%		15.7
L-10-A	L	t/4	132.6	143.9	15.6%	32.9%		15.5
L-11-A	L	t/4	132.4	143.8	16.6%	34.4%		15.4
L-12-A	L	t/4	134.1	144.2	17.0%	32.9%		15.8
L-13-A	L	t/4	135.1	144.7	19.2%	34.2%		15.6
14824C-T-L-14-A	L	t/4	140.2	147.6	18.5%	39.0%	16.2	15.5
L-15-A	L	t/4	138.7	146.0	18.0%	39.2%	16.3	15.1
L-16-A	L	t/4	137.9	146.3	11.6%	36.8%		15.9
L-17-A	L	t/4	137.4	145.4	17.5%	36.5%		15.6
L-18-A	L	t/4	136.5	144.8	16.8%	35.2%		16.0
L-19-A	L	t/4	135.8	144.3	18.2%	35.6%		15.6
L-20-A	L	t/4	135.0	143.5	16.2%	33.5%		15.8
L-21-A	L	t/4	134.8	143.1	16.5%	33.7%		15.6
L-22-A	L	t/4	134.6	142.6	16.8%	33.7%		15.8
L-23-A	L	t/4	134.5	142.9	16.3%	33.7%		15.5
L-24-A	L	t/4	134.4	143.6	18.6%	37.3%		15.7
L-25-A	L	t/4	134.4	143.6	18.4%	33.0%		16.0
L-26-A	L	t/4	134.7	143.7	18.8%	33.7%		15.4

Approved for public release; distribution unlimited.

14824E-T-L-27-A	L	t/4	137.7	145.0	19.2%	41.9%	16.1	15.7
L-28-A	L	t/4	136.4	144.2	18.5%	33.4%	16.1	15.5
L-29-A	L	t/4	135.6	143.7	17.9%	34.4%		15.6
L-30-A	L	t/4	135.2	142.6	16.2%	37.1%		15.3
L-31-A	L	t/4	134.6	142.0	16.2%	33.9%		15.8
L-32-A	L	t/4	133.4	141.1	15.7%	32.6%		15.5
L-33-A	L	t/4	133.8	141.7	17.4%	36.5%		15.7
L-34-A	L	t/4	134.0	141.9	14.8%	31.7%		15.4
L-35-A	L	t/4	133.1	140.9	17.2%	32.4%		15.3
L-36-A	L	t/4	133.8	141.9	18.8%	31.9%		15.9
L-37-A	L	t/4	134.4	142.2	17.2%	34.9%		15.7
L-38-A	L	t/4	133.2	140.7	15.7%	35.9%		15.6
L-39-A	L	t/4	134.5	141.8	16.0%	34.4%		15.6
14824G-T-L-40-A	L	t/4	141.5	148.7	18.0%	42.0%	16.1	15.4
L-41-A	L	t/4	138.5	145.5	17.6%	40.2%	16.0	15.1
L-42-A	L	t/4	137.7	144.5	20.0%	39.4%		15.1
L-43-A	L	t/4	137.4	145.2	17.8%	34.9%		15.6
L-44-A	L	t/4	136.3	143.8	18.6%	34.1%		15.1
L-45-A	L	t/4	136.1	144.0	18.0%	41.0%		15.8
L-46-A	L	t/4	135.7	143.7	18.1%	36.1%		15.4
L-47-A	L	t/4	137.2	144.6	18.1%	37.5%		15.3
L-48-A	L	t/4	136.1	143.9	15.6%	32.2%		16.0
L-49-A	L	t/4	136.2	144.7	18.5%	27.5%		15.5
L-50-A	L	t/4	136.6	144.5	17.9%	32.5%		15.6
L-51-A	L	t/4	135.7	144.2	18.1%	35.0%		15.2
L-52-A	L	t/4	136.2	144.4	14.9%	23.1%		15.4
AMS-T-9046			135	145	8%			16.0[a]
AMS-T-9047 (1"-3")			131	143	10%	20%		
AMS-T-9047 (3"-4")			129	137	10%	20%		

(a): Typical value per MMPDS-04

Approved for public release; distribution unlimited.

(b) Longitudinal orientation, t/2 thickness location

	Orientation	Thickness Location	Yield Strength (ksi)	Ultimate Tensile Strength (ksi)	% Elongation	% Reduction of Area	Elastic Modulus, E111 (msi)	Elastic Modulus, E8 (msi)
14824A-T-L-1-B	L	t/2	138.4	146.9	17.4%	41.7%	16.3	15.8
L-2-B	L	t/2	137.4	146.1	17.7%	40.3%	16.4	15.8
L-3-B	L	t/2	136.9	145.9	19.0%	38.1%		15.5
L-4-B	L	t/2	135.3	143.9	13.7%	30.3%		15.5
L-5-B	L	t/2	134.7	143.2	17.1%	38.4%		15.1
L-6-B	L	t/2	134.6	142.8	17.4%	37.7%		15.3
L-7-B	L	t/2	134.1	142.5	17.8%	32.8%		15.1
L-8-B	L	t/2	135.3	143.2	16.8%	34.4%		15.8
L-9-B	L	t/2	134.0	141.6	16.8%	34.9%		15.3
L-10-B	L	t/2	135.0	142.5	16.3%	29.2%		15.7
L-11-B	L	t/2	135.1	142.5	16.9%	32.4%		15.9
L-12-B	L	t/2	135.9	144.5	16.8%	31.2%		15.8
L-13-B	L	t/2	134.9	142.8	16.1%	37.5%		15.5
14824C-T-L-14-B	L	t/2	138.8	147.4	19.8%	35.6%	16.6	15.8
L-15-B	L	t/2	137.3	146.0	17.1%	34.3%	16.6	15.5
L-16-B	L	t/2	137.8	146.5	16.0%	28.4%		15.9
L-17-B	L	t/2	133.4	141.6	17.0%	40.0%		15.7
L-18-B	L	t/2	135.0	143.6	15.6%	26.3%		15.8
L-19-B	L	t/2	134.4	142.5	17.9%	33.2%		15.7
L-20-B	L	t/2	135.8	144.4	16.9%	33.5%		15.9
L-21-B	L	t/2	134.9	143.0	17.0%	31.6%		15.8
L-22-B	L	t/2	134.1	141.9	16.7%	35.0%		15.7
L-23-B	L	t/2	134.4	141.9	16.0%	34.4%		15.7
L-24-B	L	t/2	134.7	142.1	16.2%	36.2%		15.6
L-25-B	L	t/2	134.6	143.0	17.7%	30.7%		15.6
L-26-B	L	t/2	133.6	141.6	18.9%	26.8%		15.7

Approved for public release; distribution unlimited.

14824E-T-L-27-B	L	t/2	137.6	145.8	16.9%	36.9%	16.1	15.7
L-28-B	L	t/2	135.9	144.7	17.5%	37.7%	16.2	15.7
L-29-B	L	t/2	135.5	144.4	17.3%	32.1%		15.8
L-30-B	L	t/2	133.8	142.7	16.2%	32.3%		15.4
L-31-B	L	t/2	133.6	142.5	18.4%	36.6%		15.7
L-32-B	L	t/2	133.5	141.7	17.5%	31.7%		16.0
L-33-B	L	t/2	133.7	142.1	16.1%	33.1%		15.2
L-34-B	L	t/2	133.8	142.1	16.4%	37.4%		15.1
L-35-B	L	t/2	134.1	142.4	17.3%	35.8%		15.0
L-36-B	L	t/2	134.0	142.2	15.4%	33.8%		16.0
L-37-B	L	t/2	133.6	141.4	15.1%	30.1%		15.7
L-38-B	L	t/2	133.2	141.2	17.4%	25.5%		15.8
L-39-B	L	t/2	133.0	141.0	21.1%	35.7%		15.7
14824G-T-L-40-B	L	t/2	139.8	147.7	18.1%	44.1%	16.1	15.7
L-41-B	L	t/2	137.1	145.8	18.6%	39.7%	16.1	15.6
L-42-B	L	t/2	135.8	143.7	15.8%	32.8%		15.4
L-43-B	L	t/2	135.7	143.3	15.1%	37.1%		15.7
L-44-B	L	t/2	134.2	141.9	18.9%	34.3%		15.5
L-45-B	L	t/2	134.8	143.2	17.6%	34.5%		15.7
L-46-B	L	t/2	134.5	143.0	17.4%	34.3%		15.4
L-47-B	L	t/2	134.7	141.9	15.7%	34.6%		15.7
L-48-B	L	t/2	134.0	141.5	16.5%	36.3%		15.7
L-49-B	L	t/2	134.7	142.8	18.1%	33.6%		15.6
L-50-B	L	t/2	133.8	141.0	17.9%	36.7%		15.3
L-51-B	L	t/2	134.5	142.1	14.8%	26.5%		16.0
L-52-B	L	t/2	132.7	140.1	18.1%	34.3%		14.8
AMS-T-9046			135	145	8%			16.0[a]
AMS-T-9047 (1"-3")			131	143	10%	20%		
AMS-T-9047 (3"-4")			129	137	10%	20%		

(a): Typical value per MMPDS-04

Approved for public release; distribution unlimited.

(c) Longitudinal orientation, 3t/4 thickness location

	Orientation	Thickness Location	Yield Strength (ksi)	Ultimate Tensile Strength (ksi)	% Elongation	% Reduction of Area	Elastic Modulus, E111 (msi)	Elastic Modulus, E8 (msi)
14824A-T-L-1-C	L	3t/4	139.9	147.8	18.1%	39.3%	16.3	15.6
L-2-C	L	3t/4	139.1	147.0	19.3%	41.2%	16.5	15.8
L-3-C	L	3t/4	138.2	146.6	18.6%	32.1%		15.5
L-4-C	L	3t/4	136.7	145.0	18.1%	32.9%		15.8
L-5-C	L	3t/4	136.4	144.5	15.7%	39.1%		15.9
L-6-C	L	3t/4	136.4	144.8	13.7%	24.0%		16.1
L-7-C	L	3t/4	136.6	144.7	15.7%	35.9%		15.9
L-8-C	L	3t/4	136.2	145.2	15.8%	34.0%		15.7
L-9-C	L	3t/4	136.0	144.7	16.9%	34.8%		15.4
L-10-C	L	3t/4	135.6	145.4	15.7%	30.5%		15.1
L-11-C	L	3t/4	135.1	145.2	15.0%	27.7%		15.2
L-12-C	L	3t/4	135.1	145.2	15.7%	34.6%		15.1
L-13-C	L	3t/4	134.7	145.0	15.9%	34.8%		15.0
14824C-T-L-14-C	L	3t/4	141.0	148.2	17.9%	36.6%	16.1	15.8
L-15-C	L	3t/4	139.4	146.8	14.6%	33.9%	16.5	15.5
L-16-C	L	3t/4	138.2	145.8	16.4%	38.6%		16.0
L-17-C	L	3t/4	137.9	145.7	16.8%	33.7%		16.0
L-18-C	L	3t/4	136.0	144.5	16.4%	28.4%		15.8
L-19-C	L	3t/4	136.1	144.8	14.2%	35.3%		15.7
L-20-C	L	3t/4	135.1	143.4	16.0%	38.6%		15.5
L-21-C	L	3t/4	136.6	145.0	19.2%	38.3%		15.5
L-22-C	L	3t/4	136.3	145.2	17.1%	34.4%		15.4
L-23-C	L	3t/4	135.6	144.4	16.6%	38.5%		15.8
L-24-C	L	3t/4	135.1	144.3	18.7%	36.4%		15.2
L-25-C	L	3t/4	134.9	144.1	18.2%	35.1%		15.4
L-26-C	L	3t/4	134.6	144.0	18.1%	37.5%		15.6

Approved for public release; distribution unlimited.

14824E-T-L-27-C	L	3t/4	138.1	145.3	17.0%	34.9%	16.1	15.3
L-28-C	L	3t/4	135.5	143.8	19.2%	42.5%	16.1	15.1
L-29-C	L	3t/4	136.1	144.3	17.7%	38.2%		15.8
L-30-C	L	3t/4	133.5	141.7	16.9%	35.3%		15.5
L-31-C	L	3t/4	133.0	140.8	16.8%	36.4%		15.5
L-32-C	L	3t/4	133.0	141.3	16.2%	31.6%		15.6
L-33-C	L	3t/4	134.5	142.5	16.2%	34.3%		15.9
L-34-C	L	3t/4	134.3	142.9	18.7%	34.7%		15.6
L-35-C	L	3t/4	134.9	142.3	13.3%	32.2%		15.6
L-36-C	L	3t/4	133.4	141.4	15.7%	35.3%		15.8
L-37-C	L	3t/4	133.3	141.4	16.6%	35.2%		15.7
L-38-C	L	3t/4		142.2	17.4%	33.9%		15.6
L-39-C	L	3t/4	133.0	140.3	15.5%	36.0%		15.8
14824G-T-L-40-C	L	3t/4	140.1	147.5	17.5%	43.1%	16.0	15.2
L-41-C	L	3t/4	138.5	146.3	17.4%	34.8%	16.1	15.5
L-42-C	L	3t/4	137.2	144.8	16.6%	34.7%		15.6
L-43-C	L	3t/4	136.6	144.4	18.5%	33.6%		15.8
L-44-C	L	3t/4	135.7	143.6	17.5%	35.0%		14.9
L-45-C	L	3t/4	134.8	143.4	13.7%	28.0%		15.6
L-46-C	L	3t/4	135.2	143.7	16.3%	32.7%		15.5
L-47-C	L	3t/4	135.9	144.2	18.7%	37.7%		15.9
L-48-C	L	3t/4	136.4	144.1	15.3%	30.3%		15.4
L-49-C	L	3t/4	135.6	144.3	18.1%	34.8%		15.8
L-50-C	L	3t/4	135.6	144.5	21.0%	32.7%		15.8
L-51-C	L	3t/4	134.4	143.2	16.9%	34.0%		15.4
L-52-C	L	3t/4	135.1	143.8	18.4%	34.7%		15.2
AMS-T-9046			135	145	8%			16.0[a]
AMS-T-9047 (1"-3")			131	143	10%	20%		
AMS-T-9047 (3"-4")			129	137	10%	20%		

(a): Typical value per MMPDS-04

(d) Short-transverse orientation, t/2 thickness location

	Orientation	Thickness Location	Yield Strength (ksi)	Ultimate Tensile Strength (ksi)	% Elongation	% Reduction of Area	Elastic Modulus, E111 (msi)	Elastic Modulus, E8 (msi)
14824A-T-S-1-B	S	t/2	135.9	144.6	12.4%	24.8%	15.6	15.2
S-2-B	S	t/2	135.3	144.1	14.2%	31.4%	15.6	14.9
S-3-B	S	t/2	135.1	143.9	12.8%	23.9%		14.8
S-4-B	S	t/2	135.0	143.3	12.9%	28.4%		14.8
S-5-B	S	t/2	135.4	144.2	11.7%	20.9%		15.2
S-6-B	S	t/2	135.1	142.9	12.3%	26.1%		15.0
S-7-B	S	t/2	135.1	142.4	15.2%	21.2%		14.7
S-8-B	S	t/2	135.1	143.0	12.5%	23.6%		14.9
S-9-B	S	t/2	135.1	141.7	13.3%	28.2%		15.1
S-10-B	S	t/2	135.4	142.3	14.1%	24.1%		15.0
14824C-T-S-11-B	S	t/2	134.3	142.3	13.6%	24.0%	15.8	14.2
S-12-B	S	t/2	135.5	143.9	14.8%	25.1%	15.9	14.7
S-13-B	S	t/2	134.6	143.8	11.6%	19.9%		15.1
S-14-B	S	t/2	134.4	144.6	13.6%	20.5%		14.6
S-15-B	S	t/2	135.0	144.1	13.0%	25.6%		14.8
S-16-B	S	t/2	133.7	142.7	11.1%	19.5%		14.8
S-17-B	S	t/2	135.5	143.5	13.2%	23.2%		15.0
S-18-B	S	t/2	135.3	142.8	10.1%	19.4%		15.1
S-19-B	S	t/2	135.8	143.0	12.7%	20.3%		14.8
S-20-B	S	t/2	135.8	143.4	12.6%	18.6%		14.5
14824E-T-S-21-B	S	t/2	135.1	143.4	12.7%	25.1%	15.9	15.0
S-22-B	S	t/2	134.5	143.3	13.3%	22.7%	15.8	14.8
S-23-B	S	t/2	135.7	143.7	12.8%	27.1%		15.0
S-24-B	S	t/2	136.3	144.3	13.9%	27.9%		15.6
S-25-B	S	t/2	135.1	143.5	13.2%	23.3%		15.7
S-26-B	S	t/2	135.1	143.9	12.1%	22.4%		14.8
S-27-B	S	t/2	134.8	142.9	13.5%	22.8%		15.4
S-28-B	S	t/2	134.2	142.4	13.2%	24.3%		15.0
S-29-B	S	t/2	135.2	143.6	13.7%	24.1%		14.9
S-30-B	S	t/2	134.1	142.5	13.8%	26.9%		15.0

Approved for public release; distribution unlimited.

14824G-T-S-31-B	S	t/2	134.8	143.2	13.0%	22.4%	15.7	14.9
S-32-B	S	t/2	135.1	143.7	13.1%	22.5%	15.8	15.3
S-33-B	S	t/2	135.5	143.6	11.1%	20.5%		15.0
S-34-B	S	t/2	136.2	144.5	13.1%	19.5%		15.3
S-35-B	S	t/2	134.7	142.9	11.7%	22.2%		14.8
S-36-B	S	t/2	135.7	144.3	13.7%	23.9%		14.8
S-37-B	S	t/2	135.8	144.6	12.5%	22.6%		14.7
S-38-B	S	t/2	133.8	141.7	11.2%	21.7%		14.8
S-39-B	S	t/2	135.3	143.6	13.7%	26.8%		15.1
S-40-B	S	t/2	135.0	142.7	13.8%	23.0%		14.8
AMS-T-9046 (L-orientation)			135	145	8%			16.0[a]
AMS-T-9047 (1"-3")			131	143	10%	20%		
AMS-T-9047 (3"-4")			129	137	8%	15%		

(a): Typical value per MMPDS-04

Table 3. Preliminary reasonable lower bound tensile properties for Ti-6Al-6V-2Sn billet (14824).

Yield Strength (ksi)	Ultimate Tensile Strength (ksi)	% Elongation	% Reduction of Area	Elastic Modulus (msi)
131	139	10%	19%	14.2

Fatigue (force-controlled) – The results of force-controlled axial fatigue testing are shown graphically in Figure 9. Individual results are tabulated in Table 4. In Fig. 9, the results for each stress ratio (R) have been fit with a best-fit power-law curve for graphical purposes only. Also included in this figure are curves based on an equivalent stress equation from MMPDS Figure 5.4.2.1.8(a). As stated in Fig. 4, the fatigue specimens used herein were manufactured using low-stress grinding operations to a surface finish (Ra) of 8 per the ASTM E466 standard. The MMPDS reference data curves were generated using specimens having a surface roughness of 32 RMS. Although the specimens used in this effort had a smoother surface finish than those used in the reference data, and a longer life would typically be expected, it is not known whether low-stress grinding was used on the reference specimens. This aspect, along with the fact that the material from which the referenced specimens were extracted exhibited higher tensile strength than the billet

material tested in this program, could potentially have contributed to the difference between the data sets.

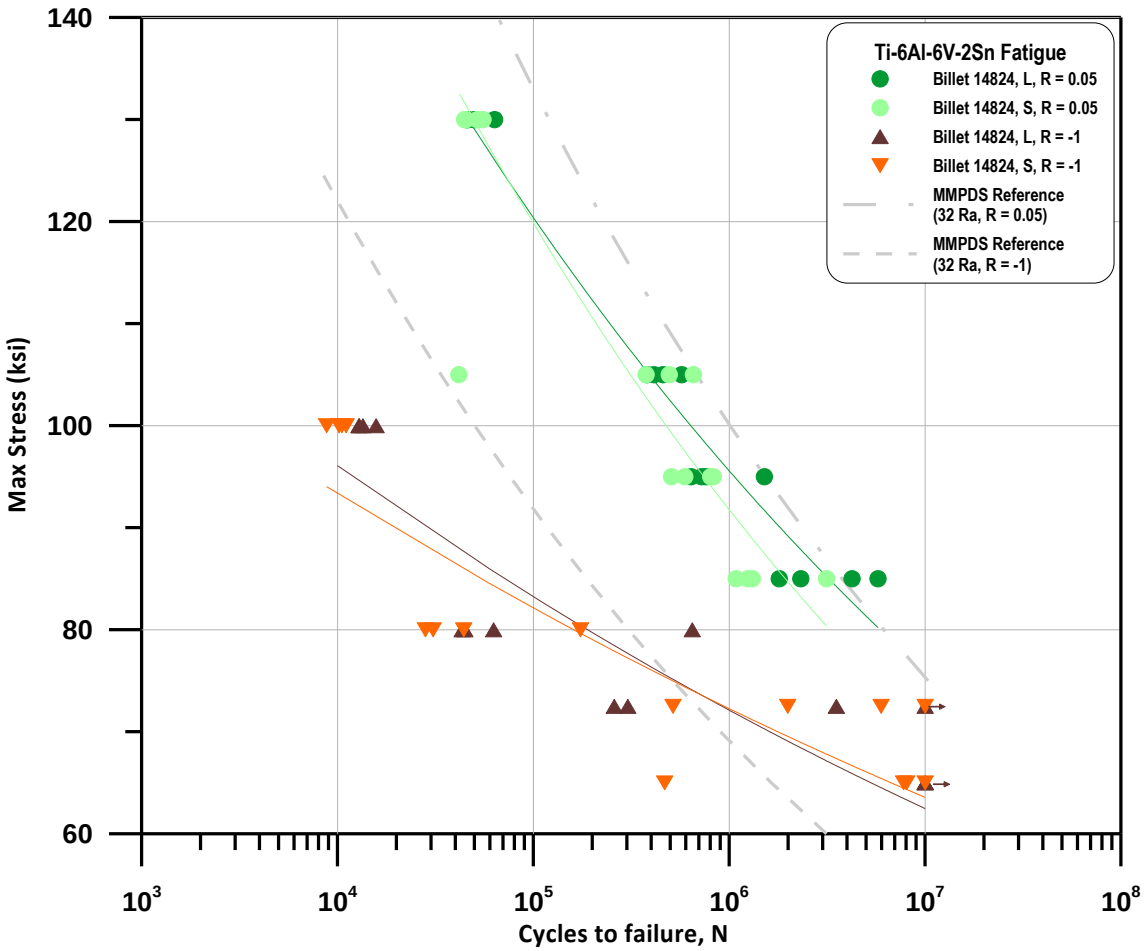


Figure 9. Ti-6Al-6V-2Sn billet (14824) force-controlled axial fatigue test results.

Table 4. Ti-6Al-6V-2Sn billet (14824) force-controlled axial fatigue test results.

(a) R = 0.05

	Thickness Location	Orientation	Max Stress (ksi)	Stress Ratio, R	Cycles to Failure
14824G-F-L-23-A	t/4	L	130	0.05	49,960
14824G-F-L-24-B	t/2	L	130	0.05	45,560
14824A-F-L-6-B	t/2	L	130	0.05	46,310
14824G-F-L-24-C	3t/4	L	130	0.05	63,310
14824C-F-L-11-A	t/4	L	105	0.05	571,360
14824C-F-L-12-A	t/4	L	105	0.05	458,750
14824G-F-L-23-B	t/2	L	105	0.05	412,460
14824G-F-L-23-C	3t/4	L	105	0.05	380,140
14824A-F-L-6-A	t/4	L	95	0.05	722,170
14824C-F-L-12-B	t/2	L	95	0.05	759,790
14824A-F-L-5-B	t/2	L	95	0.05	1,510,660
14824A-F-L-6-C	3t/4	L	95	0.05	638,540
14824A-F-L-5-A	t/4	L	85	0.05	2,318,580
14824C-F-L-11-B	t/2	L	85	0.05	4,234,190
14824C-F-L-12-C	3t/4	L	85	0.05	1,800,530
14824A-F-L-5-C	3t/4	L	85	0.05	5,747,450
14824G-F-S-62-B	t/2	S	130	0.05	44,520
14824C-F-S-30-B	t/2	S	130	0.05	45,290
14824A-F-S-13-B	t/2	S	130	0.05	51,720
14824G-F-S-61-B	t/2	S	130	0.05	55,290
14824A-F-S-15-B	t/2	S	105	0.05	656,190
14824A-F-S-14-B	t/2	S	105	0.05	494,000
14824C-F-S-31-B	t/2	S	105	0.05	41,630
14824A-F-S-16-B	t/2	S	105	0.05	375,630
14824G-F-S-64-B	t/2	S	95	0.05	803,510
14824C-F-S-32-B	t/2	S	95	0.05	592,680
14824E-F-S-48-B	t/2	S	95	0.05	507,230
14824E-F-S-45-B	t/2	S	95	0.05	828,590
14824C-F-S-29-B	t/2	S	85	0.05	1,242,760
14824G-F-S-63-B	t/2	S	85	0.05	3,140,860
14824E-F-S-46-B	t/2	S	85	0.05	1,309,470
14824E-F-S-47-B	t/2	S	85	0.05	1,083,620

Approved for public release; distribution unlimited.

(b) R = -1

	Thickness Location	Orientation	Max Stress (ksi)	Stress Ratio, R	Cycles to Failure
14824-F-L-1-B	t/2	L	100	-1	13,472
14824-F-L-7-B	t/2	L	100	-1	12,908
14824-F-L-13-B	t/2	L	100	-1	15,715
14824-F-L-19-C	3t/4	L	100	-1	12,848
14824-F-L-2-A	t/4	L	80	-1	44,660
14824-F-L-8-A	t/4	L	80	-1	647,083
14824-F-L-14-A	t/4	L	80	-1	43,194
14824-F-L-20-C	3t/4	L	80	-1	62,630
14824-F-L-4-A	t/4	L	72.5	-1	10,000,000 *
14824-F-L-10-A	t/4	L	72.5	-1	3,524,291
14824-F-L-16-B	t/2	L	72.5	-1	258,479
14824-F-L-22-B	t/2	L	72.5	-1	303,350
14824-F-L-3-C	3t/4	L	65	-1	10,000,000 *
14824-F-L-9-C	3t/4	L	65	-1	10,000,000 *
14824-F-L-21-C	3t/4	L	65	-1	10,000,000 *
14824-F-S-3-B	t/2	S	100	-1	11,054
14824-F-S-19-B	t/2	S	100	-1	8,802
14824-F-S-35-B	t/2	S	100	-1	10,514
14824-F-S-51-B	t/2	S	100	-1	10,177
14824-F-S-6-B	t/2	S	80	-1	28,051
14824-F-S-22-B	t/2	S	80	-1	173,807
14824-F-S-38-B	t/2	S	80	-1	30,723
14824-F-S-54-B	t/2	S	80	-1	44,031
14824-F-S-12-B	t/2	S	72.5	-1	515,879
14824-F-S-28-B	t/2	S	72.5	-1	10,000,000 *
14824-F-S-44-B	t/2	S	72.5	-1	1,988,113
14824-F-S-60-B	t/2	S	72.5	-1	5,951,147
14824-F-S-9-B	t/2	S	65	-1	8,056,352
14824-F-S-25-B	t/2	S	65	-1	10,000,000 *
14824-F-S-41-B	t/2	S	65	-1	7,756,287
14824-F-S-57-B	t/2	S	65	-1	467,916

** : indicates runout*

Fatigue (strain-controlled) – The results of strain-controlled axial fatigue testing are shown graphically in Figure 10, with individual results tabulated in Table 5.

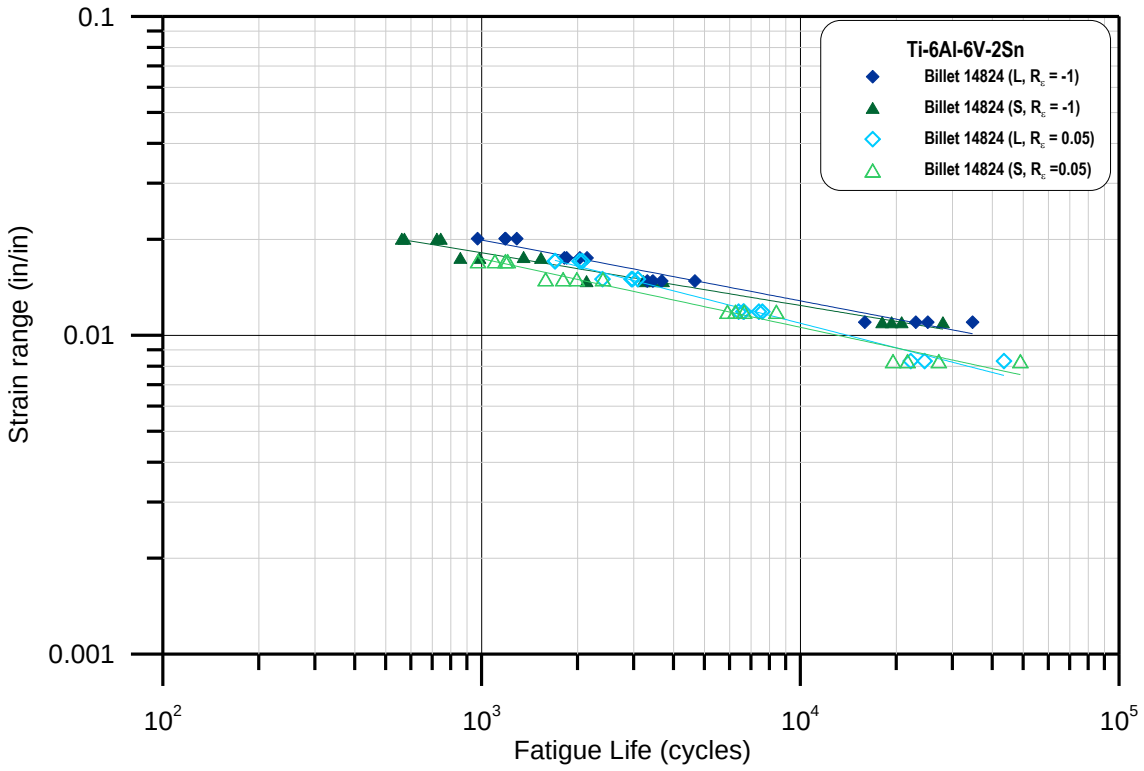


Figure 10. Ti-6Al-6V-2Sn billet (14824) strain-controlled axial fatigue test results.

Approved for public release; distribution unlimited.

Table 5. Ti-6Al-6V-2Sn billet (14824) strain-controlled axial fatigue test results.

(a) $R_\varepsilon = 0.05$

	Thickness Location	Orientation	Strain Range (in/in)	Strain Ratio, R_ε	Cycles to Failure
14824E-F-L-16-A	t/4	L	0.0171	0.05	1,697
14824A-F-L-4-C	3t/4	L	0.0171	0.05	1,700
14824C-F-L-10-C	3t/4	L	0.0171	0.05	2,071
14824G-F-L-22-C	3t/4	L	0.0171	0.05	2,028
14824G-F-L-20-A	t/4	L	0.0150	0.05	3,090
14824A-F-L-2-B	t/2	L	0.0150	0.05	2,394
14824C-F-L-8-B	t/2	L	0.0150	0.05	2,952
14824E-F-L-13-C	3t/4	L	0.0150	0.05	2,975
14824A-F-L-3-A	t/4	L	0.0119	0.05	6,625
14824C-F-L-9-A	t/4	L	0.0119	0.05	7,597
14824G-F-L-22-A	t/4	L	0.0119	0.05	6,643
14824E-F-L-14-B	t/2	L	0.0119	0.05	6,398
14824G-F-L-20-B	t/2	L	0.0119	0.05	7,404
14824A-F-L-3-B	t/2	L	0.0083	0.05	22,178
14824C-F-L-9-B	t/2	L	0.0083	0.05	43,500
14824E-F-L-14-C	3t/4	L	0.0083	0.05	24,521
14824A-F-S-11-B	t/2	S	0.0171	0.05	1,100
14824C-F-S-27-B	t/2	S	0.0171	0.05	1,206
14824F-F-S-43-B	t/2	S	0.0171	0.05	1,187
14824G-F-S-59-B	t/2	S	0.0171	0.05	974
14824A-F-S-2-B	t/2	S	0.0150	0.05	1,586
14824C-F-S-18-B	t/2	S	0.0150	0.05	2,402
14824E-F-S-34-B	t/2	S	0.0150	0.05	1,988
14824G-F-S-50-B	t/2	S	0.0150	0.05	1,800
14824A-F-S-5-B	t/2	S	0.0119	0.05	6,254
14824C-F-S-21-B	t/2	S	0.0119	0.05	5,900
14824E-F-S-37-B	t/2	S	0.0119	0.05	8,408
14824G-F-S-53-B	t/2	S	0.0119	0.05	6,660
14824A-F-S-8-B	t/2	S	0.0083	0.05	27,157
14824C-F-S-24-B	t/2	S	0.0083	0.05	19,525
14824F-F-S-40-B	t/2	S	0.0083	0.05	21,687
14824G-F-S-56-B	t/2	S	0.0083	0.05	48,994

(b) $R_\varepsilon = -1$

	Thickness Location	Orientation	Strain Range (in/in)	Strain Ratio, R_ε	Cycles to Failure
14824C-F-L-10-B	t/2	L	0.0201	-1	1,288
14824E-F-L-16-C	3t/4	L	0.0201	-1	1,185
14824G-F-L-21-B	t/2	L	0.0201	-1	970
14824A-F-L-4-B	t/2	L	0.0201	-1	1,188
14824E-F-L-13-A	t/4	L	0.0175	-1	2,141
14824G-F-L-19-A	t/4	L	0.0175	-1	1,848
14824A-F-L-1-A	t/4	L	0.0175	-1	1,817
14824C-F-L-7-A	t/4	L	0.0175	-1	2,033
14824E-F-L-15-A	t/4	L	0.0148	-1	3,309
14824G-F-L-19-B	t/2	L	0.0148	-1	4,667
14824A-F-L-1-C	3t/4	L	0.0148	-1	3,444
14824C-F-L-7-C	3t/4	L	0.0148	-1	3,672
14824E-F-L-15-B	t/2	L	0.0110	-1	15,921
14824G-F-L-21-A	t/4	L	0.0110	-1	23,017
14824A-F-L-2-C	3t/4	L	0.0110	-1	34,656
14824C-F-L-8-C	3t/4	L	0.0110	-1	25,101
14824A-F-S-10-B	t/2	S	0.0201	-1	562
14824C-F-S-26-B	t/2	S	0.0201	-1	572
14824E-F-S-42-B	t/2	S	0.0201	-1	744
14824G-F-S-58-B	t/2	S	0.0201	-1	724
14824C-F-S-17-B	t/2	S	0.0176	-1	1,354
14824A-F-S-1-B	t/2	S	0.0175	-1	984
14824E-F-S-33-B	t/2	S	0.0175	-1	1,535
14824G-F-S-49-B	t/2	S	0.0175	-1	857
14824C-F-S-20-B	t/2	S	0.0148	-1	3,218
14824E-F-S-36-B	t/2	S	0.0148	-1	2,133
14824A-F-S-4-B	t/2	S	0.0148	-1	3,704
14824G-F-S-52-B	t/2	S	0.0148	-1	3,418
14824C-F-S-23-B	t/2	S	0.0110	-1	19,318
14824E-F-S-39-B	t/2	S	0.0110	-1	27,989
14824G-F-S-55-B	t/2	S	0.0110	-1	20,768
14824A-F-S-7-B	t/2	S	0.0110	-1	18,042

Fatigue Crack Growth Rate – Fatigue crack growth rate test result summary curves are shown in Figures 11 and 12 for stress ratios (R) of 0.1 and 0.7, respectively. Individual specimen curves are located in Appendix A of this report.

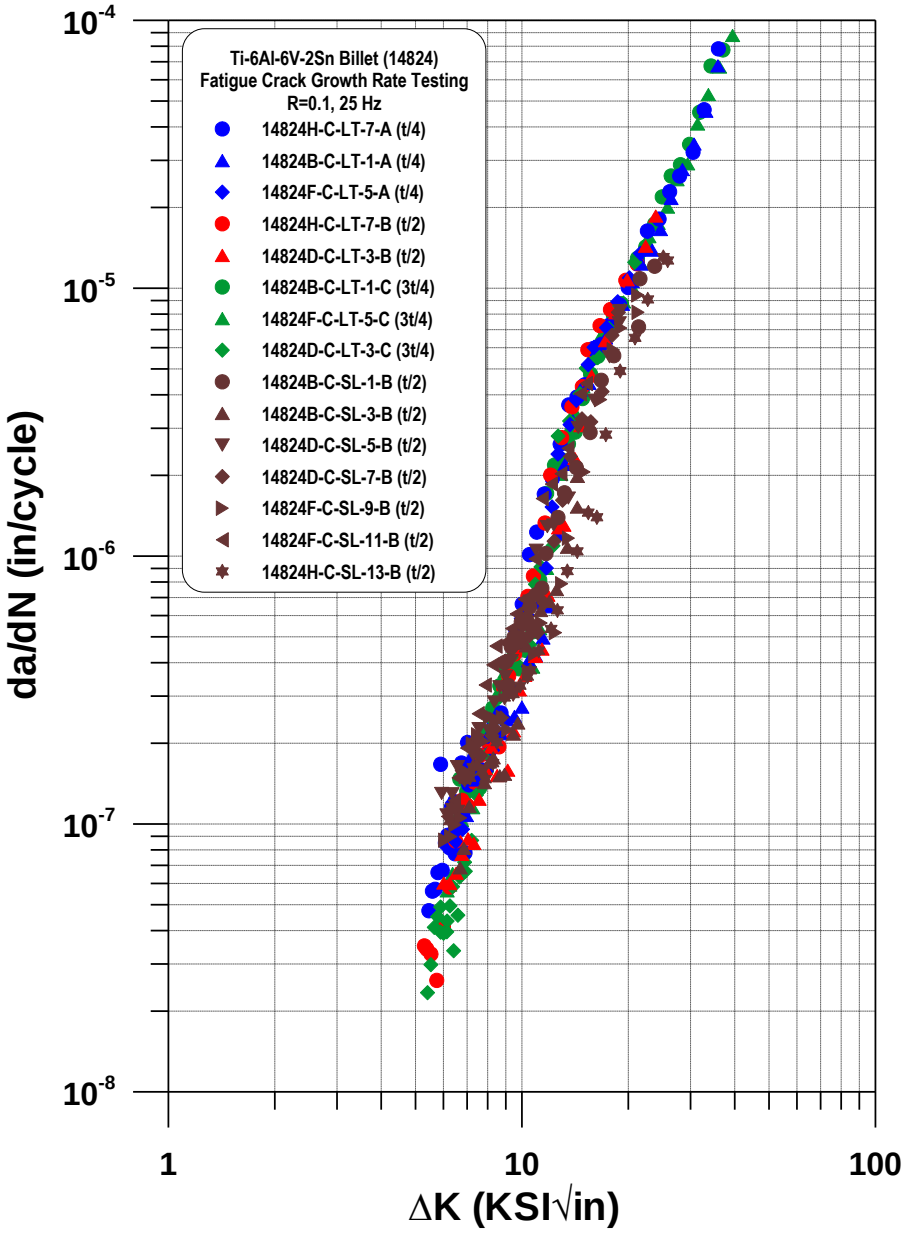


Figure 11. Ti-6Al-6V-2Sn billet (14824) fatigue crack growth rate test results (R=0.1).

Approved for public release; distribution unlimited.

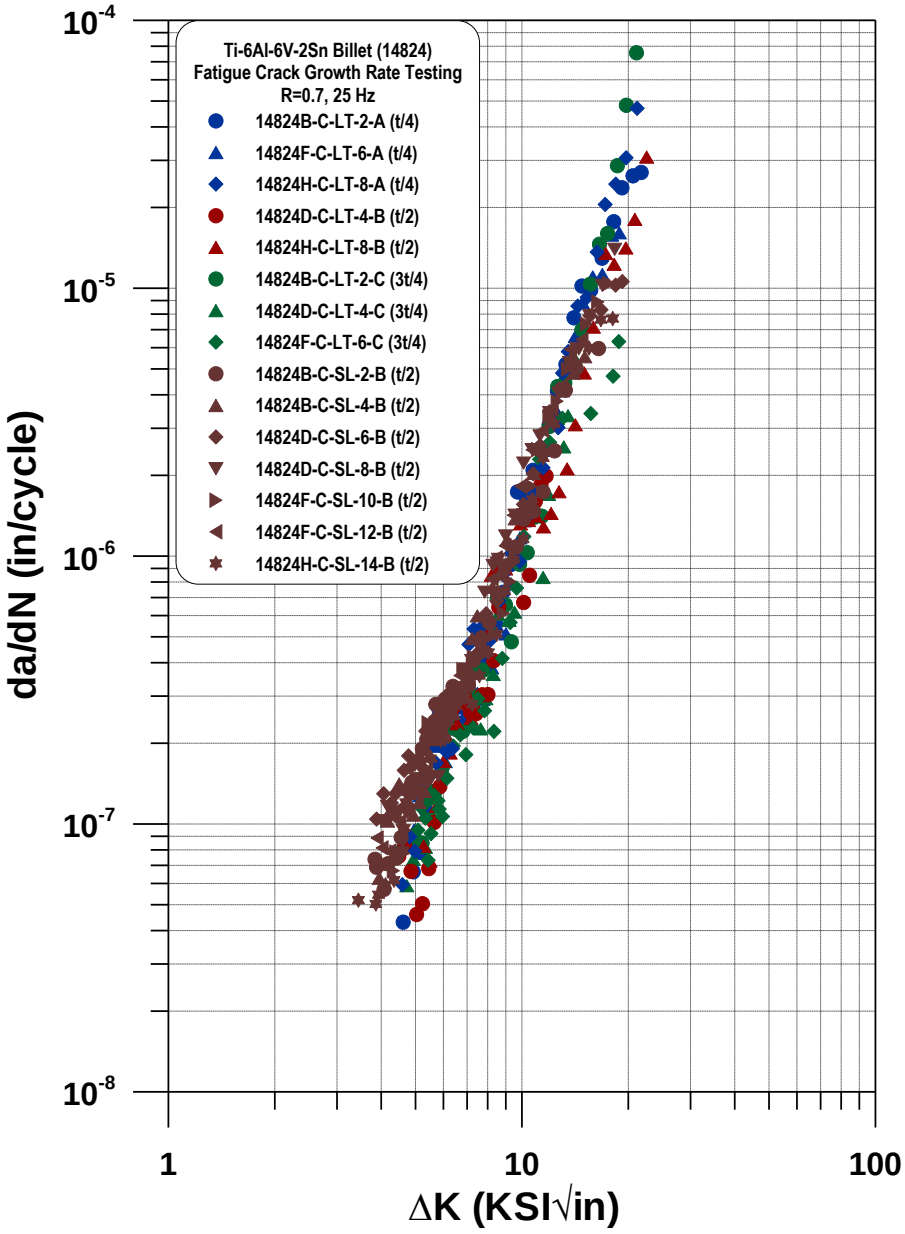


Figure 12. Ti-6Al-6V-2Sn billet (14824) fatigue crack growth rate test results (R=0.7).

Approved for public release; distribution unlimited.

Fracture Toughness – Plane-strain fracture toughness test results are shown in Table 6. For this investigation, only the L-T orientation was tested. The specimens excised from the t/2 location had slightly higher fracture toughness than those specimens taken from the t/4 or 3t/4 planes, although the population sizes are quite limited.

Also shown in this table is a reference value the Damage Tolerant Design Handbook **[*2*]** for mill annealed billet. The pedigree for the billet material shown in the reference is unknown however.

Table 6. Ti-6Al-6V-2Sn billet (14824) fracture toughness test results.

	Thickness Location	K_{Ic} (ksiVin)	
14824B-K-LT-1-A	t/4	80.0	
14824F-K-LT-3-A	t/4	81.9	
14824H-K-LT-4-A	t/4	81.1	
14824B-K-LT-1-B	t/2	84.0	
14824H-K-LT-4-B	t/2	87.9	
14824B-K-LT-1-C	3t/4	80.0	
14824D-K-LT-2-C	3t/4	84.0	
14824F-K-LT-3-C	3t/4	81.8	
14824H-K-LT-4-C	3t/4	79.5	← Preliminary reasonable lower bound
Damage Tolerant Design Handbook *Table 6.18.1.1 (Billet) Mean*		52.3	

Stress Corrosion Cracking – Axial, smooth bar stress corrosion cracking tests were performed on 22 test specimens, representing two orientations (L and S). As stated previously, the specimens were loaded at a stress of 101.3 ksi (75% of the specification yield strength of 135 ksi) for 40 days in an alternate immersion 3.5% NaCl solution. No failures occurred during testing. After testing, specimens were rinsed in deionized water and visually inspected for evidence of corrosion damage. No evidence of pitting or other corrosion-related damage was indicated.

Approved for public release; distribution unlimited.

8" Ti-6Al-6V-2Sn Billet (14828)

Tension – The results of tensile testing are shown in Tables 7(a) through 7(d). Strength levels for a portion of specimens from both orientations were below the specification minimum values shown in AMS-T-9046 (plate) and AMS-T-9047 (1"-3" bar) for this alloy. Elastic modulus values (based on E8 tensile test results) were generally below the range expected for this alloy. On average, there was approximately a 5% difference between those modulus results from ASTM E111 tests and those obtained from the E8 tensile test record. In addition, there did not appear to be a difference between specimens excised from the three different thickness locations.

Although the "reasonable lower bound" for the alloy will be calculated and identified in a future report, for this billet a preliminary reasonable lower bound was calculated using the procedures described in MMPDS Section 9.4.1 and assuming normality in the data population. The equation used for the calculation of these preliminary values (for strength only) was:

$$Minimum\ S = \overline{X} - s * k_{99}$$

where

$\overline{X}$ = sample mean

s = standard deviation

k_{99} = one-sided tolerance-limit factor corresponding to a proportion at least 0.99 of a normal distribution and a confidence coefficient of 0.95 based on the number of specimens in the given population. For this billet, a k_{99} factor of 2.58 was used, representing a population size of 192.

It should be noted that the AMS-T-9046 specification does not list minimum properties for the short-transverse orientation. Due to information indicating that non conforming materials have been cut-down from billet and purported as plate or bar, the expected orientation system may not have been known during component fabrication. Therefore, the results from the two orientations tested have been grouped together in order to provide reasonable lower bound properties. These preliminary reasonable lower bound properties are shown in Table 8. For modulus, elongation, and reduction of area, the minimum value from the data has been used as the preliminary reasonable lower bound.

Approved for public release; distribution unlimited.

Table 7. Ti-6Al-6V-2Sn billet (14828) tensile test results.

(a) Longitudinal orientation, t/4 thickness location

	Orientation	Thickness Location	Yield Strength (ksi)	Ultimate Tensile Strength (ksi)	% Elongation	% Reduction of Area	Elastic Modulus, E111 (msi)	Elastic Modulus, E8 (msi)
14828A-T-L-1-A	L	t/4	137.6	145.8	16.7%	34.8%	15.8	16.5
L-2-A	L	t/4	137.0	144.8	20.4%	30.5%	16.2	15.6
L-3-A	L	t/4	136.6	143.8	18.1%	33.9%		15.8
L-4-A	L	t/4	134.4	140.8	17.7%	37.6%		15.4
L-5-A	L	t/4	135.8	142.6	17.5%	30.3%		15.6
L-6-A	L	t/4	135.7	142.5	18.7%	37.8%		15.8
L-7-A	L	t/4	135.2	142.3	18.3%	30.8%		15.5
L-8-A	L	t/4	134.6	141.4	18.4%	31.6%		15.4
L-9-A	L	t/4	134.4	140.8	17.8%	32.3%		15.1
L-10-A	L	t/4	135.7	141.9	18.1%	30.6%		15.4
L-11-A	L	t/4	134.1	140.8	16.6%	33.6%		15.3
L-12-A	L	t/4	135.8	142.4	18.9%	36.1%		15.4
L-13-A	L	t/4	134.7	141.0	20.4%	31.8%		15.6
14828C-T-L-14-A	L	t/4	139.9	146.6	17.4%	33.0%	16.5	15.1
L-15-A	L	t/4	139.6	145.8	18.6%	33.4%	16.6	15.3
L-16-A	L	t/4	138.3	144.3	18.7%	31.5%		15.5
L-17-A	L	t/4	136.5	141.6	16.0%	33.7%		14.9
L-18-A	L	t/4	136.9	141.6	18.8%	35.1%		15.1
L-19-A	L	t/4	135.5	139.7	19.4%	35.7%		14.8
L-20-A	L	t/4	134.9	139.6	16.2%	30.6%		14.9
L-21-A	L	t/4	136.9	141.7	18.0%	34.2%		15.2
L-22-A	L	t/4	134.1	138.9	17.4%	36.4%		15.1
L-23-A	L	t/4	134.2	138.2	15.8%	32.8%		14.6
L-24-A	L	t/4	134.7	139.6	17.9%	27.8%		15.1
L-25-A	L	t/4	135.4	139.7	17.9%	34.8%		14.8
L-26-A	L	t/4	136.2	140.8	17.0%	30.5%		14.9

Approved for public release; distribution unlimited.

14828E-T-L-27-A	L	t/4	136.5	145.0	19.0%	35.0%	16.2	15.4
L-28-A	L	t/4	135.7	143.5	18.5%	36.4%	16.1	15.8
L-29-A	L	t/4	135.7	143.0	17.7%	33.6%		15.0
L-30-A	L	t/4	135.5	141.8	17.9%	34.2%		15.4
L-31-A	L	t/4	135.1	141.3	18.8%	36.7%		15.1
L-32-A	L	t/4	134.7	141.2	18.3%	33.7%		15.5
L-33-A	L	t/4	135.6	142.3	17.7%	33.6%		15.4
L-34-A	L	t/4	136.8	143.7	17.1%	33.3%		15.4
L-35-A	L	t/4	135.8	141.9	17.0%	34.2%		15.6
L-36-A	L	t/4	136.1	143.1	16.0%	31.9%		15.6
L-37-A	L	t/4	136.6	143.1	15.7%	29.6%		15.7
L-38-A	L	t/4	133.9	139.9	15.4%	31.5%		14.3
L-39-A	L	t/4	136.3	142.5	16.5%	31.2%		15.5
14828G-T-L-40-A	L	t/4	138.4	145.3	17.3%	38.8%	15.7	15.5
L-41-A	L	t/4	138.5	145.4	17.6%	35.5%	16.0	14.4
L-42-A	L	t/4	138.1	144.7	17.5%	35.9%		15.5
L-43-A	L	t/4	137.9	144.1	16.7%	34.6%		15.7
L-44-A	L	t/4	137.6	143.9	16.6%	29.6%		16.1
L-45-A	L	t/4	135.5	141.3	17.1%	36.2%		15.0
L-46-A	L	t/4	136.4	142.6	17.5%	36.2%		15.4
L-47-A	L	t/4	137.1	143.6	17.4%	36.9%		15.4
L-48-A	L	t/4	137.6	143.8	17.4%	35.2%		15.4
L-49-A	L	t/4	135.6	141.8	17.9%	35.3%		14.8
L-50-A	L	t/4	136.5	142.4	17.3%	35.3%		15.6
L-51-A	L	t/4	136.9	142.8	16.8%	35.3%		14.8
L-52-A	L	t/4	137.8	143.9	17.7%	32.5%		15.6
AMS-T-9046			135	145	8%			16.0[a]
AMS-T-9047 (1"-3")			131	143	10%	20%		
AMS-T-9047 (3"-4")			129	137	10%	20%		

(a): Typical value per MMPDS-04

Approved for public release; distribution unlimited.

(b) Longitudinal orientation, t/2 thickness location

	Orientation	Thickness Location	Yield Strength (ksi)	Ultimate Tensile Strength (ksi)	% Elongation	% Reduction of Area	Elastic Modulus, E111 (msi)	Elastic Modulus, E8 (msi)
14828A-T-L-1-B	L	t/2	137.5	145.2	16.8%	33.9%	15.8	15.2
L-2-B	L	t/2	136.1	143.5	16.7%	28.7%	15.8	15.3
L-3-B	L	t/2	135.0	142.6	18.2%	32.5%		15.5
L-4-B	L	t/2	134.2	141.3	19.8%	36.0%		15.4
L-5-B	L	t/2	134.3	141.4	19.6%	33.7%		15.3
L-6-B	L	t/2	133.0	140.1	18.9%	33.4%		15.3
L-7-B	L	t/2	132.1	139.1	19.5%	31.4%		14.8
L-8-B	L	t/2	134.2	142.1	19.8%	31.4%		15.5
L-9-B	L	t/2	131.6	138.8	20.7%	36.9%		14.9
L-10-B	L	t/2	133.3	141.1	15.3%	32.3%		15.3
L-11-B	L	t/2	134.3	142.4				15.7
L-12-B	L	t/2	131.8	138.3	18.0%	37.4%		14.7
L-13-B	L	t/2	134.3	141.4	18.9%	35.3%		15.2
14828C-T-L-14-B	L	t/2	138.2	144.3	16.6%	36.1%	16.1	14.6
L-15-B	L	t/2	137.3	143.2	17.1%	32.6%	16.3	14.6
L-16-B	L	t/2	138.0	144.4	17.2%	33.9%		14.9
L-17-B	L	t/2	138.3	145.1	19.6%	28.3%		15.0
L-18-B	L	t/2	136.5	142.4	16.2%	33.5%		15.3
L-19-B	L	t/2	134.6	140.2	17.6%	33.8%		14.8
L-20-B	L	t/2	132.7	137.3	17.9%	31.5%		14.4
L-21-B	L	t/2	133.8	138.9	18.0%	34.8%		15.6
L-22-B	L	t/2	133.3	138.2	18.0%	34.1%		15.5
L-23-B	L	t/2	132.6	138.3	20.7%	37.2%		15.4
L-24-B	L	t/2	132.4	137.1	18.5%	37.4%		14.9
L-25-B	L	t/2	133.6	139.2	19.7%	32.4%		15.2
L-26-B	L	t/2	135.2	140.8	18.9%	32.3%		15.6

Approved for public release; distribution unlimited.

14828E-T-L-27-B	L	t/2	134.7	142.8	16.7%	30.6%	15.9	15.2
L-28-B	L	t/2	135.2	143.0	17.9%	33.0%	16.1	15.4
L-29-B	L	t/2	135.7	143.6	17.1%	29.9%		15.7
L-30-B	L	t/2	135.0	142.1	19.8%	30.5%		15.3
L-31-B	L	t/2	133.6	140.1	18.0%	37.7%		15.3
L-32-B	L	t/2	134.2	140.6	17.8%	36.1%		15.1
L-33-B	L	t/2	132.3	138.9	20.2%	36.2%		15.1
L-34-B	L	t/2	136.5	143.2	16.6%	32.6%		15.2
L-35-B	L	t/2	132.7	140.1	18.5%	30.4%		15.7
L-36-B	L	t/2	131.2	137.0	16.7%	35.6%		15.1
L-37-B	L	t/2	132.8	139.9	18.8%	35.9%		15.5
L-38-B	L	t/2	132.6	139.2	17.8%	35.2%		15.4
L-39-B	L	t/2	134.0	140.4	16.1%	32.5%		14.9
14828G-T-L-40-B	L	t/2	137.7	144.9	17.4%	37.0%	15.5	14.7
L-41-B	L	t/2	137.2	143.1	17.7%	34.2%	15.9	15.0
L-42-B	L	t/2	137.1	144.8	17.5%	33.0%		15.6
L-43-B	L	t/2	136.1	142.1	17.7%	31.4%		15.2
L-44-B	L	t/2	135.1	140.6	18.4%	36.5%		14.9
L-45-B	L	t/2	135.7	141.6	17.7%	31.3%		15.7
L-46-B	L	t/2	136.3	143.0	18.5%	34.8%		15.7
L-47-B	L	t/2	135.9	142.3	18.9%	35.8%		15.7
L-48-B	L	t/2	135.5	142.2	17.8%	37.0%		15.6
L-49-B	L	t/2	134.1	140.4	17.3%	39.6%		15.2
L-50-B	L	t/2	134.8	141.4	18.7%	36.8%		14.4
L-51-B	L	t/2	135.6	141.9	19.8%	37.7%		15.2
L-52-B	L	t/2	136.3	142.9	19.2%	39.5%		15.3
AMS-T-9046			135	145	8%			16.0[a]
AMS-T-9047 (1"-3")			131	143	10%	20%		
AMS-T-9047 (3"-4")			129	137	10%	20%		

(a): Typical value per MMPDS-04

Approved for public release; distribution unlimited.

(c) Longitudinal orientation, 3t/4 thickness location

	Orientation	Thickness Location	Yield Strength (ksi)	Ultimate Tensile Strength (ksi)	% Elongation	% Reduction of Area	Elastic Modulus, E111 (msi)	Elastic Modulus, E8 (msi)
14828A-T-L-1-C	L	3t/4	138.8	146.8	17.0%	36.5%	16.0	15.6
L-2-C	L	3t/4	138.0	146.0	18.5%	32.8%	16.5	15.7
L-3-C	L	3t/4	136.5	143.4	18.7%	31.3%		15.0
L-4-C	L	3t/4	135.6	141.7	16.8%	36.2%		14.9
L-5-C	L	3t/4	136.3	142.9	18.2%	33.0%		15.2
L-6-C	L	3t/4	134.9	141.4	19.4%	25.2%		15.1
L-7-C	L	3t/4	135.6	143.0	18.2%	33.4%		15.3
L-8-C	L	3t/4	136.1	142.8	17.1%	31.9%		14.9
L-9-C	L	3t/4	136.6	143.6	17.9%	33.0%		15.3
L-10-C	L	3t/4	135.0	142.2	17.1%	30.8%		15.4
L-11-C	L	3t/4	136.6	143.7	19.2%	32.1%		15.2
L-12-C	L	3t/4	134.0	140.8	18.7%	37.9%		14.9
L-13-C	L	3t/4	134.1	139.9	16.7%	32.7%		14.8
14828C-T-L-14-C	L	3t/4	139.2	146.0	17.4%	35.4%	16.3	15.0
L-15-C	L	3t/4	138.1	144.1	19.9%	34.5%	16.4	14.8
L-16-C	L	3t/4	136.8	142.1	18.0%	38.1%		14.5
L-17-C	L	3t/4	137.5	142.8	18.6%	33.7%		15.4
L-18-C	L	3t/4	136.3	141.0	17.5%	32.8%		14.7
L-19-C	L	3t/4	137.2	141.8	16.3%	32.5%		15.3
L-20-C	L	3t/4	135.9	140.7	19.3%	37.0%		14.9
L-21-C	L	3t/4	136.1	140.9	17.7%	32.6%		15.3
L-22-C	L	3t/4	135.0	138.9	15.7%	34.4%		14.6
L-23-C	L	3t/4	137.3	142.6	15.4%	27.6%		15.5
L-24-C	L	3t/4	136.2	141.0	18.0%	36.1%		15.0
L-25-C	L	3t/4	136.2	141.1	17.2%	30.1%		15.0
L-26-C	L	3t/4	136.6	141.3	19.0%	32.1%		15.1

14828E-T-L-27-C	L	3t/4	135.6	144.1	18.2%	37.2%	16.1	14.9
L-28-C	L	3t/4	137.1	145.0	16.9%	31.8%	16.5	15.4
L-29-C	L	3t/4	135.8	142.8	17.1%	33.6%		15.2
L-30-C	L	3t/4	136.5	143.6	17.5%	31.3%		15.6
L-31-C	L	3t/4	134.8	141.0	17.1%	32.4%		15.2
L-32-C	L	3t/4	135.7	142.6	18.6%	36.3%		15.5
L-33-C	L	3t/4	137.6	146.8	14.3%	27.2%		15.3
L-34-C	L	3t/4	134.2	141.1	17.9%	31.4%		15.6
L-35-C	L	3t/4	134.8	141.8	17.8%	29.4%		15.6
L-36-C	L	3t/4	135.5	141.9	15.5%	29.6%		15.0
L-37-C	L	3t/4	136.2	142.8	17.0%	30.9%		15.2
L-38-C	L	3t/4	135.5	141.4	17.2%	32.6%		15.1
L-39-C	L	3t/4	135.1	141.4	16.2%	25.8%		15.3
14828G-T-L-40-C	L	3t/4	139.6	146.6	17.7%	37.7%	16.0	15.2
L-41-C	L	3t/4	137.3	143.9	17.3%	35.2%	15.7	14.9
L-42-C	L	3t/4	137.8	144.0	17.6%	37.7%		15.0
L-43-C	L	3t/4	136.7	142.6	18.6%	37.2%		15.0
L-44-C	L	3t/4	137.9	144.0	19.1%	37.8%		15.5
L-45-C	L	3t/4	136.8	143.1	17.2%	34.3%		14.9
L-46-C	L	3t/4	137.9	143.9	16.8%	31.7%		15.2
L-47-C	L	3t/4	138.8	144.8	17.9%	33.6%		15.7
L-48-C	L	3t/4	138.2	145.9	17.9%	33.1%		15.1
L-49-C	L	3t/4	137.2	143.3	18.3%	37.0%		15.1
L-50-C	L	3t/4	138.1	144.7	19.0%	34.4%		15.4
L-51-C	L	3t/4	138.7	145.8	17.8%	33.2%		15.7
L-52-C	L	3t/4	138.0	144.3	16.3%	32.3%		15.6
AMS-T-9046			135	145	8%			16.0[a]
AMS-T-9047 (1"-3")			131	143	10%	20%		
AMS-T-9047 (3"-4")			129	137	10%	20%		

(a): Typical value per MMPDS-04

Approved for public release; distribution unlimited.

(d) Short-transverse orientation; t/4, t/2, and 3t/4 thickness locations

	Orientation	Thickness Location	Yield Strength (ksi)	Ultimate Tensile Strength (ksi)	% Elongation	% Reduction of Area	Elastic Modulus, E111 (msi)	Elastic Modulus, E8 (msi)
14828A-T-S-1-A	S	t/4	140.8	149.9	15.9%	30.9%	17.2	16.3
S-2-A	S	t/4	136.6	145.1	11.4%	23.9%	16.5	15.1
S-3-A	S	t/4	136.6	145.1	13.3%	26.8%		14.9
14828C-T-S-4-A	S	t/4	140.5	147.7	16.1%	29.5%	15.9	15.7
S-5-A	S	t/4	138.0	145.2	11.9%	25.6%	15.6	15.3
S-6-A	S	t/4	137.2	144.5	13.0%	19.0%		14.8
14828E-T-S-7-A	S	t/4	135.7	143.9	12.6%	24.6%	16.1	15.4
S-8-A	S	t/4	137.6	147.1	15.2%	26.6%	16.3	15.6
S-9-A	S	t/4	136.2	146.1	13.7%	24.8%		16.0
14828G-T-S-10-A	S	t/4	140.6	148.5	14.7%	29.6%	16.7	15.8
S-11-A	S	t/4	138.7	145.7	11.4%	31.8%	16.4	15.7
S-12-A	S	t/4	138.6	146.0	12.8%	27.2%		15.4
14828A-T-S-1-B	S	t/2	136.0	144.0	12.5%	22.6%	16.6	15.6
S-2-B	S	t/2	135.4	142.8	12.5%	29.7%	16.5	15.9
S-3-B	S	t/2	134.9	143.2	12.9%	29.8%		15.3
14828C-T-S-4-B	S	t/2	133.8	140.1	13.1%	26.9%	15.2	14.4
S-5-B	S	t/2	134.6	140.7	14.7%	26.8%	15.3	14.6
S-6-B	S	t/2	135.4	141.3	15.3%	26.0%		15.0
14828E-T-S-7-B	S	t/2	134.2	142.6	12.5%	20.2%	16.1	15.4
S-8-B	S	t/2	135.2	143.3	12.0%	23.2%	16.2	15.0
S-9-B	S	t/2	134.6	142.9	14.4%	23.6%		15.3
14828G-T-S-10-B	S	t/2	137.6	144.7	16.4%	21.8%	16.4	16.0
S-11-B	S	t/2	136.6	144.1	17.7%	28.7%	16.2	14.9
S-12-B	S	t/2	137.1	144.6	13.7%	27.1%		15.3

Approved for public release; distribution unlimited.

14828A-T-S-1-C	S	3t/4	139.8	149.5	17.8%	34.9%	16.9	15.7
S-2-C	S	3t/4	135.6	144.4	11.7%	24.8%	16.3	15.3
S-3-C	S	3t/4	136.9	145.9	14.9%	26.3%		15.0
14828C-T-S-4-C	S	3t/4	140.5	147.7	15.9%	31.6%	15.8	15.6
S-5-C	S	3t/4	138.4	145.7	14.0%	28.8%	16.5	15.3
S-6-C	S	3t/4	137.2	144.9	15.7%	23.2%		15.0
14828E-T-S-7-C	S	3t/4	139.0	148.4	14.3%	27.8%	16.6	15.9
S-8-C	S	3t/4	137.0	146.3	12.1%	27.0%	16.2	15.9
S-9-C	S	3t/4	136.2	143.8	18.9%	34.0%		15.6
14828G-T-S-10-C	S	3t/4	142.6	150.1	16.1%	34.4%	16.7	15.7
S-11-C	S	3t/4	138.9	146.3	14.2%	28.6%	16.3	15.3
S-12-C	S	3t/4	139.3	146.9	13.2%	29.1%		15.8
AMS-T-9046 (L-orientation)			135	145	8%			16.0[a]
AMS-T-9047 (1"-3")			131	143	10%	20%		
AMS-T-9047 (3"-4")			129	137	8%	15%		

(a): Typical value per MMPDS-04

Table 8. Preliminary reasonable lower bound tensile properties for Ti-6Al-6V-2Sn billet (14828).

Yield Strength (ksi)	Ultimate Tensile Strength (ksi)	% Elongation	% Reduction of Area	Elastic Modulus (msi)
131	137	11%	19%	14.3

Fatigue (force-controlled) – The results of force-controlled axial fatigue testing are shown graphically in Figure 13. Individual results are tabulated in Table 9. In Fig. 13, the results for each stress ratio (R) have been fit with a best-fit power-law curve for graphical purposes only. Also included in this figure are curves based on an equivalent stress equation from MMPDS Figure 5.4.2.1.8(a). As stated in Fig. 4, the fatigue specimens used herein were manufactured using low-stress grinding operations to a surface finish (Ra) of 8 per the ASTM E466 standard. The MMPDS reference data curves were generated using specimens having a surface roughness of 32 RMS. Although the specimens used in this effort had a smoother surface finish than those used in the reference data, and a longer life would typically be expected, it is not known whether low-stress grinding was used on the reference specimens. This aspect, along with the fact that the material from which the referenced specimens were extracted exhibited higher tensile strength than the billet material tested in this program, could potentially have contributed to the difference between the data sets.

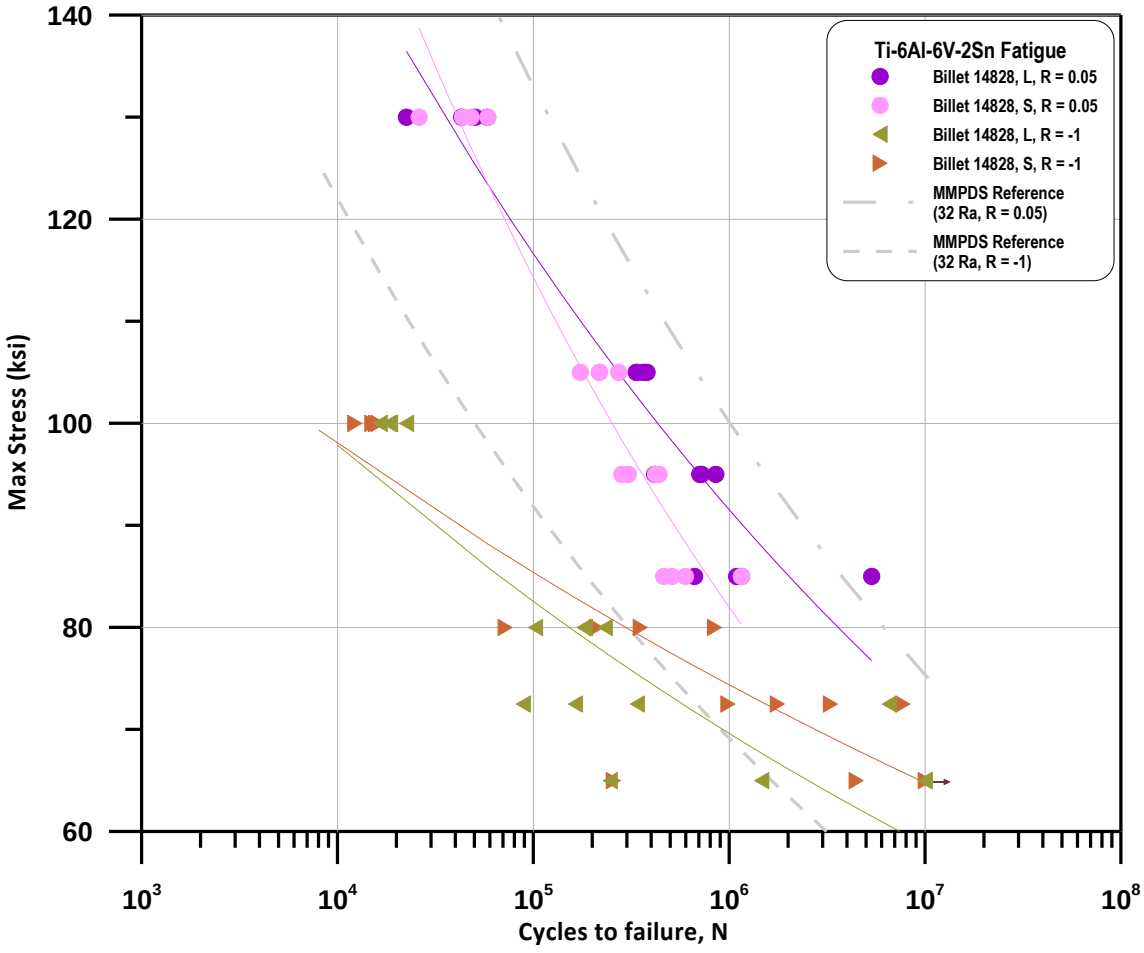


Figure 13. Ti-6Al-6V-2Sn billet force-controlled axial fatigue test results.

Approved for public release; distribution unlimited.

Table 9. Ti-6Al-6V-2Sn billet (14828) force-controlled axial fatigue test results.

(a) R = 0.05

	Thickness Location	Orientation	Max Stress (ksi)	Stress Ratio, R	Cycles to Failure
14828G-F-L-23-A	t/4	L	130	0.05	43,020
14828C-F-L-12-A	t/4	L	130	0.05	22,470
14828G-F-L-24-B	t/2	L	130	0.05	58,070
14828G-F-L-24-C	3t/4	L	130	0.05	50,390
14828G-F-L-24-A	t/4	L	105	0.05	336,630
14828C-F-L-11-A	t/4	L	105	0.05	334,840
14828E-F-L-17-C	3t/4	L	105	0.05	363,380
14828G-F-L-23-C	3t/4	L	105	0.05	380,550
14828G-F-L-23-B	t/2	L	95	0.05	721,890
14828E-F-L-18-B	t/2	L	95	0.05	852,680
14828C-F-L-11-B	t/2	L	95	0.05	416,120
14828A-F-L-5-C	3t/4	L	95	0.05	706,770
14828E-F-L-17-A	t/4	L	85	0.05	5,324,860
14828A-F-L-6-B	t/2	L	85	0.05	664,430
14828C-F-L-11-C	3t/4	L	85	0.05	1,090,170
14828C-F-L-12-C	3t/4	L	85	0.05	1,152,660
14828G-F-S-61-B	t/2	S	130	0.05	58,540
14828E-F-S-47-B	t/2	S	130	0.05	26,100
14828E-F-S-46-B	t/2	S	130	0.05	43,500
14828G-F-S-63-B	t/2	S	130	0.05	48,060
14828G-F-S-62-B	t/2	S	105	0.05	217,610
14828C-F-S-29-B	t/2	S	105	0.05	173,560
14828A-F-S-15-B	t/2	S	105	0.05	217,230
14828G-F-S-64-B	t/2	S	105	0.05	272,530
14828A-F-S-13-B	t/2	S	95	0.05	420,080
14828A-F-S-16-B	t/2	S	95	0.05	282,500
14828C-F-S-31-B	t/2	S	95	0.05	438,220
14828C-F-S-32-B	t/2	S	95	0.05	304,630
14828E-F-S-48-B	t/2	S	85	0.05	596,960
14828E-F-S-45-B	t/2	S	85	0.05	1,151,960
14828C-F-S-30-B	t/2	S	85	0.05	462,240
14828A-F-S-14-B	t/2	S	85	0.05	507,540

Approved for public release; distribution unlimited.

(b) R = -1

	Thickness Location	Orientation	Max Stress (ksi)	Stress Ratio, R	Cycles to Failure
14828A-F-L-1-A	t/4	L	100	-1	18,348
14828A-F-L-4-A	t/4	L	100	-1	18,653
14828C-F-L-9-B	t/2	L	100	-1	16,490
14828A-F-L-1-C	3t/4	L	100	-1	22,535
14828G-F-L-21-A	t/4	L	80	-1	102,617
14828C-F-L-7-A	t/4	L	80	-1	181,437
14828E-F-L-14-B	t/2	L	80	-1	232,564
14828E-F-L-13-C	3t/4	L	80	-1	184,375
14828G-F-L-19-A	t/4	L	72.5	-1	88,730
14828E-F-L-16-A	t/4	L	72.5	-1	163,743
14828A-F-L-3-B	t/2	L	72.5	-1	339,682
14828C-F-L-8-C	3t/4	L	72.5	-1	6,569,956
14828G-F-L-22-B	t/2	L	65	-1	246,786
14828C-F-L-10-B	t/2	L	65	-1	10,000,000*
14828G-F-L20-C	3t/4	L	65	-1	1,464,052
14828E-F-L-15-C	3t/4	L	65	-1	10,000,000*
14828A-F-S-1-B	t/2	S	100	-1	16,106
14828C-F-S-23-B	t/2	S	100	-1	12,230
14828E-F-S-42-B	t/2	S	100	-1	14,966
14828C-F-S-26-B	t/2	S	100	-1	15,612
14828E-F-S-36-B	t/2	S	80	-1	209,481
14828E-F-S-39-B	t/2	S	80	-1	71,617
14828A-F-S-4-B	t/2	S	80	-1	351,024
14828G-F-S-49-B	t/2	S	80	-1	840,530
14828G-F-S-58-B	t/2	S	72.5	-1	1,758,964
14828G-F-S-55-B	t/2	S	72.5	-1	983,095
14828A-F-S-10-B	t/2	S	72.5	-1	3,278,166
14828G-F-S-52-B	t/2	S	72.5	-1	7,685,823
14828A-F-S-7-B	t/2	S	65	-1	10,000,000*
14828C-F-S-20-B	t/2	S	65	-1	4,438,245
14828C-F-S-17-B	t/2	S	65	-1	255,475
14828E-F-S-33-B	t/2	S	65	-1	10,000,000*

** : indicates runout*

Fatigue (strain-controlled) – The results of strain-controlled axial fatigue testing are shown graphically in Figure 14, with individual results tabulated in Table 10. Due to material limitations, only longitudinal specimens were tested.

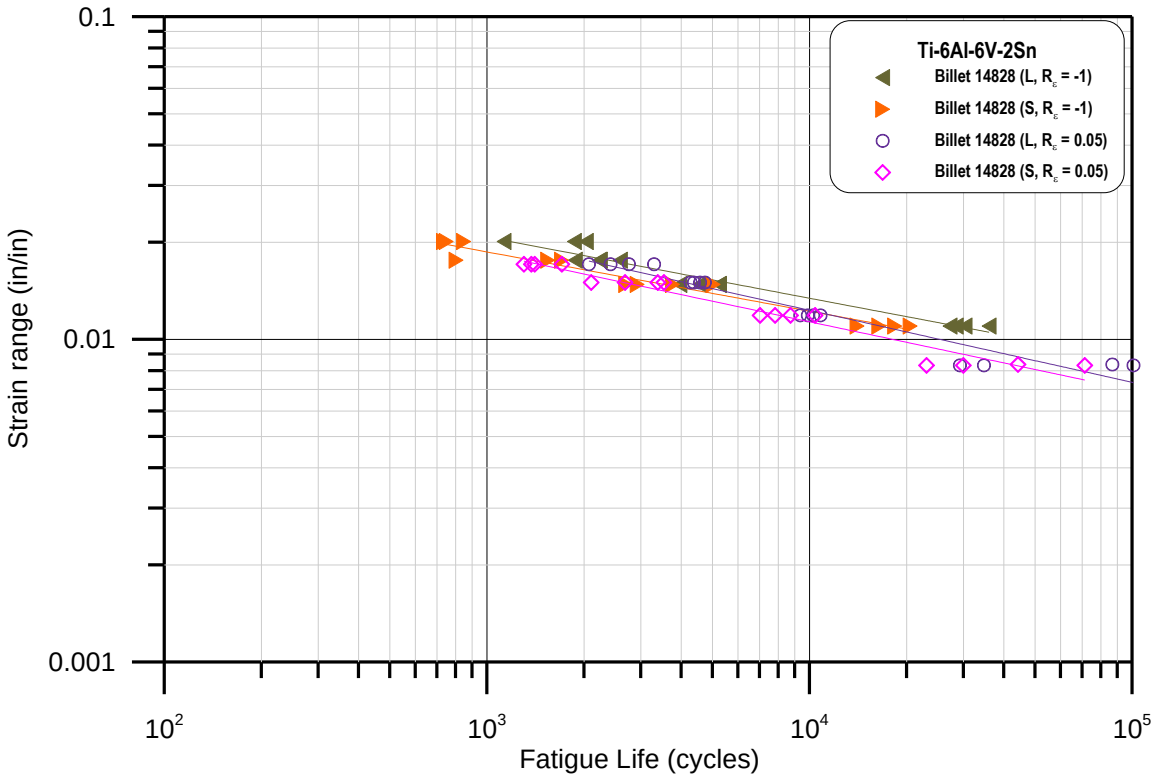


Figure 14. Ti-6Al-6V-2Sn billet (14828) strain-controlled axial fatigue test results.

Table 10. Ti-6Al-6V-2Sn billet (14828) strain-controlled axial fatigue test results.

(a) $R_\varepsilon = 0.05$

	Thickness Location	Orientation	Strain Range (in/in)	Strain Ratio, R_ε	Cycles to Failure
14828A-L-4-B	t/2	L	0.0171	0.05	2,071
14828E-L-16-B	t/2	L	0.0171	0.05	3,296
14828C-L-9-C	3t/4	L	0.0171	0.05	2,415
14828G-L-22-C	3t/4	L	0.0171	0.05	2,755
14828A-L-2-A	t/4	L	0.0150	0.05	4,277
14828E-L-13-A	t/4	L	0.0150	0.05	4,382
14828C-L-7-B	t/2	L	0.0150	0.05	4,575
14828G-L-19-B	t/2	L	0.0150	0.05	4,735
14828C-L-8-A	t/4	L	0.0119	0.05	9,869
14828G-L-20-A	t/4	L	0.0119	0.05	10,810
14828A-L-2-C	3t/4	L	0.0119	0.05	9,354
14828E-L-14-C	3t/4	L	0.0119	0.05	10,257
14828G-L-21-C	3t/4	L	0.0083	0.05	86,759
14828C-L-9-A	t/4	L	0.0083	0.05	100,888
14828E-L-15-B	t/2	L	0.0083	0.05	29,242
14828A-L-3-C	3t/4	L	0.0083	0.05	34,705
14828A-S-12-B	t/2	S	0.0171	0.05	1,301
14828C-S-28-B	t/2	S	0.0171	0.05	1,373
14828E-S-44-B	t/2	S	0.0171	0.05	1,406
14828G-S-60-B	t/2	S	0.0171	0.05	1,707
14828A-S-3-B	t/2	S	0.0150	0.05	2,103
14828C-S-18-B	t/2	S	0.0150	0.05	3,535
14828E-S-35-B	t/2	S	0.0150	0.05	3,385
14828G-S-51-B	t/2	S	0.0150	0.05	2,679
14828A-S-6-B	t/2	S	0.0119	0.05	7,019
14828C-S-22-B	t/2	S	0.0119	0.05	10,402
14828E-S-38-B	t/2	S	0.0119	0.05	7,818
14828G-S-54-B	t/2	S	0.0119	0.05	8,732
14828G-S-57-B	t/2	S	0.0083	0.05	44,240
14828A-S-9-B	t/2	S	0.0083	0.05	71,300
14828C-S-25-B	t/2	S	0.0083	0.05	29,942
14828E-S-41-B	t/2	S	0.0083	0.05	23,040

Approved for public release; distribution unlimited.

(b) $R_\varepsilon = -1$

	Thickness Location	Orientation	Strain Range (in/in)	Strain Ratio, R_ε	Cycles to Failure
14828A-L-1-B	t/2	L	0.0201	-1	1,867
14828E-L-13-B	t/2	L	0.0201	-1	1,130
14828C-L-7-C	3t/4	L	0.0201	-1	2,033
14828E-L-14-A	t/4	L	0.0175	-1	2,590
14828A-L-2-B	t/2	L	0.0175	-1	2,246
14828C-L-8-B	t/2	L	0.0175	-1	2,233
14828G-L-20-B	t/2	L	0.0175	-1	1,879
14828A-L-3-A	t/4	L	0.0148	-1	5,254
14828C-L-10-A	t/4	L	0.0148	-1	3,964
14828E-L-15-A	t/4	L	0.0148	-1	4,564
14828G-L-21-B	t/2	L	0.0148	-1	5,256
14828G-L-22-A	t/4	L	0.0110	-1	28,492
14828A-L-4-C	3t/4	L	0.0110	-1	27,271
14828C-L-10-C	3t/4	L	0.0110	-1	36,000
14828E-L-16-C	3t/4	L	0.0110	-1	30,350
14828A-S-2-B	t/2	S	0.0201	-1	733
14828E-S-34-B	t/2	S	0.0201	-1	846
14828G-S-50-B	t/2	S	0.0201	-1	747
14828A-S-5-B	t/2	S	0.0176	-1	802
14828C-S-21-B	t/2	S	0.0176	-1	1,541
14828G-S-53-B	t/2	S	0.0176	-1	1,703
14828A-S-8-B	t/2	S	0.0148	-1	3,760
14828C-S-24-B	t/2	S	0.0148	-1	2,920
14828E-S-40-B	t/2	S	0.0148	-1	2,691
14828G-S-56-B	t/2	S	0.0148	-1	5,022
14828A-S-11-B	t/2	S	0.0110	-1	18,345
14828C-S-27-B	t/2	S	0.0110	-1	14,034
14828F-S-43-B	t/2	S	0.0110	-1	16,392
14828G-S-59-B	t/2	S	0.0110	-1	20,489

Fatigue Crack Growth Rate – Fatigue crack growth rate test result summary curves are shown in Figures 15 and 16 for stress ratios (R) of 0.1 and 0.7, respectively. Individual specimen curves are located in Appendix B of this report. For both stress ratios, the S-L orientation specimens tended to have slightly faster growth rates than the L-T specimens. Fractographic and metallographic examinations of the failed specimens will be performed to investigate possible reasons for this difference in growth rates.

Approved for public release; distribution unlimited.

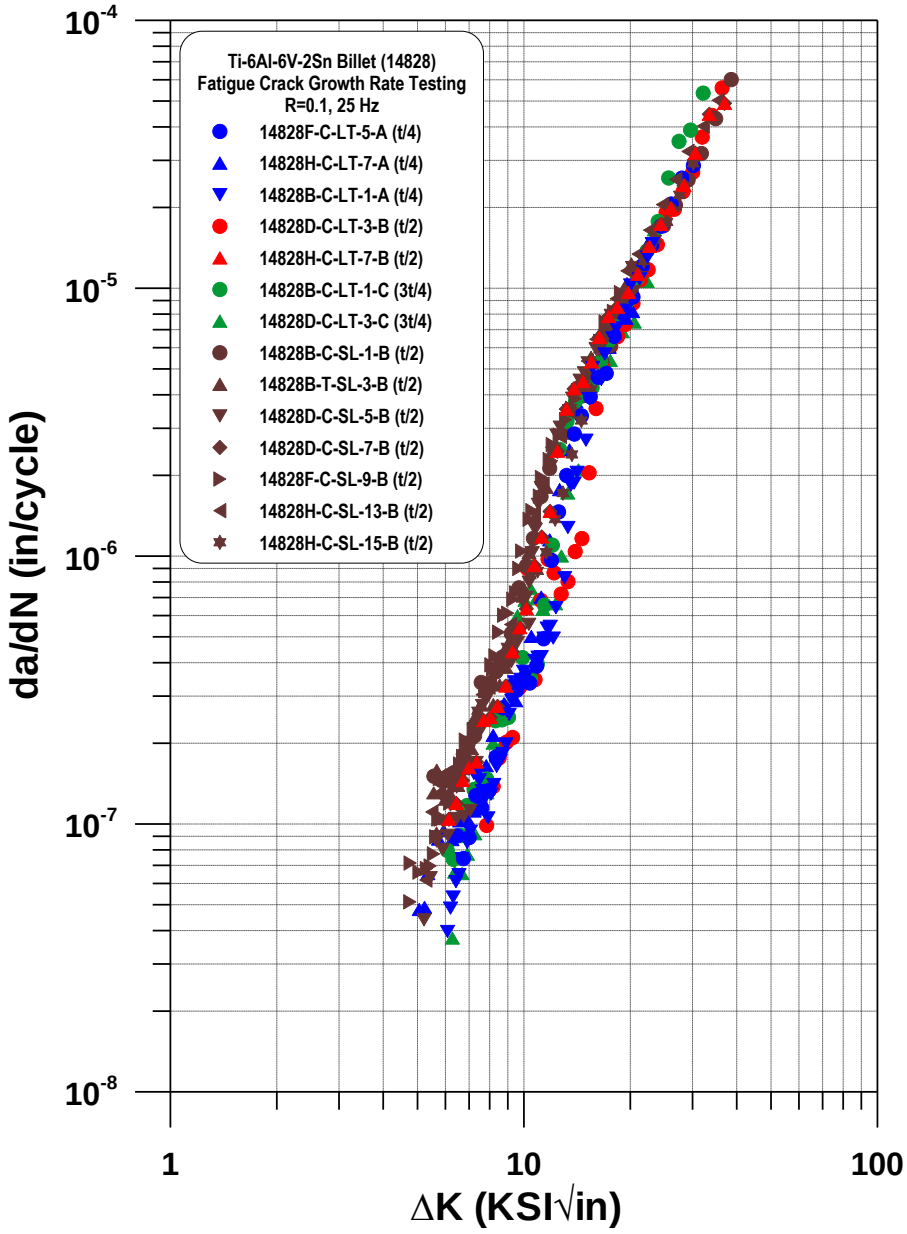


Figure 15. Ti-6Al-6V-2Sn billet (14828) fatigue crack growth rate test results (R=0.1).

Approved for public release; distribution unlimited.

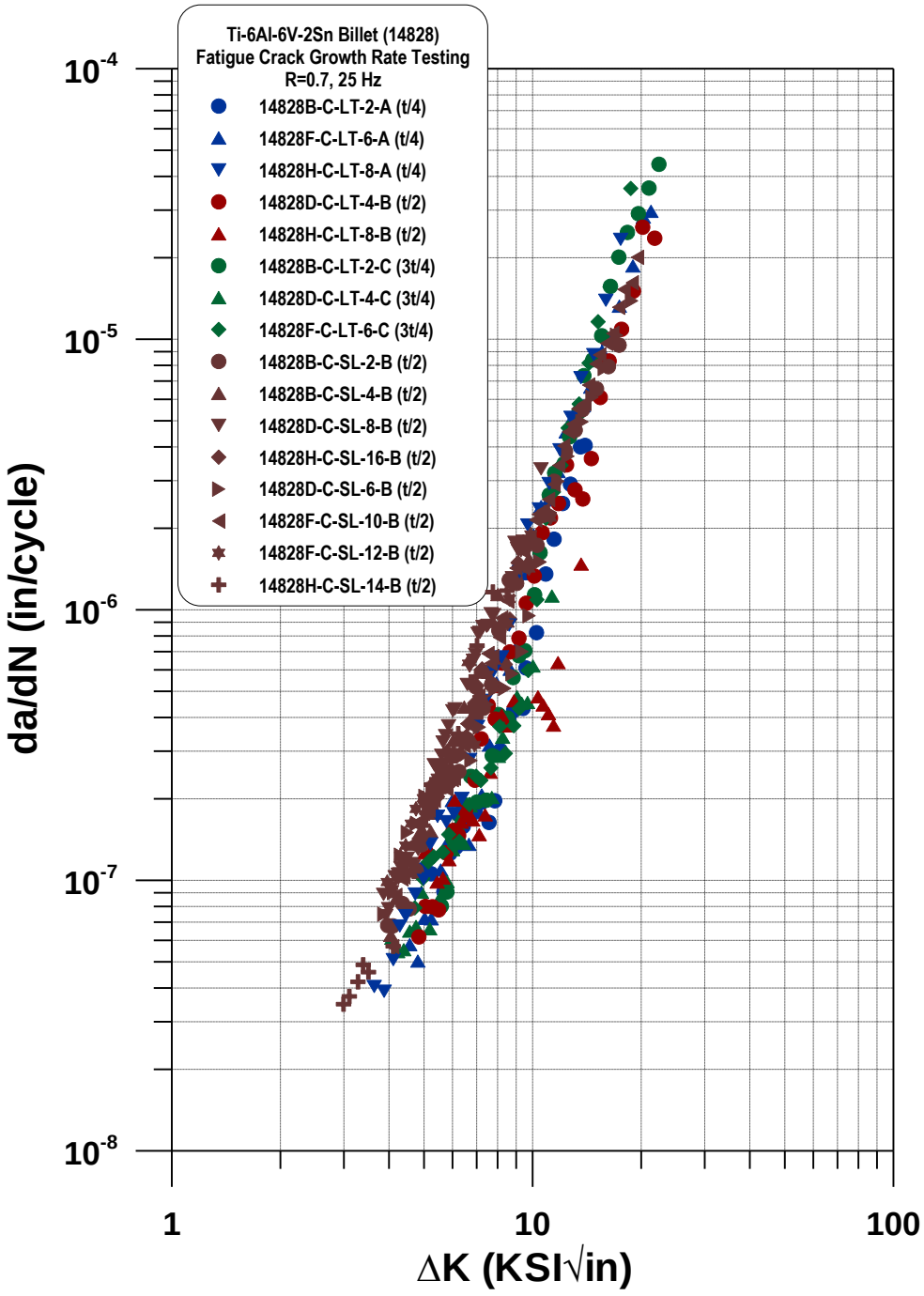


Figure 16. Ti-6Al-6V-2Sn billet (14828) fatigue crack growth rate test results (R=0.7).

Approved for public release; distribution unlimited.

Fracture Toughness – Plane-strain fracture toughness test results are shown in Table 11. For this investigation, only the L-T orientation was tested.

Also shown in this table is a reference value the Damage Tolerant Design Handbook **[*2*]** for mill annealed billet. The pedigree for the billet material shown in the reference is unknown however.

Table 11. Ti-6Al-6V-2Sn billet (14828) fracture toughness test results.

	Thickness Location	K_{Ic} (ksi√in)	
14828B-K-LT-1-A	t/4	78.2	
14828D-K-LT-2-A	t/4	77.6	
14828F-K-LT-3-A	t/4	88.6	
14828H-K-LT-4-A	t/4	82.0	
14828D-K-LT-2-B	t/2	88.5	
14828B-K-LT-1-C	3t/4	80.8	
14828D-K-LT-2-C	3t/4	69.1	
14828F-K-LT-3-C	3t/4	76.6	
14828H-K-LT-4-C	3t/4	71.8	← Preliminary reasonable lower bound
Damage Tolerant Design Handbook *Table 6.18.1.1 (Billet) Mean*		52.3	

Stress Corrosion Cracking – Axial, smooth bar stress corrosion cracking tests were performed on 24 test specimens, representing two orientations (L and S). As stated previously, the specimens were loaded at a stress of 101.3 ksi (75% of the specification yield strength of 135 ksi) for 40 days in an alternate immersion 3.5% NaCl solution. No failures occurred during testing. After testing, specimens were rinsed in deionized water and visually inspected for evidence of corrosion damage. No evidence of pitting or other corrosion-related damage was indicated.

CONCLUSIONS AND RECOMMENDATIONS

As this report dealt with mechanical properties from only two Ti-6Al-6V-2Sn billets, no specific conclusions or recommendations will be made, other than comparisons to material specifications or available reference data. Both billets had some portion of tensile strength results (yield and ultimate) that fell below the specification minimum properties for plate and bar (depending on thickness).

REFERENCES

7. *Metallic Materials Properties Development and Standardization (MMPDS)*, MMPDS-04; April 2008; Federal Aviation Administration.
8. *Damage Tolerant Design Handbook: A Compilation of Fracture and Crack Growth Data for High Strength Alloys*; Compiled by D.A. Skinn, J.P. Gallagher, A.P. Berens, P.D. Huber, J. Smith; University of Dayton Research Institute, May 1994.

ACKNOWLEDGEMENTS

The author wishes to thank Mssrs. John Ruschau, Nick Jacobs, Don Woleslagle, Eric Soppe, Cris Williams, Ron Glett, Ms. Pat Youngerman, and Ms. Sarah Kuhlman, all of the University of Dayton Research Institute (UDRI); Mssrs. Dan Laufersweiler, Ed Porter, and Dave Roberts of Universal Technology Corporation (UTC); and Mr. Nick Blommel of AFRL/RXSCE for their engineering and technical support of this program. Acknowledgement is also given to Westmoreland Mechanical Testing & Research, Inc. for the machining of all of the test specimens.

Approved for public release; distribution unlimited.

PREPARED BY

SIGNED

STEVEN R. THOMPSON, Senior Materials Engineer
Materials Test & Evaluation Team
Acquisition Systems Support Branch
Systems Support Division

REVIEWED BY

SIGNED

NEAL ONTKO, Team Lead
Materials Test & Evaluation Team
Acquisition Systems Support Branch
Systems Support Division

PUBLICATION REVIEW: This report has been reviewed and approved.

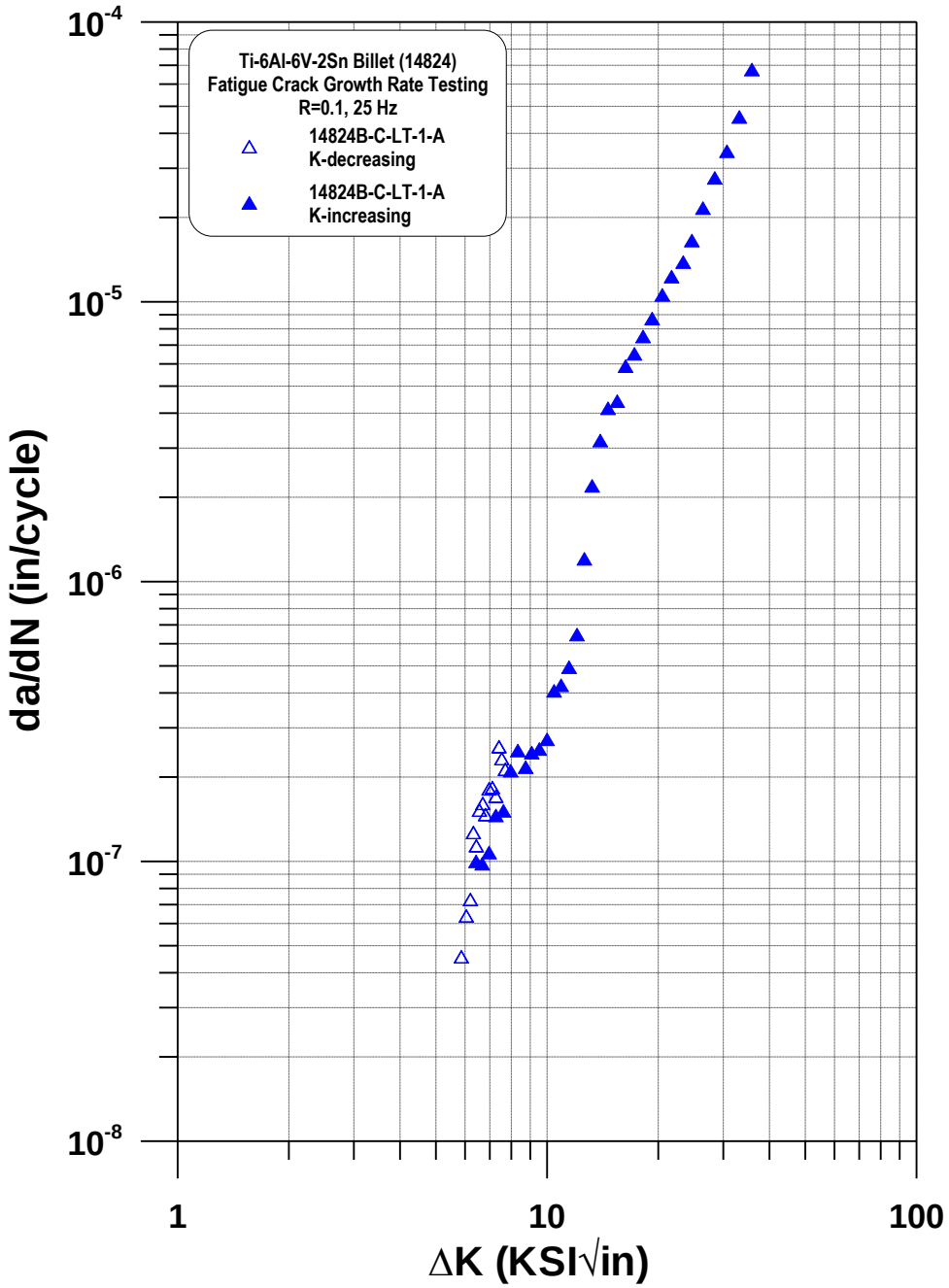
SIGNED

CHARLES WAGNER, Branch Chief
Acquisition Systems Support Branch
Systems Support Division

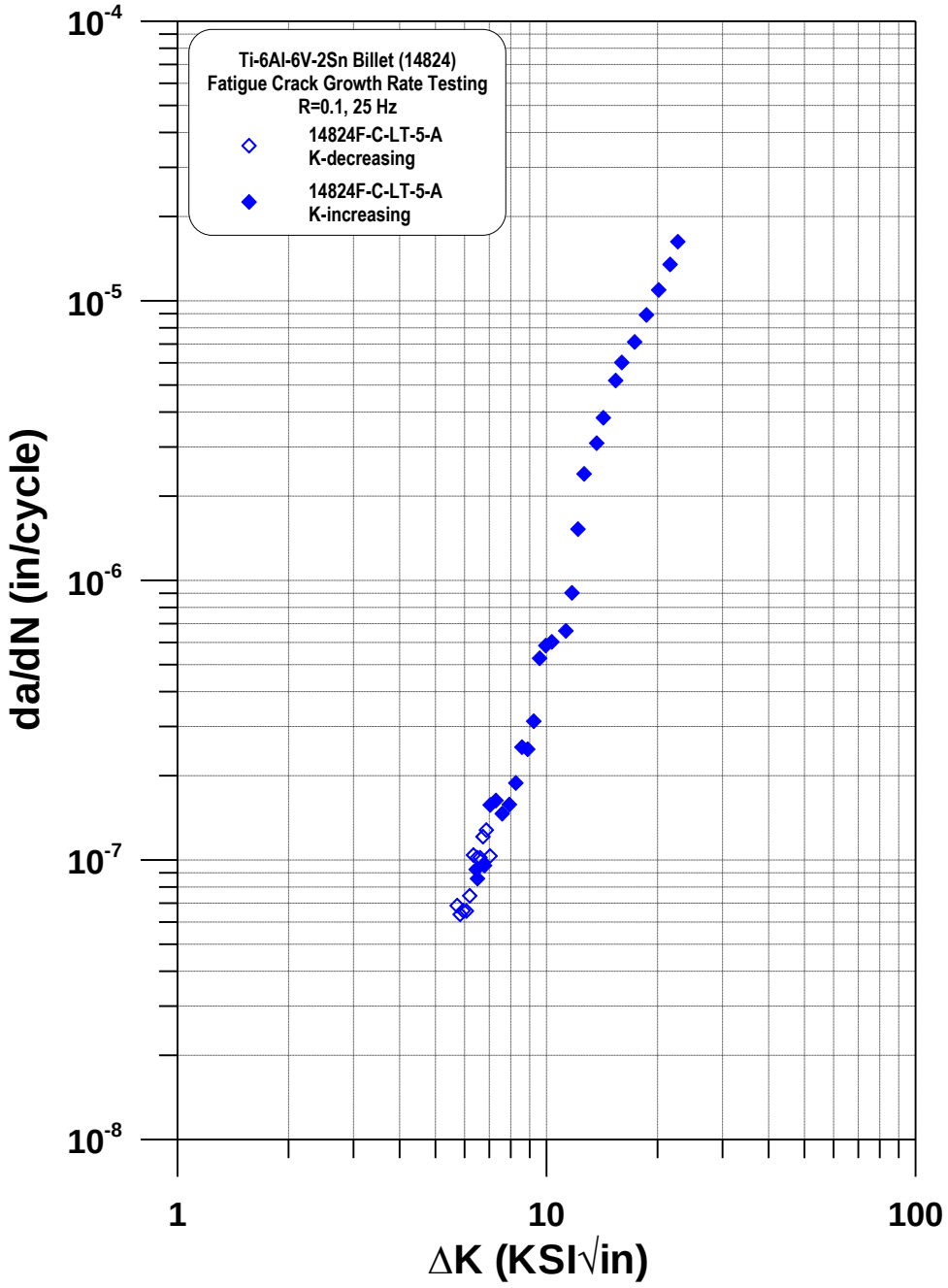
Approved for public release; distribution unlimited.

Appendix A
Individual fatigue crack growth rate curves for Ti-6Al-6V-2Sn billet (14824).

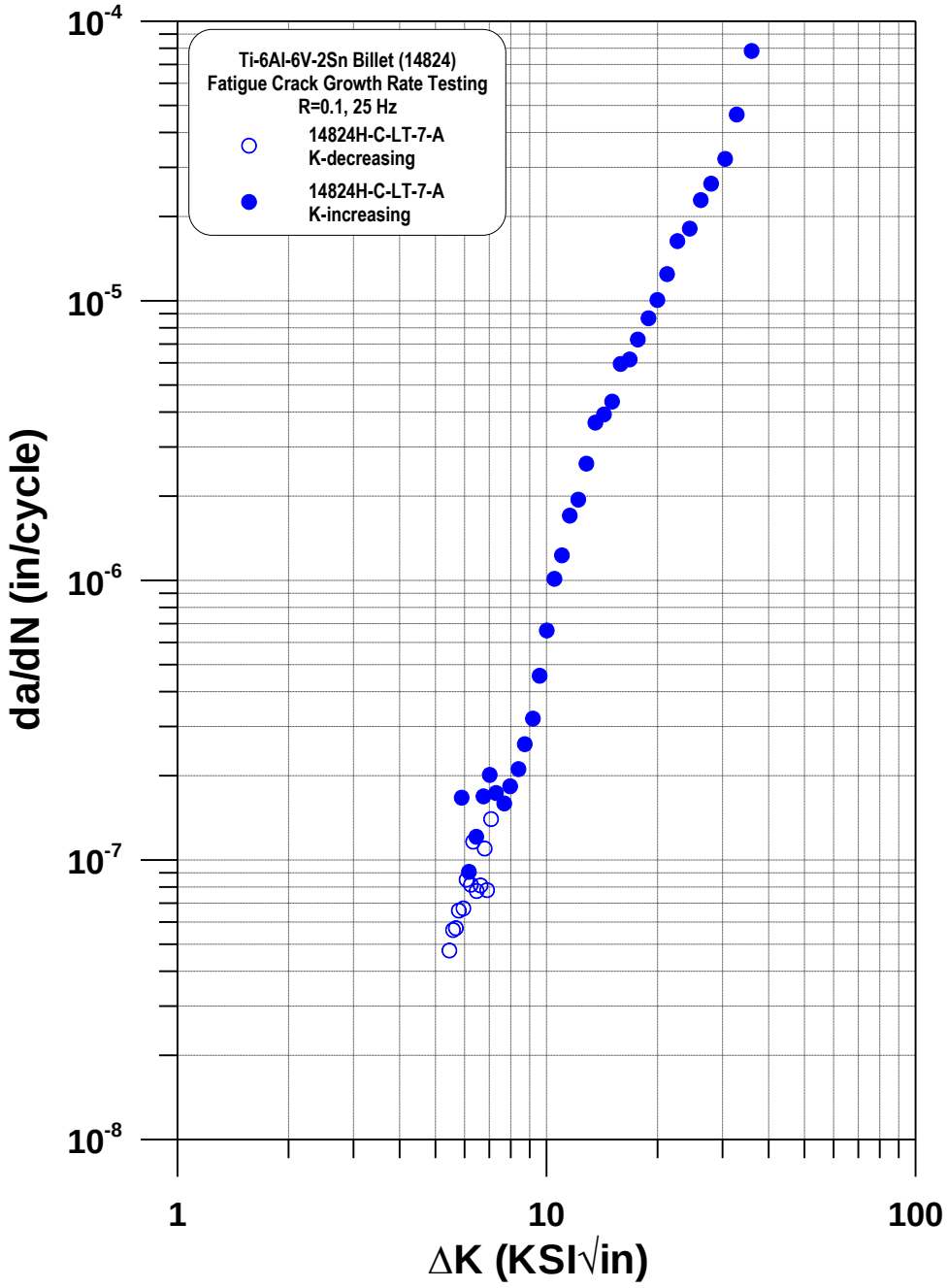
Approved for public release; distribution unlimited.



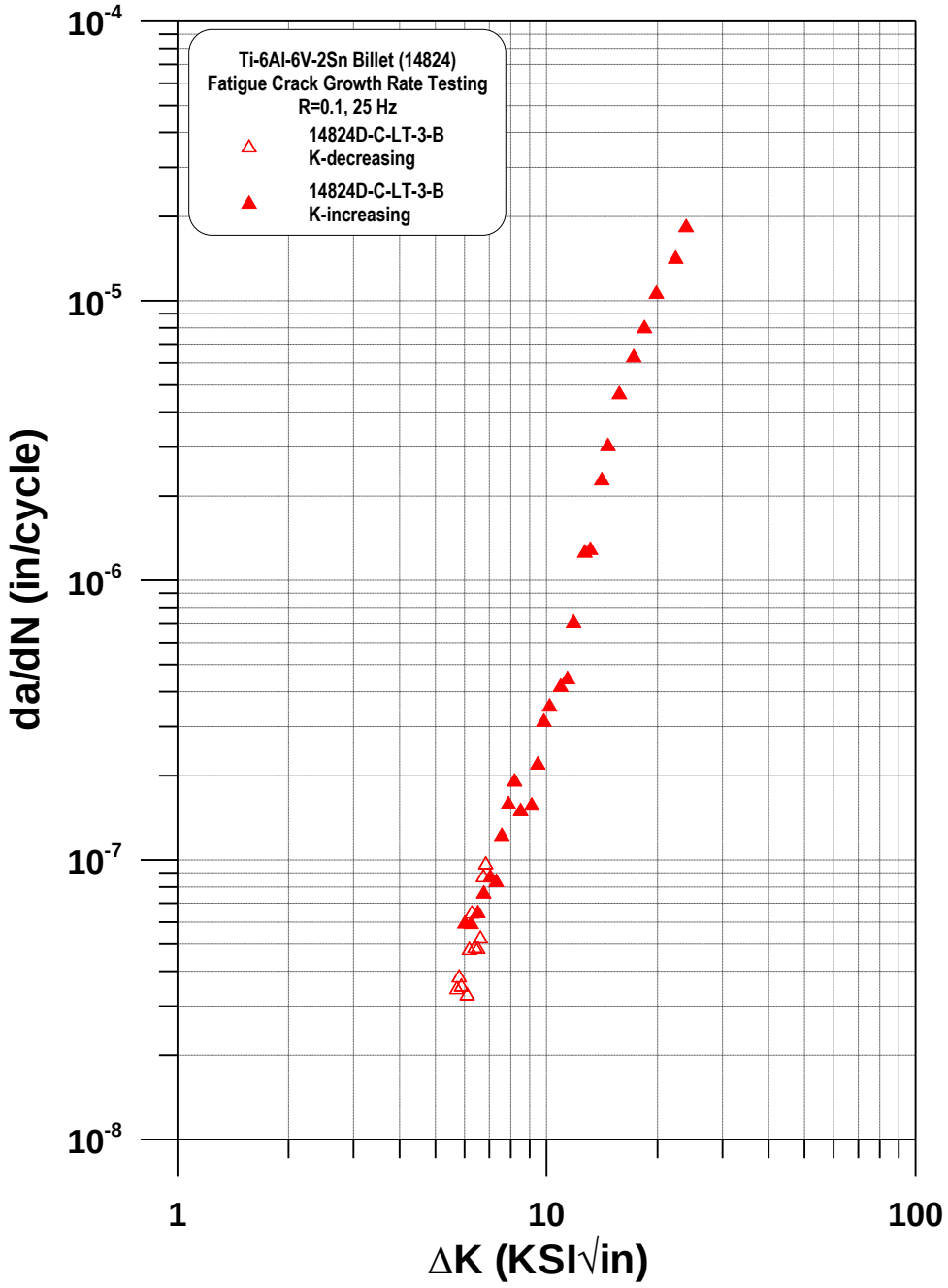
Approved for public release; distribution unlimited.



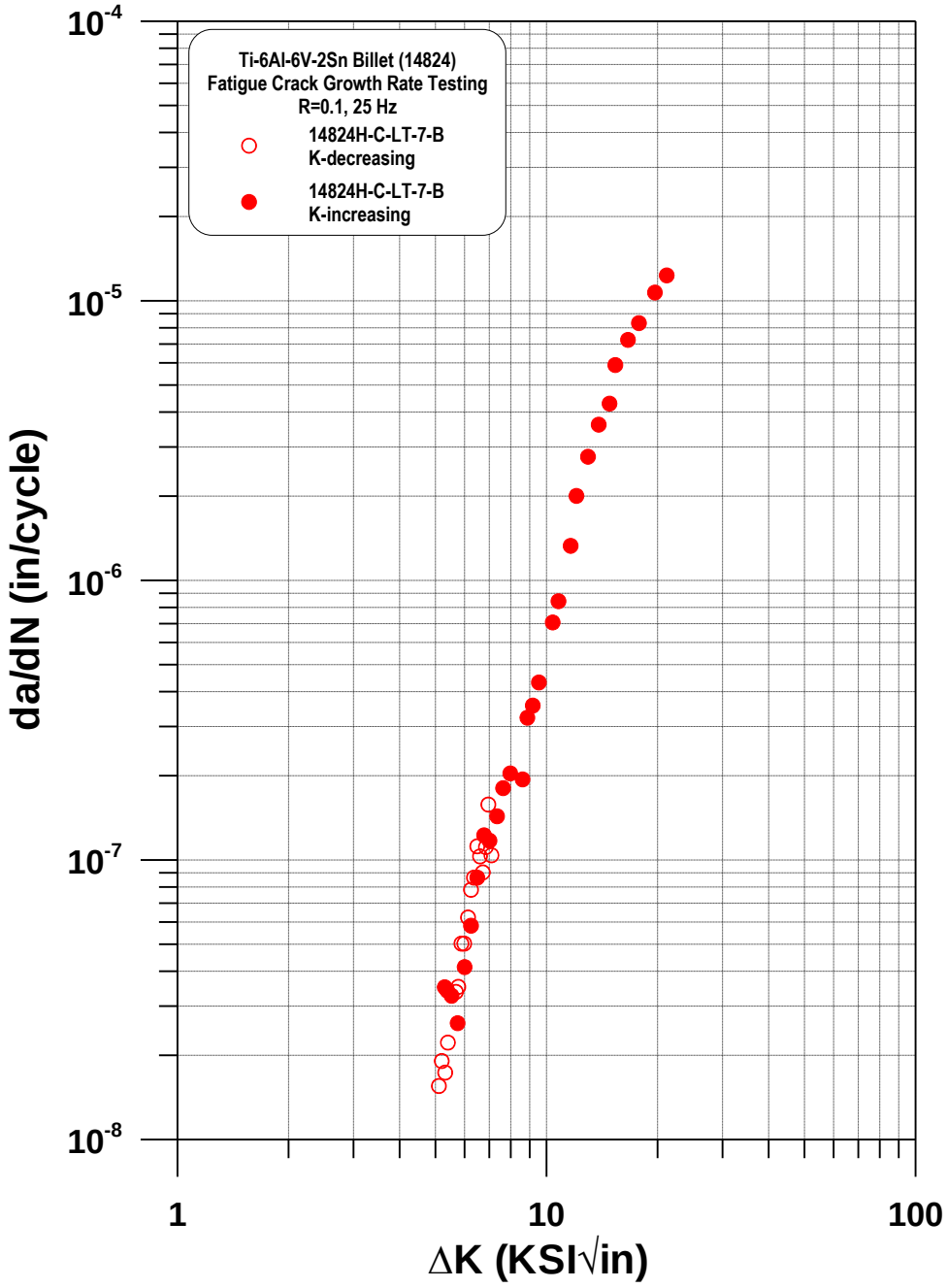
Approved for public release; distribution unlimited.



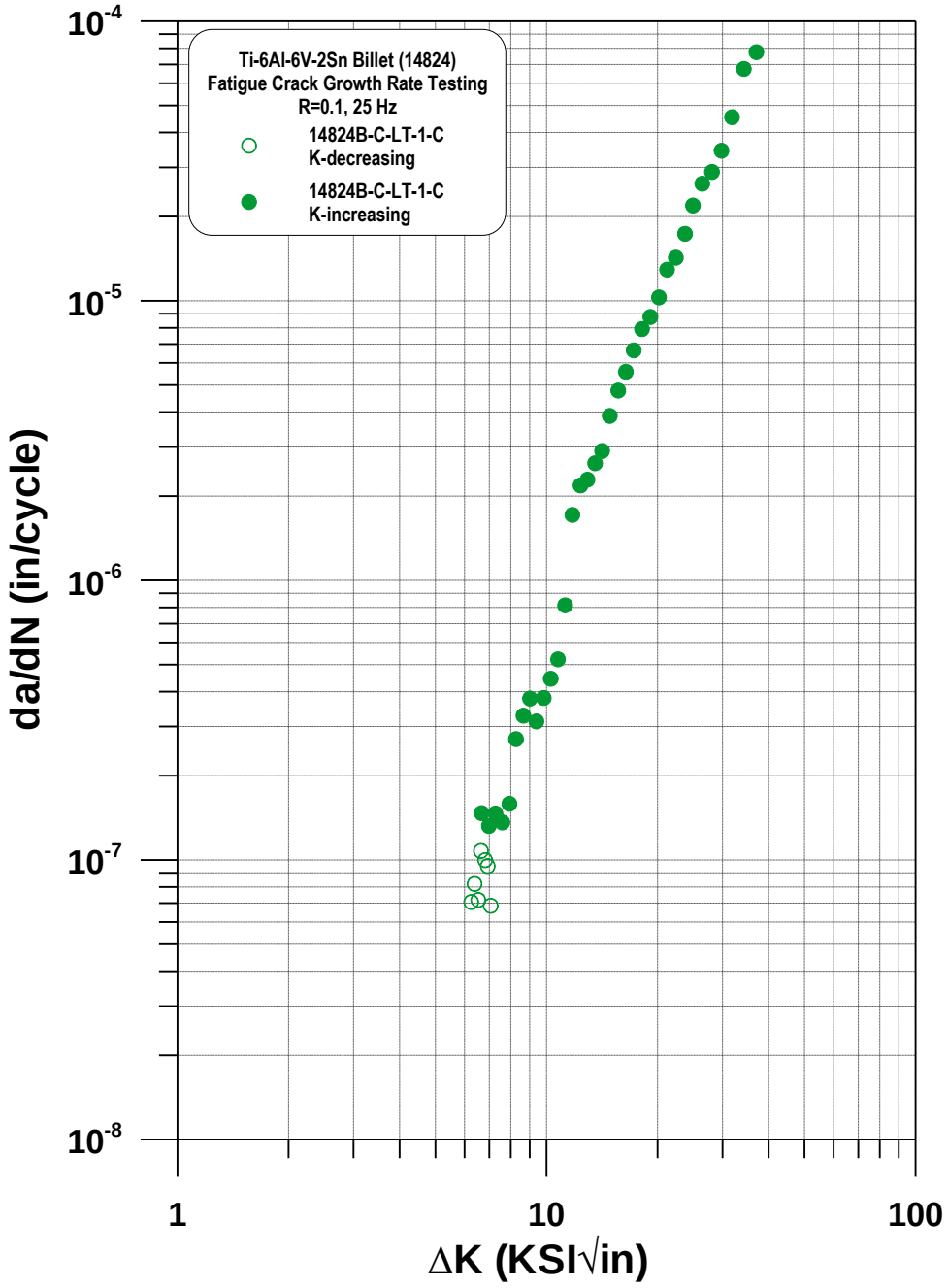
Approved for public release; distribution unlimited.



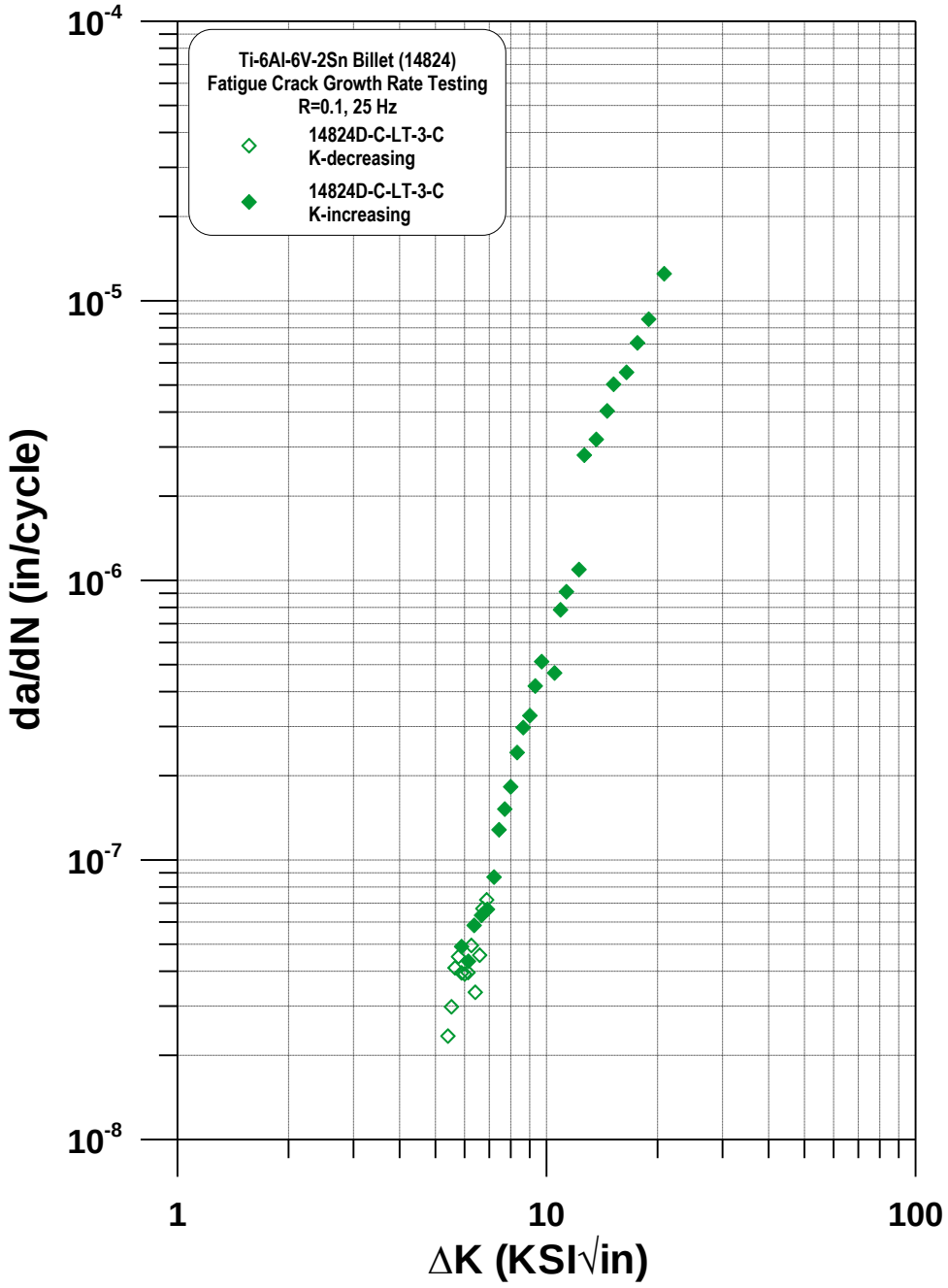
Approved for public release; distribution unlimited.



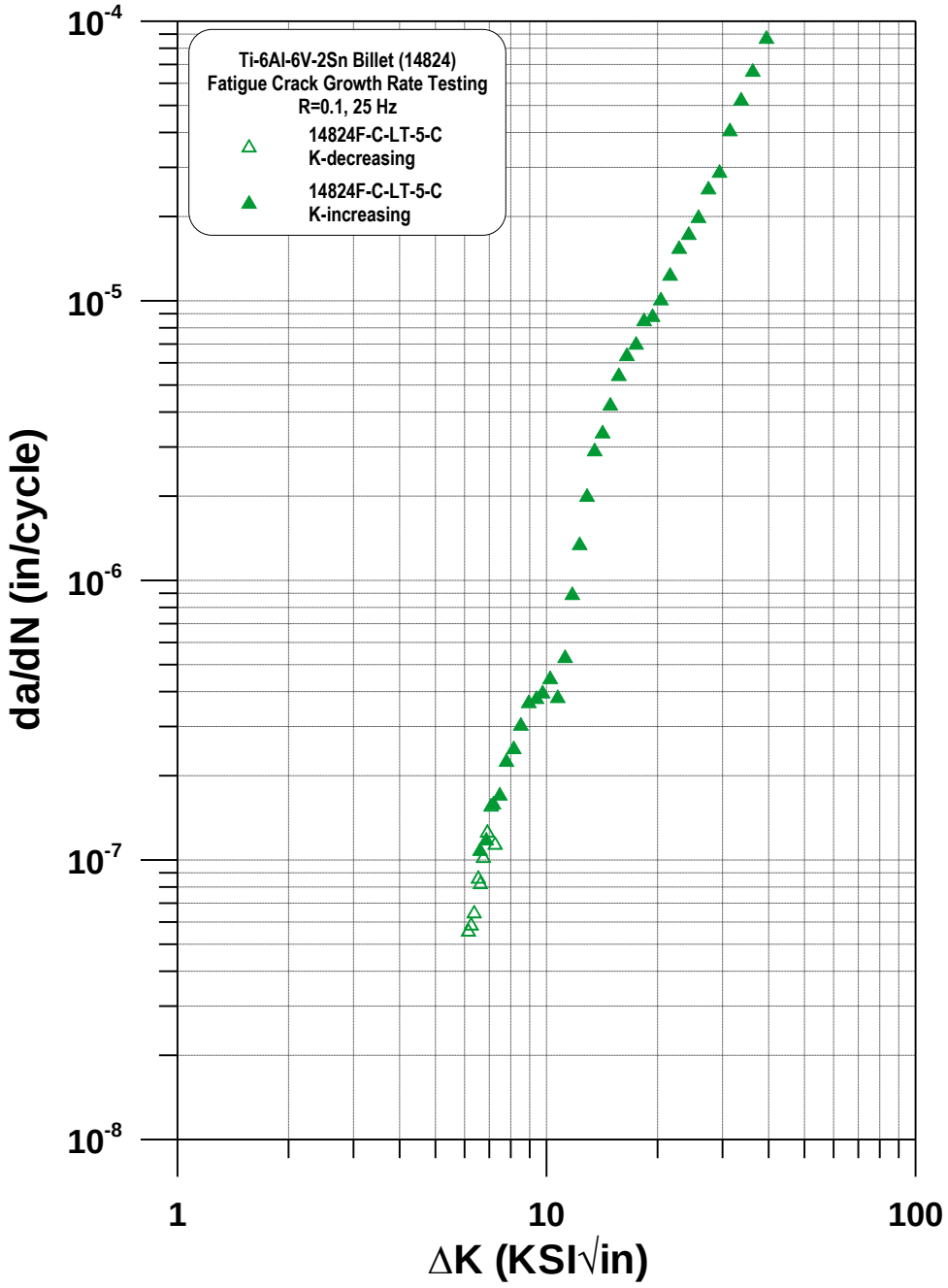
Approved for public release; distribution unlimited.



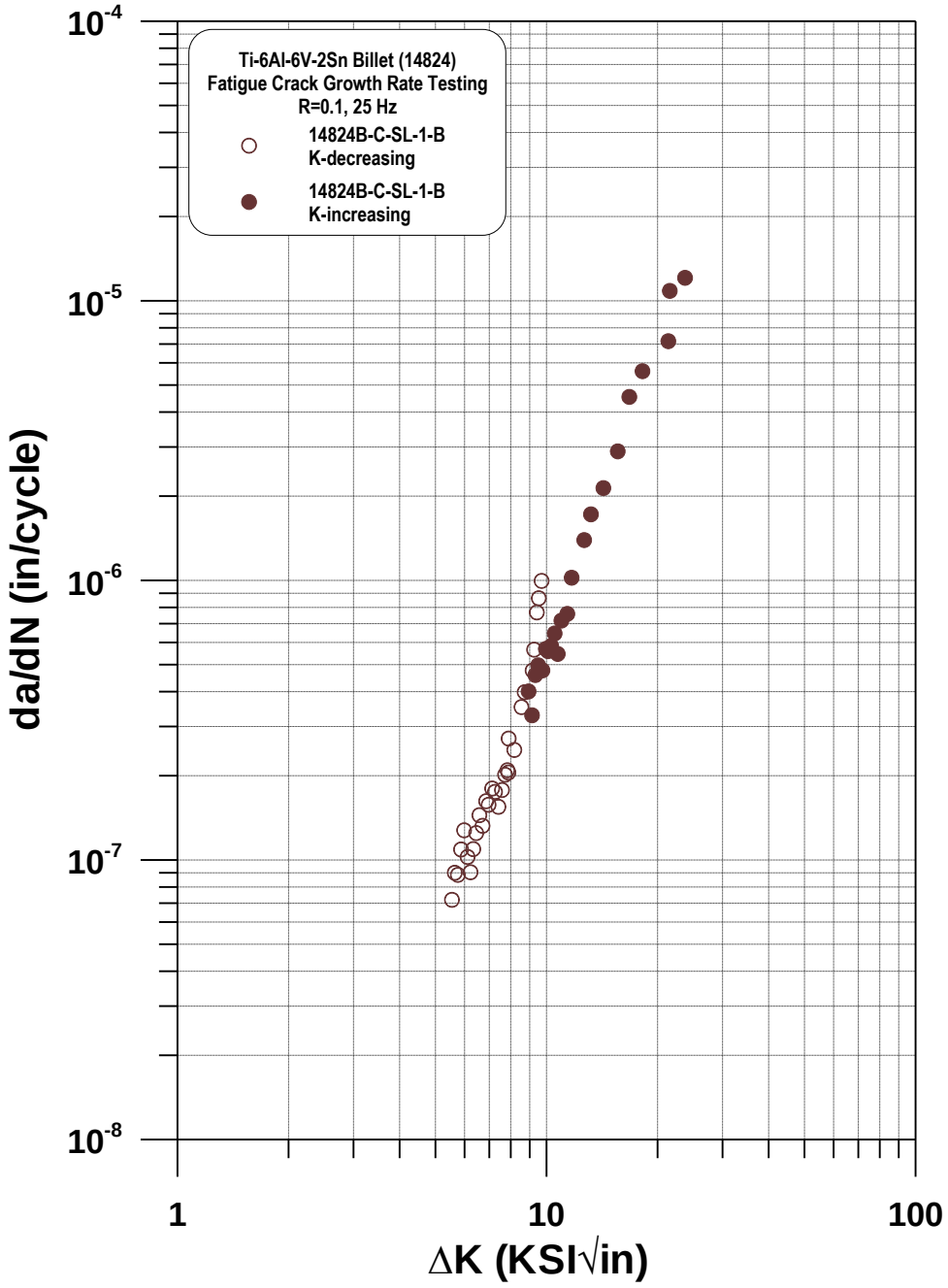
Approved for public release; distribution unlimited.



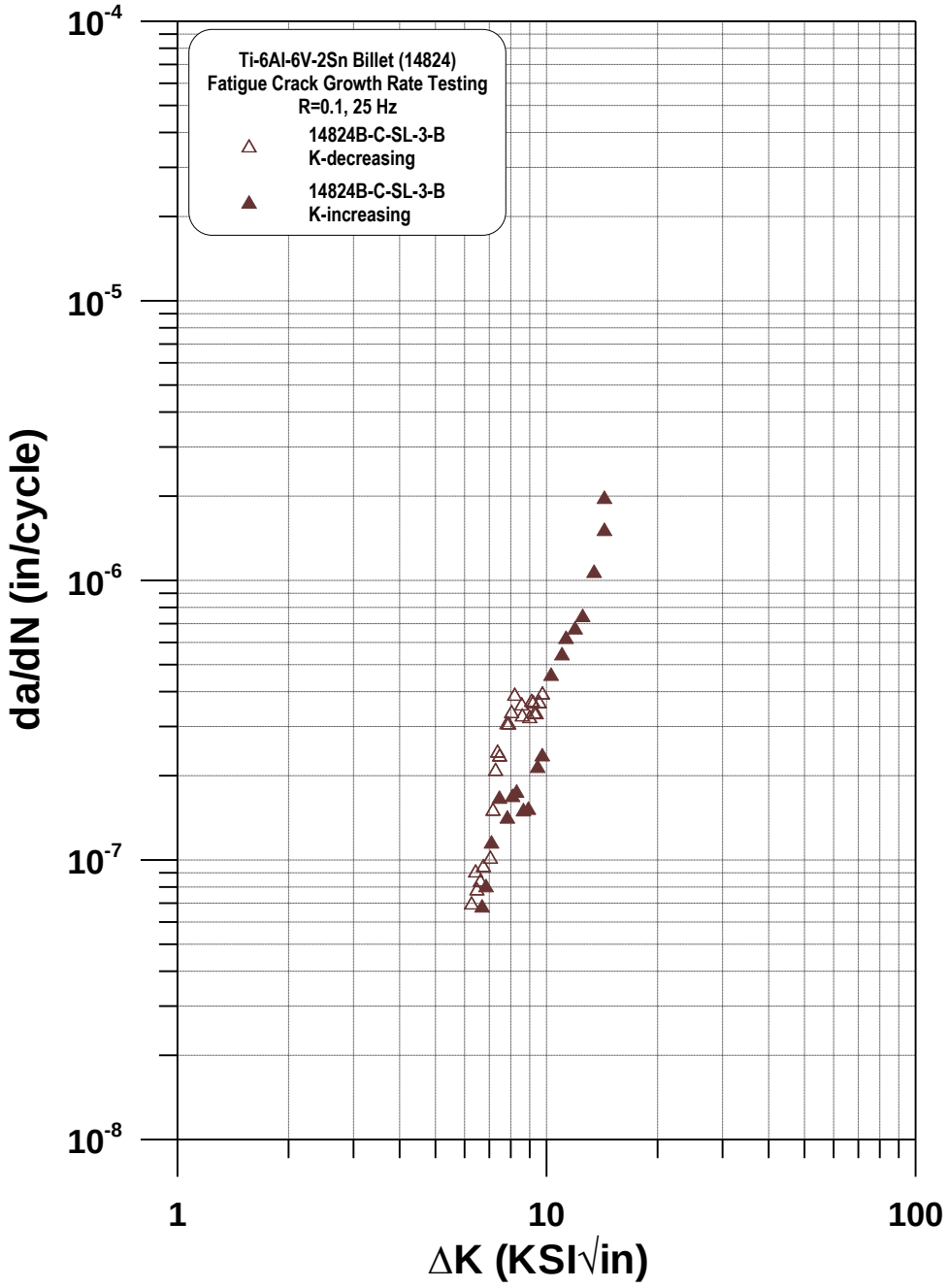
Approved for public release; distribution unlimited.



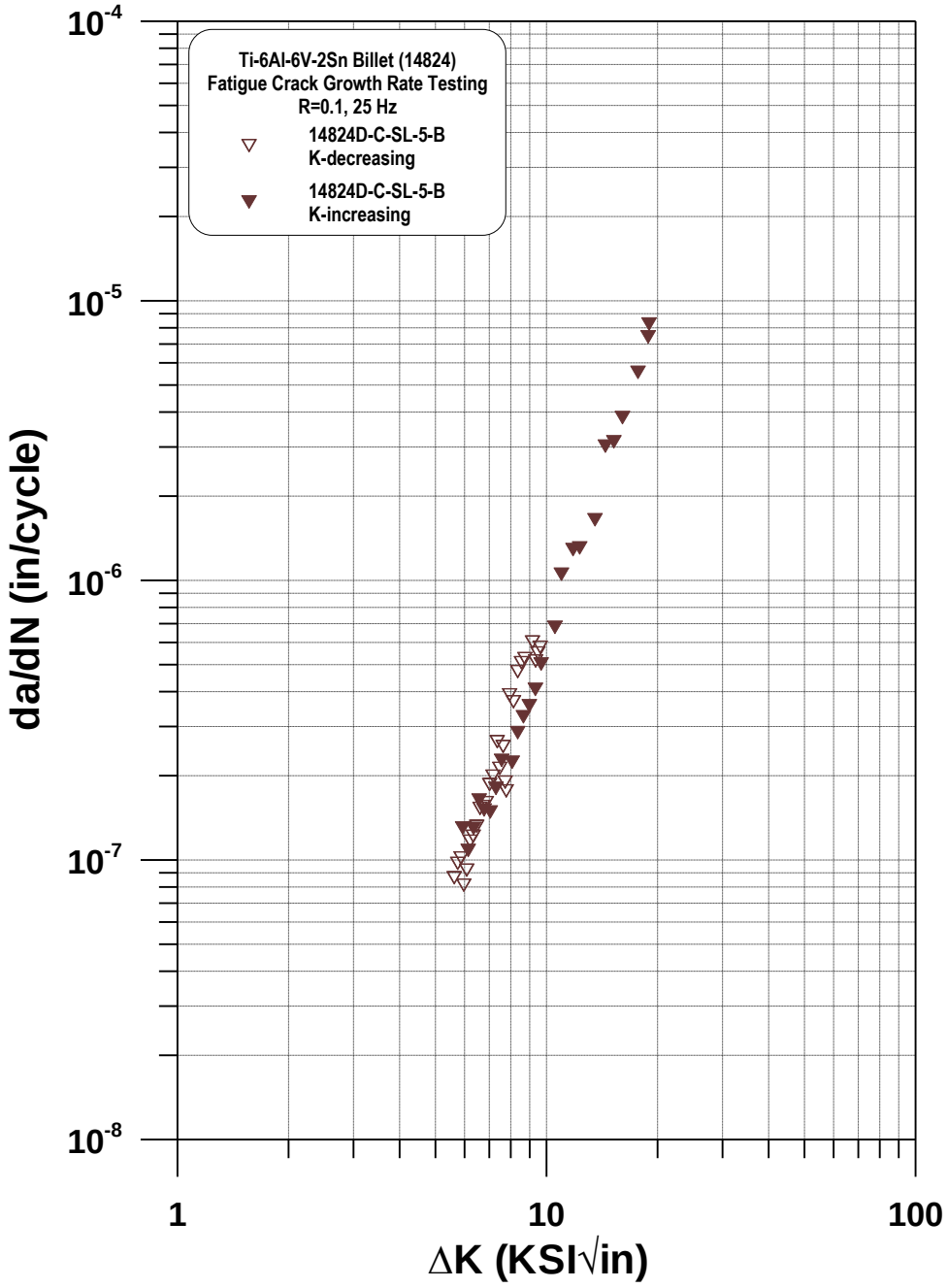
Approved for public release; distribution unlimited.



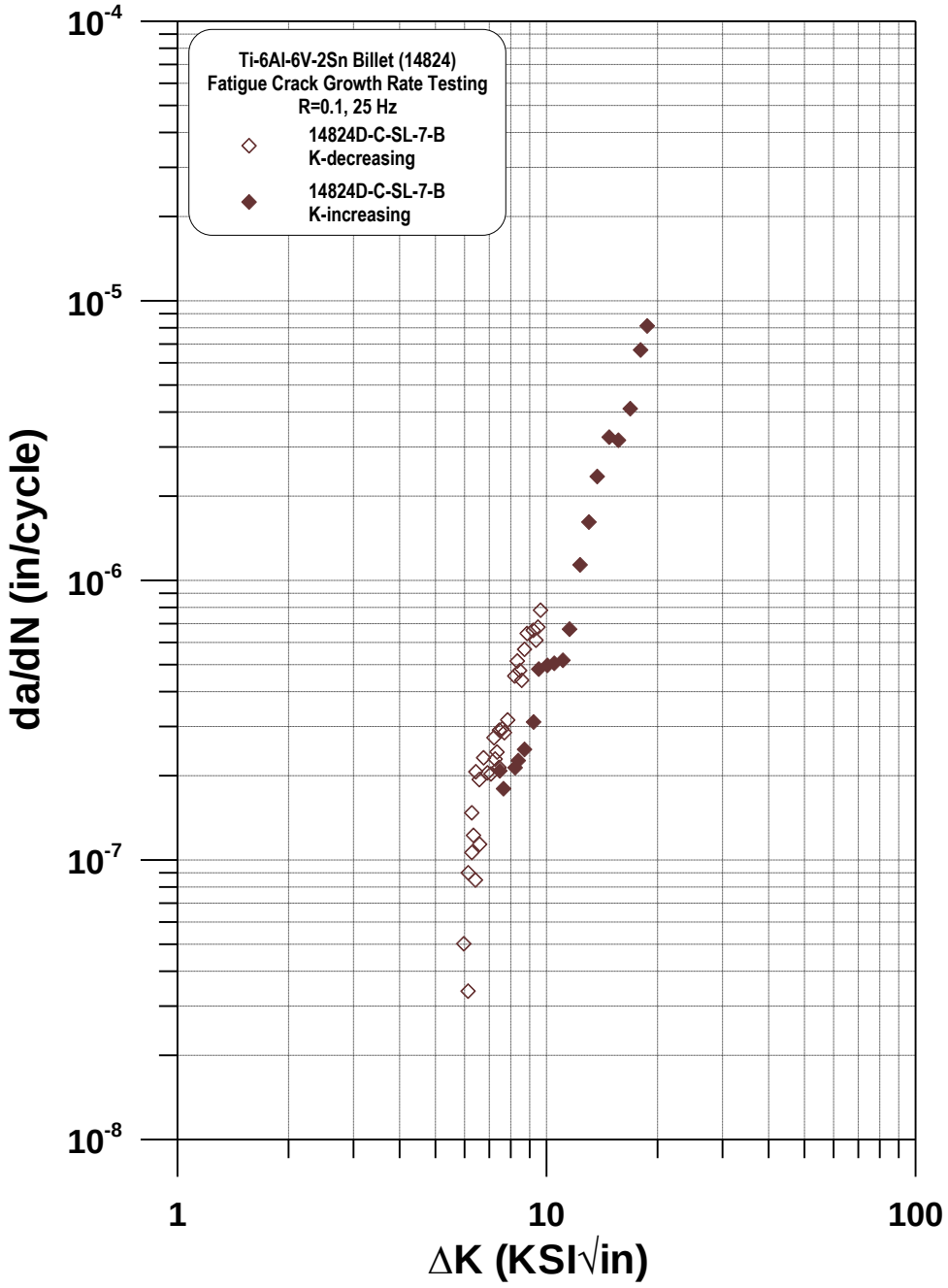
Approved for public release; distribution unlimited.



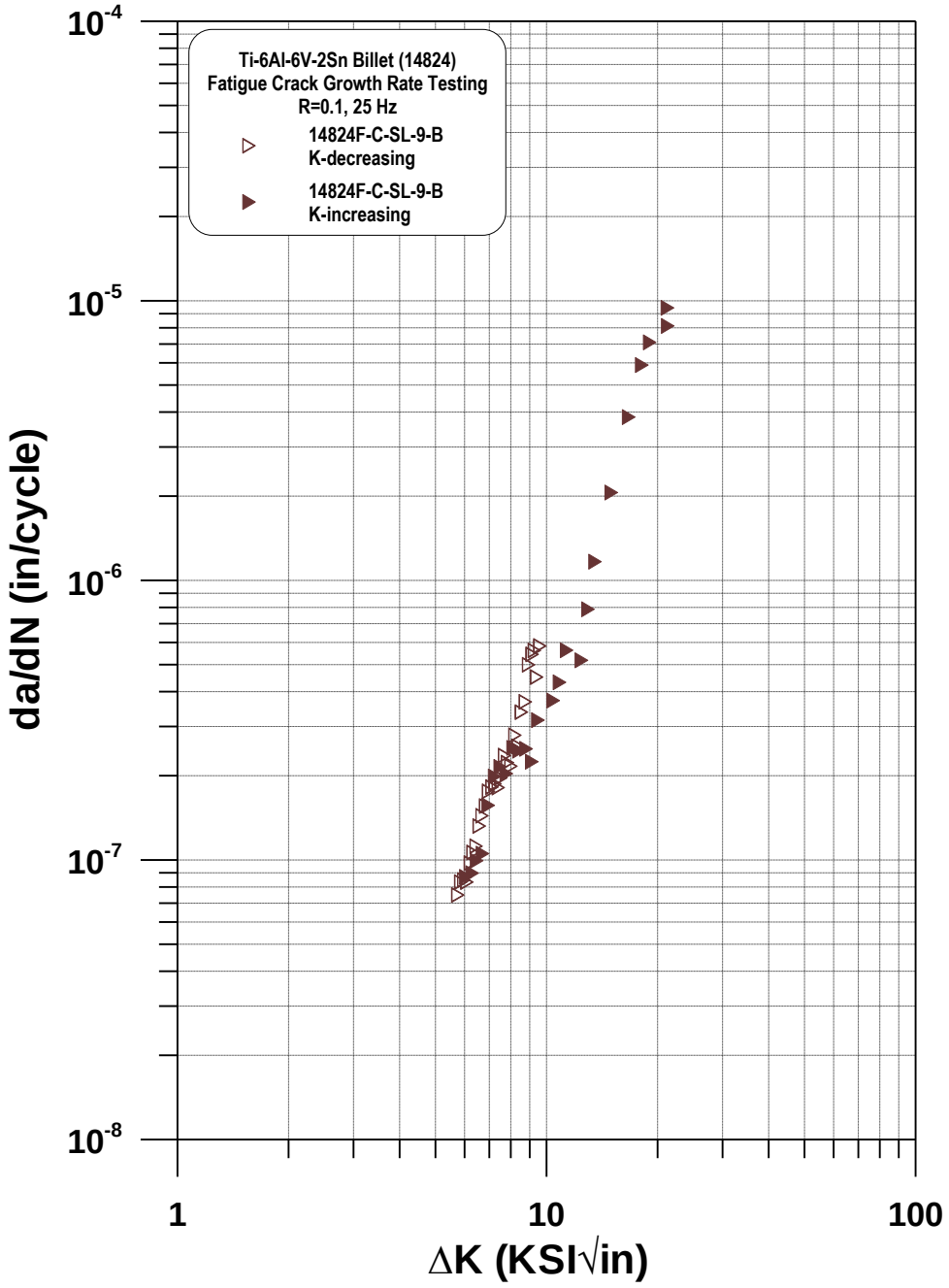
Approved for public release; distribution unlimited.



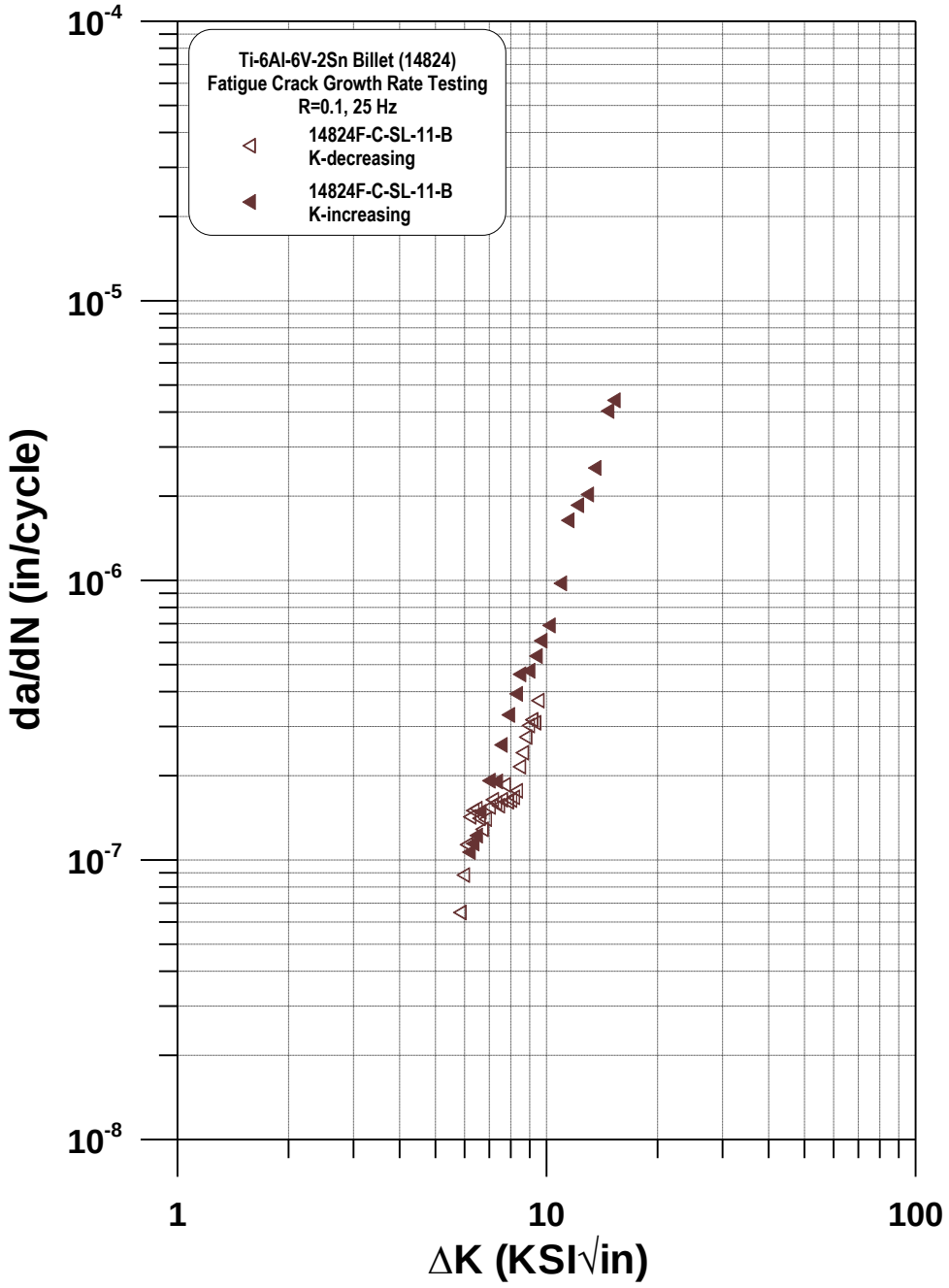
Approved for public release; distribution unlimited.



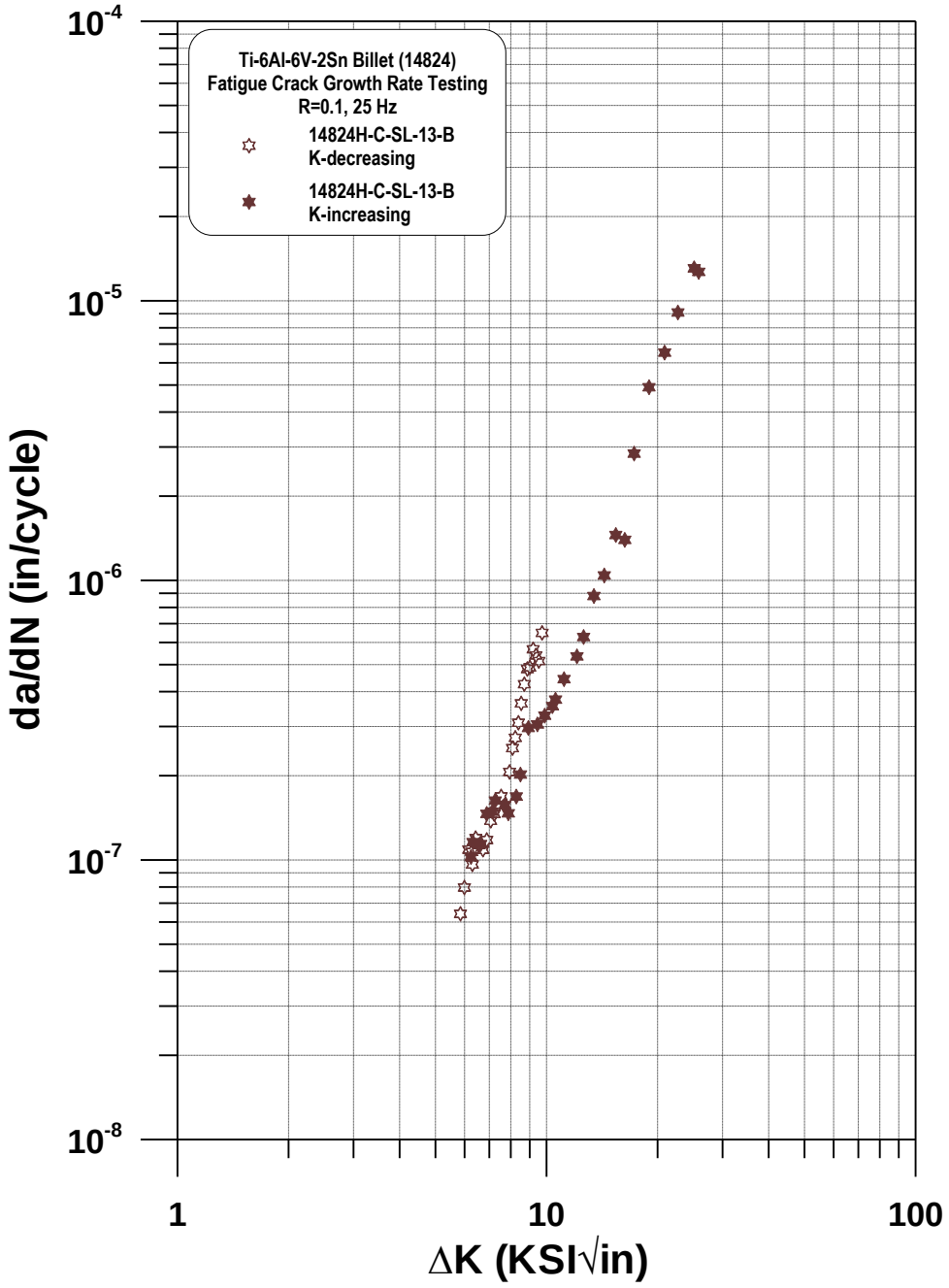
Approved for public release; distribution unlimited.



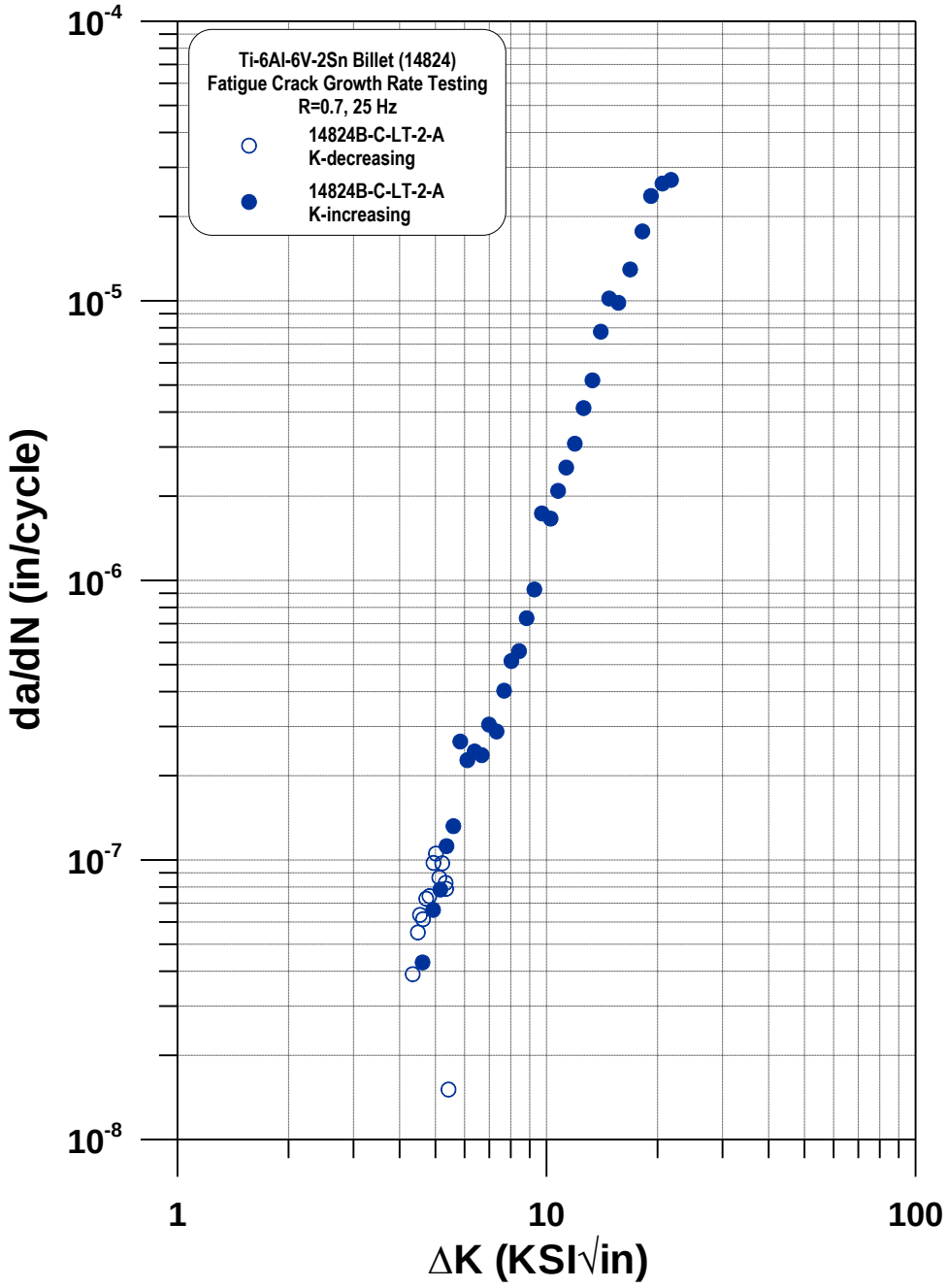
Approved for public release; distribution unlimited.



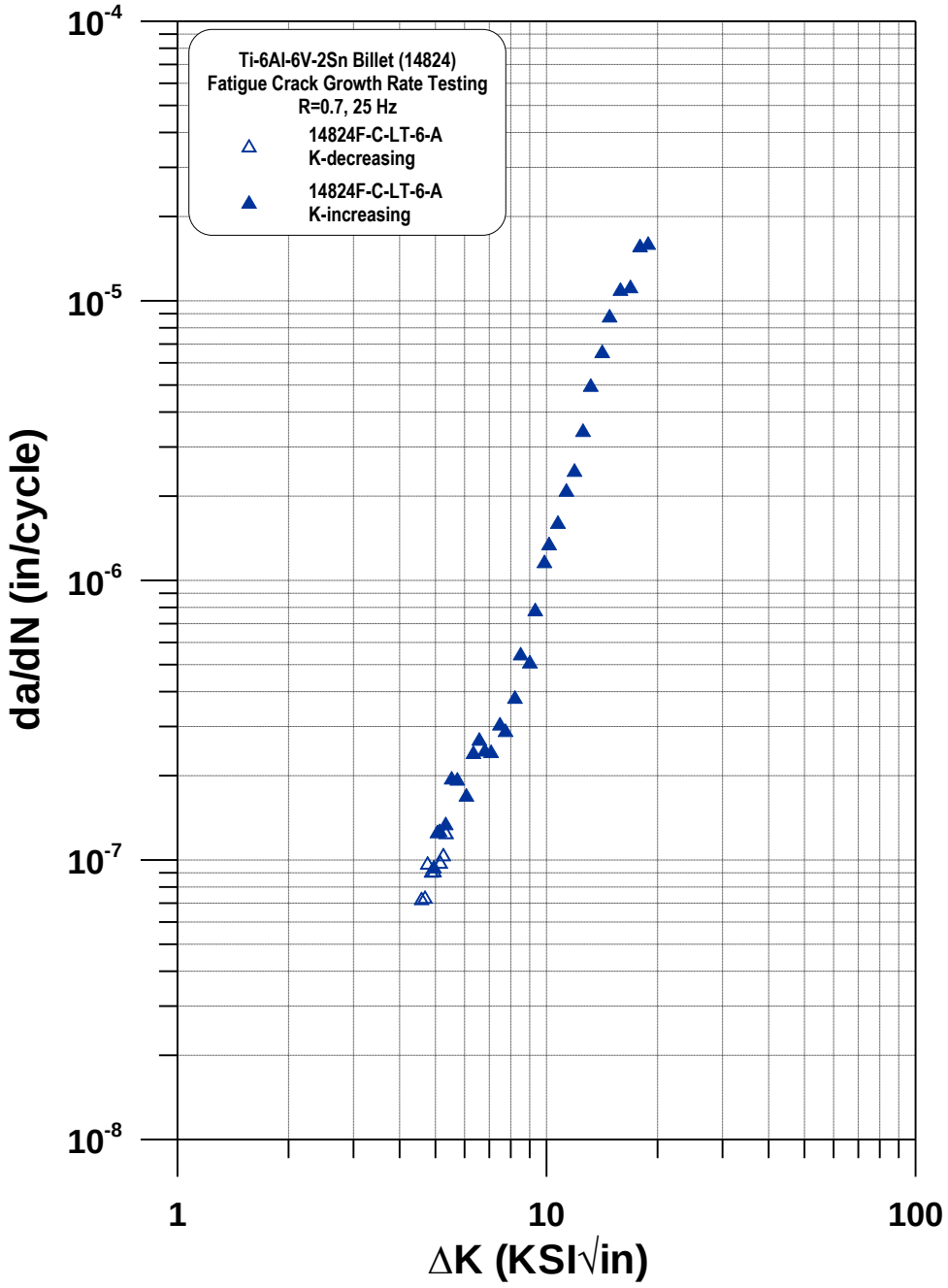
Approved for public release; distribution unlimited.



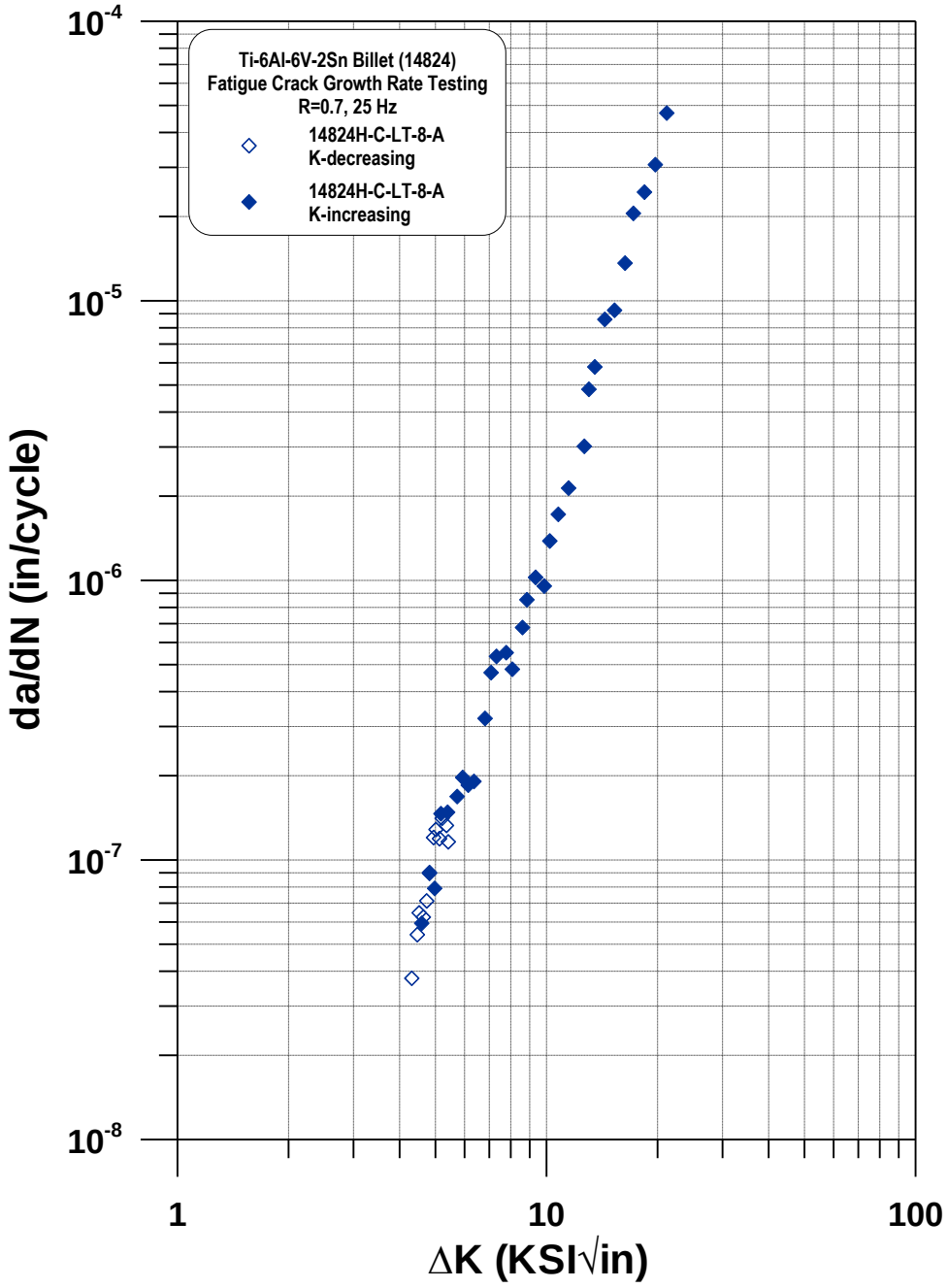
Approved for public release; distribution unlimited.



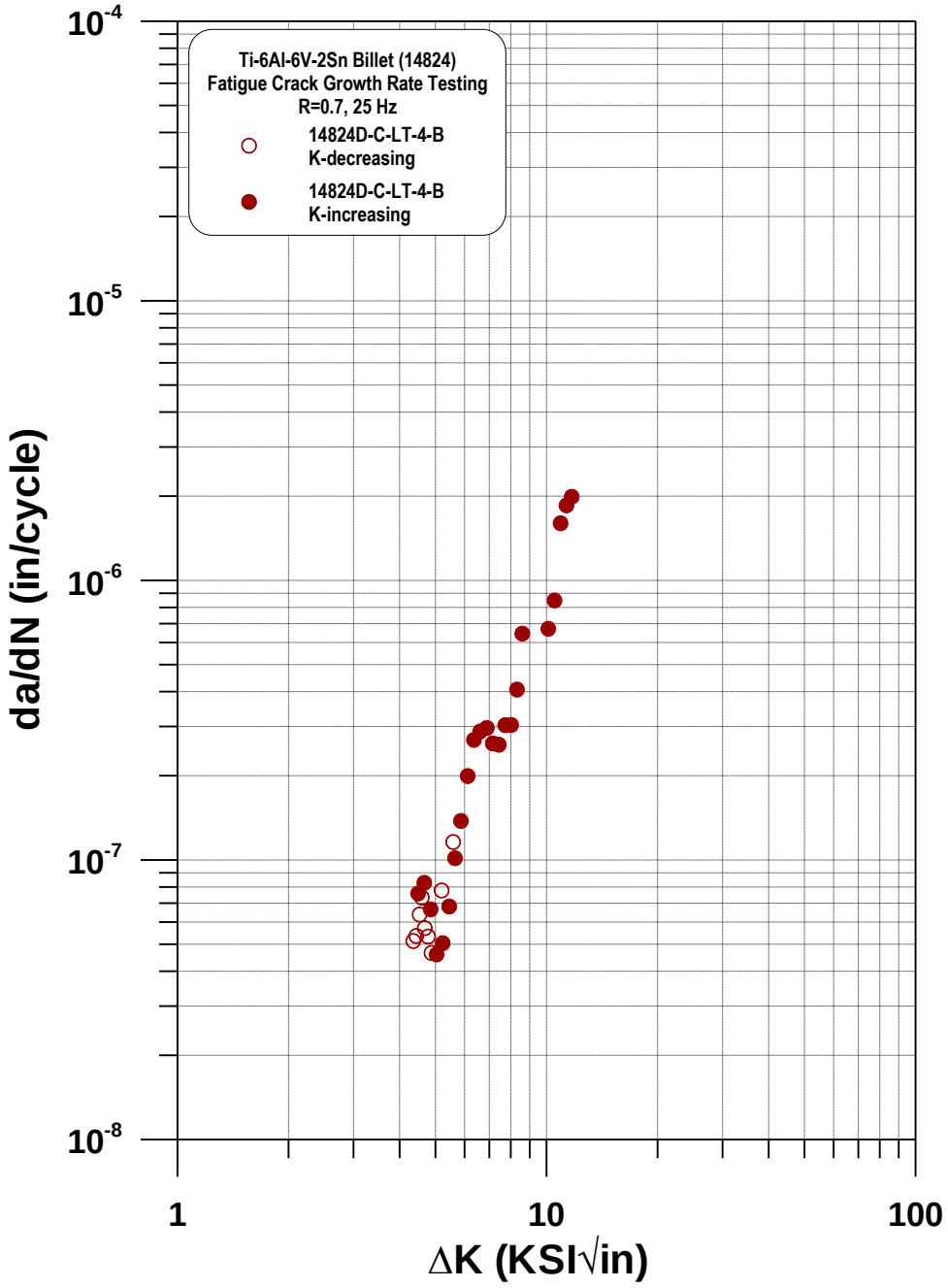
Approved for public release; distribution unlimited.



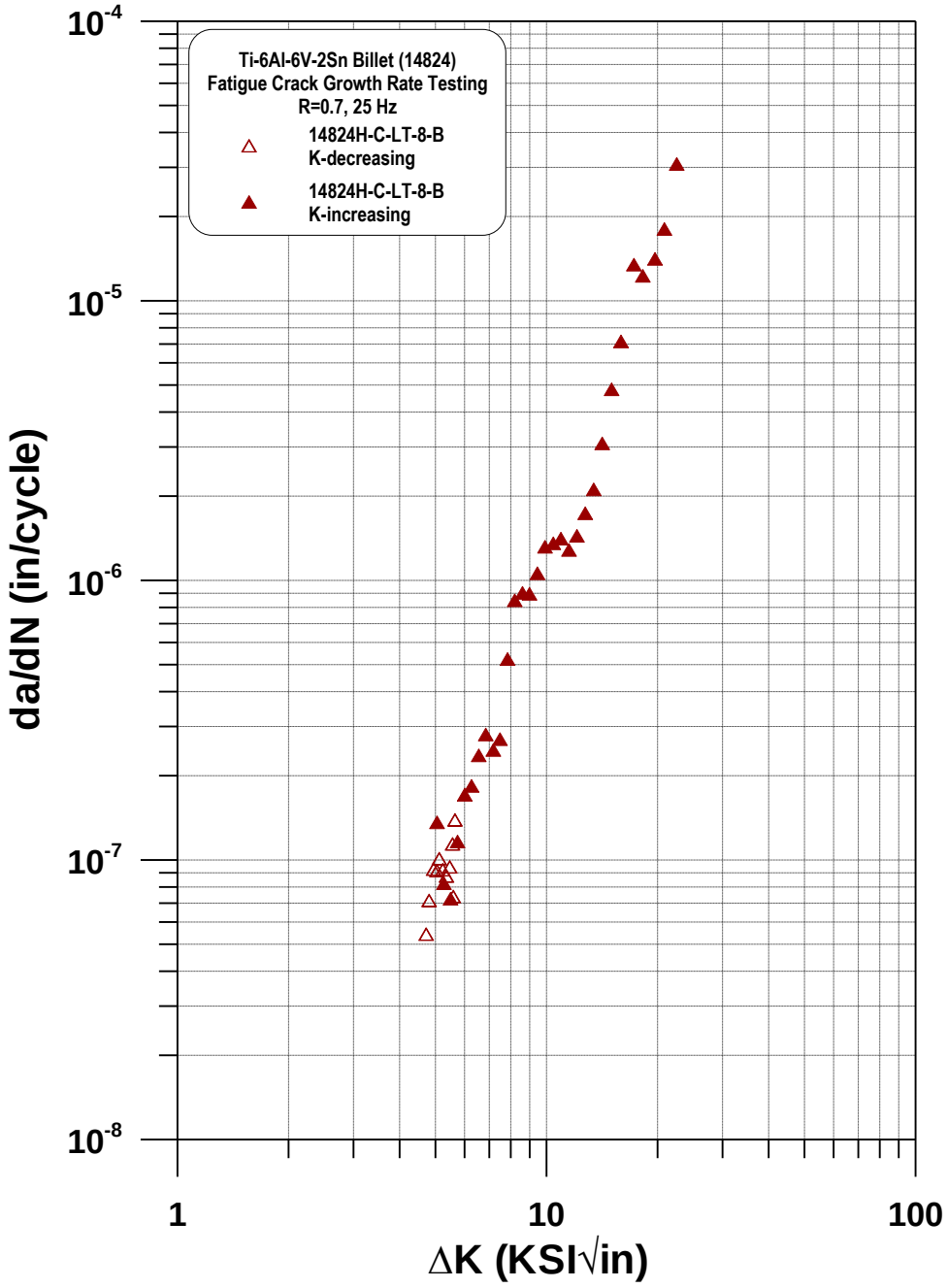
Approved for public release; distribution unlimited.



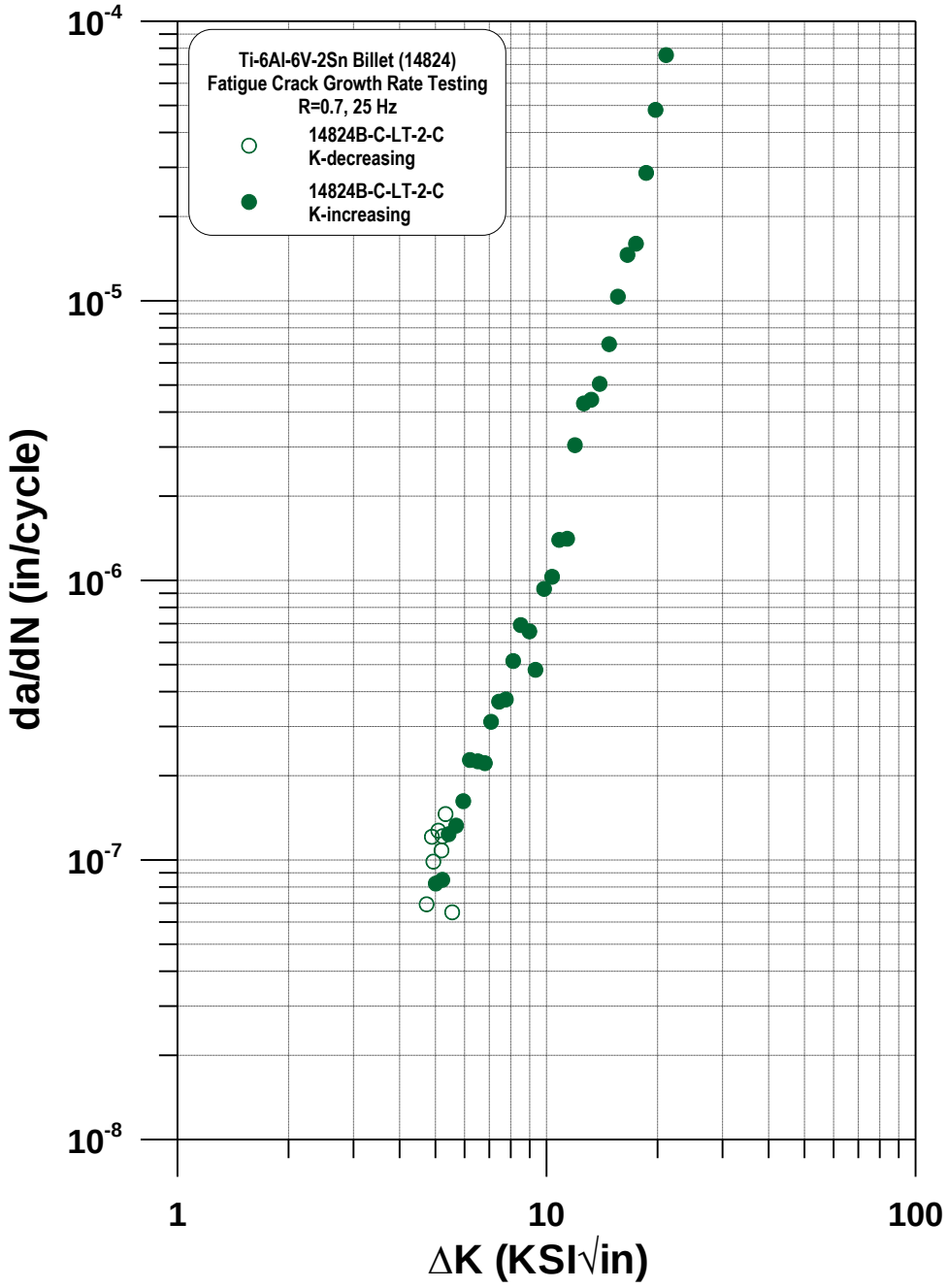
Approved for public release; distribution unlimited.



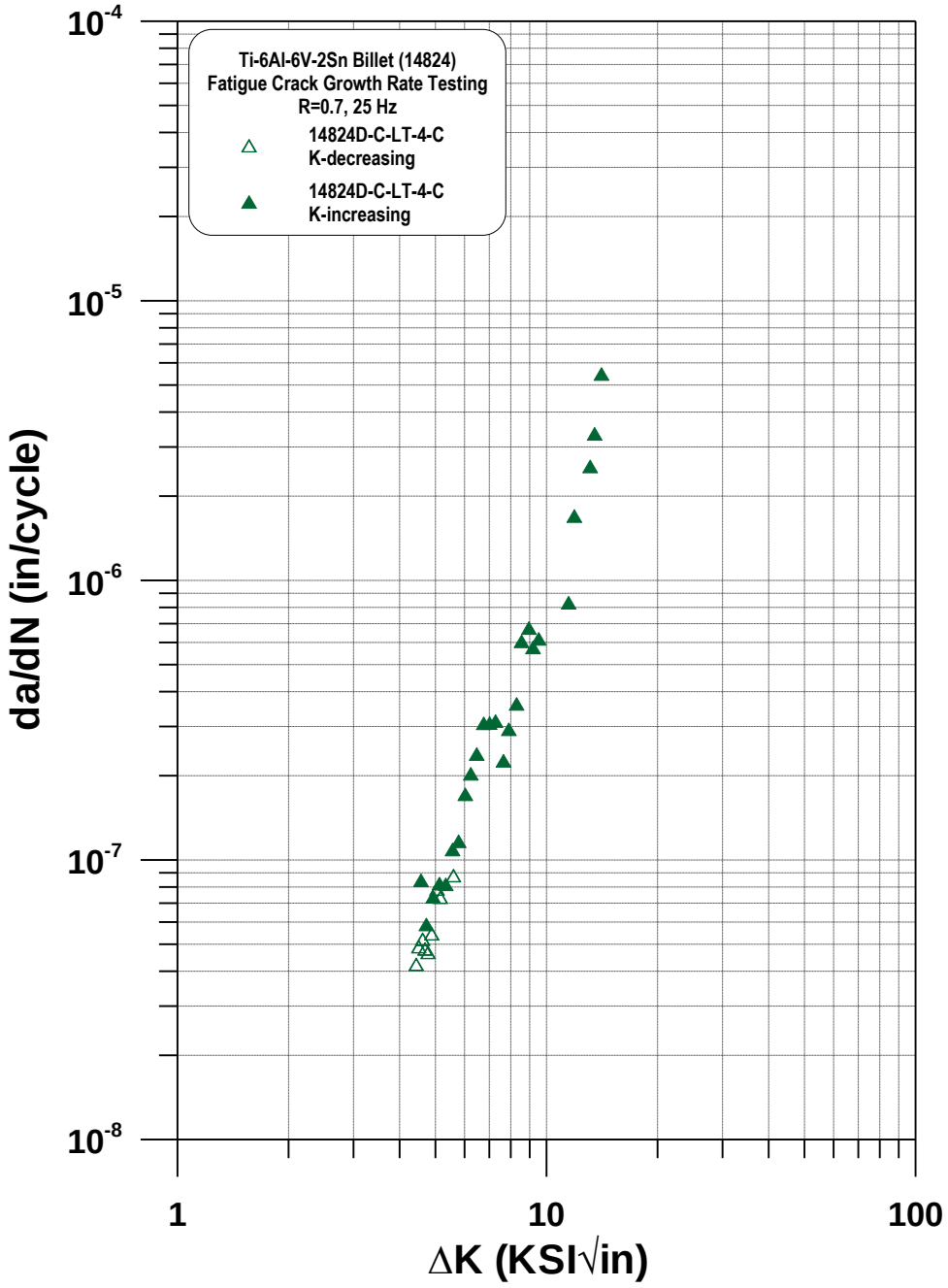
Approved for public release; distribution unlimited.



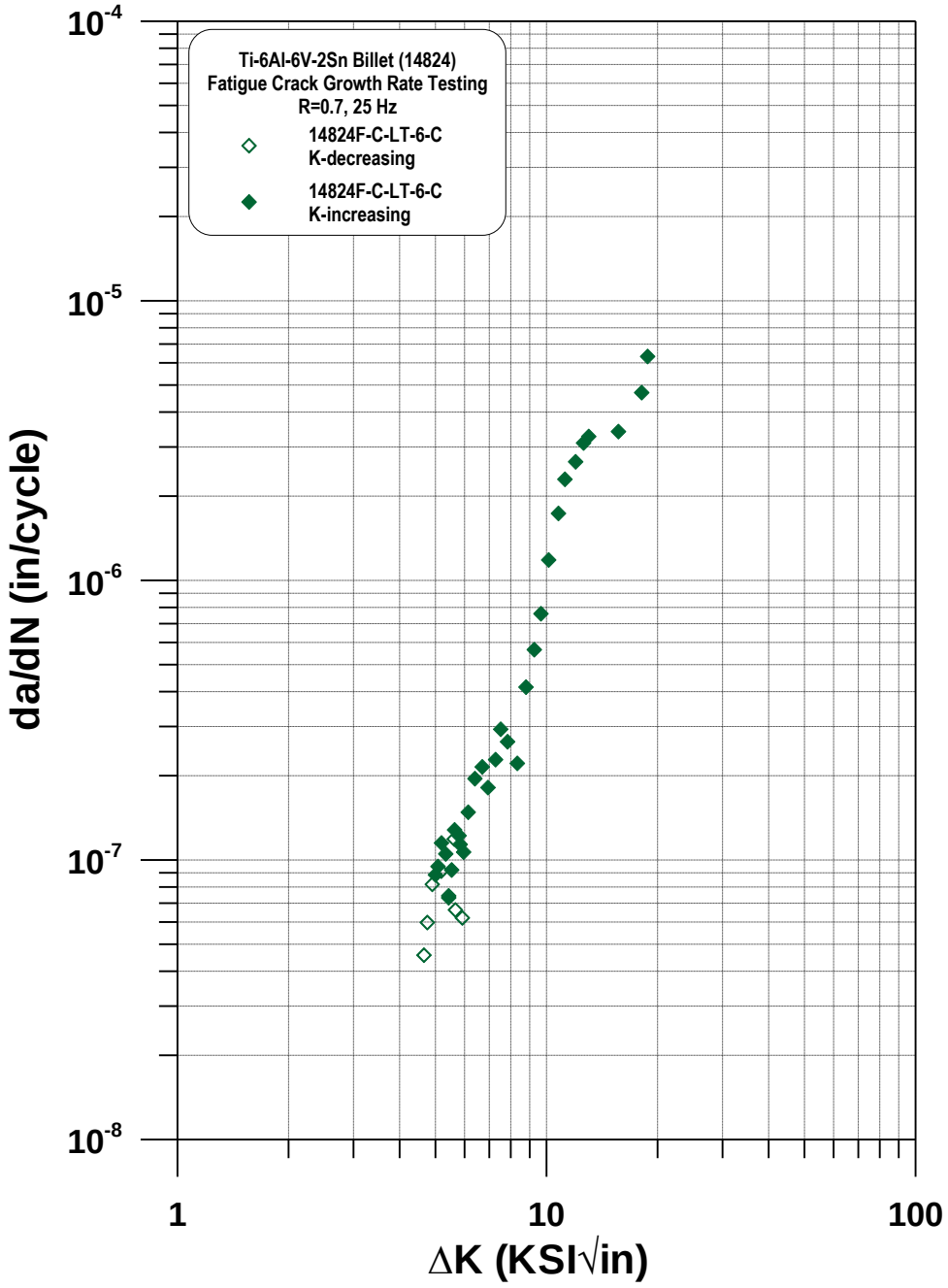
Approved for public release; distribution unlimited.



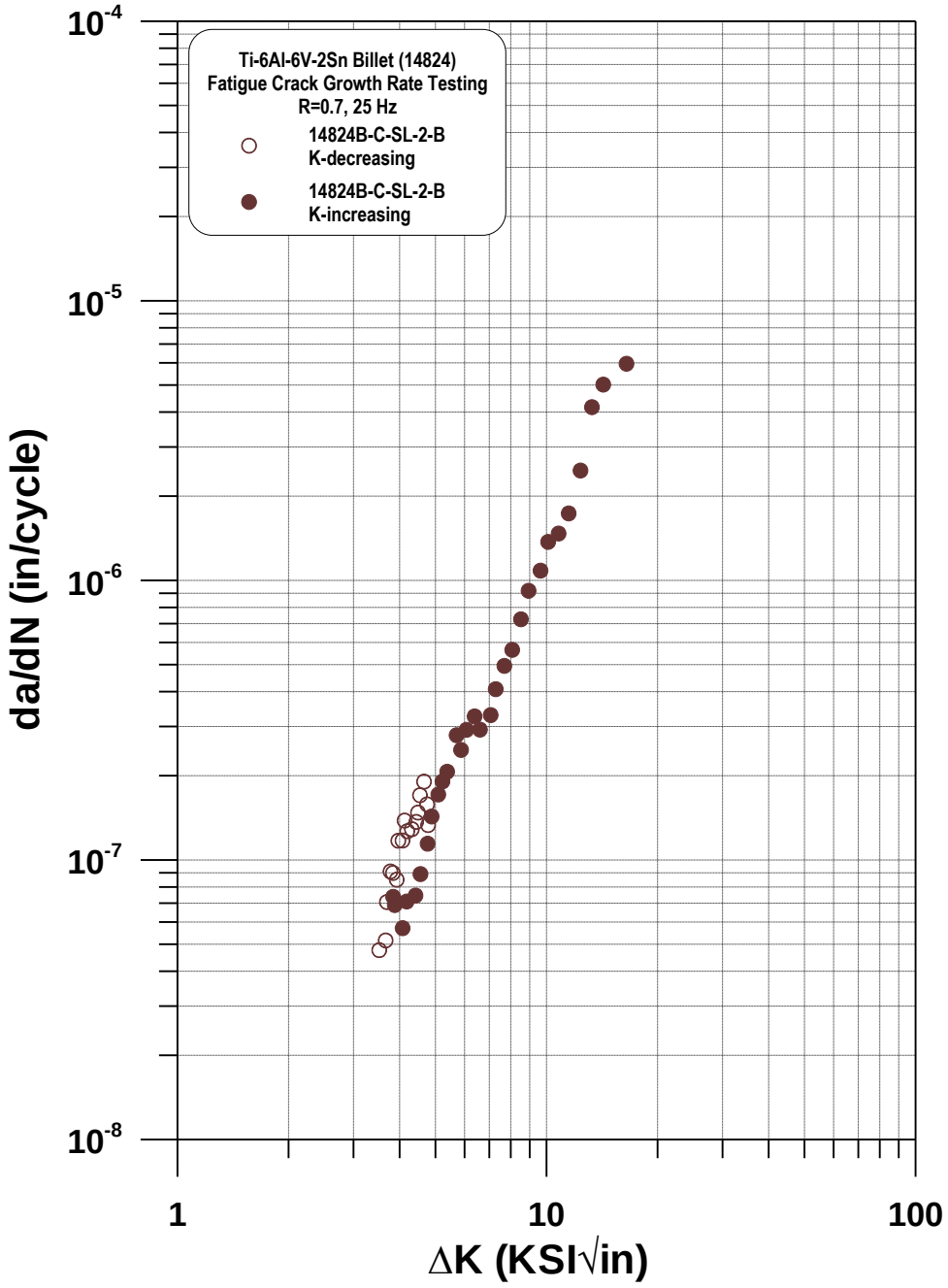
Approved for public release; distribution unlimited.



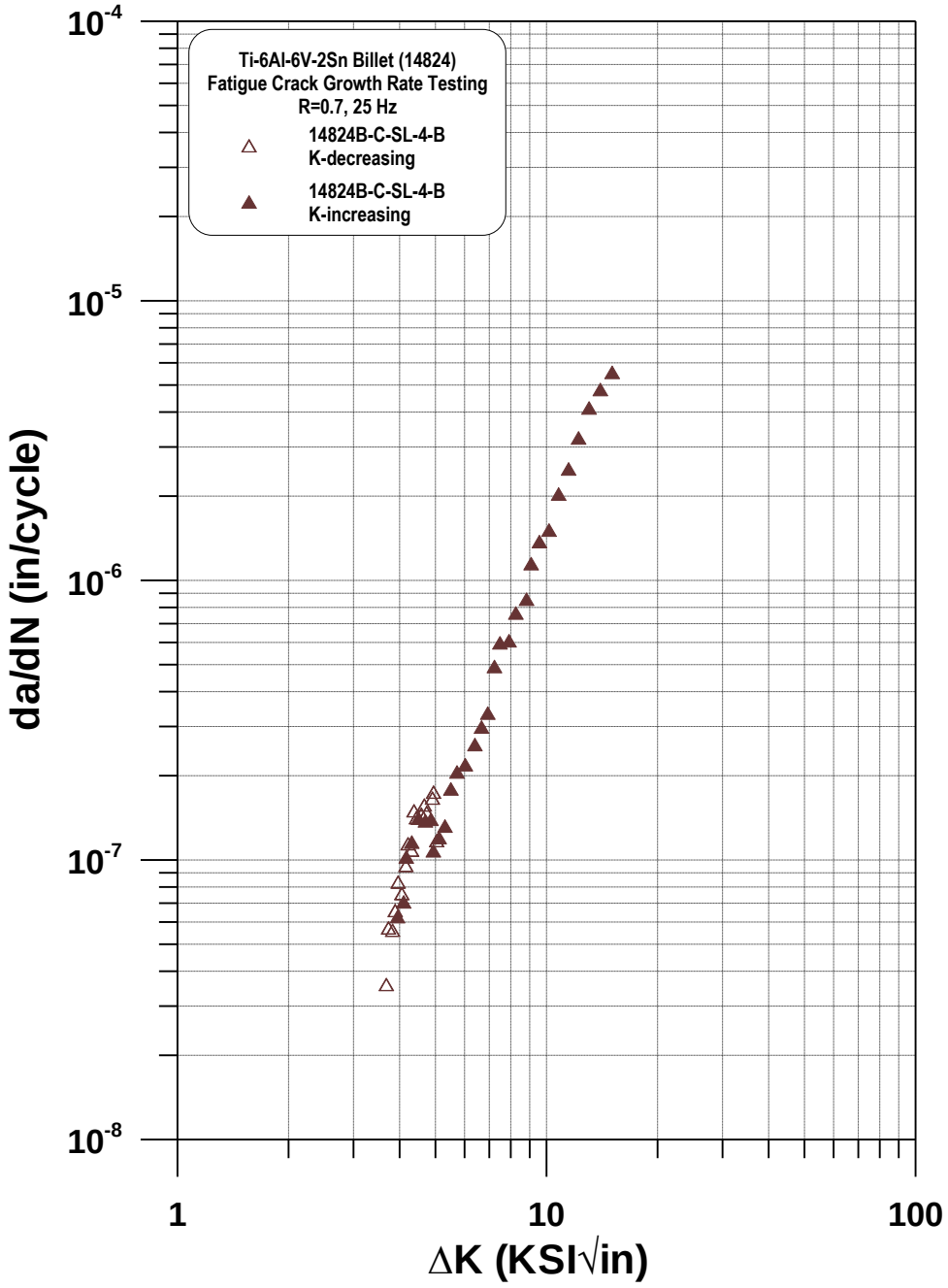
Approved for public release; distribution unlimited.



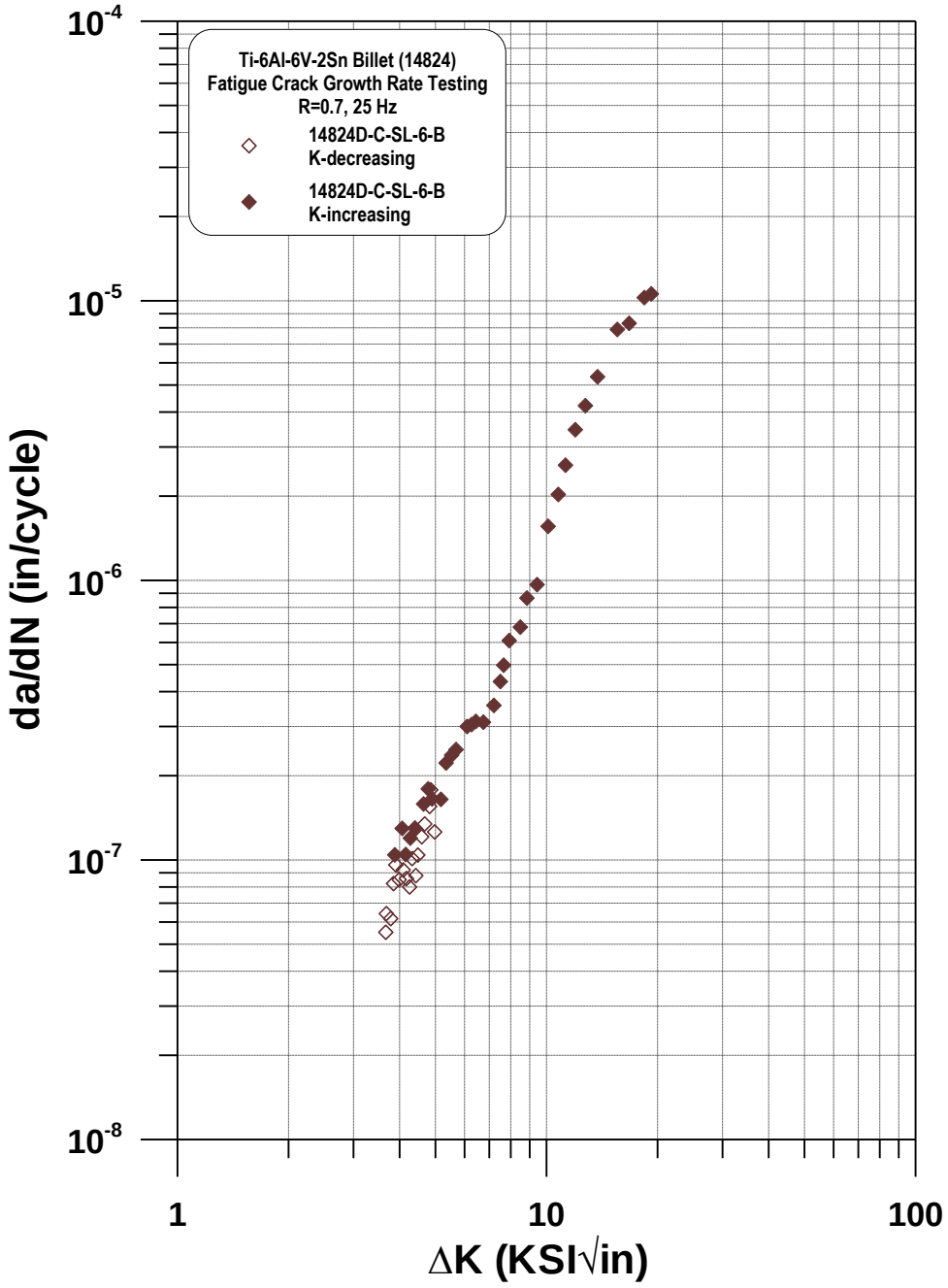
Approved for public release; distribution unlimited.



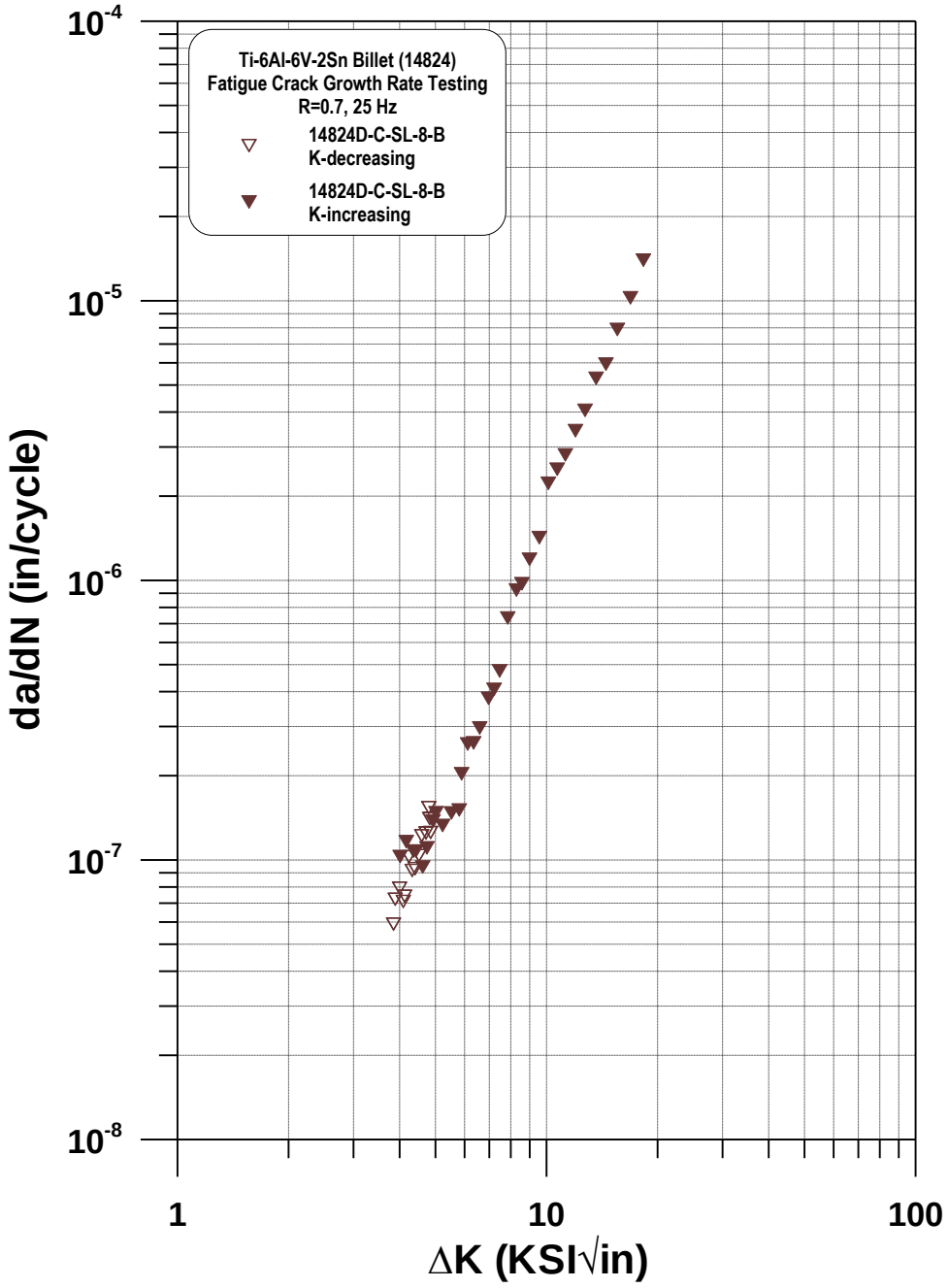
Approved for public release; distribution unlimited.



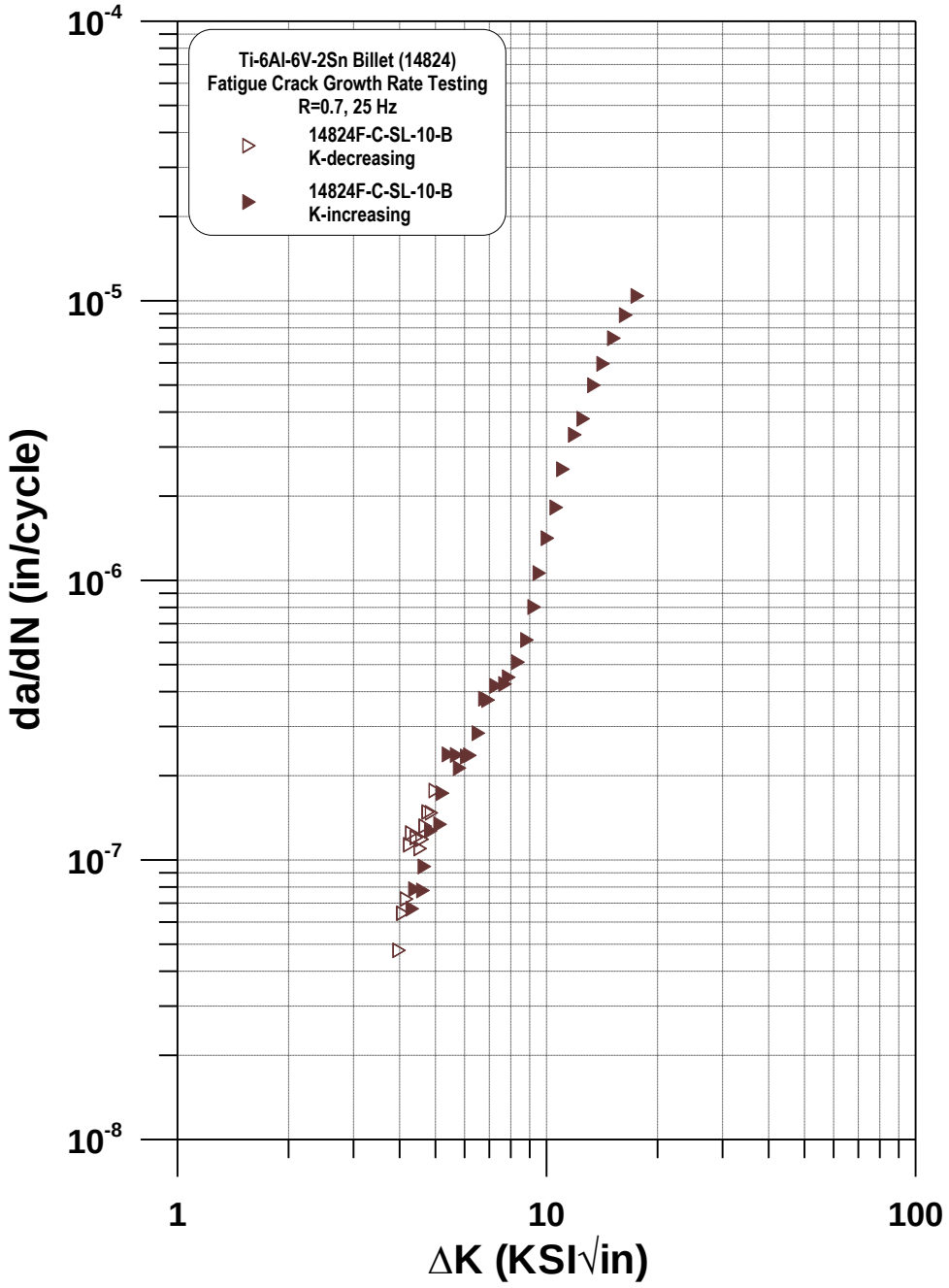
Approved for public release; distribution unlimited.



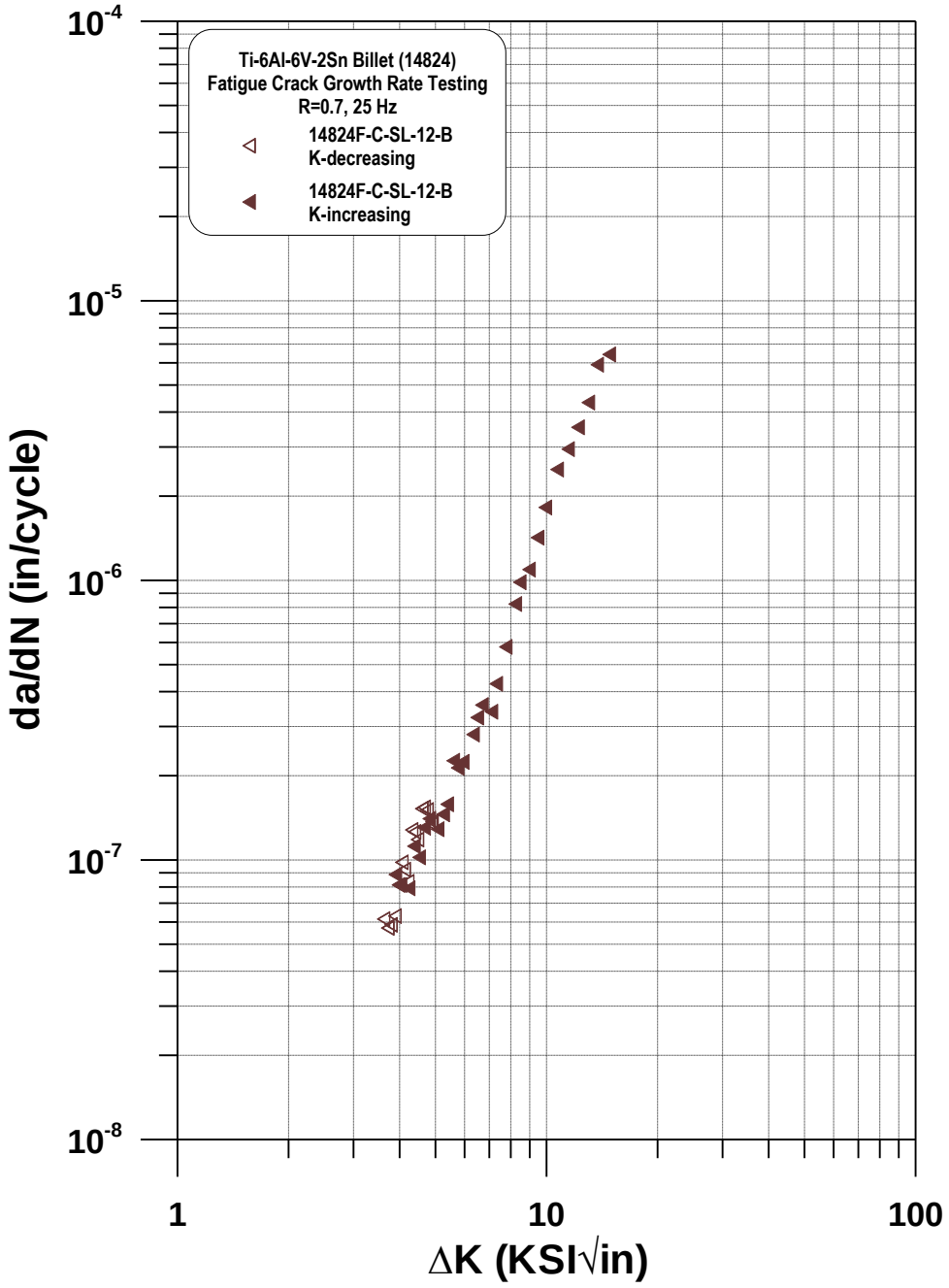
Approved for public release; distribution unlimited.



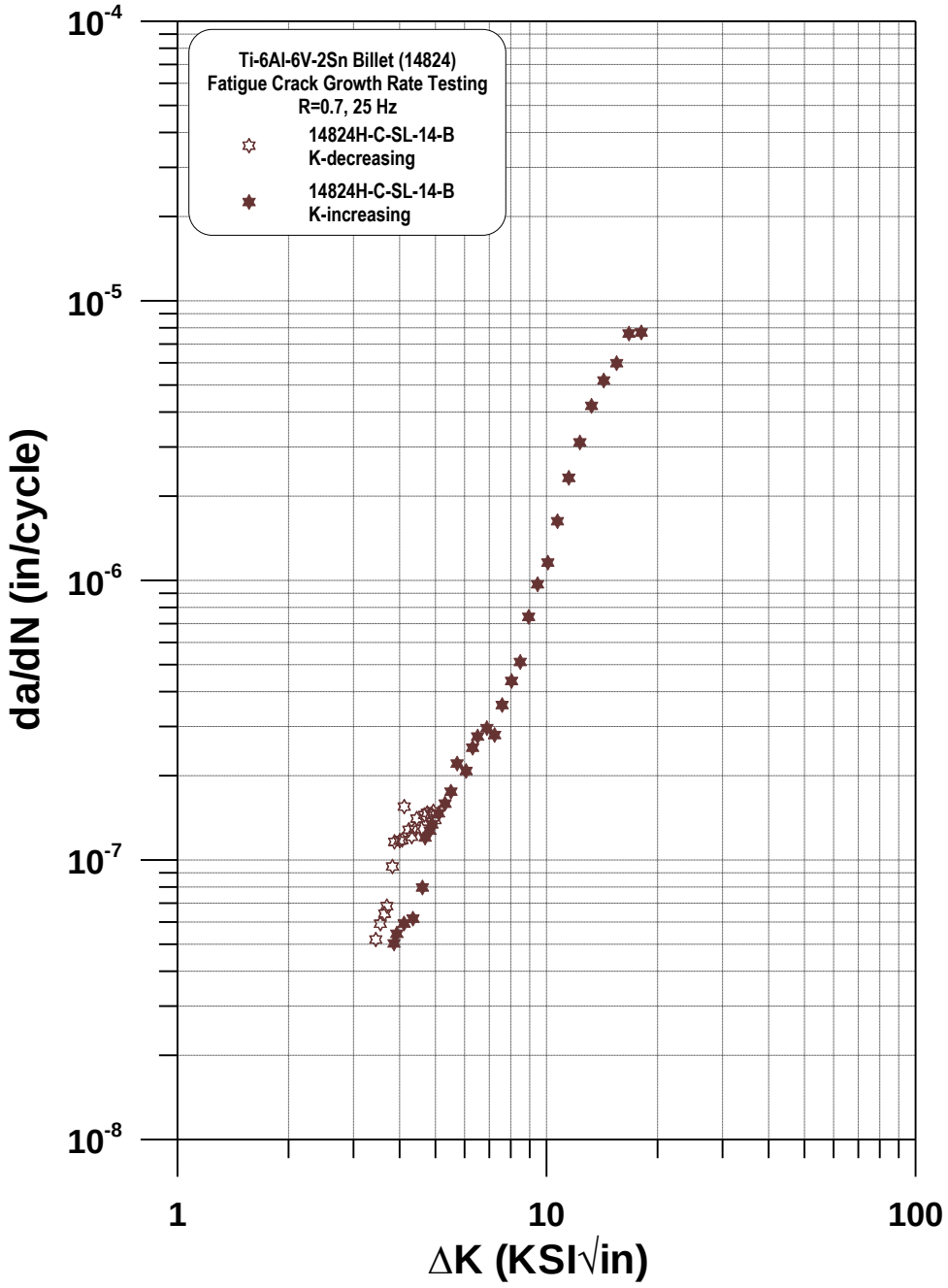
Approved for public release; distribution unlimited.



Approved for public release; distribution unlimited.



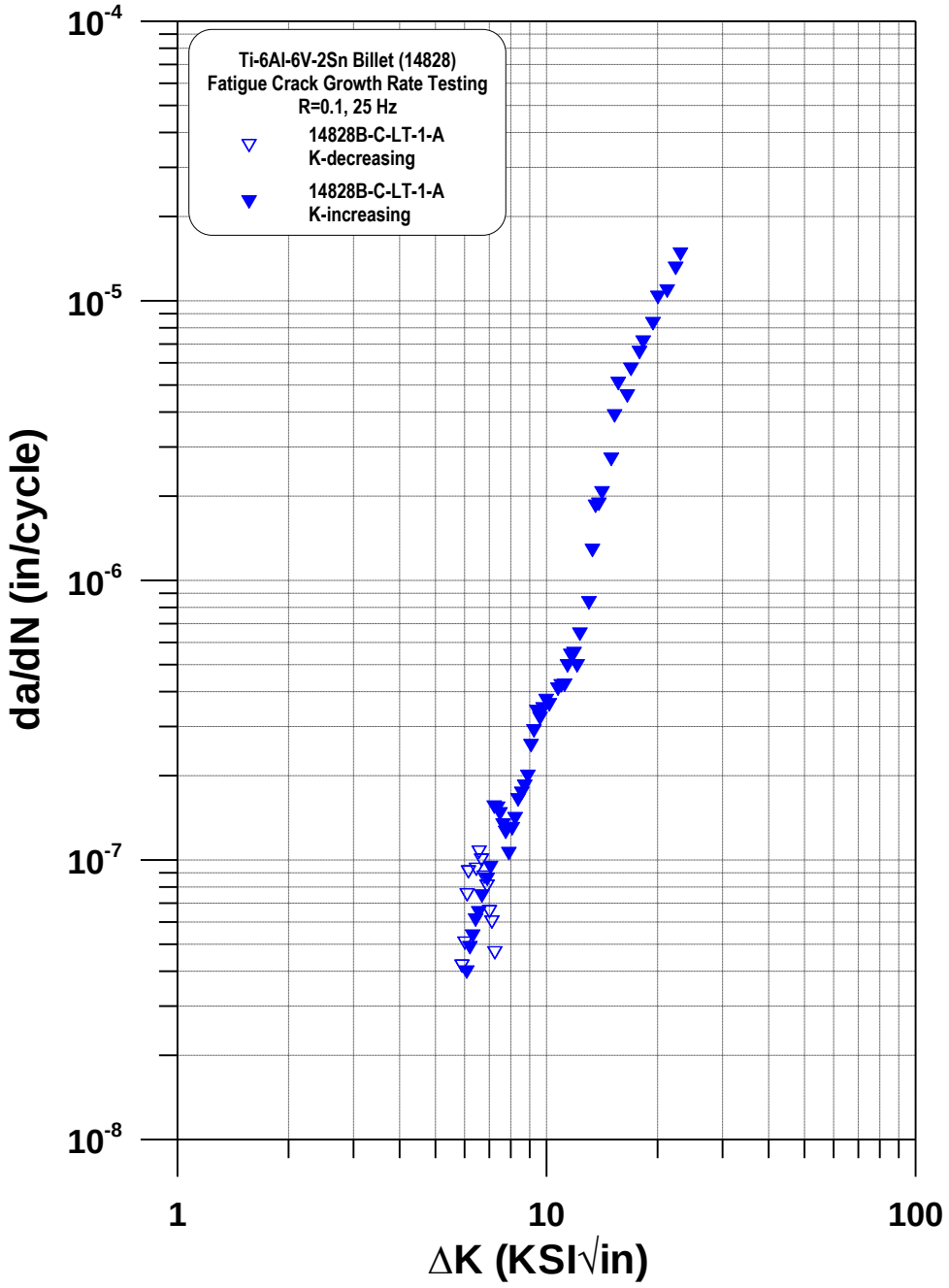
Approved for public release; distribution unlimited.



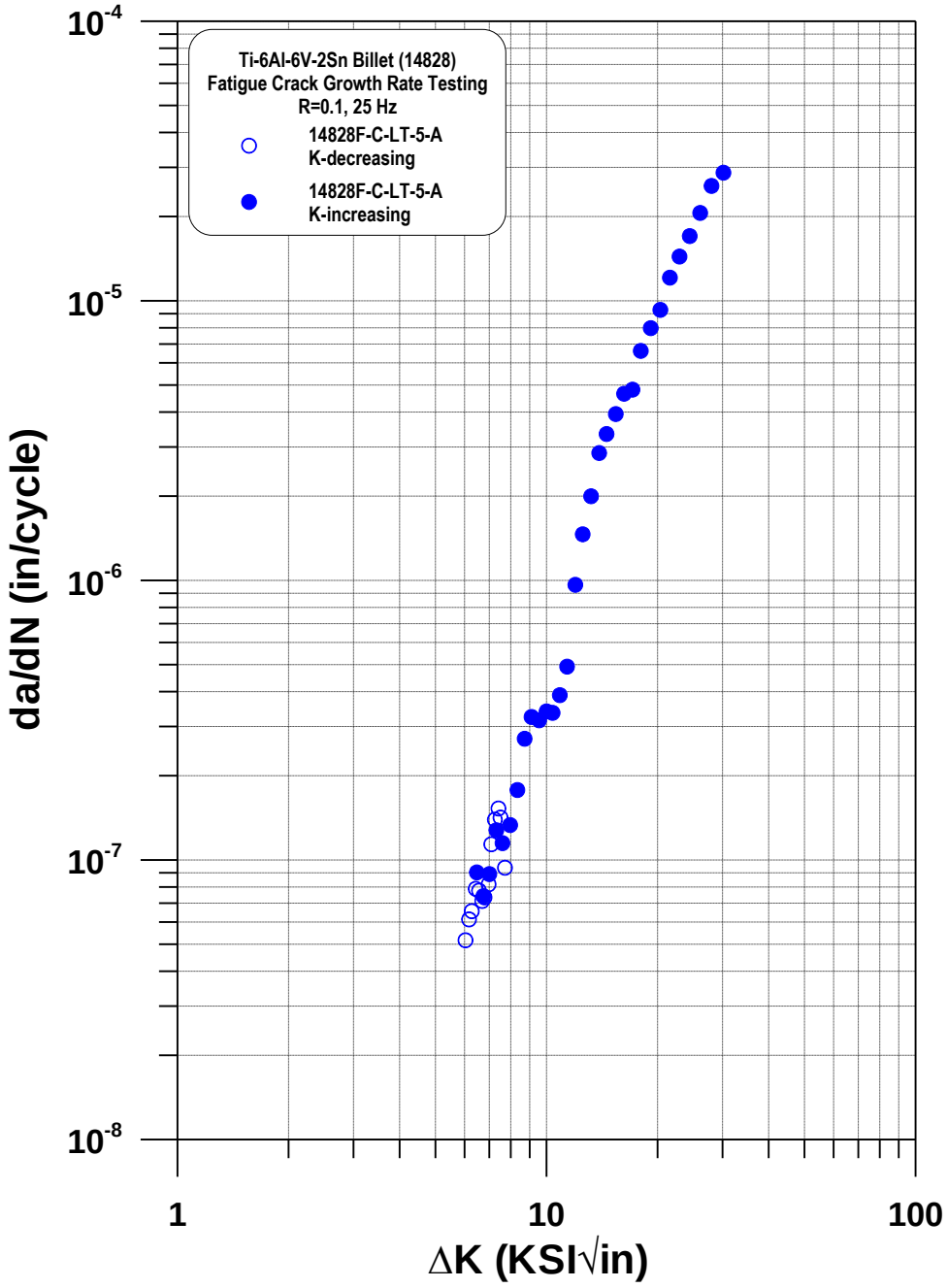
Approved for public release; distribution unlimited.

Appendix B
Individual fatigue crack growth rate curves for Ti-6Al-6V-2Sn billet (14828).

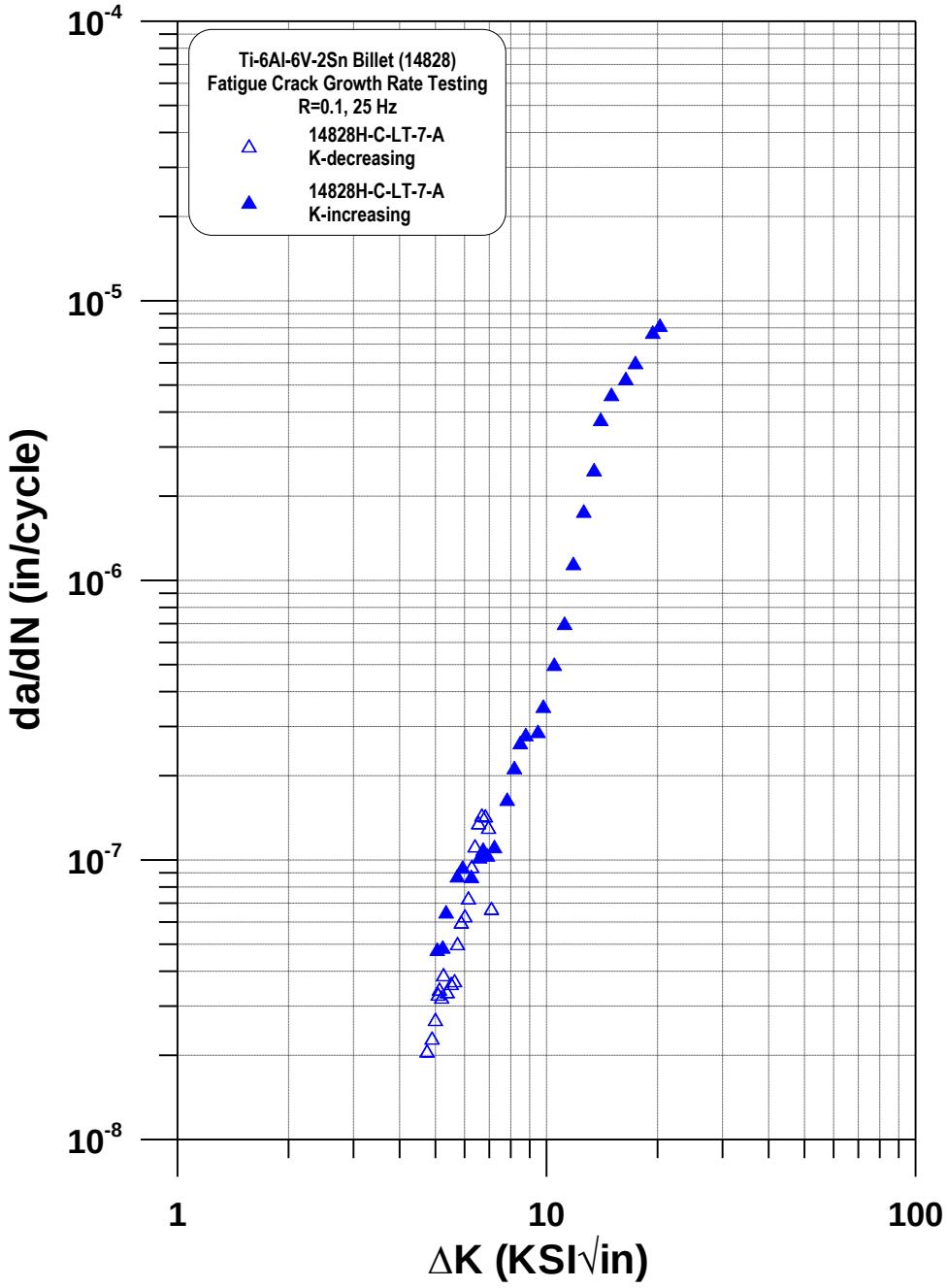
Approved for public release; distribution unlimited.



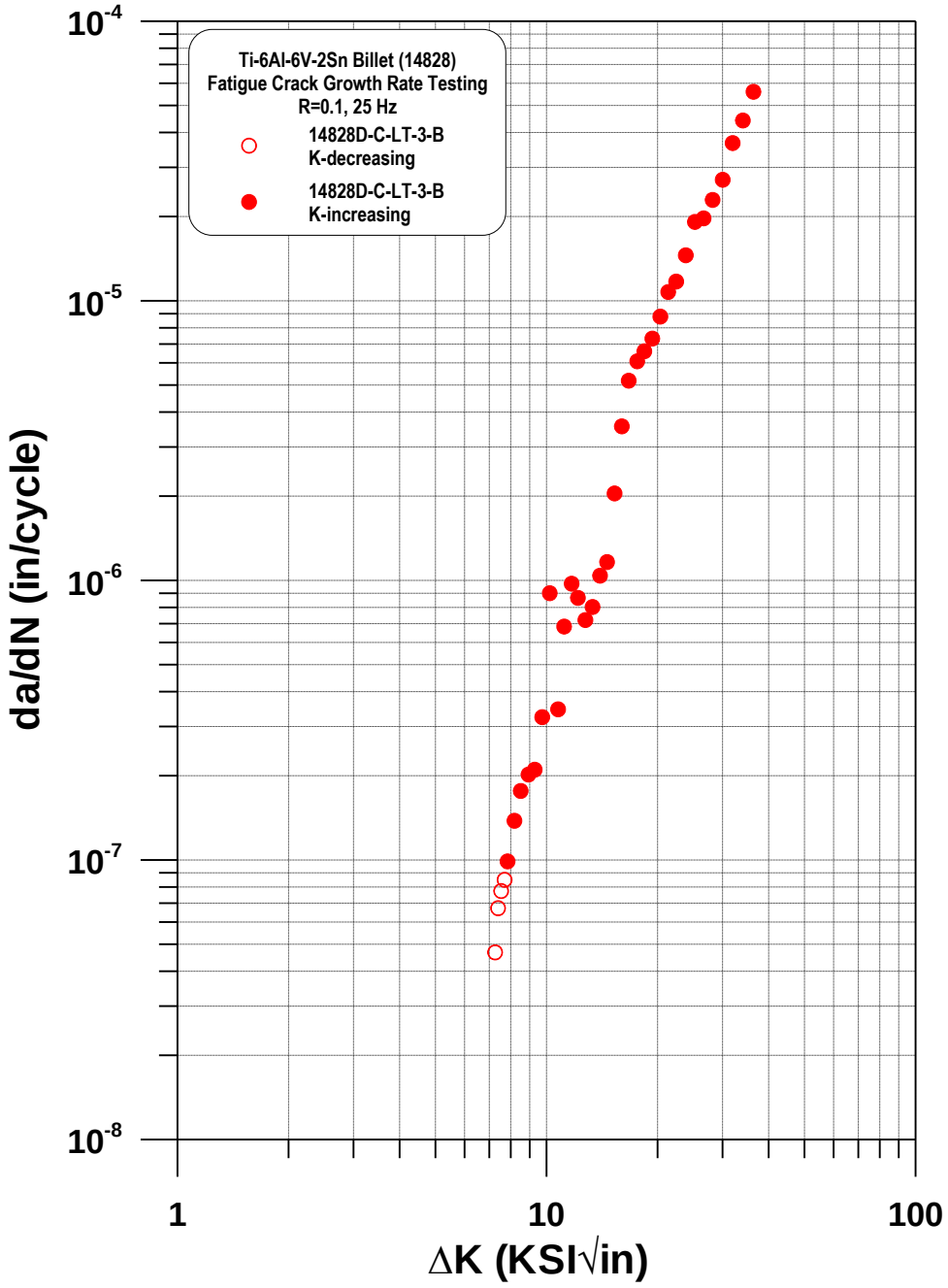
Approved for public release; distribution unlimited.



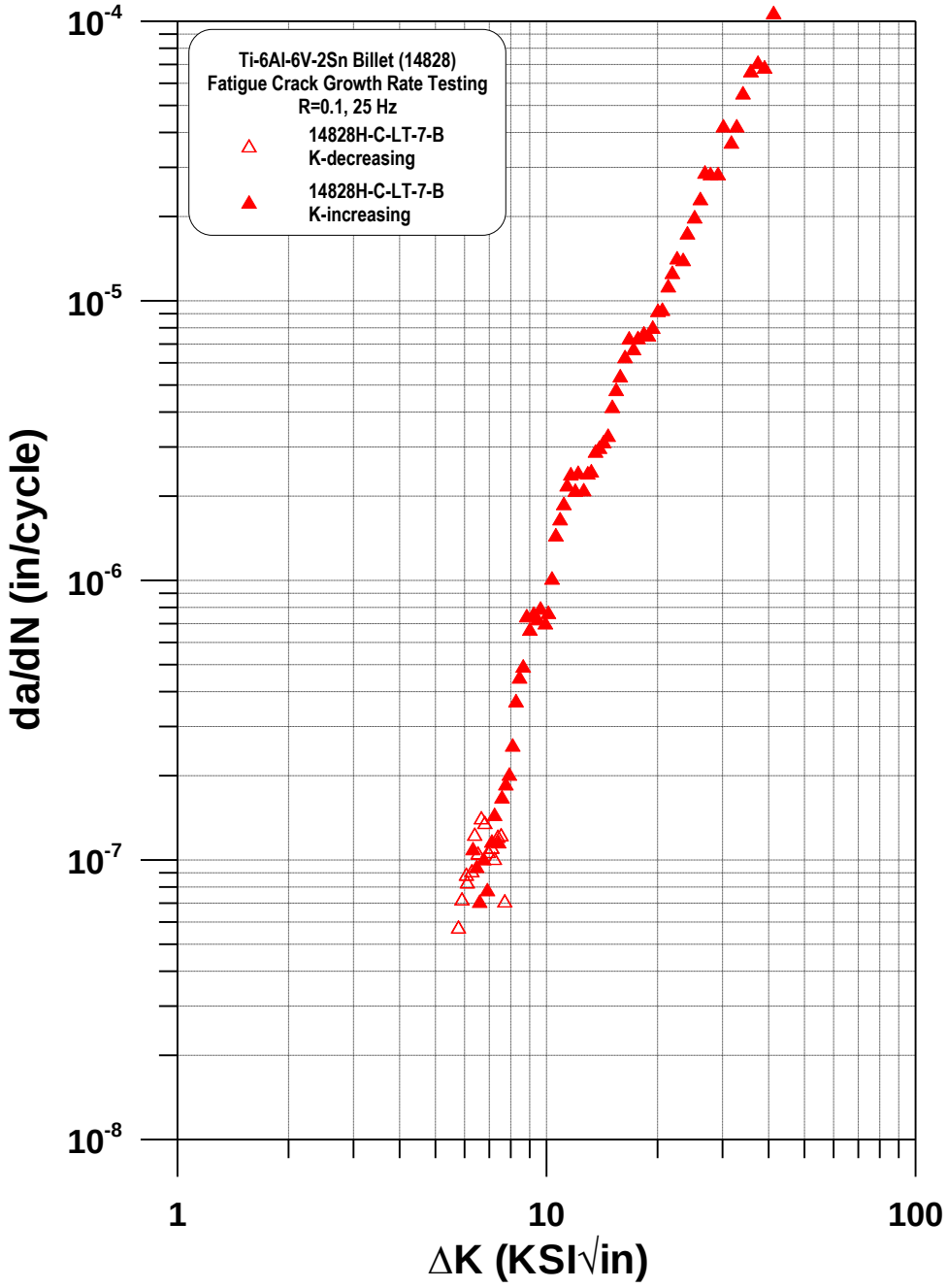
Approved for public release; distribution unlimited.



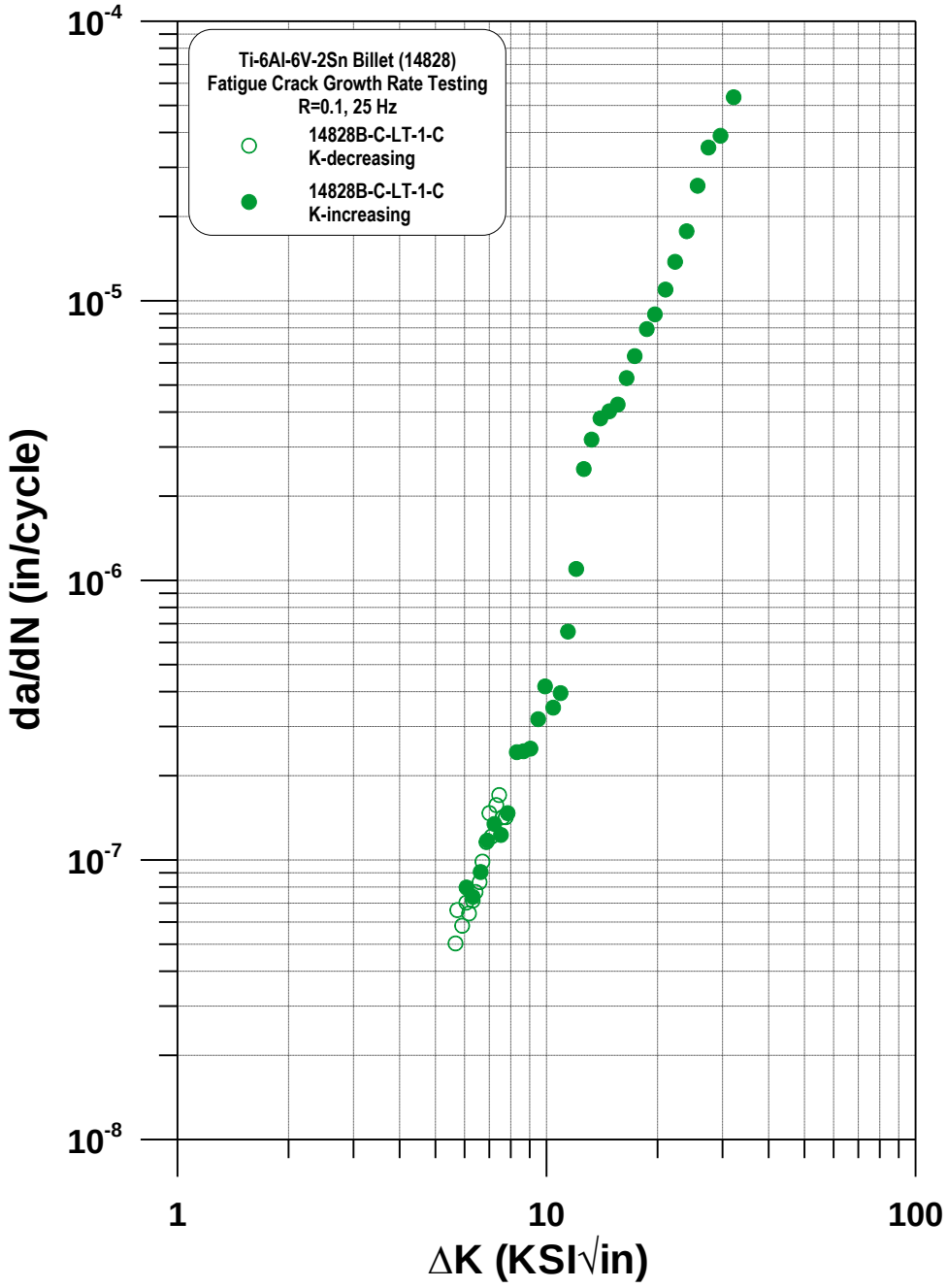
Approved for public release; distribution unlimited.



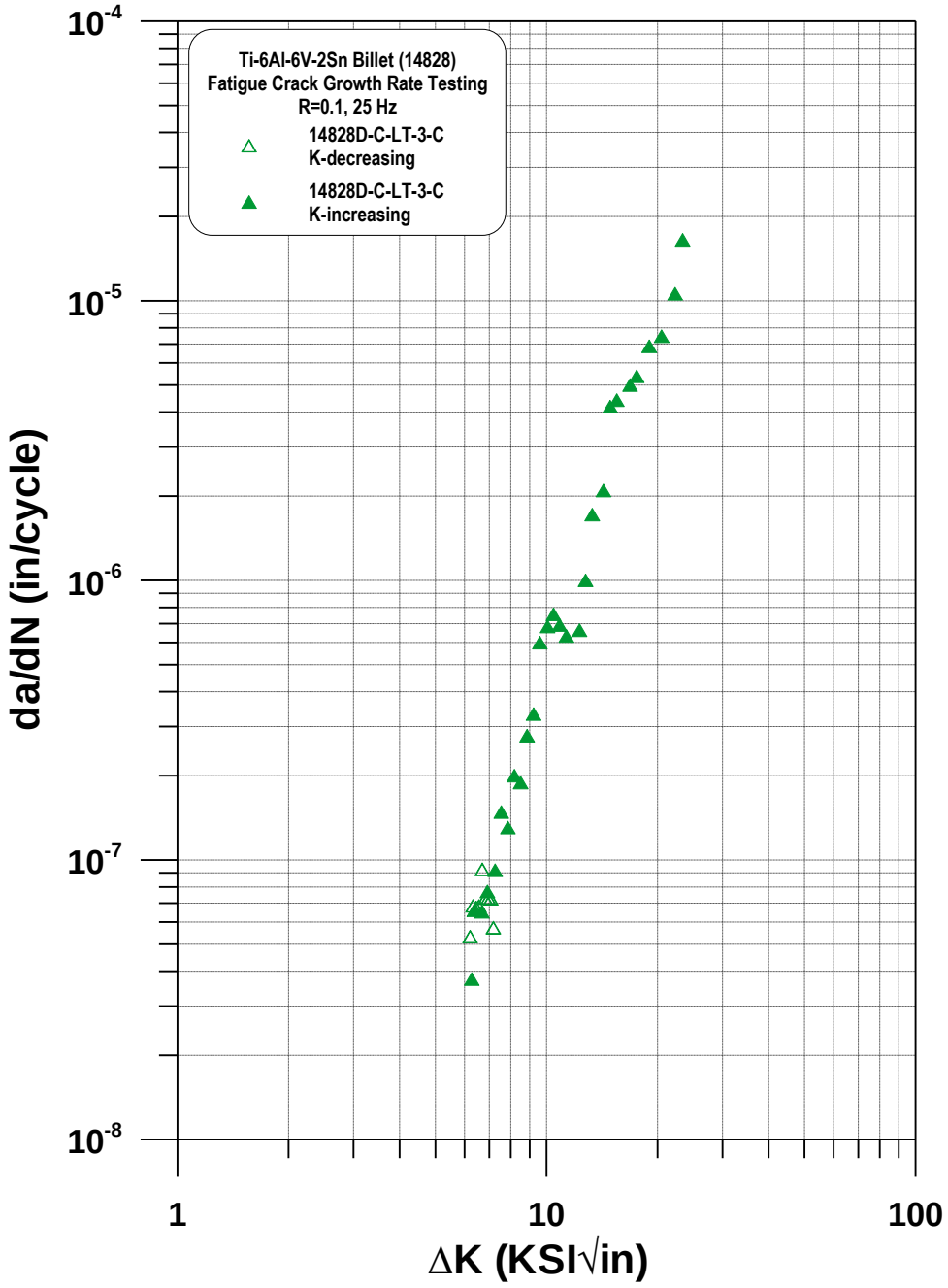
Approved for public release; distribution unlimited.



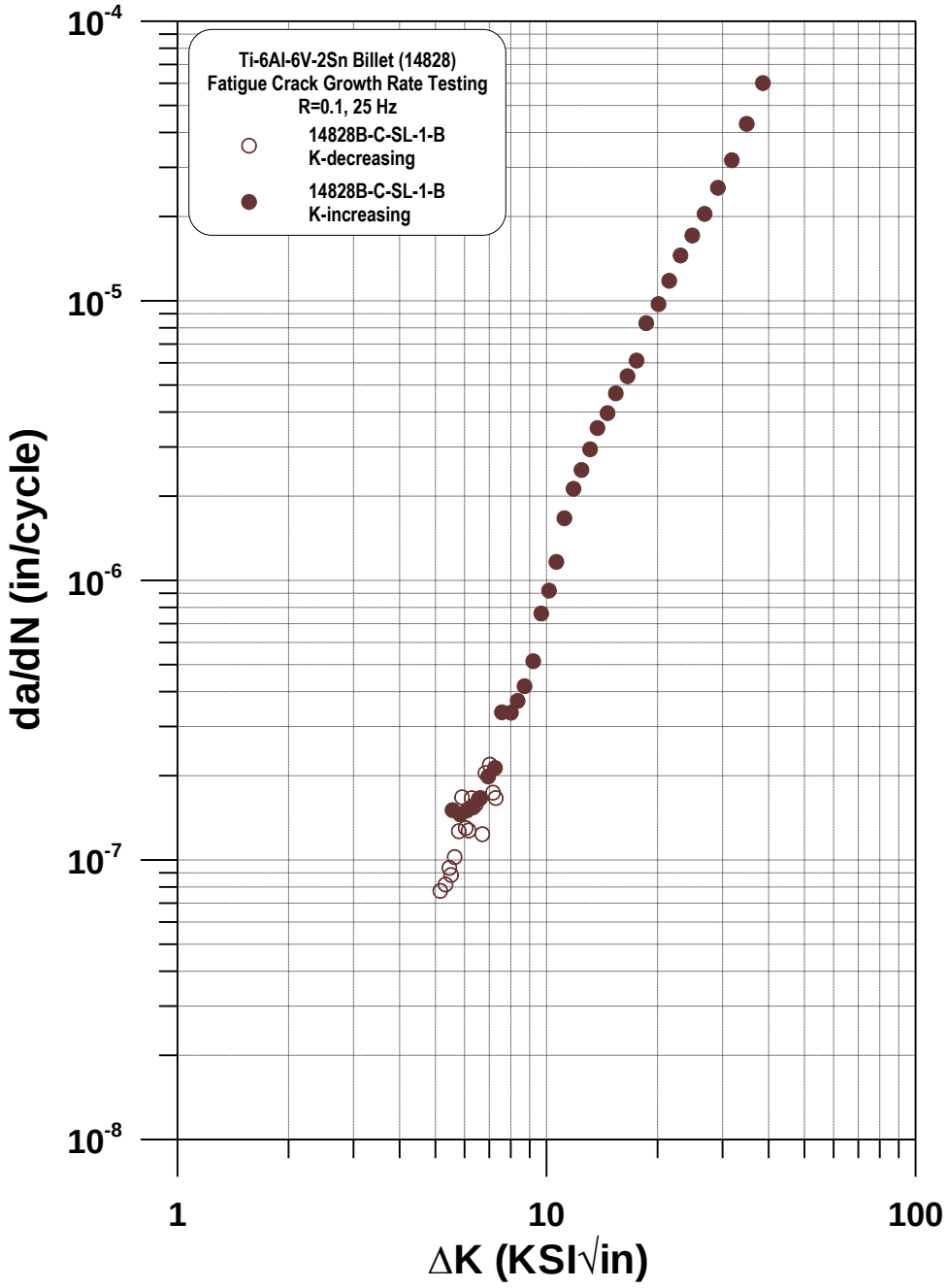
Approved for public release; distribution unlimited.



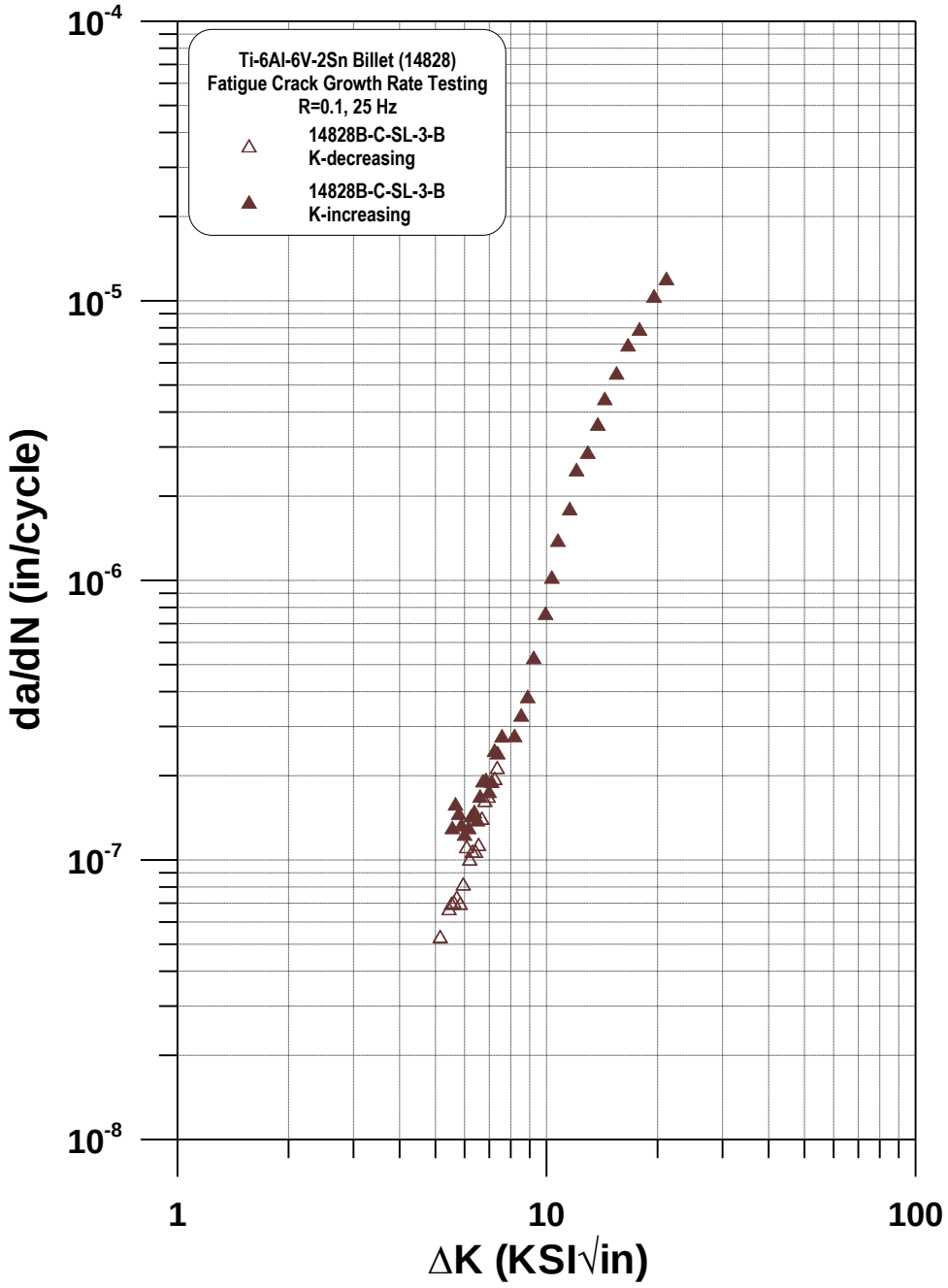
Approved for public release; distribution unlimited.



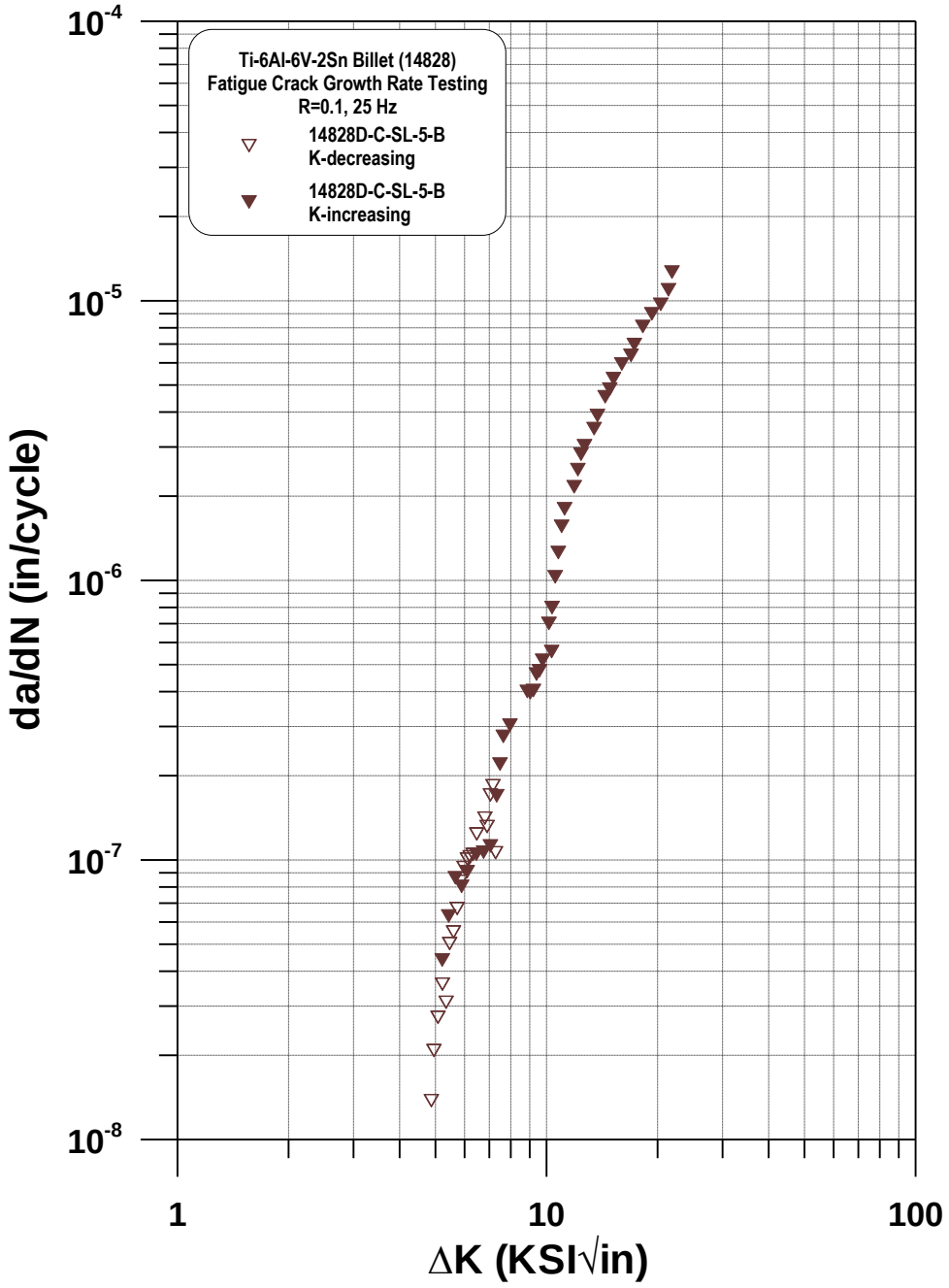
Approved for public release; distribution unlimited.



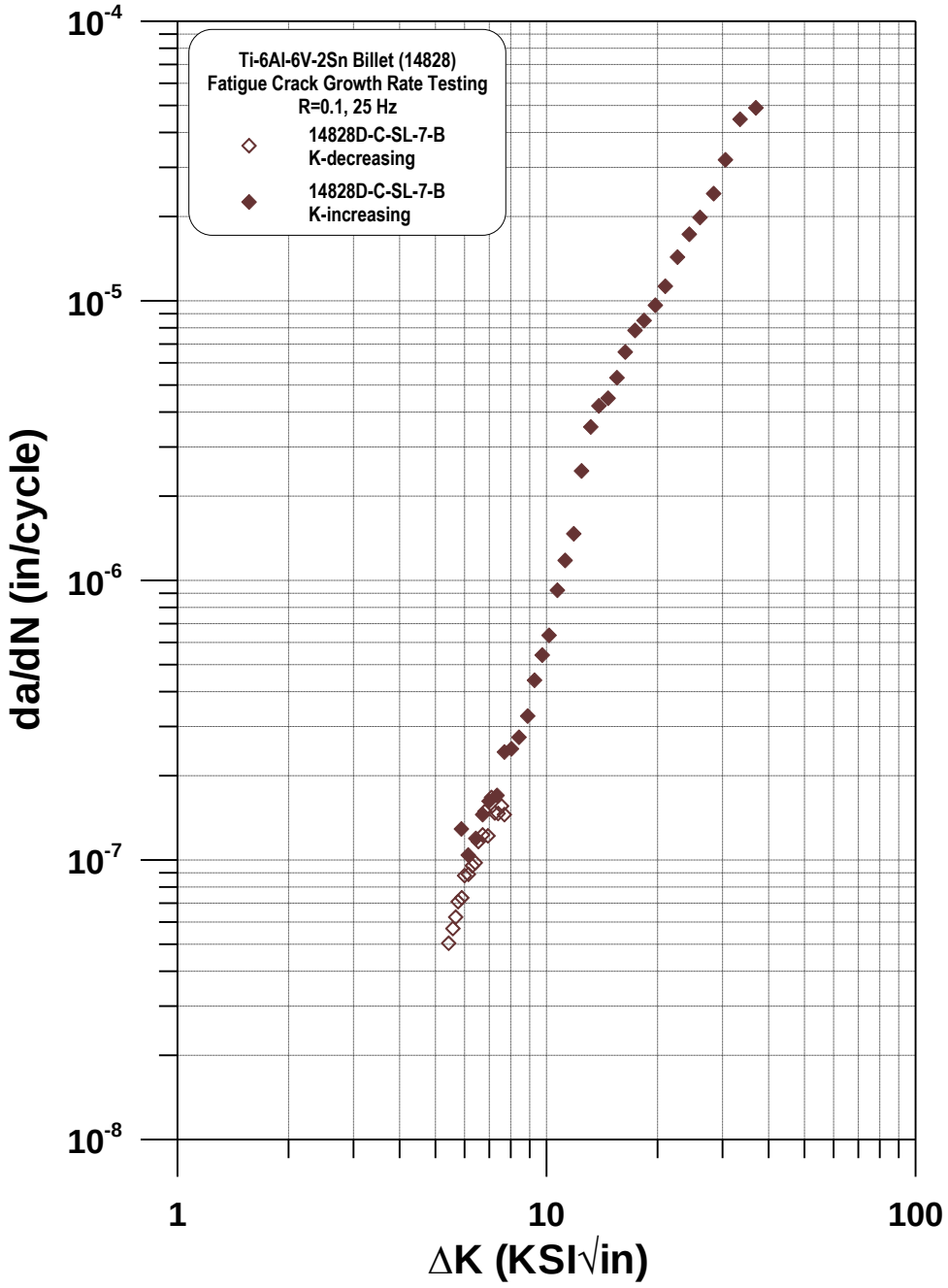
Approved for public release; distribution unlimited.



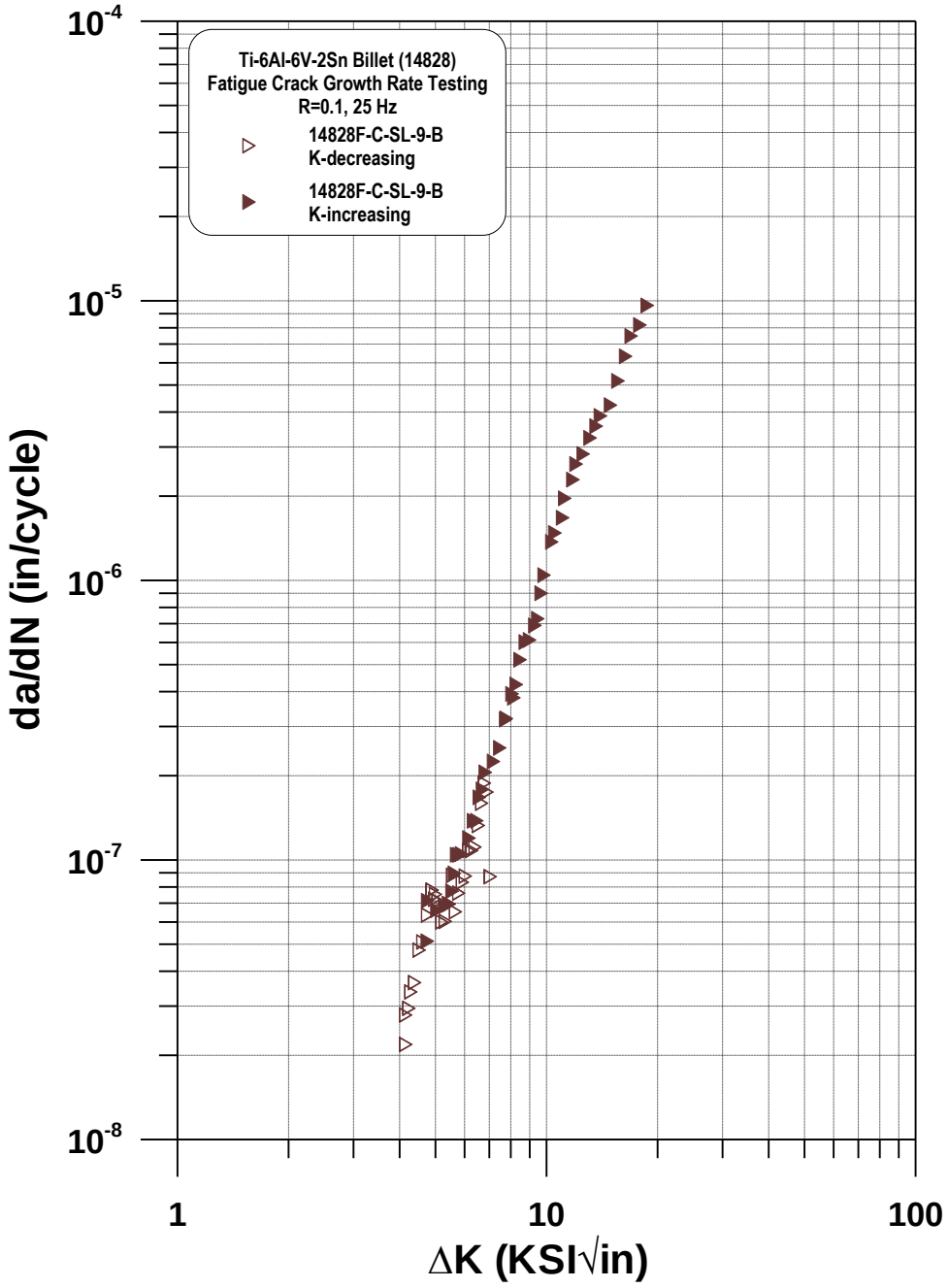
Approved for public release; distribution unlimited.



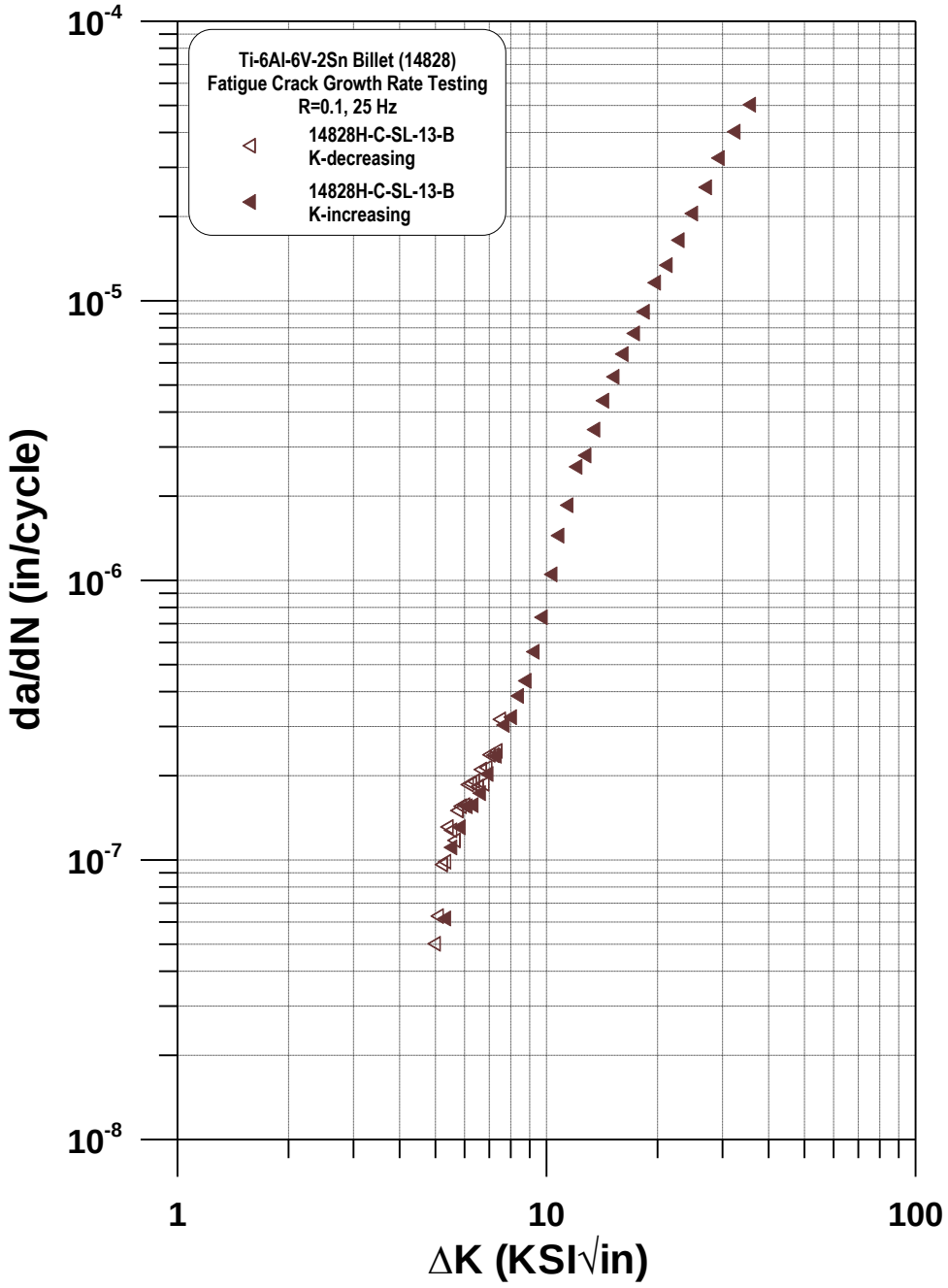
Approved for public release; distribution unlimited.



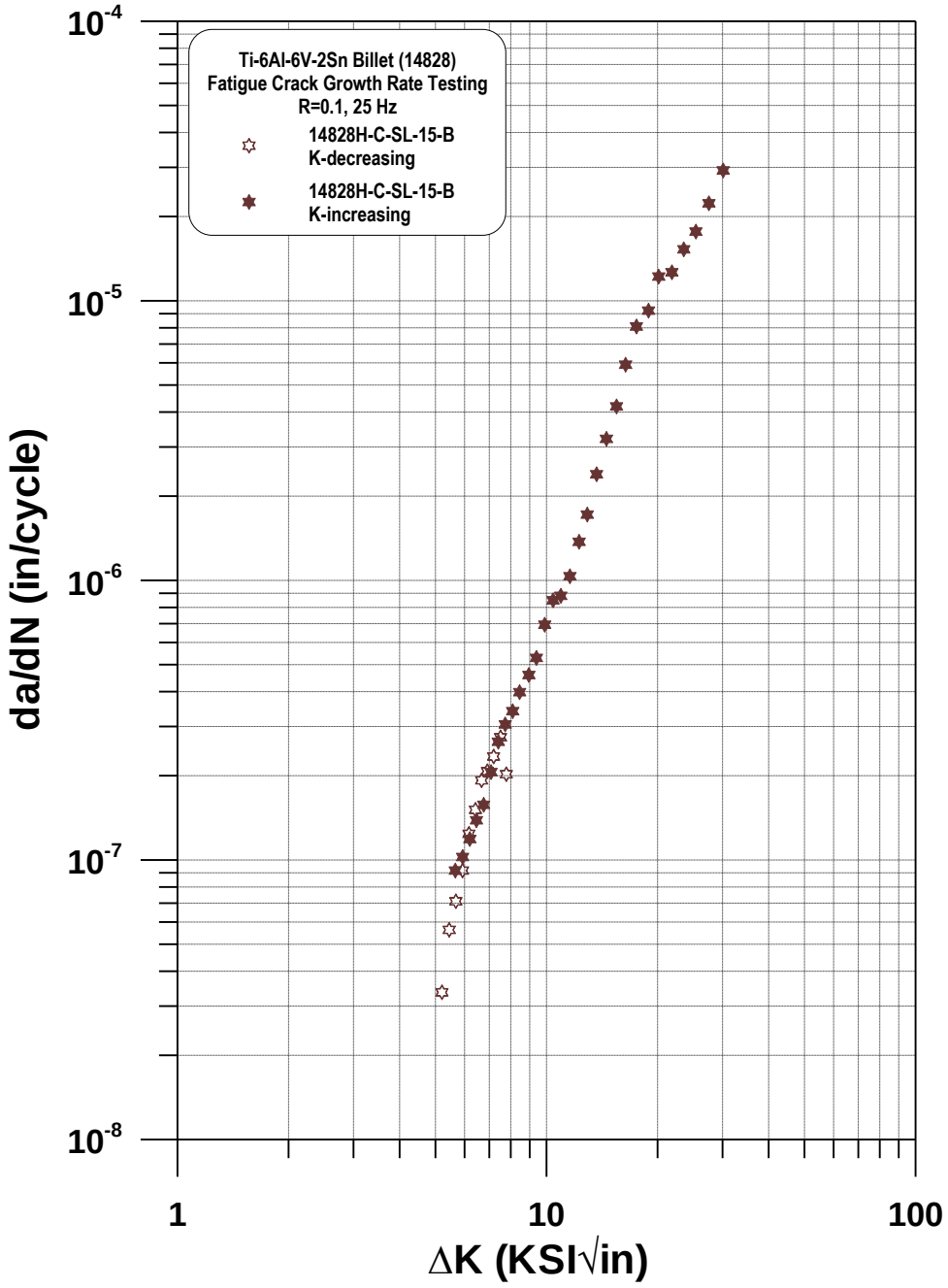
Approved for public release; distribution unlimited.



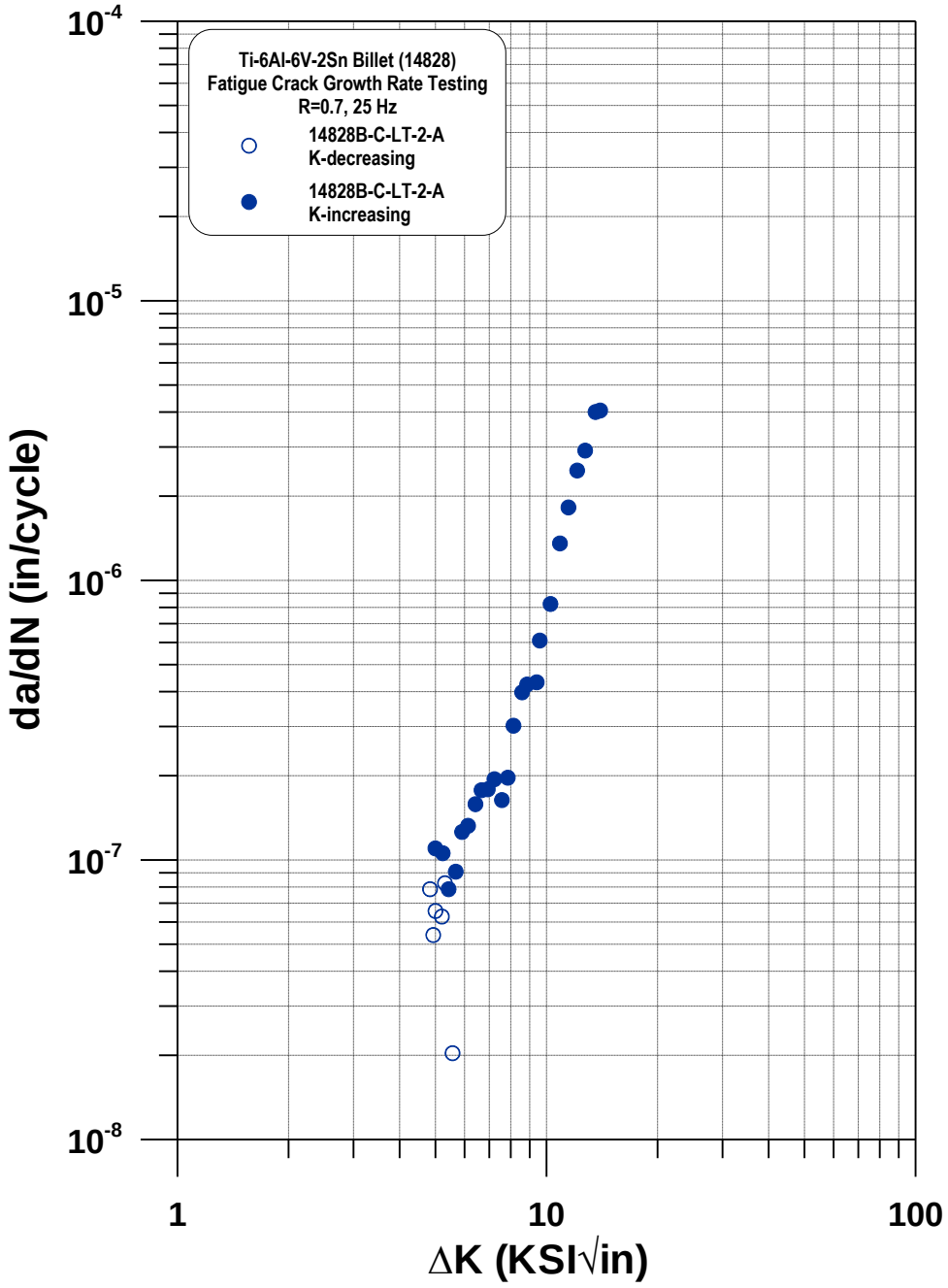
Approved for public release; distribution unlimited.



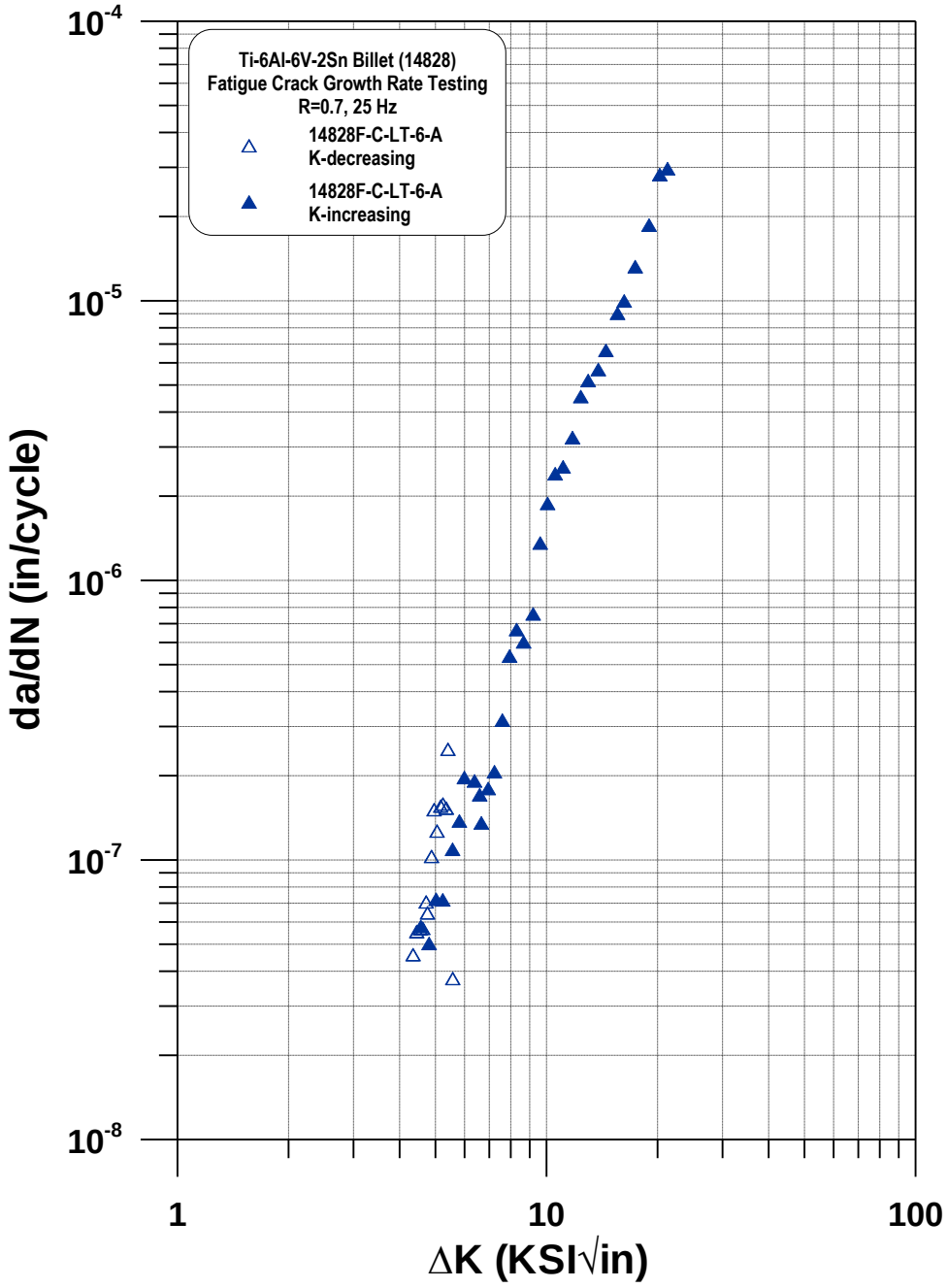
Approved for public release; distribution unlimited.



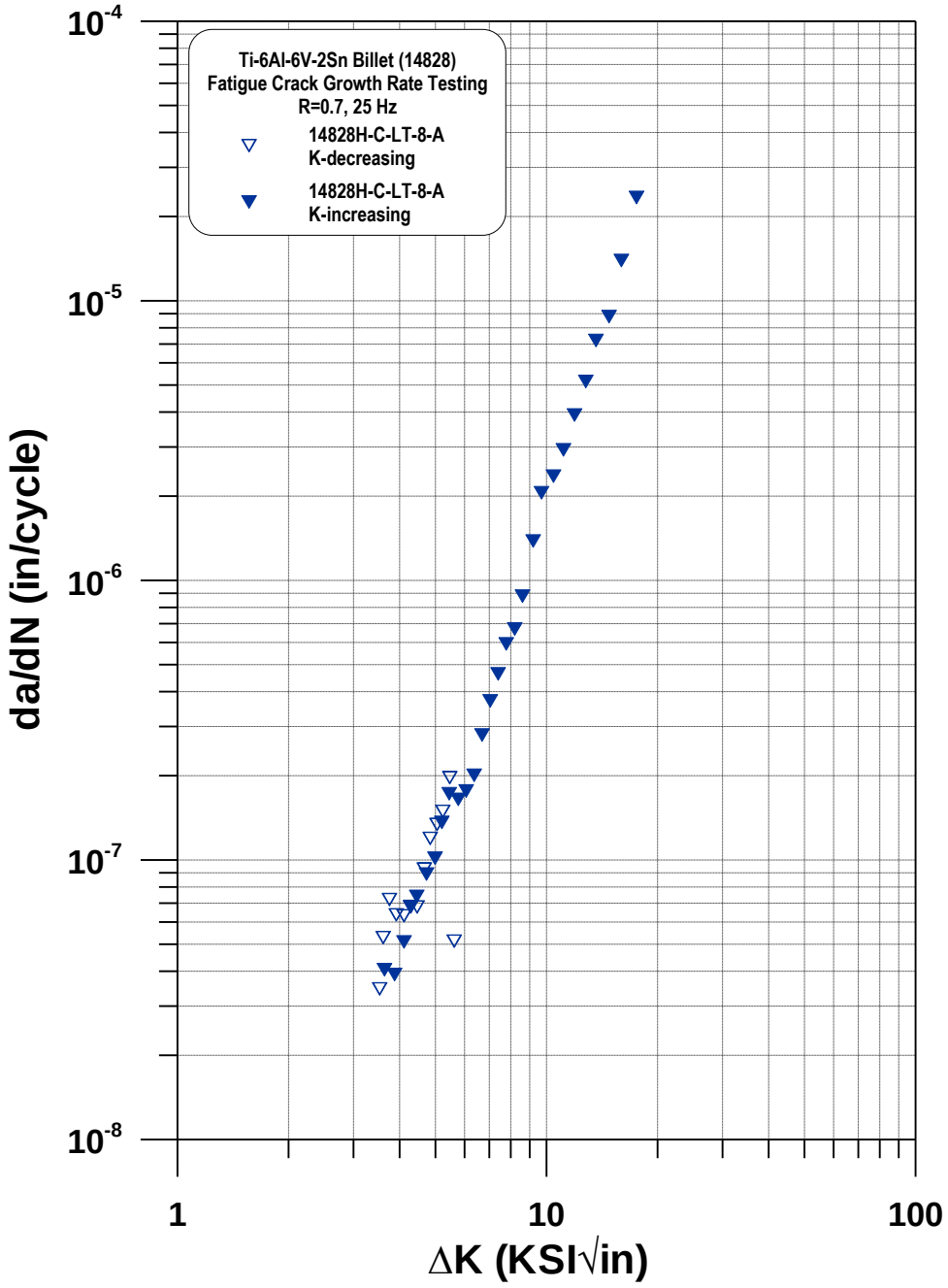
Approved for public release; distribution unlimited.



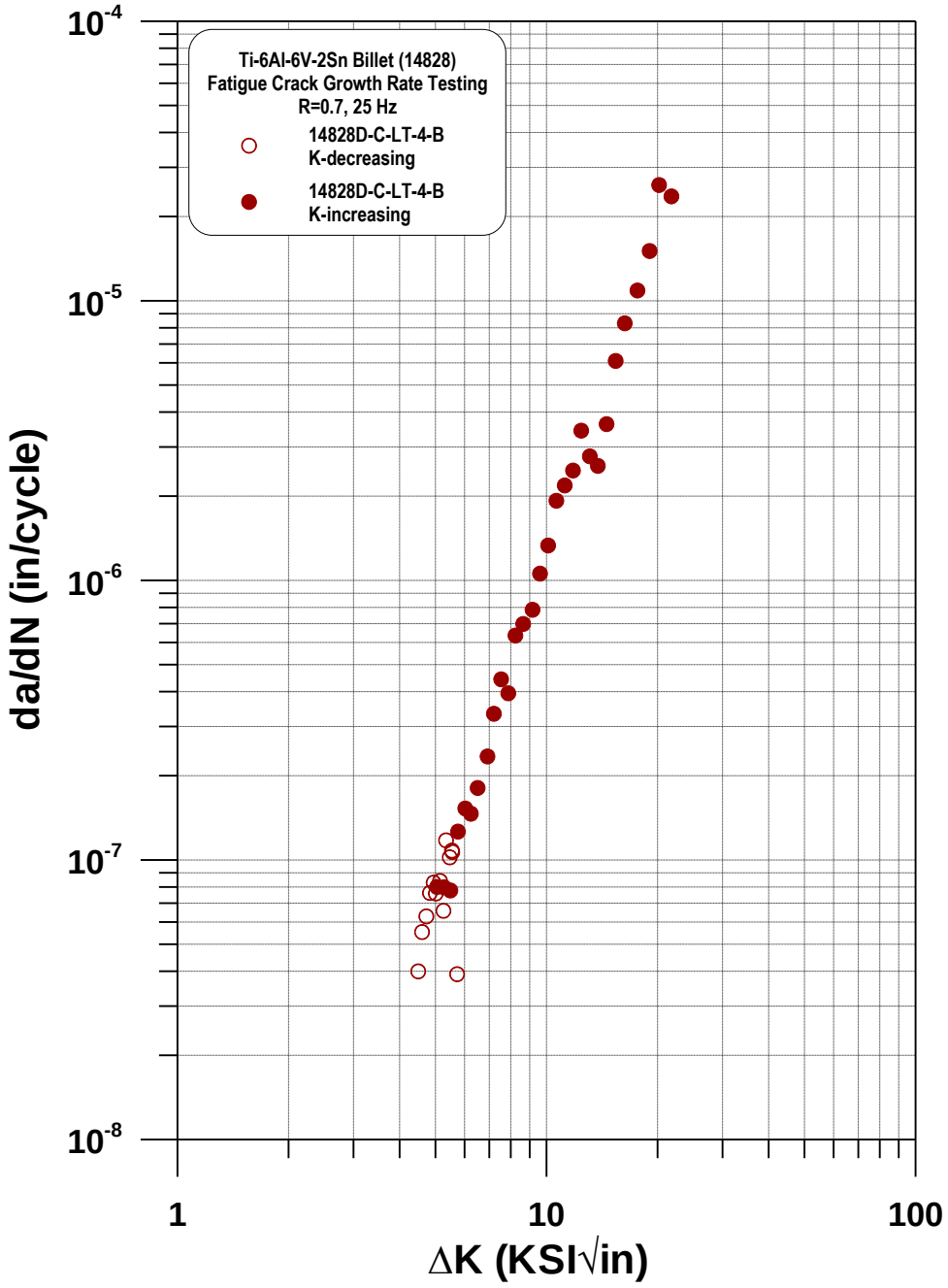
Approved for public release; distribution unlimited.



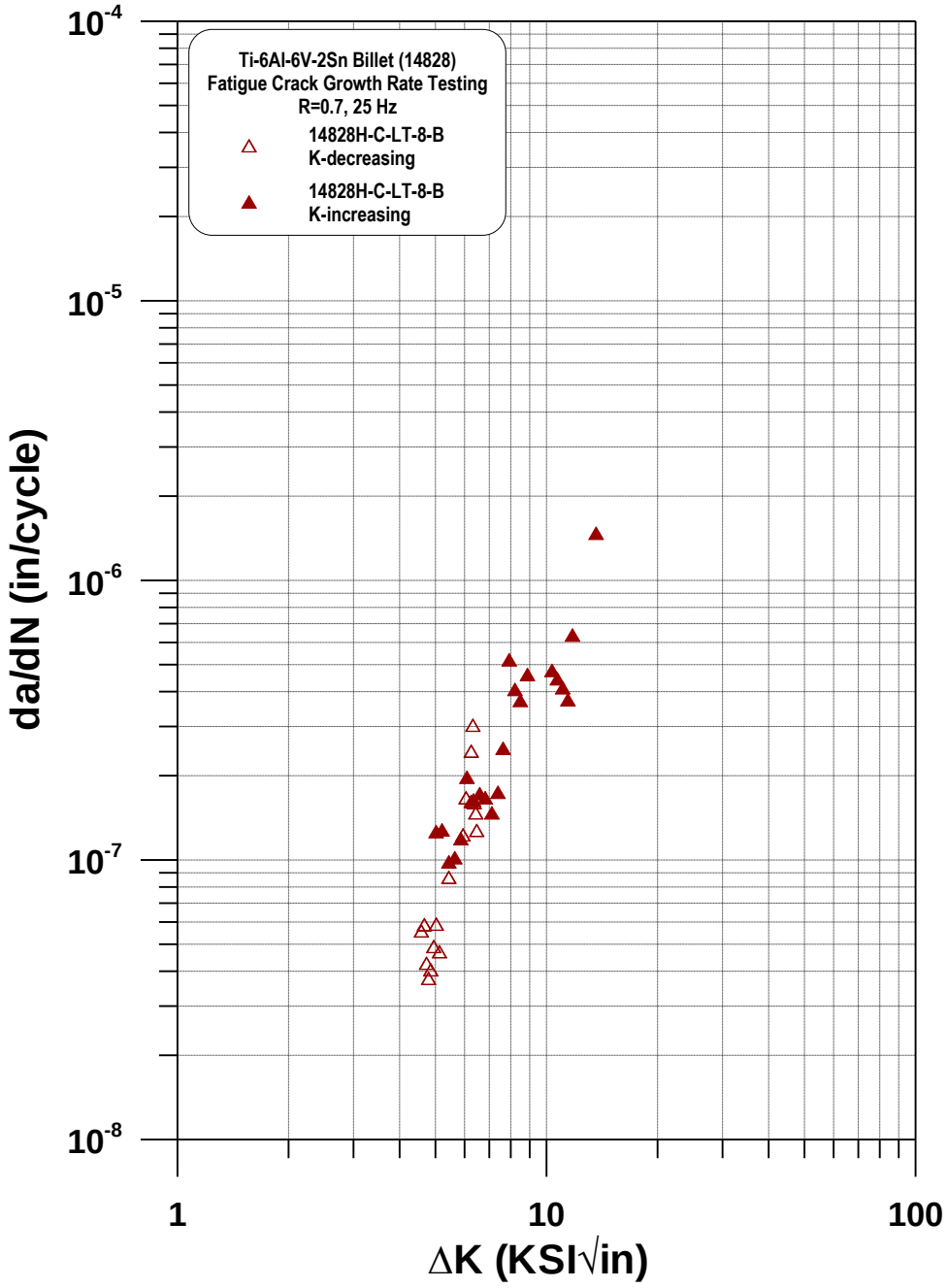
Approved for public release; distribution unlimited.



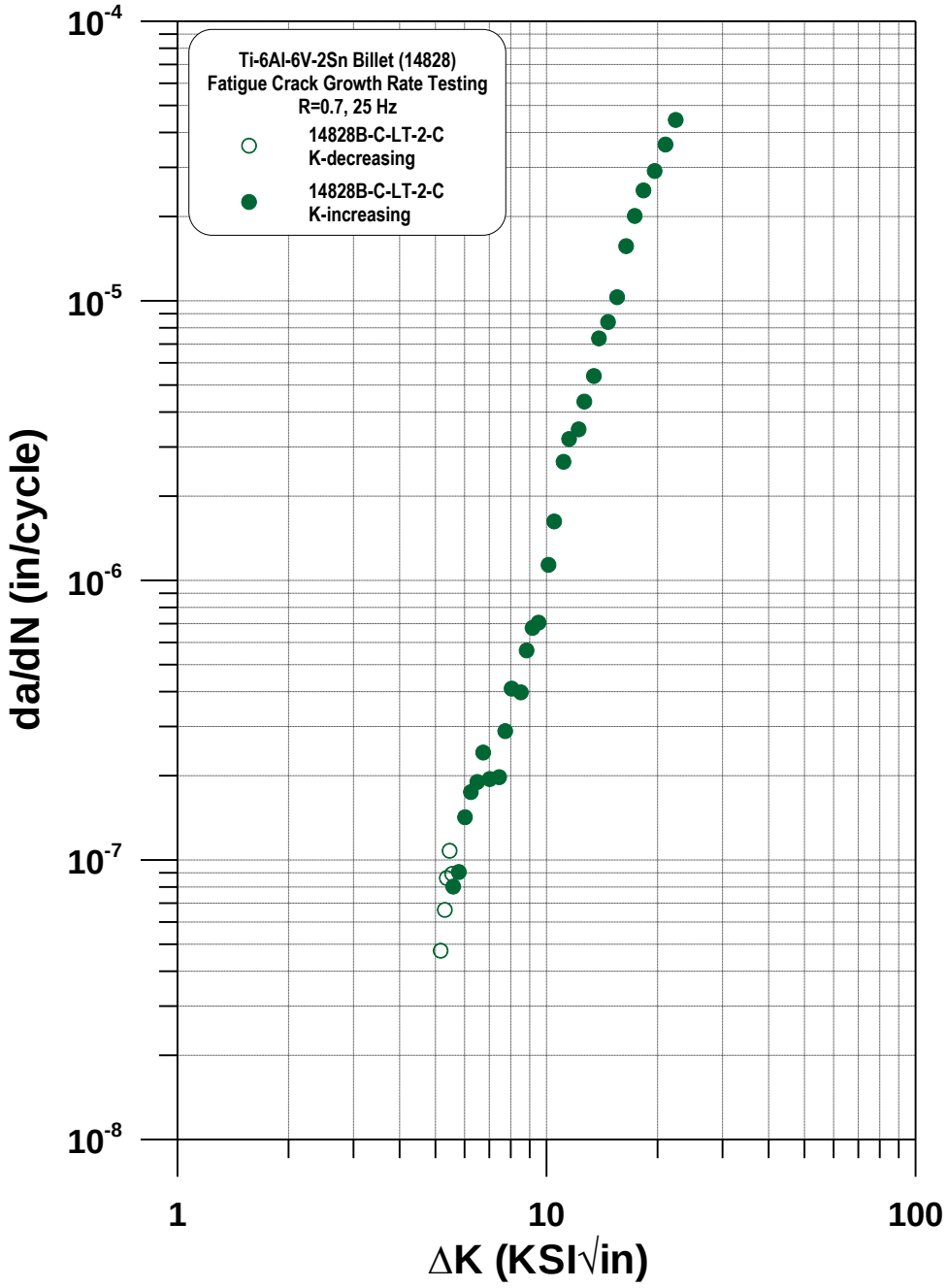
Approved for public release; distribution unlimited.



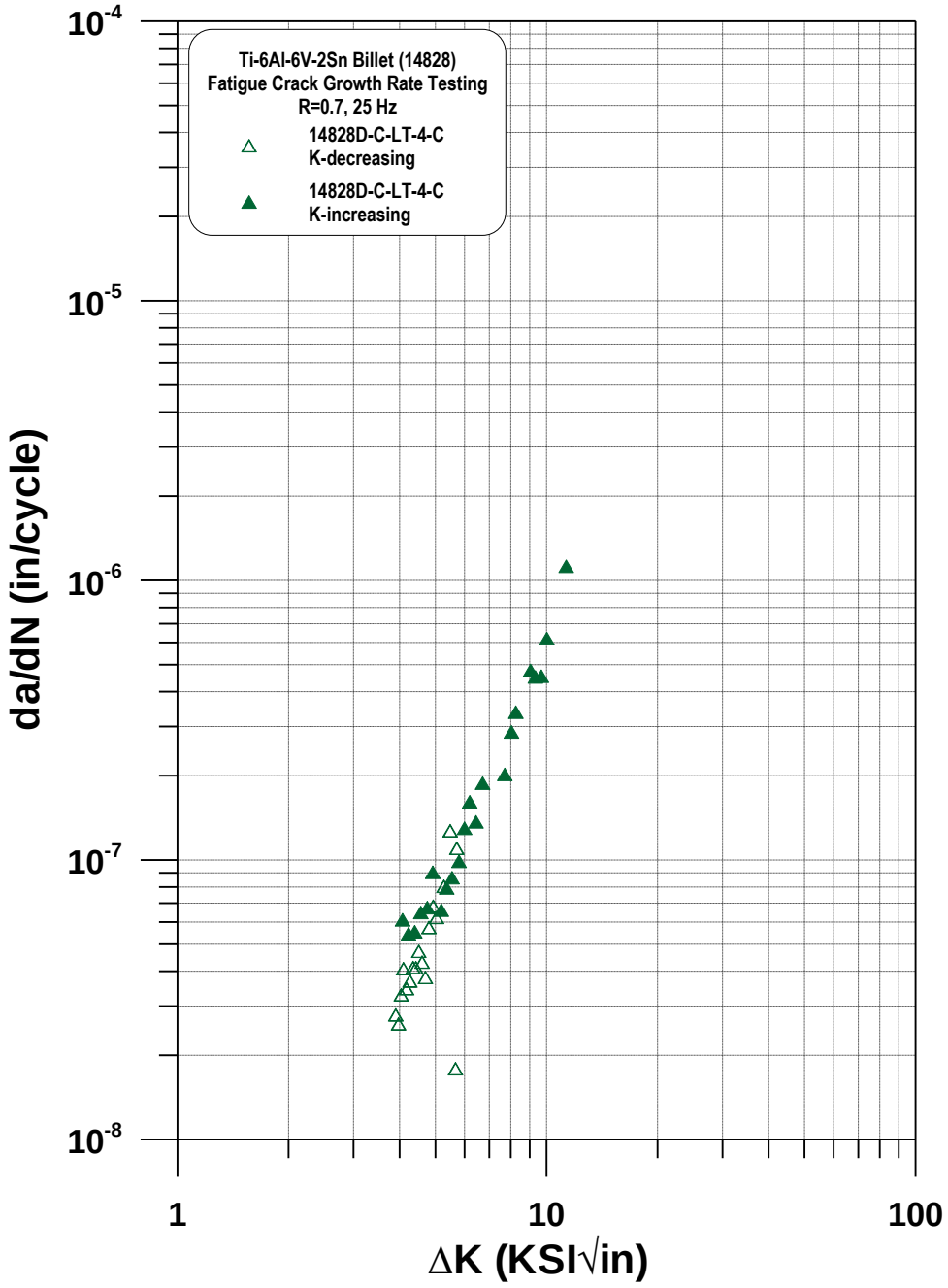
Approved for public release; distribution unlimited.



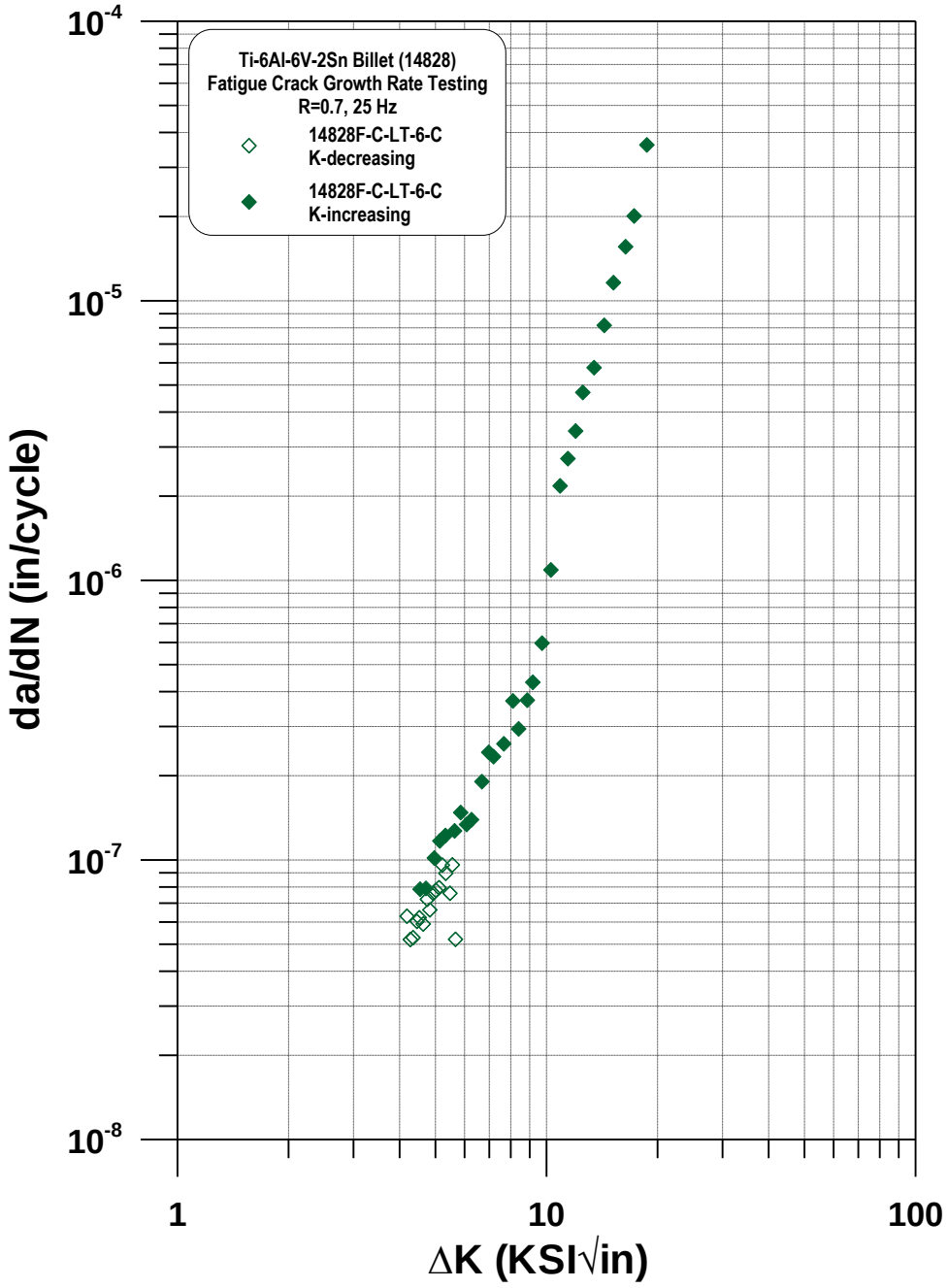
Approved for public release; distribution unlimited.



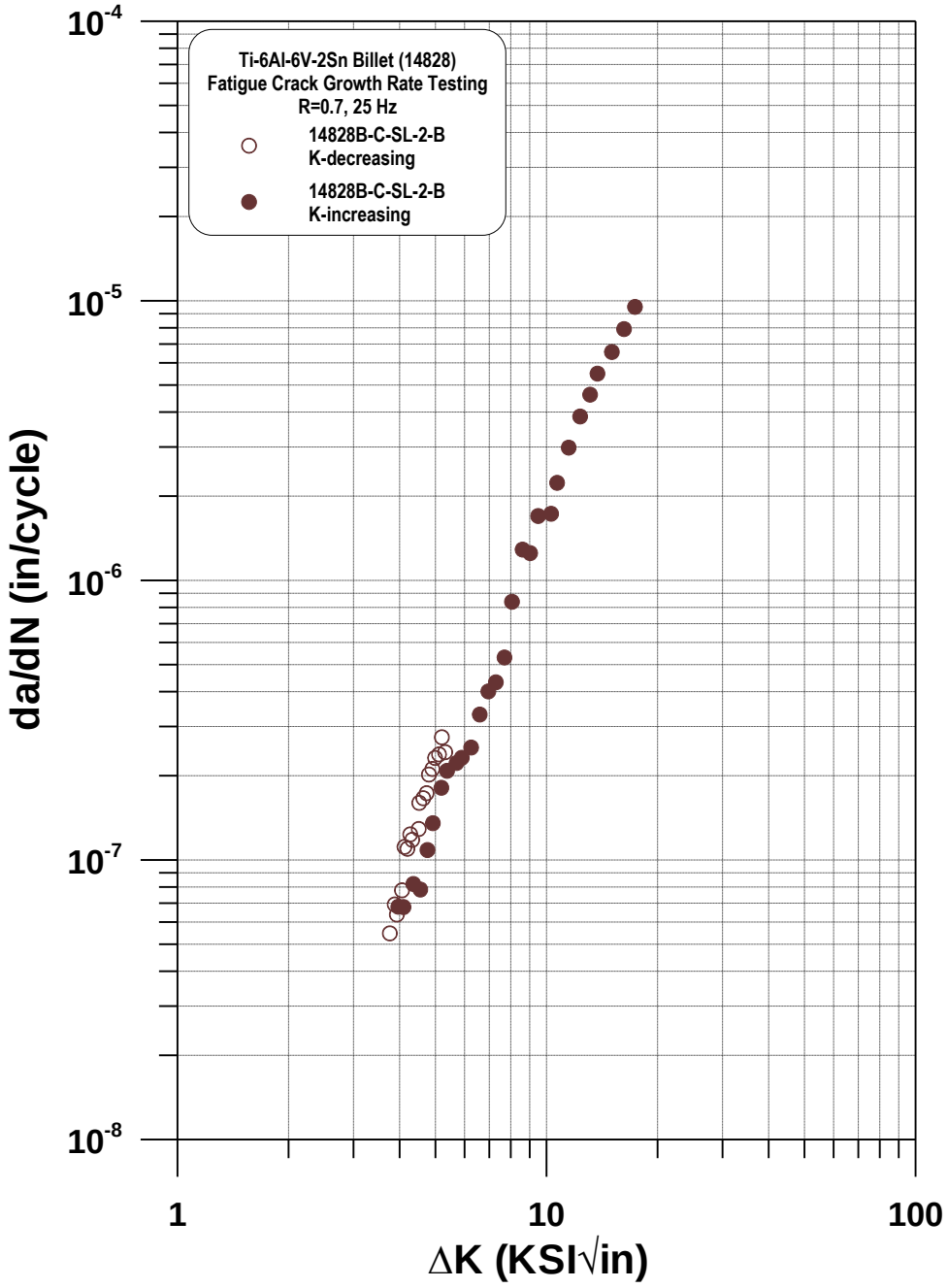
Approved for public release; distribution unlimited.



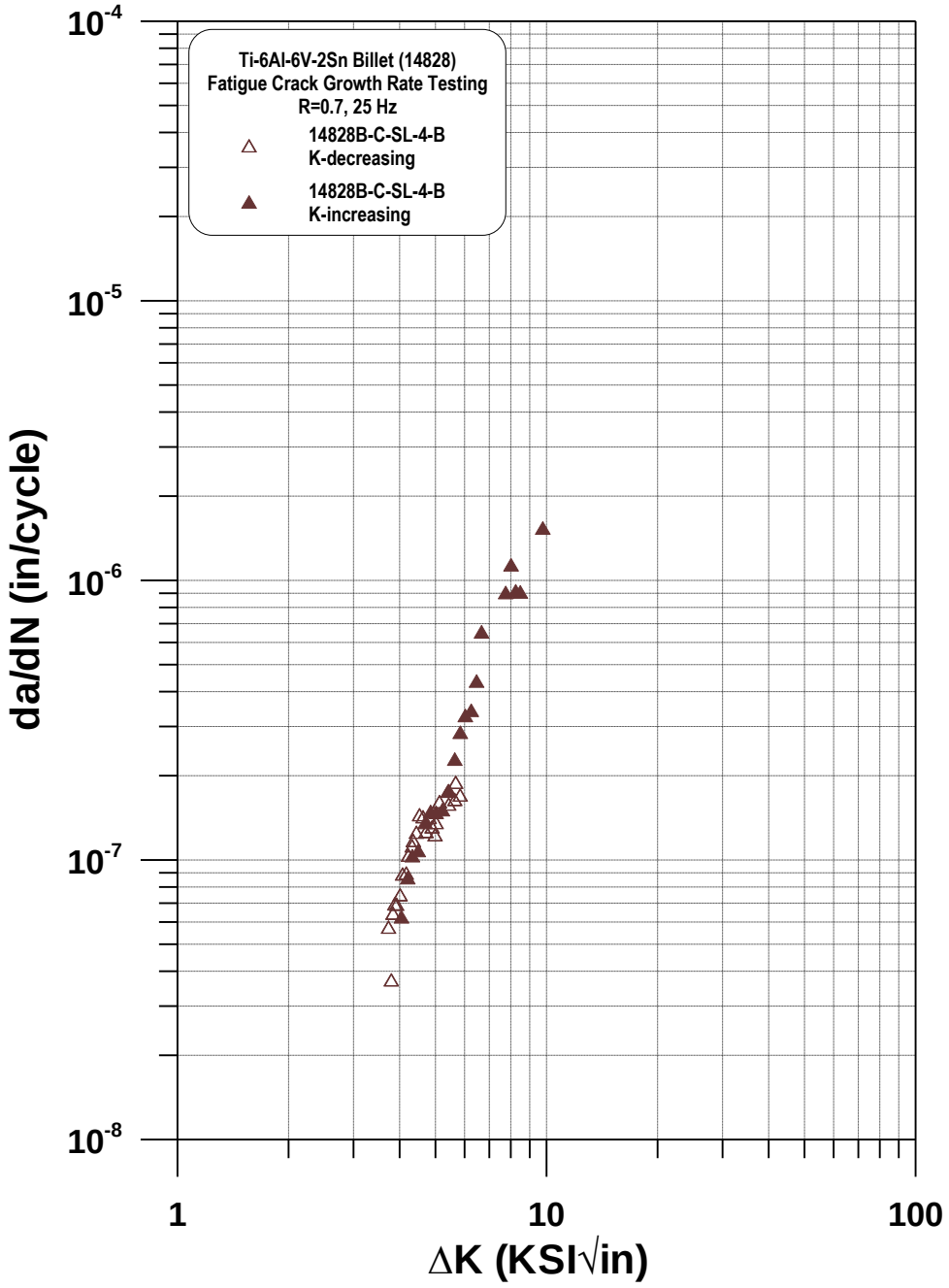
Approved for public release; distribution unlimited.



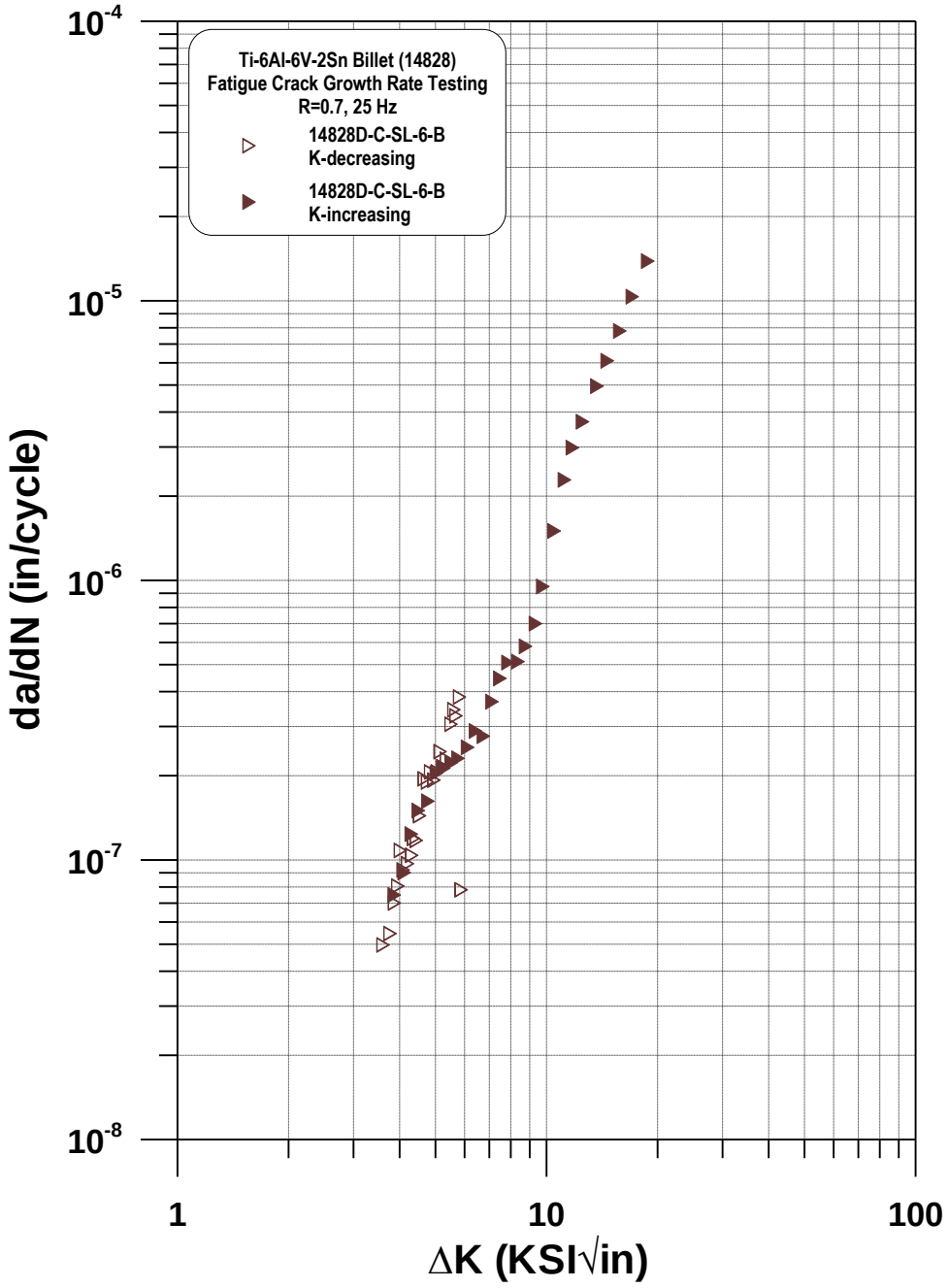
Approved for public release; distribution unlimited.



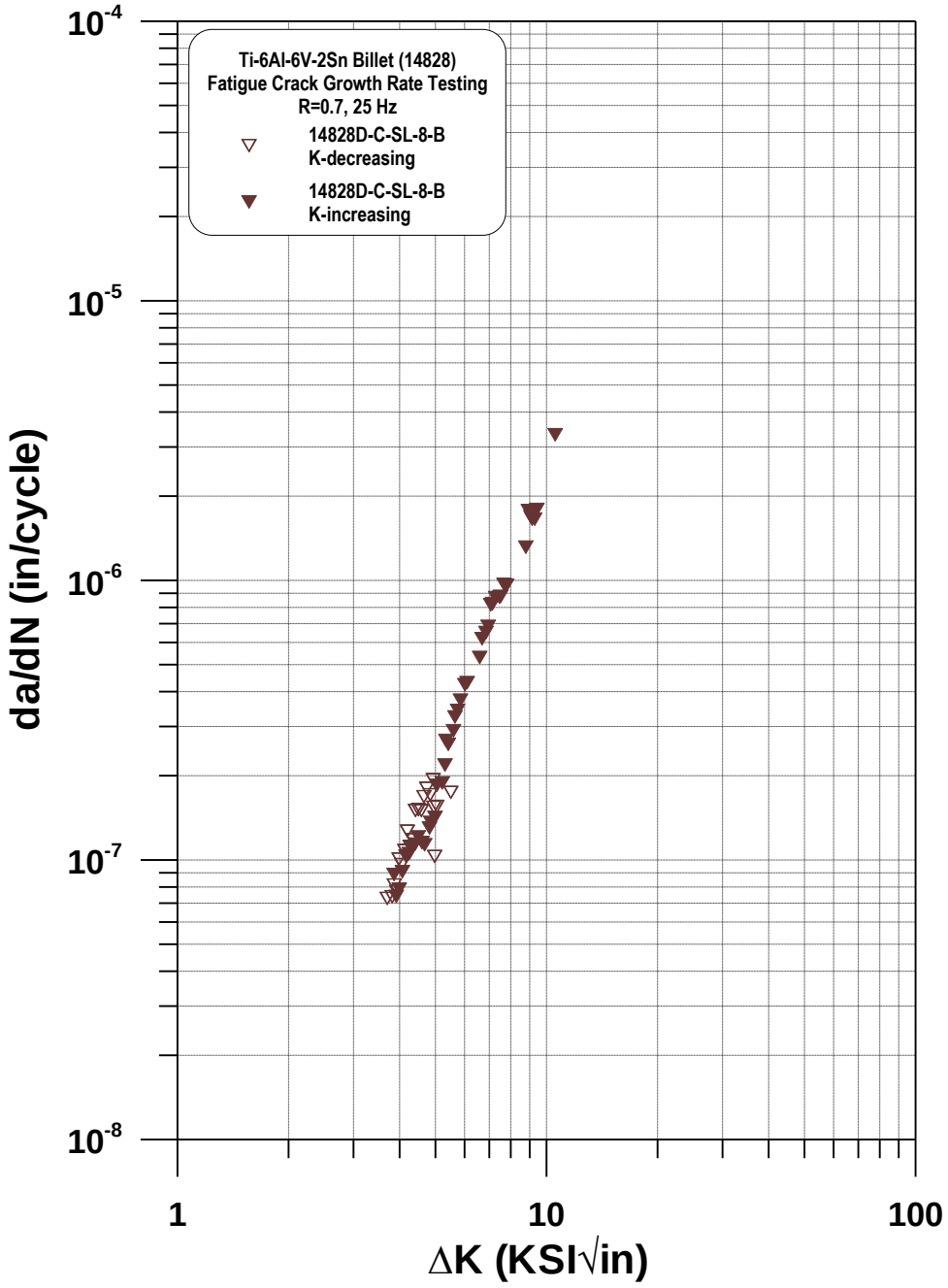
Approved for public release; distribution unlimited.



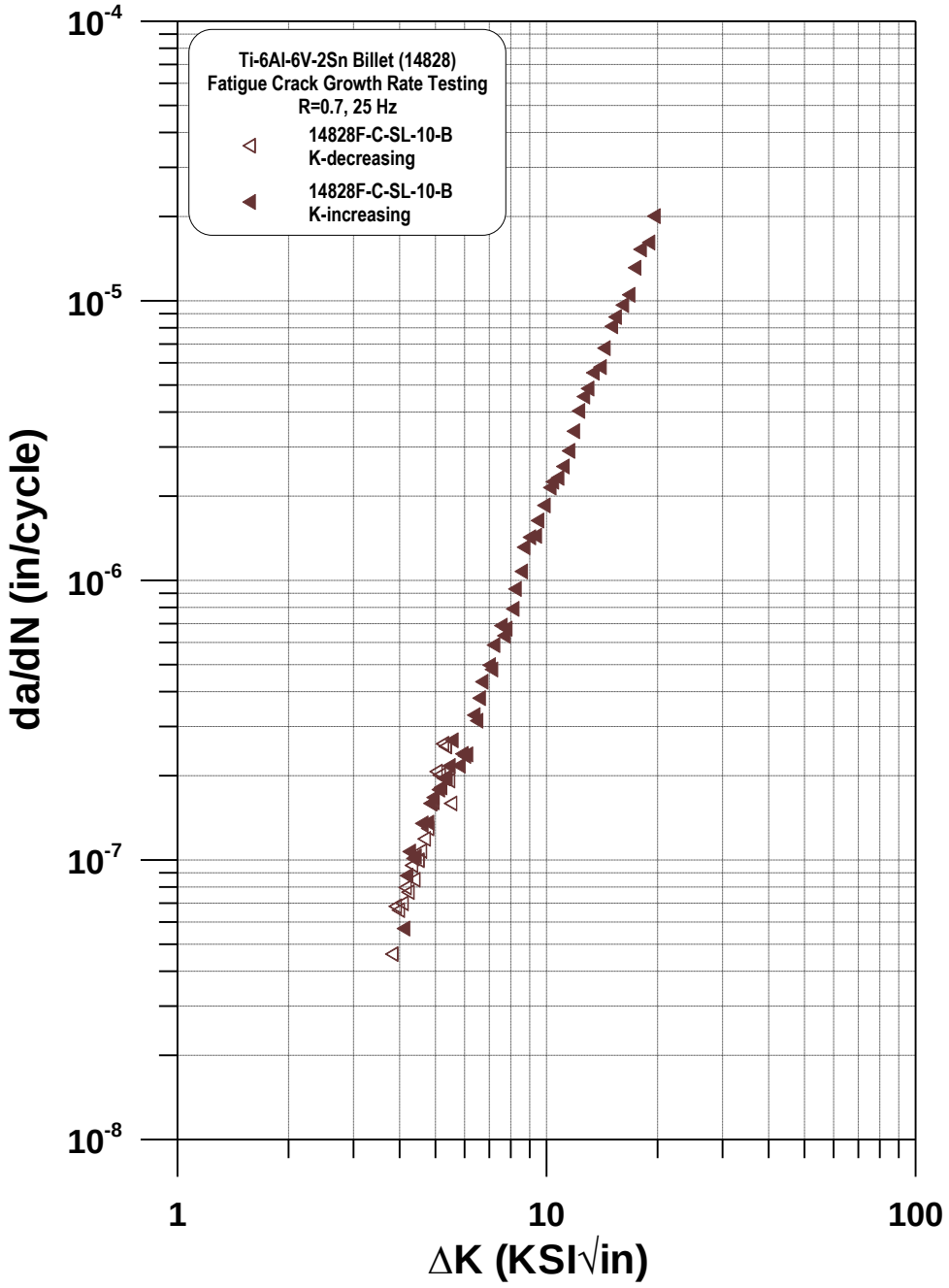
Approved for public release; distribution unlimited.



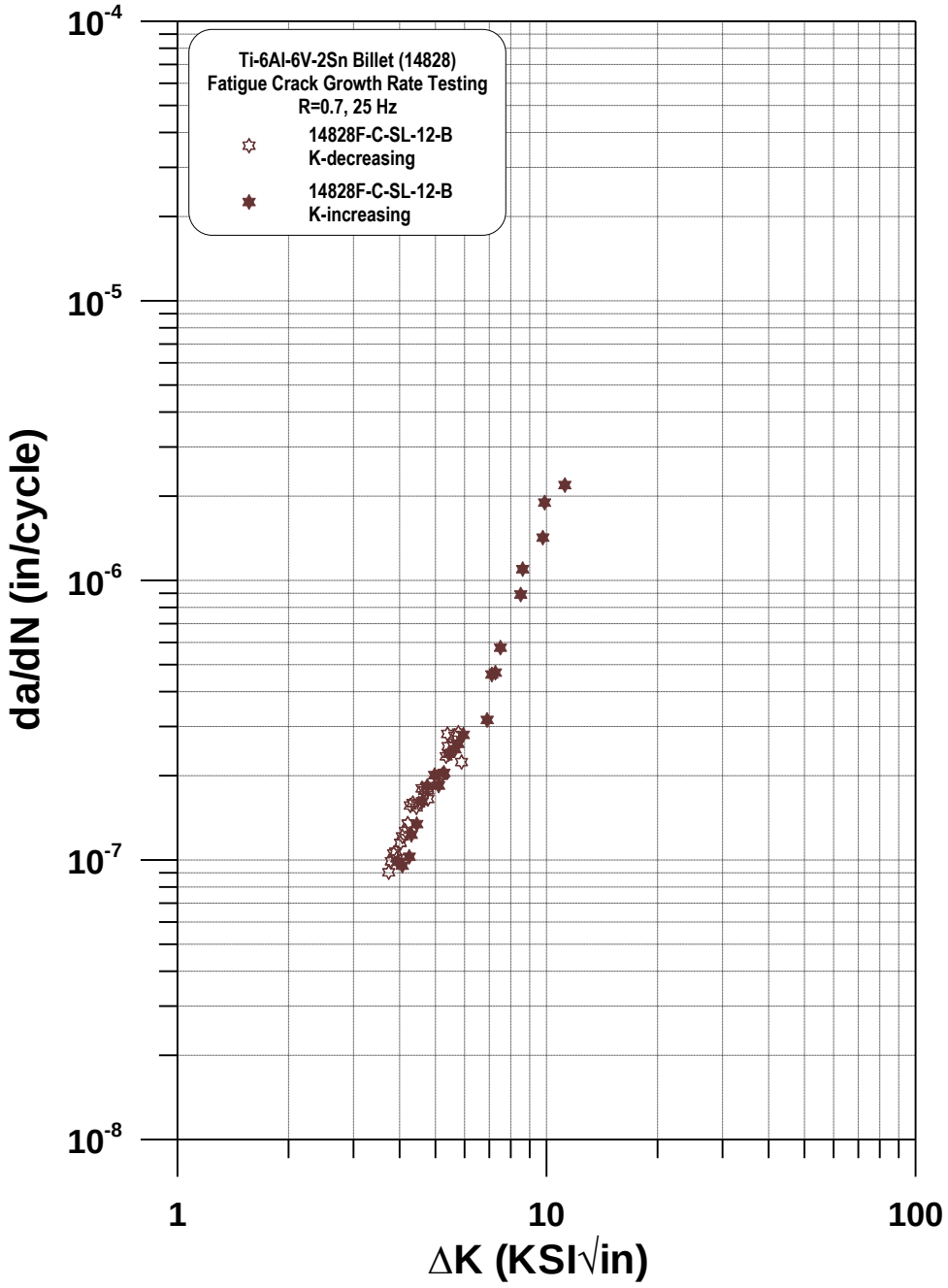
Approved for public release; distribution unlimited.



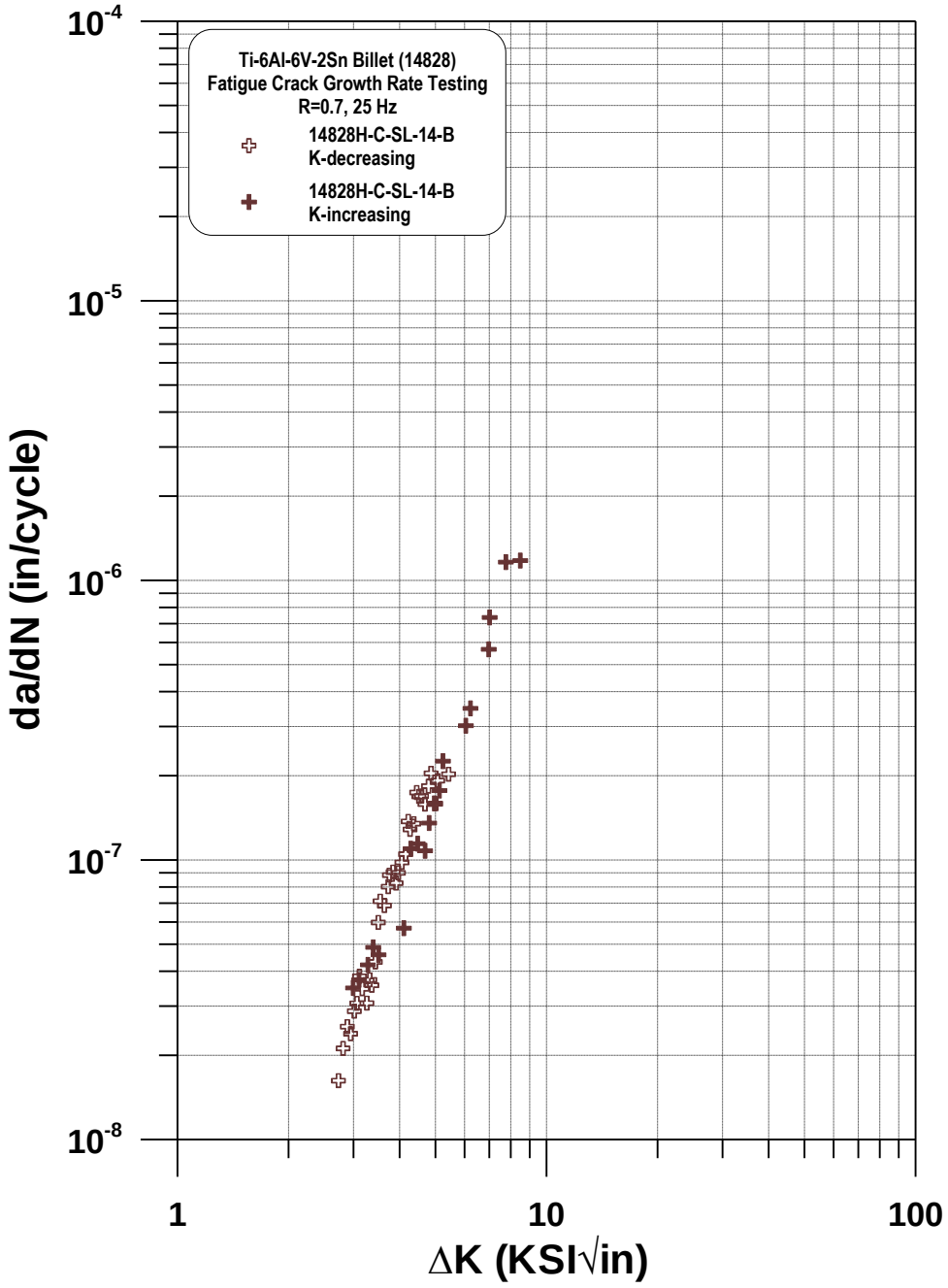
Approved for public release; distribution unlimited.



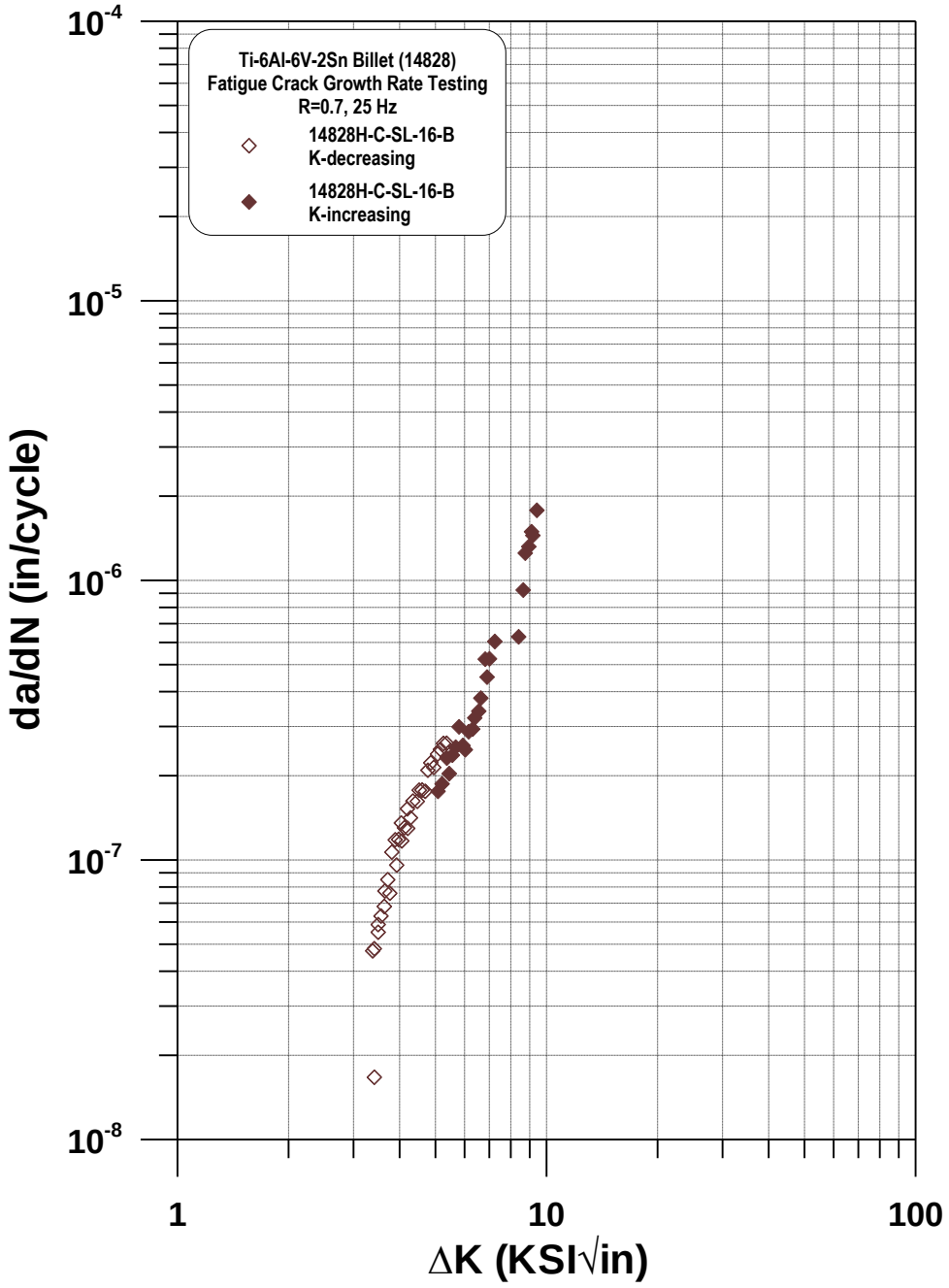
Approved for public release; distribution unlimited.



Approved for public release; distribution unlimited.



Approved for public release; distribution unlimited.



Approved for public release; distribution unlimited.

APPENDIX E

NON CONFORMING TITANIUM – REASONABLE LOWER BOUND ANALYSES

12 August 2011

EVALUATION REPORT

REPORT NO. AFRL/RXS 11-51

AUTHOR

Steven R. Thompson
Acquisition Systems Support Branch (AFRL/RXSCE)

Building 652, Room 122
2179 12th Street
Wright-Patterson AFB, Ohio 45433-7718

REQUESTER
AFMC/EN (Thomas Fischer, Robert Reifenberg)

CAUTION

This information consists of reasonable lower bound properties for titanium billet.
This information should be used **only** to evaluate the potential impact of improperly substituted titanium.
This information should **not** be used for design purposes in place of material properties from specifications or MMPDS entries covering titanium plate, bar, or other product forms.
This information should **not** be used to analyze components manufactured from titanium stock that is known to be compliant with applicable specifications.

CAUTION

DISTRIBUTION STATEMENT A: Approved for public release; distribution unlimited.

EXECUTIVE SUMMARY

This report is intended to summarize the analyses used for the determination of "reasonable lower bound" (RLB) properties for Ti-6Al-4V and Ti-6Al-6V-2Sn billet materials. Key results of the testing described in this report are shown in the table below. Statistical analyses were utilized to determine RLBs/life factors for tensile strength (ultimate and yield), fatigue, and fatigue crack growth rate. Tensile ductility (elongation and reduction of area), elastic modulus, and fracture toughness RLBs were determined by the lowest value in the test population.

Improperly processed materials can have material properties that do not meet specifications and requirements. This report has documented this for the titanium alloys Ti-6Al-4V and Ti-6Al-6V-2Sn.

Engineers and designers must account for reduced properties when assessing the integrity and safety of components that are, or may have been, made with improperly processed materials. This report provides data for Ti-6Al-4V and Ti-6Al-6V-2Sn that should be used in such assessments.

Approved for public release; distribution unlimited.

Property	Alloy	Reasonable Lower Bound / Life Factor	Difference from Specification Minimum Value
F_{tu}	Ti-6Al-4V	130 ksi	*MMPDS A-basis*
	Ti-6Al-6V-2Sn	137 ksi	8 ksi lower than AMS-T-9046 (2"-4") 6 ksi lower than AMS-T-9047 (1"-3")
F_{ty}	Ti-6Al-4V	118 ksi	*MMPDS A-basis*
	Ti-6Al-6V-2Sn	131 ksi	4 ksi lower than AMS-T-9046 (2"-4")
% elongation	Ti-6Al-4V	6.7%	3.3% lower than AMS-T-9046, 9047
	Ti-6Al-6V-2Sn	8%	*AMS-T-9046 (2"-4") Spec Min*
% reduction of area	Ti-6Al-4V	10%	15% lower than AMS-T-9047 (<4") 10% lower than AMS-T-9047 (4"-6")
	Ti-6Al-6V-2Sn	19%	1% lower than AMS-T-9047 (L-orientation)
E	Ti-6Al-4V	15.3 msi	0.7 msi lower than MMPDS typical
	Ti-6Al-6V-2Sn	14.2 msi	1.8 msi lower than MMPDS typical
K_{Ic}	Ti-6Al-4V	59.8 ksi√in	n/a
	Ti-6Al-6V-2Sn	55.7 ksi√in	
S-N Fatigue*	Ti-6Al-4V	0.61	n/a
	Ti-6Al-6V-2Sn	0.14	
ε-N Fatigue*	Ti-6Al-4V	0.70	n/a
	Ti-6Al-6V-2Sn	0.69	
Fatigue Crack Growth Rate*	Ti-6Al-4V	1x	n/a
	Ti-6Al-6V-2Sn	2x	

where:
F_{tu}*: ultimate tensile strength*
F_{ty}*: tensile yield strength*
E*: elastic modulus*
K_{Ic}*: plane strain fracture toughness*
*: *Fatigue & crack growth rate life factors discussed in this report that describe the relationship between titanium billet and plate should be used for initial screening purposes only. These factors represent worst case comparisons FOR ONLY TWO STRESS RATIOS; factors approach 1.0 at certain regions of the curves from which the factors were derived. If a program's initial screening indicates that sufficient maintenance intervals continue to exist for titanium components, no further analysis is required. However, if maintenance intervals are found to be unacceptable during an initial screening using the published factors, a program may conduct further analysis using the full range of the test data provided by AFRL supplemented, as appropriate, with test data and analysis generated by the program.*

Approved for public release; distribution unlimited.

BACKGROUND

A federal investigation identified a risk associated with improperly processed titanium (Ti) material being used in the fabrication of critical safety items and safety-of-flight components in USAF, DoD, NASA, and FAA. At the direction of AFMC/CC, the USAF Titanium Task Force (led by AFMC/EN) was formed to further define risk to USAF systems and to assist with mitigation efforts. The suspect Ti material (e.g., "billet," "reforging stock") was never intended to be machined to the final forms in which it is now possibly being used. This R&D testing program will develop new baseline (reasonable lower bound) properties on a heretofore not fully characterized form of Ti. The decision to refer to these baseline values as "reasonable lower bounds" is based on the fact that an insufficient quantity of material heats and lots were represented for the calculation of traditional MMPDS **[*1*]** A- or B-, or even S-basis allowables. However, the number of specimens tested (often in replicate) is significant. Thus "reasonable lower bound" (RLB) was chosen as the proper phrase to describe properties derived from the testing of multiple specimens from the two heats (per alloy) of material in this program. While they do not meet the requirements for standard baseline property determination, these data are, nevertheless, significant.

This report is intended to summarize the analyses used for the determination of "reasonable lower bounds" of Ti-6Al-4V and Ti-6Al-6V-2Sn billet materials.

Approved for public release; distribution unlimited.

MATERIAL DESCRIPTION

The titanium materials summarized in this report were described and reported on in previous reports ***[2-5]***. Two Ti-6Al-4V billets, two Ti-6Al-6V-2Sn billets, one Ti-6Al-4V plate, and one Ti-6Al-6V-2Sn plate were tested for this effort. The billets were produced to AMS-T-9047 and the plates were produced per AMS-T-9046.

TEST PLAN

Test Specimens – The test specimens used in this program were machined to the final required geometries as shown in Figures 1 through 5. All of the geometries were in accordance with the applicable test method (as described in the next section). All of the specimens were fabricated using the same machine shop per specimen drawings provided by AFRL/RXSCE, in order to minimize possibility of variability due to specimen machining. Special care was given to the traceability of the specimen back to a general location within the billet. Test specimens were given a unique identification that would allow for this tracking.

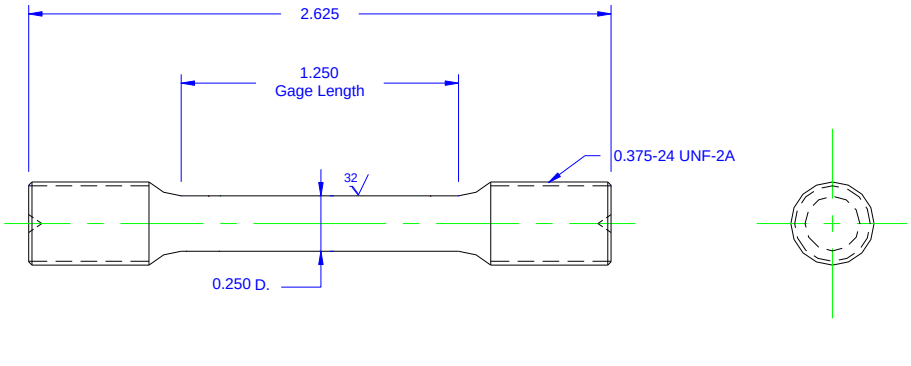


Figure 1. Geometry of tensile test specimen.

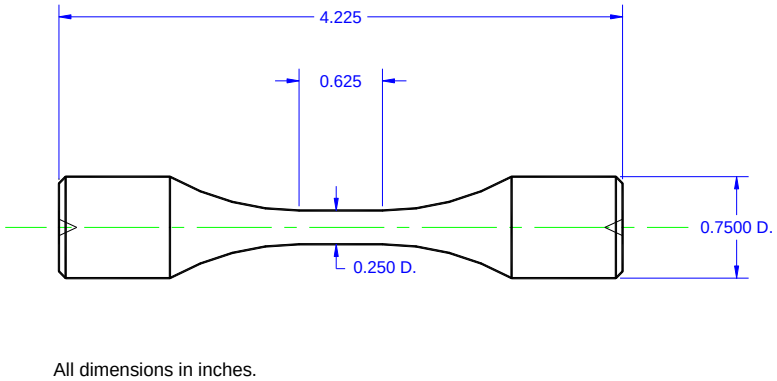
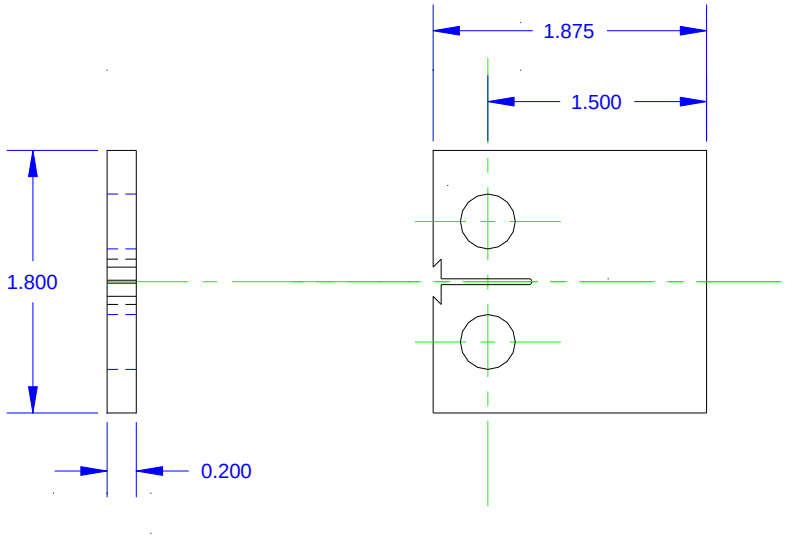


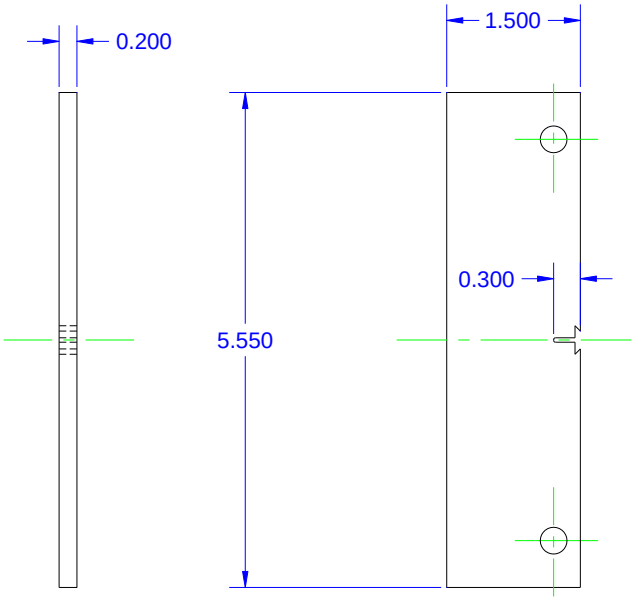
Figure 2. Geometry of fatigue test specimen. (Note: gage section was low-stress ground to a final surface finish of 8 Ra and then hand-polished longitudinally to remove all circumferential scratches.)

Approved for public release; distribution unlimited.



All dimensions in inches.

(a)



all dimensions in inches

(b)

Figure 3. Geometry of fatigue crack growth rate (a) C(T) and (b) ESE(T) test specimens.

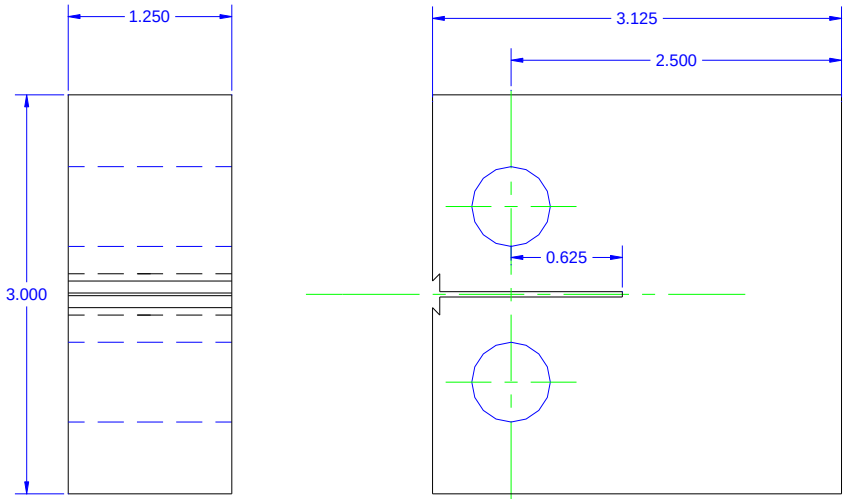


Figure 4. Geometry of fracture toughness C(T) test specimen.

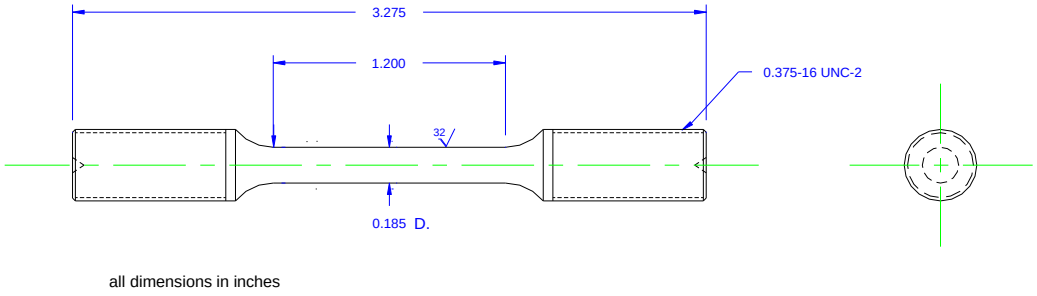


Figure 5. Geometry of stress corrosion cracking (SCC) test specimen.

Test Methods – The test methodologies used in this investigation are listed in Table 1. With the exception of stress corrosion cracking, all of the tests were performed in accordance with applicable ASTM standards. All testing was performed in ambient laboratory conditions (approximately 72°F and 50% relative humidity).

Table 1. Test Methodology

Test	ASTM Method
Tension (Modulus)	E 111-04 "Standard Test Method for Young's Modulus, Tangent Modulus, and Chord Modulus"
Tension	E 8/E 8M-08 "Standard Test Methods for Tension Testing of Metallic Materials"
Fatigue (force-controlled)	E 466-07 "Standard Practice for Conducting Force Controlled Constant Amplitude Axial Fatigue Tests of Metallic Materials"
Fatigue (strain-controlled)	E 606-04 "Standard Practice for Strain-Controlled Fatigue Testing"
Fatigue Crack Growth Rate	E 647-08 "Standard Test Method for Measurement of Fatigue Crack Growth Rates"
Fracture Toughness	E 399-08 "Standard Test Method for Linear-Elastic Plane-Strain Fracture Toughness K_{Ic} of Metallic Materials"
Stress Corrosion Cracking	Similar to G 64-99 "Standard Classification of Resistance to Stress-Corrosion Cracking of Heat-Treatable Aluminum Alloys" Applied stress = 75% of specification tensile yield strength / 40 days 3.5% NaCl solution – alternate immersion (10 min wet/50 min dry)

Tension (Modulus) – Prior to performing full-range tension testing, approximately 10% of the machined tension specimens were used to generate modulus data using the procedures outlined in ASTM E111. For this testing the specimens were loaded to a maximum stress below the proportional limit, so as to remain within the linear region of the stress-strain curve. The test was repeated three times per specimen, with the specimen being rotated 120° between test runs. Strain was measured using an MTS averaging extensometer (B-1 classification) with a one-inch gage length. The average modulus from the three runs was recorded as the final elastic modulus.

Tension – Tension testing was performed on an Instron electro-mechanical test machine in accordance with ASTM E8. Strain was measured using an Instron one-inch gage length extensometer. The extensometer was removed from the specimen prior to reaching ultimate load to prevent damage to the instrument during specimen breakage. Elongation and reduction of area measurements were made using the "fit-back" method.

Fatigue (Force-controlled) – Axial fatigue testing was performed under force-controlled conditions using an MTS servo-hydraulic test machine in accordance with ASTM

E466. Stress ratios (R) of 0.05 and -1 were used in this investigation. Replicate specimens were tested at four applied stress levels for each of the stress ratios.

Fatigue (Strain-controlled) – Axial fatigue testing was performed under strain-controlled conditions using an MTS servo-hydraulic test machine in accordance with ASTM E606. An MTS one-inch gage length extensometer was used for strain measurement. The testing frequency used was 1 Hz. Strain ratios ($R_\varepsilon = \varepsilon_{min}/\varepsilon_{max}$) of 0.05 and -1 were used for these specimens.

Fatigue Crack Growth Rate – Fatigue crack growth rate testing was performed on an MTS servo-hydraulic test machine per ASTM E647 using computer data acquisition and control systems developed in-house. Crack length was measured via compliance techniques with standard crack-opening-displacement (COD) gages. Testing was performed under K-control (normalized K-gradient, C=-2) until a near-threshold growth rate was obtained, at which point the test was then run under constant amplitude (constant load) conditions for the remainder of the test. Initial and final crack lengths were measured optically for use in post-test crack correlation calculations. A test frequency of 25 Hz was used throughout the test, with humidity maintained at 50% ±10% for the duration of the test. Specimens were tested using stress ratios (R) of 0.1 and 0.7. Two orientations were tested for this program, L-T and S-L, where the first letter indicates the loading direction and the second letter indicates the direction of crack propagation. The compact, C(T), specimen geometry was utilized for the S-L orientation specimens extracted from the 4.5" thick billet material (14824) due to thickness limitations which would prevent the eccentrically-loaded single edge crack tension, ESE(T), specimen from being used.

Fracture Toughness – Plane-strain fracture toughness tests were performed in accordance with ASTM E399 on a Tinius-Olsen electro-mechanical test machine. Specimen precracking was performed on an MTS servo-hydraulic test machine. Crack length was monitored via compliance techniques using an MTS COD gage as previously described. Initial and final crack lengths were measured optically post-test.

Stress Corrosion Cracking – The theory behind this testing was that since the billet material had not been subject to final hot working, the microstructure may not have been fully homogenized, increasing the potential for localized aluminum segregation. If this were to occur, aluminum-rich areas would be more susceptible to the effect of stress corrosion cracking, particularly at the applied stress levels employed in this investigation.

For this investigation, stress corrosion cracking tests were therefore performed to obtain pass/fail results. As there is currently no ASTM test method for SCC of titanium alloys, the procedure outlined in ASTM G64 ("A" level) was used. This procedure was previously adopted for use within AFRL/RXSCE as a standard SCC test. Specimens were axially loaded (statically) in an alternate immersion, 3.5% NaCl solution such that the specimens were submerged in the solution for 10 minutes and then allowed to dry for the next 50 minutes each hour. The specimens were loaded at 75% of the specification yield

Approved for public release; distribution unlimited.

strength (for plate and bar). For Ti-6Al-4V, the applied stress was 90 ksi. For Ti-6Al-6V-2Sn, the applied stress was 101.3 ksi. The test duration was set at 40 days. To pass the test, no specimen could fail during this 40 day loading cycle; failure being breakage of the test specimen or evidence of corrosion-related damage (i.e. pitting).

FACTUAL DATA

For the testing described above, analyses were performed to establish RLBs for each property, excluding stress corrosion cracking. Statistical methodologies were utilized in the analysis of tensile strength (ultimate and yield), fatigue (S-N and e-N), and fatigue crack growth rate. RLBs for tensile ductility (elongation and reduction of area), elastic modulus, and fracture toughness were based on the lowest property in the population. It should be noted that the elastic modulus results used for the RLB determination were those generated from the tensile test stress-strain curve. Since there was a relatively small difference between the ASTM E111 testing and those from the tensile test, the larger population from the latter was used for the analysis population. As stress corrosion cracking consisted of pass/fail testing, no further analysis was performed on the results from this testing.

As the populations for testing consisted of billet materials rather than properly processed plate or bar, billet-to-billet and L vs. S orientation combinabilities were forced during the analyses. For example, the longitudinal and short-transverse orientation results from Billet A were combined together with the same from Billet B to create one complete population. For the control plate materials, only data from the L-orientation was used in the analyses.

The statistical analyses used on tensile strength results were performed by Battelle using methodologies similar to those prescribed for MMPDS “A” basis allowables. For this investigation, normal-distribution statistical methods were used for the determination of the RLBs for ultimate tensile strength and tensile yield strength. In statistical terms, the RLBs presented herein for tensile strength are the one-sided lower tolerance limit, representing a 95% confidence limit on the first percentile of the distribution. These preliminary RLB values were then compared against the material specification minimum values and MMPDS “A” basis allowables (where available). The lower of these values were used as the final RLB.

Fatigue analyses were also performed by Battelle, again using procedures similar to those used in MMPDS. Equivalent stress (or strain) equations were developed on the data sets for billet and plate. In order to establish lower bounds for the populations, -2 sigma curves were calculated from the equivalent stress (or strain) equations for each dataset. Since there weren’t established lower bound properties to compare against, the plate data developed under this program was used as the baseline for comparison. The life factors for fatigue stated in the following sections are based on the worst case difference where billet had a lower life than plate.

Approved for public release; distribution unlimited.

The statistical analyses for fatigue crack growth rate were performed by the University of Dayton. Power-law curves were initially fit to the data populations to represent the mean behavior. In order to establish a bound on the population, 95% confidence limits were calculated for log (da/dN) at given values of log (ΔK). As with fatigue testing, since there weren't established lower bound properties to compare against, the plate data developed under this program was used as the baseline for comparison. The life factors for fatigue crack growth rate stated in the following sections are based on the worst case difference where billet had a lower life than plate.

Fatigue & fatigue crack growth rate life factors discussed in this report that describe the relationship between titanium billet and plate should be used for initial screening purposes only. These factors represent worst case comparisons FOR ONLY TWO STRESS RATIOS; factors approach 1.0 at certain regions of the curves from which the factors were derived. If a program's initial screening indicates that sufficient maintenance intervals continue to exist for titanium components, no further analysis is required. However, if maintenance intervals are found to be unacceptable during an initial screening using the published factors, a program may conduct further analysis using the full range of the test data provided by AFRL supplemented, as appropriate, with test data and analysis generated by the program.

Ti-6Al-4V

Tension – Histograms for the tensile strength, elongation, and elastic modulus results are shown in Figures 1-4. Also shown on these histograms are the AMS-T-9046 specification minimum values (MMPDS typical value shown for elastic modulus). It is readily apparent from Figures 1 and 2 that the control plate exhibited higher strength properties when compared to the two billets. It is also obvious that, with the exception of a few ultimate strength values, the billets were able to meet the specification minimum properties for strength. However, for elongation, Billet 75838 had multiple (11 of 100 total specimens) results that fell below the plate specification minimum value. With respect to elastic modulus, although the minimum value is to be used as the RLB, the mean values for the billet populations were equal to or higher than the MMPDS typical value.

Sample statistics for ultimate tensile strength and tensile yield strength are shown in Table 2. As stated earlier, normal distribution statistics were applied to the population in order to determine the preliminary RLB. These values were then compared with the specification minimum properties and the MMPDS A-basis allowables. The lower of these values have been designated as the final RLB.

Approved for public release; distribution unlimited.

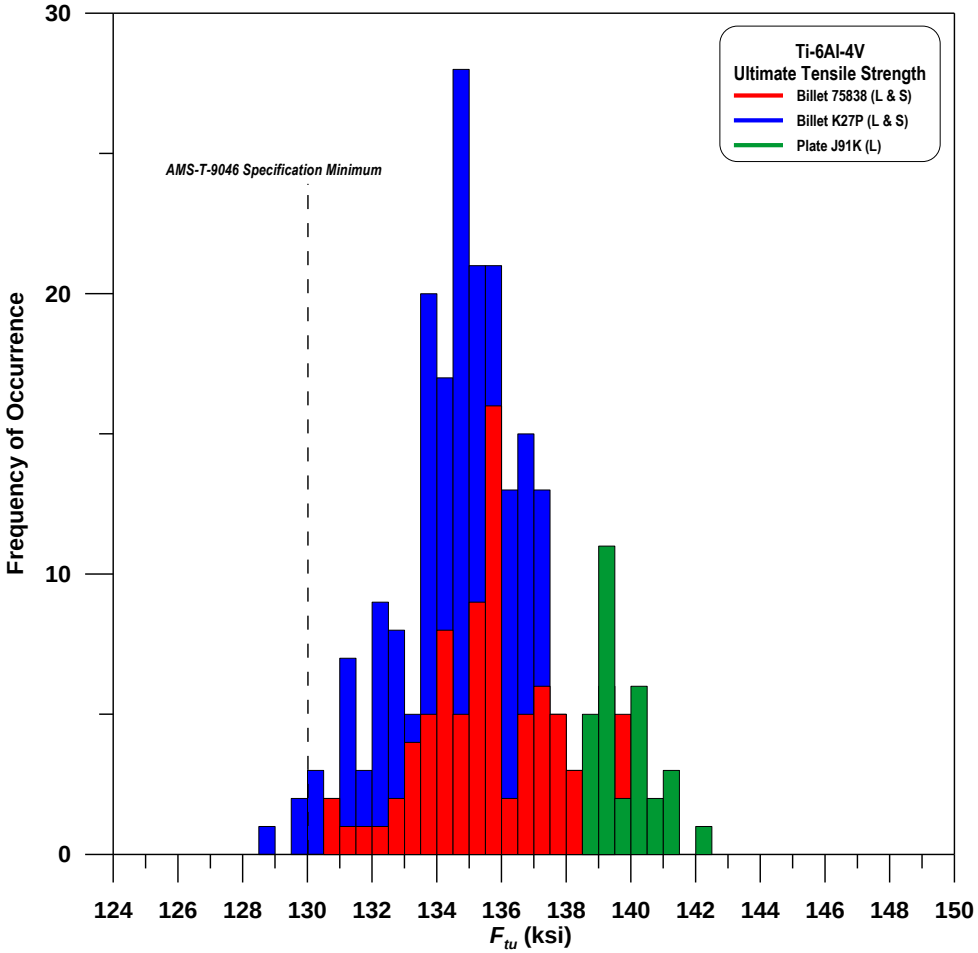


Figure 1. Histogram of Ti-6Al-4V ultimate tensile strength results.

Approved for public release; distribution unlimited.

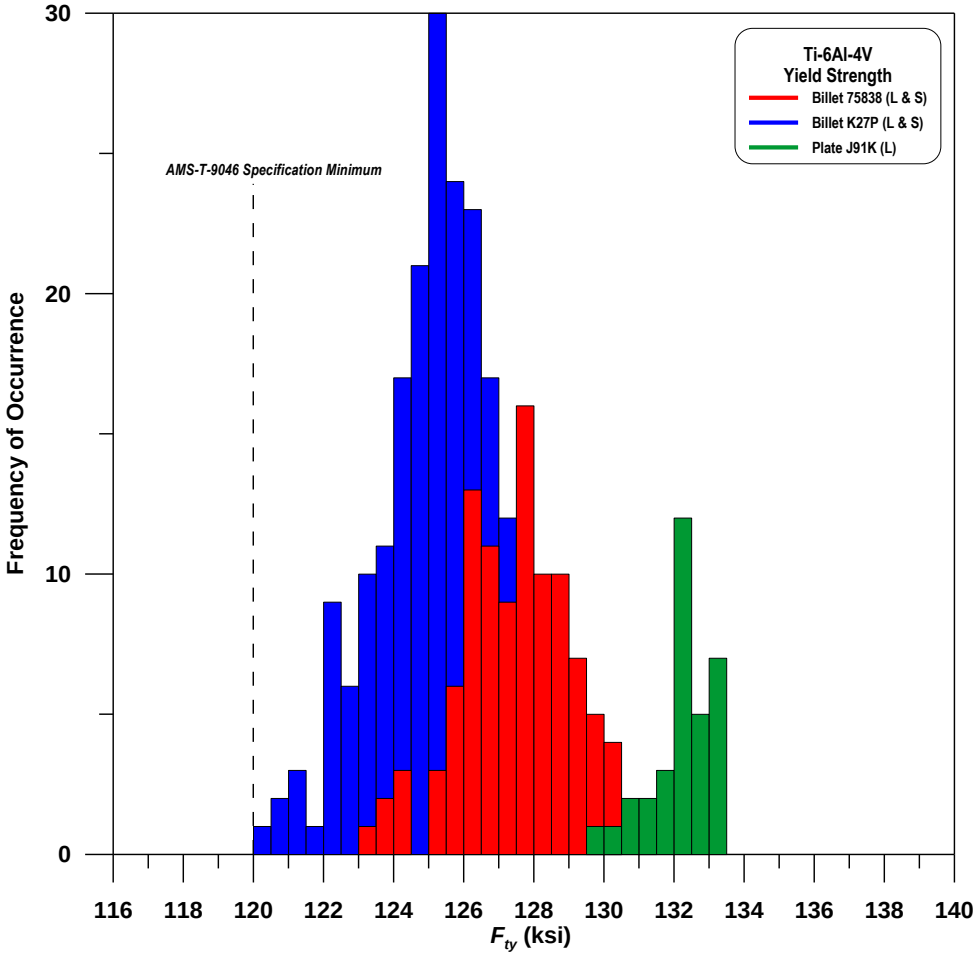


Figure 2. Histogram of Ti-6Al-4V tensile yield strength results.

Approved for public release; distribution unlimited.

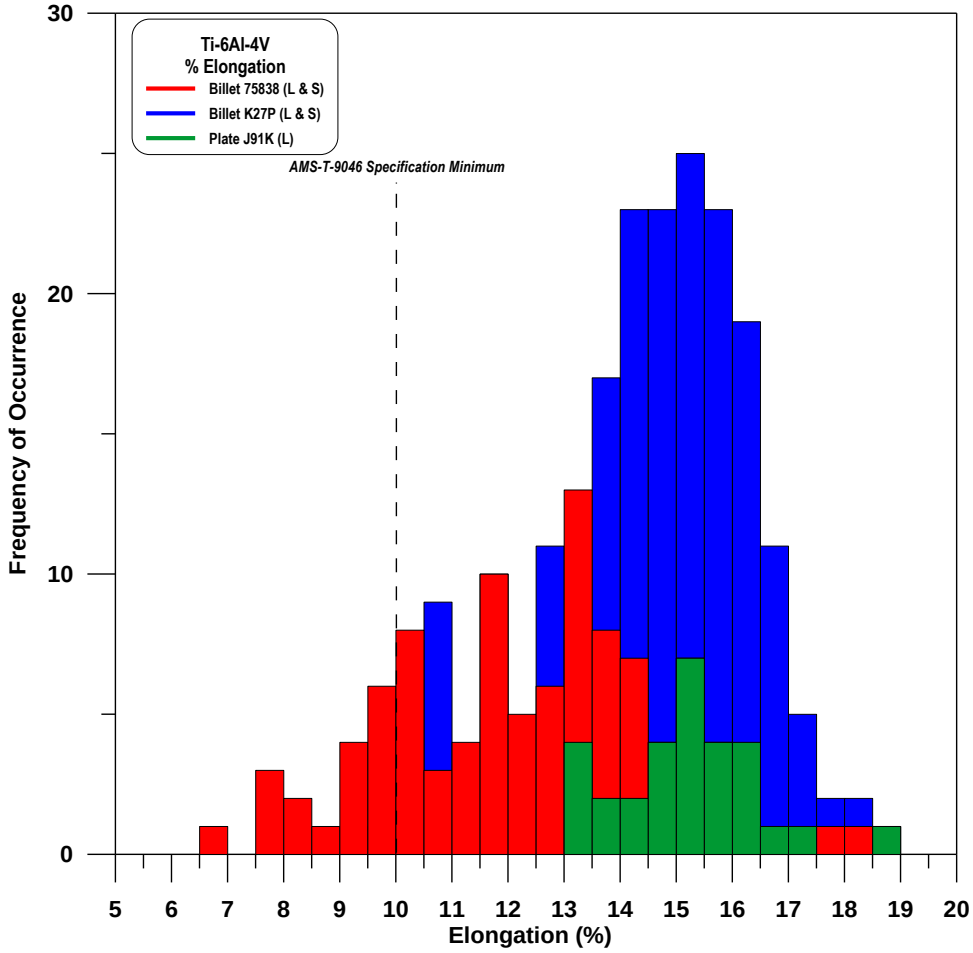


Figure 3. Histogram of Ti-6Al-4V tensile elongation results.

Approved for public release; distribution unlimited.

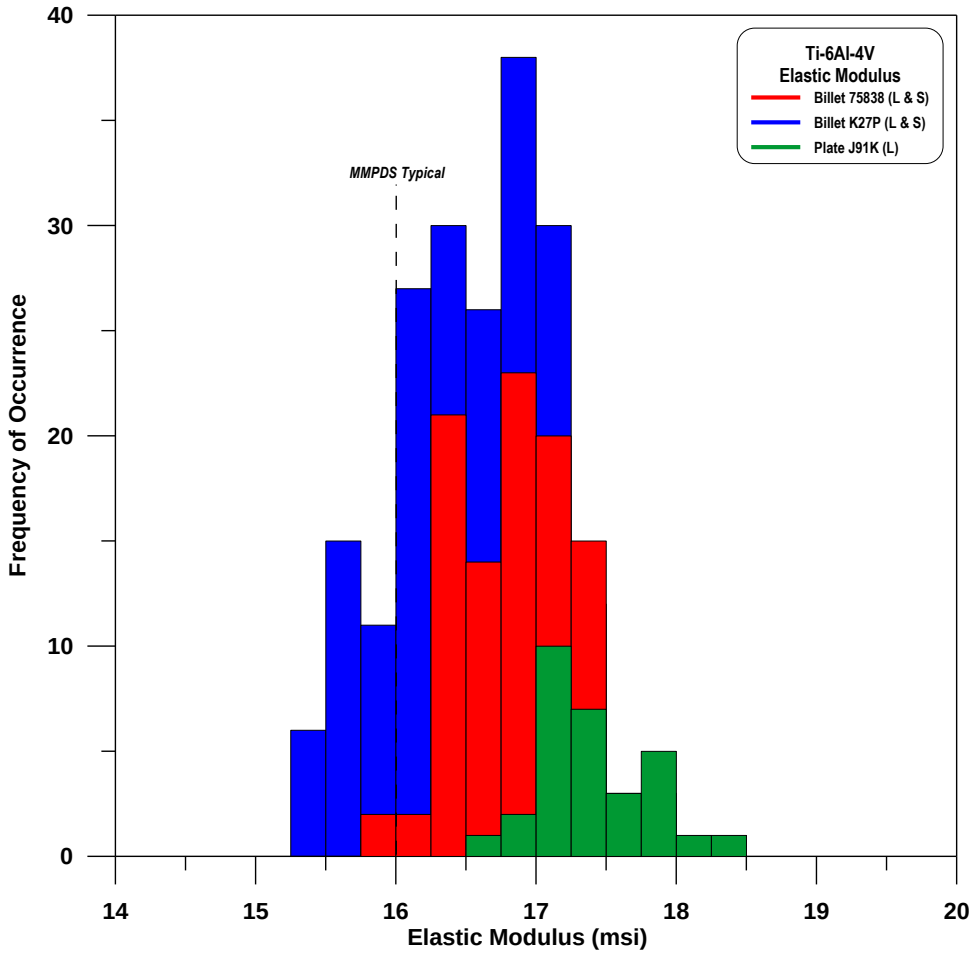


Figure 4. Histogram of Ti-6Al-4V elastic modulus results.

Approved for public release; distribution unlimited.

Table 2. Ti-6Al-4V tensile property analysis.

Statistic	F_{tu} (ksi)	F_{ty} (ksi)	Elongation (%)	Reduction of Area (%)	Elastic Modulus (msi)
Mean	135.34	126.62	13.8	24.8	16.7
Std. Dev.	2.31	1.77	2.23	4.77	0.53
COV	1.71%	1.40%	-	-	-
Skewness	0.15	-0.25	-	-	-
Sample Size	301	301	299	301	301
Preliminary RLB	***130***	***122***	***6.7***	***10***	***15.3***
AMS-T-9046 Spec Min	130	120	10	n/a	n/a
AMS-T-9047 Spec Min	130	120	10	25 [< 4”] 20 [4”-6”]	n/a
MMPDS A-basis allowable	130	118	10*	n/a	16.0†
Final RLB	**130**	**118**	**6.7**	**10**	**15.3**

*: MMPDS S-basis
†: MMPDS typical

Fatigue (force-controlled) – The -2 sigma analysis of force-controlled axial fatigue test results are shown graphically in Figure 5. The curves shown were based on equations of the form:

$$\log N_f = A_1 + A_2 \log(S_{max} - A_3),$$

where:
N_f is the number of cycles to failure,
S_{max} is the maximum applied stress, and
A_1, A_2, A_3 are coefficients determined by analysis.

Coefficients for each curve are shown in Table 3. The curves are plotted only between the stress levels applied during testing. No further extrapolation was performed.

As can be seen in Figure 5, the largest decrement for billet, when compared against plate, occurs at the 120 ksi stress level for R=0.05. At this stress level, the billet specimens only exhibited 61% of the plate specimens' fatigue life. Therefore, the life factor for force-controlled fatigue is 0.61, as shown in Table 4. As stated earlier, this life factor is based on a worst-case difference where billet had a lower life and was based on comparisons for only two stress ratios. In some cases, the factors are equal to or greater than 1.0. This factor should be used for initial screening purposes only.

Approved for public release; distribution unlimited.

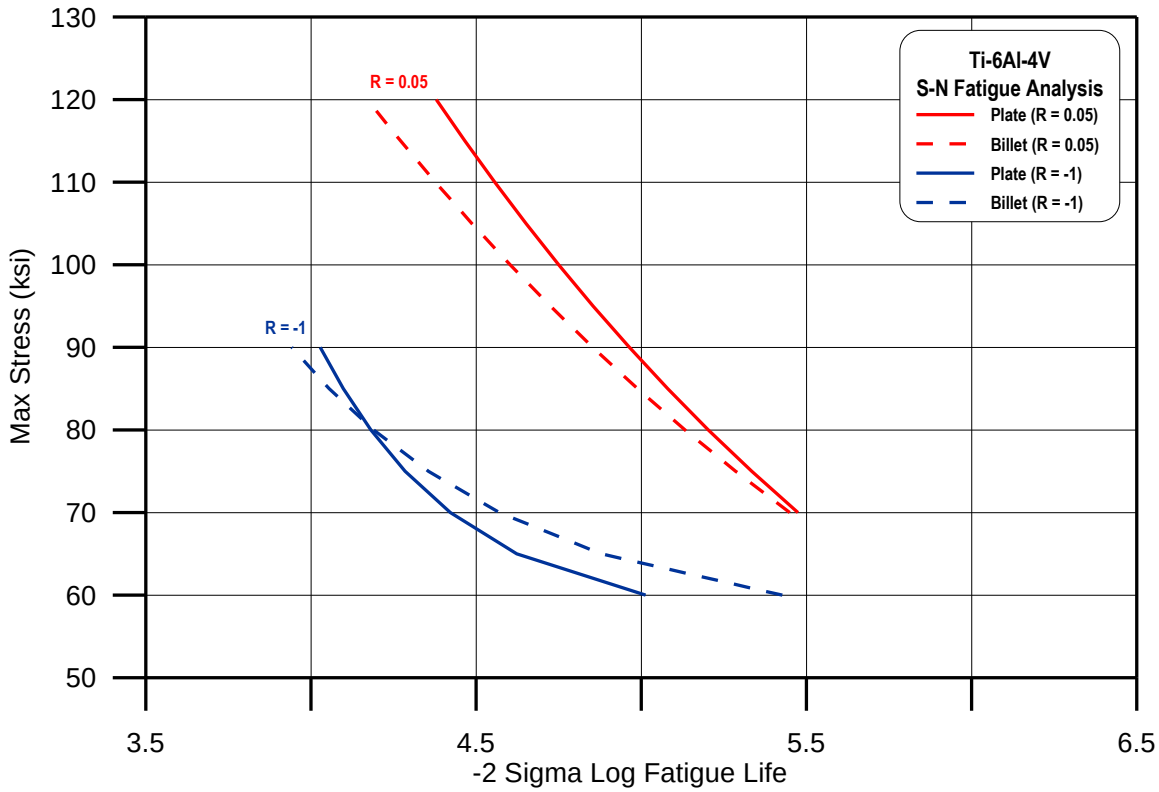


Figure 5. Ti-6Al-4V force-controlled axial fatigue analysis results.

Table 4. Ti-6Al-4V force-controlled axial fatigue -2 sigma equation coefficients.

Product Form	Stress Ratio	-2 Sigma Equation Coefficients		
		A_1	A_2	A_3
Plate	0.05	14.104	-4.677	0.00
	-1	5.541	-0.993	56.60
Billet	0.05	15.531	-5.464	0.00
	-1	6.497	-1.663	55.60

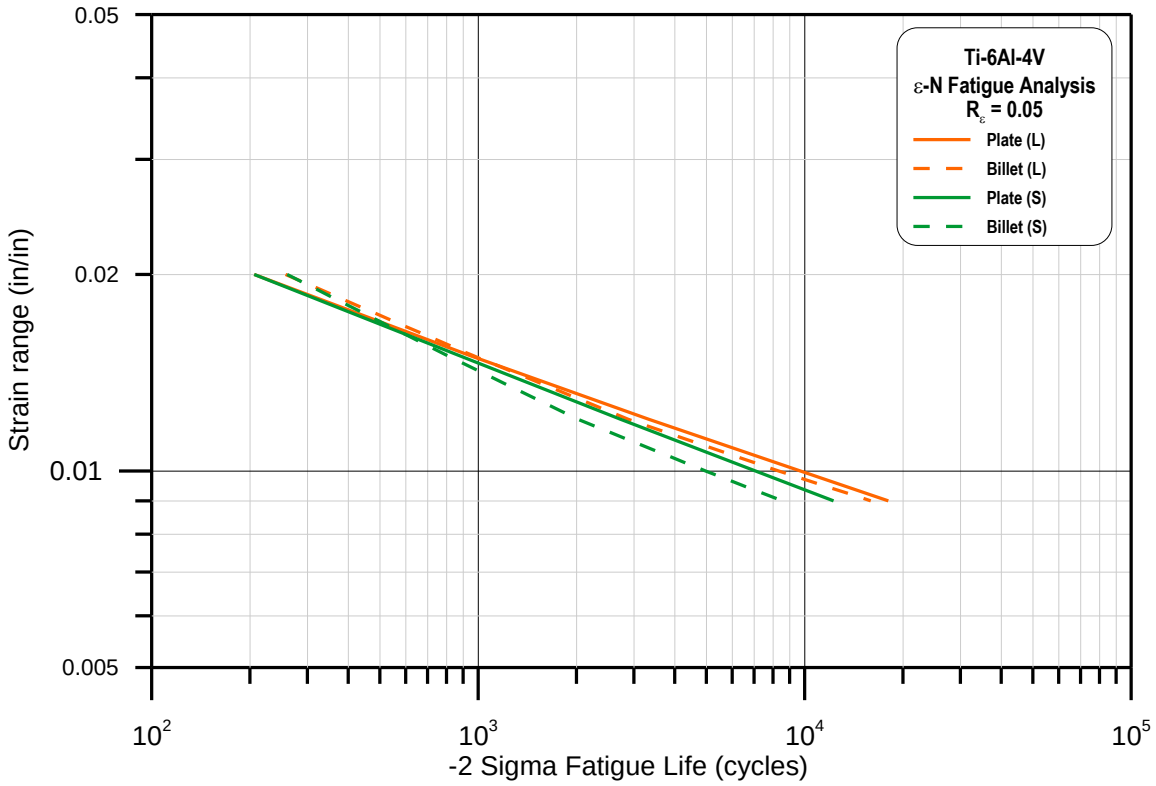
Table 5. Life factor for Ti-6Al-4V force-controlled axial fatigue.

Ti-6Al-6V-2Sn S-N Life Factor
0.61

Approved for public release; distribution unlimited.

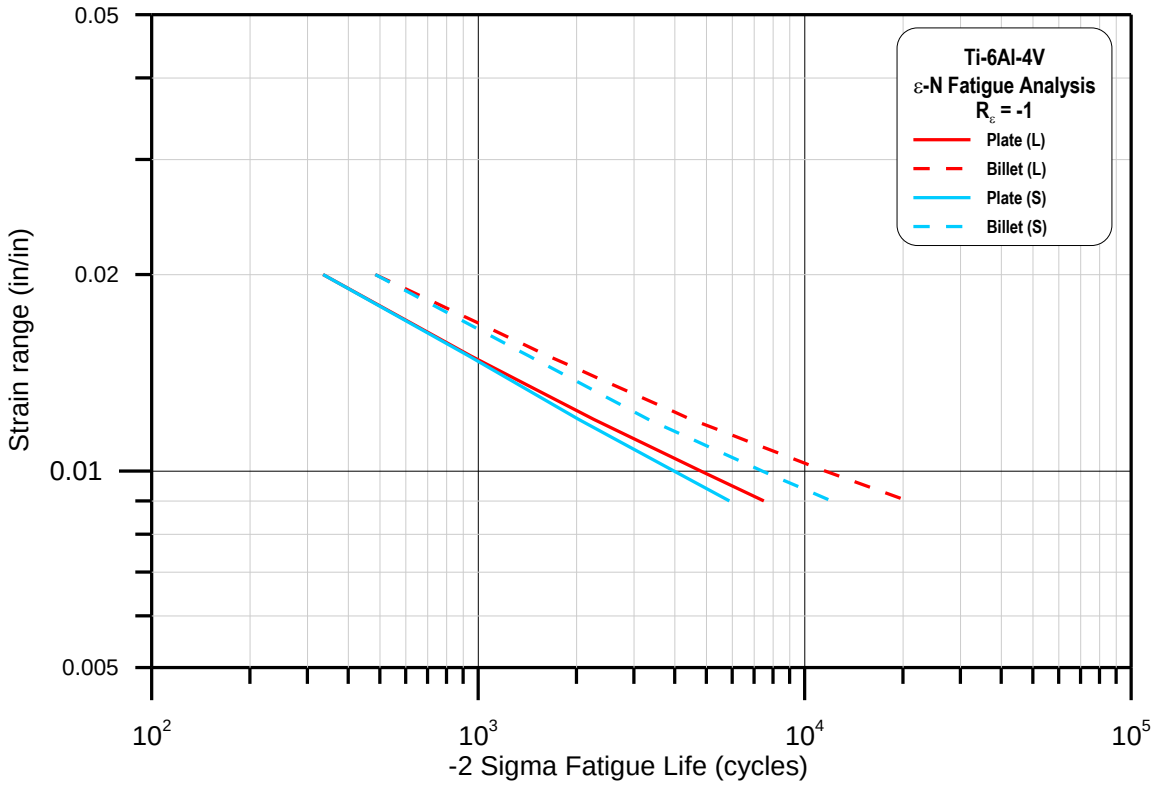
Fatigue (strain-controlled) – The results of strain-controlled axial fatigue analysis are shown graphically in Figure 6, with individual results tabulated in Table 5 for specific strain ranges. Since there were significant differences in the cyclic response and strain-control fatigue resistance between the L and S orientation for both plate and billet, the decision was made to not combine these results during the determination of the -2σ curves.

As can be seen in Figure 6(a), the largest decrement for billet, when compared against plate, occurs at the strain range of 0.009 in/in for R=0.05, in the S-orientation. At this strain range, the billet specimens only exhibited 70% of the plate specimens fatigue life. Therefore, the life factor for strain-controlled fatigue is 0.70, as shown in Table 6. As stated earlier, this life factor is based on a worst-case difference where billet had a lower life and was based on comparisons for only two stress ratios. In some cases, the factors are equal to or greater than 1.0. This factor should be used for initial screening purposes only.



(a)

Approved for public release; distribution unlimited.



(b)

Figure 6. Ti-6Al-4V strain-controlled axial fatigue analysis results for (a) $R_\varepsilon = 0.05$ and (b) $R_\varepsilon = -1$.

Approved for public release; distribution unlimited.

Table 5. Ti-6Al-4V strain-controlled axial fatigue analysis.

(a) $R_\varepsilon = 0.05$

Product Form	Orient-ation	Strain Range	Strain Ratio	Fatigue Life, cycles	
				Avg.	-2 Sigma
Plate	L	0.0090	0.05	9,120	5,880
	S	0.0090	0.05	19,710	12,260
Billet	L	0.0090	0.05	19,380	12,060
	S	0.0090	0.05	13,490	8,540
Plate	L	0.0100	0.05	6,040	3,980
	S	0.0100	0.05	11,050	7,070
Billet	L	0.0100	0.05	11,620	7,410
	S	0.0100	0.05	7,640	4,970
Plate	L	0.0120	0.05	2,980	2,030
	S	0.0120	0.05	4,070	2,730
Billet	L	0.0120	0.05	5,000	3,320
	S	0.0120	0.05	2,970	2,020
Plate	L	0.0150	0.05	1,320	940
	S	0.0150	0.05	1,240	880
Billet	L	0.0150	0.05	2,060	1,430
	S	0.0150	0.05	1,130	810
Plate	L	0.0200	0.05	450	330
	S	0.0200	0.05	270	210
Billet	L	0.0200	0.05	660	490
	S	0.0200	0.05	340	260

(b) $R_\varepsilon = -1$

Product Form	Orient-ation	Strain Range	Strain Ratio	Fatigue Life, cycles	
				Avg.	-2 Sigma
Plate	L	0.0090	-1.00	11,750	7,500
	S	0.0090	-1.00	29,590	18,050
Billet	L	0.0090	-1.00	34,160	20,690
	S	0.0090	-1.00	25,960	15,940
Plate	L	0.0100	-1.00	7,380	4,810
	S	0.0100	-1.00	15,410	9,700
Billet	L	0.0100	-1.00	18,530	11,560
	S	0.0100	-1.00	13,140	8,330
Plate	L	0.0120	-1.00	3,340	2,260
	S	0.0120	-1.00	5,010	3,330
Billet	L	0.0120	-1.00	6,860	4,490
	S	0.0120	-1.00	4,300	2,880
Plate	L	0.0150	-1.00	1,340	950
	S	0.0150	-1.00	1,340	950
Billet	L	0.0150	-1.00	2,380	1,640
	S	0.0150	-1.00	1,370	970
Plate	L	0.0200	-1.00	450	330
	S	0.0200	-1.00	270	210
Billet	L	0.0200	-1.00	660	490
	S	0.0200	-1.00	340	260

Table 6. Life factor for Ti-6Al-4V strain-controlled axial fatigue.

Ti-6Al-6V-2Sn ε-N Life Factor
0.70

Fatigue Crack Growth Rate – Fatigue crack growth rate analysis results curves are shown in Figures 7 and 8 for stress ratios (R) of 0.1 and 0.7, respectively. These curves were based on a 95% statistical upper bound on predicted values of da/dN. To accomplish this, a linear regression was fit to determine a linear model relating log (da/dN) to log (ΔK). The 95% prediction limits were calculated such that there was a 95% confidence that the prediction limits would contain any future data value of log (da/dN) at a given value of log (ΔK). The equations for these predictions are shown in the figures.

As previously reported ***[2, 3, 4]*** the fatigue crack growth rate results for both billet and plate were below those as shown in MMPDS-04 Figure 5.4.1.1.9(a1) for Ti-6Al-4V

plate. Therefore, although there is a small statistical difference between the combined billet data and the tested control plate, since both datasets exhibited slower growth rates than reference data for both stress ratios tested, the life factor for this alloy was determined to be 1x (as shown in Table 7), indicating an equivalent life. (The reference data is not shown in the following figures since it represents the mean of the data and not a 95% upper bound.) As stated earlier, this life factor is based on a worst-case difference where billet had a lower life and was based on comparisons for only two stress ratios. In some cases, the factor approaches 1.0. This factor should be used for initial screening purposes only.

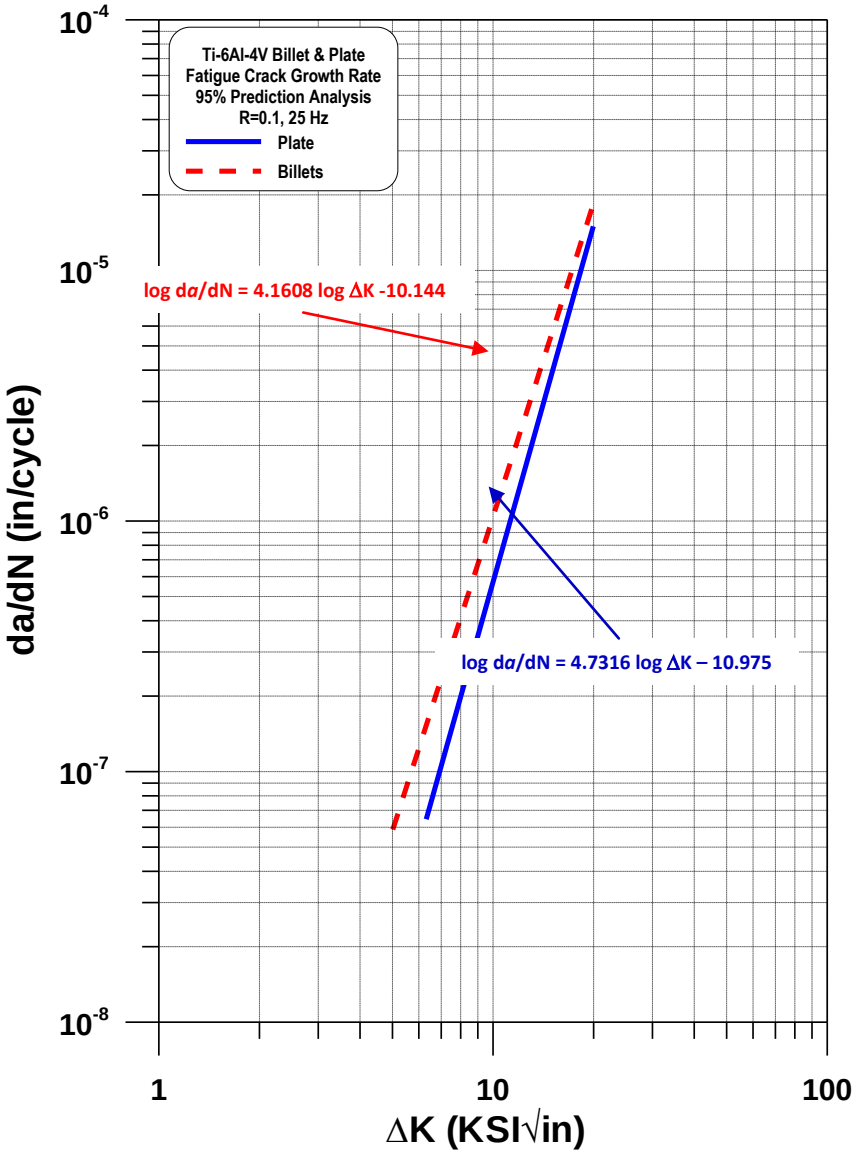


Figure 7. Ti-6Al-4V fatigue crack growth rate analysis results (R=0.1).

Approved for public release; distribution unlimited.

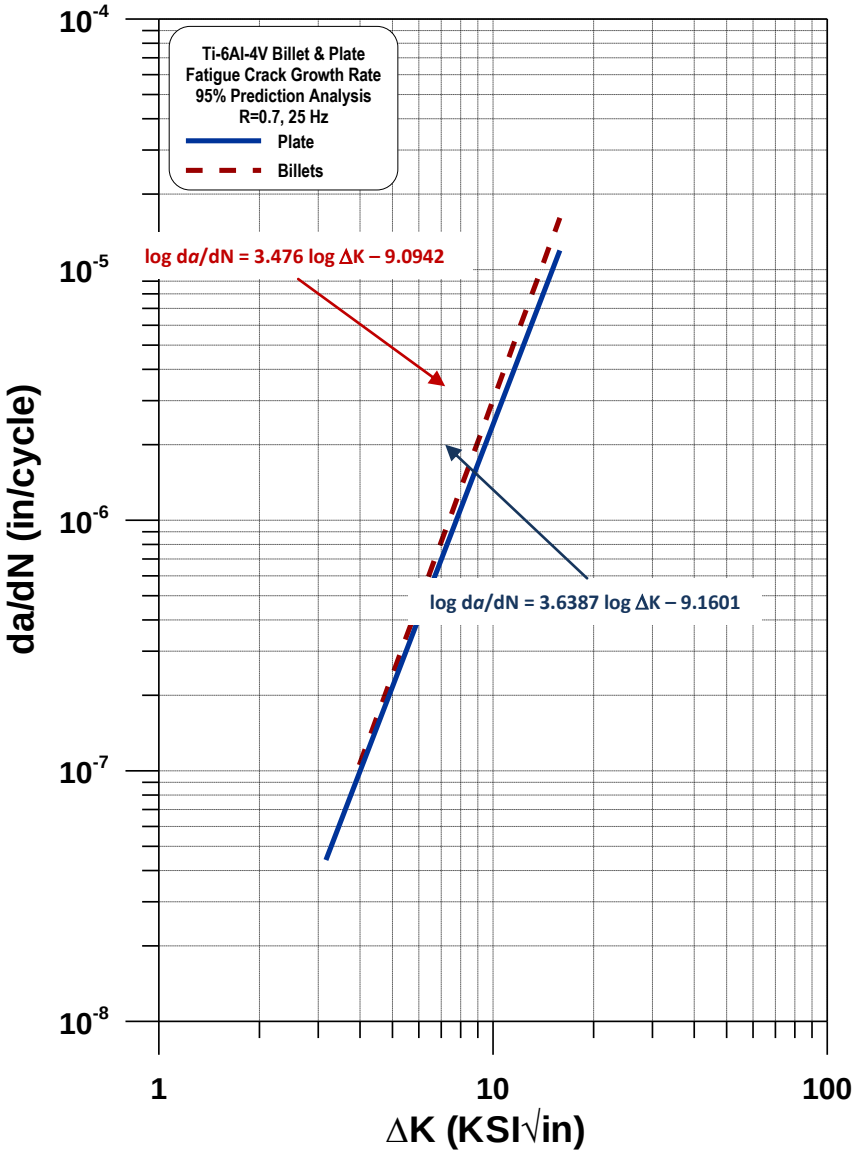


Figure 8. Ti-6Al-4V fatigue crack growth rate analysis results (R=0.7).

Table 7. Life factor for Ti-6Al-4V fatigue crack growth rate.

Ti-6Al-4V Fatigue Crack Growth Rate Life Factor
1x

Approved for public release; distribution unlimited.

Fracture Toughness – Plane-strain fracture toughness test results were not statistically analyzed, with the RLB being based on the lowest value determined during testing. This result is shown in Table 8.

Table 8. Reasonable lower bound for Ti-6Al-4V plane strain fracture toughness.

Ti-6Al-4V RLB
59.8 ksi√in

Stress Corrosion Cracking – Stress corrosion cracking tests had only a pass/fail criteria, therefore no analysis was performed. All specimens tested passed without issue.

Ti-6Al-6V-2Sn

Tension – Histograms for the tensile strength, elongation, and elastic modulus results are shown in Figures 9-12. Also shown on these histograms are the AMS-T-9046 and AMS-T-9047 specification minimum values (MMPDS typical value shown for elastic modulus). It is readily apparent from Figures 9 and 10 that the control plate exhibited higher strength properties when compared to the two billets. It is also obvious that the billets were unable to meet the specification minimum properties for plate (AMS-T-9046) a majority of the time. As previously reported ***[3]***, there were a few (3 of 26, longitudinal orientation) control plate specimens that also fell below specification minimum properties for ultimate tensile strength. When compared to the minimum properties in AMS-T-9047, the billet material had a significant amount (~36%) of specimens that fell below the specification properties for ultimate tensile strength, particularly in the 1"-3" specification thickness range. With respect to elastic modulus, although the minimum value is to be used as the RLB, even the mean values for the billet populations were lower than the MMPDS typical value.

Also included in the final analysis was tensile data from earlier investigations [***6, 7, 8]*** on components suspected of being manufactured from non-conforming material. These investigations reported numerous specimens having below specification strength results and lower than expected modulus results.

Sample statistics for ultimate tensile strength and tensile yield strength are shown in Table 9. As stated earlier, normal distribution statistics were applied to the population

in order to determine the preliminary RLB. MMPDS A-basis allowables have never been published for this alloy.

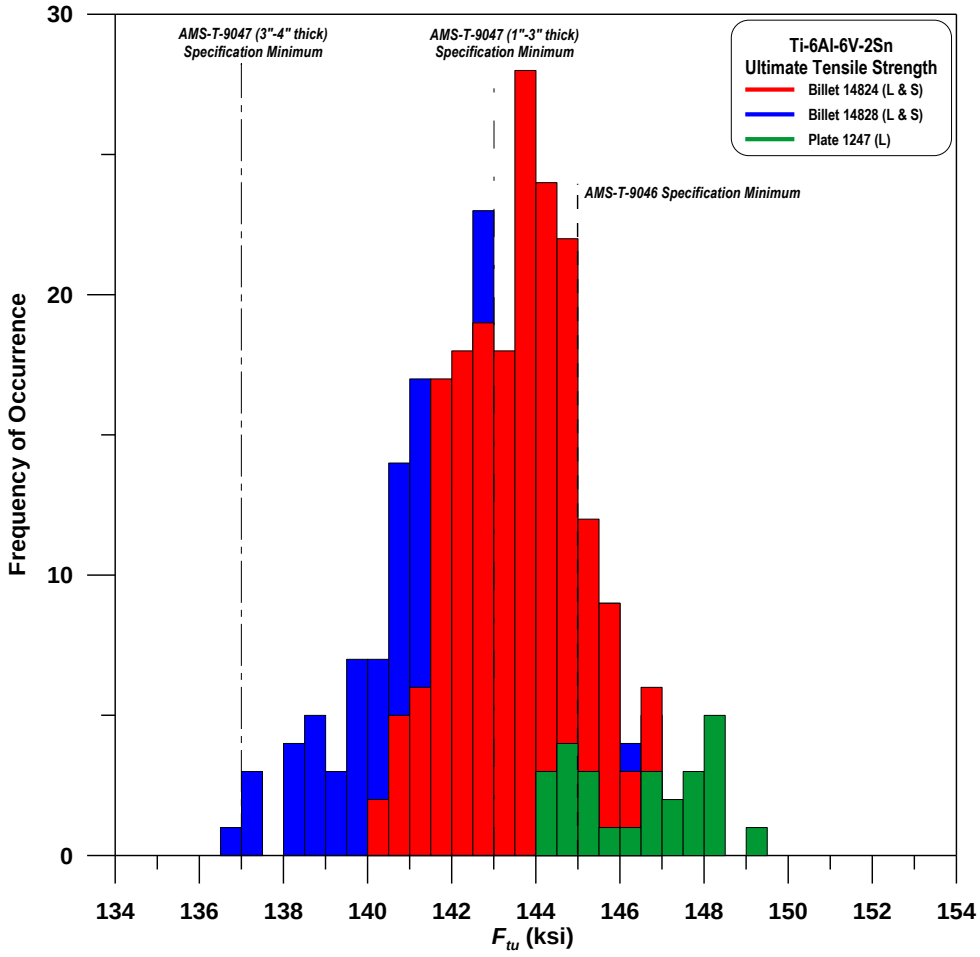


Figure 9. Histogram of Ti-6Al-6V-2Sn ultimate tensile strength results.

Approved for public release; distribution unlimited.

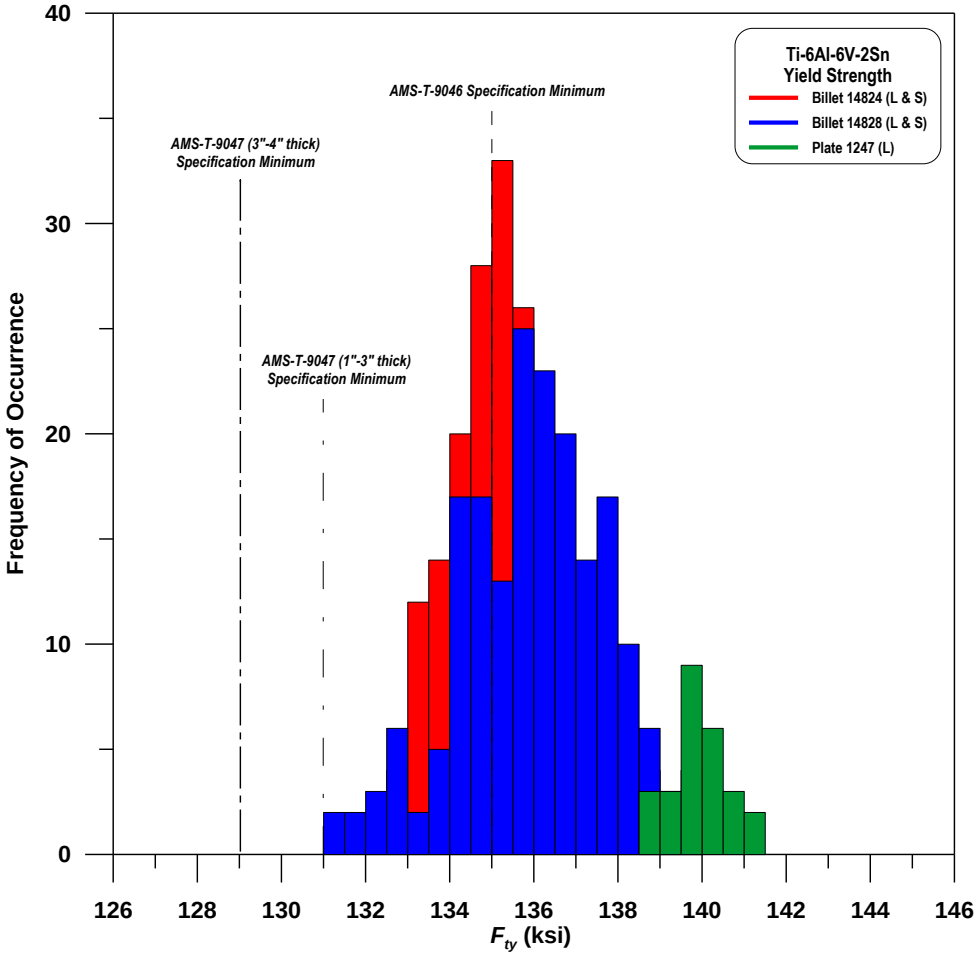


Figure 10. Histogram of Ti-6Al-6V-2Sn tensile yield strength results.

Approved for public release; distribution unlimited.

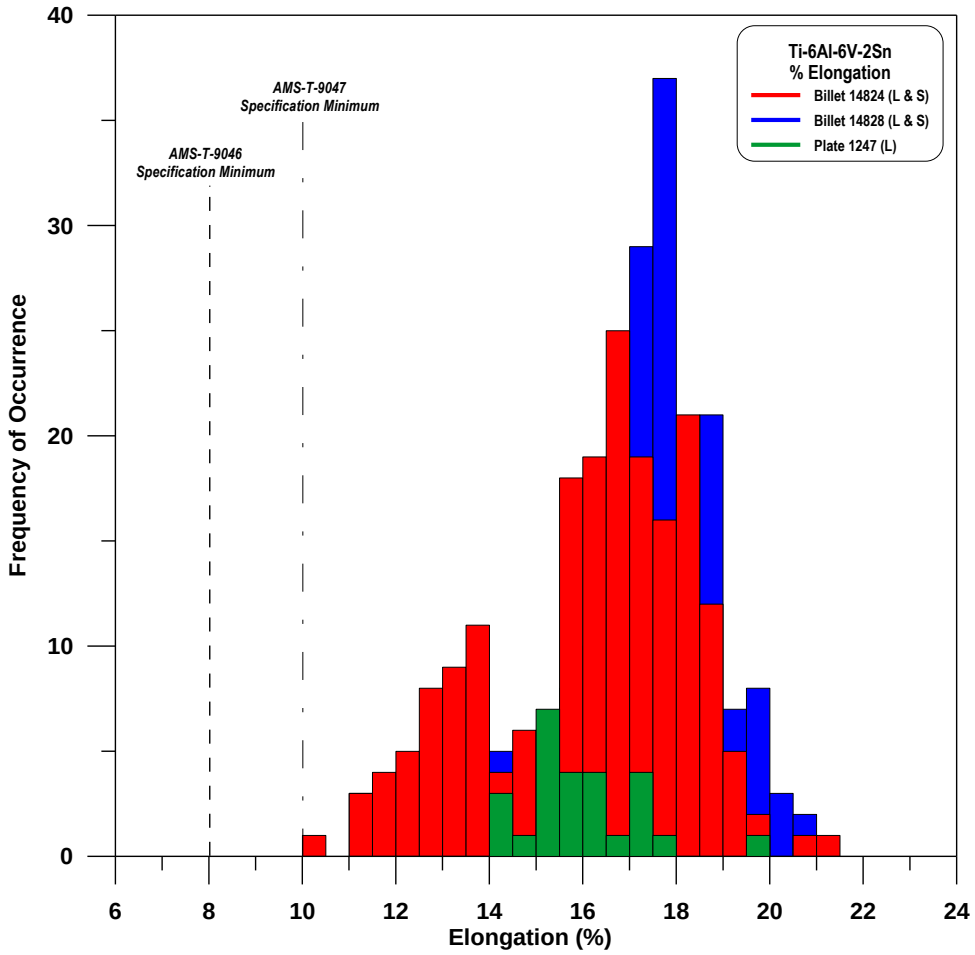


Figure 11. Histogram of Ti-6Al-6V-2Sn tensile elongation results.

Approved for public release; distribution unlimited.

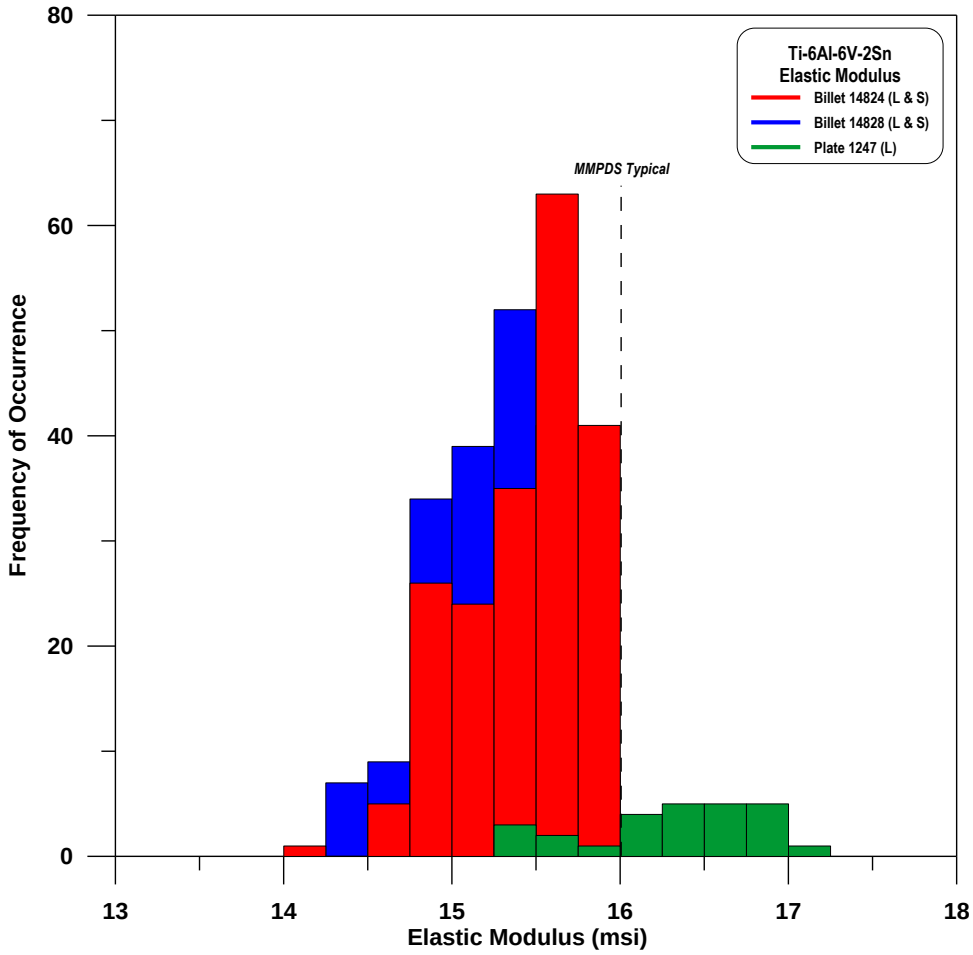


Figure 12. Histogram of Ti-6Al-6V-2Sn elastic modulus results.

Approved for public release; distribution unlimited.

Table 9. Ti-6Al-6V-2Sn tensile property analysis.

Statistic	F_{tu} (ksi)	F_{ty} (ksi)	Elongation (%)	Reduction of Area (%)	Elastic Modulus (msi)
Mean	143.29	135.81	16.7	32.5	15.4
Std. Dev.	2.119	1.812	2.113	4.936	0.381
COV	1.48%	1.33%	-	-	-
Skewness	0.04	0.55	-	-	-
Sample Size	388	387	387	387	388
Preliminary RLB	***137***	***131***	***10%***	***19%***	***14.2***
AMS-T-9046 Spec Min	145	135	8%	n/a	16.0†
AMS-T-9047 Spec Min	143 (1"-3") 137 (3"-4")	131 (1"-3") 129 (3"-4")	10%	20%	n/a
Final RLB	**137**	**131**	**10%**	**19%**	**14.2**

†: MMPDS typical

Fatigue (force-controlled) – The -2 sigma analysis of force-controlled axial fatigue test results are shown graphically in Figure 13. Due to the fact that the data for the two stress ratios were not well represented with the equivalent stress model (as used for Ti-6Al-4V), the data was analyzed separately and had separate standard error of estimate curves (-2 SEE). The curves shown were based on equations of the form:

$$N_{-2SEE} = 10^{\log N_f - 2SEE},$$

$$Log\ N_f = A_1 + A_2 \log(S_{max} - A_3),$$

where:
SEE varies with S_{max},
N_f is the number of cycles to failure,
S_{max} is the maximum applied stress, and
A_1, A_2, A_3 are coefficients determined by analysis.

Coefficients for each curve are shown in Table 10. The curves are plotted only between the stress levels applied during testing. No further extrapolation was performed.

As shown in Figure 13, the largest decrement for billet, when compared against plate, occurs at the 65 ksi stress level for R = -1. At this stress level, the billet specimens only exhibited 14% of the plate specimens' fatigue life. Therefore, the life factor for force-controlled fatigue is 0.14, as shown in Table 11. As stated earlier, this life factor is based on a worst-case difference where billet had a lower life and was based on comparisons for only two stress ratios. This factor should be used for initial screening purposes only.

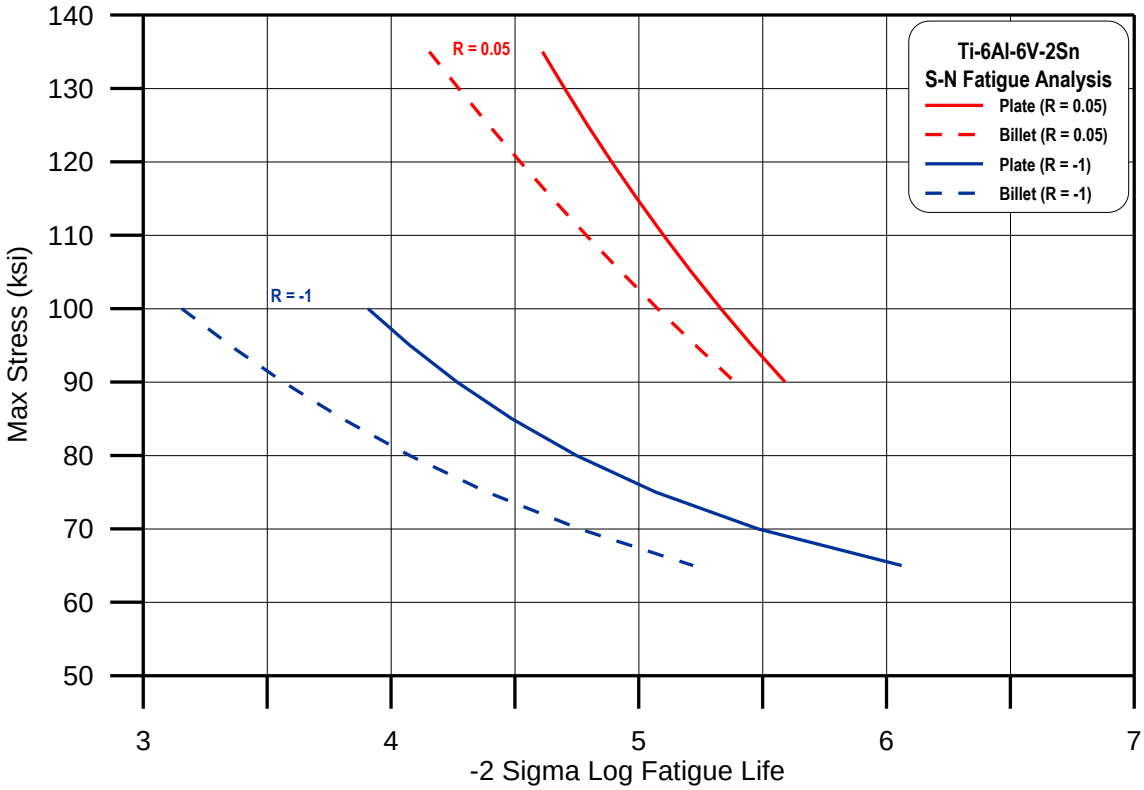


Figure 13. Ti-6Al-6V-2Sn force-controlled axial fatigue analysis results.

Table 10. Ti-6Al-6V-2Sn force-controlled axial fatigue -2 sigma equation coefficients.

Product Form	Stress Ratio	-2 Sigma Equation Coefficients			
		A_1	A_2	A_3	*SEE*
Plate	0.05	15.456	-5.140	19.10	$15.9/S_{max}$
	-1	10.550	-3.764	54.23	$19.6/S_{max}$
Billet	0.05	21.862	-8.127	0.00	$26.6/S_{max}$
	-1	14.599	-6.004	44.31	$48.1/S_{max}$

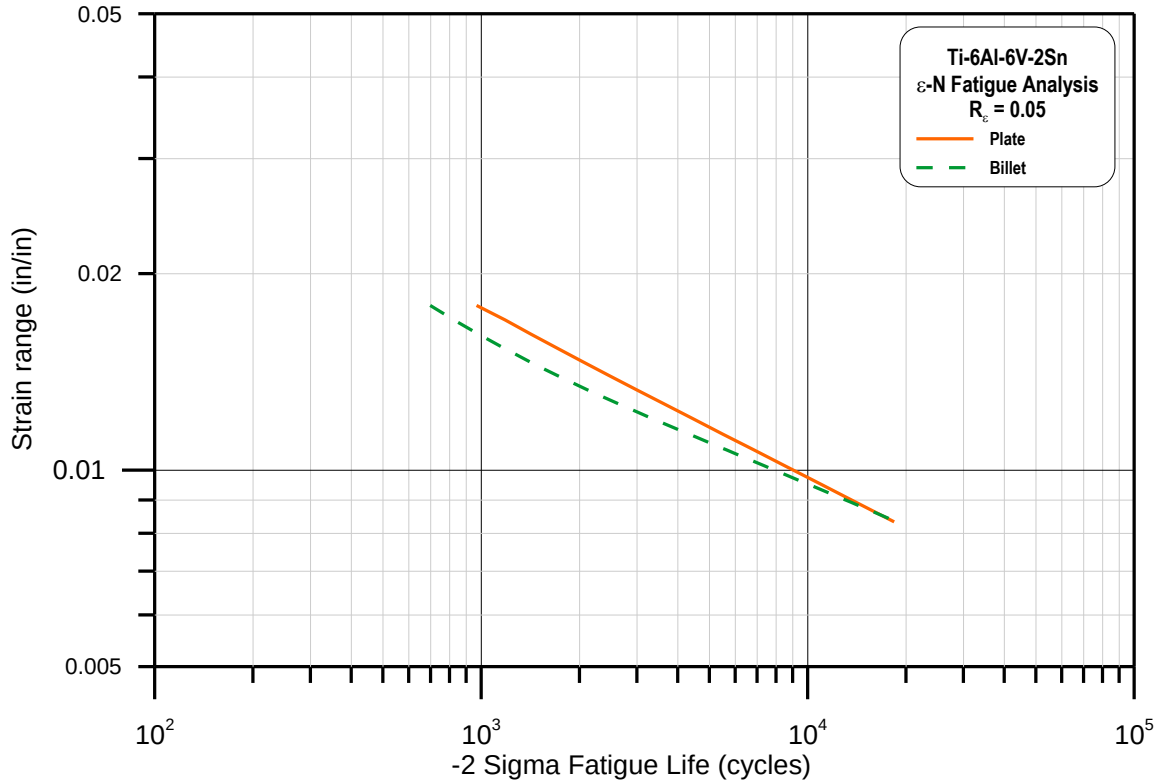
Table 11. Life factor for Ti-6Al-6V-2Sn force-controlled axial fatigue.

Ti-6Al-6V-2Sn S-N Life Factor
0.14

Approved for public release; distribution unlimited.

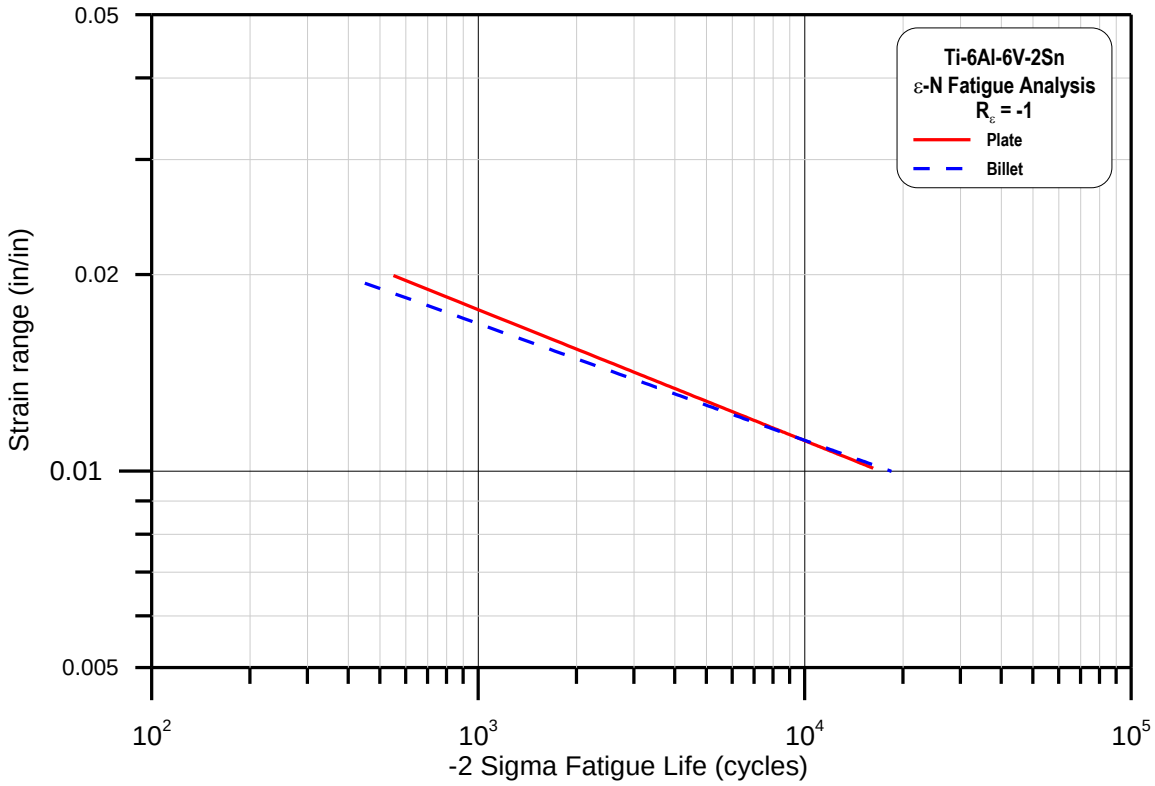
Fatigue (strain-controlled) – The results of strain-controlled axial fatigue analysis are shown graphically in Figure 14, with individual results tabulated in Table 12 for specific strain ranges. For this alloy, the decision was made to combine the L and S orientation results during the determination of the -2σ curves.

As can be seen in Figure 14(a), the largest decrement for billet, when compared against plate, occurs towards the upper strain ranges for R=0.05. At this strain range, the billet specimens only exhibited 69% of the plate specimens' fatigue life. Therefore, the life factor for strain-controlled fatigue is 0.69, as shown in Table 13. As stated earlier, this life factor is based on a worst-case difference where billet had a lower life and was based on comparisons for only two stress ratios. In some cases, the factors are equal to or greater than 1.0. This factor should be used for initial screening purposes only.



(a)

Approved for public release; distribution unlimited.



(b)

Figure 14. Ti-6Al-6V-2Sn strain-controlled axial fatigue analysis results for (a) $R_\varepsilon = 0.05$ and (b) $R_\varepsilon = -1$.

Approved for public release; distribution unlimited.

Table 12. Ti-6Al-4V strain-controlled axial fatigue analysis.

(a) $R_\varepsilon = 0.05$

Product Form	Strain Range	Strain Ratio	Fatigue Life, cycles	
			Avg.	-2 Sigma
Plate	0.0083	0.05	27,975	18,398
Billet	0.0083	0.05	36,612	18,777
Plate	0.0101	0.05	13,044	8,578
Billet	0.0101	0.05	14,501	7,437
Plate	0.0120	0.05	6,772	4,454
Billet	0.0120	0.05	6,561	3,365
Plate	0.0154	0.05	2,594	1,706
Billet	0.0154	0.05	2,288	1,173
Plate	0.0179	0.05	1,472	968
Billet	0.0179	0.05	1,361	698

(b) $R_\varepsilon = -1$

Product Form	Strain Range	Strain Ratio	Fatigue Life, cycles	
			Avg.	-2 Sigma
Plate	0.0101	-1.00	24,655	16,215
Billet	0.0101	-1.00	35,979	18,452
Plate	0.0120	-1.00	10,469	6,885
Billet	0.0120	-1.00	12,657	6,491
Plate	0.0139	-1.00	4,879	3,209
Billet	0.0139	-1.00	5,235	2,685
Plate	0.0162	-1.00	2,376	1,563
Billet	0.0162	-1.00	2,470	1,267
Plate	0.0179	-1.00	1,472	968
Billet	0.0179	-1.00	1,518	779

Table 13. Life factor for Ti-6Al-6V-2Sn strain-controlled axial fatigue.

Ti-6Al-6V-2Sn ε-N Life Factor
0.69

Approved for public release; distribution unlimited.

Fatigue Crack Growth Rate – Fatigue crack growth rate analysis results curves are shown in Figures 15 and 16 for stress ratios (R) of 0.1 and 0.7, respectively. These curves were based on a 95% statistical upper bound on predicted values of da/dN. To accomplish this, a linear regression was fit to determine a linear model relating log (da/dN) to log (ΔK). The 95% prediction limits were calculated such that there was a 95% confidence that the prediction limits would contain any future data value of log (da/dN) at a given value of log (ΔK). The equations for these predictions are shown in the figures.

The fatigue crack growth rate results from previous investigations ***[6, 8]*** on suspect F-15 components were also included in this analysis. This data actually produced the fastest growth rates when compared to both plate and billets at the stress ratio of R=0.1. Therefore, the largest statistical difference was between the component data and the tested control plate, giving the life factor for this alloy as 2x, indicating that non-conforming material had crack growth rates twice that of properly processed plate material. (It should be noted that handbook reference data was not available for this alloy.) As stated earlier, this life factor is based on a worst-case difference where billet had a lower life and was based on comparisons for only two stress ratios. In some cases, the factor approaches 1.0. This factor should be used for initial screening purposes only.

Approved for public release; distribution unlimited.

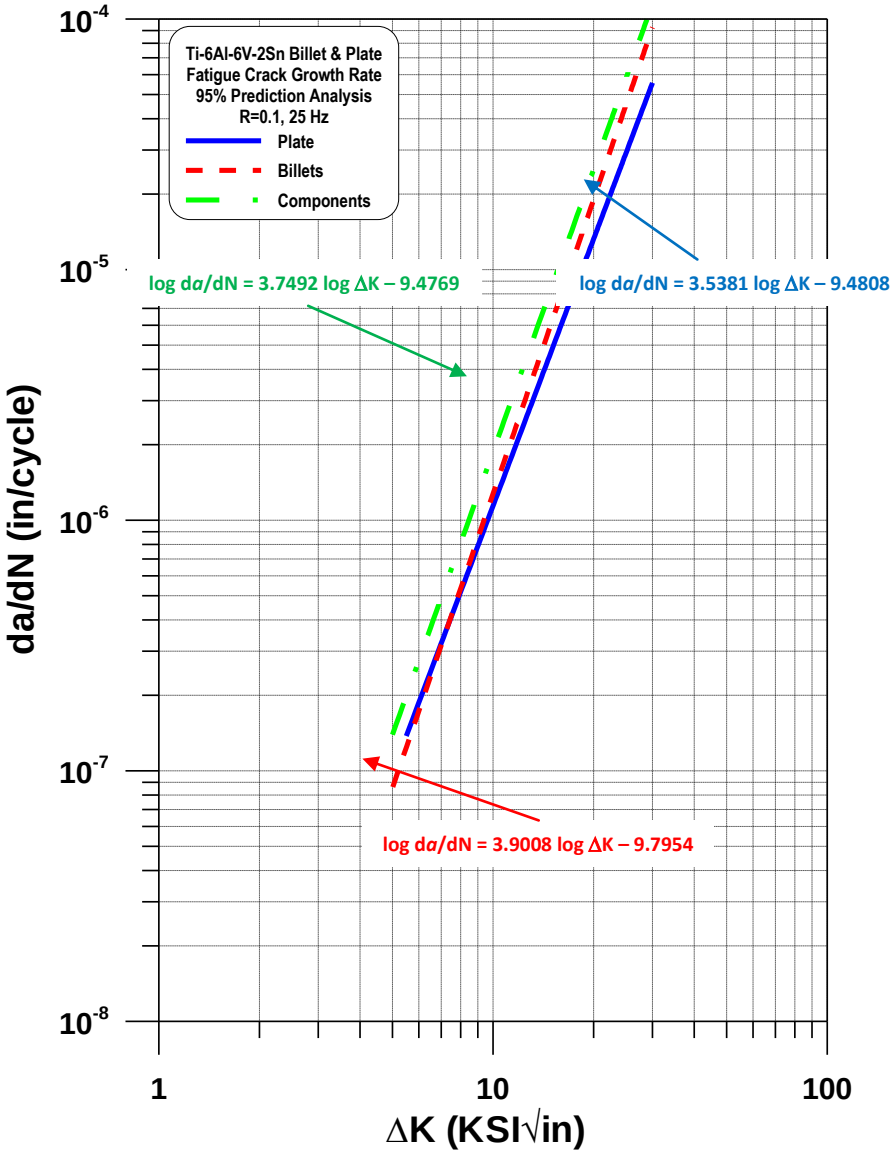


Figure 15. Ti-6Al-6V-2Sn fatigue crack growth rate analysis results (R=0.1).

Approved for public release; distribution unlimited.

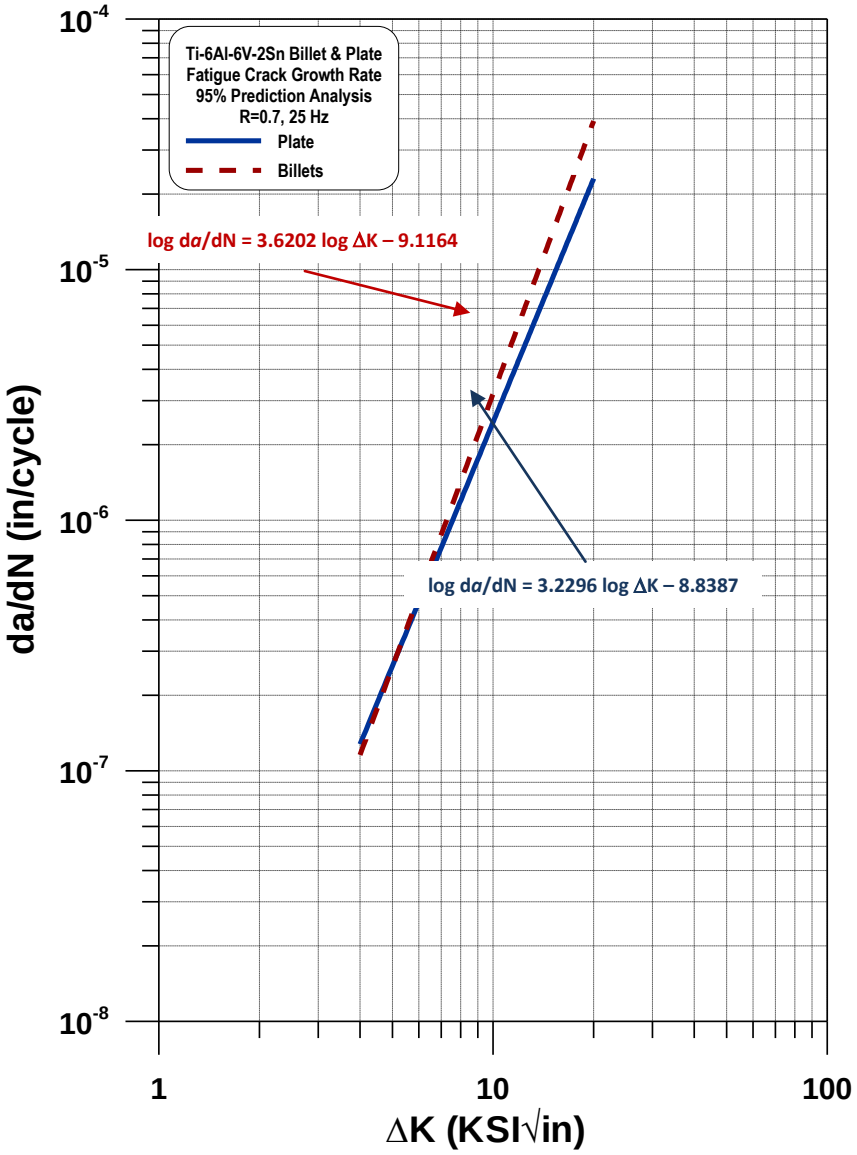


Figure 16. Ti-6Al-6V-2Sn fatigue crack growth rate analysis results (R=0.7).

Table 15. Life factor for Ti-6Al-6V-2Sn fatigue crack growth rate.

Ti-6Al-6V-2Sn Fatigue Crack Growth Rate Life Factor
2x

Fracture Toughness – Plane-strain fracture toughness test results were not statistically analyzed, with the RLB being based on the lowest value determined during testing. This result is shown in Table 16.

Table 16. Reasonable lower bound for Ti-6Al-6V-2Sn plane strain fracture toughness.

Ti-6Al-6V-2Sn RLB
55.7 ksi$\sqrt{in}$

Stress Corrosion Cracking – Stress corrosion cracking tests had only a pass/fail criteria, therefore no analysis was performed. All specimens tested passed without issue.

CONCLUSIONS AND RECOMMENDATIONS

Improperly processed materials can have material properties that do not meet specifications and requirements. This report has documented this for the titanium alloys Ti-6Al-4V and Ti-6Al-6V-2Sn.

Engineers and designers must account for reduced properties when assessing the integrity and safety of components that are, or may have been, made with improperly processed materials. This report provides data for Ti-6Al-4V and Ti-6Al-6V-2Sn that should be used in such assessments.

Approved for public release; distribution unlimited.

REFERENCES

9. *Metallic Materials Properties Development and Standardization (MMPDS)*, MMPDS-04; April 2008; Federal Aviation Administration.
10. *Non-Conforming Titanium – Billet Characterization (Ti-6Al-4V Billet),* AFRL/RXS 10-057; S.R. Thompson; July 2010.
11. *Non-Conforming Titanium – Control Plate Characterization (Ti-6Al-4V & Ti-6Al-6V-2Sn Plate),* AFRL/RXS 10-072; S.R. Thompson; August 2010.
12. *Non-Conforming Titanium – Billet Characterization (Ti-6Al-4V Billet),* AFRL/RXS 10-087; S.R. Thompson; November 2010.
13. *Non Conforming Titanium – Billet Characterization (Ti-6Al-6V-2Sn Billets),* AFRL/RXS 11-009; S.R. Thompson; January 2011.
14. *Material Evaluation of Ti-6Al-6V-2Sn Plate and Components*; AFRL/MLSC 05-082; S.R. Thompson; June 2005.
15. *Material Evaluation of Ti-6Al-6V-2Sn F-15 Engine Mounts*; AFRL/MLSC 07-011; S.R. Thompson; January 2007.
16. *Material Evaluation of Ti-6Al-6V-2Sn F-15 Engine Mounts (Part 2)*; AFRL/RXSC 08-083; S.R. Thompson; November 2008.

ACKNOWLEDGEMENTS

The author wishes to thank Mr. Richard Rice of Battelle Memorial Institute for his statistical analyses of the tensile and fatigue data, and to Dr. Gerald Shaughnessy of the University of Dayton for his statistical analyses on the fatigue crack growth rate data.

PREPARED BY

SIGNED

_____

STEVEN R. THOMPSON, Senior Materials Engineer
Materials Test & Evaluation Team
Acquisition Systems Support Branch
Systems Support Division
Materials and Manufacturing Directorate

PUBLICATION REVIEW: This report has been reviewed and approved.

SIGNED

_____

CHARLES E. WAGNER, Chief
Acquisition Systems Support Branch
Systems Support Division

Approved for public release; distribution unlimited.

UDRI
UNIVERSITY of DAYTON RESEARCH INSTITUTE

APPENDIX F

STATISTICAL EVALUATION OF FATIGUE CRACK GROWTH RATE DATA FROM TITANIUM BILLETS/PLATES

TECHNICAL EVALUATION REPORT
FA8650-09-D-5600, TO 0008

August 2011

Prepared for:

Steven Thompson
Materials Test & Evaluation Team, RXSCE
Wright-Patterson AFB, OH 45433

Prepared by:

Gerald Shaughnessy
University of Dayton
and
John J. Ruschau
Structural Integrity Division

University of Dayton Research Institute
300 College Park
Dayton, OH 45469-0120

DISTRIBUTION A: Approved for public release. Distribution unlimited.

TABLE OF CONTENTS

Page

SECTION 1 INTRODUCTION 349
SECTION 2 TECHNICAL ANALYSIS DETAIL.....350
2.1 Discussion of Models Considered and Justification for Use of the Paris Model.....350
2.2 Comparison of Billets 75838 and K27P (Combined Orientations) with 95% Prediction Values for Plate J91K (Combined Orientations) with R = 0.1 350
2.2.1 Comparison at Log(ΔK) =1 for 95% Predicted Values, R = 0.1 352
2.2.2 Comparison at Log(ΔK) =1.2 for 95% Predicted Values, R = 0.1 352
2.2.3 Comparison at Log(ΔK) =1.4 for 95% Predicted Values 352
2.3 Comparison of Combined Billets 75838 and K27P with 95% Prediction Values for Plate J91K with R = 0.7 353
2.3.1 Comparison at Log(ΔK) =0.6 for 95% Predicted Values, R =0.7 354
2.3.2 Comparison at Log(ΔK) =0.85 for 95% Predicted Values, R =0.7 355
2.3.3 Comparison at Log(ΔK) =1.1 for 95% Predicted Values, R =0.7 355
2.4 Comparison of 95% Prediction Values among Combined Billets 14824 and 14828 and Plate 1247 and Component at R = 0.1 355
2.4.1 Comparison at Log(ΔK) = 0.8 for 95% Predicted Values, R =0.1 356
2.4.2 Comparison at Log(ΔK) =1.0 for 95% Predicted Values, R =0.1 358
2.4.3 Comparison at Log(ΔK) =1.4 for 95% Predicted Values, R =0.1 359
2.5 Comparison of 95% Prediction Values among Combined Billets 14824 and 14828 and Plate 1247, R = 0.7.....359
2.5.1 Comparison at Log(ΔK) =0.6 for 95% Predicted Values, R =0.7 361
2.5.2 Comparison at Log(ΔK) =0.85 for 95% Predicted Values, R =0.7 361
2.5.3 Comparison at Log(ΔK) =1.1 for 95% Predicted Values, R =0.7 361
SECTION 3 CONCLUSIONS.....362

LIST OF FIGURES

Page

Figure 1. Comparison of Billets 75838 & K27P with J91K Plate Data at R=0.1 351
Figure 2. Comparison of Billets 75838 & K27P with J91K Plate Trend Lines at R=0.1 351
Figure 3. Comparison of Billets 75838 & K27P with Plate J91K Data at R=0.7 353
Figure 4. Comparison of Billets 75838 & K27P with Plate J91K Trendlines at R=0.7 354
Figure 5. Comparison of Billets 14824 & 14828 and Plate 1247 and 357
Component Data at R = 0.1 357
Figure 6. Comparison of Billets 14824 & 14828 and Plate 1247 and 357
Component Trendlines at R = 0.1 357
Figure 7. Comparison of Billets 14824 and 14828 and Plate 1247 Data at R=0.7 360
Figure 8. Comparison of Billets 14824 and 14828 and Plate 1247 Trendlines at R=0.7 360

Approved for public release; distribution unlimited.

SECTION 1
INTRODUCTION

An investigation was conducted at the request of USAF to evaluate the potential risk associated with improperly processed titanium material being used in the fabrication of critical safety items and safety-of-flight components in USAF, DoD, NASA, FAA, and other systems. The suspect Ti material herein referred to as "billet" or "reforging stock," was never intended to be machined to the final forms in which it is now possibly being used. As such, an R&D testing program was initiated to develop engineering design data on a heretofore not fully characterized form of Ti.

To assist in this effort to characterize mechanical properties of billet materials, UD was asked to perform statistical analysis on fatigue crack growth rate (FCGR) properties to compare several billets materials with properly-processed baseline materials. The analysis protocols, results, and conclusions are presented in the following sections.

Approved for public release; distribution unlimited.

SECTION 2
TECHNICAL ANALYSIS DETAIL

2.1 Discussion of Models Considered and Justification for Use of the Paris Model

The graphs of da/dN versus ΔK on a Log-Log showed that a linear model on that scale would fit the data very well. Other models were considered such as the Walker equation and a cubic spline fit of the relationship between da/dN versus ΔK but the goodness of the linear fit as indicated by the graphs of da/dN versus ΔK on a Log- Log scale as well as the high values of R^2 (an $R^2 = 1$ indicates a perfect linear fit of the data). The linear model relating Log(da/dN) to Log(ΔK) was determined to give a more than adequate fit to the data.

Using standard commercially available statistical software, a linear regression line was fit to determine the linear model relating Log(da/dN) to Log ΔK) For each linear regression model fit to the data, ninety five percent prediction limits of prediction were calculated The 95% prediction limits are calculated such that there is 95% confidence that the prediction limits will containing any future data value of Log(da/dN) at any given value of Log(ΔK). Since the prediction limits are two sided and only the upper value is of interest, the upper limit has 97.5 % confidence that future data values of Log(da/dN) will lie below the calculated limit.

2.2 Comparison of Billets 75838 and K27P (Combined Orientations) with 95% Prediction Values for Plate J91K (Combined Orientations) with R = 0.1

The data for the combined billets 75838 and K27P are plotted in Figure 1. Upper 95% prediction values for combined billets 75838 and K27P and plate J91K were calculated. Figure 2 shows only the upper 95% calculated limits of prediction for future values.

Next two sample t-tests were performed to determine if the differences between the billet values and the plate values were statistically significant. The tests for statistical significance were performed at fixed values of Log(ΔK).

In this case Log(ΔK) = 1.0, 1.2, and 1.4.

Approved for public release; distribution unlimited.

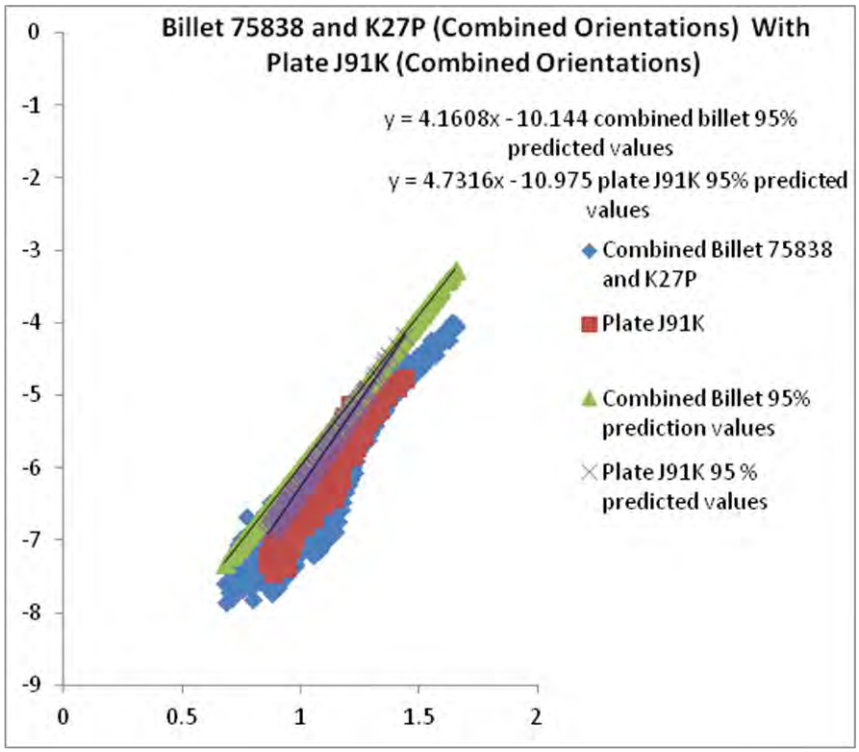


Figure 1. Comparison of Billets 75838 & K27P with J91K Plate Data at R=0.1

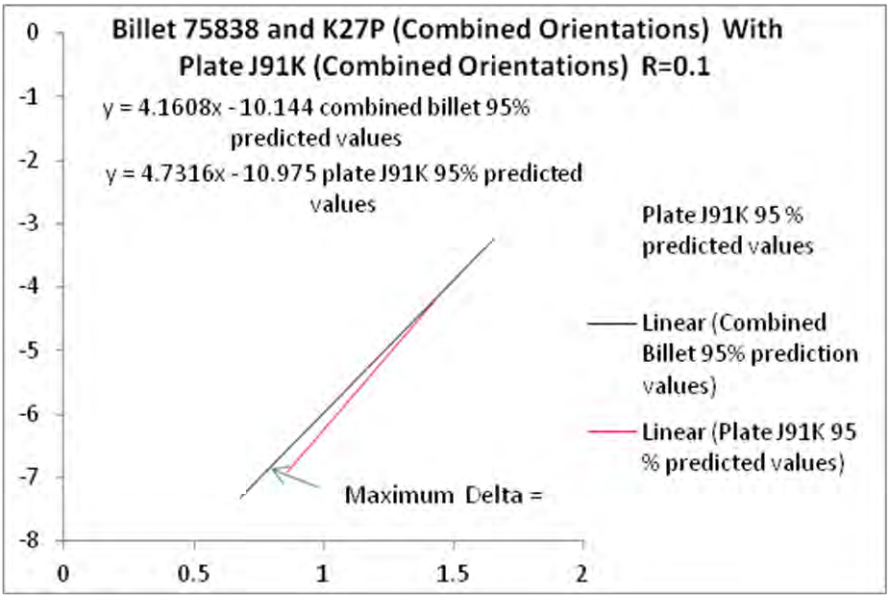


Figure 2. Comparison of Billets 75838 & K27P with J91K Plate Trend Lines at R=0.1

Approved for public release; distribution unlimited.

2.2.1 Comparison at Log(ΔK) =1 for 95% Predicted Values, R = 0.1

Two-Sample T-Test and CI: Combined Billet 75838 and K27P Log(ΔK) =1, Plate

	N	Mean	Standard Deviation	SE Mean
Billet	28	-6.0154	0.0304	0.0057
Plate	29	-6.2256	0.0769	0.014

Difference = mu (Billet Log(ΔK) =1) - mu (Plate Log(ΔK) =1)
Estimate for difference: 0.210173
95% CI for difference: (0.178967, 0.241378)
T-Test of difference = 0 (vs not =): T-Value = 13.66 P-Value = 0.000 DF = 36

- **The difference is statistically significant at the 0.05 significance level.**

2.2.2 Comparison at Log(ΔK) =1.2 for 95% Predicted Values, R = 0.1

Two-Sample T-Test and CI: Combined Billet 75838 and K27P Log(ΔK) =1.2, Plate Log(ΔK) =1.2

	N	Mean	Standard Deviation	SE Mean
Billet	22	-5.1460	0.0321	0.0068
Plate	14	-5.3173	0.0519	0.014

Difference = mu (Billet Log(ΔK) =1.2) - mu (Plate Log(ΔK) =1.2)
Estimate for difference: 0.171250
95% CI for difference: (0.138889, 0.203610)
T-Test of difference = 0 (vs not =): T-Value = 11.08 P-Value = 0.000 DF = 19

- **The difference is statistically significant at the 0.05 significance level.**

2.2.3 Comparison at Log(ΔK) =1.4 for 95% Predicted Values

Two-Sample T-Test and CI: Combined Billet 75838 and K27P Log(ΔK) =1.4, Plate Log(ΔK) =1.4

	N	Mean	Standard Deviation	SE Mean
Billet	18	-4.3264	0.0388	0.0092
Plate	7	-4.438	0.148	0.056

Difference = mu (Billet Log(ΔK) =1.4) - mu (Plate Log(ΔK) =14)
Estimate for difference: 0.111511
95% CI for difference: (-0.027386, 0.250409)
T-Test of difference = 0 (vs not =): T-Value = 1.96 P-Value = 0.097 DF = 6

- **The difference is not statistically significant at the 0.05 significance level.**

2.3 Comparison of Combined Billets 75838 and K27P with 95% Prediction Values for Plate J91K with R = 0.7

The data for the combined billets 75838 and K27P are plotted in Figure 3.Upper 95% prediction values for combined billets 75838 and K27P and plate J91K were calculated. Figure 4 shows only the upper 95% calculated limits of prediction for future values.

Next two sample t-tests were performed to determine if the differences between the billet values and the plate values were statistically significant. The tests for statistical significance were performed at fixed values of Log(ΔK).

In this case Log(ΔK) = 0.6, 0.85, and 1.1.

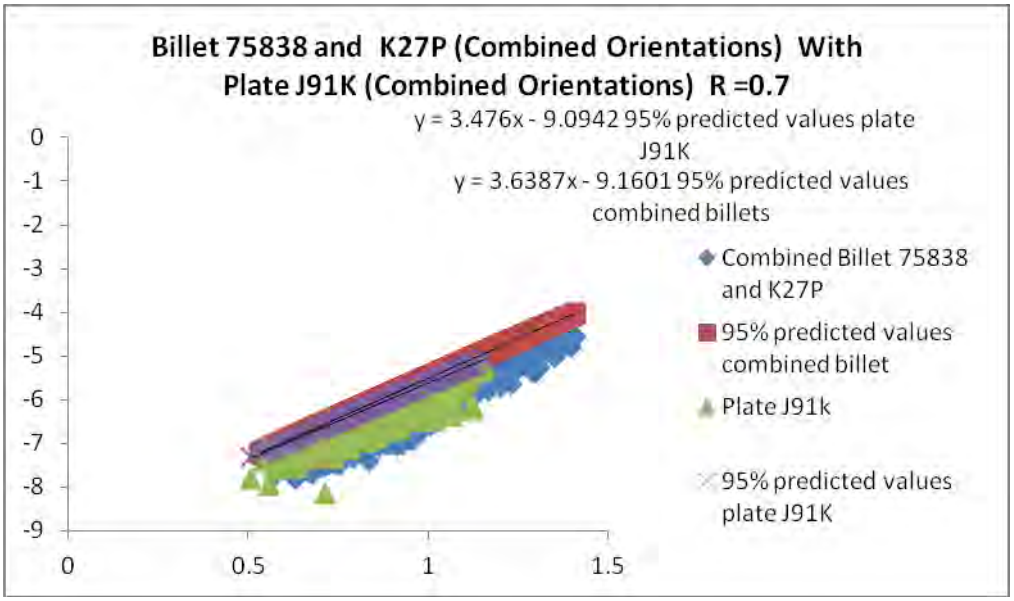


Figure 3. Comparison of Billets 75838 & K27P with Plate J91K Data at R=0.7

Approved for public release; distribution unlimited.

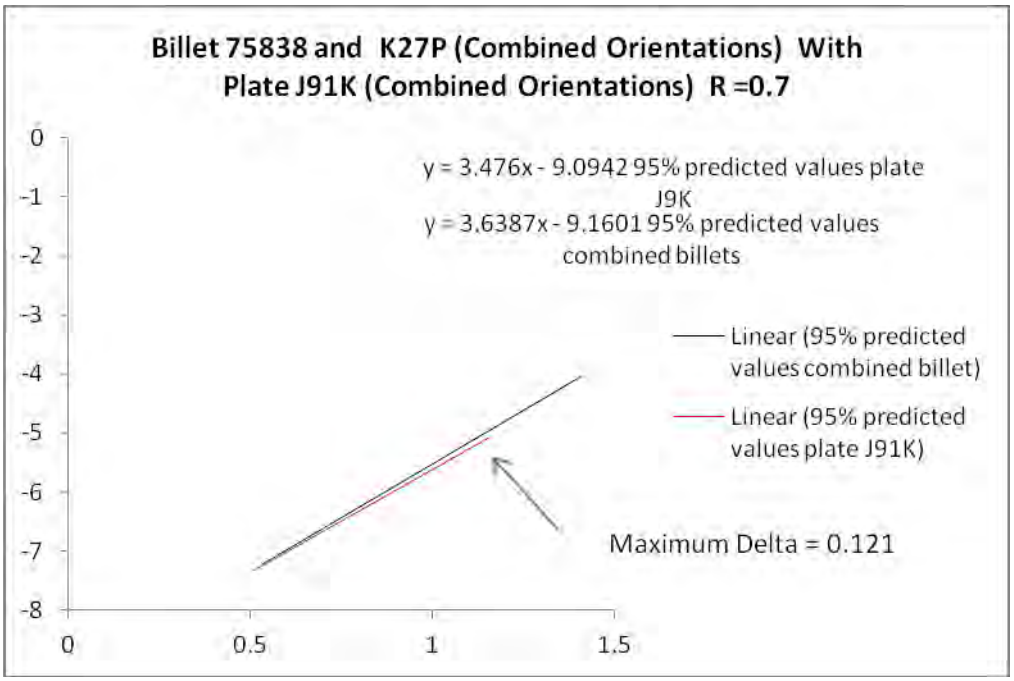


Figure 4. Comparison of Billets 75838 & K27P with Plate J91K Trendlines at R=0.7

2.3.1 Comparison at Log(ΔK) =0.6 for 95% Predicted Values, R =0.7

Two-Sample T-Test and CI: Combined Billets vs Plate J91K at Log(ΔK)=0.6

	N	*Mean*	*Standard Deviation*	*SE Mean*
Combined	*17*	*-6.9723*	*0.0321*	*0.0078*
Plate J9	*12*	*-6.9808*	*0.0852*	*0.025*

Difference = mu Combined Billets Log(ΔK)=.6 - mu Plate J91K Log(ΔK)=.6
Estimate for difference: 0.0085
95% CI for difference: (-0.0378, 0.0547)
T-Test of difference = 0 (vs not =): T-Value = 0.38 P-Value = 0.710 DF = 27
Both use Pooled StDev = 0.0598

- **The difference between the combined billet 95% predicted values and the Plate 95% predicted values is NOT statistically significant at the 0.05 significance level at Log(ΔK) =0.6.**

Approved for public release; distribution unlimited.

2.3.2 Comparison at Log(ΔK) =0.85 for 95% Predicted Values, R =0.7

Two-Sample T-Test and CI: Combined Billets vs Plate J91K for Log(ΔK) =0.85

	N	Mean	Standard Deviation	SE Mean
Combined	*10*	*-6.06966*	*0.00703*	*0.0022*
Plate J9	*10*	*-6.1657*	*0.0254*	*0.0080*

Difference = mu Combined Billets Log(ΔK)=.8 - mu Plate J91K Log(ΔK)=0.85
Estimate for difference: 0.09608
95% CI for difference: (0.07857, 0.11360)
T-Test of difference = 0 (vs not =): T-Value = 11.53 P-Value = 0.000 DF = 18
Both use Pooled StDev = 0.0186

- **The difference between the combined billet 95% predicted values and the Plate 95% predicted values is statistically significant at the 0.05 significance level at Log(Delta K) =0.85.**

2.3.3 Comparison at Log(ΔK) =1.1 for 95% Predicted Values, R =0.7

Two-Sample T-Test and CI: Combined Billets vs Plate J91K for Log(ΔK)=1.1

	N	Mean	Standard Deviation	SE Mean
Combined	*16*	*-5.1755*	*0.0163*	*0.0041*
Plate J9	*27*	*-5.2955*	*0.0839*	*0.016*

Difference = mu Combined Billets Log(ΔK)=1 - mu Plate J91K Log(ΔK)=1.1
Estimate for difference: 0.1200
95% CI for difference: (0.0770, 0.1630)
T-Test of difference = 0 (vs not =): T-Value = 5.63 P-Value = 0.000 DF = 41
Both use Pooled StDev = 0.0675

- **The difference between the combined billet 95% predicted values and the Plate 95% predicted values is statistically significant at the 0.05 significance level at Log(ΔK) =1.1.**

2.4 Comparison of 95% Prediction Values among Combined Billets 14824 and 14828 and Plate 1247 and Component at R = 0.1

The data for the combined billets 14824 and14828 are plotted in Figure 5. Upper 95% prediction values for combined billets 14824 and14828 and plate 1247 were calculated. Figure 6 shows only the upper 95% calculated limits of prediction for future values.

Approved for public release; distribution unlimited.

Next an analysis of variance was calculated to determine if any significant differences occurred among the billet values the component values and the plate values. The tests for statistical significance were performed at fixed values of Log(Delta K).

In this case Log(Delta K) = 0.8, 1.0, and 1.4.

2.4.1 Comparison at Log(ΔK) = 0.8 for 95% Predicted Values, R =0.1

One-way ANOVA: Combined Billets, Plate 1247 R=0.1, Component R=0.1, Log(ΔK)=0.8.

Source	*DF*	*SS*	*MS*	*F*	*P*
Factor	*2*	*1.5326*	*0.7663*	*69.45*	*0.000*
Error	*395*	*4.3587*	*0.0110*		
Total	*397*	*5.8914*			

S = 0.1050 R-Sq = 26.01% R-Sq(adj) = 25.64%

Level	*N*	*Mean*	*Standard Deviation*
Combined Billet	*27*	*-6.6985*	*0.0597*
Plate 1247 R=0.1	*20*	*-6.6372*	*0.1004*
Component R=0.1	*351*	*-6.4829*	*0.1079*

Individual 95% CIs For Mean Based on Pooled Standard deviation

```
Level              ---+---------+---------+---------+------
Combined Billet   (-----*-----)
Plate 1247 R=0.1       (------*-----)
Component R=0.1                          (-*)
                   ---+---------+---------+---------+------
                   -6.720    -6.650    -6.580    -6.510
```

Pooled Standard deviation = 0.1050

- **The difference between the Component 95% predicted value is statistically significant from both the Plate 1247 predicted value and the Combined Billet using the 0.05 level of significance at Log(ΔK)=0.8. The difference between the combined billet 95% predicted value and the Plate 1247 95% predicted value is not statistically significant using the 0.05 level of significance at Log(ΔK)=0.8.**

Approved for public release; distribution unlimited.

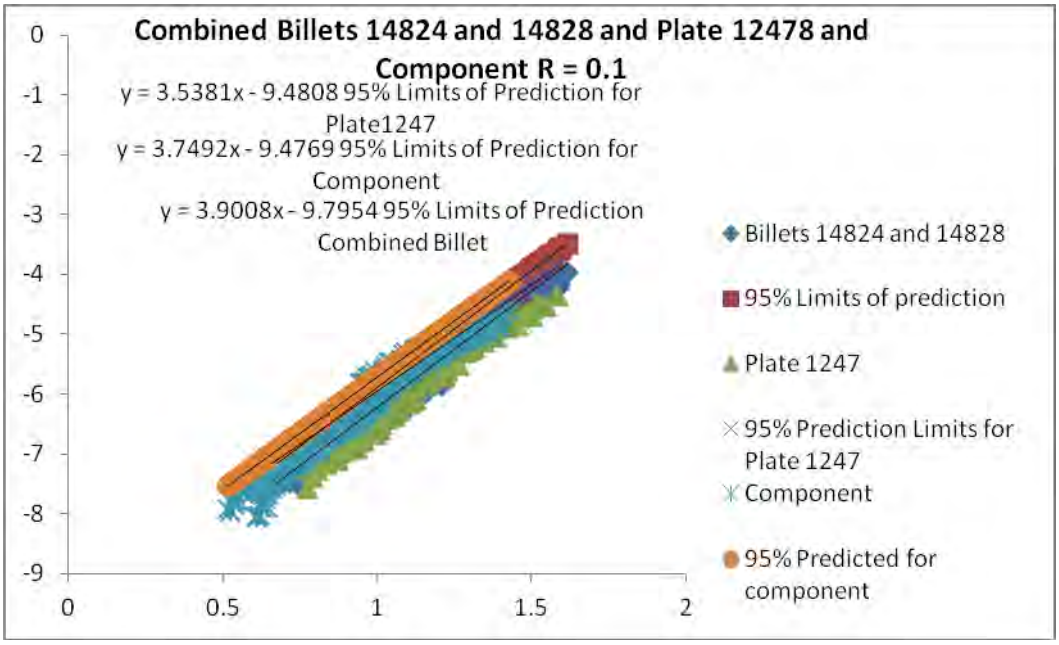


Figure 5. Comparison of Billets 14824 & 14828 and Plate 1247 and Component Data at R = 0.1

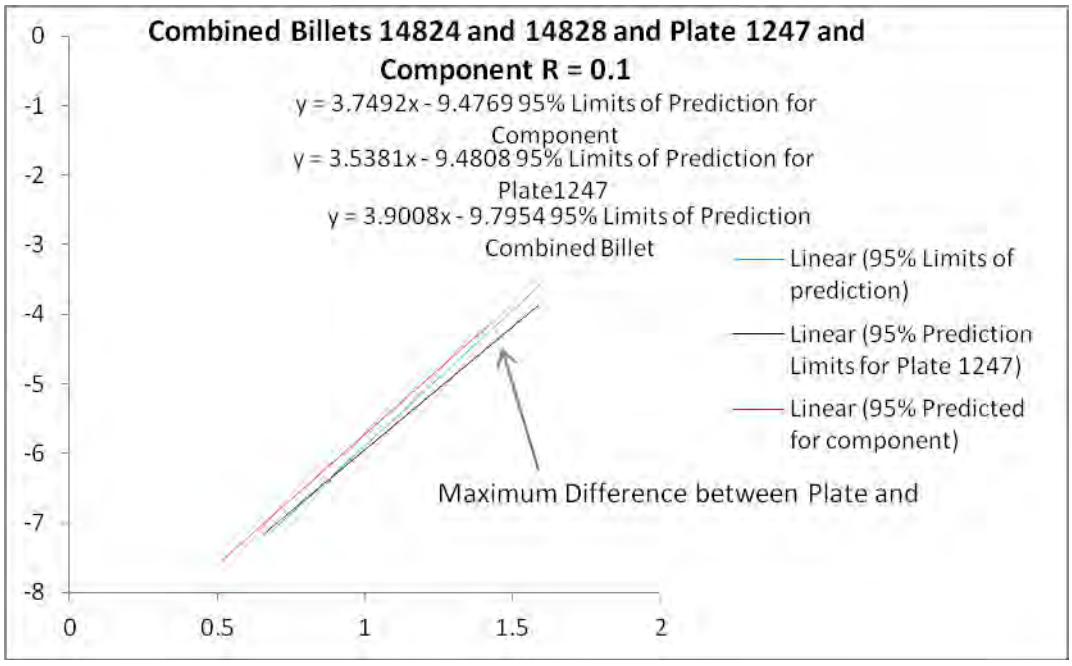


Figure 6. Comparison of Billets 14824 & 14828 and Plate 1247 and Component Trendlines at R = 0.1

Approved for public release; distribution unlimited.

2.4.2 Comparison at Log(ΔK) =1.0 for 95% Predicted Values, R =0.1

One-way ANOVA: Combined Billets, Plate 1247 R=0.1, Component R=0.1, Log(ΔK)=1.

Source	*DF*	*SS*	*MS*	*F*	*P*
Factor	*2*	*3.2127*	*1.6064*	*149.80*	*0.000*
Error	*345*	*3.6996*	*0.0107*		
Total	*347*	*6.9123*			

S = 0.1036 R-Sq = 46.48% R-Sq(adj) = 46.17%

Level	*N*	*Mean*	*Standard Deviation*
Combined Billet	*80*	*-5.9096*	*0.1155*
Plate 1247 R=0.1	*40*	*-5.9532*	*0.0934*
Component R=0.1	*228*	*-5.7236*	*0.1008*

Individual 95% CIs For Mean Based on Pooled Standard deviation

```
Level              -----+---------+---------+---------+----
Combined Billet         (--*--)
Plate 1247 R=0.1   (----*---)
Component R=0.1                      (-*-)
                   -----+---------+---------+---------+----
                    -5.950    -5.880    -5.810    -5.740
```

Pooled Standard deviation = 0.1036

- **The difference between the Component 95% predicted value is statistically significant from both the Plate 1247 predicted value and the Combined Billet using the 0.05 level of significance at Log(ΔK)=0.8. The difference between the combined billet 95% predicted value and the Plate 1247 95% predicted value is not statistically significant using the 0.05 level of significance at Log(ΔK)=1.0.**

Approved for public release; distribution unlimited.

2.4.3 Comparison at Log(ΔK) =1.4 for 95% Predicted Values, R =0.1

One-way ANOVA: Combined Billets, Plate 1247 R=0.1, Component R=0.1 Log(ΔK)=1.4.

Source	*DF*	*SS*	*MS*	*F*	*P*
Factor	*2*	*0.34320*	*0.17160*	*19.59*	*0.000*
Error	*41*	*0.35913*	*0.00876*		
Total	*43*	*0.70233*			

S = 0.09359 R-Sq = 48.87% R-Sq(adj) = 46.37%

Level	*N*	*Mean*	*Standard Deviation*
Combined Billet	*18*	*-4.4006*	*0.0910*
Plate 1247 R=0.1	*13*	*-4.5326*	*0.0903*
Component R=0.1	*13*	*-4.3039*	*0.1002*

Individual 95% CIs for Mean Based on Pooled Standard deviation

```
Level          ---------+---------+---------+---------+
Combined Billet      (----*---)
Plate 1247 R=0.1  (-----*----)
Component R=0.1                (-----*----)
               ---------+---------+---------+---------+
                 -4.50     -4.40     -4.30     -4.20
```

Pooled Standard deviation = 0.0936.

- **The differences between the Component 95% predicted value is statistically significant from both the Plate 1247 predicted value and the Combined Billet using the 0.05 level of significance at Log(ΔK)=0.8. The difference between the combined billet 95% predicted value and the Plate 1247 95% predicted value is also statistically significant using the 0.05 level of significance at Log(ΔK)=1.4.**

2.5 Comparison of 95% Prediction Values among Combined Billets 14824 and 14828 and Plate 1247, R = 0.7

The data for the combined billets 14824 and 14828 at the stress ratio R=0.7 are plotted in Figure 7. Upper 95% prediction values for the combined data sets and plate 1247 were calculated and presented in Figure 8. An analysis of variance was calculated to determine if any significant differences occurred among the billet and the plate values. The tests for statistical significance were performed at fixed values of Log(ΔK).

In this case Log(ΔK) = 0.6, 0.85, and 1.1.

Approved for public release; distribution unlimited.

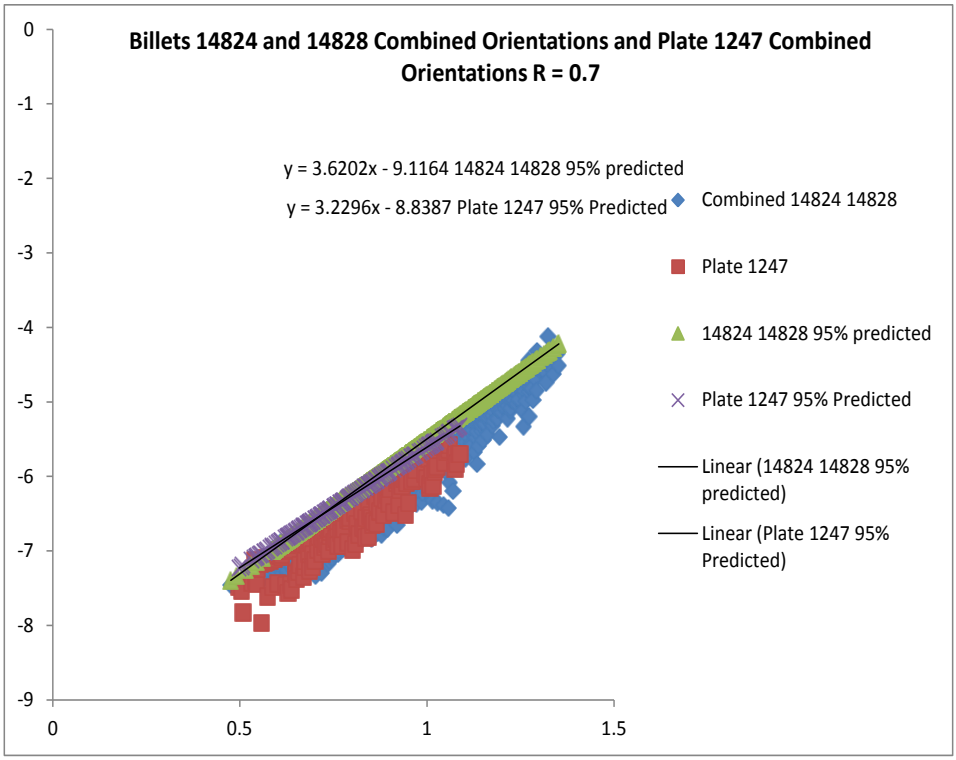


Figure 7. Comparison of Billets 14824 and 14828 and Plate 1247 Data at R=0.7

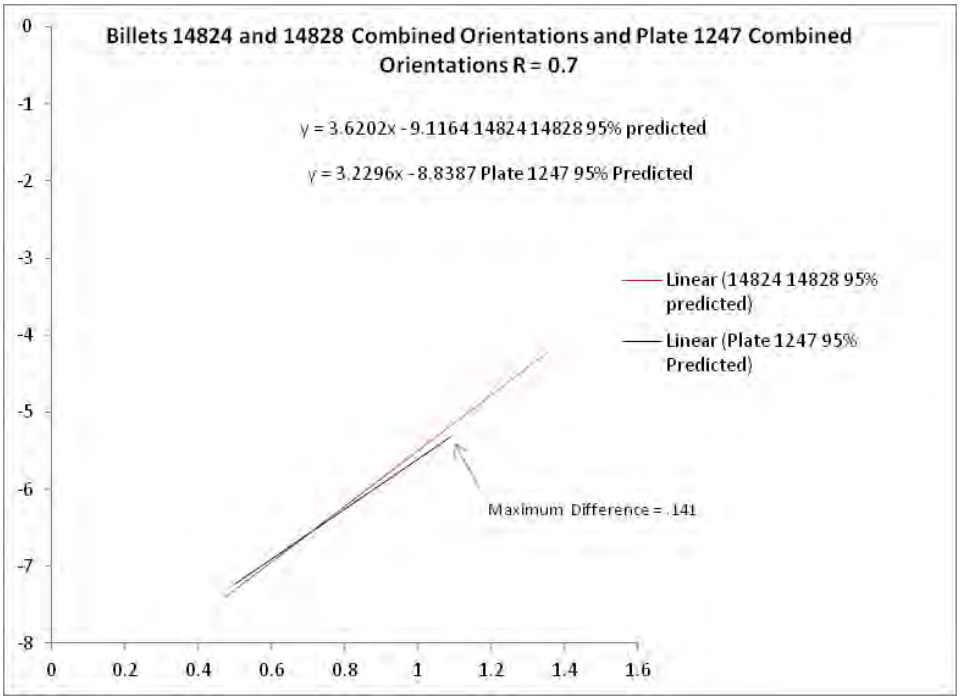


Figure 8. Comparison of Billets 14824 and 14828 and Plate 1247 Trendlines at R=0.7

Approved for public release; distribution unlimited.

2.5.1 Comparison at Log(ΔK) =0.6 for 95% Predicted Values, R =0.7

Two-Sample T-Test and CI: Billet Log(ΔK)=0.6, Plate Log(ΔK)=0.6

	N	Mean	Standard Deviation	SE Mean
Billet	14	-6.9665	0.0217	0.0058
Plate	13	-6.9766	0.0534	0.015

Difference = mu (Billet Log(ΔK)=0.6) - mu (Plate Log(ΔK)=0.6)
Estimate for difference: 0.010104
95% CI for difference: (-0.021780, 0.041989)
T-Test of difference = 0 (vs not =): T-Value = 0.65 P-Value = 0.520 DF = 25
Both use Pooled StDev = 0.0402

- **The difference is NOT statistically significant at the 0.05 significance level.**

2.5.2 Comparison at Log(ΔK) =0.85 for 95% Predicted Values, R =0.7

Two-Sample T-Test and CI: Billet Log(ΔK)=0.85, Plate Log(ΔK)=0.85

	N	Mean	Standard Deviation	SE Mean
Billet	17	-6.0422	0.0101	0.0025
Plate	7	-6.0957	0.0168	0.0064

Difference = mu (Billet Log(ΔK)=0.85) - mu (Plate Log(ΔK)=0.85)
Estimate for difference: 0.053467
95% CI for difference: (0.041994, 0.064940)
T-Test of difference = 0 (vs not =): T-Value = 9.66 P-Value = 0.000 DF = 22
Both use Pooled StDev = 0.0123

- **The difference is statistically significant at the 0.05 significance level.**

2.5.3 Comparison at Log(ΔK) =1.1 for 95% Predicted Values, R =0.7

Two-Sample T-Test and CI: Billet Log(ΔK)=1.1 vs Plate Log(ΔK)=1.1

	N	Mean	Standard Deviation	SE Mean
Billet Log	22	-5.1560	0.0252	0.0054
Plate Log	9	-5.3733	0.0400	0.013

Difference = mu (Billet Log(ΔK)=1.1) - mu (Plate Log(ΔK)=1.1)
Estimate for difference: 0.217214
95% CI for difference: (0.192914, 0.241513)
T-Test of difference = 0 (vs not =): T-Value = 18.28 P-Value = 0.000 DF = 29
Both use Pooled StDev = 0.0300

- **The difference is statistically significant at the 0.05 significance level.**

Approved for public release; distribution unlimited.

SECTION 3
CONCLUSIONS

Statistical comparisons of fatigue crack growth rate data were performed on data sets furnished by RXSC engineers. Comparisons of growth rate were made at a 95% confidence level at selected stress intensity ranges to determine if data were from the same population. Based on the data furnished, the following general conclusions are rendered:

- For the Ti 6-4 alloys examined, there were no discernable differences between the control plate and the billet materials. The billet data in fact showed slower growth rate for a given stress intensity range than reference data from MMPDS. Based on constant amplitude test results, there appears no safety impact for this alloy.
- For the Ti-6-6-2 alloy, fatigue crack growth data for the components were faster than both the billet and control plate materials.

Approved for public release; distribution unlimited.